Development of Landslide Risk Assessment Technology along Transport Arteries in Vietnam

Proceedings of the Final SATREPS Workshop on Landslides

13 October 2016, Hanoi, Vietnam

Published by
Institute of Transport Science and Technology (ITST)
International Consortium on Landslides (ICL)

Development of Landslide Risk Assessment Technology along Transport Arteries in Vietnam

Proceedings of the Final SATREPS Workshop on Landslides

13 October 2016, Hanoi, Vietnam

Published by

Institute of Transport Science and Technology (ITST)

International Consortium on Landslides (ICL)

Preface for SATREPS Final Workshop 2016

Nguyen Xuan Khang, Project Director
Kyoji Sassa, Project Leader

SATREPS Project: Development of landslide risk assessment technology along transport arteries in Vietnam

A landslide is a downslope movement of a mass of soil, rock, or both. Landslides include various type of movements, fall, topple, slide, spread and flow. Landslide disasters occur in mountainous areas all over the world. The motion of landslides results in lots of damages in human lives and properties, and huge impact on social infrastructures and system in urban and rural areas every year. Landslide causing factors include; conditions of topography, geology, tectonic and seismic activities, climate change and precipitation (rainfall, snow and snow melting), vegetation, mining, dam construction, re-profiling of slopes and other impacts from human beings during the regional development of land. Especially, due to the influence of global climate change, the increase of frequency and the intensity of extreme weather events has contributed to the increase of landslides in many of landslide prone areas.

The rate of mountainous terrain of Vietnam is up to ¾ area of its whole territory and the mountain slopes have a complex geological structure and soil layers are subjected to strong tropical weathering and the speed of weathering is fast. Vietnam is located in tropical monsoon, most of countries are affected by very high humidity and heavy rains. Vietnam is one of the strongest landslide impacted countries. Moreover, main transport arteries pass through mountainous areas where large-scale deep landslides and small scale shallow landslides occur frequently.

The cooperative research project “Development for landslide risk assessment technology along main transport arteries in Vietnam” was set up to reduce landslide disasters that block sustainable development across the country, based on developed Japanese technology and experiences of International Consortium on Landslides (ICL). Long-term objective of the Project is socialization of the new landslide risk assessment technology and early warning system suitable for Vietnam developed through the Project. Project results are expected to contribute to transport artery safety and effective implementation of disaster reduction strategy of the Government.

The Project consists of four working groups. Work Group 1- Integrated Research for Development of landslide risk assessment technology and education. Work Group 2- Wide-area landslide mapping and landslide risk identification. Work Group 3- Laboratory

soil testing & Computer simulation of landslide initiation and motion. Work Group 4- Landslide monitoring and development of early warning system.

After five years of implementation, the Project has executed many survey and research activities and capacity development activities in Vietnam and in Japan. As the results of joint research efforts, a bunch of science and technology results and the capacity development has been achieved to meet the planned project objectives

- **Main activity results of Work Group 1:**

Regarding human resource training, five long-term trainees completed master courses and two long-term trainees obtained Ph. D through the doctor courses in Japan.
Besides participating the International Programme on Landslides (IPL) meeting and IPL symposium in France, Japan and the 3rd World Landslide Forum in Beijing (June 2014), ITST assigned seven staff to join sixteen short-term training for technology transfer in Japan. As a result of short-term training, one obtained Thesis Dr. Other staffs are in the progress to pursue Thesis Dr. by submitting papers.

The Project completed landslide risk assessment guidelines which consist of thirty three guidelines both in English and in Vietnamese. These technical guidelines have key role to provide instruction tools for experts, scientists, consulting engineers as well as managers in terms of risk assessment and solution proposal in Vietnam.

The Project Website was set up to introduce widely about project activities and outputs; this is a scientific forum for people and experts in landslide area to share and update scientific knowledge.

- **Main activity results of Work Group 2:**

Field investigation and Data collection for landslide mapping was conducted along Ho Chi Minh Route, National Highway No. 1A, Hai Van area and other relevant areas through many surveys. Discussion on phenomenon types, landslide mechanism and landslide causing factors were jointly implemented based on the field survey results and the examination of already studied and published papers in scientific magazines locally and internationally.

The Work Group made six distribution inventory and landslide risk assessment maps for 60km of Ho Chi Minh Route (1:12,000); one map for Hai Van area and one susceptibility map along the road applied AHP or Fuzzy theory for evaluation and analysis. For application, a map for 10km along National Highway No. 7 (Muong Xen to Tam Quang) was made directly by Vietnamese researchers in cooperation with Japanese experts.

Identification technology by air photo of the surface of forest cover using unmanned aerial vehicle based on the pattern analysis of digital surface model has been developed from research result of the Project.

- **Main activity results of Work Group 3:**

The Work Group developed successfully a high-stress undrained dynamic-loading ring shear apparatus (ICL-2) which is used for basic landslide research and simulating landslide initiation and motion, and can be applied for landslide with the depth of more than 100m. The first application of the above apparatus was for Unzen Mayuyama landslide where landslide occurred and resulted in 15,000 deaths in Japan.

This ring shear apparatus was developed for the practical use in Vietnam and upgraded in 2014-2015 based on testing experience of Vietnamese short-term and long-term trainees. The main improvement was the development of two additional protection systems for equipment safety once operators wrongly drive the apparatus and gives damages on it during testing. The new improved apparatus was installed at ITST in June 2015 and has been used now for experiments of Vietnamese landslides (Lam Huu Quang, project report in 2016).

Testing samples were taken from the ground surface and also drilling cores in different depths at Hai Van landslide area, those samples were tested by ICL-2. Computer simulation of the Hai van landslide was conducted using the tested data and assessed landslide hazard affecting the Hai van Rail way and Station. The research by Vietnamese researcher is very successful and a research paper was written for an international journal on this research result.

Adding landslide-induced tsunami simulation function on the current landslide simulation model was achieved to integrate the tsunami simulation model developed by Intergovernmental Oceanographic Commission to current landslide simulation model. This function is applied to assess tsunami generation which can occur from a rapid large-scale landslide on Hai Van slope.

- **Main activity results of Work Group 4:**

Landslide activities behind the Hai Van station indicate potential risks of disasters (National railway runs on the landslide body). This landslide was chosen for monitoring and early warning research site. Monitoring equipment installation, topography and geology surveys were already completed. Three boreholes were drilled and undisturbed samples were taken accordingly. An integrated monitoring system including rain gauge, extensometers, inclinometers, total station and GNSS was developed and installed at this area. Rain fall and slope deformation monitoring started since May 2013 and data have been collected since September 2013 up to now.

Data transmission system was installed successfully at Hai Van and Project Office in ITST, Hanoi in March 2016. This system allows us real-time landslide monitoring from remote location.

Landslide model testing facilities, such as landslide flume, data logger and pore water pressure sensors were installed in ITST. The first landslide flume experiment using river sand was conducted in November 2015. Landslide experiment applying with strong weathered granite sand from Hai Van slopes was succeeded and provided good results. Unwired multi-depth tensiometer was developed in Japan and utilised for testing in ITST.

A proceeding of the project research results was published and reported in the project workshop. The main contents of the proceeding include: (1) Activity reports of Work Group 1, 2, 3 and 4; (2) Keynote lectures by project members; (3) Research and reports by long-term and short-term trainees in Japan, (4) Guidelines for landslide risk assessment; and (5) Report on Capacity Development in SATREPS project.

Acknowledgement

The Vietnam-Japan Joint Project "Development for landslide risk assessment technology along main transport arteries in Vietnam" was officially started in November 2011, in the frame of "Science and Technology Research Partnership for Sustainable Development (SATREPS)" program, which was jointly funded by the Japan International Cooperation Agency (JICA) and the Japan Science and Technology Agency (JST).

Success of the project is the result of collaboration between Vietnam and Japan. Representative from Vietnamese side is Institute of Transport Science and Technology, Ministry of Transport (MOT). From Japan side, there are three organizations: International Consortium on Landslides (ICL), Tohoku Gakuin University and Forestry & Forest Product Research Institute (FFPRI). Besides, the project recognizes the extensive contribution of many other organizations, research institutes, universities, and companies relating to landslide sector from both Vietnam and Japan.

On behalf of all project members, we would like to send our sincere appreciation for extensive supports from MOT, relevant ministries, state management units, universities, research institutes, companies, and also for the great contribution of Vietnamese and Japanese individual researchers and engineers. Especially, the research group acknowledges MOT (Vietnam), JICA and JST (Japan) for their instruction and financial support for the success of this project.

Nguyen Xuan Khang
Project Director
Institute of Transport Science and Technology, MOT

Kyoji Sassa
Project Leader
International Consortium on Landslides - ICL

Contents of Japan-Vietnam SATREPS Final Workshop Proceedings

JICA-JST Joint Project in Vietnam

Development of Landslide Risk Assessment Technology along Transport Arteries in Viet Nam

WG 1
Objectives and Achievements

Kyoji Sassa, Project Leader
Executive Director of ICL
Nguyen Xuan Khang, Project Director
Director of ITST

Geology and Rain fall in Vietnam

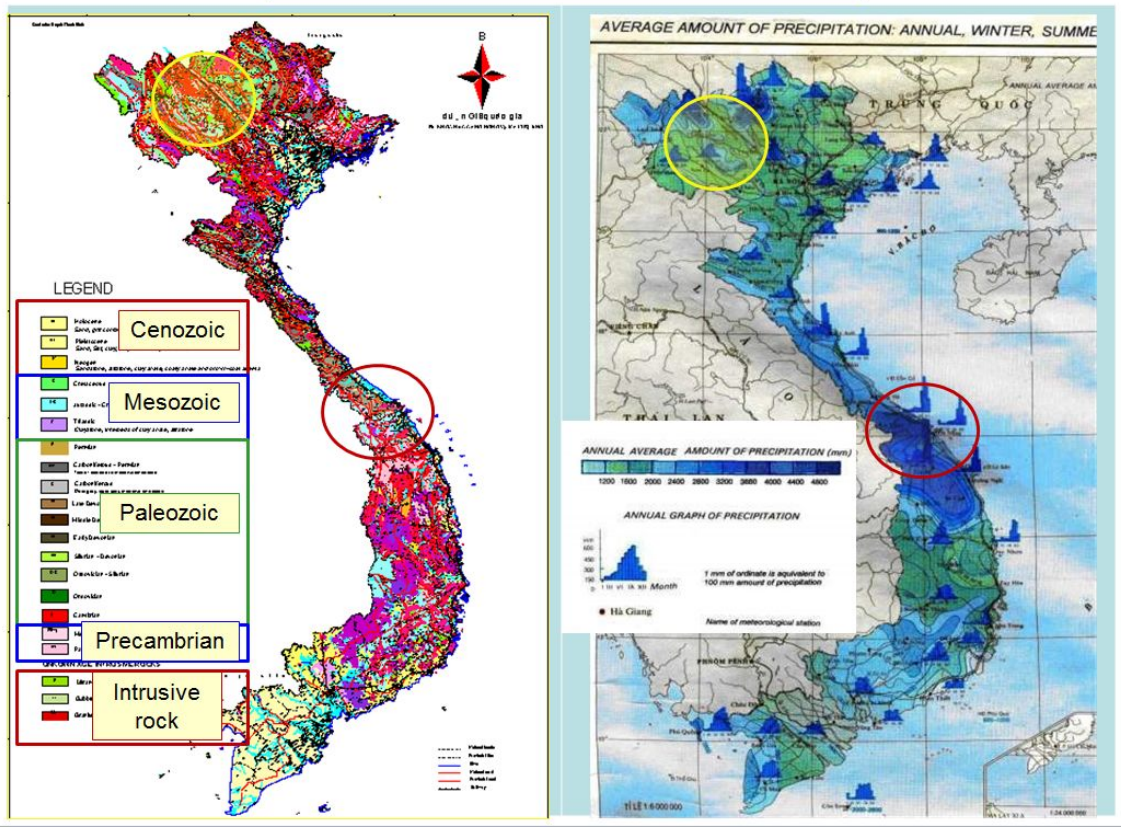

The Investigation Sites in Da Nang (MM and RD in 2011)

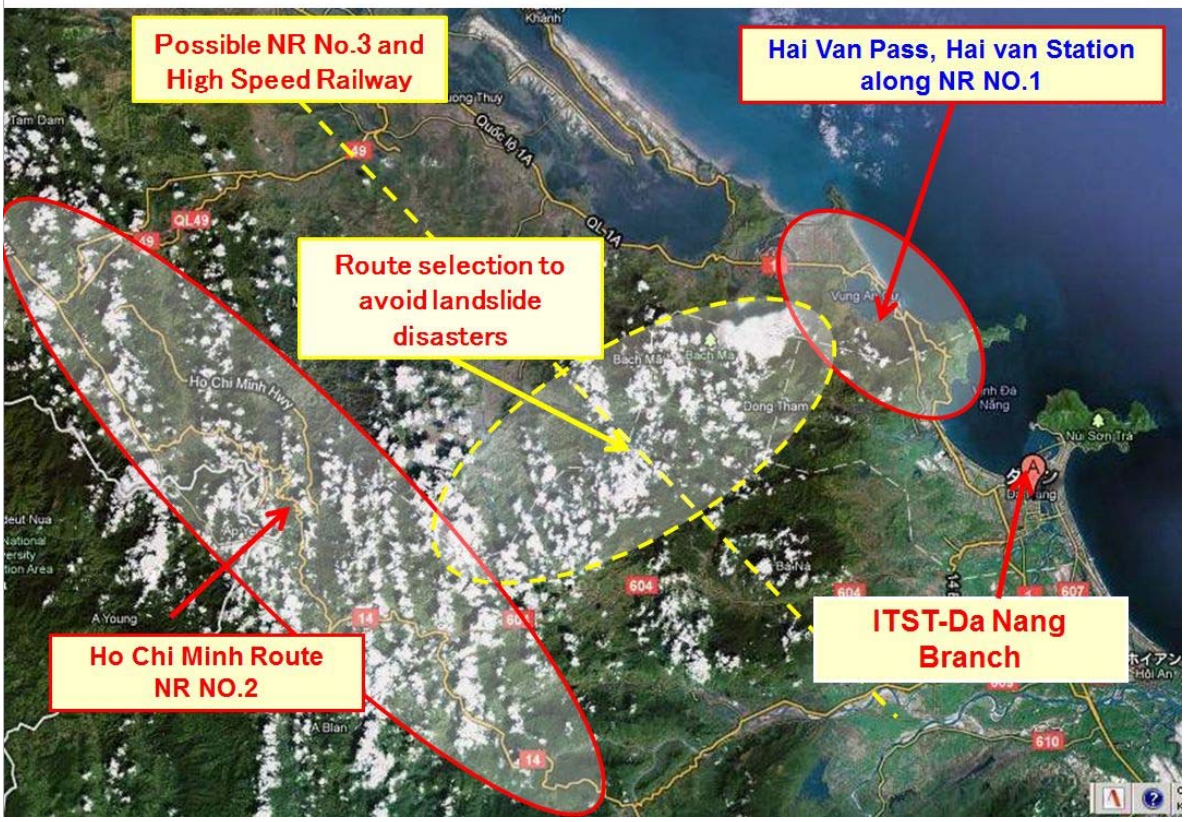

Objectives of SATREPS Joint research

- Mountainous areas of Greater Mekong Sub-region are subject to frequent slope disasters caused by a combination of weak ground, steep slopes, and tropical monsoon.
- Safety ensuring of transport arteries connecting north and south is the most important issue for national development in Vietnam.
- Establishment of an effective landslide risk assessment technology suitable for Vietnam is the key issue for disaster reduction.
- Technologies of landslide mapping, landslide risk identification, soil testing and computer simulation, landslide monitoring and early warning are jointly developed and transferred to Vietnam.
- An extensive human resources with an advanced landslide risk assessment technology are developed through capacity development in Vietnam and in Japan.
- Network for landslide risk reduction is established in Vietnam, Japan and other mountainous countries.

Development of Landslide Risk Assessment Technology along Transport Arteries in Viet Nam

Overall Objective

Social implementation of the developed landslide risk assessment technology and early warning system will contribute to the safety ensuring of transport arteries through urban and local communities in Viet Nam.

Project Purpose

Landslide risk assessment technology to reduce landslide disasters along main transport arteries areas is developed, and education and capacity development for the effective use of this technology is implemented in Viet Nam.

Outputs

1 Wide-area landslide mapping and identification of landslide risk area
2. Development of landslide risk assessment technology based on soil testing and computer simulation
3. Risk evaluation and development of early warning system based on landslide monitoring
4. Preparation of Integrated guidelines for the application of developed landslide risk assessment technology

PROJECT IMPLEMENTING STRUCTURE

Institute of Transport Science and Technology (ITST)
Project Director :
Nguyen Xuan Khang (Director General)
Project Manager:
Dinh Van Tien (Director for planning)

Project Cooperation Organization
Viet Nam Landslide Association for Transport (approved in 2014)
Vietnam National University, Hanoi (establishment of joint research office with Kyoto University in 2010)

Integrated Research "Development of Landslide Risk Assessment Technology" and Education (G1)
Leaders: Kyoji Sassa, Nguyen Xuan Khang, Dinh Van Tien, Toyohiko Miyagi, Hirotaka Ochiai
- Planning and coordination of research, Implementation of integrated research, Capacity development
- Organization of symposia, workshops, research meetings, publication and information dissemination

Tohoku Gakuin Univ. (G2)
Leader:Toyohiko Miyagi
Wide-area landslide mapping & Landslide risk identification

(NPO) ICL (G3)
Leader: Kyoji Sassa
Soil testing & Computer simulation of landslide initiation and motion

FFPRI (G4)
Leader: Hirotaka Ochiai
Landslide monitoring & Development of early warming system

Review of Activities (WG1:Outline of progress)

1. Pilot study sites of the project were once moved from the central Vietnam to Son La Province in the North-West Vietnam due to the proposal from the Vietnamese side in 2012. It had to be changed again due to the strategical change in the Vietnam to major transport arteries in Danang area in 2013. Thereafter, pilot study sites have been fixed in the back slope of Hai Van station located in the center of north and south Vietnam, and the Ho Chi Minh Route between Danang and Hue.
2. Severe difficulties were faced to make the project document including the Vietnamese side budget. WG1 examined the plan of activities and necessary budget from the Vietnamese side in Vietnam and Japan and also through JCC meeting in 2012 including JICA. The project document was approved by the Government of Vietnam in December 2012

Review of Activities:Outline of Progress 2

3. Equipment to be donated are affected by the study sites, the development of equipment/software, and the understanding and interest of transferred technology. So the list of equipment to be written in A4 form should be flexible to be changed or modified. WG1 organized a joint meeting inviting seven directors/deputy directors from MOT and ITST in Kyoto, Japan on 18-22 November 2013. Then, possible modification and changes of the list were approved. The purchase of equipment and their installation started from 2014. In advance of A4 form, we started the installation and monitoring of extensometers and rail gauge purchased by JST budge in the Hai Van station landslide in 2013. It was very effective.
4. WG1 has managed the coordination of ITST, MOT and Japanese group and educated many of ITST engineers as long-term and short–term trainees in Japan and also in Vietnam. WG1 has coordinated the publication of SATREPS proceedings, a thematic issue in a journal, and publication of Landslide Teaching Tools in 2013. Based on this Landslide Teaching Tools in 2013, Landslide Dynamics: ISDR-ICL Landslide Interactive Teaching Tools in much greater and global scale is in progress. Major results of Vietnam and Croatia SATREPS project are included.

Review of Activities (WG1-Guidelines)

Based on the technological transfer from Japan to Vietnam, Vietnamese researchers have made the guidelines in the following 5 parts – 33 guidelines (GL). The guidelines will be submitted to the Ministry of Transport (MOT) to be approved as the guidelines of MOT.

- **Part 1. Mapping and Site Prediction.**
  This includes 8 GLs (No.1-No.8), covers on Landslide classification, Field Work for Landslide Engineers, Geotechnical , topo survey, inventory, occurred landslide risk evaluation Hazard, susceptibility mapping.
- **Part 2. Material Tests**
  This includes 8 GLS (No.9-No.16), covers the ring shear testing apparatus, 5 types of test, direct shear test and portable direct shear test.
- **Part 3. Monitoring**
  This includes 9 GLs (No.17-No.25) covers on parameters for Landslide Monitoring Systems for conventional landslide (slow and middle velocity)and high velocity landslide (Debris flow)
- **Part 4. Landslide experiment**
  This includes 5 GLs (No.26-No.30), covers on Introduction, relationship between Landslide Motion and Cumulative rainfall, Pore water Pressure Distribution, Volumetric Strain, Velocity
- **Part 5. Software and simulation**
  This includes 3 GLs (No.31-No.33) which support for landslide study and mapping

Review of Activities (WG1-Teaching Tools)

The United Nations World Conference on Disaster Risk Reduction (WCDRR) was organized in Sendai, Japan from 14-18 March 2015. **The Sendai Partnerships 2015-2025 for Global Promotion of Understanding and Reducing Landslide Disaster Risk** was proposed by ICL and agreed and signed by 17 international and national organizations (UNISDR,UNESCO, WMO, FAO, UNU, ICSU, WFEO, Gov. of Japan, Italy, Croatia et al.). One of the proposed activities in this partnerships is to develop an integrated teaching tools on landslides, **Landslide Dynamics: ISDR-ICL Landslide Interactive Teaching Tools (LITT) .** It contains 102 text tools, 1,700 pages in two volumes. Within 102 tools, 18 tools come from this SATREPS projects in Vietnam and in Croatia. The video manual for the undrained dynamic-loading ring-shear apparatus (ICL-2) and its testing was produced by Lam Huu Quang et al., ITST

LITT includes PPT tools for lesson and PDF tools of papers/reports and manuals as well as text tools. This LITT is always updated in WEB by the interactive response between users and authors. A new updated version will be periodically published. The publication of LITT aims to provide the successful and effective technologies and experiences from many countries to the world and to create the latest landslide risk reduction technologies for the UN sustainable development goals and the Sendai Framework for Disaster Risk Reduction 2015-2030.

Review of Activities (WG1:Capacity Development)

Name	ITST/ VNU	University	Doctor/ Mater	Period
Khang Dang Quang	VNU	Kyoto Univ.	Doctor	10/1/2012-9/30/2015
Le Hong Luong	ITST	Tohoku G. U.	Doctor	4/1/2013-3/31/2016
Pham Van Tien	ITST	Kyoto Univ.	Master	4/1/2013-3/31/2015
		Kyoto Univ. (KU Scholarship)	Doctor	4/1/2015 3/31/2018
Doan Huy Loi	ITST	Kyoto Univ.	Master	4/1/2013-3/31/2015
Do Ngoc Ha	ITST	Shimane Univ.	Master	10/1/2012-9/30/2014
Pham Thi Chien	ITST	Shimane Univ.	Master	10/1/2013-9/30/2015
Vu The Truong	ITST	Shizuoka Univ.	Master	10/1/2013-9/30/2015

Review of Activities (WG1-Capacity Development in Japan-Continued)

Name	ITST/ VNU	University	Doctor/ Mater	Period
Short term training engineers (studying for Ph.D)				
Dinh Van Tien	ITST	Tohoku G. U.	Thesis Doctor	2016.9.15
Lam Huu Quang	ITST	Kyoto Univ.	For Thesis Doctor	Expected to complete in 2017.
Do Ngoc Ha	ITST	Kyoto Univ.	For Thesis Doctor	Studying
Ngo Doan Dung	ITST	Tohoku G. U.	For Thesis Doctor	Studying
Doan Huy Loi	ITST	Kyoto Univ.	For Course/ Thesis Doctor	Studying

Review of Activities (WG2)

1. Mapping group has investigated slopes along Ho Chie Minh Route (HCM) between Khan Duc to Prau and the Haivan pass land mass area.
2. The group has established six sheets of landslide inventory map for HCM and 60 km long detail scale landslide distribution map (1:12000)
3. Technological development of identifying slope deforming area by tree crown DSM (Digital Surface Model) data which carried at mangrove forest in Iriomote island, Okinawa.
4. The tree crown deformation are measured in several centimeter scale by the comparative study of UAV and aerial photo data. The application to the identify the initial stage landslide deformation is trying to the Aratozawa landslide, Kurikoma, Japan.
5. The Vietnamese counterpart applied the transferred technology to other sites than the project target areas as one of overall objective of this project.
6. The selected application site is National Road No.7 from Muong Xan to Tam Quang.

   The Vienamese counterpart with advices from Japanese experts made the landslide distribution map (1:12000) along the National Road No.7.
7. It is a verifying evidence that the technology of landslide mapping has been well transferred to the counterpart organization.

Review of Activities (WG3)

WG3 has successful developed the world first high-stress (up to 3 MPa) undrained dyanamic-laoding ring-shear apparatus (ICL-2) to simulate large-scale landslides (100-200 m in depth) using the budget provided by the Japan Science and Technology Agency (JST) which was reported in Landslides Vol.11, No.5.

- A practical version of ICL-2 has been developed to donate it to Vietnam together with technological transfer. The practical and sustainable version of ICL-2 used in Vietnam needs many of technological development, to change the loading system for easy handling, to change the rubber edge system to keep undrained condition for easy maintenance, and the many of safety systems to avoid damages of apparatus by miss-handling.
- After ICL-2 donated version has been completed, it has been tested by Vietnamese long term and short term trainees for around two years. All trouble sources are solved, and all trainees had confident to use ICL-2. The trainees has developed video manuals in addition to the written manuals for teaching engineers who have not visited Japan. The video manual made by ITST is included in Landslide Dynamics: ISDR-ICL Landslide Interactive Teaching Tools.
- ICL2 was applied by Lam Huu Quang and other Vietnamese engineers to test the samples taken from drilling in the Hai van Station and succeeded to test those samples. This is the world first successful application of the undrained dynamic-loading ring-shear apparatus to test samples taken from the potential sliding surface found from the drilled cores in the precursor stage of Landslides.
- WG3 main objectives has been completed within the project period.

Review of Activities (WG3)

WG3 has published or submitted five papers to Landslides (2015 Impact Factor is 3.049) as below.

1.Sassa K, Dang K, He B, Takara K, Inoue K, Nagai O (2014) A new high-stress undrained ring-shear apparatus and its application to the 1792 Unzen–Mayuyama megaslide in Japan. Landslides 11 (5):827-842.

2.Sassa K, Dang K, Yanagisawa H, He B (2016) A new landslide-induced tsunami simulation model and its application to the 1792 Unzen-Mayuyama landslide-and-tsunami disaster. Landslides (published online first. DOI 10.1007/s10346-016-0691-9).

3.Dang K, Sassa K, Fukuoka H, Sakai N, Sato Y, Takara K, Lam H Q, Doan H L, Pham V T, Nguyen D H (2016) Mechanism of two rapid and long runout landslides in the 16 April 2016 Kumamoto earthquake using a ring-shear apparatus and computer simulation (LS-RAPID), Landslides (published online first. DOI: 10.1007/s10346-016-0748-9).

4.Lam H Q, Doan H L, Sassa K, Takara K, Dang K, Abe S, Asano S (2016) Risk Assessment of a Precursor Stage of Landslide Threatening the Haivan Railway Station in Vietnam (Submitting to Landslides).

5.Doan H L, Lam H Q, Sassa K, Takara K, Dang D, Nguyen K T ,Pham V T (2016) The 28 July 2015 rapid landslide at Ha Long city, Quang Ninh, Vietnam (Submitting to Landslides).

Review of Activities (WG4)

1. Monitoring group developed an integrated monitoring system including rain gauges, extensometers, inclinometers, total station, and GNSS, which provided the newest information of landslide activity and risks for early warning.
2. Three bore holes were drilled including a 80m inclinometer casing and the integrated monitoring system was installed in Hai Van Station landslide.
3. Rainfall and slope deformation monitoring was started in may 2013 and number of slope deformation records during heavy rainfalls have been monitored.
4. Installation of the data transfering and displaying system was finished in Haivan and the project office in ITST, Hanoi in March 2016.
5. The landslide experimental facilities including landslide flume and data logging system and sensors were provided and adjusted for ITST. The 1st landslide experiment was conducted in November 2015. A landslide reproduction of weathered granite soil from Hai van slope was succeeded. And new multi-depth wireless tensiometers was developed in Japan and utilized in landslide experiment in ITST. Important information about relationship of landslide activity and landslide risks have provided.
6. A training course of the data analysis of landslide monitoring and experiment for Mr. Ha from August 17th to September 17th, 2016 in FFPRI was finished successfully.
7. These activities will contribute to reduce the landslide disaster triggered by heavy rain in Vietnam

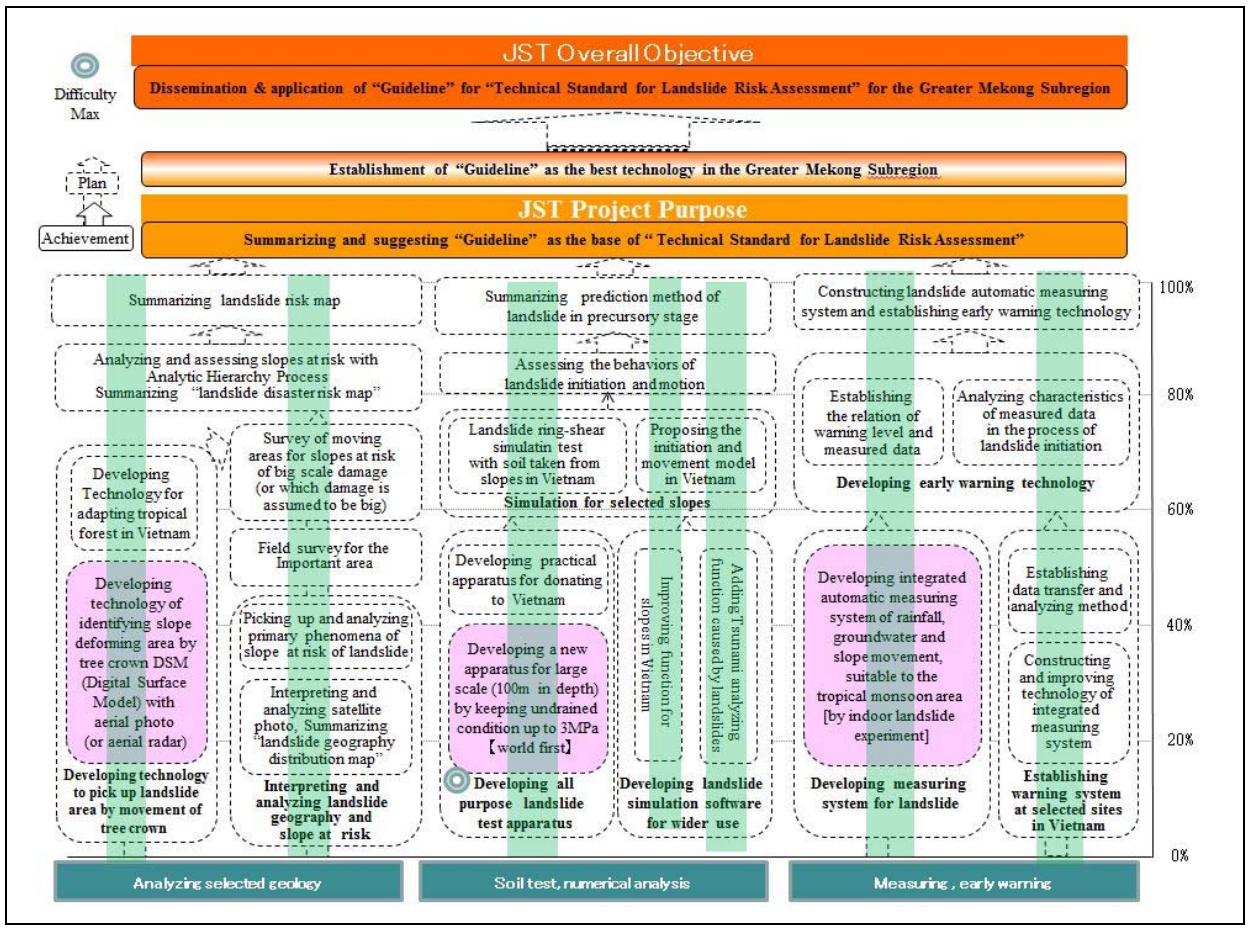
JST Overall Objective
Difficulty
Max
Dissemination & application of "Guideline" for "Technical Standard for Landslide Risk Assessment" for the Greater Mekong Subregion
Plan
Establishment of "Guideline" as the best technology in the Greater Mekong Subregion
Achievement
JST Project Purpose
Summarizing and suggesting "Guideline" as the base of " Technical Standard for Landslide Risk Assessment"
Summarizing landslide risk map
Summarizing prediction method of landslide in precursory stage
Constructing landslide automatic measuring system and establishing early warning technology
Analyzing and assessing slopes at risk with Analytic Hierarchy Process Summarizing "landslide disaster risk map"
Assessing the behaviors of landslide initiation and motion
Establishing the relation of warning level and measured data
Analyzing characteristics of measured data in the process of landslide initiation
Developing early warning technology
Survey of moving areas for slopes at risk of big scale damage (or which damage is assumed to be big)
Landslide ring-shear simulatin test with soil taken from slopes in Vietnam
Proposing the initiation and movement model in Vietnam
Simulation for selected slopes
Developing Technology for adapting tropical forest in Vietnam
Field survey for the Important area
Developing practical apparatus for donating to Vietnam
Improving function for slopes in Vietnam
Adding Tsunami analyzing function caused by landslides
Developing integrated automatic measuring system of rainfall, groundwater and slope movement, suitable to the tropical monsoon area [by indoor landslide experiment]
Establishing data transfer and analyzing method
Developing technology of identifying slope deforming area by tree crown DSM (Digital Surface Model) with aerial photo (or aerial radar)
Picking up and analyzing primary phenomena of slope at risk of landslide
Developing a new apparatus for large scale (100m in depth) by keeping undrained condition up to 3MPa 【world first】
Constructing and improving technology of integrated measuring system
Developing technology to pick up landslide area by movement of tree crown
Interpreting and analyzing satellite photo, Summarizing "landslide geography distribution map"
Developing all purpose landslide test apparatus
Developing landslide simulation software for wider use
Developing measuring system for landslide
Establishing warning system at selected sites in Vietnam
Interpreting and analyzing landslide geography and slope at risk
100%
80%
60%
40%
20%
0%
Analyzing selected geology
Soil test, numerical analysis
Measuring , early warning

Proceedings of the SATREPS Workshop on Landslides in Vietnam, 2016

WG2 Landslide mapping and susceptibility evaluation along the Ho Chi Minh Route and Haivan Area

Toyohiko Miyagi[(1)], Dinh Van Tien[(2)], Ngo Doan Dung[(2)]

1) Tohoku-Gakuin University,Graduate School of Human Informatics, Sendai, Japan, e-mail: miyagi@mail.tohoku-gakuin.ac.jp

2) ITST, Min. of Transport, Hanoi, Vietnam, e-mail: dvtien@gmail.com; ngodoandung@gmail.com

Abstract WG 2 has been carried the programme of a part the SATREPS project titled " Development of landslide risk assessment technology along transport arteries in Vietnam" by JICA/JST/ITST. The project will clarify the characteristics of landslide disaster in a humid tropical strongly weathered zone. We have two tasks. One is identification, mapping, the disaster risk evaluation of each landslide area, and susceptibility evaluation along the HCM Route and related areas, the other is search the landslide feature through the forest canopy dislocation.

The results are as follows. The wider area landslide mapping carried from Kham Duck to Prao and Haivan mountains central Vietnam. 685 landslide topographic areas are identified and carried the AHP risk evaluation. Susceptibility evaluation along the HCM route is also carried. The data preparation of weathered soil strength is just finished. The report will submit to journal. Identify and risk evaluation is important but the management is also necessary for disaster reduction.

Search the early stage landslide movement through the forest canopy dislocation has been tried in Japan and in Vietnam. The UAV and FsM technology of this matter is advancing very recently. The application just started. The clear evidence of landslide deformation in Vietnam case is not yet prepare. We will promote the data collection.

Keywords Landslide mapping, Risk evaluation, AHP, UAV research, Tropical strongly weathered zone, Vietnam

Outline, typology and the causes of landslide disasters in Vietnam

In Vietnam, landslide disasters frequently occur in connection with rapid infrastructure construction. However, few research reports have discussed landslides in Vietnam to date. Particularly, very few if any studies address Vietnam comprehensively. This deficit has hindered sufficient responses to landslide disasters, has delayed development construction, has increased economic liability, and has even affected people's safety.

Firstly, we report extracts common causes of numerous landslide disasters and discusses landslide mechanisms based on landslide surveys in various parts of Vietnam. Consequently, landslide activities in landslide disasters in Vietnam are classified according to geological features, geology, and weathering. Moreover, the relation between construction works and landslide occurrence is discussed with respect to a mechanism.

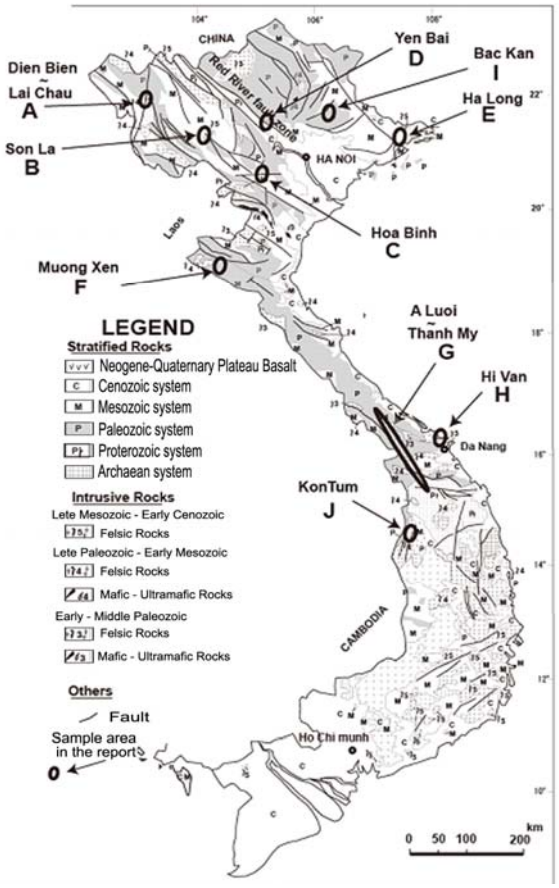

Fig.1 Outline of the Vietnam geology and notable landslide disasters (Tien et al, 2016).

Landslides occur in sedimentary rocks with bedding and schistosity, weakly converted crystalline schist, and granitic rocks. Landslides move as a translational slide when the beds are gently sloping, and otherwise as a wedge type slide at an intersection with a crack. It is often the case that organic layers such as crushed coal bed, black mudstone, black shale, and black schist act as a slip plane in sedimentary rocks with developed bedding. Granitic rocks slide as rock falls of granite core stones formed at shallow layers by weathering and as rotational slides where deep layers are weathered.

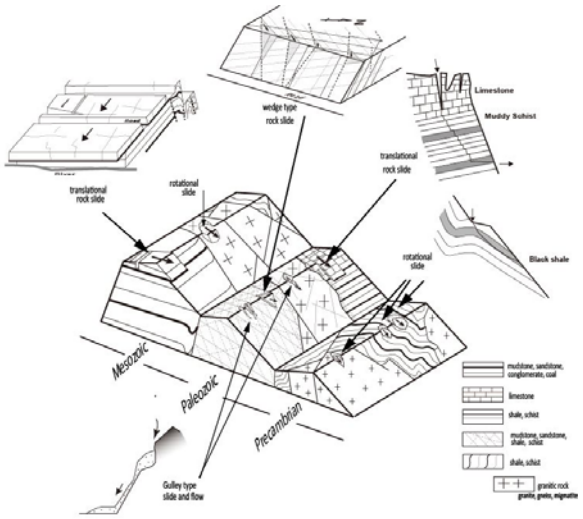

Fig.2 Idea of the relationships between the landslide type, geological structure and geomorphic setting in case of Vietnam Landslide (Tien et al, 2016).

Large scale landslide topography mapping and inventory in central Vietnam

Landslide distribution mapps and the inventory has been made for area between Prao and Kham Duc. The inventory was prepared by interpretating landslide observed on over 100 aerial photographs at a scale of 1:33,500 that were taken in 1999. We used these photographs because, at the time of this study, only 1999s aerial photographs are available. Interpretation of aerial photographs was locally aided by field checks. By this way, all the unstable areas were mapped at a scale of 1:25000 onto topographical maps. The map was tranfered to GIS and contains on 685 landslides, corresponding to an average density of 0.6 landslides per square kilometre. Landslides range in size from 3071 m2 to 3.08 km2, and the most frequent (abundant) landslide has an area of about 25,400 m2. They classified into five categories. 324 of which are classified as rotational slide, 66 are classified as translational slide, 4 are classified as compound slide, 275 are classified as debris slide and, 16 are classified as debris flow. For each landslide, 13 characteristics were recorded and listed in accompanying database table. Combine with geolgical map, among 685 landslides were maped, 314 landslide topographys belong to Mesozoic; 178 landslide units belong to Paleozoic; 171 landslide units belong to Precambrian; 22 landslide units belong to Quaternary. Most of landslides occur at Mesozoic zone, occupy 46% of recorded landslides (Le et al., 2016).

The maps show interesting distribution features: 1) the spatial distribution seems to have some relation with geological periods. The large-scale landslide topography concentrates to the area of the Mesozoic geology. The Paleozoic geology has few large-scale landslides except in areas of plutonic rocks such as gabbro and granitic rocks. Especially, the largest landslide topography is located at the gabbro. The Quaternary and Precambrian geology also have several characteristics. The movement features are categorized to five types: Rotational slide, Translational slide, Compound slide, Debris slide, and Debris flow (Le et al., 2016).

On the other hand, an interesting characteristic observing at Thon A So in the study area. This located

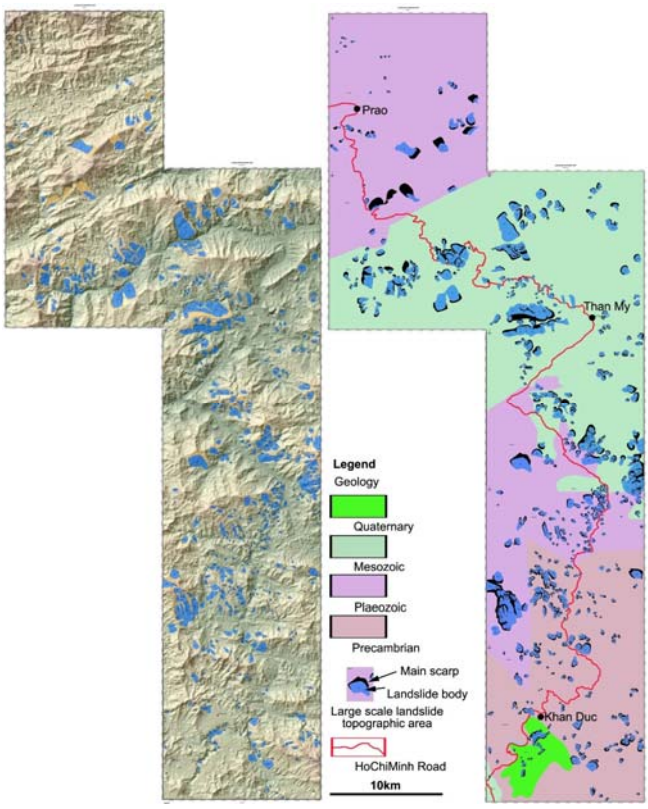

Fig.3 Maps of landslide topographic area from Prao to Khan Duc along the Ho Chi Minh Road, central Vietnam (Le et al., 2016). The map is a combination of six sheets.

at the part of northward homo-clinal slope at a southern part of major Mesozoic syncline. I observed a big number of landslides and scars are distributed, and there are very remarkable topographic features identified, the scars are distributed at the northward dip slope, on the contrary many types of landslide topographies locate to other direction of slope the size of landslides are relative of small but it easy to indentify in size, and such landslides and scars distribution are strongly reflective the geology structure. It means in case of landslide distribution and the type in case of the Mesozoic sedimentary rock controls the characteristics (Le et al, 2014b).

Landslide risk evaluation

Landslide risk evaluation by AHP approach (Saaty, 1980) has been carried. Application to the large scale landslide topography is carried by aerial photo interpretation and the inspection sheet. The basic study had been carried by Japanese scientists (Miyagi et al, 2004). The possibility or adoptability of AHP inspection sheets were discussed by our special high level engineer. The inspection carried by Vietnamese and Japanese inspectors. Based on the discussion and the cross check the sheet, the AHP sheet was a bit modification, and the no necessity of geological factors contribution is also confirmed.

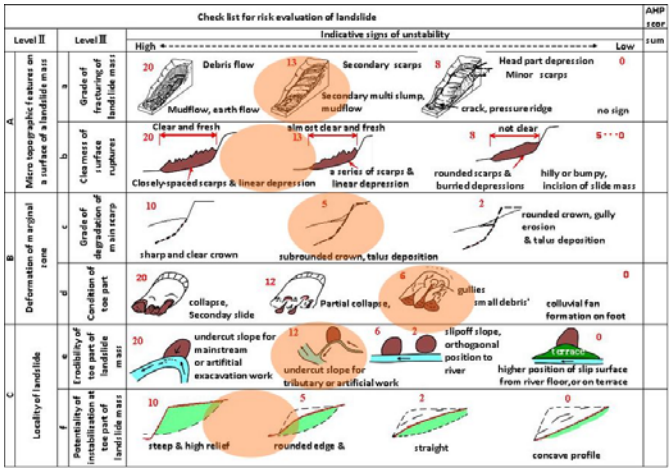

Fig. 4 The inspection sheet for latge scale landslide reactivation risk evaluation (Dung, et al., submitting).

One of the main targets of landslide mechanism analysis in the Humid Tropical Strongly Weathered Zone is characterize the residual strength of weathered rocks. We are accumulating the field data and tried the soil strength testing during the project. There is a clear relationship between the geological age, clay mineral components, the weathering features and the soil strength (Dung et al., submitting, Fig. 5, Table 1). That is similar tendency in case of Japan (Mayumi et al, 2003). The result will applicate the background knowledge for make decision of the particular countermeasure.

Table 1. Result of ring shear tests in case of weatherd soil in central Vietnam, (Dung et al., submitting)

Sample No.	Location	Fully Softened Strength		Residual Strength			
						Cr'=0	Cr'≠0
		Cs' (kPa)	φs' (°)	σN' (kPa)	τf/σN'	Secant φr' (°)	Cr' (kPa) / φr' (°)
1	Loc.2	7.6	33.5	50	0.736	36.4	3.9 / 32.9
				99	0.672	33.9	
				150	0.675	34.0	
2	Loc.11	13.3	32.4	47	0.602	31.1	5.0 / 28.6
				86	0.647	32.9	
				147	0.569	29.6	
3	Loc.16	6.8	34.0	45	0.734	36.3	2.2 / 34.9
				81	0.737	36.4	
				129	0.711	35.4	
4	Loc.21	16.1	30.0	34	0.790	38.3	9.0 / 27.0
				80	0.611	31.4	
				126	0.585	30.3	
5	Loc.29-1	11.7	33.4	99	0.651	33.0	11.6 / 28.0
				199	0.609	31.3	
				299	0.565	29.4	
6	Loc.29-2	10.8	32.8	45	0.665	33.6	18.9 / 14.0
				100	0.447	24.1	
				145	0.376	20.6	
7	Loc.33	12.1	23.2	99	0.267	15.0	8.2 / 10.9
				191	0.237	13.3	
				292	0.219	12.4	
8	Loc.103	14.9	20.1	98	0.222	12.5	6.6 / 9.4
				201	0.191	10.8	
				300	0.185	10.5	
9	Loc.101	13.2	24.3	100	0.275	15.4	6.7 / 8.3
				200	0.207	11.7	
				301	0.163	9.3	
10	Loc.102	11.0	27.1	97	0.506	26.8	18.0 / 11.0
				200	0.307	17.1	
				300	0.249	14.0	

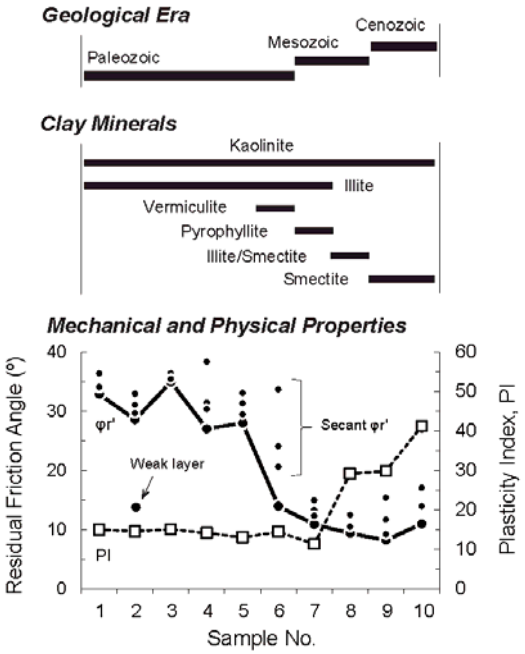

Fig.5 Influence of geological settings on residual strength of soils collected from Ho Chi Minh route at central Vietnam (Dung et al., submitting).

The susceptibility evaluation and the mapping:

The susceptibility of landslide disasters has been discussed by Tien et al (2016).

According to the study results of the landslide susceptibility map of the study area along corridor HCM route from QuangTri to Kontum and with the division of the landslide index of Galang Method applied, the Galang Method was introduced from 2004, with landslide susceptibility divided into four classes from low to very high landslide sensitivity. The number of landslide occurred in lower is a half of higher zone. Overlapping of the landslide distribution map and landslide susceptibility map showed that 26, 80, 255, and 244 landslides in all of 604 recorded landslides were respectively located in low, average, high, and very high susceptibility areas for landslides. Therefore, 40.40% of the landslides were in the very high susceptibility areas; 42.22% of the landslides occurred in high susceptibility areas; 13.25% of the landslides occurred in middle susceptibility areas; only 4.14% of landslides occurred in low susceptibility areas. Specifically regarding high and very high susceptibility areas, 82.66% all landslides occurred there.

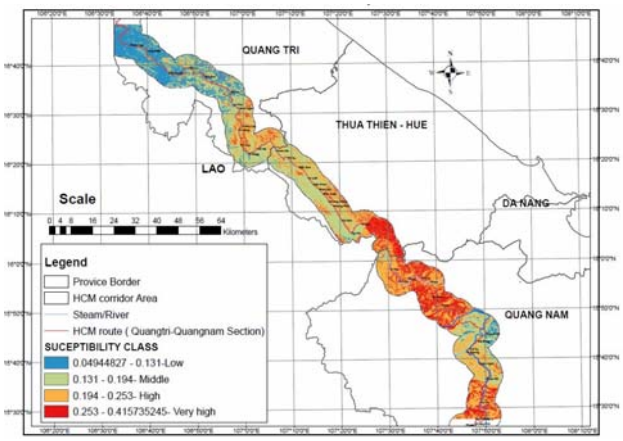

Fig. 6: Landslide susceptibility map of the study area, along HCM route from QuangTri to Kontum.

Limitations and future study of susceptibility evaluation

Landslides in this study were slope failures mainly located along a road. Positions of artificial slope failures were recorded as points measured from an intersection between the landslide boundary and the road. Therefore, landslides spatial arrangements were only distributions along the road. The susceptibility map scale was large, 1 : 500,000, so the areas and micro-features of respective landslides were not considered.

In general, three basic methods exist for creating a landslide distribution map: collecting historical data, conducting field surveys, and interpreting aerial photos. However, for this study, the field survey method was applied to create a landslide distribution map. Landslide surveys are related to human capabilities of recognizing them in terms of number, space, and time, all of which introduce error.

For susceptibility mapping, aside from the causal factors which were considered, i.e., Slope angle, Total annual average precipitation, Land use, Rock type, Distance to road, and Fault density, other sensitive causal factors such as fault depth, distance to water stream, and alignment were not examined because of their poor relevance and lack of available data sources. Although most landslides occurred in high and very high risk zones, some landslides occurred in other zones, perhaps because of low-probability causes such as slope cutting for road construction.

Landslides are regarded as a dangerous phenomenon that often occurs in mountainous regions of Vietnam. They directly affect the lives of the people in the region, destroy traffic infrastructure and road systems. The center section of the HCM route is a mountainous road that is heavily influenced by landslides. Therefore, reducing landslide susceptibility for this important corridor is the target of this study.

Landslides have various possible causes with complex mutual relations. Detailed assessments to ascertain the main causes of each landslide are not feasible in most cases. The selection of causative factors for a landslide susceptibility map is usually based on experts' subjective experience. In this study, to analyze landslide manifestation, causative factors were derived: slope angle, rock type, fault density, distance to the road, land use, and precipitation. Maps for causative factors were created, with causes divided into classes.

Positions of 604 artificial slope failures were found along the HCM route. From them, a landslide distribution was produced. The sensitivity to landslide of each zone of causative factor maps was calculated and then evaluated using NOL and DOL values derived from a comparison of the landslide distribution map and causative factor maps using GIS.

An analytical hierarchical process was used to combine these maps for landslide susceptibility mapping. Consequently, based on the inventory map of observed landslide from 2006–2009, a landslide susceptibility zonation map with four landslide susceptibility classes is derived, with low, moderate, high and very high susceptibility for landslides. This map shows that 82.66% of all landslides have occurred in highly and very highly susceptible areas.

Although limited by matters of map scale and available data, the landslide susceptibility map of this study for corridor along this road is expected to be useful for landslide mitigation.

Landslide mapping and related geological study at Haivan Mountains

The large scale landslide mapping and the study of landslide mechanism is carried and report by Dr. Abe in this occasion.

Monitoring the Forest canopy dislocation by UAV/SfM for landslide studies

By processing aerial photographs of Iriomote Island, Okinawa captured in 1978 and low-altitude aerial photographs obtained in June and December 2015 using the SfM-MVS technology. Uchiyama and Miyagi (2016) reported the results of forest cover changes of mangrove habitat at Nakama river delta Iriomote Island. This monitoring technology is originates by the technology of 3 dimensional data creation and photo preparation technology. Recently the two important skill can use by low cost, safely and easily.

The high precision ortho image created from three stages. Photo 1 is the ortho image of a part of Nakama river mangrove habitat. We are easy to realize the detail of the forest canopy.

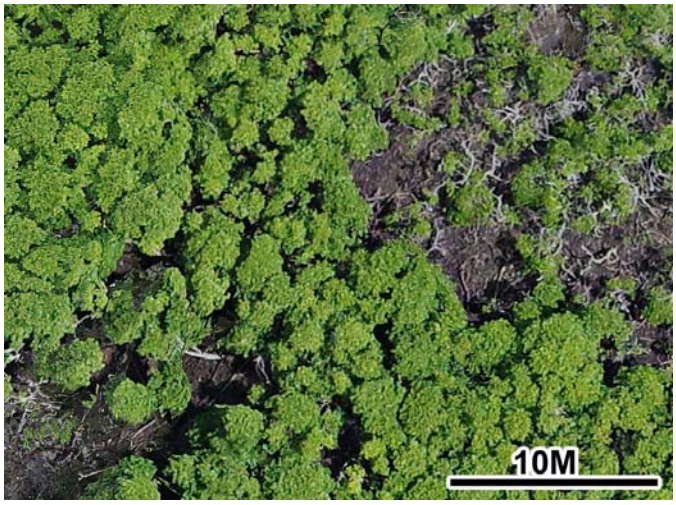

Fig. 7 Ortho photo image by UAV SfM of a small part of mangrove habitat in Nakama river delta, Iriomote island, Okinawa Japan (Data taken by Mr. Uchiyama, 2015)

The Ortho data image is transfer to DSM by soft-wear Photo Scan. It means that we are able to clarify the change of forest canopy condition by plural stage data collection. In this case we detected the forest height changes between 1978 to July 2015 (Fig.8) and July 2015 to December 2015 (Fig.9).

There are several interesting changes were revealed. That is, tree heights increases along the channel and decline at the inter channel flat area, some strongly destroyed forest by typhoon were identified as the abrupt decline the forest canopy heights (Fig. 8). And from the other result as Fig. 9, the new height decline zone appeared along the area of prior decline area.

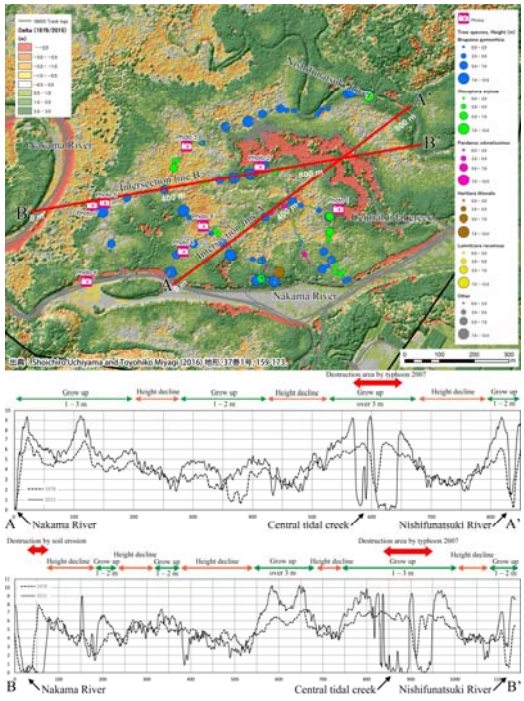

Fig. 8. Change detaction of DSM for 37 years from 1978 to 2015. Dark red area along the Central tidal channel and red bold arrows in the closs-sectional diagram indicate the area in which trees were felled by typhoons. Red area along the both sides of Nakama river and red bold arrows in the cross-sectional diagram are estimqted to be the area in which fallen tree damage was aggravated by soil erosion due to shear waves from shifting boats. The cplors and sizes of circles in the figure indicate tree species and tree height, respectively Uchiyama and Miygai, 2016.

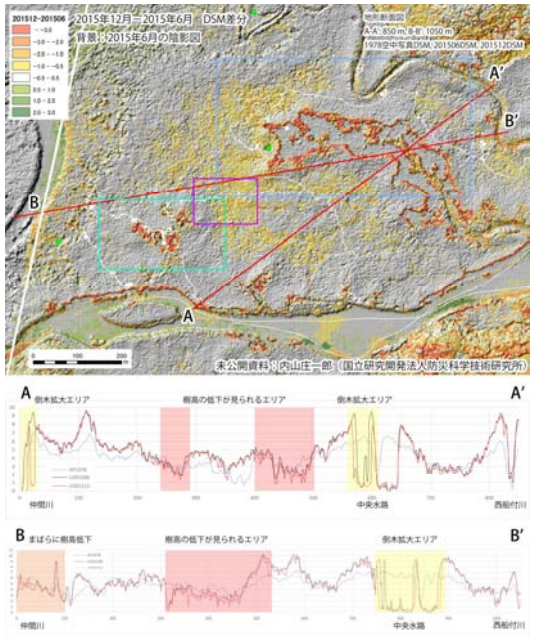

Fig.9 Change detection of DSM between 1978, July to December 2015. The forest height decline zone clarified (By Uchiyama data, 2016).

Application to the landslide deformation monitor

If we applicate the technic to monitor the landslide deformation which will became the very useful tool. Hereupon we have trying now in Japan and in Vietnam. Fig. 10 and 11 is a result of case study of the small landslide monitoring at Koei Minami landslide in Kurihara City, Japan. The landslide had occurred in 2008 and moved sometimes. Small crucks, bulge, trenches are still very clearly remaining there. The two times (At Oct. 2015 and June 2016) of the aerial photo preparation by UAV has been carried by us. The data analysis has been also carried by Mr. Uchiyama. By the realization of the forest canopy deformation at this landslide area among the period which is not identified. The landslide looks no deformation among these 8 months.

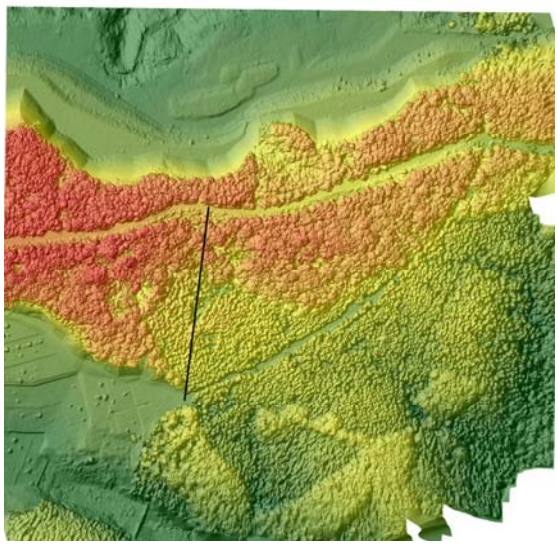

Fig. 10. DSM data of small landslide at Koei Minami, Kurihara City Japan. Black line is the cross profile of A line in Fig. 11 (Created by Uchiyama and Miyagi, 2016)

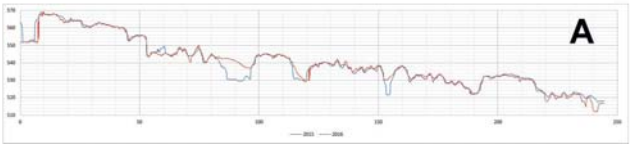

Fig. 11 Monitor the forest canopy dislocation during the 8 months at the line in Fig.10, Koei Miami landslide area (Calculated by Uchiyama, 2016).

Some early stage trial for implementation of the project

WG2 members are challenging to some further study based of the results of the project. The landslide topographic area identification and the mapping, landslide mechanism analysis, safety factor calculation of a number of landslides disasters are carrying along the Ho Chi Minh route, National Road No.7. This trial is the combination work of the using ALOS W3D data, field investigation, in site topography measurement, soil testing and simulation by Ad-calc 3D. The landslide distribution maps is established along the National Road No. 7 is completed based on the ALOS W3D data and more than 1000 landslide areas are identified (Dung et al, 2016).

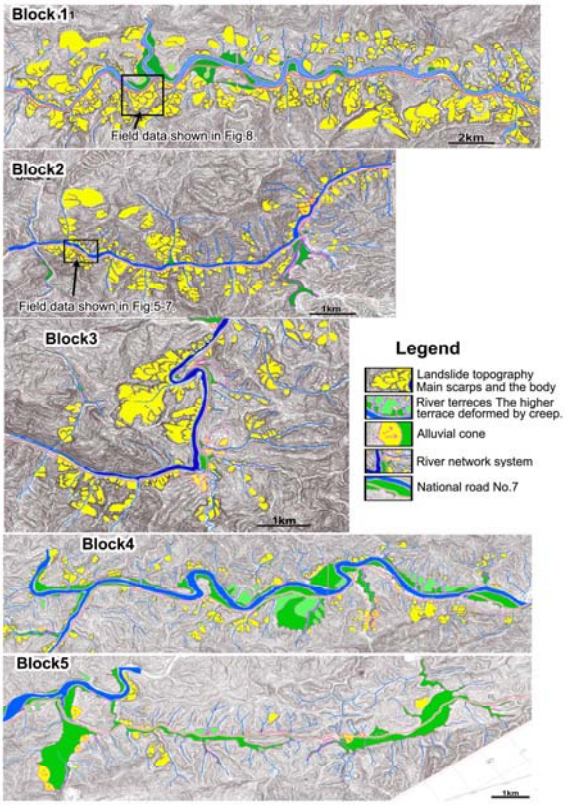

Fig. 12. Landslide distribution along the National road No. 7 by ALOSW3D data (Dung et al., 2016)

The combination works of contour from W3D data, field investigation, soil testing and simulation lead us the presence of real phenomenon and will suggests the alternative countermeasure strategy setting. Fig. 13 and Fig.14 is a sample of investigation. Fig. 13 is the small landslide occurred in rainy season 2009. It looks one block wedge type slump. Based on the detail investigation, the slip structure is composed by three small slip surfaces.

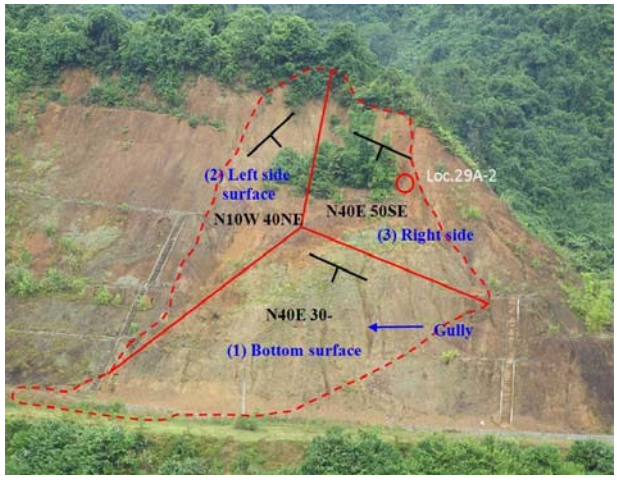

Fig. 13. Landslide No.029 on HCM route

The two steep surfaces follow the geological structures. The bottom surface stretches to a part of road. Soil strength mentions in table 1. Fig. 14 is the result of simulation of RBSM3D analysis. According the trial calculation, SF value changes from 1.2 to 0.92 according with the increase the ground water level.

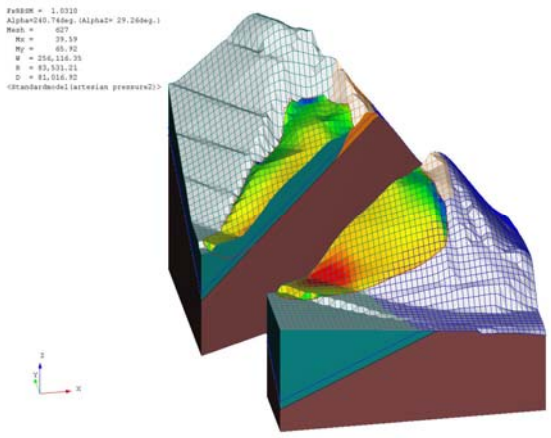

Fig. 14. Result of simulilation safty factor by Ad-calc 3D at Landslide No.029 on HCM route

Recommendation of alternative landslide investigation, risk evaluation and support the decision making for landslide management

WG2 has been carried the series of programme i.e. identify the landslide area by aerial photo interpretation and ALOS W3D data contour analyse, wider area mapping, field investigations, soil strength evaluation, susceptibility and reactivation risk evaluation, monitoring by field check and UAV/SfM processing, Boring for identify the geological structure and identify the slip surface etc.

The trial covers almost of all area of landslide management in the field. Actually there is poor advancing or the improvement of landslide management technology yet (Dung et al, 2016). It looks the technological development will start by the project.

We like to recommend the new framework of landslide investigation and the management for landslide disaster prevention, mitigation and the control.

The idea of workflow is shown in Fig. 15.

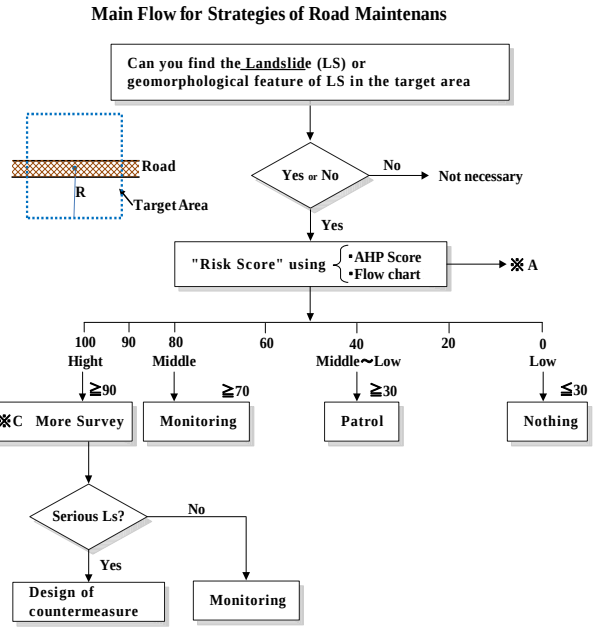

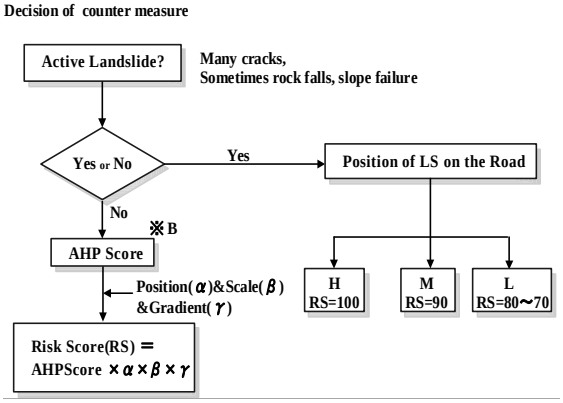

Fig.15. Mail flow of landslide management (ubove) and sub flow (below) along the roads (Dung et al. 2016)

Results of the project

1. Field data prepared by the number of field investigations by Vietnamese and Japanese engineers and scientists. The intellectual sense or ability of thinking improved in each other. Two of Doctors, Doctoral candidacies and many aggressive engineers were created by the study and discussion.
2. The project has been carried and established the landslide distribution maps, inventory data preparations.
3. Risk evaluation foe each identified landslide topographic area and susceptibility evaluation of landslide hazard potential has been clarified along the HoChiMinh route in central part of Vietnam.
4. Soil strength data arranged based on the many soil samples along the HoChiMinh route.
5. The detection of the landslide deformation through the forest clone dislocation has been tried in Japan and in Vietnam.
6. Several trial of implementation has been carried in and around the project area.

Acknowledgments

The all researches were conducted at the project "Development of landslide risk assessment technology along transport arteries in Vietnam" as a JICA/JST/ITST/ICL project. We would like to acknowledge the all the institutions involved. The

authors say deeply thanks to Professor Sassa in ICL, project leader, Professor Khang Director of ITST.
We also very deep thanks to all project contributes, Dr. Yoshimatsu, Dr. Abe, Dr. Hamasaki, Dr. Daimaru, Dr. Shibasaki, Mr. Uchiyama, Dr. Hayashi, Mr. Katoh, Mr. Chiba in Japan side, Dr. Luong, Mr. Thang, Ms. Anh, and Mr. Adachi in Vietnam side.

References

Dung, N.D., T. Shibasaki, T. Miyagi and E. Hamasaki (2016), Residual strength characteristics of weatherd rocks in Central Vietnam. (Submitting now)

Dung, N.D., T. Miyagi and E. Hamasaki, T. Shibasaki,K. Hayashi, Tien, D.V., and Luong, L.H. (2016), Study of new road side landslide disaster management structure in Vietnam. (Submitting now)

Dung N.D, Tien D. V., Khang N.X (2016), The current manual and standards for the survey and design works for Landslide prevention in Vietnam - Transactions, Japanese Geomorphological Union, vol.37-1, pp. 5-31.

Dung N.D., T. Miyagi, L.H. Luong, E. Hamasaki, K. Hayashi, Tien D.V (2016), Trial of landslide topography mapping using W3D data – Case study along the National Road No. 7 in central Vietnam, Transactions Japanese Geomorphological Union, p.127-140, vol.37-1.

Luong L.H, T. Miyagi, Tien P.V (2016), Mapping of large scale landslide topographic area by aerial photograph interpretation and possibilities for application to risk assessment for the Ho Chi Minh route – Vietnam. Transactions, Japanese Geomorphological Union, pp. 97-118.

Mayumi, T., T. Shibasaki, and T. Yamasaki (2003), Evaluation of the shear strength on undisturbed slip surface by newly developed Slip Surface Direct Shear (SSDS) apparatus. Journal of the Japan landslide Society, 40(2):273-282.

Miyagi, T., G.B. Prasada, C. Tanavud, A. Potichan, E. Hamasaki (2014), Landslide Risk evaluation and Mapping - Manual of Aerial photo Interpretation for Landslide Topography and Risk Managemen. Reprinted from Report of the National Research Institute for Earth Science and Disaster Prevention No.66.

Tien D. V., S. Abe, Dung N.D, Ha D.N, T. Miyagi (2016), Outline, typology and the causes of landslides disasters in Vietnam - Transactions, Japanese Geomorphological Union, vol.37-1.

Tien D. V., T. Miyagi, S. Abe, E. Hamasaki, H. Yoshimatsu, (2016), Landslide susceptibility mapping along the HCMR in the Central of Vietnam - an application of an AHP approach to humid tropical area - Transactions, Japanese Geomorphological Union, vol.37-1.

Tien D. V., H. Yoshimatsu, K. Hayahi, T. Miyagi, (2016), Landslide type Classification by pattern recognition using fuzzy inference method along the HCMR in central Vietnam - Transactions, Japanese Geomorphological Union, vol.37-1.

Saaty, T.L. (1980) The analytic hierarchy process: McGraw-Hill Book Co., New York.

Uchiyama, S and T. Miyagi (2016), Acquisition and utilization of high-definition digital surface models through aerial photography using a small unmanned aerial system: an example of typhoon damage in Iriomote Island mangrove forests - Transactions, Japanese Geomorphological Union, vol.37-1.

SATREPS

Science and Technology Research Partnership for Sustainable Development Program

Development of new undrained ring-shear apparatus for large-scale landslides and application of the new apparatus to the samples of drilled cores from the Hai Van landslide

Kyoji Sassa
Lam Huu Quang

Contents

Introduction

Hai Van station

The New High Stress Undrained Ring Shear Apparatus (ICL-2)
(International Consortium on Landslide)

Geological features và the average rainfall of the regions in Vietnam

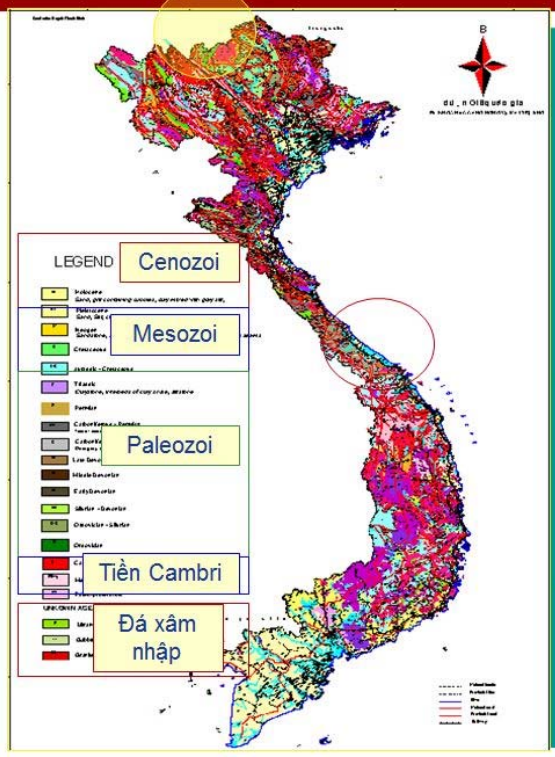

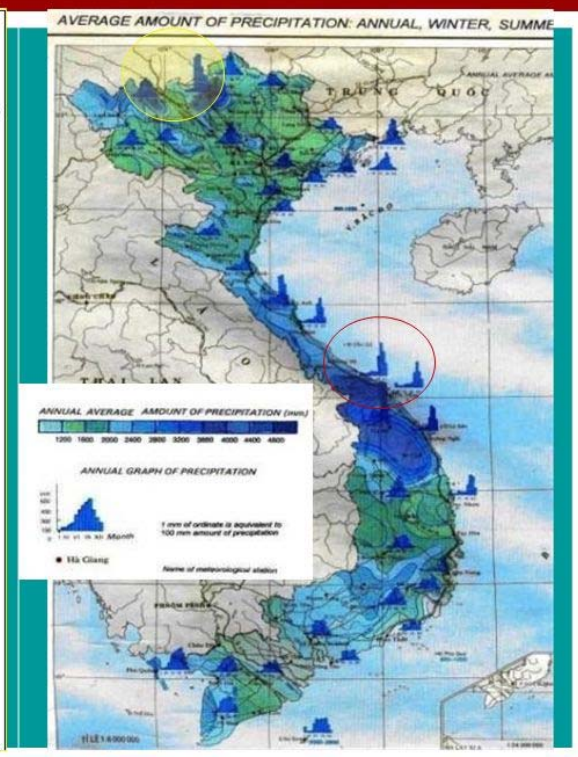

The Study Area (Hai Van station)

- Located at Haivan pass, Danang province in the center part of Vietnam
- National railway runs through this area.

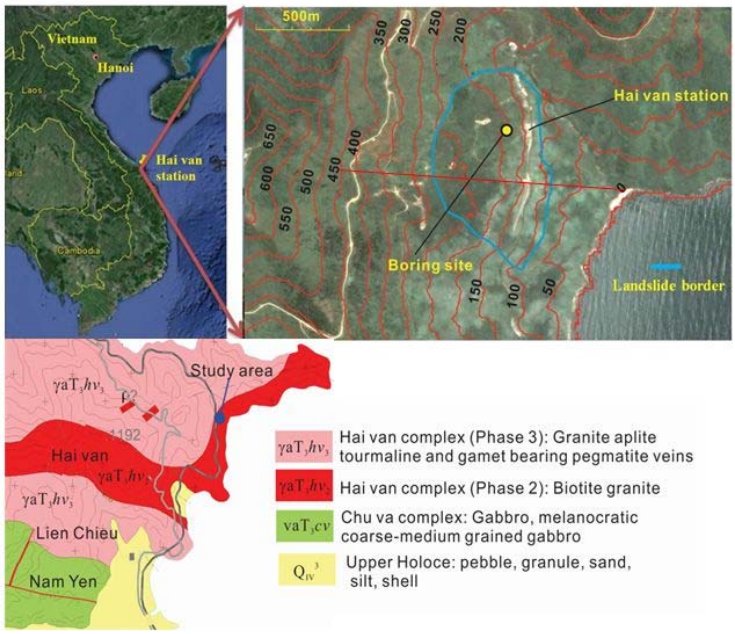

The influence of the landslides in the Hai Van Pass

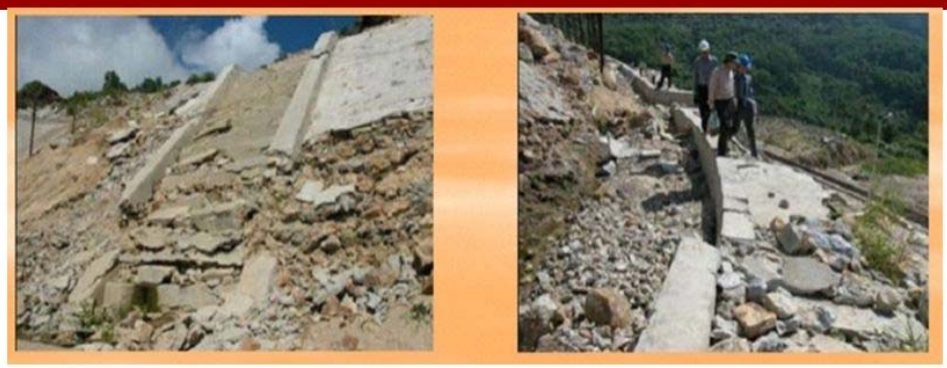

The influence of the landslides in the Hai Van Pass

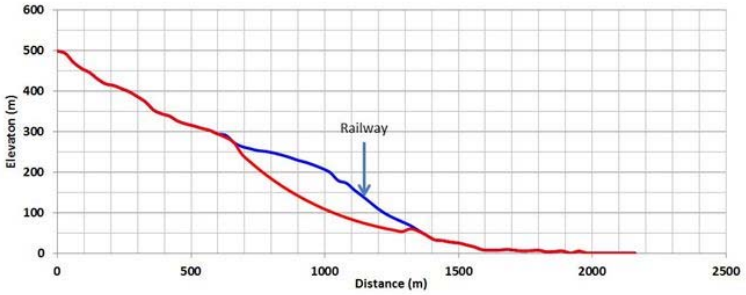

Where is the hazard area

?

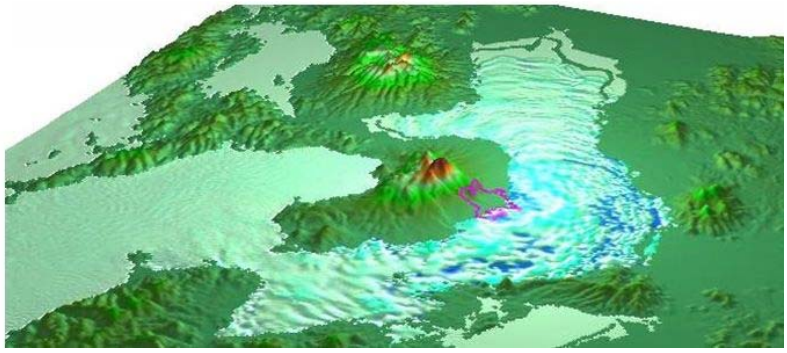

Theoretical research

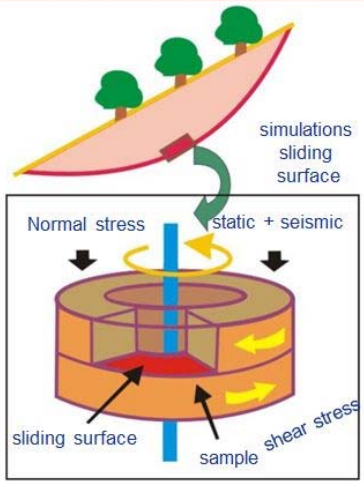

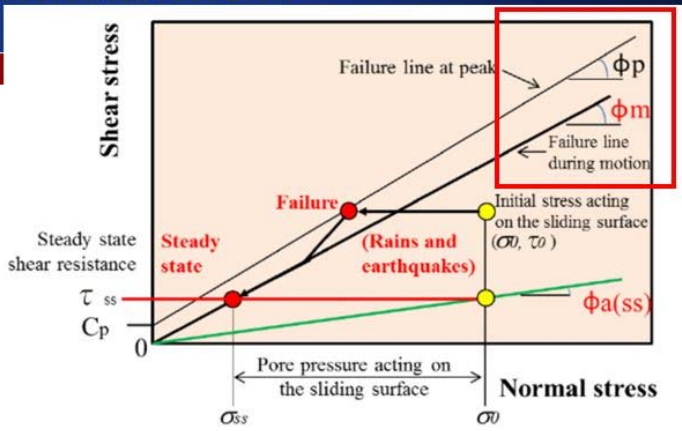

Fig.20 The steady state shear resistance and the apparent friction angle at the steady state

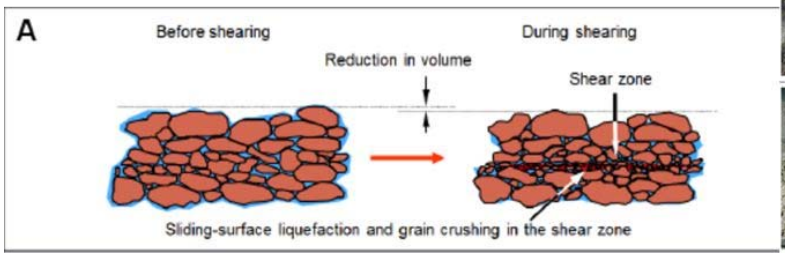

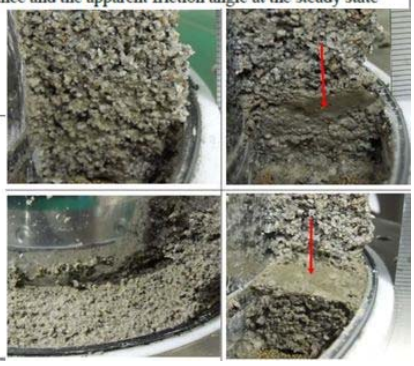

Theoretical research

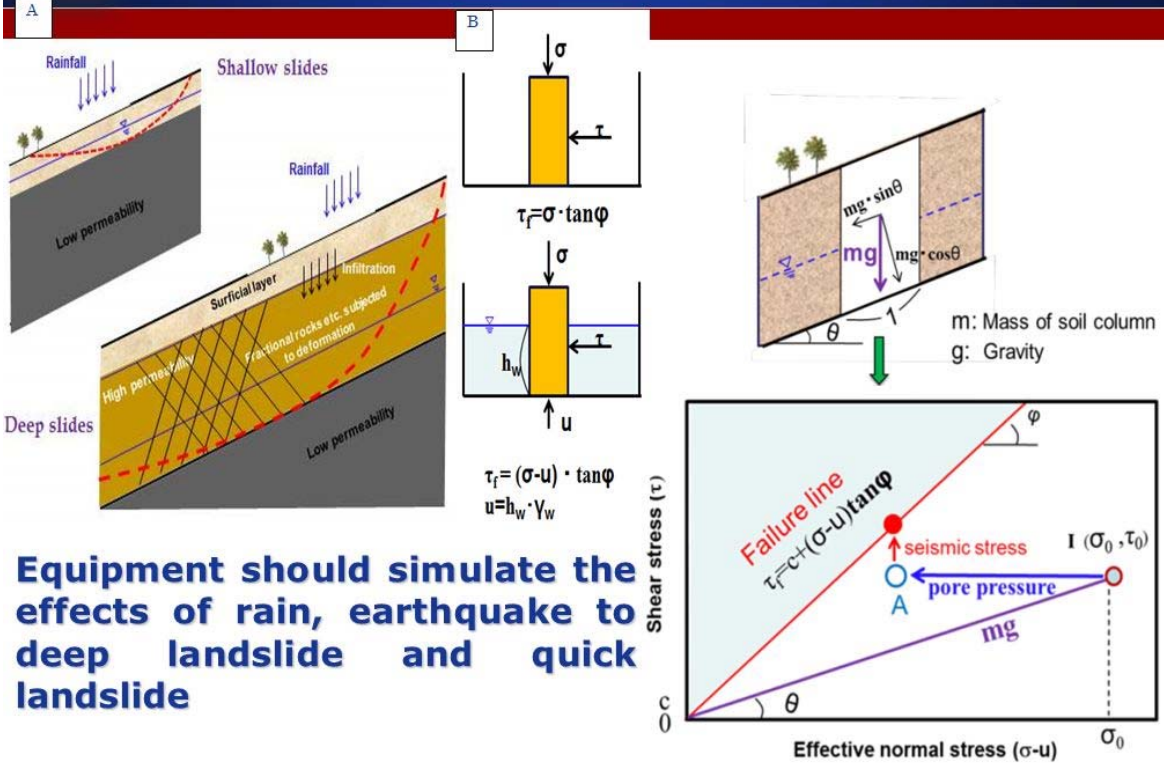

Equipment should simulate the effects of rain, earthquake to deep landslide and quick landslide

Direct shear test

ISO 9001 : 2008

1. Purpose:

This test is performed to determine the consolidated-drained shear strength of a sandy to silty soil.

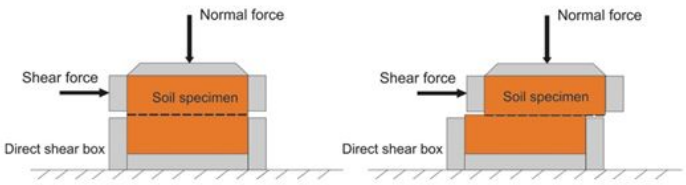

Not satisfactory

2. Advantage and disadvantage

+Equipment are simple, low-cost devices, popular in the laboratory

+Conduct experiments are simple, fast

- Low normal stress (**1.5MPa**), experiments only for deep landslide and shallow landslide.
- Maximum shear speed **1cm/minute**
- The length of the sliding surface is short, only determine the largest shear strength, not determine residual shear strength; Not determine the impact of pore water pressure
- The pre-determined sliding surface, can not match the actual sliding surface.

Triaxial compression testing

1. Purpose

Determination of shear resistance in the conditions: not consolidation - undrained; consolidation - undrained; and cohesion - drained.

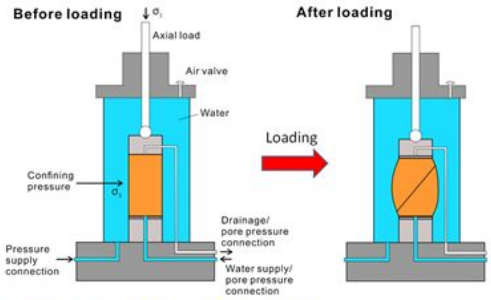

Not satisfactory

2. Advantage and disadvantage

+Sliding surface is not determined in advance, similar to the more practical sliding surface.

- The length of the sliding surface is short; normal stress is not high **(1.7MPa)**, in accordance with the shallow sliding surface and medium sliding surface. Maximum shear speed **1cm/minute; Can not be determined rapid landslides**
- Complex equipment, equipment costs are relatively high
- Conducting experiments are complex, take time.

Ring shear apparatus

1. Purpose

Determination of residual shear resistance of soil.

2. Advantage and disadvantage

+High normal stress (3MPa), Simulation be the deep slide; Max shear speed **50cm/minute; Simulation be rapid landslide**

+The length of the sliding surface is not limited

+Simulations are landslides triggered by: : **earthquake**, Groundwater level changes

+The equipment is very complex, high-cost equipment

+Conducting experiments are complex, take time

–Only conducted experiments with soil samples were prepared

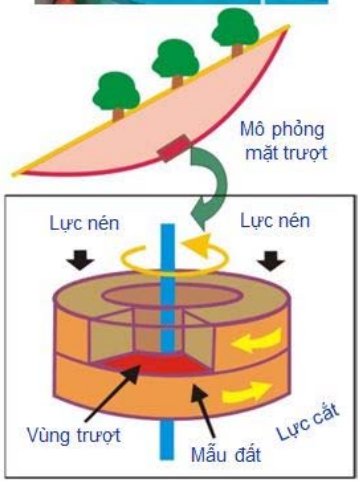

Features of the ring-shear apparatuses from DPRI-3 to ICL-2

Version	Sassa (1992) DPRI-3	Sassa (1996) DPRI-4	Sassa (1997) DPRI-5	Sassa (1997) DPRI-6	Sassa (2004) DPRI-7	Sassa (2011) ICL-1	Sassa (2012) ICL-2
Inner diameter (cm)	21.0	21.0	12	25.0	27.0	10.0	10
Outer diameter (cm)	31.0	29.0	18	35.0	35.0	14.0	14.2
Max. height of sample (cm)	9.0	9.5	11.5	15.0	11.5	5.2	5.2
Shear area (cm2)	408.41	314.16	141.37	471.24	389.56	75.36	79.79
Max. shear speed (cm/s)	30.0	18.0	10.0	224.0	300.0	5.4	50
Max. normal stress (kPa)	500	3,000	2,000	3,000	500	1000	3000
Max. pore-water pressure (kPa)	-	490	400-600	400-600	400-600	1000	3000

The design and construction of RSA (ICL-2) (International Consortium on Landslide)

A

B

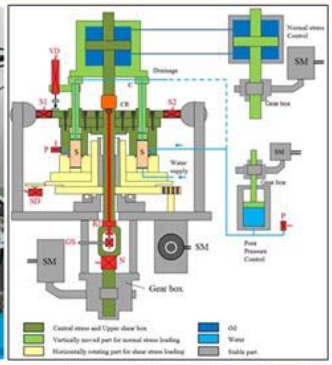

C

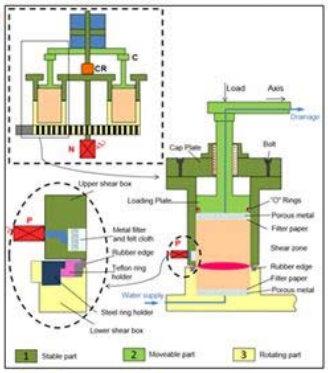

D

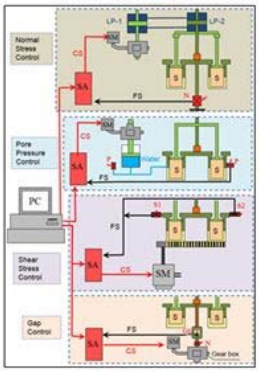

The latest version, ICL-2, developed in 2013.

High-stress ring shear apparatus for large-scale landslides.
Maximum normal stress and undrained capacity is 3 MPa.

A: Photo of the main apparatus.
B: Mechanical structure
C: Close up view of the shear box and sealing.
D: Servo-control system for Normal stress, shear stress, pore pressure and gap.
Red arrow: control signal
Black arrow: feed-back signal
Blue line is for water control

The design and construction of RSA (ICL-2) (International Consortium on Landslide)

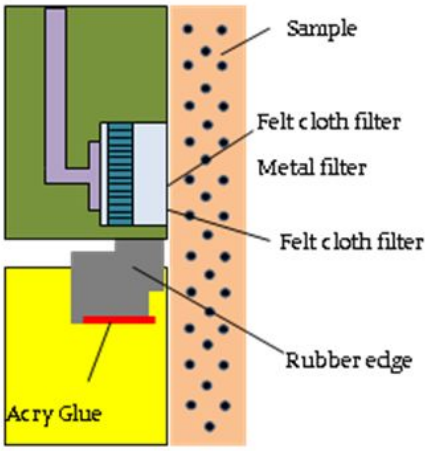

DPRI - 6

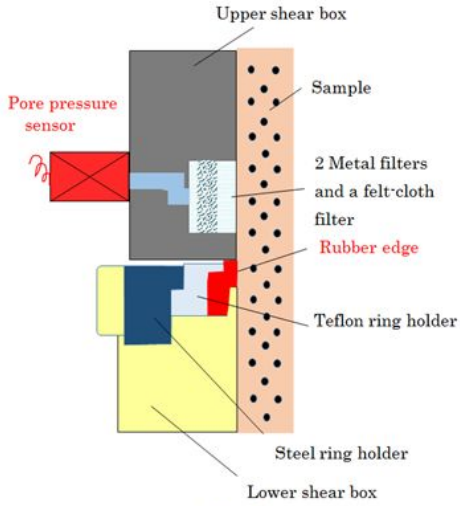

ICL-2

3. The application of the new high-stress ring shear apparatus to the samples of drilled cores from the Hai van landslide

Sampling

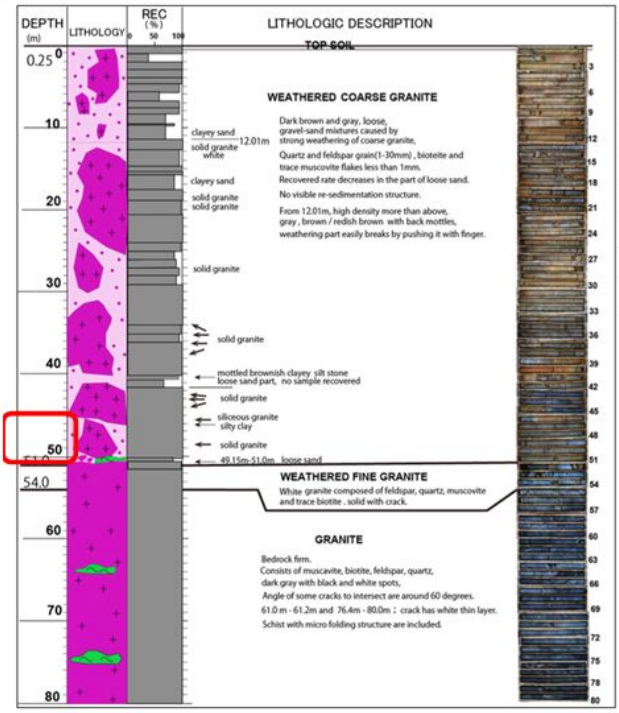

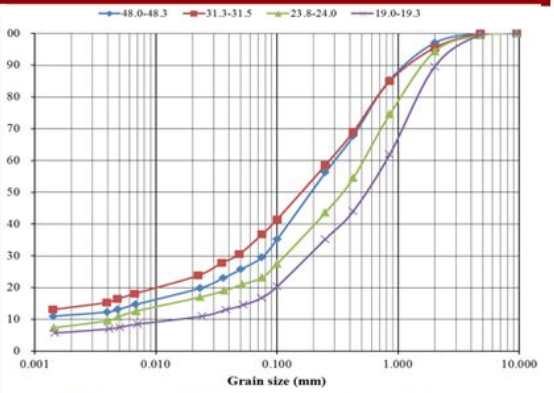

Grain size distribution of sample Hai Van-3 (50m)

Drained Speed Control Test

ISO 9001 : 2008

1. The sample was fully saturated
2. Consolidation to close to:
   - 780 kPa
3. Shear at 0.2 cm/s in the drained condition.
4. After the shear surface reached peak shear resistance, the drained normal stress was reduced to zero at a rate of $\Delta\sigma$=5 kPa/s
5. The peak friction angle and friction angle during motion remained = 39.0°.

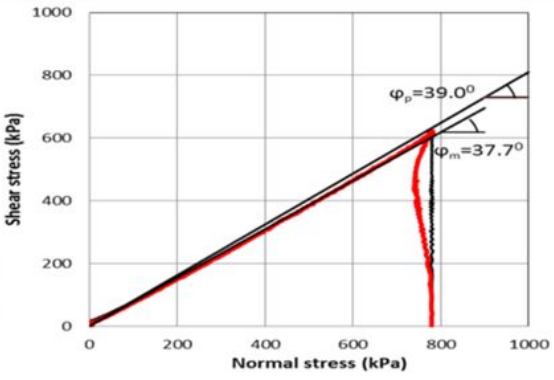

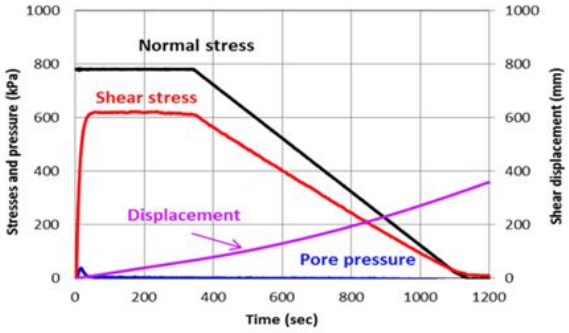

Undrained Monotonic Stress Control Test

1. The sample was fully saturated
2. Consolidation to close to:
❖780 kPa
3. Increase the shear stress value with rate Δσ = 1 kPa / s
4. The peak friction angle and friction angle during motion remained = 39,8^0.

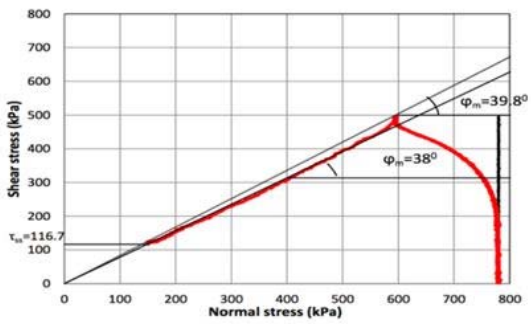

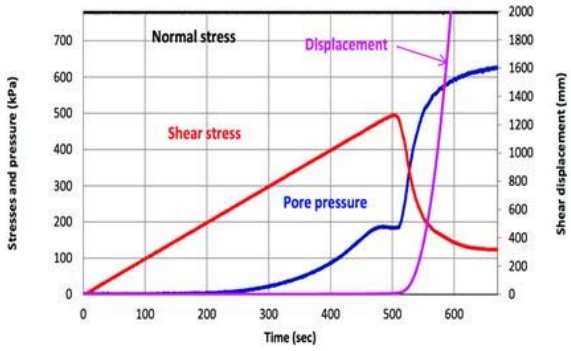

Pore Water Pressure Control Test

1. The sample was fully saturated
2. Consolidation to close to:
❖c) σ:780 kPa, τ = 360 kPa
3. Increase the pore water pressure value with rate Δσ = 1 kPa / s
4. The peak friction angle = friction angle during motion remained= 39,9^0.

Ru = u/σ = 360/780 = 0,46

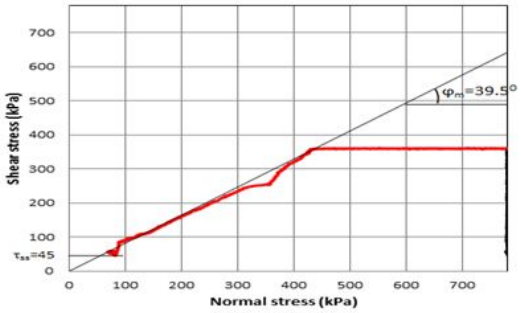

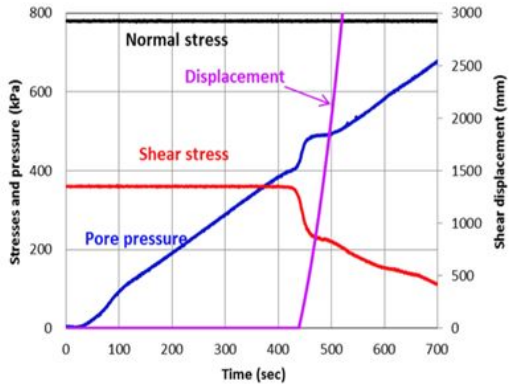

Computer simulation (theoretical)

Integrated Landslide Simulation Model (*LS-RAPID*)

Kyoji SASSA (International Consortium on Landslides)

An Integrated Landslide Simulation Model (*LS-RAPID*) is a computer simulation code integrating the initiation and motion of rapid landslides which are triggered by earthquakes, rains, or their combined effects. A vertical column is considered within a landslide mass. The model calculates the discharge (M, N) and the height (h) of soil mass by assuming that the balance of all forces acting to this column (Self-weight (W), Seismic forces, Lateral pressure, Shear resistance including the effect of pore water pressure) will accelerate the soil mass (m) by acceleration (a) on the horizontal plane (1) and the discharge flowing into the column is the same with the change of the height of soil (2).

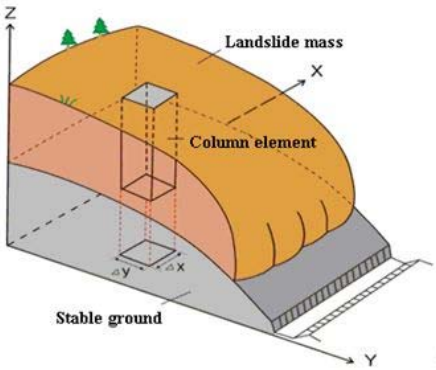

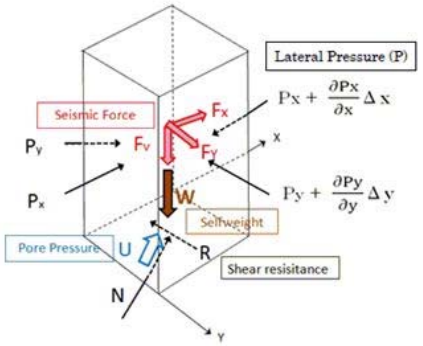

$$am = (W + Fv + Fx + Fy) + \left(\frac{\partial Px}{\partial x}\Delta x + \frac{\partial Py}{\partial y}\Delta y\right) + R \quad \cdots (1)$$

$$\frac{\partial h}{\partial t} + \frac{\partial M}{\partial x} + \frac{\partial N}{\partial y} = 0 \quad \cdots (2)$$ (M, N: Discharge of X, Y direction)

R includes effect of pore pressure (U) and normal force (N).
P includes effect of vertical seismic force (Fv).

Parameters used in LS-RAPID simulation

Parameters	Value (scenario 1/2)	Source
Parameters of Soil in the moving area (deeper area)		
Steady state shear resistance (τ_{ss}, kPa)	116/85	Test data
Lateral pressure ratio ($k=\sigma_h/\sigma_v$)	0.4-0.9	Estimated
Friction angle at peak (ϕ_p, degree)	39.8	Test data
Cohesion at peak (c, kPa)	20	Estimated
Friction angle during motion (ϕ_{cv}, degree)	38.0	Test data
Shear displacement at the start of strength reduction (DL, mm)	300	Test data
Shear displacement at the start of steady state (DU, mm)	3000	Test data
Pore pressure generation rate (B_{ss})	0.7-0.9	Estimated
Total unit weight of the mass (γ_t, kN/m^3)	19	Test data
Parameters of Soil in the moving area (shallower area)		
Steady state shear resistance (τ_{ss}, kPa)	22	Test data
Lateral pressure ratio ($k=\sigma_h/\sigma_v$)	0.8-0.9	Estimated
Friction angle at peak (ϕ_p, degree)	39.8	Test data
Cohesion at peak (c, kPa)	20	Estimated
Friction angle during motion (ϕ_{cv}, degree)	38.0	Test data
Pore pressure generation rate (B_{ss})	0.7-0.9	Estimated
Total unit weight of the mass (γ_t, kN/m^3)	19	Test data
Triggering factor		
Pore pressure ratio changing during rain in the potential shear zone (r_u)	0-0.50	Test data
Other factors		
Slope angle (θ, degree)	20-25	Investigated
Unit weight of water (γ_w, kN/m^3)	9.8	Normal value

Computer simulation (Result)

Computer simulation with pore pressure ratio Ru=0.25

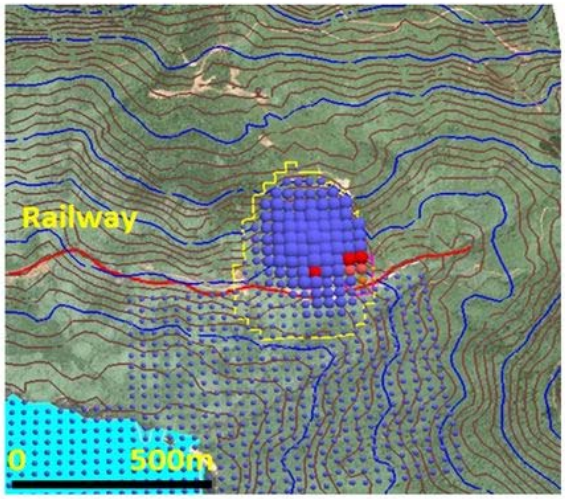

Computer simulation (Result)

Computer simulation with pore pressure ratio Ru=0.3

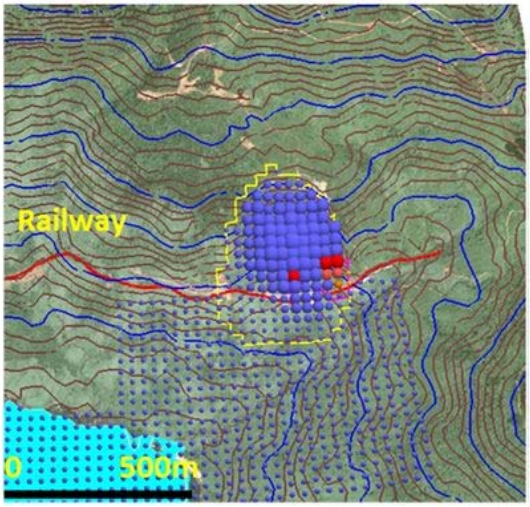

Computer simulation (Result)

Computer simulation with pore pressure ratio Ru=0.46

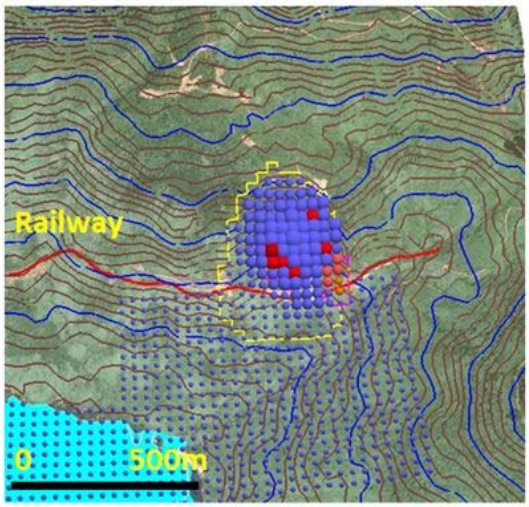

Computer simulation (Result)

Computer simulation with pore pressure ratio Ru=0.5

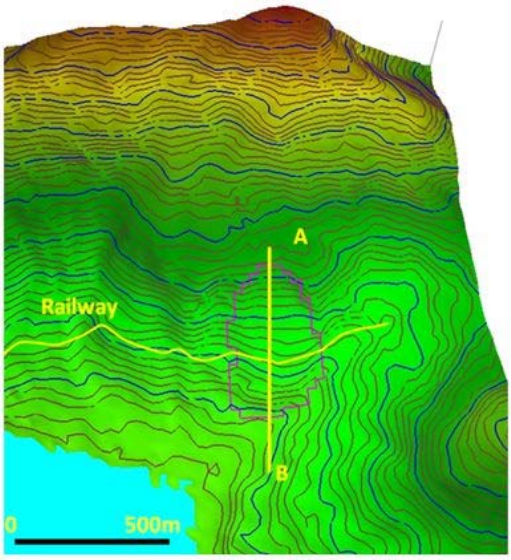

Computer simulation (Result)

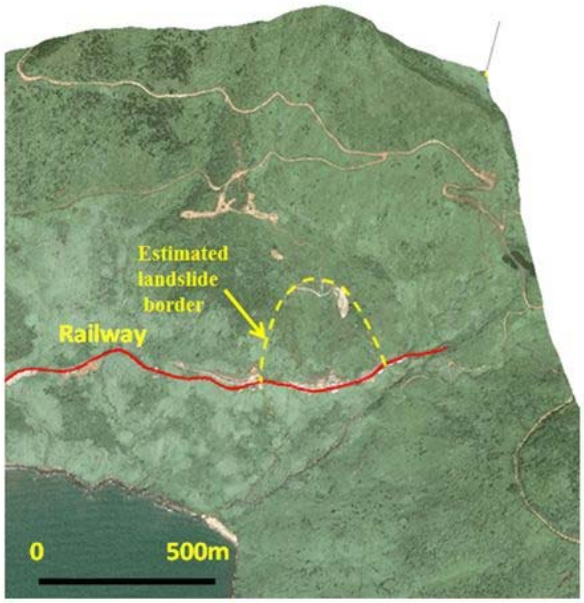

Computer simulation (Result)

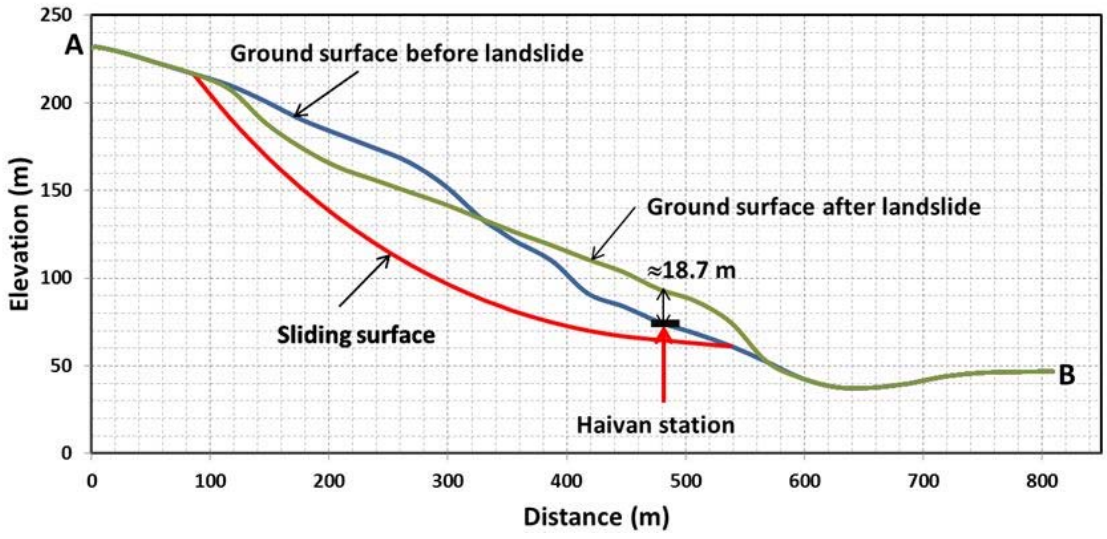

Landslide development process (τss= 116 kPa) (a. ru=0.4501, t=1 s; b. ru=0.4510, t=10 s c. ru=0.4527, t=27 s; d. ru=0.4550, t=50 s)

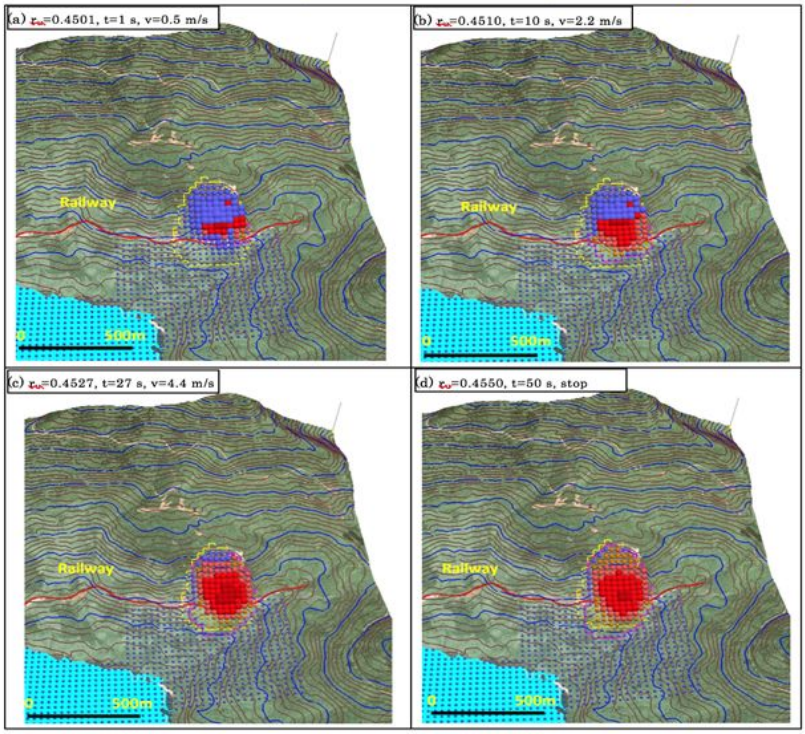

Landslide development process (τss= 116 kPa) (a. ru=0.4501, t=1 s; b. ru=0.4510, t=10 s c. ru=0.4527, t=27 s; d. ru=0.4550, t=50 s)

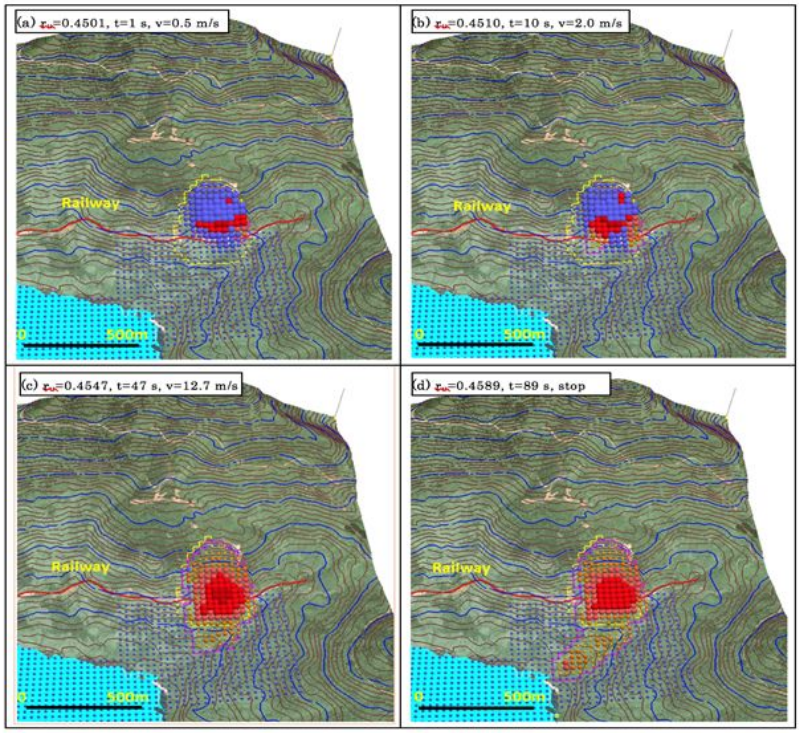

Conclusion

From the ring shear test results, the conclusions can be described as follows:

1) Undrained tests were successful in the monotonic speed-control test, monotonic stress-control test, pore-pressure control test on Hai van core samples.

2) The pore-pressure control tests for simulating the initiation of the landslide indicated that a pore-pressure ratio of 0.46 could have caused the landslide.

Conclusion

5) Using ring shear tests with computer simulation, we can determine hazard area in Haivan area.

ICL-2

LS-Rapid

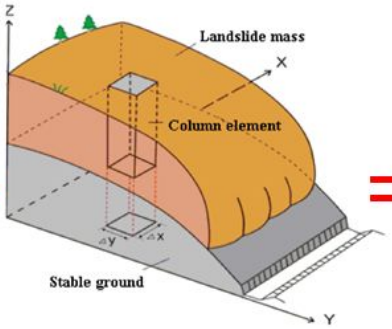

Hazard area

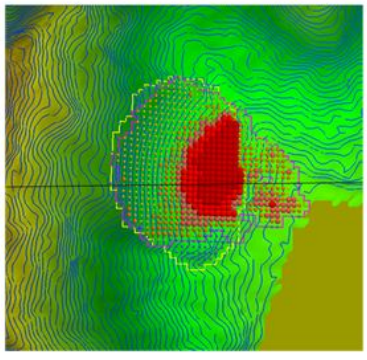


iTST
JST
jICA
ICL
Thank you very much
for yor attention

Japan-Vietnam SATREPS Final Workshop

Monitoring system in Hai Van and landslide flume construction in ITST

Hirotaka Ochiai, Shiho Asano (Forestry and Forest Products Research Institute),
Huynh Dang Vinh, Do Ngoc Ha (Institute of Transport Science and Technology)

Purpose of Landslide monitoring and flume test

Landslide prone slope is estimate the mapping method or actual slope deformation. And It's need to consider about risk level of collapse.

Specific landslide risk level and estimation of collapse time for escape from disaster is able to be considered based on the actual landslide phenomenon.
For estimation of risk level, the landslide monitoring is important.

Web based the landslide monitoring system is developed and installed on the landslide prone slope.

This system is consisted by many sensors that has any kind of method and accuracy and presented the real time monitoring data on web.
It can be useful for clarification of landslide mechanism and early warning.
It can be prototype model of landslide monitoring in Vietnam in a future.

Relationship between slope failure and landslide displacement that is different each landslide is necessary for forecasting and early warning.
The landslide flume equipment by rainfall simulator is installed in ITST and landslide examination is started for early warning.

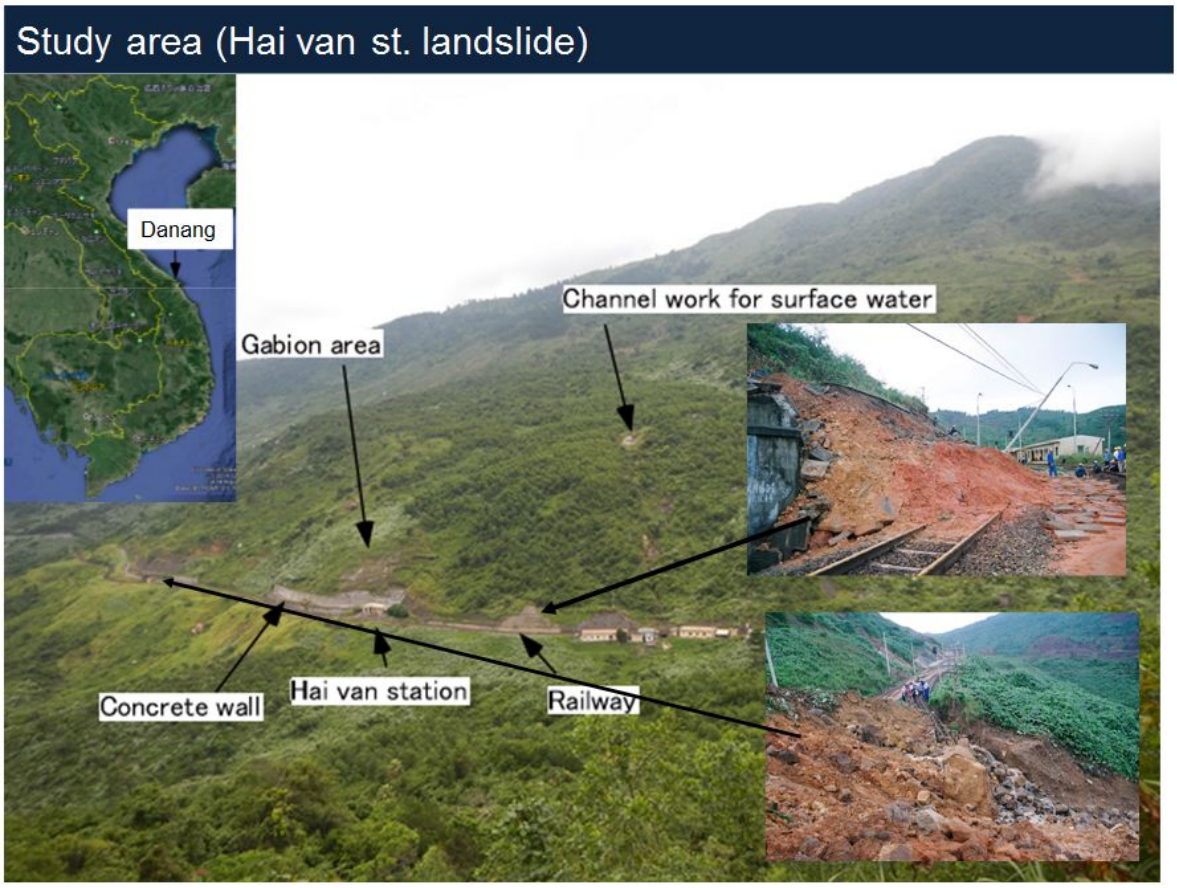
Study area (Hai van st. landslide)
Danang
Channel work for surface water
Gabion area
Concrete wall
Hai van station
Railway

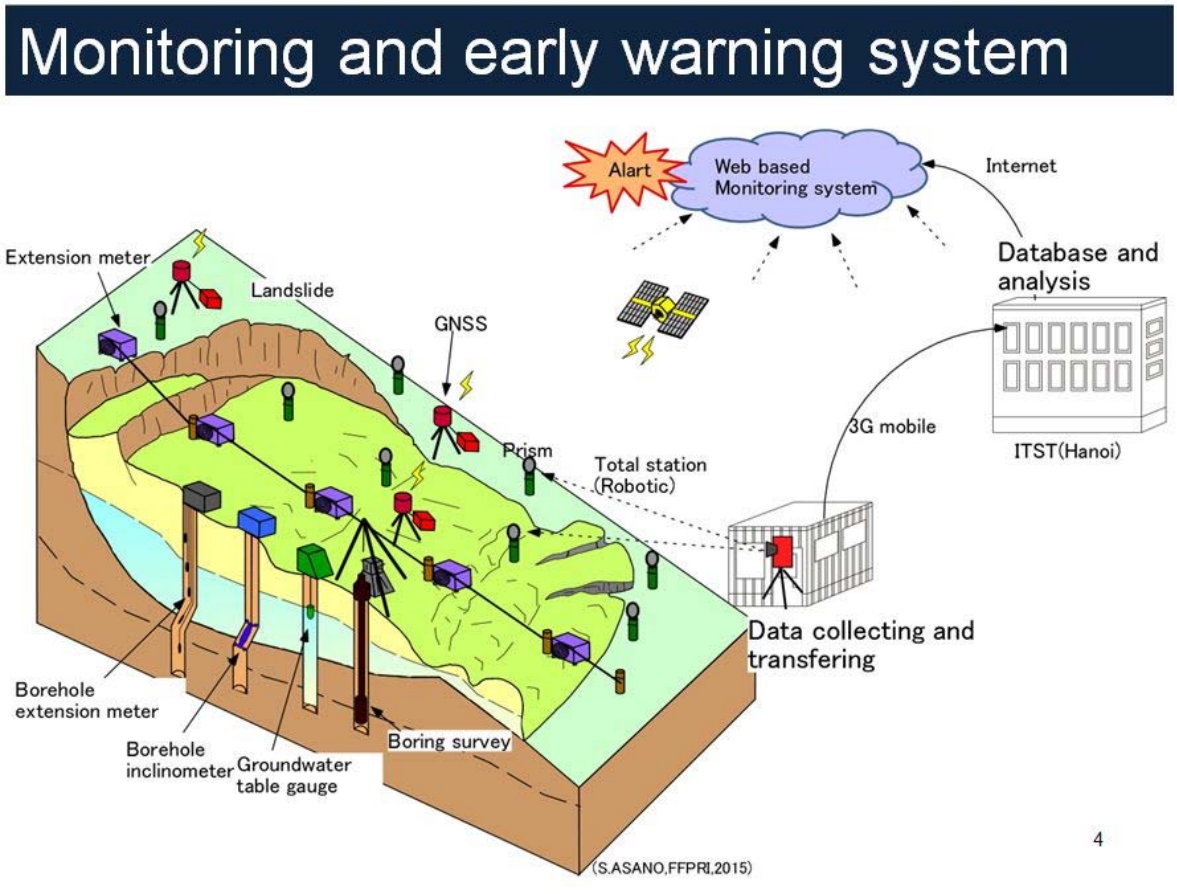
Monitoring and early warning system
Alart
Web based
Monitoring system
Internet
Database and
analysis
Extension meter
Landslide
GNSS
Prism
Total station
(Robotic)
3G mobile
ITST(Hanoi)
Data collecting and
transfering
Borehole
extension meter
Borehole
inclinometer
Groundwater
table gauge
Boring survey
(S.ASANO,FFPRI,2015)
4

Topography and sensor location

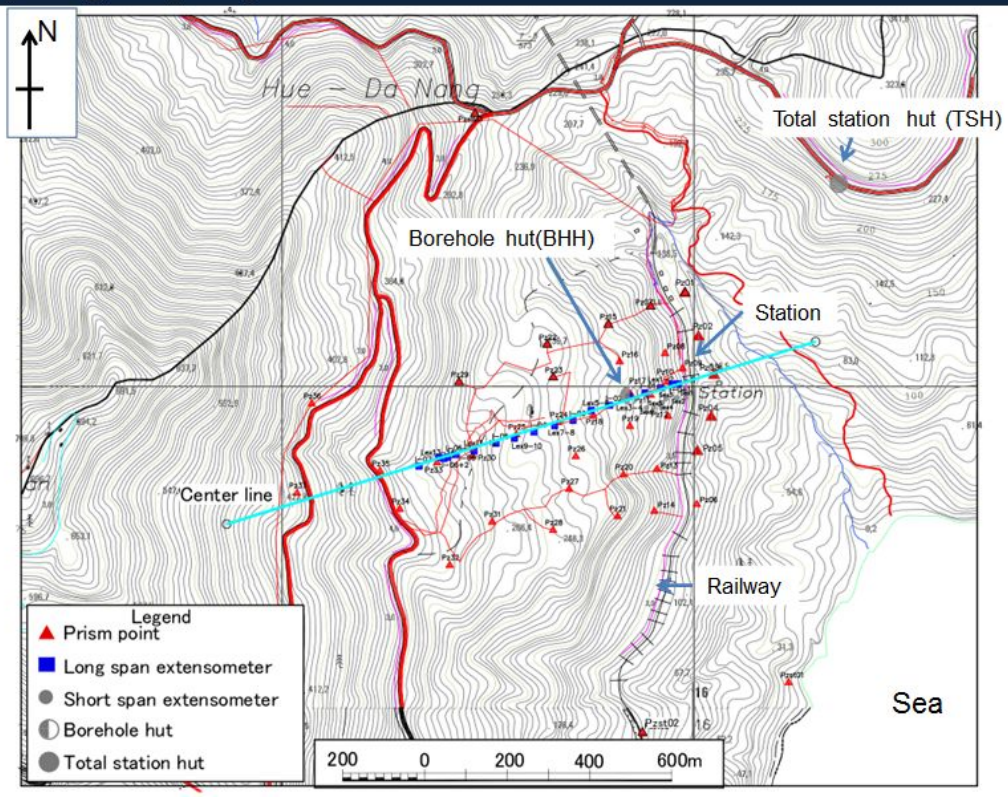

Boring and geological survey

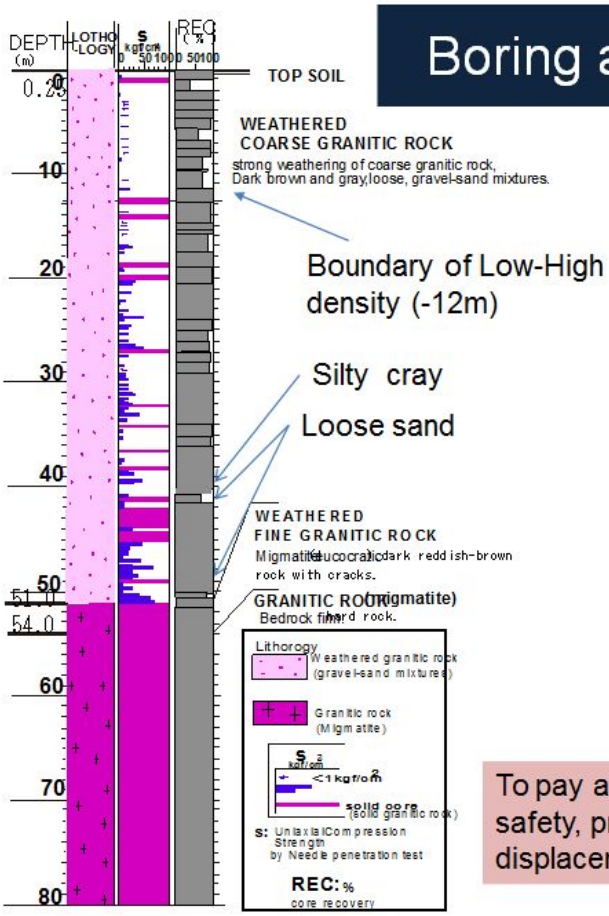

To pay attention on the installation work for safety, preliminary observation of rain and displacement was conducted.

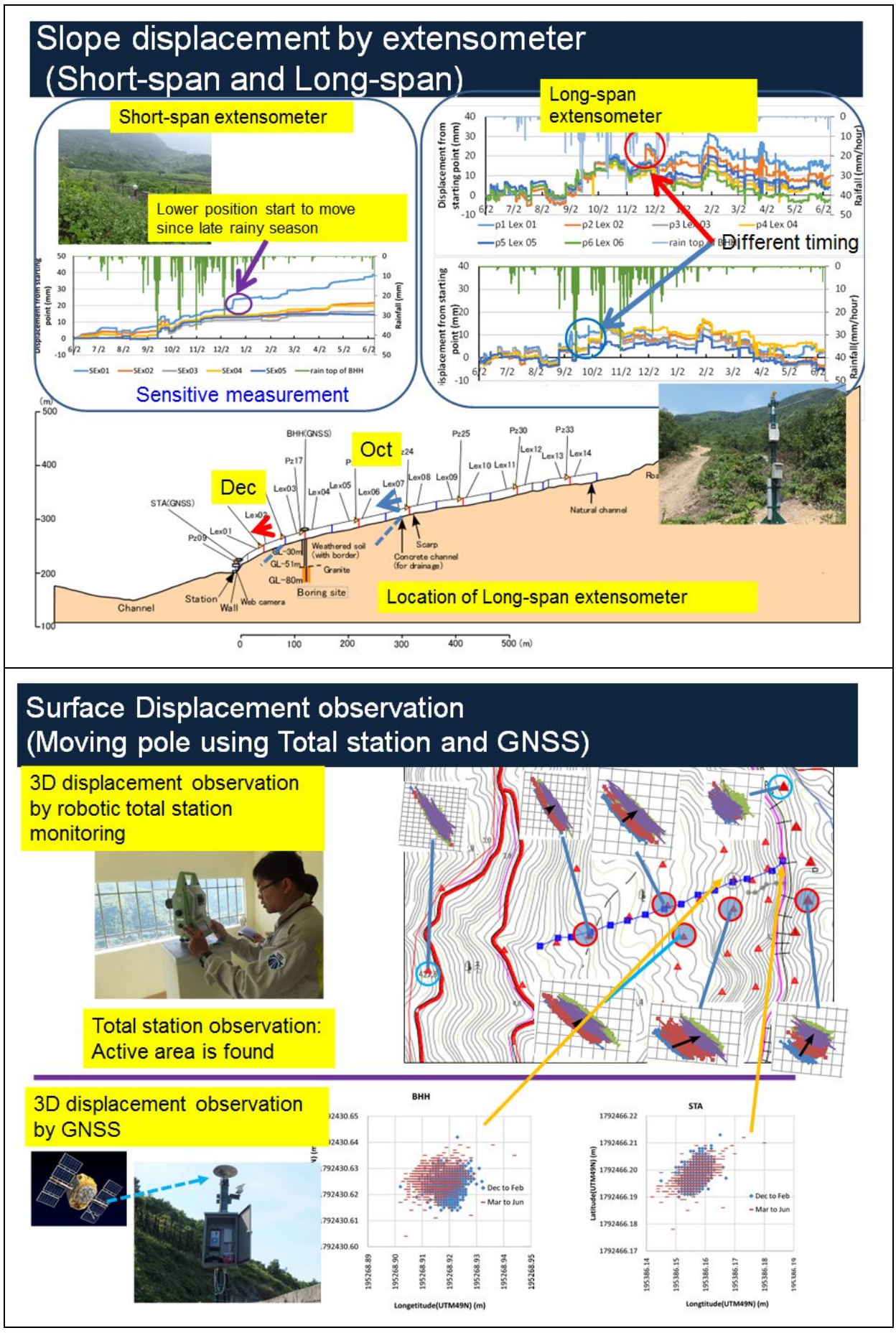
Slope displacement by extensometer
(Short-span and Long-span)
Short-span extensometer
Lower position start to move
since late rainy season
Sensitive measurement
Long-span
extensometer
Different timing
Oct
Dec
Location of Long-span extensometer
Surface Displacement observation
(Moving pole using Total station and GNSS)
3D displacement observation
by robotic total station
monitoring
Total station observation:
Active area is found
3D displacement observation
by GNSS
BHH
STA
Dec to Feb
Mar to Jun
Longetitude(UTM49N) (m)
Longtitude(UTM49N) (m)
Latitude(UTM49N) (m)

Groundwater table (Groundwater pressure gauge)

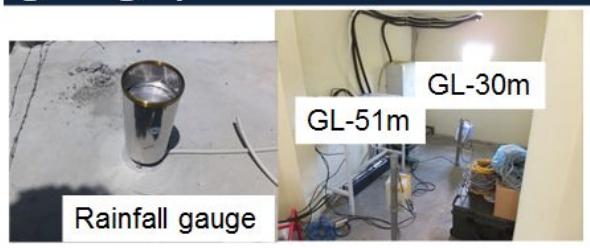

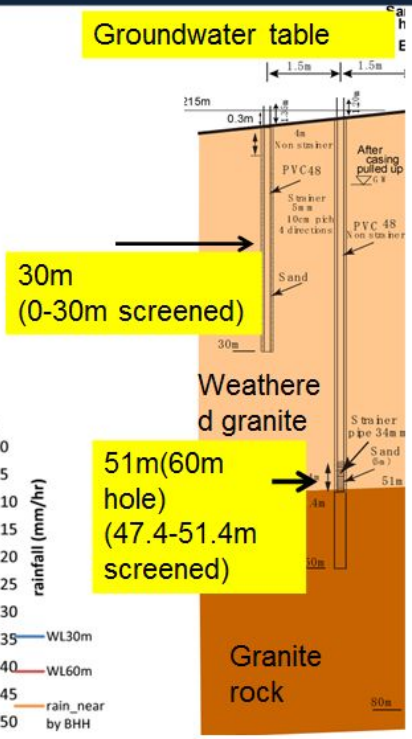

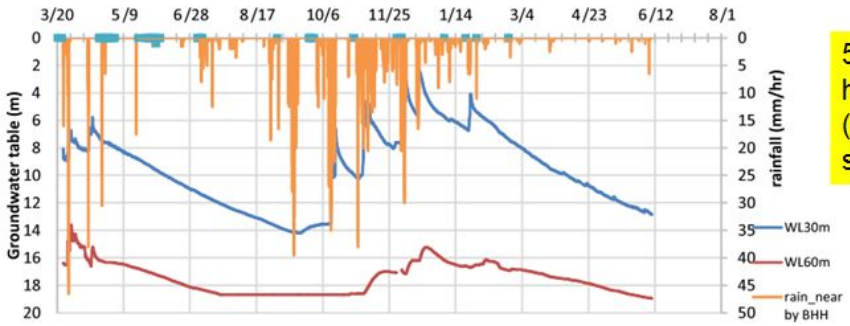

Underground displacement (Borehole inclinometer and Vertical extensometer)

From periodical to continuous monitoring of inclinometer

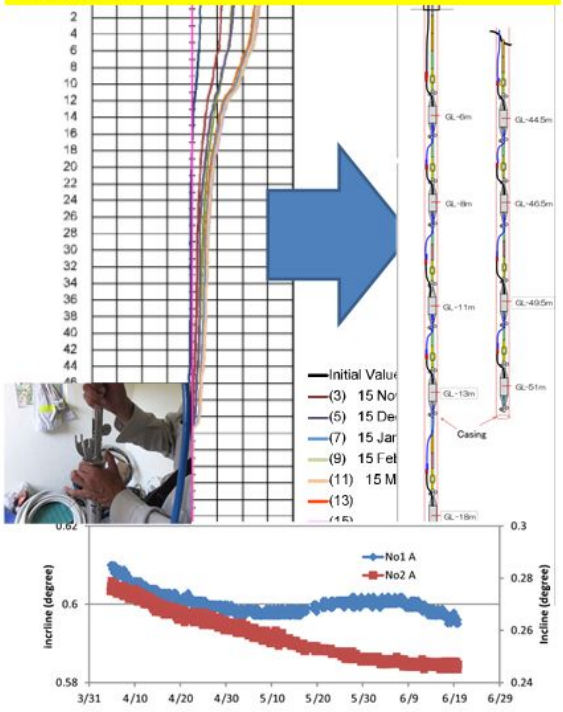

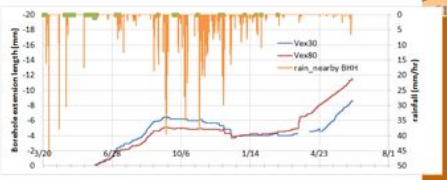

Data transferring system

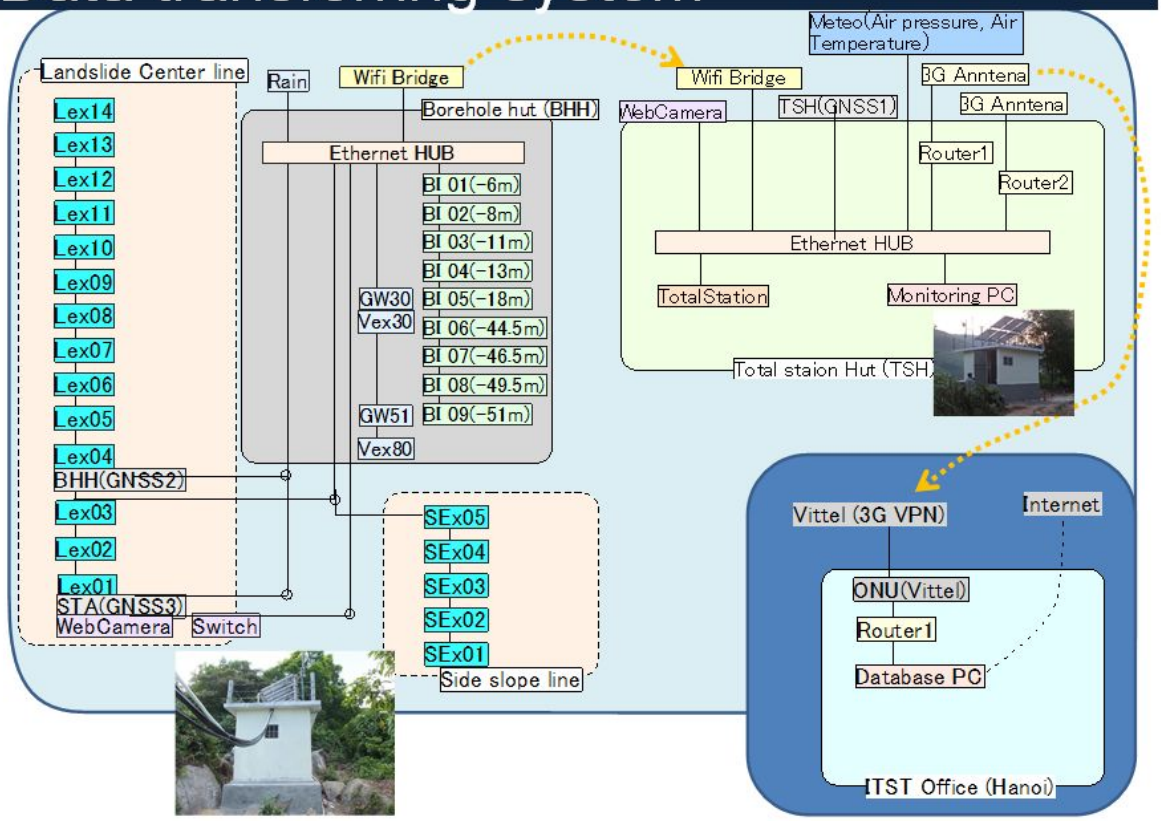

Web observation

・All data can be seen and downloaded on the web-site.
・The web site needs to be accessed by the parties concerned of Hai van landslide monitoring.
・Access level (ex. High or low) of web site will be set in order to use effectivly.

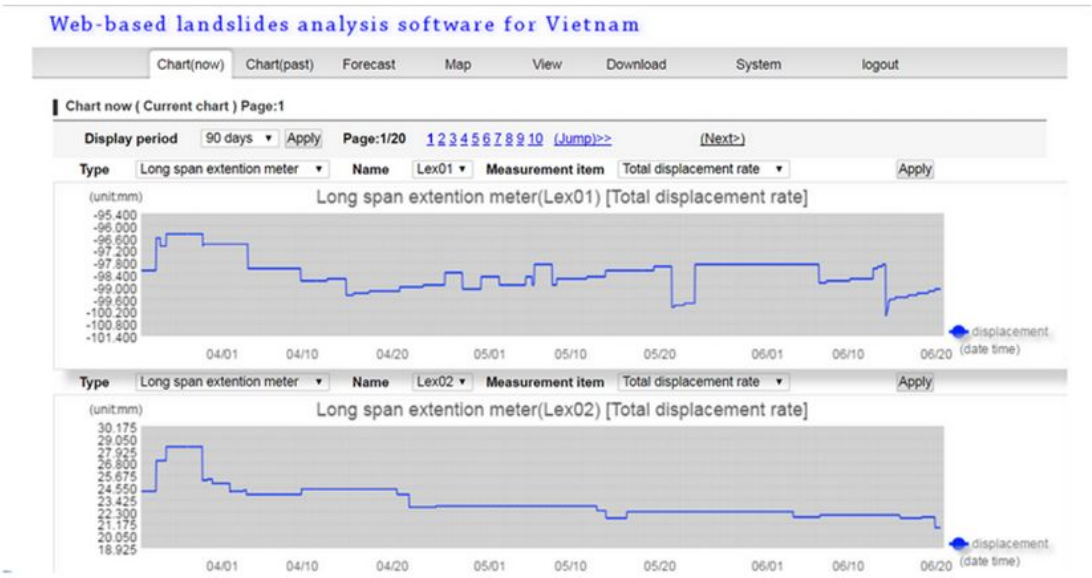

"Map"

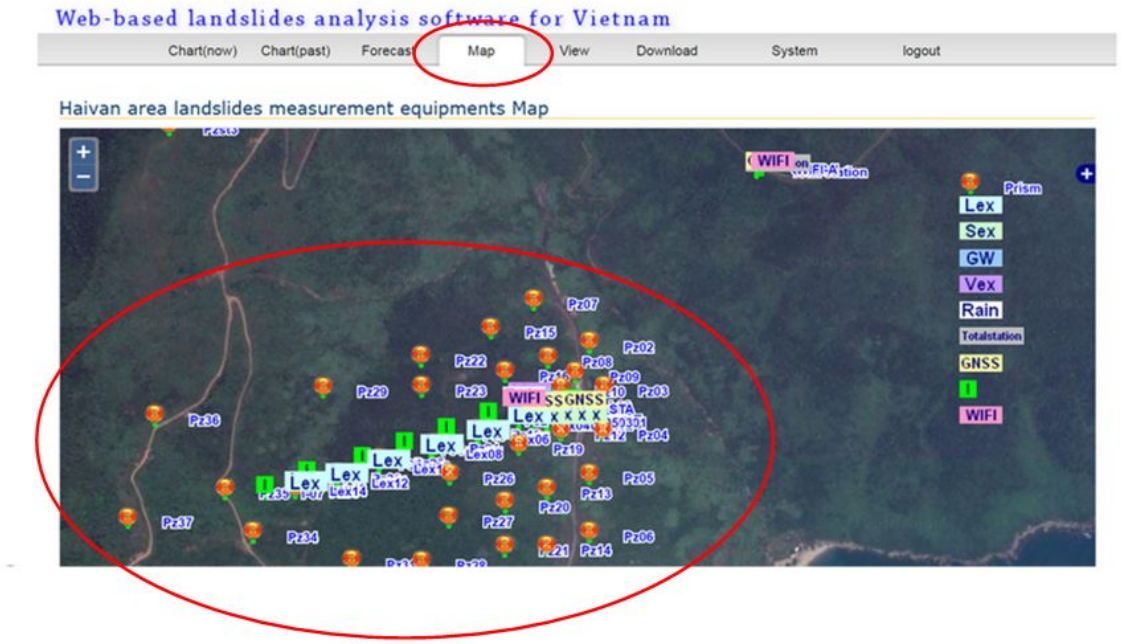
Web-based landslides analysis software for Vietnam
Chart(now)
Chart(past)
Forecast
Map
View
Download
System
logout
Haivan area landslides measurement equipments Map
WIFI
Prism
Lex
Sex
GW
Vex
Rain
Totalstation
GNSS
I
WIFI

"View"

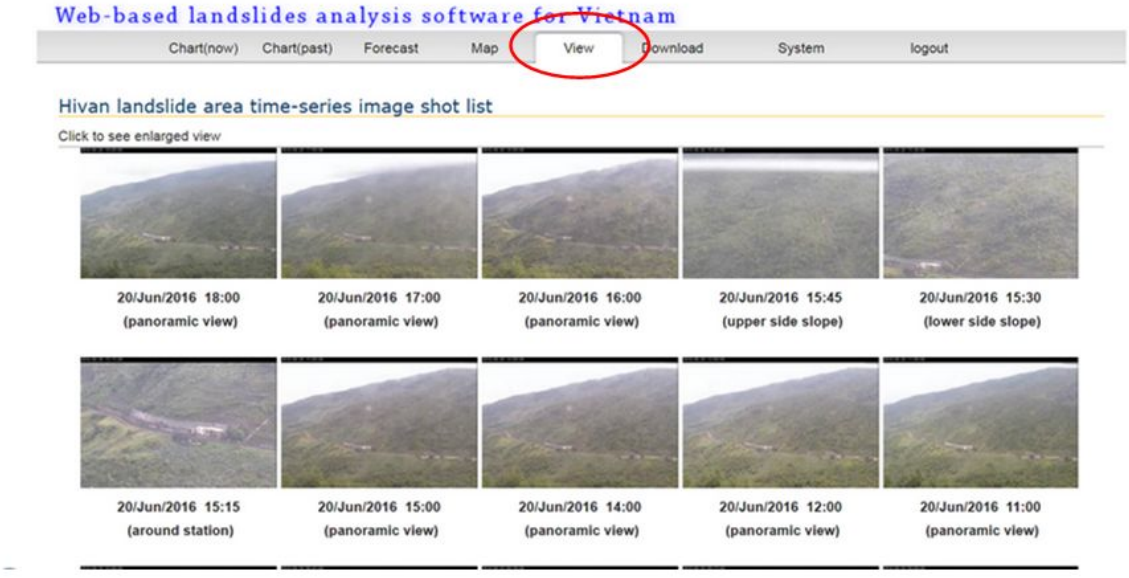
Web-based landslides analysis software for Vietnam
Chart(now)
Chart(past)
Forecast
Map
View
Download
System
logout
Hivan landslide area time-series image shot list
Click to see enlarged view
20/Jun/2016 18:00 (panoramic view)
20/Jun/2016 17:00 (panoramic view)
20/Jun/2016 16:00 (panoramic view)
20/Jun/2016 15:45 (upper side slope)
20/Jun/2016 15:30 (lower side slope)
20/Jun/2016 15:15 (around station)
20/Jun/2016 15:00 (panoramic view)
20/Jun/2016 14:00 (panoramic view)
20/Jun/2016 12:00 (panoramic view)
20/Jun/2016 11:00 (panoramic view)

Construction of landslide experimental facilities

In 2013, landslide experimental facility was designed and the building was made. In 2014, the data logging system and sensors are donated. The landslide flume was designed based on the soil properties of the weathered granite of Hai Van area. In 2015, the landslide flume with rainfall simulator was constructed and first landslide experiment in Vietnam was conducted in ITST in November 2015.
Vietnamese researchers participate in developing these facilitie, are encouraged for human resources development. They are expected to be key persons after the project finished.

15

Landslide flume

Landslide experiment started in ITST from November 2015.

16

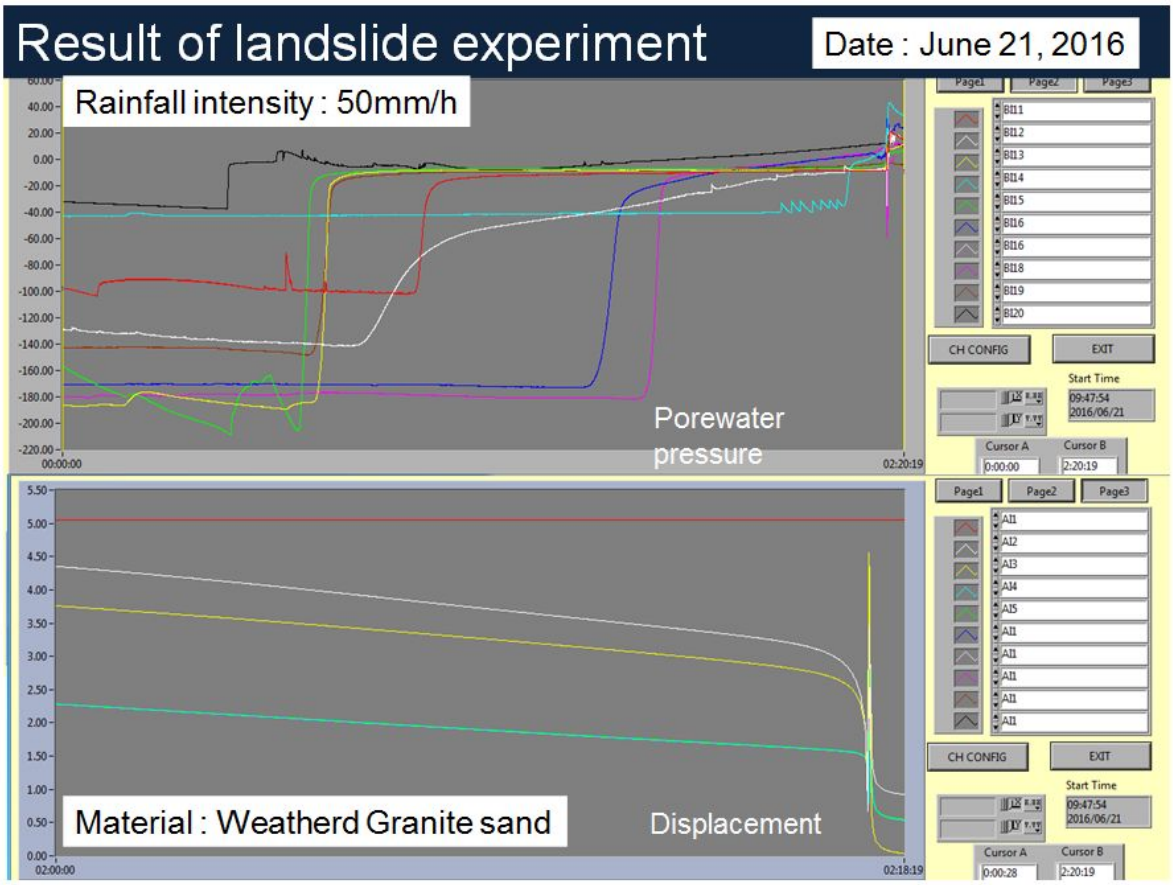
Result of landslide experiment
Date : June 21, 2016
Rainfall intensity : 50mm/h
Porewater pressure
Material : Weatherd Granite sand
Displacement
CH CONFIG
EXIT
Start Time
09:47:54
2016/06/21
Cursor A
Cursor B
Page1
Page2
Page3

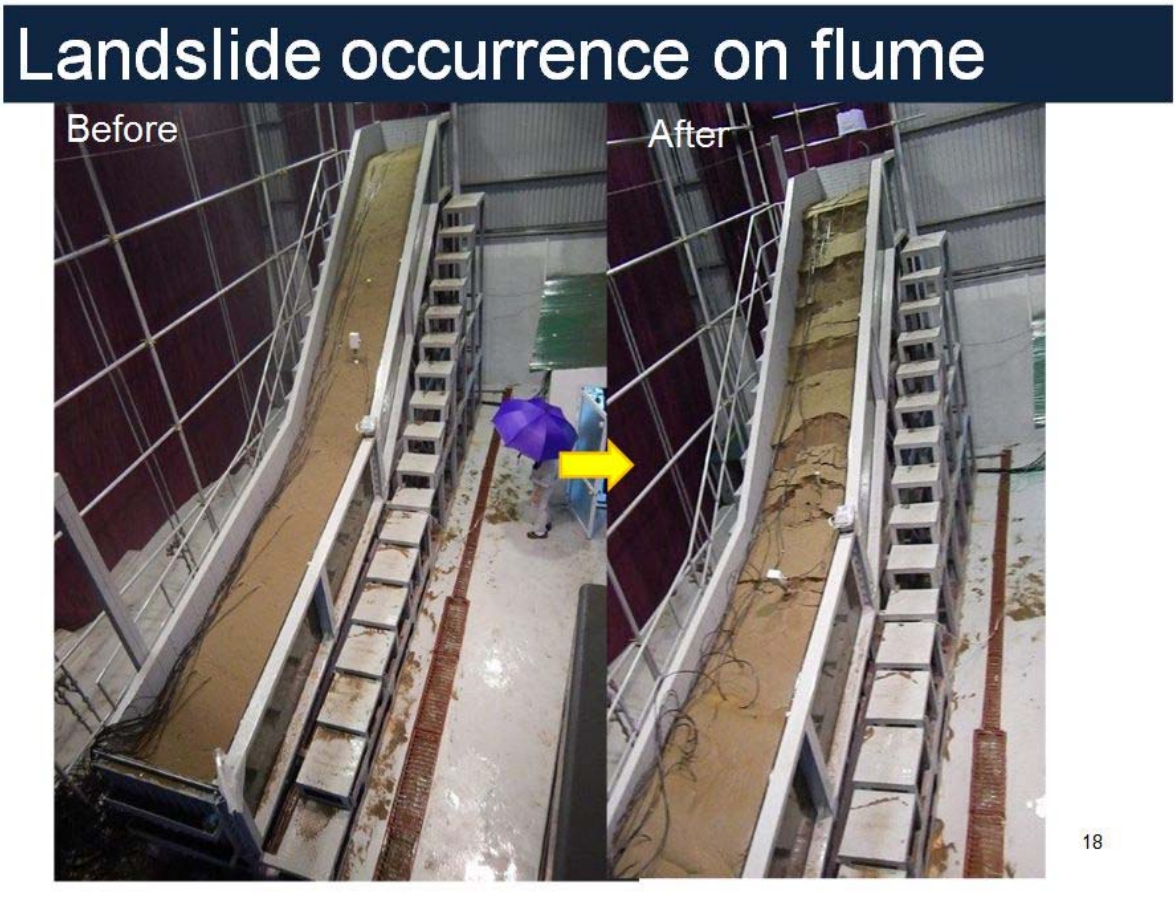
Landslide occurrence on flume
Before
After
18

Trial test of forecasting with observed data in Hai van

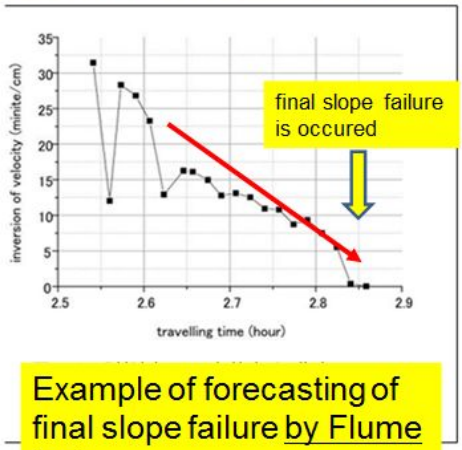

Example of forecasting of final slope failure by Flume test

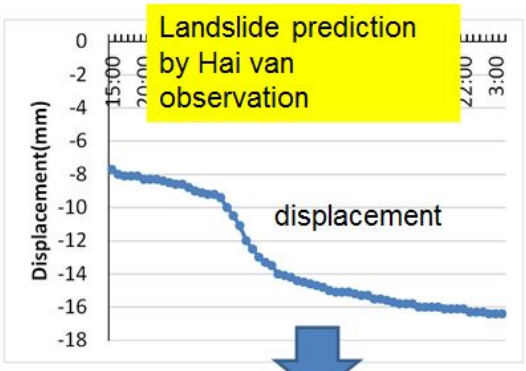

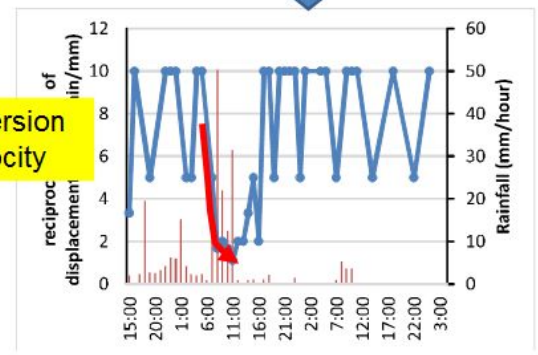

Final slope failure can be estimated by "Inversion velocity of slope displacement"

Conclusion

Landslide monitoring system was developed and installed in Hai van slope.

It provided the newest information of landslide activity and risks for early warning.

Landslide flume examination was started. It is provided the important information about relationship of landslide activity and landslide risks

These system will contribute to reduce the large-scale landslide disaster triggered by heavy rain.

This system is specialized for the specific landslide.
When the estimation of landslide risk for the transportation system of wide area, other warning system will be needed to consider (ex. rainfall and soil water forecasting)

Proceedings of the SATREPS Workshop on Landslides in Vietnam, 2016

Report of the Guidelines developed by this Project for Landslide Risk Assessment

MsC. Bui Ngoc Hung [(1)], Dr. Dinh Van Tien [(1)]

1) Institute of transport science and technology, Viet Nam, e-mail: bnhungitst@itst.gov.vn (WG1)

Abstract Based on the technological transfer from Japan to Vietnam, Vietnamese researchers have drafted a intergrade guidelines for landslide risk assessment in the following 6 parts with 33 guidelines (GL), which cover on (1)Mapping and Site Prediction,(2)Material Tests,(3) Monitoring,(4)Landslide flume experiment and (5)Software application. Those guidelines will be first step for strategy of national standard development for landslide risk assessment in Vietnam.

Keywords guidelines, Vietnamese standards, basis standards.

1. Landslides Risk assessment Project

For more insight into the phenomenon of landslides in general as well as to control and mitigate the loss of this natural phenomenon to the under-operated traffic system as well as the new projects in a mountainous area,

A Technical Cooperation Project named "Development of Landslides Risk Assessment Technology along Transport Arteries in Vietnam" was proposed by Vietnam institute of transportation science and technology (ITST) and ICL. It was the second Satreps project, which was established in 2008 as a part of the new "Science and Technology Diplomacy" implemented jointly by the Ministry of Foreign Affairs **(MOFA)** though (JICA) and the Ministry of Education, Culture, Sports, Science and Technology (**MEXT** through JST) regarding landslide .

Overall objective of project is to socially implement the developed landslide risk assessment technology and early warning system will contribute to the safety ensuring of transportation arteries and residents in mountainous communities in Vietnam.

The project was implementation time starting from 2011 and ending at 2016 with full time of 5 years.

All results of the project was divided in to 4 work groups (WG) as following:

- Preparation of integrated guidelines for the application of developed landslide risk assessment technology and capacity development by WG1 Joint Team of all groups.
- Wide-area landslide mapping and identification of landslide risk area by WG2 Mapping Group.
- Development of landslide risk assessment technology based on soil testing and computer simulation by WG3 Testing Group.
- Risk evaluation and development of early warning system based on landslide monitoring by WG4 Monitoring Group.

Using MEXT budget and JST budget, ICL landslide teaching tools (TEXT, PDF and PPT) have been developed by Japanese members and cooperated international researchers from ICL. All text tools were translated into Vietnamese by long-term and short-term Vietnamese trainees. Those tools will be the base of the guidelines for the landslide risk assessment technology of the Government of Vietnam.

Vietnamese researchers have drafted an intergrade guidelines for landslide risk assessment based on the technological transfer from Japan to Vietnam. GL includes 6 parts with 33 guidelines, which cover on (1) Mapping and Site Prediction, (2) Material Tests, (3) Monitoring, (4) Landslide flume experiment and (5) Software application.

2. Basis and purpose of Guideline making

According to the Project Design Matrix (PDM), guideline making is one of an important output results of the Project. The guideline (GL) will be developed mainly base on research results of Work Groups in the Project and mentioned main points in Teaching Tool provided by ICL.

Purpose of the GL is to make standardized document as manual for researching and implementation of the Project. The GL is also consider as basic teaching tool for students, researchers regarding to landslide risk assessment

The next step of strategy of dissemination of the project is to develop GL to ITST basic standards and then become National Vietnamese Standards in order to enhance nationwide application technology development for landslide prevention and mitigation in Vietnam.

3. Structure and form of Guideline

Vietnamese Project Management Unit (PMU) issued instruction on structure and form of GL to each Work Group and individuals who were in charge of GL making.

Form of GL is referred as in National Vietnam Standards (TCVN).

Main content of GL includes:

- Abstract
- Scope
- Reference documents
- Terms, definitions
- Main content of GL
- Conclusion

Regulations on the arrangement of the main content of the GL as following:

(1). Structure and name of the guideline in front cover is described as Figure 1.

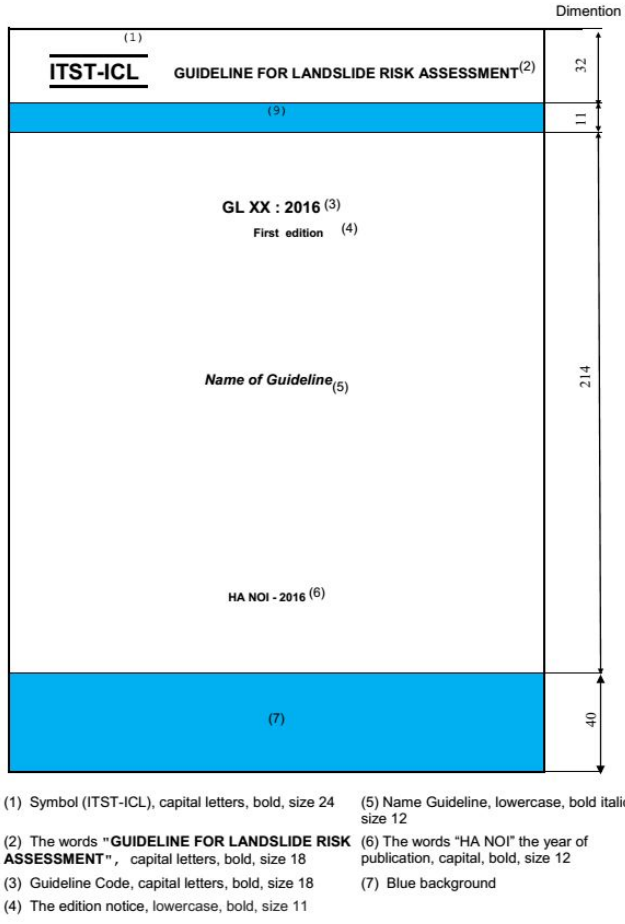

Figure 1: Regulation form of the structure and drafting of Guideline in front cover (the first page)

(2). Structure and the abstract section (the second page) is described as Figure 2.

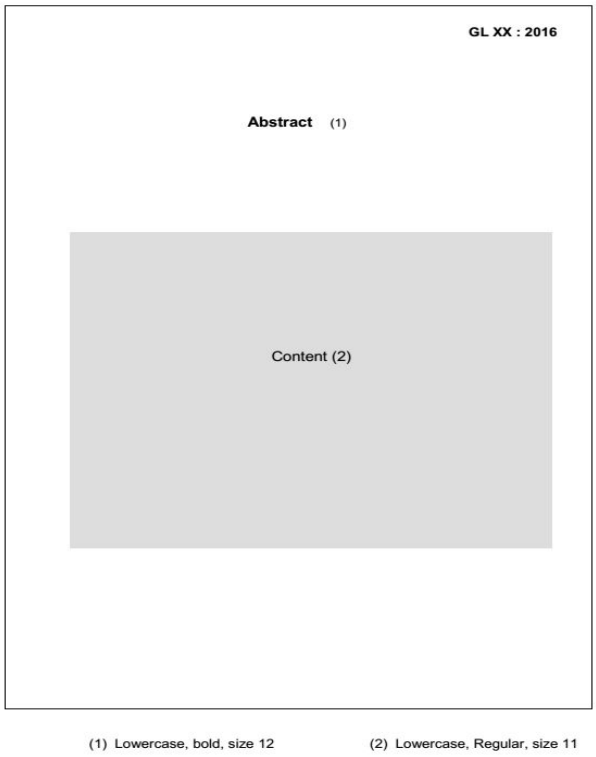

Figure 2: Regulation form of the structure of the abstract section

(3). Structure and the Table of Contents (the third page) is described as Figure 3.

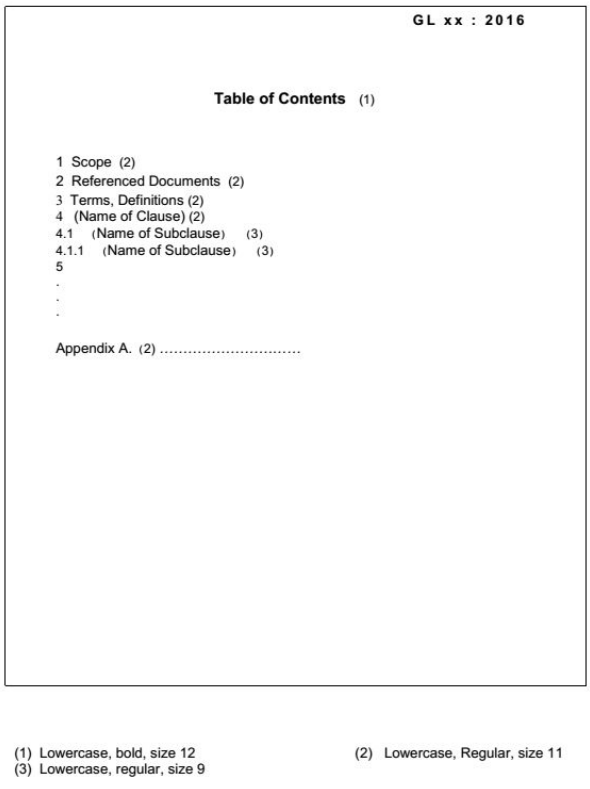

Figure 3: Regulation form of the structure and of the Table of Contents

(4)From the fourth page to the end presents the guideline contents and is described as Figure 4.

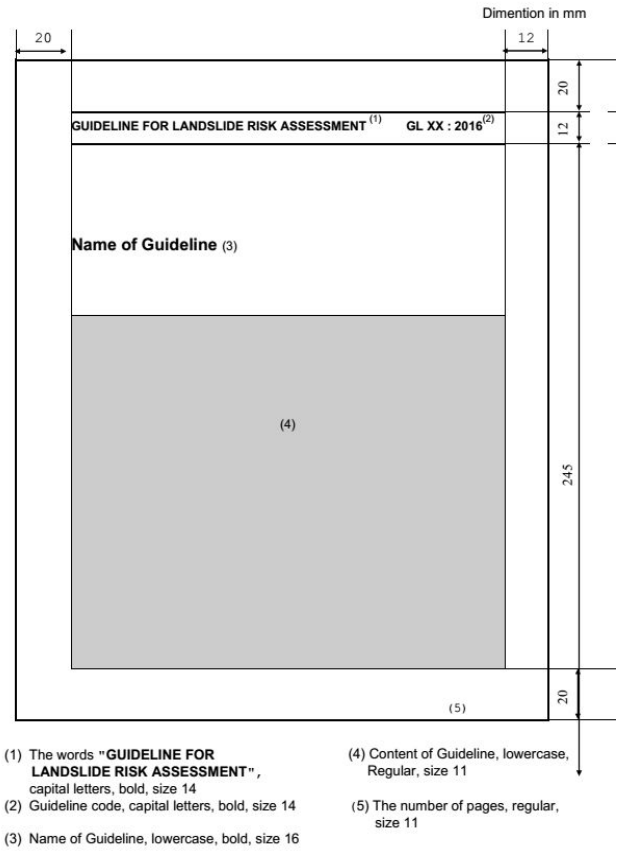

Figure 4: Regulation form of pages from the fourth page to the end of the guideline contents

4. Number and group of integrated Guideline

The intergraded guidelines for landslide risk assessment is divided in to the following 6 parts with 33 guidelines (GL), which cover on (1) Mapping and Site Prediction,(2)Material Tests,(3) Monitoring,(4)Landslide flume experiment and (5)Software application .

Detailed list of intergraded Guideline and person-in-charge as following (Table 1):

Table 1: Detailed list of Guideline and Name of the person-in-charge

`	Name of guildeline	Code	Participants (Vietnamese members)
I	**Part 1. Mapping and Site Prediction**		
1	Landslide topography mapping through aerial photo interpretation	GL 01 2016	:PhD. Le Hong Luong
2	Field Work for Landslide Engineers	GL 02 2016	:MSC. Ngo Doan Dung
3	SFM base DSM establishing	GL 03 2016	:MSC. Nguyen Kim Thanh
4	Risk Evaluation of occurred landslide using the Analytic Hierarchy Process (AHP)	GL 04 2016	:PhD. Le Hong Luong
5	Landslide susceptibility mapping along the Ho Chi Minh route in central Vietnam	GL 05 2016	:PhD. Dinh Van Tien
6	Hazard zonation for Landslide Risk Reduction	GL 06 2016	:MSC. Nguyen Kim Thanh
7	Geological survey for landslide	GL 07 2016	:MSC. Doan Huy Loi
8	Landslide disaster and mitigation for region. Guideline for vulnerability of Landslide mitigation in humid tropical region	GL 08 2016	:PhD. Dinh Van Tien
II	**Part 2. Material Tests**		
9	High Stress Un-drained Ring Shear Apparatus (RSA) Introduction	GL 09 2016	:MSC. Hoang Tuan Nam
10	Drained shear speed control test using RSA Ring shear test - Testing method of drained shear speed control test	GL 10 2016	:MSC. Lam Huu Quang
11	Un-drained shear stress control test using RSA	GL 11 2016	:MSC. Lam Huu Quang
12	Pore water pressure control test using RSA Ring shear test - Testing methodof pore pressure control test	GL 12 2016	:MSC. Lam Huu Quang
13	Cyclic stress control test using RSA	GL 13 2016	:MSC. Lam Huu Quang
14	Undrained pore water pressure and seismic loading test using RSA Ring shear test - Testing method of Undrained pore water pressure and seismic loading test	GL 14 2016	:MSC. Lam Huu Quang
15	Soil shearing test in lab – Direct shear test	GL 15 2016	:MSC. Doan Huy Loi
16	Portable Direct shear apparatus and testing	GL 16 2016	:MSC. Doan Huy Loi
III	**Part 3. Monitoring**		
17	Landslide Monitoring Systems	GL 17 2016	:MSC. Do Ngoc Ha
18	Measurement of slope surface displacement using Robotic total station	GL 18 2016	:Eng. Mai Van Nam
19	Measurement of slope surface displacement using Global Navigation Satellite System (GNSS)	GL 19 2016	:MSC. Vu The Truong
20	Measurement of slope surface displacement using Extensometer	GL 20 2016	:MSC. Pham Thi Chien
21	Measurement of slip surface displacement in borehole using Inclinometer	GL 21 2016	:Eng. Nguyen Van Hung
22	Measurement of slip surface displacement in borehole using Vertical extensometer	GL 22 2016	:MSC. Nguyen Duc Thien

23	Rainfall gauge and others Meteorological equipment	GL 23 : 2016	Eng. Vu Kim Tra My
24	Groundwater observation using water pressure gauge	GL 24 : 2016	MSC. Chu Quoc Dung
25	Early warning system	GL 25 : 2016	MSC. Do Ngoc Ha
IV	**Part 4. Landslide experiment**		
26	Outline of landslide experiment	GL 26 : 2016	MSC. Do Ngoc Ha
27	Infiltration properties of testing material – for permeameter	GL 27 : 2016	Eng. Nguyen Minh Hien
28	Testing method (displacement measurement, porepressure measurement)	GL 28 : 2016	MSC. Huynh Thanh Binh
29	Analysis of measured data (Landslide motion and porewater pressure)	GL 29 : 2016	MSC. Huynh Thanh Binh
30	Mechanism of landslide initiation	GL 30 : 2016	MSC. Huynh Thanh Binh
V	**Part5. Software and Simulations**		
31	Alcalc 3D Software	GL 31 : 2016	MSC. Ngo Doan Dung
32	Arc View Software - Arc GIS10.1/ Spatial Analysis Software	GL 32 : 2016	MSC. Doan Huy Loi
33	LS rapid	GL 33 : 2016	MSC. Nguyen Kim Thanh

5. Abstract of Content of Guidelines

Part 1. Mapping and Site Prediction

- **GL1-Landslide topography mapping through aerial photo interpretation**

The production of a landslide inventory map is a very important preliminary step to determine landslide susceptibility, hazard, and risk assessment. There are a number of methods for producing land-slide inventory maps, such as geomorphological field mapping and visual interpretation of stereoscopic aerial photographs, lidar... The exact choice of method depends on the quality of collected data, type of data, purpose of the map, map scale and availability of aerial photographs etc. In this guideline visual interpretation of stereo-scopic aerial photography is used to prepare an inventory map because of the type of data collected on landslide occurrence. These features are clearly discernible in terms of morphological features that manifest as changes in the form, shape and appearance of the topographic surface. Most of these features can be recognized and appropriately classified through the interpretation of aerial photographs. Recognizing and mapping of landslide topographic area using aerial photograph interpretation remains a challenging task. Formal standards for identification as yet do not exist, and the interpreter classifies landslide morphological forms based on experience, and on the analysis of a set of characteristics (signatures) that can be identified on the images

- **GL2-Field Work for Landslide Engineers**

While we are in the field, we can enjoy a beautiful landscape. But on theother hand, sometimes we recognize the wounded nature here and there. Forthe researchers in regarding to landslide engineering, they always have totake account these points, when you enter the nature. In this article you will find many points helpful when you take a fieldinvestigation. From the way to see slopes from the view point ofgeomorphology, to prediction of slope failure, many key points in fieldwork for landslide engineering are described here.

- **GL3-SFM base DSM establishing**

Aerial photo technology application has been conducted in Vietnam in various sectors but mainly in military. This technology is recently applied in Vietnam for landslide analysis by Japanese experts via ODA landslide project. Unmanned Aerial Vehicles (UAV) has been used widely in many countries applying in different sectors. Photo shots, as a result of UAV, could be used for SFM base DSM establishing. Purposes of guideline is to instruct using of UAV as inputs for SFM base DSM.

- **GL4-Risk Evaluation of occurred landslide using the Analytic Hierarchy Process (AHP)**

In Vietnam, we only know of landslides after they occur. Countermeasures must be quite simple because of lack of funds. They include retaining walls, surface water drainage works, and earth removal works... These countermeasures require large budgets, although the government cannot supply them sufficiently because disasters increase year by year. Therefore, risk evaluation is extremely important. We must ascertain the probability of landslide occurrence and take time to prepare sufficient necessary sources for reduction. In this case Analytic Hierarchy Process (AHP) method is used to evaluate the risk. It aims to rank decision alternatives and select the best one for a complex multi-criteria decision-making problem using pairwise comparison of those criteria. This work will be implemented through several times discussion at the working group. Each person in the working group implements AHP evaluations. The score is calculated intuitively based on the experiences of a geomorphologist. In this way, landslides are classified from special high risk to low risk based on the AHP score evaluation.

- **GL5-Landslide susceptibility mapping along the Ho Chi Minh route in central Vietnam**

Landslide is considered as one of the dangerous phenomenon that often occurs in the mountainous region of Vietnam and directly affects to the lives of the people in the region, destroys the traffic infrastructure the road system. This paper introduces an overview of the

natural conditions of the studied area locates along the corridor of the HCMR, in the provinces of Quang Tri and Thua Thien-Hue, Quang Nam in order to focus on the spatial analysis of landslide susceptibility in this area. There are various possible causes for land sliding with complex inter–relationships. However, in practice a detailed assessment to find the main causes of each landslide is not feasible in most cases. The selection of causative factor for landslide susceptibility map is usually base on expert's subjective experience. In this study, to analyze landslide manifestation, causative factors are derived of slope anger, type of rock, fault density, distance to the road, land used and precipitation. Maps for causative factors were created, in which each one was divided in to classes. From position of 604 artificial slope failures appeared along the HCMR a landslide distribution was build up. The sensitiveness to landslide of each classis zone of causative factor maps is calculated and then evaluated thought the value of number occurred landslide -NOL and density of occurred landslide DOL. These values were the result of comparison of landslide distribution map and each causative factor maps using GIS application. An analytical hierarchical process is used to combine these maps for landslide susceptibility mapping. As the result, A landslide susceptibility zonation map with 4 landslide susceptibility classes, i.e low, moderate, high and very high susceptibility for land sliding, is derived based on the inventory map of observed landslide from 2006-2009. This map indicates that 82.66% total number of occurred landslide, which have been reported fall into highly and very highly susceptible zone. Even there was limited matter concerning relevant, scale and available data, the landslide susceptibility map of this study for corridor along this road is credible for landslide mitigation.

- **Gl6-Hazard zonation for Landslide Risk Reduction**

Landslides, especially rapid mass landslides, is a natural phenomena disaster danger threatening human life, destruction and loss of property of the society. For the specific locations of landslides, mechanisms of displacement of motion can be analyzed and forecasted by result of testting. By knowledge from simulation modeling, scale of each position sensitivity can be predicted based on laboratory cutter integrated within the shifting conditions. The forecasting incidence occurs with a frequency of movement will help people minimize the damage of this natural phenomenon. The Map to forecast area effect of landslides phenomenon establish on this idea.

- **GL7-Geological survey for landslide**

This report aims at providing guidelines for geological survey for landslide. This guideline is based on the guideline of Japan Landslide Society (2002). To understand the mechanism of origination of disasters associated with slope movement and to predict the resulting deformation, geological survey is most important

- **GL8-Landslide disaster and mitigation for region. Guideline for vulnerability of Landslide mitigation in humid tropical region**

For landslide prevention, response and mitigation, a Landslide Hazard Vulnerability in tropical region a Guideline was proposed. The author approach is to answer for questions " What-Where-When-How"to landslides. Concept and classification of landslide in study area will be discussed for "What" question. Landslide moving mechanism is mentioned, in which the effect of the pore-pressure rise by raining is confirmed then the relationship between dynamic factor and displacement (signal of landslide recognition) is tagged for observation. As the result, basic data for landslide management and regional monitoring system are advised that will answer for "When" question. The integrated maps for landslide hazard vulnerability such as landslide inventory map, landslide risk assessment map, landslide susceptibility map and landslide hazard map are presented as basic tools to answer for "Where" question as site prediction. The application of research for landslide prevention, response and mitigation plan, in which metioned landslide knowlerges and tools used will discuss for question "How". This guideline will contribute for landslide hazard management as a basic document in center of Vietnam.

Part 2. Material Tests

- **GL9-High Stress Un-drained Ring Shear Apparatus (RSA) Introduction**

This apparatus that can geotechnically simulate the formation of the shear zone and the post-failure mobility of rapid landslides. It measures the consequences of mobilized shear resistance, as well as the post- failure shear displacement and generated pore water pressure. A series of different modifications of the apparatus (DPRI-3, 4, 5, 6, and 7) were developed from 1992 to 2004. The concept of the simulator is illustrated in Fig. 1. A remolded sample from a slope is placed in the shear box. Then normal and shear stresses including seismic stress and pore-water pressure are reproduced in the apparatus. The apparatus can maintain undrained conditions during shear while monitoring pore-water presssure. All stresses are reproduced and generated pore-water pressure, mobilised shear resistance during measured shear displacement and shear speed are monitored. Fig.2 is a view of the largest apparatus in this series.

- **GL10-Drained shear speed control test using RSA Ring shear test**

Testing method of drained shear speed control test.The sample the sample was first fully saturated (BD values ≥ 0.95) and consolidated to simulate natural initiation in drained condition. Shearing sample in drained condition to measure the specifications of the soil

- **GL11-Un-drained shear stress control test using RSA**

The sample the sample was first fully saturated (BD values from 0.93 to 0.96) and consolidated to simulate natural initiation in drained condition. Shearing in undrained condition to simulate landslides.

- **GL12-Pore water pressure control test using RSA**

Pore pressure control test used to determined values largest pore water pressure to happen landslides. The sample the sample was first fully saturated (BD values from 0.93 to 0.96) and consolidated to simulate natural initiation in drained condition. Cyclic shear stress in undrained condition to simulate landslides.

- **GL13-Cyclic stress control test using RSA**

Undrained cyclic loading test is performed to simulate dynamic-loading induced landslide. The sample the sample was first fully saturated (BD values from 0.93 to 0.96) and consolidated to simulate natural initiation in drained condition. Cyclic shear stress in undrained condition to simulate landslides.

- **GL14-Un-drained pore water pressure and seismic loading test using RSA**

The sample the sample was first fully saturated (BD values from 0.93 to 0.96) and consolidated to simulate natural initiation in drained condition. Seismic Shearing in undrained condition to simulate landslides triggered by rainfall and earthquakes

- **GL15-Soil shearing test in lab – Direct shear test**

This report aims at providing guidelines for Soil shearing test in lab – Direct shear test. This guideline is based on manual of Portable Direct shear apparatus and testing. To understand the mechanism of origination of disasters associated with slope movement and slope analysis, shear test is most important.

- **GL16-Portable Direct shear apparatus and testing**

This report aims at providing guidelines for Portable Direct shear apparatus and testing. This guideline is based on manual of Portable Direct shear apparatus and testing. To understand the mechanism of origination of disasters associated with slope movement and slope analysis, shear test is most important.

Part 3. Monitoring

- **GL17-Landslide Monitoring Systems**

This report aims at providing guidelines for setting up field monitoring programs for landslides. Recognizing that many parameters may be involved in landslide monitoring, the report concentrates on ground displacement, rainfall and groundwater conditions as the key elements. The types of instrumentations involved and their field installations are presented. The options of using automated electrical or optical fiber sensor systems are described. A few cases of applying fully automated field monitoring schemes for slope stability monitoring are presented to demonstrate the capabilities of currently available techniques.

- **GL18-Measurement of slope surface displacement using Robotic total station**

Monitoring of slope movement monitoring data through change the coordinates of the grids covered area with video- shift device electronic total station to automatically find and catch the target with high accuracy to ± 1.0 mm . Especially electronic total stations automatically measure meets the requirements for the progress and monitoring data at the time of reporting . Through our dedicated software installed deformation values allowed limit , when the value of monitoring points shift received value exceeds the permitted limit values , the sirens will sound at the same time the alert will automatically be sent to those in charge of managing unit works with SMS, EMAIL , FAX to get timely treatment measures

- **GL19-Measurement of slope surface displacement using Global Navigation Satellite System (GNSS)**

Global Navigation Satellite System (GNSS) is constituted as a constellation (a group or a system) of the satellite orbit combined with ground equipments. In the same time, in a position on the ground if it is determined the distances to three satellites (the minimum), it will calculate the coordinates of that location. GNSS operation in any weather conditions, anywhere on the earth, and 24 hours a day. With four or more satellites, the receiver can calculate three-dimensional location (latitude, longitude and altitude). When the user location is calculated by the GPS receiver can calculate other information, such as speed, direction of movement, listened closely movement, about journeys, distance to the destination, and many other parameters

- **GL20-Measurement of slope surface displacement using Extensometer**

Extensometers are devices used to measure the changing distance between two points. They are commonly used in the monitoring of landslides. Measurement points may be located on the surface of a landslide to measure ground movements, for example, spanning a tension crack to monitor its rate of opening, or in a borehole to measure differential displacements at depth, for instance to identify active landslide shear surfaces

- **GL21-Measurement of slip surface displacement in borehole using Inclinometer**

Monitoring displacement of one point at depth in bore hole by using probe inclinometer and automatic probe. The manual inclinometer equipment is used to determine the depth of sliding surface.The auto matic probe will be fix in borehole to measure the displacement with time and provide data for early warning system as well as for research the relationship between displacement and the other factor cause landslide

- **GL22-Measurement of slip surface displacement in borehole using Vertical extensometer**

The exensometer use to measure the change between two points .This device used control the landslide. The poistion to measure is installed in sliding layer when compare with fixing point,from that can determine the distance displacement of sliding mass through this device

- **GL23-Rainfall gauge and others Meteorological equipment**

Use rainfall gauge and temperature equipment to monitor rainfall and temperature with time to provide datas which have used in warning and estimate for landslide research

- **GL23-Groundwater observation using water pressure gauge**

Installation and observation to monitor the groundwwater aim to collect data of water level from well is hydrogeological investigation to collect data of water level in well . This instruction show the basic principle for installation and observation groundwater (or pore water pressure) . Procedure to operate, collect and analysis use the suitable data and ensure its quality.

- **GL 24-Early warning system**

We define landslide Early Warning Systems and present practical guidelines to assist end-users with limited experience in the design of landslide Early Warning Systems (EWSs). In particular, two flow chart-based tools coming from the results of the SafeLand project (7th Framework Program) have been created to make them as simple and general as possible and in compliance with a variety of landslide types and settings at single slope scale. We point out that it is not possible to cover all the real landslide early warning situations that might occur, therefore it will be necessary for end-users to adapt the procedure to local peculiarities of the locations where the landslide EWS will be operated.

Part 4. Landslide experiment

- **GL25-Outline of landslide experiment**

An almost real-size slope model was used to study the generation process of landslide fluidization during torrential rain. Experiments were conducted by filling an inclined flume with loose sand and spraying water over the flume with a rainfall simulator to induce the sand to collapse. Both the movement, volumetric strain and the pore water pressure of the sand were monitored throughout the experiments, from the start of spraying to the cessation of the landslide. Our experiments showed the following. (1) Landslide fluidization caused by undrained sudden loading undergoes three stages: compaction of the sand layer by the sliding mass from upper slope, generation of excess pore water pressure in saturated zone, and induction of fast shearing. (2) Fluidization at the collapse source area also undergoes three stages: destruction and compaction of sand layer skeleton by outbreak of shearing, increase of pore water pressure in saturated zone, and shift to fast shearing. But these three stages take place almost simultaneously

- **GL26- Infiltration properties of testing material**

The permeability of the material is an important indicator in landslide studies at laboratory, especially testing slide flume. Apply Laminar Darcy's law to determine the coefficient of permeability of the soil by measuring the stream flow of water through soil pores of granules, in cm / s.

- **Gl27-Testing method (displacement measurement, pore pressure measurement)**

Flume experiment is a physical model experiments in the laboratory. The experiment simulated a natural slope with minimum size and it is used to study the relationship between displacement, pore water pressure, rainfall The probes of pore water pressure and elongation probe which used to obser the changing over time of pore water pressure and displacement. This guideline will contribute for landslide hazard management as a basic document in Vietnam

- **GL28-Analysis of measured data (Landslide motion and pore water pressure)**

Analysis the data of monitoring at flume test to find to principle of behavior when during sliding process of scope when rain with pore water pressure and time. Analysis flume test is a key to understand all the proecess when scople occure sliding and this will built to the development of technical to estimate risk and warning for landslide.

- **GL29- Mechanism of landslide initiation**

Understanding landslide initiation mechanisms is the basis of landslide risk preparedness. Landslides are all types of gravitational downslope movements of masses of soil, rock or both. Landslides are initiated by separation of unstable masses from the stable part of slope. The major mechanism of separation is “shear failure” of the slope material. This text describes the mechanism of “shear failure” of soil or weathered rock due to stress changes inside the slope during rainfall. For this purpose, the gravitational initial stress acting on a potential sliding surface, pore-water pressure due to rainfall. Shear failure occurs when the stress on a potential sliding surface shifts toward and reaches the failure line of the soil or weathered rock. This process is visualized by the stress path of the “change in stress” due to rainfall, acting individually or together. This guideline will contribute for landslide hazard management as a basic documents in Vietnam.

- **GL 30-Mechanism of landslide initiation**

Currently, Hovland’s method (Hovland, 1977) and 3D Janbu method (Ukai, 1988) are used for a three-dimensional slope stability analysis.The former, Hovland’s method, expands a simplified slice method into three dimensions.Yoshimatsu (1995) has introduced the modified-Hovland's method, which are used anextended-computation to determine a minimum safety factor.Three-dimensional Janbu's method is well known

as a less error to rigorous solution byapplying a horizontal force balance equation. Also, it computes a higher effective lateralrestraint against downward force on a hillslope relative to Hovland's method. In general, at a three dimensional stability analysis using by a limit equilibrium method, asafety factor is calculated from the total resistance force of each columns which representvarious landslide causes inside sliding soil mass such as ground water etc. The columnforms triangular or quadrangular prisms and a limit equilibrium method (LEM) is used inthe calculation. In this soft ware, two type methods are adopted to analyse landslide phenomenon. One is"the squares mesh method", which mainly uses square prisms for an easier formulation.Another one is a finite element method, which uses triangular prisms for a flexible nodearrangement.We recommend the former one, "the squares mesh method", from an aspect ofextensibility.

Part5. Softwares and Simulations

- **GL31-Three Dimensional Stability Analysis for Landslides**

ADCALC3D is a software for stability analysis, offers a variety of options for 3-D slope stability analysis of the landslidessuch as Hovland, Janbu3D and RBSM3D. This program has an easy data compute/input operation which can provide full 3-D images and solid viewer functions.

The program also support to users many new features such as a wide variety of drawing performance, linked to mitigation works design, high speed control, simple input operation, and a variety of grid density to choose.

This guideline establishes to introduce main features of the ADCALC3D software and then will present a specific example, which is calculated by this software at a typical landslide on National Highway 6, HoaBinh, Vietnam.

- **GL32-Arc View Software - Arc GIS10.1/ Spatial Analysis Software**

This report aims at providing guidelines for Spatial Analysis using Arc Map 10.1 for landslide research. ArcMap is used to view, edit, create, and analyze geospatial data. ArcMap allows the user to explore data within a data set, symbolize features accordingly, and create maps. Up to now, we can order or make the raster data of landslide area. From raster data we can create slope, contour map, 3D view of landslide area and export the 3D cordinate for making topography in the landslide simulation.

- **GL33-LS rapid**

The LS-RAPID system is an application designed for Microsoft Windows based on the program, "Landslide Motion Simulation", produced by Prof. Kyoji Sassa (International Consortium on Landslides). The software uses a visual interface which enables the user to input topography parameters, sliding surface parameters, and parameters of soil characteristics to simulate results in 3D. The parameter input by High stress Ring shear apparatus. Purpose to simulation motion and development of landslide through real time.

6. Progress of Guideline compilation

After the decision of mission assignment of General Director of Institute of Transport Science and Technology in April, 2016 for the groups and individuals who compiled Guideline for Landslide Risk Assessment (GL), Leader of the groups and the individuals had been implemented promptly the missions. They usually contacted with Japanese experts and Japanese partners to get comments so as to complete their Guidelines.

According to the reports of the Groups, the progress of Guidelines compilation was reported as following:

- On 4 August, 2016, ITST gathered all 33 Guidelines in English and sending it to the Japanese experts and Japanese partners for consideration and comments.
- Until 31 August, 2016, ITST almost received the comments and edits from Japanese experts and Japanese partners for 33 Guidelines which ITST previously sent.
- Until 06 September, 2016, the Groups and individuals who were tasked, completed the English version Guideline based on the Japanese side's comments as well as translating the Guideline to Vietnamese.
- To correct the Guidelines in accordance with the Vietnamese condition, ITST sent the Guidelines to the experts of Vietnamese Landslide Association of Transport (VLAT) to review, comment and edit the Guidelines before submitting it to Ministry of Transport for approval consideration. Until 15 September, 2016, ITST received all the comments for the Guideline from 08 experts of VLAT.
- From 15 September, 2016 to 20 September, 2016, the Groups and individuals acquired, edited and completed 33 the Guideline in Vietnamese version based on the comments from experts of VLAT.
- From 23 September, 2016 to 24 September, 2016, ITST held a meeting to review all 33 the Guidelines in Vietnamese version after the Groups and individuals previously completed.
- On 30 September, 2016, all 33 the Guideline in Vietnamese version and English version completed following the comments from Japanese and Vietnamese experts.
- Expectation before 05 October, 2016, ITST is submitting Ministry of Transport for consideration and approval for all 33 the Guidelines in Vietnamese version.

7. Conclusion

Vietnamese counter part collaborated with Japanese experts to develop Guideline for Landslide Risk Assessment. This is a result within the project framework as well as a material to use, guide and reference for landslide risk assessment in future.

Basically, the progress of guideline compilation by ITST implemented with Japanese expert's support is following the plan, its contents are insured and eligible for submitting to Ministry of Transport for approval consideration.

After the Guidelines are approved by Ministry of Transport, ITST will consider proposing to Ministry of Transport to allow developing some Guidelines become basic standards and national standards to prevent landslides in Vietnam.

Vietnamese counter part collaborated with Japanese experts to develop an integrated Guideline for Landslide Risk Assessment. This is an output result within the project framework, which developed from cooperation reseach from ITST and ICL regading landslide risk assessment. Strategy for development of the Guideline bases on the new technology from Japan and to be customized to be suistable with Vietnam condiction.

The integrated guideline for Landslide Risk Assessment will be summited to Vietnamese MOT as main research result of the project for consideration. To go with this, ITST will summited MOT a report for academy research, and propose for future study to which some of GL will be upgrade study and developed to be Vietnamese standard (TCVN).

The achievement of the project and intergrade guideline is basic document, useful for students, researchers as well as management staffs of MOT but also contribute for Vietnamese movement strategy for response, mitigation and prevention of natural landslide disaster.

References

Kyoji Sassa (1), Hirotaka Ochiai (2), Toyohiko Miyagi (3), Tien D. V. (4) Nguyen Xuan Khang (5), Development of Landslide Risk Assessment Technology along Transport Arteries in Vietnam – 2015- Abstracts of the 54thannual meeting of the Japan landslide Society-(2.3);

Kyoji Sassa :Toyohiko Miyagi, Hirotaka Ochiai - Project report for final evaluation, 2016;

Sassa , Project Technical report for final evaluation 2016.

A Programme of the ICL for ISDR

the *ISDR-ICL Sendai Partnerships 2015-2025*

for Global Promotion of Understanding and Reducing Landslide Disaster Risk

Voluntary Commitment to
the Sendai Framework for Disaster Risk Reduction 2015-2030
(*Priority 1. Understanding disaster risk*) and
the United Nations Sustainable Development Goals
(*G 11. Make cities and human settlements inclusive, safe, resilient and sustainable*)

Kyoji Sassa
Executive Director of ICL
Secretariat@iclhq.org, http://www.iplhq.org/

Contents

Badakhshan mudslide, Afghanistan on 2 May 2014 (Death toll: 500)

http://www.dailymail.co.uk

Landslide in Kedarnath, Uttarakhand, India on 16 June 2013 (Death toll: 5700)

http://landslides.usgs.gov

Heavy rainfall induced landslide disaster in Rio de Janeiro, Brazil on 11 January 2011 (Death toll: >1000)

http://totallycoolpix.com/2011/01/brazils-deadly-landslides/

List of major landslide disasters (Wikipedia)

No	Date	Place	Casualties
1	21 May1792	Nagasaki , Japan	16,000
2	19 May 1919	Kelud, Indonesia	5,110
3	16 December 1920	Ningxia, China	>100,000
4	25 August 1933	Sichuan, China	~3,100
5	5 July 1938	Kwansai, Japan	~1,000
6	13 December 1941	Ancash, Peru	4,000-6,000
7	10 July 1949	Oblast,Tajikistan	800-4,000
8	18 July 1953	Wakayama, Japan	1,046
9	26 September 1958	Shizuoka, Japan	1,094
10	10 January 1962	Ranrahirca, Peru	4,000-5,000
11	09 October 1963	Longarone, Italy	≈ 2,000
12	31 May 1970	Yungay, Peru	>22,000

No	Date	Place	Casualties
13	18 March 1971	Chungar, Peru	400-600
14	13 November 1985	Tolima,Colombia	23,000
15	30 October 1998	Mt. Casita, Nicaragua	2000
16	16 December 1999	Vargas,Venezuela	30,000
17	17 January 2001	El Salvador	500-1,700
18	17 February 2006	Leyte, Philippines	1,144
19	9 August 2009	Kaohsiung,Taiwan	500-600
20	8 August 2010	Gansu, China	1,287
21	11 January 2011	Rio de Janeiro, Brazil	>1,000
22	16 June 2013	Uttarakhand, India	5,700
23	02 May 2014	Badakhshan, Afghanistan	500
24	1 October 2015	El Cambray Dos, Guatemala	220

An international Consortium on Landslides (ICL) was established during the UNESCO-Kyoto University Joint Symposium in 2002.
Participants are from UNESCO (ADG:AS-Nagy), UNISDR (Pedro Basabe), WMO (DSG:Michel Jarraud), MOFA & MEXT, KU(Kaoru Takara), Japan and others.

High-Level Panel Discussion:
Initiative to create a safer geoenvironment toward WCDR2015 and forward

High-level panel was chaired by Hans van Ginkel (Fomer Rector of UNU). UNESCO (Director-General Irina Bokova), UNISDR, WMO, ICSU/IRDR, China Geological Survey, ICL together from floor discussed.
The 2014 Beijing Declaration "Landslide Risk Mitigation : Toward a Safer Geoenvironment" was adopted on 6 June 2014 following this panel discussion, which was the preparation for the ISDR-ICL Sendai Partnerships 2015-2025 to be adopted in Sendai 2015. 531 people, 211 national and international organizations from 40 countries and 5 organizations of United Nations System participated WLF3.

ISDR-ICL Sendai Partnerships 2015-2025 for global promotion of understing and reducing landslide disaster risk

The partnerships was proposed by ICL and adopted in a session of "Underlying risk factors" of 3rd WCDRR in AM on 16 March 2015. It was agreed and signed by leaders of 16 UN, International and national organizations in PM on 16 March 2015 in Sendai, Japan. Signatories are ICL Exective Director, Ms. Margareta Wahlström (SRSG), and leaders of UNESCO, FAO, UNU, ICSU, WFEO, IUGS, IUGG, KU, SCJ, GRF and Japanese (Cabinet office and MEXT), Italian and Croatian Governments.

Implementation of Sendai Partnerships 2015-2025

- **Publication of Landslide dynamics: ISDR-ICL Landslide Teaching Tools in WEB and Print in 2017.**
  Text tools are 102 tools in 1,686 pages, PPT tools and Video tools for lessons, pdf tools including already published manuals, guidelines, papers.
- **ICL will organize the Forth World Landslide Forum (WLF4) from 29 May- 2 June 2017 in Ljubljana, Slovenia.** High-Level Discussion in WLF4 is for "Strengthening Intergovernmental Network and the International Programme on Landslides (IPL) for "ISDR-ICL SENDAI PARTNERSHIPS 2015-2025 for global promotion of understanding and reducing landslide disaster risk".
- **Vol. 1 Sendai Partnerships of WLF 4 will be published as a full color and open access book and Print book** including Forum Lectures, articles from 17 signatory organizations of Sendai Partnerships and reports of IPL(Internatinal Programme on Landslides) and WCOE(World Centres of Excellence on Landslide risk reduction) as the materials for the high-level panel discussion.
- **WLF5 in Niigata, Japan from 21-25 September 2020** is to review 5 years activities and to plan further activities for the Partnerships.

A method to assess landslide motion for vulnerability and Exposure for landslide risks: LS-RAPID simulation (Sassa et al. 2014)

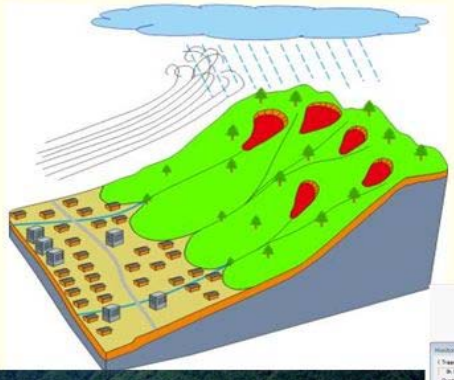

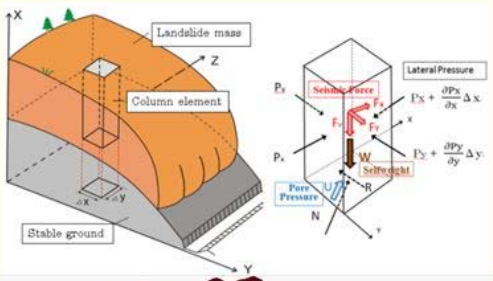

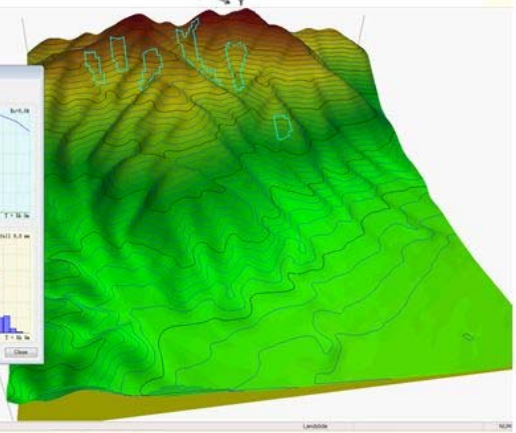

2014.8 Hiroshima Landslide Disaster

A method to assess landslide-tsunami motion for vulnerability and exposure for integrated landslide-tsunami risk: LS-Tsunami (Sassa et al 2016)

The Unzen-Mayuyama landslide-tsunami disaster in Japan. 15,000 people were killed by the landslide and its landslide-induced tsunami around Ariake Sea in 1792

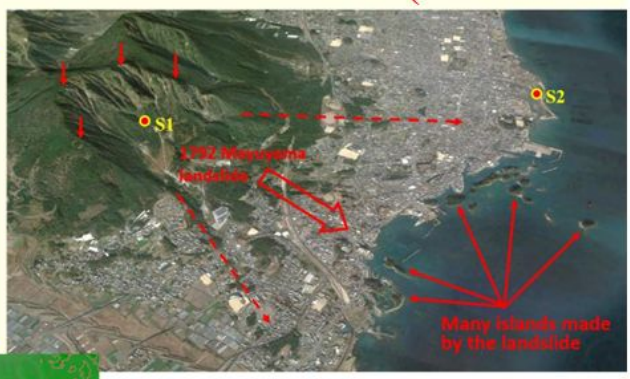

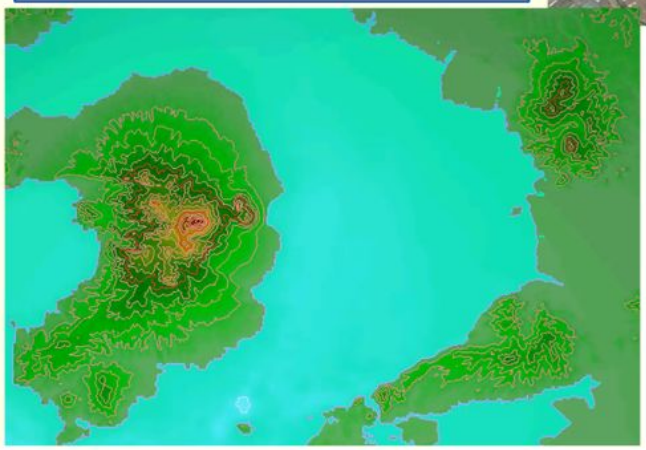

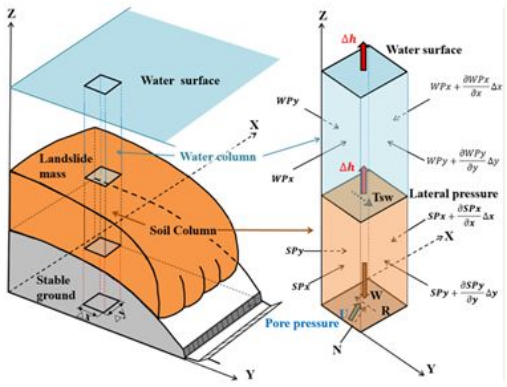

Application to Developing Countries (Case for Vietnam)

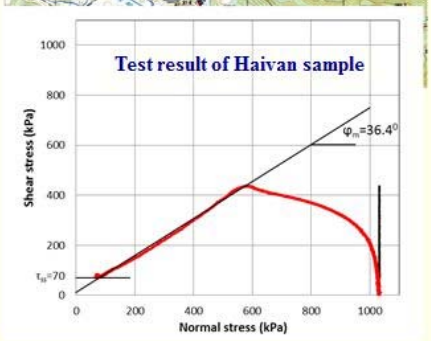

A dynamic loading undrained ring shear apparatus to meaure landslide dynamics parameters

Application of Testing and Simulation to Haivan station landslide in Vietnam

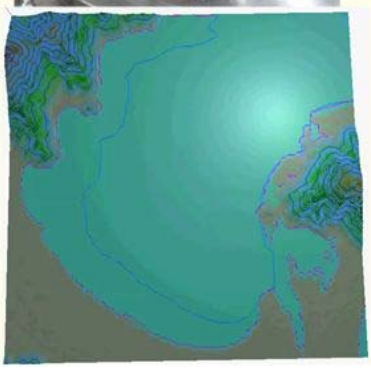

The method to assess exposure to landslides and landslide-induced tsunamis is being applied to Vietnam and other areas through ICL-network (34 countries and 62 ogranizatons). The technologies will be transferred through the planned ISDR-ICL Landslide interactive teaching tools and full color books published in the World Landslide Forum in 2017(Ljubljana, Slovenia), 2020 (Niigata, Japan) and 2023 (USA under examination) during the Sendai Partnerships.

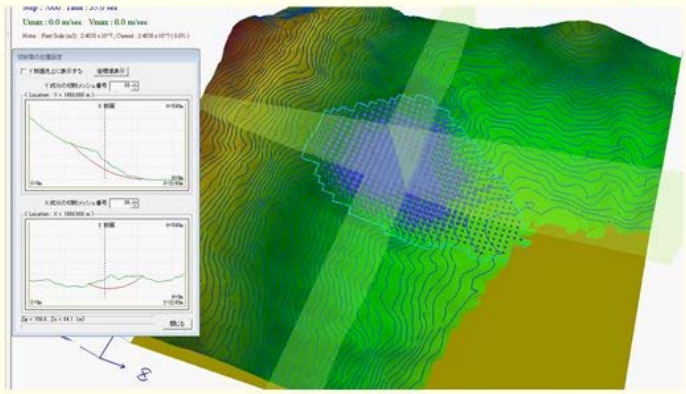

Testing of Haivan samples (Left-top), simulation by LS-RAPID (right) and LS-Tsunami (Left-bottom)

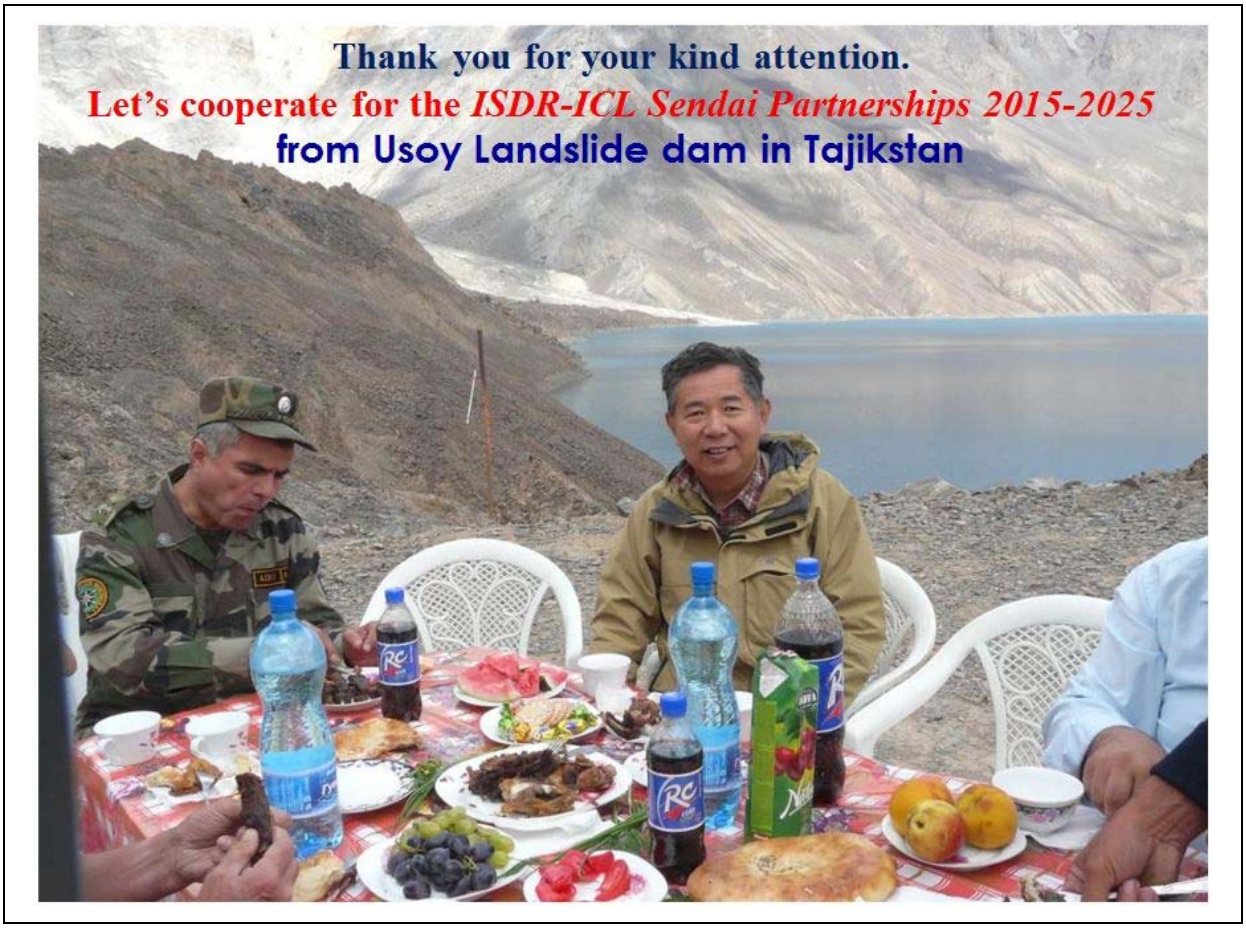
Thank you for your kind attention.
Let's cooperate for the ISDR-ICL Sendai Partnerships 2015-2025
from Usoy Landslide dam in Tajikstan

Proceedings of the SATREPS Workshop on Landslides in Vietnam, 2016

Vietnam-Japan SATREPS Project `Development of landslide risk assessment technology along transport arteries in Vietnam` and its impact to the Vietnamese society

Dinh Van Tien [(1)], Nguyen Kim Thanh [(2)]

1) Institute of transport science and technology, Viet Nam, e-mail: Dvtien.gbn@gmail.com

Abstract

On This paper beside an over view of Vietnam natural characters and landslide situation , the abstract of Vietnamese Government's strategy for response, mitigation and prevention of natural landslide disaster, the main achievement of the Vietnam-Japan SATREPS Project `Development of landslide risk assessment technology along transport arteries in Vietnam` and its impact to the Vietnamese society are presented. The research result of the project is evaluated as successful. It contributes directly to Government Strategy under effort to "proactively prevent natural disasters" to that landslide is one of the major target.

Keywords, Technical Cooperation, Landslide, Risk Assessment, Transport,

Vietnam natural characters

Vietnam is a country that has figure like letter "S", located on the eastern Indochina Peninsula between the latitudes 8°N and 24°N, and the longitudes 102°E and 110°E. It shares borders with China in north, Laos and Cambodia in the west and faces to Pacific Ocean on the east and south with its coastline is 3,444 km in length.

About 75% of its land area is mountainous, mainly located on the north and west area of Vietnam. The elevation of mountainous area is mostly lower 2000 meters above sea level. Fansipan Mountain, the highest peak (3,143 m) in Vietnam, stands in the north, whereas the Annamite Range, comprising lofty peaks of 2,000 m or higher, sits at the Laotian border in the central area of the country. The Hai Van Mountains in the central area divide northern and southern Vietnam. Vietnamese topographical map is presented in Fig.1.

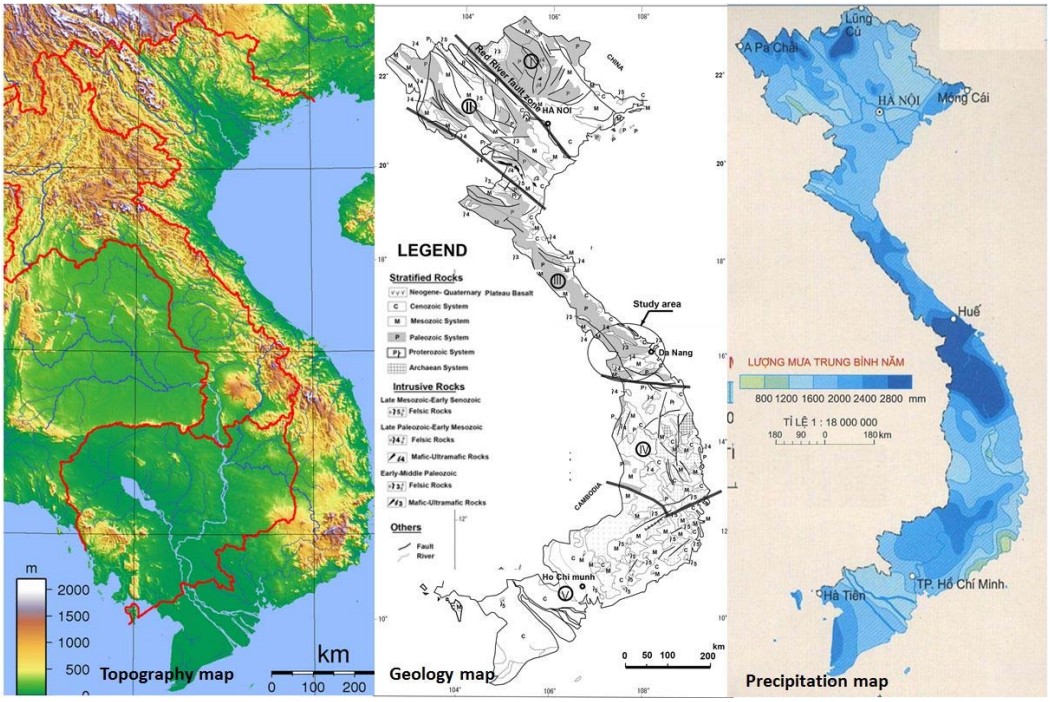

Fig 1. Topography (Atlas Vietnam) – Geology (Tran, 1995) –Precipitation map (Atlas Vietnam) of Vietnam

There are two main deltas locate in the north (Red River delta) and in the south (Mekong River delta). The coastal plain arranged along the east is small, narrow and low economic value. Almost rivers, which run over the country from the northwest to the southeast, heading towards the Eastern Sea has a short length.

The Vietnamese climate is vary from north to the south caused by the figure country expand between different

latitudes. It could be classifiable into three basic climate zones. Red river delta area has a tropical monsoon climate zone resembling the northern Vietnam climate. There are 4 clearly seasons in a year with average temperature range from 10 – 38° C. Mekong river delta area has tropical climate zone with 2 seasons in a year as dry and rainy season and temperature range from 21– 35° on average. Center area of Vietnam has transitional one. The average annual temperature is generally higher in the plains than in the mountains, and higher in the south than in the north.
Bordered by Pacific Ocean, Vietnam is influenced by the monsoon climate with the average annual rainfall from as much as. The average annual rainfall throughout the country is from 2,200mm to 3,000mm and can reach to 4,000mm per year in some particular areas of the Central and located in one of the highest rainfall area in the world. The high precipitation zone, which covers on mountainous area, distributing on the northwest and center of Vietnam could make occurrence landslide seriously. The average annual rainfall map of Vietnam is presented in Fig 1.1. As its geographical location and climate conditions, Vietnam is usually damaged by typhoons and floods with an annual density of 5 to 10 times per year.

Based on statistics, it found that the annual flood season in Vietnam is usually from June to November, equally 99% of frequency of annual floods. Typhoon density changes and tends to increase. On the distribution of typhoon by region, by monitoring data during 105 years (from 1884 to 1989) shows that major storms occur in the central region (up to 68%), followed by North (30 %) and lightest in the south (2%), (ODA Project document-2010)
About perspective geological structures, Vietnam was divided into five blocks as northeastern blocks, north-west block, Truong Son block, Kontum blocks and south blocks. Geology feature of northern zone differs from south zone significantly, separated by Kontum a Truong Son blocks.

Northeast and northwest blocks are divided by the Red-River fault. Northern Vietnam has more Paleozoic and Mesozoic formations than southern Vietnam has, and has many faults, with a complicated geological structure. Proterozoic strata are also observed in the northern Red River fault zone. Paleozoic strata are observed only from northern to central Vietnam, all of which are composed mainly of sedimentary rock such as limestone, mudstone, sandstone, and shale.

The oldest geology in Vietnam is Archean Metamorphic rocks in the northwest of the KonTum province in the central part, surrounded by Proterozoic metamorphic rocks. Southern block areas mostly Cenozoic rocks such as sand, silt, clay, clay-silt, clay mixed with gray silt. Hardly any Paleozoic rock distributes in the south of this basement rock. Basalt that erupted in the Neogene and Quaternary era is also distributed in the neighborhood of the western border (Nam, T. N., 1995) (JOGMEG - Japan Oil, 2000). Truong Son Block mainly concentrated Mesozoic and Paleozoic such as Ordovician – Silurian, carboniferous-Permian and clay stone, cretaceous. Kontum block has abundant with Mesozoic and Paleozoic rocks and pre-Cambrian rock. Geology map of Vietnam is presented in Fig 1.
Mesozoic strata are distributed over the whole country as Triassic and Jurassic marine sedimentary and volcano-sedimentary rocks and cretaceous red continental formations. They are composed mainly of limestone, sandstone, siltstone, shale, and conglomerate, and partially coal-bearing deposits known as Hongai flora. Granitic rocks distributed in the whole country include Archean, Proterozoic, Paleozoic, Mesozoic, and Cenozoic.

Landslides and damages affect to Vietnamese society

High precipitation combined with terrain, complicated geological conditions, especially destroying forested areas causes serious problems related to landslides. As a result, Vietnam is the country has the most serious landslide disasters in Southeast Asia and the Mekong sub-region.
In accordance with ITST's research results, the scientific base for Vietnamese landslide classification is close to the method provided by (Varnes, 1978) Landslides are classified following the types of movements. There are five typical types of landslide including deep landslide, shallow landslide, debris flow, rock fall and topple. As Statistics, the most popular type is shallow landslide, takes 60%. Deep landslides just take about 10-15%, however they are the most difficult and expensive for courter measure. The types above usually occur in rainy season depend on respective condition of terrain, geomorphology, geological structure and hydrology. The percentage of debris flow is around 10% but extremely dangerous. Number of rock falls and topples are small.
On the Fig 2, some pictures of landslide taken in project area are presented. According to statistics of the Central Steering Committee for Flood, from 2000 to 2014, it was occurred 250 debris flows and landslides affected residential areas. Landslides caused 646 people dead and missing, nearly 351 people injured; more than 9,700 homes poured away, more than 100,000 homes flooded and damaged, and more than 75,000 hectares of rice and vegetables flooded. The total damage was estimated at over 3,300 billion Vietnamese Dong, equivalent 150 million USD.
Provinces have frequently occurred landslides including mountainous areas of northern zone, central, central highlands and coastal provinces. The landslides concentrate distributing along transport routes with high density.
According to statistics up to 2006 of Ministry of Transport (MOT), total length of highways in Vietnam is about 17,300 km, makes up 6.87% of total length of road network in Vietnam. In which, 3/4 length of highways is on mountainous area and about 30% of those pass

through areas with complex geological structures, influenced by the tectonic destruction zone. That is why landslides usually occur every year along transport arteries in Vietnam after rainy seasons, with the annual volume up to millions of cubic meters of soil.

Fig 2.Some pictures of landslide taken in project area

Damage caused by landslides are summarized primarily by objective reasons, such as intense rainfall concentrated in a short period in areas with steep slopes, sensitive geology structural. Beside this, in many cases landslides occurrence have main distributed cause by human economic developing activities that lacks of knowledge of disasters.

Natural environments of Vietnam as the causes of landslides are exacerbated by the fact that Vietnam is a rainy region with tropical monsoon climate. Especially, the high precipitation zone, which covers on mountainous area, distributing on the northwest and center of Vietnam could make landslide occurrence seriously. Although Vietnam can be only slightly regarded as an active diastrophic zone, landslides occur frequently in Vietnam. The reasons might include abundance in a sedimentary structure with developed bedding and schistosity as described above, fold structures as a scar of ancient diastrophism, crushing of strata and development of cracks following the fold structures (Tien, D. V. et al., 2016). So, beside characters as natural steep slope, high precipitation, geology took a very importance roll to landslide in Vietnam.

Rapid infrastructure construction, forest cutting down and other customs of agricultural production contribute to increase number of landslide as artificial cause. After the historical flood in 1999 in Middle of Vietnam, landslides occurred on arterial roads caused serious traffic congestion. Vietnamese Government has allowed MOT to conduct difference measures to stabilize of slopes, especially thorough measures with permanent structures to protect and enhance the stability of the slopes along arterial roads impacted by landslides. However, due to limitation of guideline documents and technologies of landslide risk reduction, landslides have fiercely occurred in rainy seasons and continuously caused damages to communities in many parts of the country. Thus, we can say landslide phenomenon is one of the most serious natural disasters in Vietnam, and an urgent matter of Transport sector.

Abstract of Vietnamese Government's strategy for response, mitigation and prevention of natural landslide disaster

The Vietnamese government has assessed landslide is one of the considered natural disaster causes major damage to life and property of the communities. Decision No. 172/2007/QD-TTg dated on Nov. 16 2007 by the Prime Minister of Vietnam approving the national strategy for natural disaster prevention, response and mitigation to 2020 provides the responsibilities and solutions include:

- Developing science and technologies related to natural disaster prevention, response and mitigation;
- Promoting basic investigation and investment for scientific research and new technology application in disaster prevention, response and mitigation; and
- Modernizing early warning systems from

Central, regional to local levels, focusing on efficient communication methods especially for mountainous areas, territorial water and remote areas.

The State encourages the application of advanced scientific and technological achievements to improve capacities of disaster forecast, prediction, warning, and communication; to improve research capacities to observe the Earth's variability and natural changes in the region and territory; encourages the application of advanced technology and new materials for disaster prevention, response and mitigation.

Systematically, scientific sectors have been developed related to disaster: emergencies, disaster management, sustainable development, health care, post-disaster environmental and production recovery.

For natural disaster prevention, response and mitigation responsibilities and solutions for mountainous areas and central highlands, the approach of Government Strategy applied for the areas is to "proactively prevent natural disasters", for which the following solutions are focused to:

- Define and map areas highly prone to flash floods, landslides, geological hazards; make residential planning, evacuate population in dangerous areas, make land use planning, restructure crops, manage mineral exploitation to prevent harmful impacts on the environment and landslide risks, properly plant and exploit forests;
- Establish warning and communication systems down to commune and village levels; build structures to prevent landslides and flash floods; expand flood discharge openings of sluices and bridges on traffic roads to ensure flood drain ability; build reservoir system for both flood and drought control; and
- Strengthen the cooperation with bordering countries in forecasting, warning, search and rescue.

Vietnam-Japan SATREPS Project `Development of landslide risk assessment technology along transport arteries in Vietnam` and its impact to the Vietnamese society

Under the efforts to forecast and mitigate the impacts of landslides, an ODA project has been suggested. The name of project is "Development of landslide risk assessment technology along transport arteries in Vietnam". Short-term objectives is the landslide risk assessment technology to reduce disasters caused by landslides on transport arteries is developed by joint research based on experimental technology from Japan and human resources development to effectively use the technology in implementation in Vietnam. Long-term objectives is Socialization of development of landslide risk assessment technology and early warning system to ensure transport arteries and mountainous resident areas in Vietnam. The Investigation Sites for project scope is presented in Fig 3

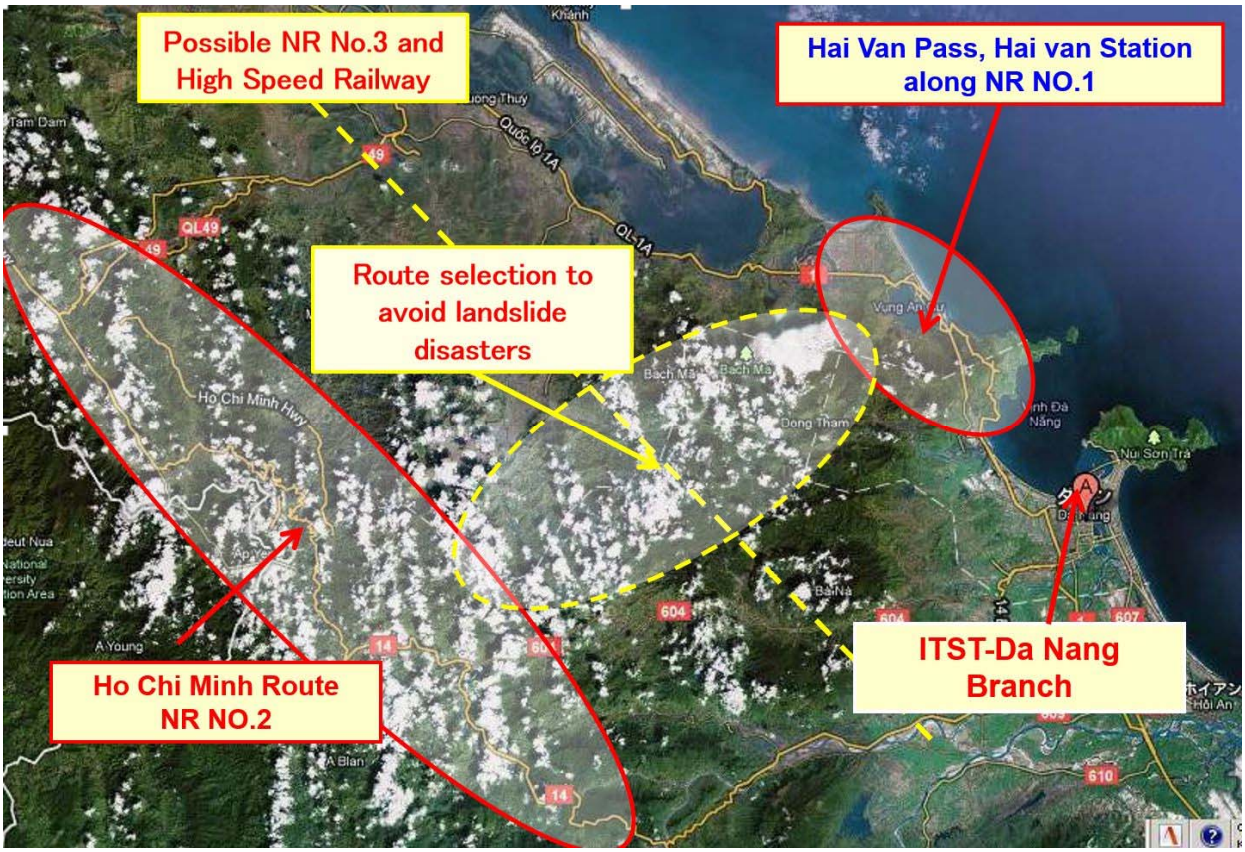

Fig 3.The Investigation Sites for project scope.

The contend of project include (1) Development of Landslide Risk Assessment Technology and Education; (2) Wide-area Landslide Mapping and Landslide Risk Identification; (3) Soil Testing – Computer Simulation of Landslide Initiation and Motion and (4) Landslide Monitoring and Development of Early Warning System.

From research results of the project we consider their impact to the Vietnamese society as following:

To Development of Landslide Risk Assessment Technology and Education

Based on the technological transfer from Japan to Vietnam, Vietnamese researchers have drafted a intergrade guidelines for landslide risk assessment in the following 6 parts with 33 guidelines (GL), which cover on (1)Mapping and Site Prediction,(2)Material Tests,(3)

Mapping group has investigated slopes along Ho Chie Minh Route (HCM) between Khan Duc to Prau and the Haivan pass land mass area. During the investigation landslide position, type of movement, micro features, causative factors were recorded as basic data. National No.7 highway was the additional target for application of landslide inventory by air-photo interpretation

Fig 4. Picture of group discussion during project time.

landslide investigation data and discussion, a landslide type classification in consideration of fuzzy nature and geological mechanisms of landslide generation in center of Vietnam were studied and published. Picture of group discussion during project time is presented in Fig4. Research results of Landslide distribution and Geology Zone A, B, C and Landslide classification and geology characters in study area are presented in fig 5

Monitoring,(4)Landslide flume experiment and (5) Software application. Those guidelines will be first step for strategy of national standard development for landslide risk assessment in Vietnam. (Sassa, Project report 2016). When they will be the national standard, they will nationwide contribute for national strategy for natural disaster prevention, response and mitigation.

As to Education and human resources development, 3 doctors and 5 masters which were educated in Japan. They will contribute for development science human resources of ITST particular as well as of Vietnamese landslide association in transport sector (VLAT).

To Wide-area Landslide Mapping and Landslide Risk Identification.

After 5 years the group has established six sheets of landslide inventory map and risk assessment map for HCM and 60 km long detail scale landslide distribution map (scale 1:12000); A landslide inventory map for Haivan area for designation of landslide monitoring site; a landslide susceptibility for road corridors a long HCM route (Dakrong to Khamduc section, scale 1: 250.000). More Further, a LS inventory map for around 10 km along National No.7 highway (Muong Xen to Tam Quang section) was established as Vietnamese application with advices from Japanese experts. The combination of the landslide risk assessment map and the landslide susceptibility map will be made an effective tool for prevention and mitigation of Landslide.

Technology of Identification of the precursor stage of landslides by the pattern analysis of digital surface model (DSM) of forest cover and others was developed from the project. The technical analysis from tree crown deformation by the comparative study of UAV and aerial photo data for landslide survey was developed at mangrove forest in Iriomote island, Okinawa then applied for Halong landslide trial site (The application to the identify the initial stage landslide deformation is trying to the Aratozawa landslide, Kurikoma, Japan (Myiagi, project report,2016). This achievement will be first step for development of new technology for not only landslide identification but also for topo survey. And it will be hopeful application in transport sector for developing infrastructures in survey and design. Pictures of landslide Site survey and UAV application in Vietnam and Japan is presented in fig 6

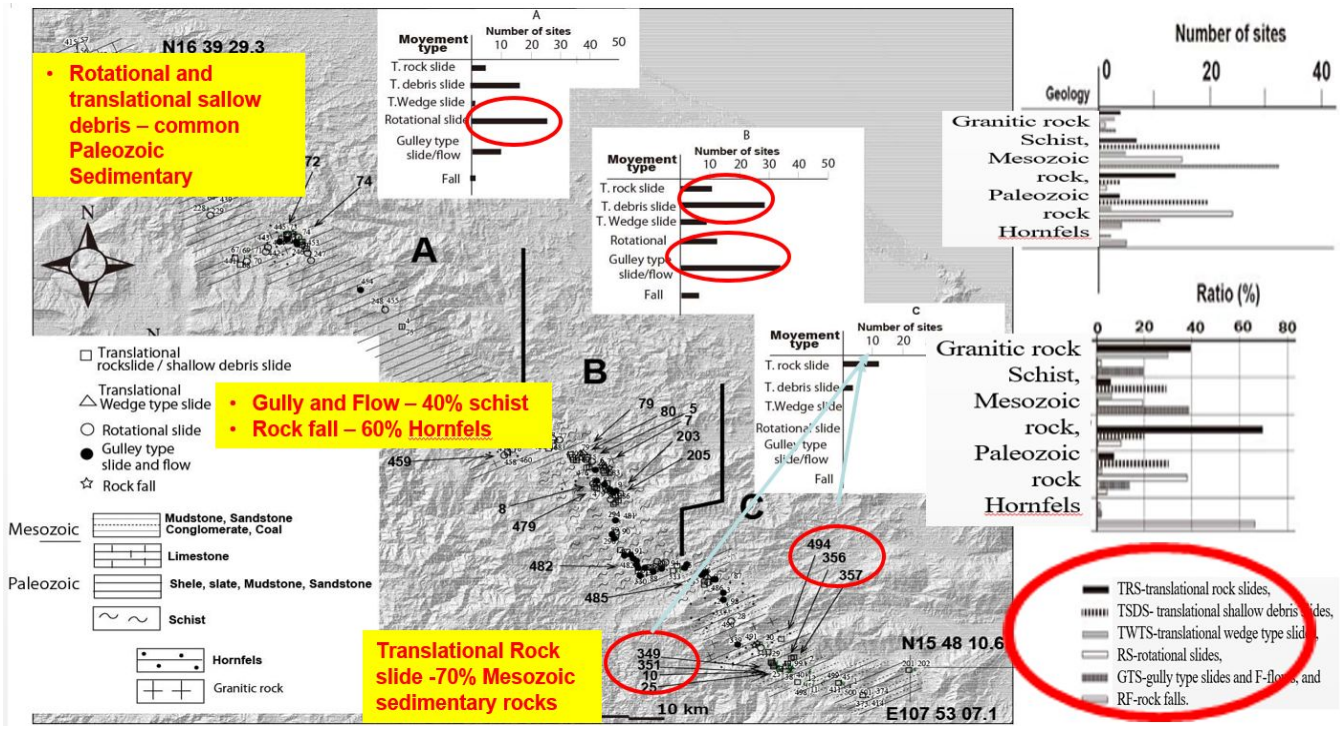

Fig 5. Research results of Landslide distribution and Geology Zone A, B, C and Landslide classification and geology characters

Fig 6. Pictures of landslide Site survey and UAV application in Vietnam and Japan

The main research results were published on special issue of transaction, Japanese geomorphological union (a journal recognized by the international Association of Geomorphologists, Volume 37 number1 January 2016

Soil Testing – Computer Simulation of Landslide Initiation and Motion

Testing group developed a high-stress undrained dynamic loading ring shear apparatus (ICL-2) which can be applied to deep landslides more than 100m. Pictures of a high-stress undrained dynamic loading ring shear apparatus (ICL-2) in Lab. ITST, Vietnam is presented in fig 7.The development and its first application to the Unzen Mayuyama Landslide killed 15,000 people in Japan was reported in Landslides (Impact factor 3.049) Vol.11, No.5 in 2014. The methodology and testing from this apparatus is useful for understanding the landslide moving mechanism, especially to depth seat one. For Vietnamese research and scientist field, it is also considered the newest one. The developed ring shear apparatus was revised in 2014-2015 based on the experiences of testing by Vietnamese short-term trainees as well as long-term trainees. Major revision was to add new two safety systems to protect the apparatus from miss-handling by testing persons. The revised apparatus was installed in ITST in June 2015 and now it is available for testing. (Lam.H.Q, project report 2016).

Fig 7. Pictures of a high-stress undrained dynamic loading ring shear apparatus (ICL-2) in Lab. ITST, Vietnam

Samples were taken from the ground and the drilled cores at various depths in the Hai van Landslide were tested using ICL-2 and computer simulation was conducted based on the measured parameters by Vietnamese researchers. Output of WG3 "Development of landslide risk assessment technology based on soil testing and computer simulation" was completed. Undrained stress control test result on Haivan-2 with time series data is presented in fig 8.

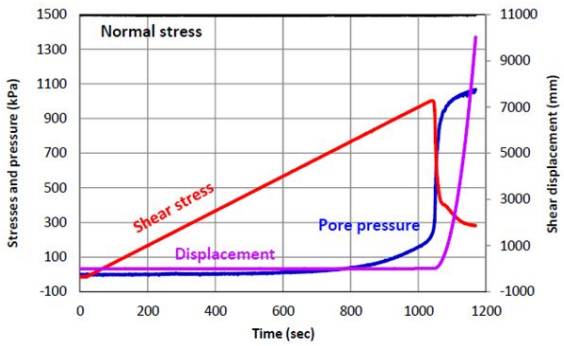

Fig 8. Undrained stress control test result on Haivan-2 with time series data

Adding the function simulating tsunami generated by landslides as one of target of JST research was completed to integrate the tsunami simulation code developed by the Intergovernmental Oceanographic Commission (IOC) and the landslide simulation code (LS-RAPID). This function was applied to assess tsunami level possibly triggered by a large-scale rapid landslide from the Hai van slope. However, Haivan case is just the first experiment for risk forecast and evaluation. Multi stages of movement of landslide simulation extracting from LS-RAPID for Haivan landslide is presented in fig 9. The application of ICL-2 apparatus and LS-RAPID will be very powerful tool for buildup landslide hazard map. And it will directly contribute for Vietnamese's Government strategy of Developing science and technologies related to natural disaster prevention, response and mitigation

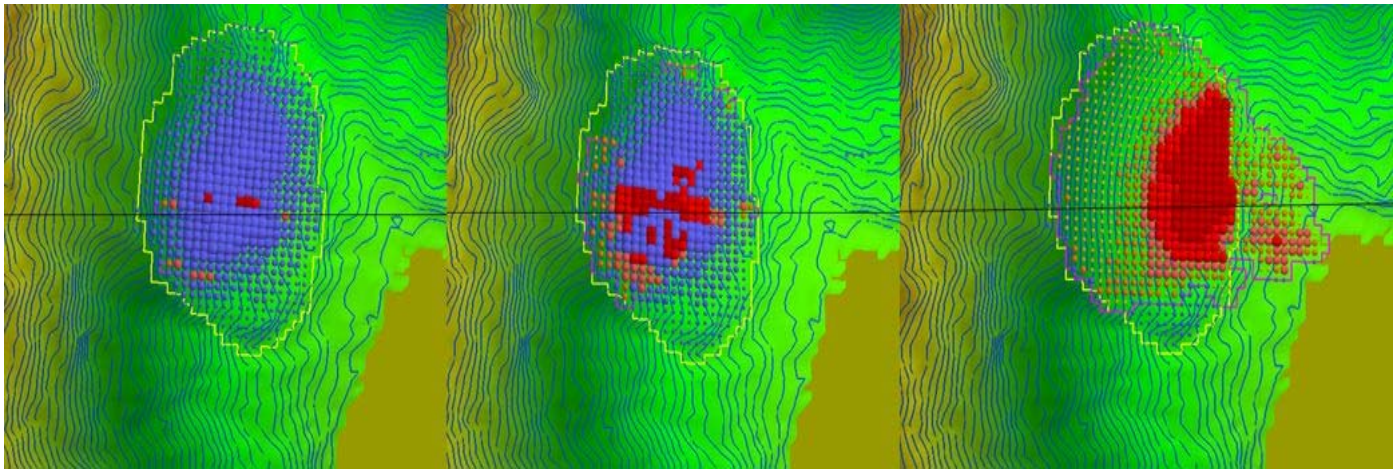

Fig 9. Multi stages of movement of landslide simulation extracting from LS-RAPID for Haivan landslide

- **Landslide Monitoring and Development of Early Warning System.**

Haivan landslide is one of the deep sheet landslide, where is national railway run over on its landslide body. It was selected as target area for monitoring and early warning. Haivan air photo and landslide inventory map for Haivan area presented in fig 10.The installation equipment for monitoring, topographic and geology survey had been done. Three boreholes were drilled by special techniques. The uniform cores was taken for testing and understand historical process of morphology and geology, from which landslide mechanism and classification could be explained. Figure4 presents the 80m depth bored hold log at Haivan Landslide.

An integrated monitoring system including rain gauges, extensometers, inclinometers, total station, and GNSS was developed here. Almost monitoring equipment installed in Hai Van Station landslide until March 2015. Monitoring the displacement result of Haivan slope by short extensometer in Haivan landslide area is presented in fig 11.

However rainfall and slope deformation monitoring was started in May 2013 and number of slope deformation records during heavy rainfalls have been monitored from September 2013 to now. An Installation of the data transferring and displaying system was finished in Haivan and the project office in ITST, Hanoi in March 2016. This monitoring system could be able to allow monitoring real-time. The Haivan landslide monitoring site is the modernist and biggest monitoring site in Vietnam up to now and it should be maintained not only for its functions but also remained as site training for Vietnamese researchers as well as community.

The landslide experimental facilities including landslide flume and data logging system and pore water pressure sensors were provided and adjusted for ITST. Outside and inside picture of landslide experimental facilities including landslide flume and monitoring equipment at ITST, Vietnam is presented in fig 12.The first landslide experiment using river sand was conducted in November 2015.

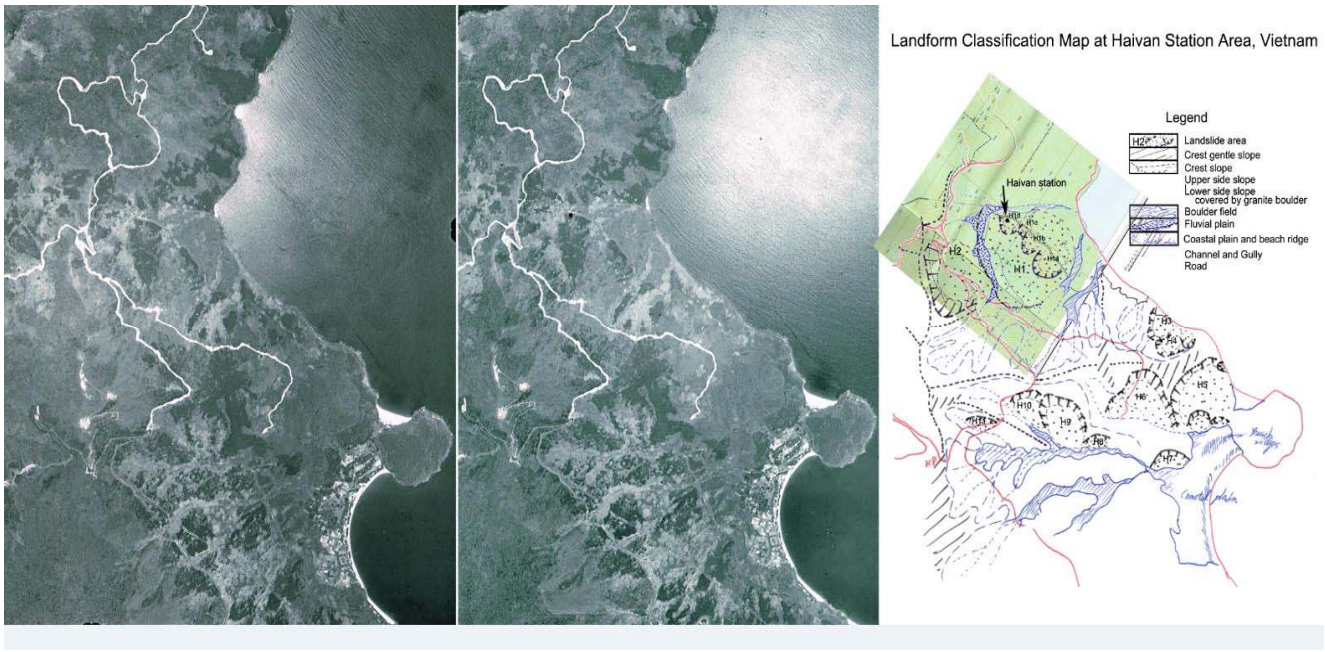

Fig 10. Air photo and landslide inventory map for Haivan area

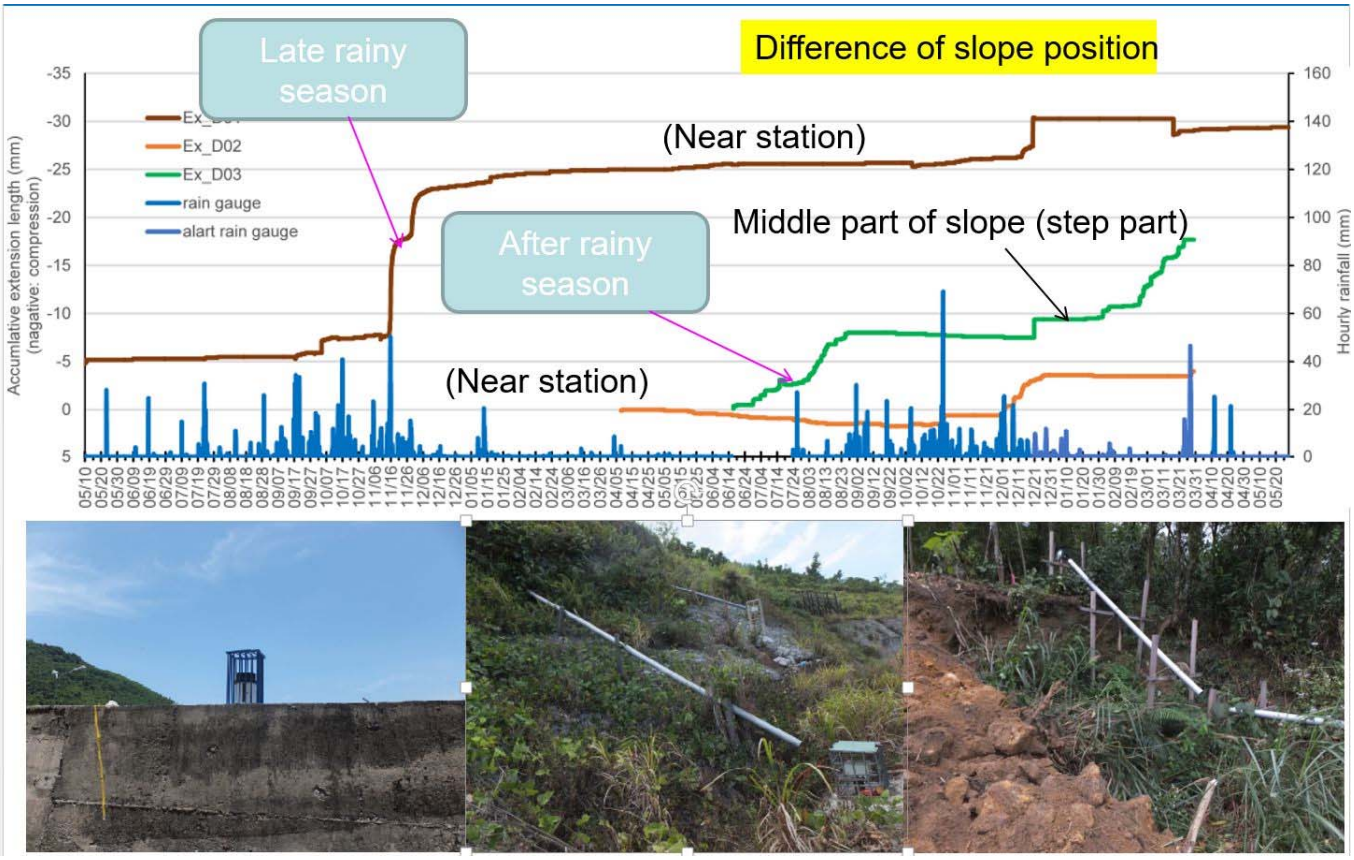

Fig 11. Monitoring the displacement of Haivan slope by short extensometer in Haivan landslide area

Fig 12. Outside and inside pictures of landslide experimental facilities including landslide flume and monitoring equipment at ITST, Vietnam

Re-production of a landslide test using the granitic soils taken from the Hai van slope was succeed. And new multi-depth wireless tensor meters has developed in Japan and utilized in landslide experiment in ITST.

Conclusions

The achievement of The Technical assistance Project "Development of Landslide Risk Assessment Technology along Transport Arteries of Vietnam" is evaluated as successful. It contributes directly for natural disaster prevention, response and mitigation of Government Strategy under effort to "proactively prevent natural disasters" and has deep impact to Vietnamese society.

As to scientific side, Landslides is a complex and unpredictable issue. The unpredictable factors increase in all the steps of the landslides settlement process, from the landslide area operation description, the quantity of physical and mechanical properties of soil and rock to the analysis, offer the effective treatment and evaluation solutions. The current trend in landslides research is to make rigorous and systematic process to officialise the implementation related to landslide treatment technique and management. So, landslides risk assessment technology now becomes an important tool in reducing the unpredictable factors.

Landslide risk assessment also gets concern of scientists and professionals in Vietnam. The joint research between Japanese and Vietnamese scientists for the first time on the issue of landslides through the technical assistance project "Development of Landslide Risk Assessment Technology along Transport Arteries in Viet Nam" will be one more step in the landslides research field in Vietnam. This is also a good opportunity for Vietnamese scientists to access to advanced technologies from Japan and enhance technical human resources to protect infrastructure systems.

On socio-economic side, the landslide risk assessment technology, including zoning of areas at landslide risk, monitoring of sliding block movement and simulation of the landslide formation and development, is a key platform in the landslide risk assessment and management system. This technology is the basis for the system to predict the risk level, decide whether or not and make the reasonable control measures to minimize for the unacceptable risk level. The evaluation which supplied by the system will help the management to have full awareness on landslide risks of and make appropriate decisions, including budget distribution planning for landslide treatment before the disaster actually occurred, thus it contribute to reducing the loss of human, economic and other negative impacts on society caused by landslides.

Besides the above scientific and socio-economic significant, the development of landslide risk assessment technology, including early warning system also have great humanity meaning for communities in large landslides risk areas. Early warning system will help people know about the risk and protect themselves before the risk occurs.

References

Kyoji Sassa (1), Hirotaka Ochiai (2), Toyohiko Miyagi (3), Tien D. V. (4) Nguyen Xuan Khang (5), Development of Landslide Risk Assessement Technology along Transport Arteries in Vietnam – 2015- Abstracts of the 54thannual meeting of the Japan landslide Society-(2.3);

Kyoji Sassa :Toyohiko Miyagi, Hirotaka Ochiai - Project report for final evaluation, 2016

Sassa , Project Technical report for final evaluation 2016.

Tien D. V. (1) Toyohiko Miyagi (2), Shinro Abe (3), Eisaku Hamasaki (4), Hiroyuki YOSHIMATSU (5) - Landslide susceptibility mapping along the HCMR in central Vietnam - an application of an AHP approach to humid tropical area - Transactions, Japanese Geomorphological Union, vol.37-1; January, 2016;

Tien D. V. (1). Vulnerability of landslide hazard in tropical region – dissertation, 2016

Tien D. V.(1), Toyohiko Miyagi(2),Eisaku Hamasaki (3), Shinro Abe(4), Nguyen Xuan Khang (5)- Landslide prevention and mitigation for road in humid tropical region - The 4th volume of World Landslide Forum 3 (WLF3) -2-6 June 2014, Beijing;

Proceedings of the SATREPS Workshop on Landslides in Vietnam, 2016

Origin of Landslide Geography in Hai Van Area, Vietnam

Shinro Abe[(1)], Dinh Van Tien[(2)], Do Ngoc Ha[(2)], Takashi Hoshide [(3)], Tadashi Nishitani[(3),] Toyohiko Miyagi[(4)]

1) Okuyama Boring Co., Ltd, Yokote, Japan, abeshinro@gmai.com
2) Institute of Transportation Science and Technology, Ministry of Transportation, Hanoi, Vietnam
3) Akita University , Centre for Disaster Studies, Akita, Japan
4) Tohoku Gakuin University, Faculty of Liberal Arts, Sendai, Japan

Abstract The area surrounding the Hai Van pass in central Vietnam, over which granitic rocks are distributed, has sustained numerous landslides during the heavy rains that occur there every year. Most of these landslides have occurred as small-scale flow type landslides or slump type landslides as general landslides occurring in a granite zone. However, the horseshoe-shaped landslide topography of width and length of about 1 km or more enclosing these landslides is observed at multiple sites on the surrounding slopes. To elucidate the generation mechanism of frequent landslides in the Hai Van area and to support their future risk assessment, it is necessary to ascertain the origin and the evolution process of large-scale landslide topography and to ascertain their relation with landslides observed at present. This study specifically examines deep weathering of granitic rocks, heavy rains in tropical monsoon regions, the generation history of large-scale landslides, and rock mass crushing resulting from local differences in constituent minerals and geological structure, with denudation such as differential weathering and corrosion, as factors of landslide occurrence or landslide topography formation. Landslide topography analysis by field investigation and aerial photography analysis, observation of lithology and movement history with drilling core, analysis of constituent minerals in the surrounding area, direction analysis of propagating cracks and faults developed into granitic rocks, and investigation of past landslide movements using magnetic direction analysis of remanent magnetism were conducted. Results reveal that the large-scale landslide topography has not been formed by a past single landslide, but by cracks on base rocks, a granite dome formed because of crushing of the base rocks and denudation by weathering and corrosion accompanied by the crack propagation, and by frequent landslides occurring on the surrounding slope of the dome.

Keywords Hai Van pass, granitic rock, landslide topography

Introduction

An area surrounding the Hai Van pass located 10 km to the north of Da Nang, Vietnam (Fig. 1) has suffered from frequent slump or flow type shallow slides having width and length of tens of meters on slopes over which granitic rocks are distributed. A landslide that occurred at the rear of Hai Van Station during a heavy rain in November, 2007 destroyed some tracks and station facilities, causing temporary suspension of railroad transportation. This section is a main route of transportation through northern and southern Vietnam. Therefore, this landslide damage strongly affected traffic and the economy throughout Vietnam. Cracks are growing on neighboring slopes even today, to the degree that future landslide occurrence can be reasonably expected.

Regarding the landslide of granitic rocks, although there was a case in which a moving body of 5,500,000 m3 slid down a slope for 1.5 km (Brian, 2008), most cases are shallow flow-type landslides of slopes of granite weathered to sands triggered by a heavy rain, as observed in Hiroshima, Japan, which killed 76 people in 2014 (Wang et al., 2015). Nevertheless, horseshoe-shaped landslide topography is observed, with width and length of about 1 km or more at multiple sites on slopes around the Hai Van pass. This topography, which has no clear microtopography such as a main scarp, a side face, or a toe (Cruden and Varnes 1996), resembles the landslide topography formed by a large-scale landslide from a considerably ancient period. Numerous frequent small-scale landslides at heavy rains in recent years have occurred inside such large-scale horseshoe-shaped landslide topography.

To elucidate the generation mechanism of frequent landslides in the Hai Van area and their risk assessment in the future, it is necessary to ascertain the origin and evolution processes of large-scale landslide topography and to comprehend the relation with landslides observed at present. Accordingly, we particularly examine the history of occurrence of large-scale landslides occurring at the rear of Hai Van Station in this study, and conduct landslide topography analysis by field investigations and

aerial photographic analyses conducted over the Hai Van pass, with analysis of constituent minerals in the surrounding area, direction analysis of propagating cracks and faults developed into granitic rocks, investigation of past landslide movements by magnetic direction analysis of residual magnetism, and observation of the lithology and movement history of the slopes at the rear of Hai Van Station with a drilling core. We have strived to elucidate the factors of landslide topography formation and landslide occurrence from comprehensive discussion of these results.

This article defines large-scale landslide topography formed on a slope by an ancient landslide showing width and length of 500 m to 1 km or more as "large-scale landslide topography" for convenience irrespective of the origin, and refers to the whole large-scale landslide topography on the rear of Hai Van Station as the "Hai Van landslide."

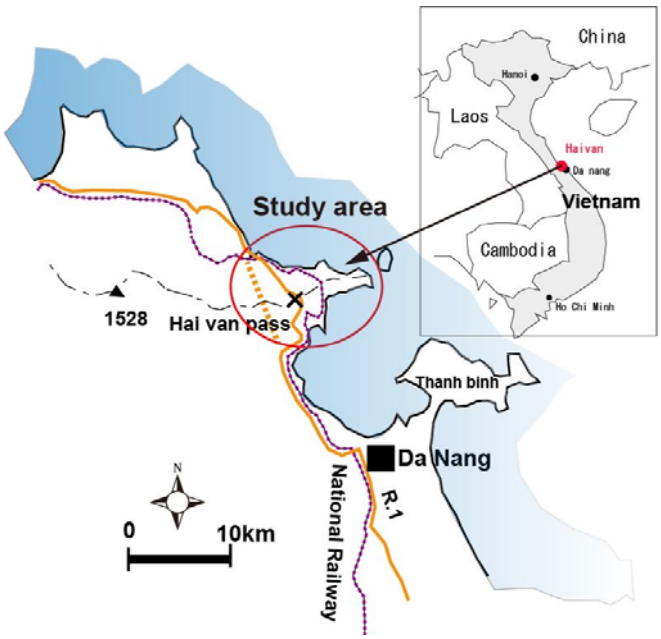

Figure 1 Study area.

Outline of study area

Landslide Topography and Recent Landslide History

The Hai Van pass and its periphery, constituting an area that divides the culture and climate of northern and southern Vietnam, is an important point of traffic over which the National Route 1A (QL1A) and the National North–South Railway pass (Fig. 1). The National Railroad crosses coastal slopes keeping an altitude of 100 m and passes through Hai Van Station on the way.

The landslide topography is recognized at many sites on the mountainous slopes around the Hai Van pass (Fig. 2), most of which are recognized as small-scale landslides having dimensions of 100 m or less, but large-scale landslide topography of a width or length of 500 m to 1000 m or more is recognized at some sites. The Hai Van landslide is a scale of a width and length of about 1 km enveloping the Hai Van Station, and forms horseshoe-shaped landslide topography open to the sea (Figs. 2 and 3). Neither the main scarp of the landslide head nor the outline of side faces is as blurred as typically observed in ancient landslide topography, but it might appear as though a small mound on the head has slid down the steep slope on the rear as a moving block. There occurred a landslide inside the Hai Van landslide topography in the rear slope of the station near the landslide toe in the event of a heavy rain in November, 2007, with another landslide of detailed occurrence time unknown at the site of forest road construction on the head slope of the Hai Van landslide (Fig. 4). Both were slump type landslides having width and length of about 20–30 m.

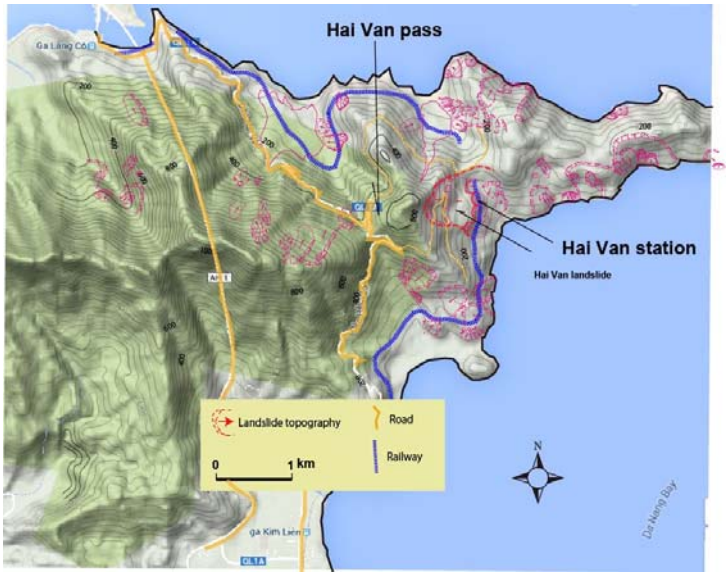

Fig. 2 Landslide topography over Hai Van pass and Hai Van landslide, extracted from aerial photography.

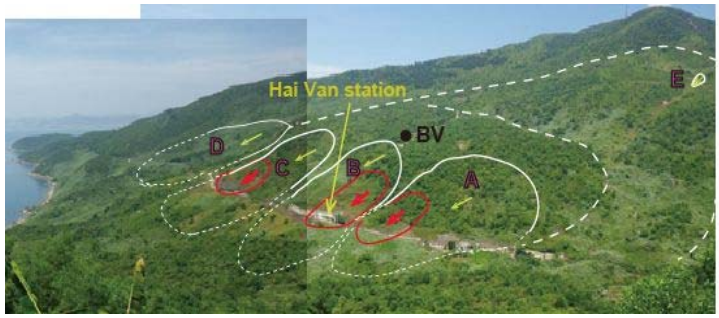

Fig. 3 Hai Van landslide: white line denotes landslide units determined by aerial photography, and red lines indicate the positions of landslide occurrence during the 2007 heavy rain.

Fig. 4 Recent landslides taking place within the Hai Van landslide: 1–2, Landslide at heavy rain in November, 2007 (Units A, C of Fig. 3). ;3, Landslide at forest road construction site, year unknown (Unit E of Fig. 3).

Climate

This area falls under the tropical monsoon region, where a year is divided into two seasons: a rainy season extending from August through December and a dry season extending from January through July. The annual mean temperature is 25.9 °C, the annual mean rainfall is about 2,500 mm, the monthly average rainfall in October–November of the peak period is about 500–1,000 mm/month, and the monthly average rainfall in March–April of the dry season is 23–40 mm/month. Roads and the railroad around the Hai Van pass have sustained serious damage from landslide activity during heavy rains. The movement of landslides is mostly falling of corestones attributable to the weathering of granitic rocks and a little flowable slump type landslides. Details of the relation between a rainfall and a landslide are unknown because the correct date of landslide occurrence is ambiguous and rainfall observed at the coast differs considerably from that of the mountainous land. However, a tendency for the rapidly enhanced landslide disaster around the Hai Van pass is recognized when the amount of daily rainfall at the coast reaches 500 mm/day in general (Fig. 5) (Tho et al., 2015).

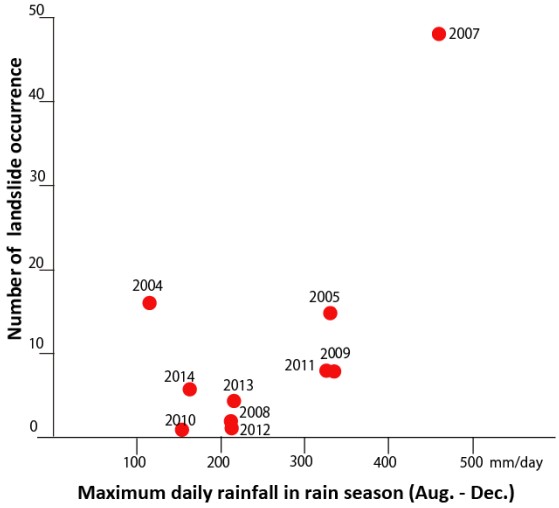

Fig. 5 Maximum daily rainfall near Hai Van pass (August–November) and annual landslide occurrence~~; suffixes denote~~

Geology

The geology of the ground around the study area is the Mesozoic Hai Van Migmatite Complex (Nakano, 2013), which is a mixture of granite comprising biotite, feldspar, muscovite, and quartz as major minerals and gneiss as a metamorphic rock (hereinafter "granitic rocks"). There are scattered corestones (Durgin 1977), rounded gravels containing those with 10 m or greater diameter formed by weathering of granitic rocks on the slopes.

Analysis results

Investigation of geology and landslide histry with drilling core

Boring surveys were conducted to collect drilling core samples to a depth of 80 m at almost the center of the Hai Van landslide (Fig. 3). The digging procedure was the rotary sampling drilling method using a sleeve incorporating a core barrel, diamond bit, and polymer mud (Abe et al., 2016). The apparatus has attracted attention for use at landslide research locations in Japan in recent years for collection of high-quality cores. The geology shows gravelly sand of granitic rock origin to 51 m depth, which then changes to fresh and hard granitic rocks underneath (Fig. 6). The drilling method described above enabled us to collect gravelly sand, which is regarded as the most difficult to core by boring surveys, in a mostly undisturbed state to 51 m depth. We conducted observations with specific attention to whether the origin of the gravelly sand clastics to 51 m depth was re-segmentation caused by past large-scale landslides, or deep weathering at the original position peculiar to granitic rocks (Ollier, 1969). Geological features usually observed in the drilling core of a landslide moving block include mixing of trees, humus soil, and accidental clasts involved in with landslide movement, blocks crushed and fractured into sand because of disturbance in the event of movement, a banded or fluidal sedimentary structure accompanying secondary sedimentation, and a slip-plane structure. Clastics to 51 m depth comprised gravelly sand that can be fractured easily by finger pressure of 1–50 kgf/cm^2, as indicated by needle penetration tests. The components were loosely accumulated particularly down to the depth of 12 m, whereas the structure was continuous beneath 12-m depth, comprising gravelly sand maintaining rock composition of granitic rocks, with color tone attributable to weathering also changing continuously and gradationally. Neither contamination of humus soil, wood pieces, accidental clasts, rounded gravels, etc., nor existence of a sedimentary structure, slip planes, and slip-plane clay was observed.

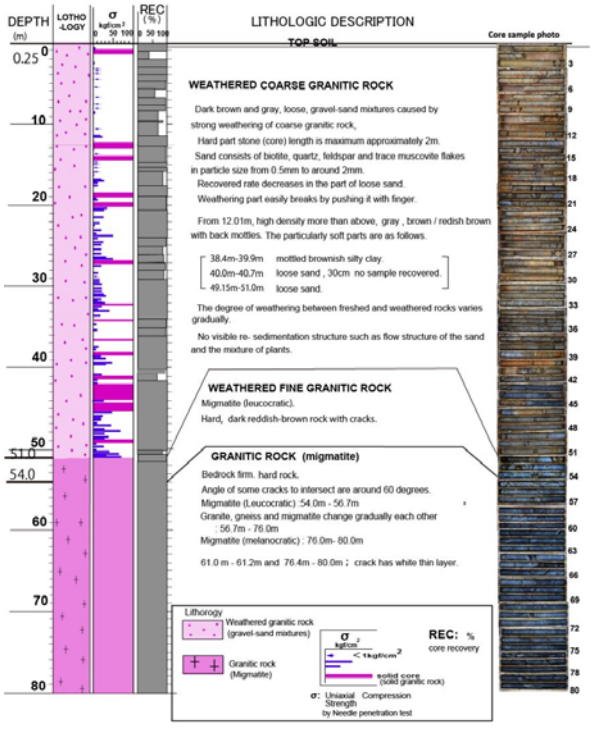

Fig. 6 Geologic column in Hai Van landslide.

Remanent magnetism analysis

Specimens

Magnetic minerals contained in a rock acquire remanent magnetism corresponding to the terrestrial magnetism prevailing during the period of rock synthesis. Consequently, past ground movement can be investigated using the intensity and direction of remanent magnetism as indices.

Studies of remanent magnetism have strongly affected the field of earth science from geomagnetic reversal and polar wandering from the early 1960s to the elucidation of plate tectonics (Holmes, 1978; Konno, 2009). Recent studies of diverse disciplines include examinations of the global environment (Sakai et al., 2000), studies of age determination in archaeology (Hirooka et al., 1988), lava flow accompanying volcanic activity (Urrutia-Fucugauchi et al., 2004), and studies of mud-flow on hills because of debris avalanche (Mimura et al., 1982, 2003; Sakai et al., 2003). Remanent magnetism measurements were conducted for this study in specimens obtained from corestones scattered on the ground surface in the Hai Van landslide and drilling cores, and specimens from exposed base rocks outside the Hai Van landslide (Fig. 7). Then the experiences of past landslide movements were examined from the variation in magnetic direction. Rock fragments were collected using a rock hammer and a base rock twist drill to prepare specimens from the corestone and eight exposed base rocks outside the landslide (Fig. 8). The selected target corestones were too gigantic to have been moved by human power. Specimens obtained from drilling cores were six specimens from cylindrical cores taken from strongly weathered granitic rocks and four specimens from fresh base rocks (Fig. 9(d)). A core of a diameter of about 3 cm was gouged out of a rock fragment fixed with concrete using a water-cooled engine twist drill with a diamond-bit (Natsuhara Giken Ltd.). Then the gouged piece was shaped to a height of 1.5–2.5 cm for magnetic measurements using a rock cutter (Fig. 9).

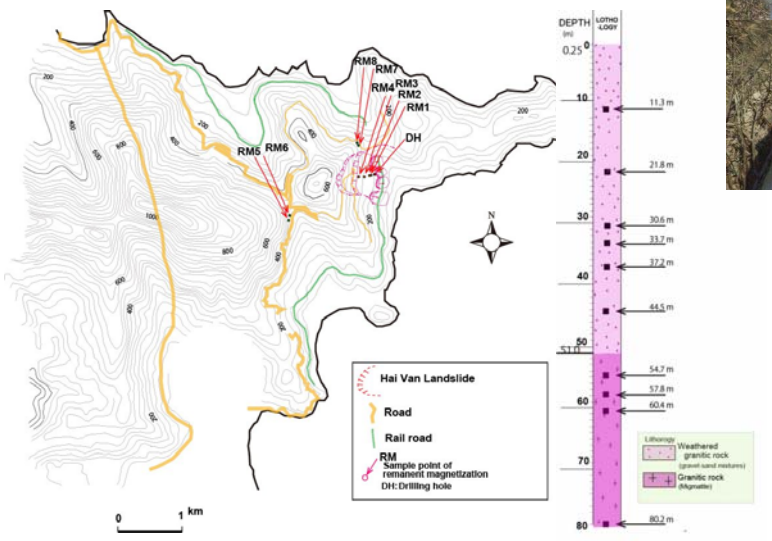

Fig.7 Sampling position of remanent magnetism measurement specimen . Left, sampling point at exposures; Right, depth of sampling from the drilling core.

Fig. 8 Sampling of remanent magnetism measurement specimens from exposures

Fig. 9 Sampling and shaping of remanent magnetism measurement specimens: a, b, c, specimen gouging from exposed rock fragments; d, e, drilling core samples and specimen gouging; and f, g: shaping and completed specimens.

Remanent Magnetism Measurement

A spinner magnetometer (SMM-85; Natsuhara Giken Ltd.) was used for residual magnetism measurements. Residual magnetism intensity *M*, horizontal component *H*, magnetic dip *I*, the downward angle from the horizontal plane, and magnetic declination *D*, which is an angle clockwise from the true north direction, were computed from magnetization components converted into the coordinate system (*x*, *y*, *z*) at the actual site. Figure 10 depicts the definition of each parameter.

The magnetic declination and dip at the sampling position were -1.08° and 20.78°, respectively. Specimens were collected according to the magnetic north standard. Then -1.08° was added to the obtained declination to convert the measured declination into the value according to the true north standard. Declination cannot be defined for a drilling specimen because of rotation at drilling. Therefore, only the magnetic dip was adopted for measurements, assuming the direction of an arrow indicating the bottom of a specimen as north.

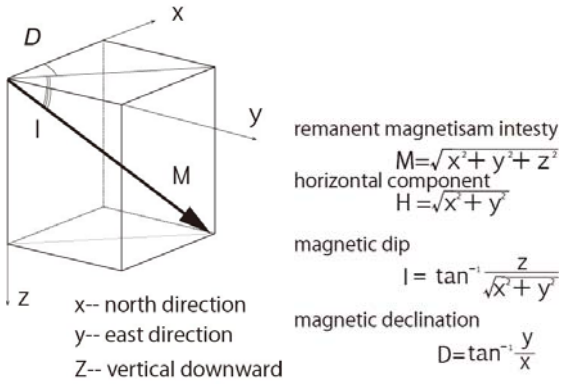

Fig. 10 Definitions of remanent magnetism intensity, magnetic dip, and magnetic declination.

Change of remanent magnetism intensity and magnetization direction by progressive AC demagnetization

Progressive AC demagnetization was carried out for each specimen to erase secondarily acquired magnetized components, in contrast to natural remanent magnetism (NRM), a value in the state with no processing. It is difficult to reproduce the direction of geomagnetism when remanent magnetism was acquired only by NRM measurement because NRM includes magnetized components acquired secondarily in many cases. AC demagnetization is an operation by which a specimen is rotated at random under no magnetic field. Then the specimen is imposed by the AC magnetic field, and the magnetic field decreases gradually to zero. This operation erases the coercive force component up to the magnetic field provided. An AC demagnetization system (DEM-93C; Natsuhara Giken Ltd.) was used for this study. The magnetic field at AC demagnetization was varied to 19 stages of 0.2, 0.4, 0.7, 1.0, 1.3, 1.6, 2.0, 2.5, 3.0, 3.5, 4.0, 4.5, 5.0, 5.5, 6.0, 7.0, 8.0, 9.0, and 10.0 mT following NRM measurement (0 mT), and remanent magnetism was measured at each demagnetization stage in principle. However, in cases where a primary magnetization component had been erased and the intensity, magnetic declination or magnetic dip of remanent magnetism varied in an unusual manner, the following demagnetization steps were skipped. Figures 11 and 12 respectively portray the intensity variation of remanent magnetism to AC magnetic field of exposed ground surface specimens and drilling core specimens.

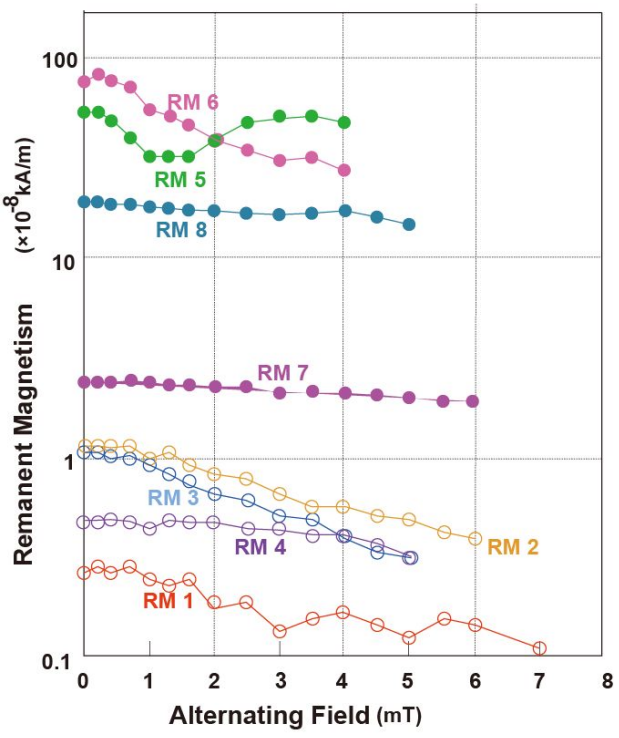

Fig. 11 Remanent magnetism intensity variation in an AC magnetic field: RM1-RM4: Exposed corestone; RM5-RM8: Exposed base rock.

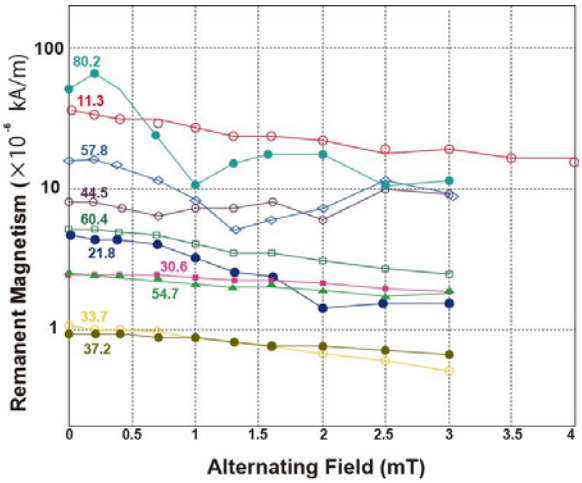

Fig. 12 Remanent magnetism intensity variation in AC magnetic field: drilling core specimen.

As for the intensity variation of remanent magnetism of the exposed ground surface specimens, the remanent magnetism intensity of specimens collected from base rocks outside the Hai Van landslide (RM 5–8) was generally high, although that of highly weathered corestone specimens (RM 1–4) was low. Almost all specimens indicated a decline of remanent magnetism intensity at enhanced magnetic field intensity of AC demagnetization. The observed tendency for a slight intensity increase at 0.2 mT and 0.4 mT is considered because secondary magnetization component impressed to the reverse direction was erased. It was generally observed that the remanent magnetism intensity dropped from 1.0 mT to 2.0 mT, and that it fluctuated up and down under a magnetic field at the demagnetization stage. Accordingly, the optimal magnetic field at a demagnetization stage was obtained between 1.0–2.0 mT for each specimen, and magnetic declination and magnetic dip after AC demagnetization were computed (Table 1). For drilling specimens, the vertical direction can be determined, but it is impossible to ascertain how much it was rotated during boring, so that the magnetic dip of remanent magnetism is measurable but the magnetic declination is not.

Accordingly, we discuss the magnetic dip only. Figure 12 suggests that the remanent magnetism intensity of drilling specimens indicates an almost constant slope generally at an AC magnetic field over 0.7–2.0 mT. Therefore, the optimal magnetic field at a demagnetization stage was determined in this range. The magnetic dip was computed after AC demagnetization (Table 1).

Table 1 Remanent magnetism and magnetism directions post-demagnetization.

Specimen condition	Sample No	Magnetic declination (°) Before demagnetization	Magnetic declination (°) After demagnetization	Optimal magnetic field for demagnetization (mT)	Magnetic dip (°) Before demagnetization	Magnetic dip (°) After demagnetization	Optimal magnetic field for demagnetization (mT)
Corestpne	RM1	−9.5	−16.99	2	31.56	32.55	2
	RM2	−3.93	−14.26	2	21.87	25.85	2
	RM3	135.47	135.29	1	24.29	25.46	1
	RM4	53.71	−30.64	2	73.92	81.46	2
Exposed base rock	RM	−48.27	95.2	1.6	38.69	54.3	1.6
	RM6	88.18	122.86	1.6	51.44	61.63	1.6
	RM7	82.26	78.27	1.6	62.61	63.57	1.6
	RM8	2.64	−5.04	1	−31.92	−30.42	1
Drilling core	11.3				41.59	46.3	1.3
	21.8				−31.9	−55.66	1.3
	30.6				−43.72	−51.04	1.3
	33.7				29.02	28.13	1.3
	37.2				−61.61	−58.4	1.3
	44.5				−57.89	−62.23	0.7
	54.7				−22.1	−33.81	1.3
	57.8				−36.92	−3.66	1.3
	60.4				−47.14	−55.28	1.3
	80.2				−25.22	−53.35	1

Crack analysis

Cracks propagating into granitic rocks are assumed to result from faults and joints because of the stress of a geological structure, crushing accompanying weathering, and removal of pressure of vertical load because of corrosion (Ollier, 1969). This section explains analyses of the prevailing direction of crack propagation in granitic rocks around the Hai Van pass, and elucidates some characteristics of the geological structure as its background. The direction of crack propagation was found using a clinometer at exposures around the Hai Van pass, with emphasis on continuous cracks of about 1 m or more. The result is shown in the Schmidt's net and Rose diagram (Fig. 13), which also classifies the degree of weathering of exposures by color, into strongly weathered gravelly sand, weakly weathered rocks in which the cracks are developing to produce corestones, and fresh and hard rocks with few cracks.

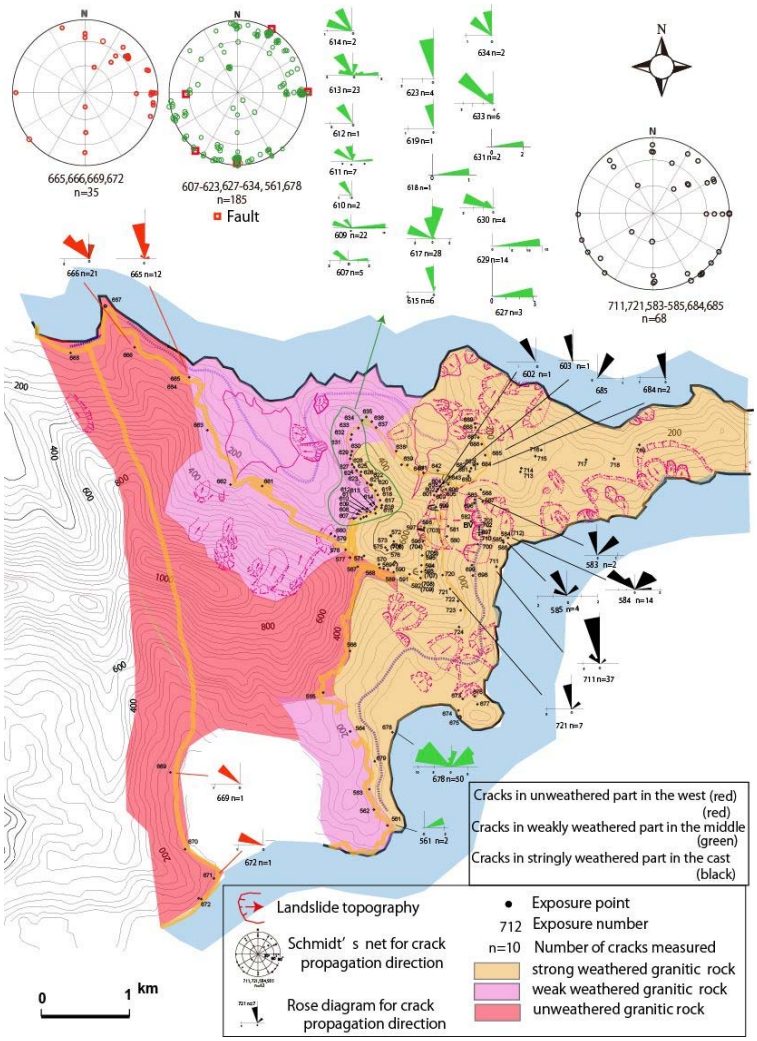

Fig. 13 Weathering and crack propagation of granitic rocks and landslide topography near Hai Van pass.

Discussion

This study was conducted to elucidate the origin and formation process of the Hai Van landslide topography and to elucidate the relation with the present landslide, in order for future elucidation and risk assessment of the generation mechanism of a landslide that occur frequently in the Hai Van area.

Remanent Magnetism Analysis Result and Landslide Activity History

The magnetic declination and magnetic dip (Table 1) along the direction of remanent magnetism after AC demagnetization of specimens obtained from corestones in the Hai Van landslide and exposures outside the landslide (Fig. 7) were projected on Schmidt's net in Fig. 14. RM 5, 6, and 7 representing base rock exposure apparently having experienced no movement show almost the same direction of magnetic declination and magnetic dip. RM8 had been considered as a stable base rock when sampled, but it is likely to have been an unstable slope or a great bounding stone. The fact that the magnetic declination of every specimen obtained from the corestones scattered on the ground surface at the Hai Van landslide differs from the direction indicated by RM5–RM7 suggests the possibility of past movement. However, all the normal magnetic dips are considered not to reflect large-scale past landslide movements accompanying rotary motion of a slope, but local movement or displacement of a corestone itself under advanced weathering.

Figure 15 shows the magnetic dip direction after AC demagnetization of drilling core specimens excavated from the Hai Van landslide. The magnetic dip of remanent magnetism of drilling core specimens shows partial variation, but is about -50° along the reverse direction in general. However, that at depths of 11.3 m and 33.7 m of strongly weathered had partially turned to the normal direction. The assumption that the weathered granitic rocks to 51 m depth had moved from a rear slope by a past large-scale landslide anticipates a greater variation of magnetic dip by the disturbance of moving blocks. However, no such tendency was found. Today some opening cracks can be observed around the drilling point, which are considered to represent whether an unstable state attributable to a shallow slide at about 30 m depth or the result of local displacement accompanying deep weathering. Variation in the magnetic dip of corestones on the ground surface or drilling cores represents the actual past movement, but besides, it includes errors because of weak remanent magnetism intensity because the target granitic rocks contain less magnetic minerals than basalt and andesite, and attributable to deteriorated magnetic intensity by advanced weathering. However, the direction of remanent magnetism of the drilling core specimens and corestones in this study presents little variation, which supports occurrence of a past large-scale landslides during which the whole weathered layer moved.

Unsolved questions include some anomalies. First many drilling core specimens exhibit reverse direction of remanent magnetism in the underground part, different from that in the ground surface part, in contrast to most specimens of corestones in the landslide and exposed base rocks outside the landslide that indicate the same normal direction as the present magnetic dip. The age of granitic rock formation in this area is assumed as 239 Ma–219 Ma (Mesozoic Triassic period) by the age determination at 10 sites by Nakano et al. (2013). Therefore, most of this study area is supposed to have been formed in almost the same period. Geomagnetism had repeatedly reversed in this age at an interval of the order of 1 Ma (Muttoni et al., 2010). Therefore, the inconsistency in remanent magnetism might be attributed to a difference in a cooling period according to the depth or the effect of multiple pegmatite of a width of about 10–20 m penetrating north and south in the Hai Van landslide, but the details remain unknown at present.

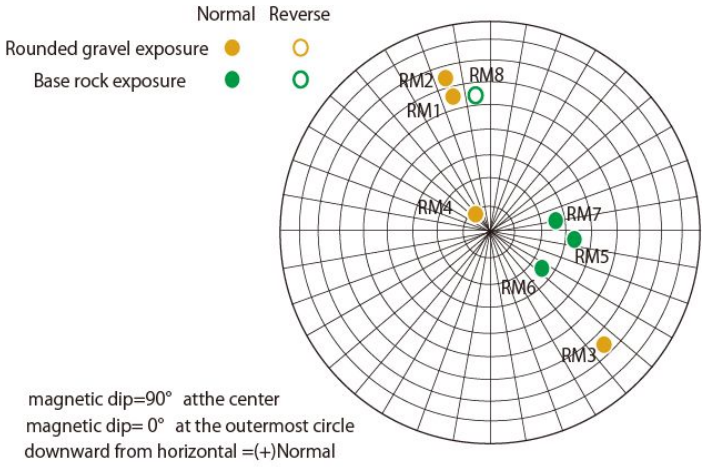

Fig. 14 Remanent magnetism in exposed specimens after demagnetization.

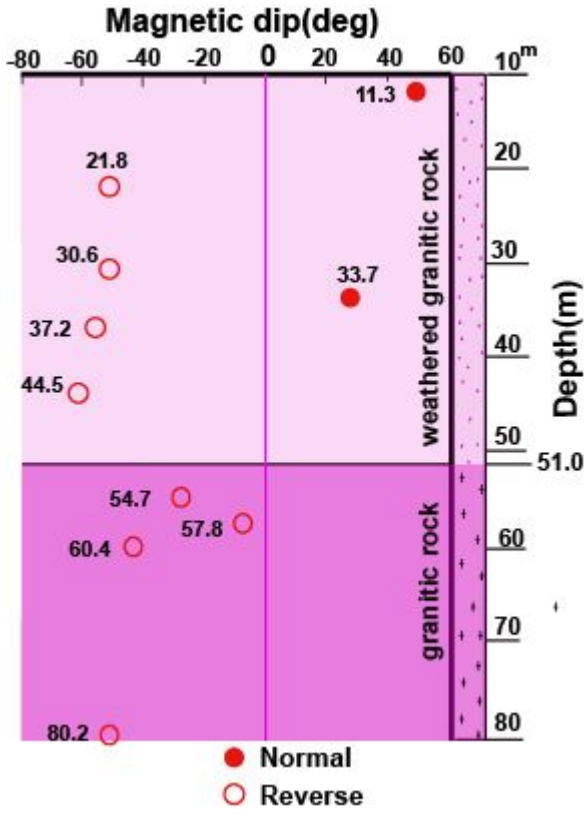

Fig. 15 Remanent magnetism and magnetic dip of drilling cores; suffixes denote depth.

Cracks and weathering of base rocks and landslide topography

As described above, the granitic rocks over the Hai Van pass exhibit transition from fresh and hard base rocks of the mountains to the west of the pass to the weakly weathered belt in the east where corestones are produced, then the strongly weathered gravelly sand belt from the Hai Van landslide to the coast. As for the direction of crack propagation in the base rocks, northwest direction is prevalent in fresh granitic rocks to the west, then east–west, northwest and north–south directions catch up near the coast of the east side with advanced weathering, where the crack density also tends to be higher. The crack gradient is generally as high as about 70–90°. Some minor faults are observed running northwest or north–south around the Hai Van pass (Fig. 13). Figure 16 presents the topographic slope distribution map of this area created from the ALOS satellite image superimposed by the crack analysis result of granitic rocks, indicating clear linear structures L1, L2, and L3 along the direction of northwest–southeast. Linear structure L2 located near the multiple minor faults described above might be a fault itself. This structure running northwest is in agreement with the direction of the red river fault zone in northern Vietnam (Tran, 1995; JOGMEC, 2000) and the tectonic line that cuts granite and gneiss along the Ho Chi Minh Route in central Vietnam (Tien et. al, 2016), which shows agreement with the direction of the structure line from central to the whole northern Vietnam. Furthermore, L1 forms a gentle arc open to west, and although ambiguous, it produces concentric circles with L2 and L3.

There are often observed an onion-shaped spheroidal structure over this area, which is formed by concentric exfoliation of rock lumps between cracks propagated into a granitic rock by being weathered and denuded at the edge (Fig. 17). The fresh part left behind to the center of weathering becomes a corestone to be scattered on the ground surface. Moreover, many fresh exposed granitic rocks around the Hai Van pass form a gentle dome or a round hill (Fig. 17). That is, dome topography is formed at a fresh part with few cracks, whereas a corestone or a mound is formed at a strongly weathered part with many cracks. Such topography is interpreted to be peculiar to a granite belt formed by differential weathering and exfoliation regulated by cracks (Linton, 1955; Ollier, 1969). Weathering over the Hai Van pass is regulated by the concentric linear structure and is advancing gradually toward the coast. This result suggests that this area is involved in a vast onion-shaped spheroidal structure bordered by a linear structure containing a fault. Landslide topography is mostly observed to be distributed over the strongly weathered belt with crack development along with L2 and L3. Especially, the Hai Van landslide has occurred on weathered slopes close to the coast with developed cracks in northwest, east–west, and north–south directions. The convex part of a landslide head is interpreted as a mound formed by such an onion-like spheroidal weathering structure.

Therefore, we infer that the topography around the Hai Van pass was not formed by occurrence of a single large-scale landslide in the past, but by the complex action of a granite dome and multiple mounds that were formed by denudation because of cracks propagating into a granitic rock and accompanying differential weathering and corrosion, and a landslide that occurred on the slopes (Fig. 17).

The possible causes of landslides taking place frequently within such large-scale landslide topography include that ground surface rain water flows down a fresh

base rock slope forming the core of a granitic rock, permeates into a weathered belt in which cracks developed at the middle of the slope fractured rocks into sand, and increases ground water rapidly (Fig. 17). As discussed above, it is necessary to recognize the large-scale landslide topography distributed around Hai Van in the future as an area with high risk of frequent landslides. These findings are expected to serve as an effective index for the landslide risk assessment not only of the Hai Van pass and its periphery, but also of other granite zones in the future.

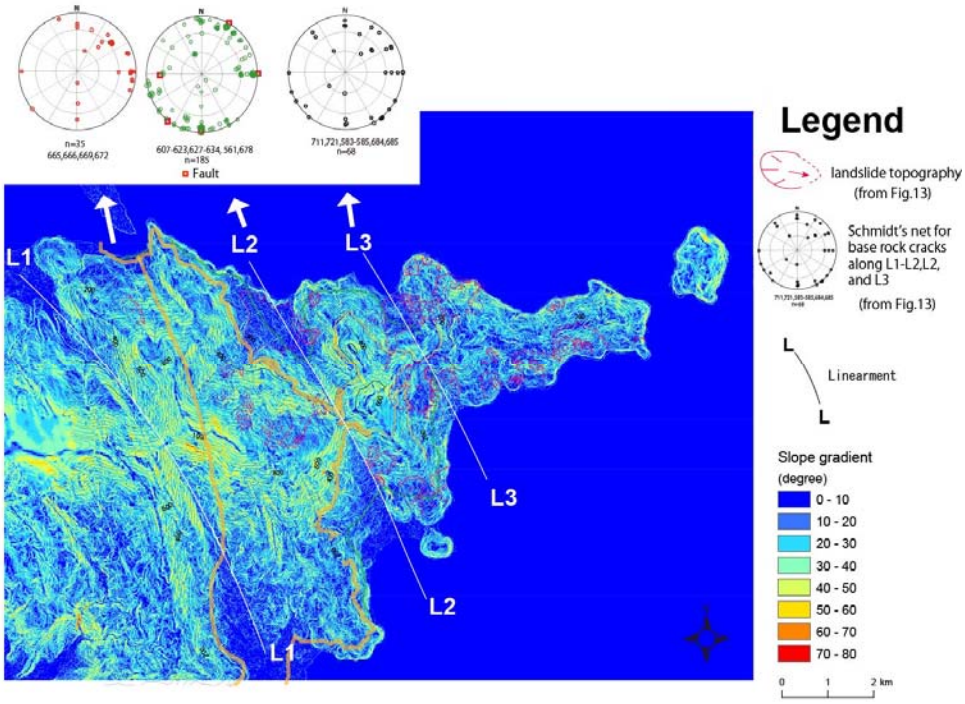

Fig. 16 Slope distribution, cracks, and lineaments: slope gradient map of the Hai Van pass based on ALOS W3D data.

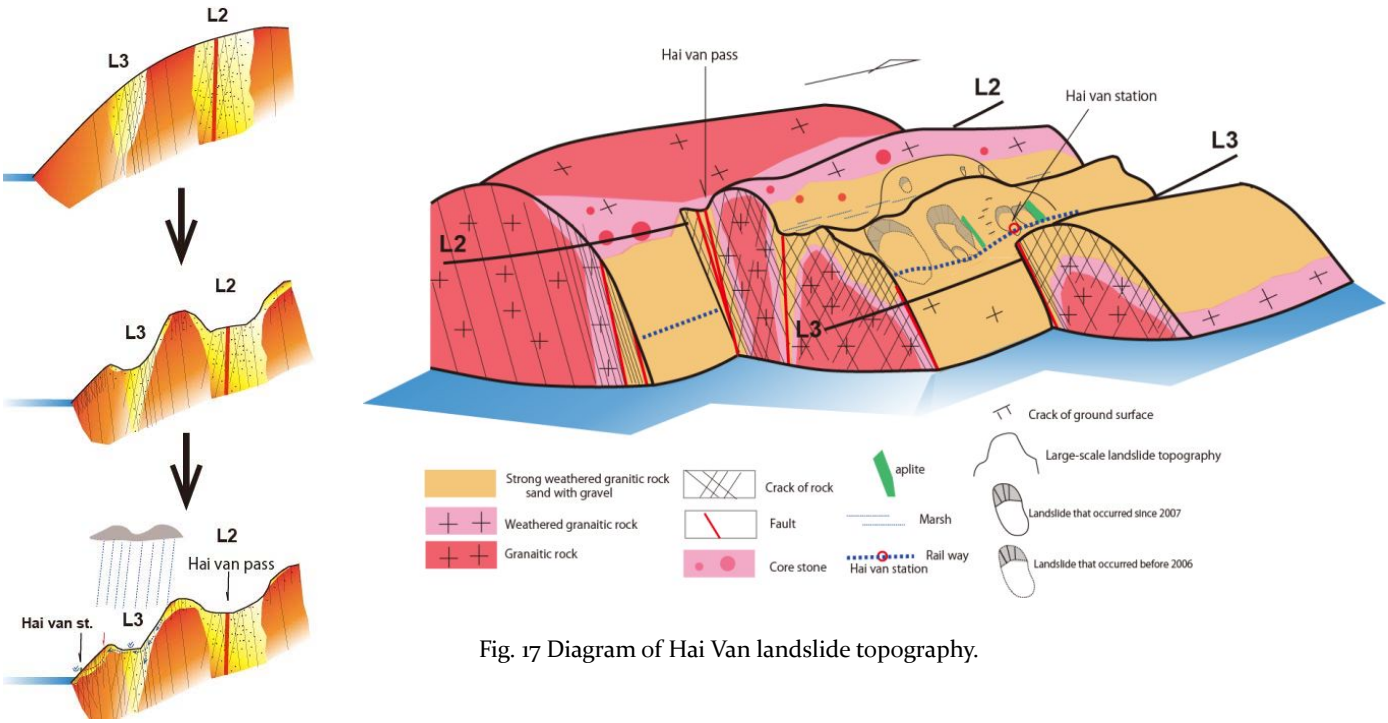

Fig. 17 Diagram of Hai Van landslide topography.

Conclusion

This study was conducted to elucidate the origin and the formation process of the Hai Van landslide topography in a granitic rock zone and to ascertain their relation with the present landslide. The study results have revealed the following findings.

The large-scale landslide topography of the Hai Van landslide was not formed by a large-scale landslide in the past, but by a landslide that occurred on the gentle slope of a granite dome and mounds formed by denudation accompanied by weathering according to crack propagation direction and crack density because drilling cores show no trace of secondary sedimentary structure or a slip-plane structure. No variation in the direction of remanent magnetism was found to the extent that any disturbance accompanying a large-scale movement of the ground is indicated.

However, the large-scale landslide topography of this area should be recognized as a region in which landslides occur frequently because of the advance of weathering or crack propagation. Moreover, in cases where a mound remaining as a less weathered base rock in large-scale landslide topography turns to have been weathered to the depths as observed by the drilling result of the Hai Van landslide, the possibility of large-scale movement of such a mound in the future should be examined carefully.

References

Abe S, Sato N, Tien DV, Ha DN, An LN, Khoat LX (2006) Rotary Sampling Drilling Technology to Extract High-Quality Cores Using a Sleeve-Incorporating Core Barrel and Polymer Mud Based on Drilling in Landslide Areas of Japan and Vietnam, Landslide Dynamics: ISDR-ICL Landslide Interactive Teaching Tools.

Arther H (1978) Holmes Principles of Physical Geology by Auther Homes 3 rd edition, Thomas Nelson and Sons Ltd., 730p.

Brian FG (2008) The Marucus landslide 'An ancient landslide in the McDowell Mountains, Arizona' The Arizona geological survey web : http://www.azgs.az.gov/MarcusLandslide_2008.shtml, 5 June,2016

Cuden DM, Varnes DJ (1996) Landslide types and processes, Landslide investigation and mitigation, Special reporet 247 (A Keith Turner and Robert L Schuster eds.), TRB, National Academy Press, Washinton D, C. pp.36-75.

Durgine PB (1977) Landslides and the weathering of granitic rocks, Geological Society of America Reviews in Engineering Geology, Volume III, pp.127-131.

Fucugauchi J.U, Valdivia L.M.A, Goguitchaichvili,A, Rivas M.L and Morales J. (2004) Palaeomagnetic, rock-magnetic and microscopy studies of historic lava flows from the Paricutin volcano, Mexico: implications for the deflection of palaeomagnetic directions, Geophysical Journal International, 156 (3), pp.431-442.

Hirooka K (1988): Paleo magnetic archeomagnetic age dating, The Memoirs of the Geological Society of Japan (29), pp.306-318.

JOGMEG (Environmental research on resources development, Japan Oil, Gas and Metals National Corporation (2000) : The Socialist Republic of Vietnam. 52p.

Konno M (2009) Geomagnetism in Perspective, Treatise on Geophysics, Geomagnetism, Vol.5, ELSEIER, pp.1-31.

Linton DL (1955) The Problem of tors, The Geographical Journal, 121(4), pp.470-487.

Mimura K, Kawachi S, Fuzimoto U, Taneichi M, Hyuga T, Ichikawa S, Koizumi M (1982) Debris avalanche hills and their natural remanent magnetization, Nirasaki Devris avalanche, central Japan, Jurnal of the Geological Society of Japan(88), 8, pp.653-663.

Muttoni G, Kent DV, Jadoul F, Olsen EO, Rigo M, Galli MT, Nicora A (2010) Rhaetian magneto-biostratigraphy from the Southern Alps (Italy): Constraints on Triassic chronology, Palaeogeography, Palaeoclimatology, Palaeocology, 285, 1-16.

Nakano N, Osanai Y, Owada M, Nam TN, Charusiri P, Khamphavong K (2013) Tectonic evolution of high-grade metamorphic terranes in central Vietnam: Constraints from large-scale monazite geochronology, Journal of Asian Earth Sciences 73, pp520-539.

Ollier CD (1969) Weathering, Geomorphology texts 2, Oliver & Boyd Edinburgh, 304p.

Sakai H, Nomura S, Horii M, Kashiwaya K, Tanaka A, Kawai T, Kravchinsky V, Peck j and King J (2000) Paleomagnetic and Rock-magnetic studies on Lake Baikal sediments -BDP96 borehole at Academician Ridge-, Lake Baikal, K. Minoura (editor), Elsevier Science B.V., pp.35-52.

Sakai H, Watanabe K, Inoguchi T (2003) Rockmagnetic Studies on Volcanic Deposits in Boring Cores from Mt.Bandai, Report of the Japan National Research Institute for Earth Science and Disaster Prevention, No.64, pp.19-31.

Tien DV, Abe S, Yoshimatsu H, Shibasaki T, Miyagi T (2016) Geological mechanisms of landslide generation along Ho Chi Minh route in central Vietnam, Journal of the Japan Landslide Society, Vol.52 (4), pp.25-35.

Tho PD, Ninh TD, Vu NMH, Nam TD, Ha DN, Abe S (2015) The occurrence mechanism of landslide in Haivan and Sontra mountainous area, Proceeding of Young Scientists research dynamically and contribute effectively to the qualified and effective development of Transportation Engineering in 2015,Wang F, Wu YH, Yang H, Tanida Y, Kamei A (2015) Preliminary investigation of the 20 August 2014 debris flows triggered by a severe rainstorm in Hiroshima City, Japan Geoenvironmental Disasters, December 2015, 2:17, Springer open Journal.

Tran NN (1995): The Geology of Vietnam, A brief summary and problems. Geosci. Repts. Shizuoka Univ., 22, pp.1-10.

Proceedings of the SATREPS Workshop on Landslides in Vietnam, 2016

Landslide Risk evaluation for large-scale landslides by AHP

Le Hong Luong[(1)], Toyohiko Miyagi[(2)], Eisaku Hamasaki[(3)]

1) Institute of Transport Science and Technology, 1253 Lang road, Dongda, Hanoi, 084, Vietnam, e-mail: lehongluong@gmail.com

2) Tohoku Gakuin University, Izumi Campus/2-1-1 Tenjinzawa, Izumi-ku, Sendai, 0081, Japan, e-mail: miyagi@izcc.tohoku-gakuin.ac.jp

3) Advantechnology Co., Ltd, Aoba, Sendai, 0081, Japan, e-mail: hamasaki@advantechnology.co.jp

Abstract In Vietnam a numerous landslide occurs as a re-active old landslide. Understanding possibility of landslide re-occurrence is very important to local people and manager, they can prepare time and necessary things in the case of emergency. This paper will briefly present Japan's inspection sheet for large-scale landslide risk evaluation base on AHP approach, application of the sheet in Vietnam and limitation of the sheet also discuss and initially propose new inspection sheet due to above limitations

Keywords Landslide risk evaluation, geomorphic factors, AHP, Vietnam

Landslide risk evaluation in Japan

According to Miyagi (Miyagi et al., 2004) risk evaluation is a probability of landslide re-occurrence within a given area; risk evaluation can be conducted by analysing landslide topographies because most landslide processes result from reactivity of aged landslide topographies. For purposes of systematic and objective risk evaluation, the Japan landslide society has developed an inspection sheet (Figure 1) incorporating geomorphic factors within and beyond landslides (Miyagi et al., 2004). In this sheet, geomorphic factors are classified into major, medium, and small categories. The first major category includes characteristics of types of movement, material, and critical features of action, micro-landforms of various types and their spatial arrangement indicate activities of landslides distributed mainly within the domain of the landslide body. The second major category involves aging factors, time processes, and clearness of the top edge of the main scarp and the sharpness between the main scarp and the landslide body. The third involves the potential energy of the slip body caused by the last action. It can change the instability of the landslide body, and increasing or decreasing their geomorphic setting such as the body face attached to the slope of a river. Focusing on these geomorphic settings, one can predict the prospective transition of stability. Each major category above was classified into medium classifications including nine categories: (A) type of movement; (B) level of clearness and micro-landform components within the landslide body; (C) level of instability of the landslide body; (D) direct features of movement; (E) between the top edge of the main scarp and the upper slope; (F) between the main scarp and the body; (G) between the landslide body and the frontal slope; (H) toe part of the landslide body; and (I) lower part of the landslide body. The items of the medium classifications are further divided into smaller categories, which will be checked and evaluated using aerial photograph interpretation.

To set up standard evaluating score for each criteria items; AHP approach was used. Every each criteria items were evaluated by paired comparison; standard score system was created for all criteria items. For convenience, all items were arranged to decrease the risk from the left to the right. The score of definitely landslide location is calculated intuitively based on features recognizing from aerial photograph and experiences of a geomorphologist.

Application of Japan's Inspection sheet in Vietnam

By using this sheet, we applied this approach in area between Prao and Kham Duc, central Vietnam for trial purposes with 261 landslide locations along Ho Chi Minh road were evaluated and developed six sheet of landslide risk map. Figure 2 is an example of this map. The colour will represent level of risk with four level: strongly assume "moving", potential of reactivation, relatively low potential and low potential of reactivation.

Limitation of Japan's inspection sheet when apply in Vietnam and initially propose new inspection sheet

As mentioned above, risk evaluation relating to aerial photograph interpretation. In Vietnam we face to challenging tasks with regard to source data, accessing aerial photograph is very difficult; sometimes it's impossible for scientific works. At the time of this study, only 1999s aerial photographs are available. And all the photographs are monochromatic and in scale of 1:33.000. There are many items in inspection sheet concerning micro feature that very difficult recognize on aerial photo.

Many reports and interpreters agree that the best scale for interpreting is smaller than 1/15.000. And in Japan they have lot of type of aerial photo and in many stage and time of taking. Limitations of data sources make difficulty to identify landslides and evaluate risk in Vietnam.

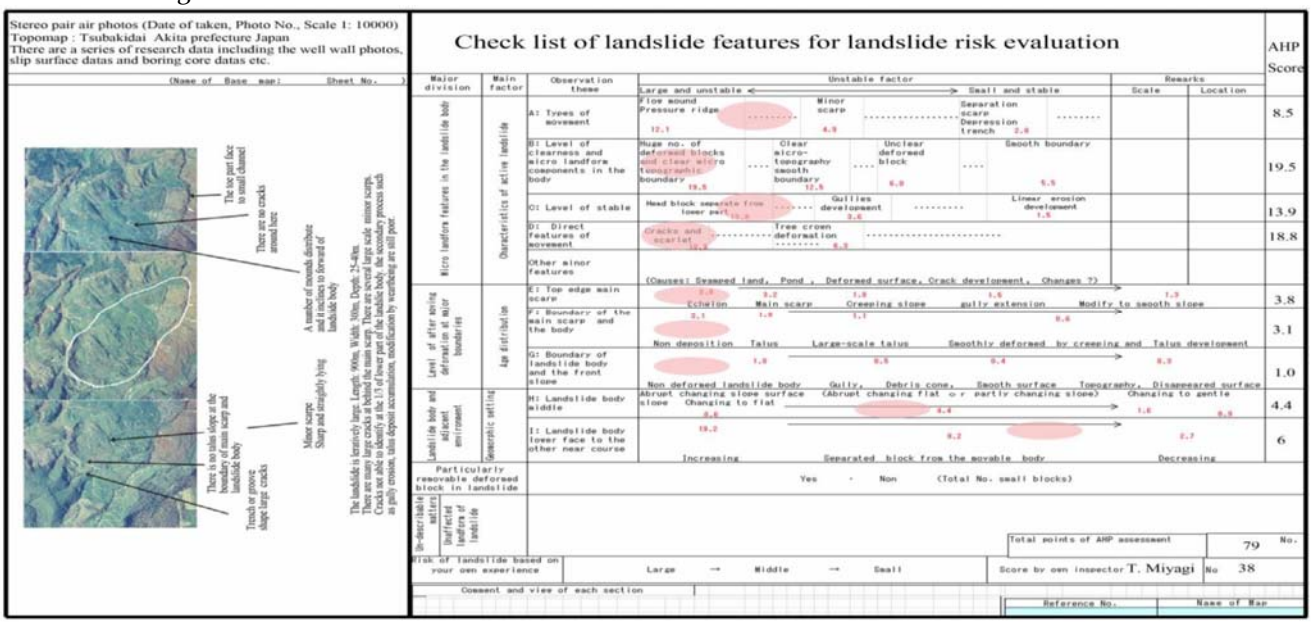

Figure 1 Example of Japan landslide society's inspection sheet (Miyagi, 2014)

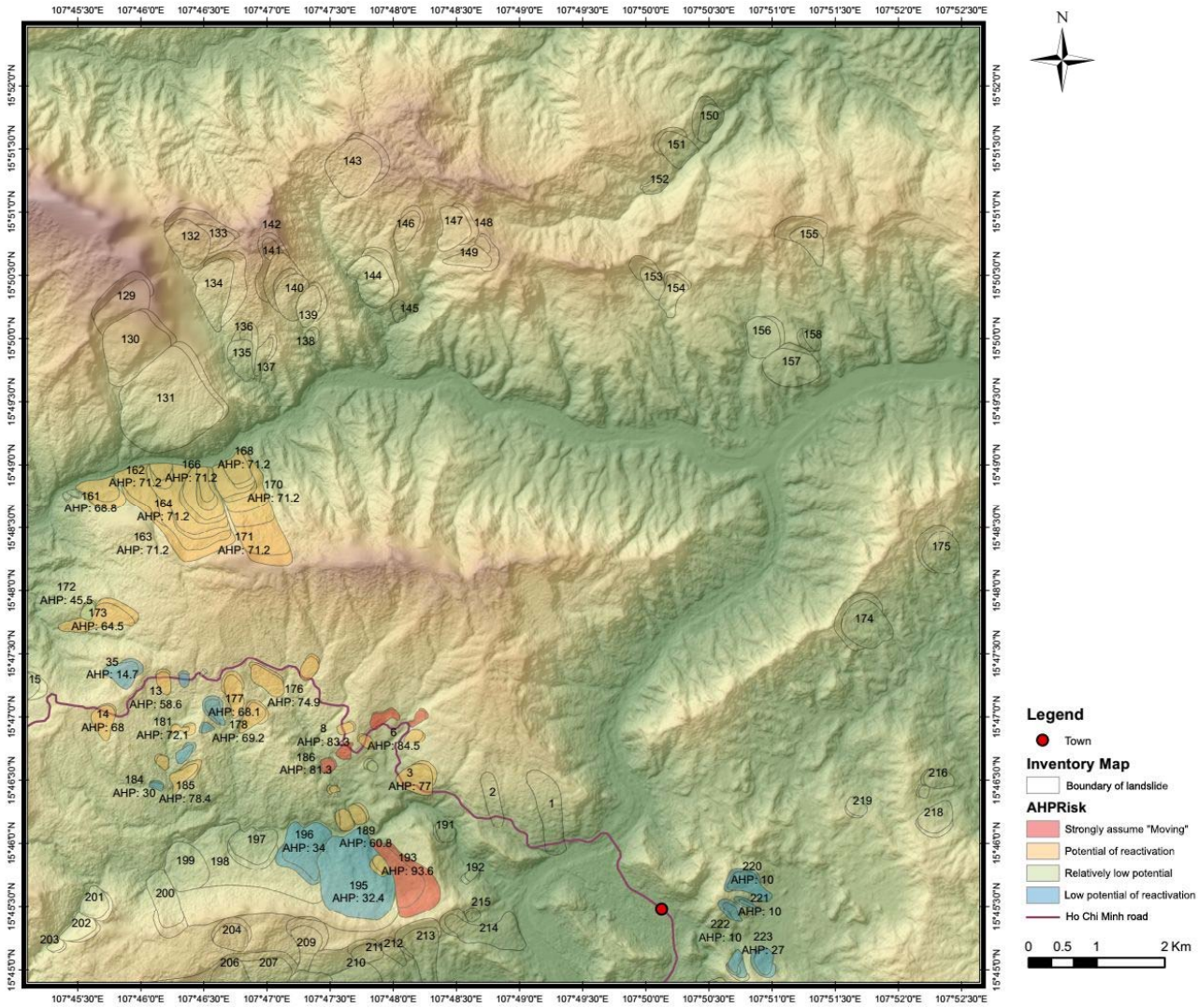

Figure 2 Example of landslide risk map at Thanh My area

Thus, the inspection sheet should be modified because of limitations of data sources. In 2014, in his report, Hamasaki proposes new inspection sheet for risk evaluation in Vietnam (Figure 3) (Hamasaki, 2014). In this sheet he divided geomorphic items into 3 large categories. The first is micro topographic features on surface of landslide mass; the second is deformation of marginal zone. And the final is locality of landslide. All above main categories were divided into six medium categories: (A): grade of fracturing of landslides mass; (B): clearness of surface ruptures; (C): grade of degradation of main scarp; (D): condition of toe part; (E): erodibility of toe part of landslide mass; (F): potentiality of instabilization at toe part of landslide mass. Each medium category was further divided into small items as mentioned in Figure 3. Compare with old inspection sheet, all geomorphic items in new inspection sheet quite are simple and it's easy for evaluating corresponding to limitation of source data. For example, in old inspection sheet there are two medium categories for evaluating: between the main scarp and the body and between the landslide body and the frontal slope; but new inspection sheet only mention as grade of degradation of main scarp with three small items depicting by well-illustrated image.

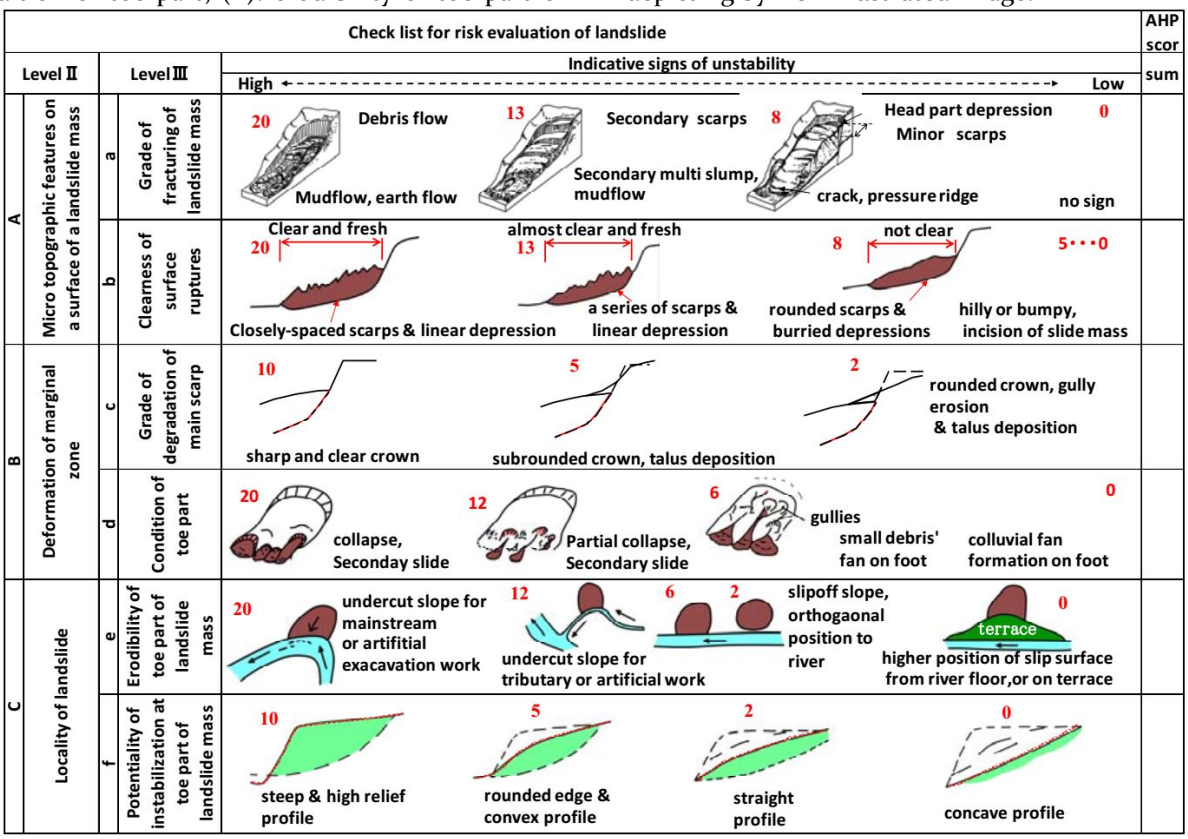

Figure 3 Example of New inspection sheet proposing by Hamasaki (Hamasaki, 2014)

Geology	Geology age	Geology age	Primary geologic unit (Rock type)	Mesozoic (Triassic to the Jurassic sedimentay rock: Conglomerate, Gritstone,	Quarternary (River soil	Precambrian (Schist and Granit gneiss)	Paleozoic (Schist, Quazt-sericite Schist, ...)	
				2.63	2.38	1.16	0.74	
	Bedrock Lithology and Structure	Bedrock Lithology and Structure	Attitude of beds	Beds of rock that parallel or dip in the same direction as the slope			Beds that dip into the slope	
				2.86			0.95	
			Presence and degree of fractures, joints, and foliation	Numerous (distance between fractures, joints, and foliation less than 20cm)	Few (distance between fractures, joints, and foliation ranging from 20cm to 50cm)		Few (distance between fractures, joints, and foliation greater than 50cm)	
				13.54	7.45		4.10	
			Tratigraphy (Sensitive key layer)	Numerous (distance between fractures, joints, and foliation less than 20cm)	Numerous (distance between fractures, joints, and foliation less		Numerous (distance between fractures, joints, and foliation less than 20cm)	
				3.43	3.34		0.98	
	Level of weathering	Level of weathering	Degree of weathering	Completely	Highly	Moderately weathered	Slightly weathered	
				10.87	5.08	2.05	1.17	

Figure 4 A part of new inspection sheet proposing by Luong mentioning geologic condition (Luong, 2016)

All above inspection sheets mention only geomorphic features. They do not mention geologic features. In Vietnam where has a richly varied geologic composition, creating a profile with various characteristics and thicknesses of rock and soil. In 2016, in his study, Luong concluded that geologic condition has

an important role in landslide occurrence in Vietnam, particularly in area between central provinces in Vietnam (Luong, 2016). So geologic condition must be mentioned in inspection sheet and he proposed new inspection sheet (Figure 4) in which both geomorphic features and geologic condition were used for risk evaluation and trial application for some landslide location along Ho Chi Minh road in Vietnam. Final evaluation show that both inspection sheet give out the same result; a little bit differences are apparent between the two results but are acceptable results.

All above inspection sheets are in initial stage and require more discussion. That is further works.

Concluding and remarks

Landslide risk evaluation is very important in landslide reduction in Vietnam. In scope of joint venture project funded by Jica, we applied Japan Inspection sheet and initially proposed new inspection sheet for risk evaluation in Vietnam. Of course it remains some limitations and requiring more discussion because it has been not discussed much.

Acknowledgments

This study is conducted under budget of JICA. First of all, I would like to thank to JICA for our support during this study. We also acknowledge and express our sincere thanks to Prof. Sassa, Ms Akemi Yoda, Mr. Masaru Iizuka and all other members of group 2 for supporting us and and assistances we received during this study.

References

Le Hong Luong, Miyagi Toyohiko, Pham Van Tien, (2016). Mapping of large scale landslide topographic area by aerial photograph interpretation and possibilities for application to risk assessment for the Ho Chi Minh route – Vietnam. Transactions, Japanese Geomorphological Union, pp. 97-118.

Miyagi Toyohiko, Gyawali B. Prasad, Charlchai Tanavud, Aniruth Potichan and Eisaku Hamasaki, (2004). Landslide Risk Evaluation and Mapping - Manual of Aerial Photo Interpretation for Landslide Topography and Risk Management. Report of the National Research Institute for Earth Science and Disaster Prevention. Pp. 75-137

Miyagi Toyohiko, Eisaku Hamasaki, Dinh Van Tien, Le Hong Luong, Ngo Doan Dung, (2014). Landslide mapping and the risk evaluation by aerial photo interpretation in Vietnam. Proceedings of the SATREPS Workshop on Landslides in Vietnam, 2014. Pp 87-95.

Eisaku Hamasaki, Toyohiko Miyagi, Dinh Van Tien, Ngo Doan Dung, (2014). Objective Function based AHP Risk Evaluation System in Humid Tropical Regions. Proceedings of the SATREPS Workshop on Landslides in Vietnam, 2014. Pp 123-127.

Proceedings of the SATREPS Workshop on Landslides in Vietnam, 2016

Simulation of landslide initiation and motion based on the measured parameters of soils taken from Unzen-Mayuyama landslide in Japan

Khang Dang[1,2], Kyoji Sassa[1]

1) International Consortium on Landslides, Kyoto, Japan, e-mail: sassa@iclhq.org

2) VNU University of Science, Hanoi, Vietnam, e-mail: khang@iclhq.org, khangdq@gmail.com

Abstract This paper presents simulation result of a historical 1792 Unzen-Mayuyama landslide in Japan based on the research published in Landslides journal "Development of a new high-stress undrained ring shear apparatus and its application to the 1972 Unzen-Mayuyama megaslide in Japan".

A new high-stress ring-shear apparatus named ICL-2 was developed in 2012–2013 to simulate the initiation and motion of megaslides of more than 100m in thickness. The successful undrained capacity of ICL-2 is 3MPa. This apparatus was applied to simulate possible conditions for the initiation and motion of the 1792 Unzen–Mayuyama megaslide (volume, $3.4\times10^8 m^3$; maximum depth, 400m) triggered by an earthquake. The megaslide and resulting tsunami killed about 15,000 people. Samples were taken from the source area (for initiation) and the moving area (for motion). The hazard area was estimated by the integrated landslide simulation model LS-RAPID, using parameters obtained with the ICL-2 undrained ring-shear apparatus. The estimated hazard area agrees reasonably with the landslide moving area reported in the Ministry leaflets.

Keywords Unzen-Mayuyama landslide, Computer simulation, LS-RAPID, Ring-shear apparatus, ICL-2

Introduction

There are many historical and recent megaslides and large-scale landslides which trigger Tsunami, landslide dams causing great debris flows or floods as well as causing direct damages. Some cases of megaslides have been studied in detail such as the 2006 Leyte landslide in the Philippines (Catane et al. 2007, Araiba et al. 2008, Sassa et al. 2010), the 2008 Aratozawa landslide in Japan (Konagai et al. 2008, Miyagi et al. 2011). The depths of these megaslides are from 120 m to 200m (Leyte landslide), or over 150 m (Aratozawa landslide). So far dynamics of such megaslides has not been well-studied. Development of Landslide dynamics needs a tool to measure the mobilized geotechnical parameters after the formation of a sliding surface—the post-failure strength reduction to its value at steady-state motion. It also needs an integrated computer model to simulate both the initiation and the motion of the landslide within the same programme using the geotechnical parameters mobilized in the landslide motion (Sassa et al. 2014). Based on this purpose, series of landslide ring-shear simulator and computer simulation model have been developed in three decades for measuring dynamic geotechnical parameters and simulating landslide from the initiation to the motion.

The latest high-stress dynamic-loading undrained ring-shear apparatus ICL-2 which developed since 2012 by the International Consortium on Landslides (ICL) (Sassa et al. 2014, Dang 2014, Dang et al. 2016) will be presented in this study. It is the most improved and advanced types in ring-shear apparatus series so far.

The LS-RAPID is an integrated landslide simulation model developed to assess the initiation and motion of landslides triggered by rainfalls, earthquakes or the combination of rainfalls and earthquakes (Sassa 2010, Sassa 2012, He 2014, Gradiski 2014). This software is the first simulation model can reproduce the whole process of landslide from initial stable state to deposition based on the measured parameters from the ring-shear apparatus (peak friction angle, friction angle during motion, shear resistance at the steady state, and other with physical meaning) (Sassa et al. 2004). Landslide simulated by LS-RAPID can be triggered by pore water pressure (pore water pressure ratio) due to rainfall and resulting groundwater rise or by seismic loading (real seismic record or simple cyclic waves) (Sassa et al. 2014).

Study area

Earthquake-induced landslides are among the most destructive phenomena related to failure of slopes during earthquakes (Trandafir 2006). Globally, many locations have over steepened and highly weathered hillsides, where large landslides could cause significant harm to local communities-many of which are already vulnerable in terms of housing structures and poverty. The 2001 earthquakes in El Salvador are a notable example in this regard, causing over 600 landslides and resulting in many hundreds of fatalities, with 585 deaths in the community of Las Colinas alone (Figure 1) (Anderson 2013).

Fig. 1 Area view of earthquake-triggered landslide in Las Colinas, El Salvador, January 13, 2001 (Source: wikipedia.org)

Unzen is the site of Japan's most destructive volcanic disaster on record. Mt. Mayuyama, one of the Unzen Volcanoes, is situated in the eastern part of the Shimabara Peninsula, and in the west of Shimabara city. It is a lava dome composed of dacite. Following a period of eruptive activity on May 21, 1792 a megaslide was triggered by an earthquake in the Mayuyama lava dome with a volume of about 3.4 x 10^8 m^3 and the maximum depth of 400m (Sassa 2014) (Figure 2). The debris of the lava dome swept through Shimabara city and slammed into the Shimabara Bay, caused a massive tsunami over 10m high that wreaked havoc the Shimabara city and Higo (current Kumamoto Prefecture) on the opposite shore. This catastrophe resulted in 15,000 deaths by landslide and its resulting tsumani making it the most serious volcanic disaster in Japan (Unzen Restoration Office of the Ministry of Land, Infrastructure and Transport of Japan 2002; 2003).

Figure 3 presents the section of the Unzen-Mayuyama landslide before and after the event modified form the Unzen Restoration Office of the Ministry of Land, Infrastructure and Transport of Japan (2002). According to the estimated ground surface before landslide and the bedrock surface in the source area of the upper slope and the bedrock in the lower area, we suggest that there were two landslide blocks occurred in this area. Firstly, a main sliding block (block with red dots) on the upper slope moved toward the lower part and applied undrained loading on the soil mass of the lower slope (black dots). This process caused a secondary motion of the lower slope. The average slope angles of the sliding surfaces in the upper slope and lower slope are 28.10 and 6.50 respectively (Sassa et al. 2014).

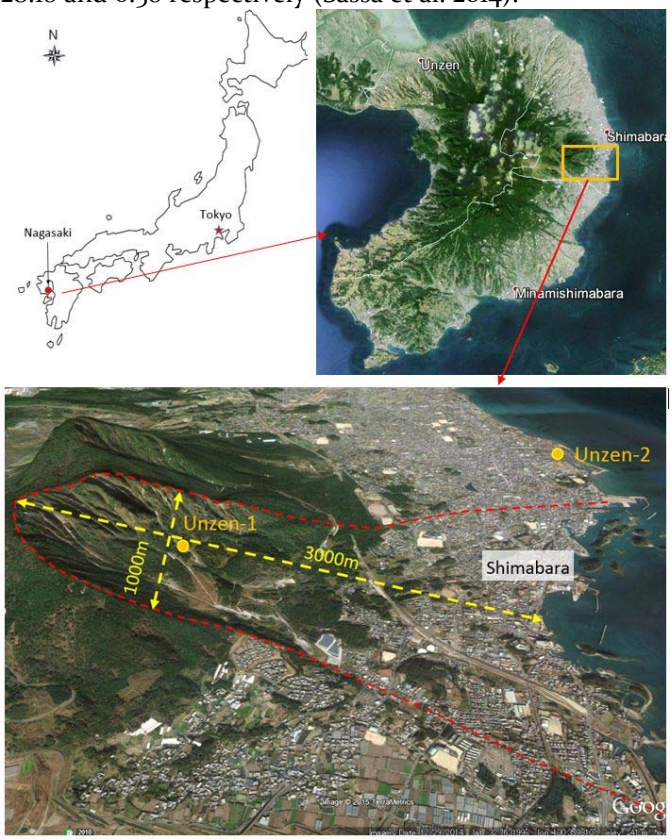

Fig. 2 Location map of the Unzen-Mayuyama landslide and sampling positions (from Google Earth)

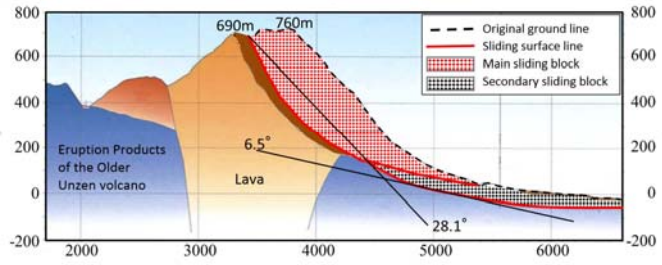

Fig. 3 Section of Mayuyama landslide and its interpretaton

During the investigation of Unzen-Mayuyama area for researching this historical megaslide, we chose two samples, one in the source area and one from the coastal area outside the landslide moving area. The location of sampling is shown in Figure 2 and the sample site is shown in Figure 4. Sample Unzen-1 was taken from a sand layer exposed along a torrent gully in the source area of the landslide. Sample Unzen-2 was taken from the coastal area outside the landslide area to represent the soil overridden by the landslide. The mountain consists of volcanic lava rock and unconsolidated eruption products (debris and sands). The sliding surface of the landslide probably formed within a sandy layer rather than in the strong intact lava rocks and boulders. We took samples from a sandy zone exposed along a torrent gully side slope in the source area. The grain-size distribution of the samples is shown in Figure 5 in which the Unzen-1 sample is finer than the Unzen-2 sample. The component of the sample 1 was 91% sand and 9% fine, while sample 2 was almost sandy particles.

Fig. 4 Photos show the sampling locations: a) Sample Unzen-1 was taken from an exposed slope along the upstream of a check dam constructed in 2012-2013; b) Sample Unzen-2 was taken from the coastal area

Figure 6 presents the unit weight of soils in the Unzen volcano. We consolidated the sample in the ring-shear apparatus under different normal stress from 0 to 3 MPa in a saturated condition. The saturated unit weight of Unzen sample was 21 kN/m3 at 3 MPa normal stress, and the dry unit weight was 19 kN/m3 at 3 MPa. In shallower areas, the value would be smaller and we assumed a single value of 19.5 kN/m3 for the entire area.

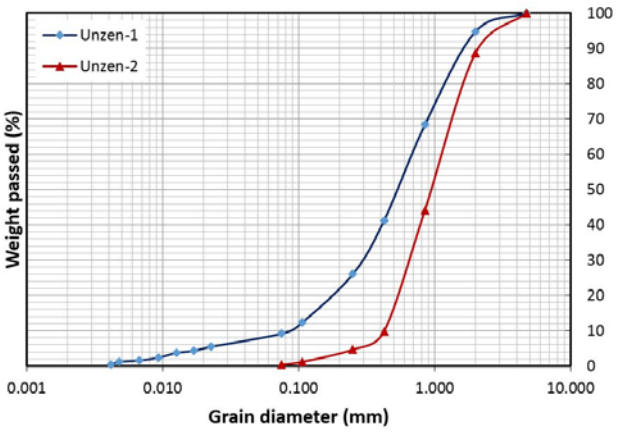

Fig. 5 Grain size distribution of sample Unzen-1 and Unzen-2

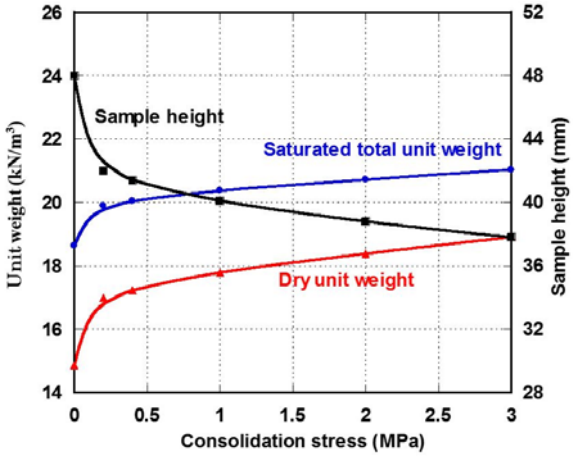

Fig. 6 Dry and saturated unit weight of Unzen-1 sample at different consolidation pressure

Ring-shear tests on the Unzen samples

A series of tests were conducted on sample S1 and S2 taken from this megaslide.

Drained speed-control test

A drained test is the best way to measure the friction angle of a sample and also to check the apparatus without any effect of pore-water pressure. A drained speed-controlled test was conducted as a basic test.

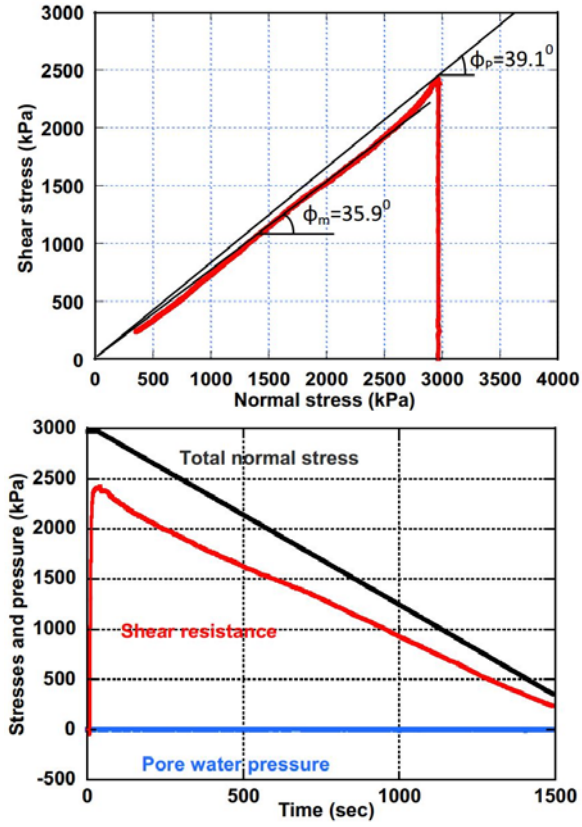

Fig 7 Drained speed-control normal-stress-reducing test on Sample 1.BD=0.97, velocity=0.2 cm/s. After reaching the peak, the normal stress was reduced at a rate of $\Delta\sigma$=5 kPa/s

First, the sample was fully saturated to BD=0.97, consolidated to close to 3 MPa and then sheared at 0.2 cm/sec in the drained condition. After the shear surface had reached peak shear resistance, the drained normal stress was reduced to zero at a rate of $\Delta\sigma$=5 kPa/sec to obtain the drained stress path and friction angle of the sample (Fig. 7). The peak friction angle for S1 was 39.1°, and the friction angle during motion was 35.9°. The stress path and the friction angles appeared to be reasonable for the nature of the sample. The lower graph in Fig. 7 is the time-series data for total normal stress, shear resistance and pore pressure. Pore pressure remained zero throughout the test, since the test was under a drained condition.

This drained, speed-controlled test result indicated that each of the ICL-2 servo-control system for normal-stress loading and unloading, the monitoring system, and the undrained capability of the apparatus could successfully function even under the very high normal stress of 3 MPa.

Undrained monotonic stress-control tests

The ring-shear test able to simulate the landslide phenomena is a stress-controlled test which can provide appropriate shear stresses under rainfall, earthquake or undrained loading in the moving landslide mass. Undrained monotonic shear-stress-control tests were conducted under four different normal stresses as tests of undrained capability, stress-control capability and precision of stress and pore-pressure monitoring.

For each test, normal stress was first loaded in the drained condition to close to the planned normal stress (0.3 MPa to 3.0 MPa). The shear box was then changed to the undrained condition, and shear stress was loaded gradually at a rate of $\Delta\tau$=1–5 kPa/sec. When the effective stress path reached the failure line, it began to decrease due to pore-pressure generation (the mechanism for this is sliding-surface liquefaction) along the failure line until the steady-state shear resistance was reached. Shearing was continued in each test until there was 3 m or more of shear displacement.

The stress paths and time-series data for each test are shown in Fig. 8 A to D. The stress path at a normal stress of 375 kPa (A) reached the failure line (39.8°) showing dilative behavior and then decreased along the failure line until it reached a steady-state shear resistance of 37 kPa. Negative pore-pressure was measured just before failure. After failure, the pore pressure increased during shear displacement. This is a typical sliding-surface liquefaction behaviour for a dense material: dilation of the sample near failure caused negative pore pressure, and grain crushing occurred in the shear zone. The resulting volume reduction, together with the accumulating post-failure shear displacement, generated positive pore pressure, even in the dense material.

Shear behavior at 1,030 kPa (B) normal stress was similar, but there was no negative pore pressure, although a zero pore pressure was measured just before failure. The steady-state shear resistance was 45 kPa, slightly higher than in the test at 375 kPa. The friction angle of the peak failure line was 41.2°, which also was slightly higher than at 375 kPa.

Shear behavior at 1,970 kPa (C) normal stress was contractive. Pore-water pressure was generated during shearing before failure. The steady-state shear resistance was 80 kPa.

Ring-shear tests to simulate initiation of the Unzen-Mayuyama landslide

A series of earthquakes struck the Shimabara area in April, 1792. The largest earthquake hit the area on 21 May 1792.

The magnitude of this nearby earthquake is estimated to have been M=6.4±0.2 (Usami 1996). Usami estimated that the seismic intensity at Shimabara was at least V and possibly VI. The Unzen Restoration Office, however, estimates that the seismic intensity which triggered the Unzen-Mayuyama landslide was VII, because more than 30% of the houses were destroyed in the Shimabara area. Exact seismic accelerations may never be known, but probably were around 400 cm/sec2 or greater.

The Japanese seismic intensities (Usami 1996) are:

V: 80–250 cm/sec2 (where walls and fences are cracked, and Japanese gravestones fall down)

VI: 250–400 cm/sec2 (where less than 30% of Japanese wooden houses are destroyed)

VII: More than 400 cm/sec2 (where more than 30% of the houses are destroyed, landslides are triggered and surface fault rupture is seen).

The estimate of an acceleration of more than 400 cm/sec2 by the Restoration Office is probably correct, as it is based on a detailed study of house damage.

There are no seismic records of the 1792 earthquake so we chose to use a record from a recent earthquake. The 2008 Iwate-Miyagi Nairiku Earthquake (M=7.2) triggered the Aratozawa landslide (67 million cubic meters) in Miyagi Prefecture.

The maximum recorded acceleration was 739.9 cm/sec2 at MYG004 (National Research Institute for Earth Science and Disaster, Prevention (NIED)). We have used the Iwate-Miyagi earthquake wave form recorded in Miyagi Prefecture (MYG004) for the ring-shear simulation test and also in the computer simulation for 1792 Unzen-Mayuyama landslide.

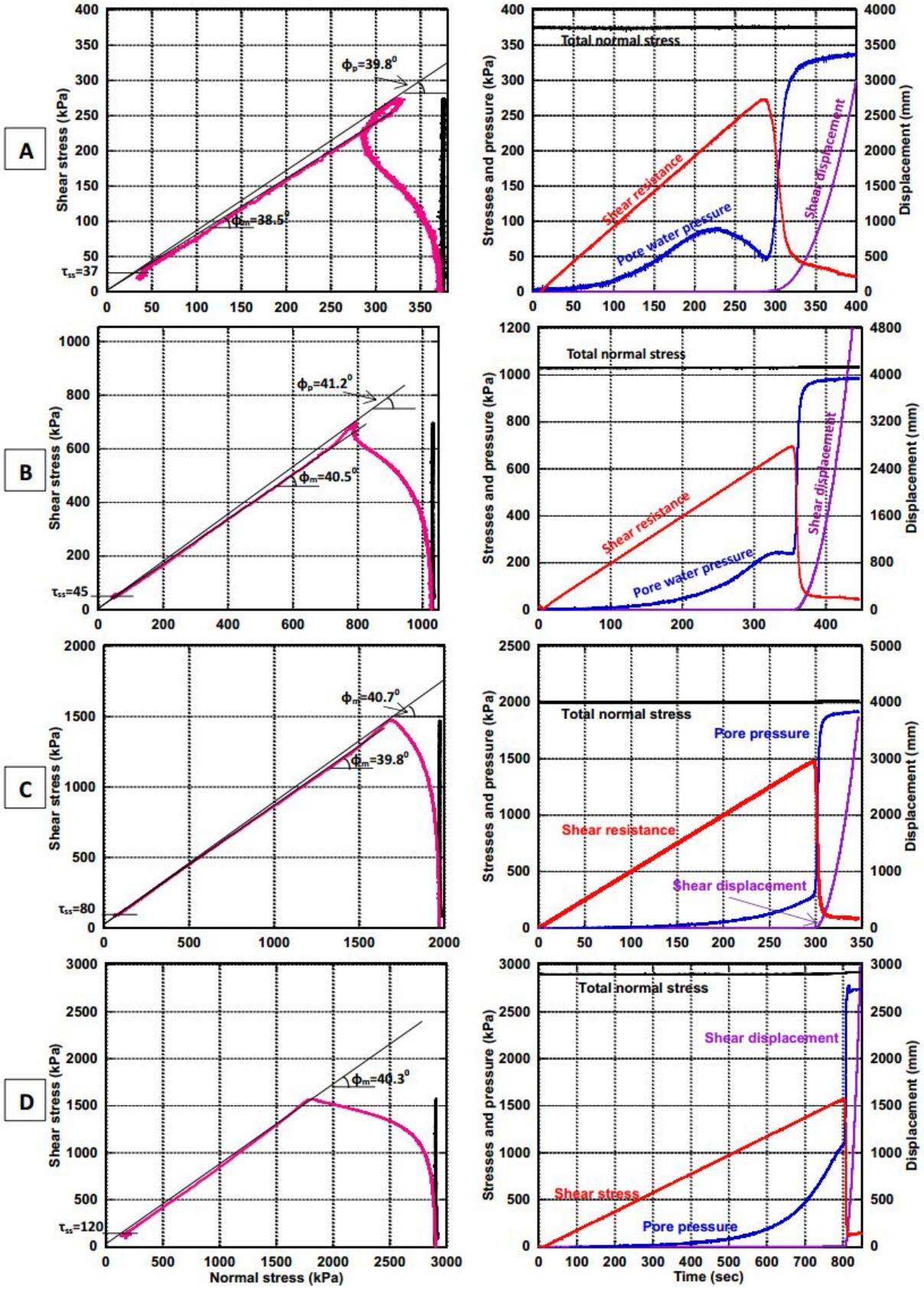

Fig 8 Undrained monotonic stress control tests at different normal stresses. Sample: S1 from Unzen–Mayuyama. A Normal stress =375 kPa, BD=0.93, Δτ/s =1 kPa/s. b Normal stress =1,030 kPa, BD=0.95, Δτ/s =2 kPa/s. c Normal stress =1,970 kPa, BD=0.95, Δτ/s =5 kPa/s. d Normal stress =2,900 kPa, BD=0.96, Δτ/s =2 kPa/s

We performed three tests on the sample (S1) taken from the source area of Unzen-Mayuyama (Fig. 2) to investigate the initiation of the landslide block in the upper slope (block with red dots in Fig. 3) using the ICL-2 apparatus.

Pore-water pressure control test

The first basic test for this landslide (Fig. 9) was to trigger landslide failure by increasing only the pore-water pressure.

Firstly , the sample was saturated (BD value, 0.98), then consolidated to 3.0 MPa normal stress and 1.5 MPa shear stress in a drained condition. This preparatory stage was to reproduce the initial stress in the slope, and is shown as a black line in Fig. 9.

This initial stress corresponded to a slope of arctan (1.5/3.0)=26.5°. This is a similar slope to the landslide block in Fig. 3.

Then, in order to simulate the pore-pressure-induced landslide process, the pore-water pressure was gradually increased at a rate of $\Delta\sigma$ = 5 kPa/sec. Failure occured at a pore-water presure of 1.2 MPa (a pore-water pressure ratio ru=1.2/3.0=0.4). The friction angle at failure was 39.4°.

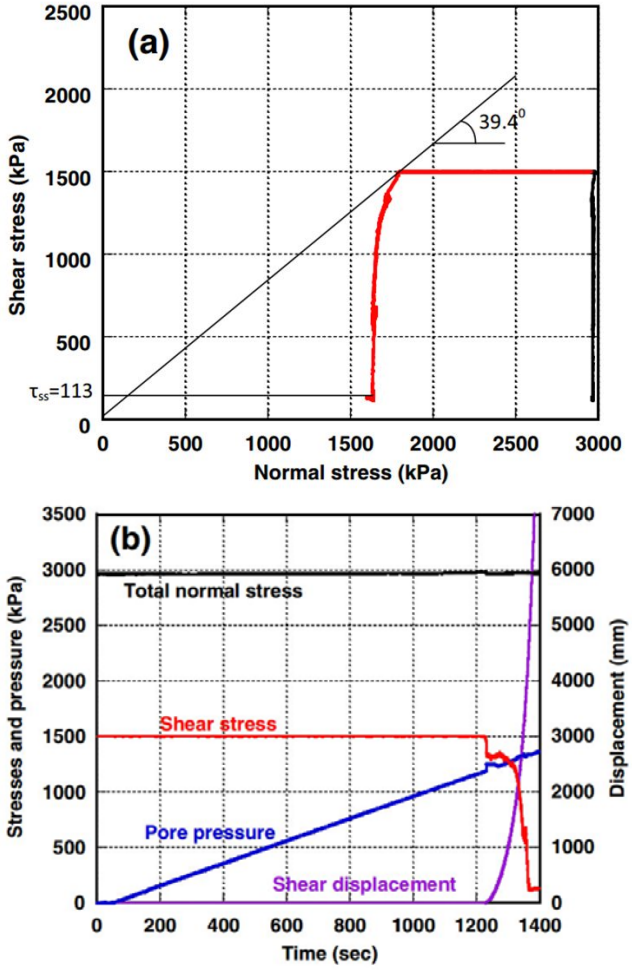

Fig 9 Pore pressure control test on sample 1. Sample: S1 from Mayuyama source area.BD=0.98

Undrained cyclic loading test

The second basic test (Fig. 10) was an undrained cyclic loading test on the saturated Sample S1.

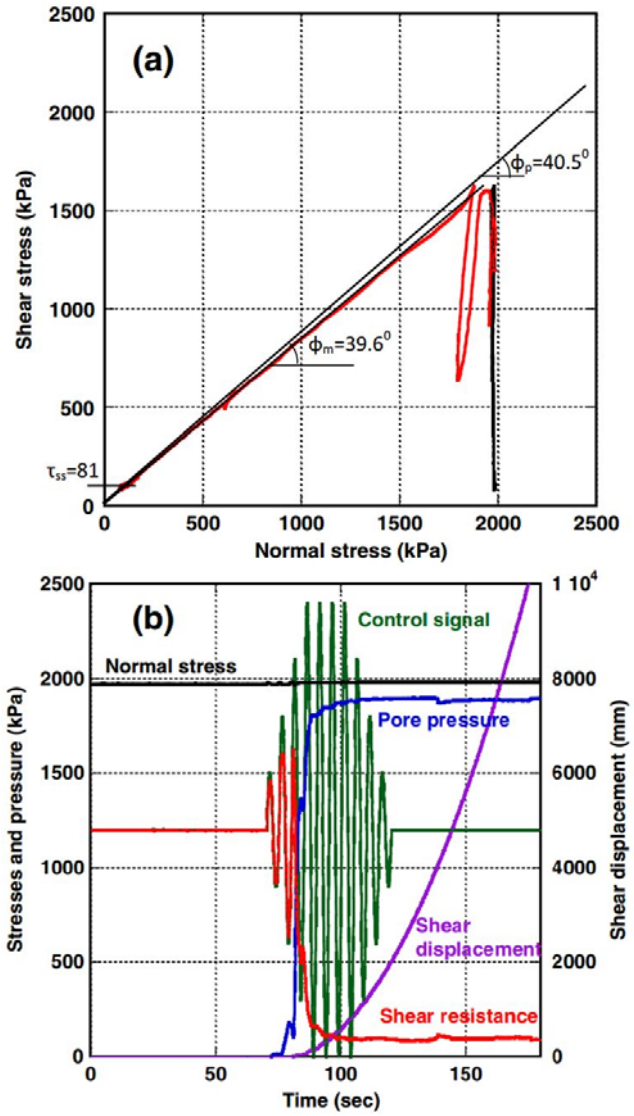

Fig 10 Undrained cyclic loading test on Sample 1. BD=0.98, cycle rate: 0.2 cycle/s, shear stress step: 300kPa

Initially, the saturated sample was consolidated at 2.0 MPa normal stress, then a 1.2 MPa shear stress was loaded in the drained state to create the initial stress state. The slope angle for this combination of normal and shear stresses corresponded to arctan (1.2/2.0), i.e. 31.0°. The shear box was then switched to the undrained state for the undrained cyclic loading test. We applied the control signal for the computer as follows: an initial cycle of shear stress increment of ±300 kPa was to be loaded as a sine curve, in which the second, third and fourth cycles of shear stress were to be loaded as increasing ±300 kPa in each step. (Normal stress was 2 MPa. It was expected that the soil would fail before the loading of the 4th cycle when the total shear stress would be 2.4 Mpa). Thereafter, three cycles would be kept constant before the cyclic shear stress was reduced to zero. This computer signal

was sent to the servo-amplifier for shear stress, while the control signal for normal stress was held constant.

The pore-water pressure generation during the test, mobilised shear resistance, and shear displacement were each monitored continuously during the test. The stress path and the time-series data for this test are shown in Fig.10. The shear stress reached the failure line during the second shear-stress cycle and shear stress decreased after the peak of the third cycle due to generation of high pore-water pressure. This phenomenon is what we have called sliding surface liquefaction. Then, the rate of shear displacement (the purple line in Fig. 10) accelerated and displacement reached to more than 10 meters. The peak friction angle was 40.5°, and the friction angle during motion was 39.6°. The steady state shear resistance was 81 kPa.

Seismic-loading test

The third test (Fig. 11) was a seismic-loading ring-shear test to simulate the landslide initiation of the Mayuyama landslide by the combined effect of pore-water pressure and earthquake shaking. Initially, the sample (S1) was saturated (BD=0.94) and consolidated to 3MPa in normal stress and 1.5 MPa in shear stress (the corresponding slope angle was artanc (1.5/3.0) = 26.6°). Then pore-water pressure was increased up to 800 kPa, (a pore water pressure ratio ru=800/3000=0.27) as the initial slope condition. An exact value remains unknown, but it must have been smaller than 0.4. A preparatory test (Fig. 9) showed that ru=1.2/3.0=0.4 was a critical pore-water pressure which could cause a landslide without an earthquake. The earthquake which triggered the 1792 Unzen-Mayuyama landslide was estimated to be Magnitude M=6.4±0.2, with a seismic intensity of VII during the earthquake; in the Japanese standard this corresponds to a seismic acceleration of more than 400 cm/sec2, as explained above.

The maximum recorded seismic acceleration in the 2008 Iwate-Miyagi earthquake was 739.9 cm/sec2, which caused the Aratozawa landslide. We loaded the N-S component of the 2008 Iwate-Miyagi earthquake record (maximum acceleration is 739.9 cm/sec2) at MYG004 as the additional shear stress. For precise pore-pressure monitoring, as well as to maintain servo-stress control, a five-times slower rate was used in applying the recorded seismic acceleration. The test result is shown in Fig. 11.

The green line indicates the control signal. The maximum value is 2,469 kPa (1500+969 kPa) and the minimum value is 369 kPa (1500–1131). The loaded acceleration (a) is calculated from the ratio of seismic acceleration and gravitational acceleration: a/g= 969/1500 or a/g=1131/1500, because ma=969 kPa, and mg=1500 kPa, expressing the landslide mass at unit area as m. The acceleration corresponds to +633 cm/sec2 and -739 cm/sec2. Therefore, the control signal for shear stress sent to the ring-shear apparatus exactly corresponded to the monitored acceleration record.

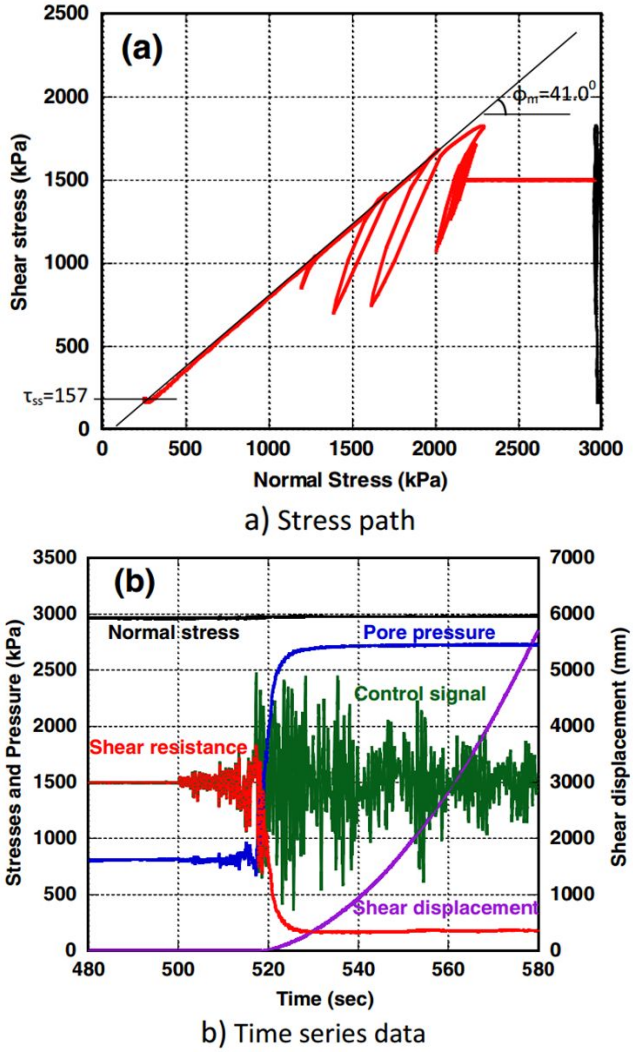

Fig 11 Undrained pore water pressure and seismic loading test. Sample: S1 from Mayuyama source area. BD=0.94

As Fig. 11 shows, failure occurred around 1,825 kPa, namely a/g=(1825–1500)/1500=0.22; the necessary acceleration to failure was 216 cm/sec2. This test result suggested that a lesser earthquake shaking (of around 216/633=0.34) than occurred in the Iwate-Miyagi earthquake could have caused failure under a slope condition with a pore-pressure ratio of 0.27. The steady-state shear strength was 157 kPa.

Ring-shear tests to simulate the motion of the Unzen-Mayuyama landslide

We collected two samples during the Unzen-Mayuyama field investigation. One sample (S1) was taken from the current ground in the soure area (red dot zone of Fig. 3) of the Unzen-Mayuyama landslide to study the initiation of the landslide.

In order to investigate the motion of the landslide, we took another sample (S2) from a location close to the landslide area, but not covered by the landslide source area mass, i.e. from exposed ground along the coast. We assumed that S2 could represent soils in the lower slope and deposits along the coast (black dot zone of Fig. 3).

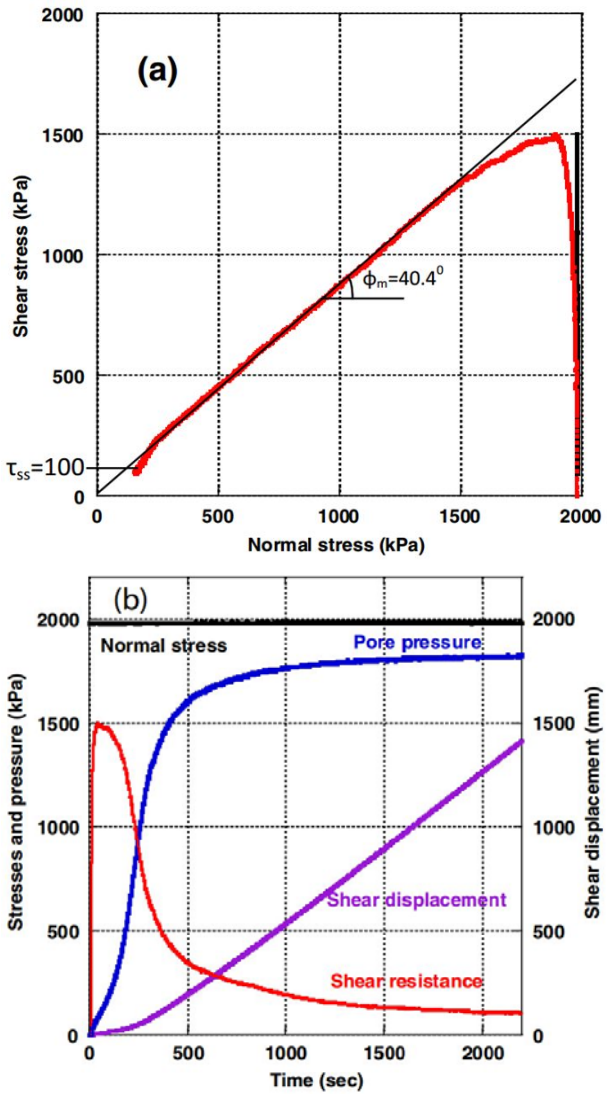

Fig 12 Undrained speed-control test on sample 2.BD=0.95, shear velocity=0.1 cm/s

We first carried out a basic undrained monotonic speed-control test on S2 (Fig. 12). The peak shear strength appeared below the failure line. The friction angle during motion was 40.4°, and steady-state shear resistance was 100 kPa. The friction angle and the steady-state shear resistance were similar to S1 (40.3° and 120 kPa). Thus, both samples were very similar in their undrained shearing behaviour, even though they were sampled from different points.

When a landslide mass on the upper slope moves, it applies undrained loading to the soil mass on the lower slope and initiates motion of the lower slope in addition to the motion from the upper slope. A study of a landslide-induced debris flow, where the landslide mass in the slope moved onto and mobilized a torrent deposit, was reported in Sassa et al. (2004), although the stress level is much different.

ICL-2 was used to simulate undrained loading on the black-dot layer in the lower slope (Fig. 3) using the displaced mass from the upper slope (red-dot block). Fig. 13 presents the test result of an undrained dynamic loading test simulating this scenario.

Firstly, the initial normal stress and the initial shear stress (σ_0 = 1,000 kPa, τ_0 = 150 kPa, corresponding to an 8.5° slope) were loaded in the drained condition to reproduce the initial stress state at the bottom of the black-dot layer. The normal stress was increased to 2,790 kPa (which is close to the 3 MPa capacity of the apparatus) as the undrained load, although a 400-m-deep initial landslide will result in a greater normal stress. If the lower slope mass can resist the undrained load from the upper slope without raised pore-water pressure, it may resist around 2,374 kPa (2,790 x tan(40.4°) in this dynamic loading. However, as seen in Fig. 13, a high pore-water pressure was generated in the undrained loading. The sample failed at 720 kPa and its steady-state stress was 80 kPa. The landslide mass from the upper slope should scrape off a layer of the lower slope and move together as a combined greater mass toward the sea. This scenario was proven to be possible by this landslide simulation test using ICL-2.

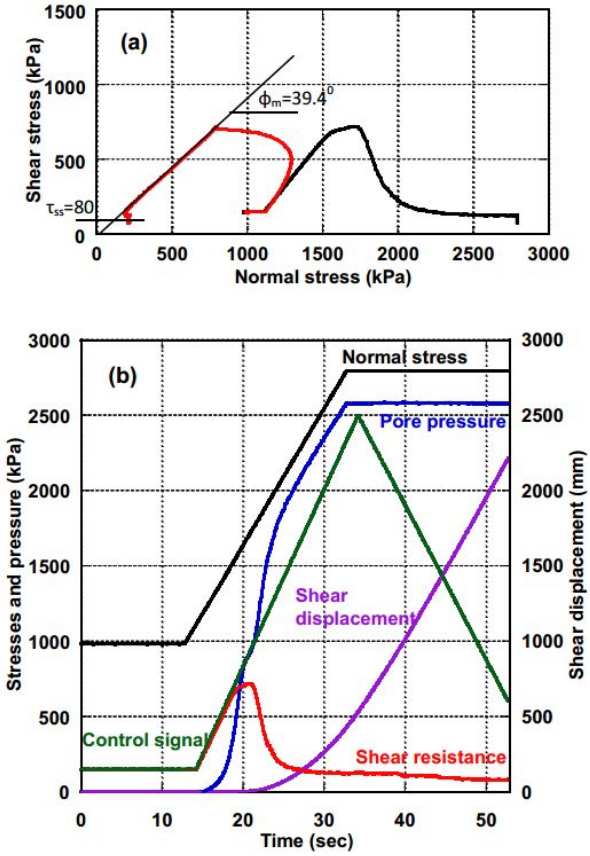

Fig 13 Undrained dynamic loading test on sample 2.BD=0.97, initial stresses (σ_0=1,000 kPa, τ_0=150 kPa)

Simulation of the 1792 Unzen-Mayuyama Megaslide in Japan

LS-RAPID model was tried to apply to the 1792 Unzen-Mayuyama megaslide triggered by a nearby earthquake. From the result of the testing and research presented in previous parts, the geotechnical parameters obtained in the ring-shear tests and the 2008 Iwate-Miyagi

earthquake record were used to simulate in the model. Those parameters are listed in Table 1.

(1) The most important parameter is the steady state shear resistance (τss) (Sassa et al. 2010). From the undrained monotonic stress control tests results (Figure 8), the steady state shear strength is 120 kPa in the landslide source area (deeper area), and 37-80 kPa in the landslide moving area (shallower area).

(2) Peak friction angle (ϕp) in the tests is from 39.80 to 41.20. The tests were conducted in saturated condition and the maximum loading stress (near 3 MPa- corresponding to less than 200m depth) is smaller than the real stress of the landslide (maximum depth was 400m). So we selected the peak friction angle of 42.00 for this landslide.

Table 4.1 Parameters used for Unzen-Mayuyama landslide simulation in LS_RAPID model (from Sassa et al. 2014)

Parameters used in simulation	Value	Source
Parameters of Soils in the source area (Deeper area)		
Steady state shear resistance (τ_{ss})	120 kPa	Test data
Lateral Pressure ratio ($k=\sigma_h/\sigma_v$)	0.7–0.8	Estimation (see text)
Friction angle at peak (ϕ_p)	42.0°	Test data
Cohesion at peak (c)	10 kPa	Assuming small
Friction angle during motion (ϕ_m)	40.0°	Test data
Shear displacement at the start of strength reduction (D_L)	6 mm	Test data
Shear displacement at the start of steady state (D_U)	90 mm	Test data
Pore pressure generation rate (B_{ss})*	0.7–0.9	Estimated
Total unit weight of the mass (γ_t)	19.5 kN/m^3	From the test
Parameters of Soils in the moving area (shallower area)		
Steady state shear resistance (τ_{ss})	30–80 kPa	Test data
Lateral Pressure ratio ($k=\sigma_h/\sigma_v$)	0.8–0.9	Estimated
Friction angle at peak (ϕ_p)	40.0°	Test data
Cohesion at peak (c)	10 kPa	Assuming small
Friction angle during motion (ϕ_m)	40.0°	Test data
Shear displacement at the start of strength reduction (D_L)	6 mm	Test data
Shear displacement at the end of strength reduction (D_U)	90 mm	Test data
Pore pressure generation rate (B_{ss})	0.7–0.9	Estimated
Total unit weight of the mass (γ_t)	19.5 kN/m^3	From the test
Triggering factor		
Excess pore pressure ratio in the fractured zone (r_u)	0.21	Assumption
0.5 times of the 2008 Iwate–Miyagi earthquake	Max:370 cm/s^2	Wave form of the Ground motion record at MYG004
Parameters of the function for non-frictional energy consumption		
Coefficient for non-frictional energy consumption	1.0	Data (Sassa et al. 2010)
Threshold value of velocity	100 m/s	A few times greater than maximum reported speed
Threshold value of soil height	400 m	Maximum depth of the initial source area
Other factors		
Steady state shear resistance under sea	10 kPa	Data (Sassa et al. 2004)
Unit weight of sea water	10.1 kN/m^3	Average sea water density

(3) Friction angle during motion is 40.00

(4) Critical shear displacement for start of strength reduction (DL) and the start of steady state (DU) are 6 mm and 90 mm. These values were determined from the shear stress and the shear displacement curves for the tests conducted for sample Unzen-1 and Unzen-2 (Figure 14)

(5) Pore-water pressure generation rate (Bss) is 0.7-0.9 in the source area, and 0.99 under the sea because of completely saturation. Outside of the landslide it was 0.2 as the ground was assumed to be unsaturated.

(6) Lateral pressure ratio (k) is 0.7-0.9. The ratio was assumed to be 0.9 in the coastal area and under the sea. Outside of the landslide, it was 0.4 (unsaturated).

(7)Unit weight of soils: 19.5 kN/m3, estimated from consolidation of sample and saturated and dry unit weight of sample Unzen-1 (Figure 6).

(8) Pore-water pressure ratio before earth quake was assumed to be 0.21.

(9) Seismic loading: Iwate-Miyagi earthquake

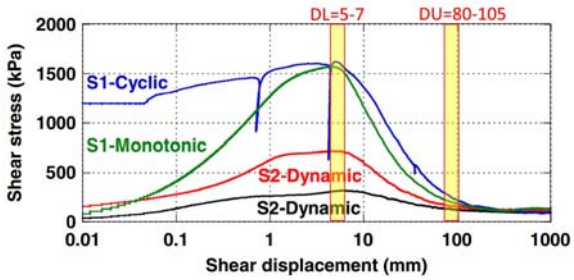

Fig. 14 Combined graph of shear strength reduction in progress of shear displacement by different ring-shear test

Then, the simulation results are demonstrated in Figure 15. Red color ball represent the moving mass, blue color balls represent the stable mass, and light green area presents the deposition area of the landslide. At 11s, the pore-water pressure reached 0.21 and the earthquake started, but no movement occurred. From 17s, the main shock of the Iwate-Miyagi earthquake struck the area, the pore water pressure ratio kept constant of 0.21, and failure was starting from the middle part of the slope and in a small part on the left edge of the slope. At 26s, the whole landslide mass was moving while the earthquake shaking. At 64s, the earthquake already stopped, the landslide mass continued moving and entered into the Shimabara bay. At 226s, the landslide mass stopped and deposited.

Figure 15f is the topographic map made by the Unzen Restoration Office of the Ministry of Land, Infrastructure and Transport of Japan (2002). It shows the similar between the area covered by simulated landslide and the actual topography. In addition, the section of line A in the topographic map (Figure 15(f)) and the E-W section (same position with line A) of the LS-RAPID model were made to compare (Figure 16). The comparison indicated that both movements were very similar. The travel distances of the landslide mass were also very close, in which the travel distance in the simulation is 6.6 km and the real distance from the field investigation is 5.9 km.

Acknowledgments

Development of ICL-2 is a part of the project “IPL-175: Development of landslide risk assessment technology and education in Vietnam and other areas in the Greater Mekong Sub-region”. This project was proposed by ICL and the Institute of Transport Science and Technology of the Ministry of Transport, Vietnam for the SATREPS programme, which is financed by the Japan Science and Technology Agency (JST) and the Japan International Cooperation Agency (JICA). The proposal including the development of ICL-2, and the donation of the developed apparatus to Vietnam was accepted. We acknowledge both agencies and their staffs for their support during this study.

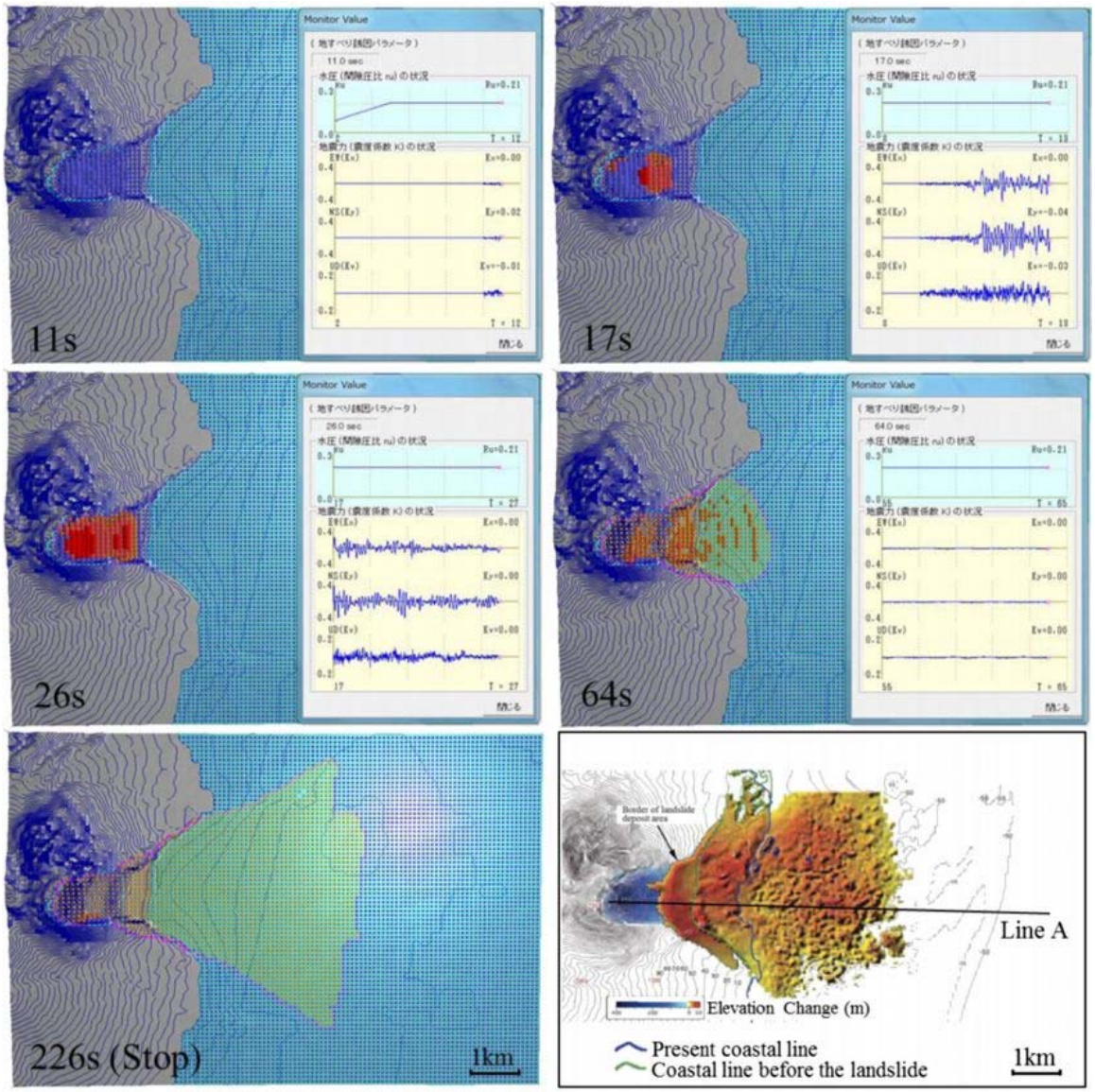

Fig. 15 Demonstration of simulation result for the 1792 Unzen–Mayuyama landslide. a-e) the whole process of landslide simulation, f) topographic map

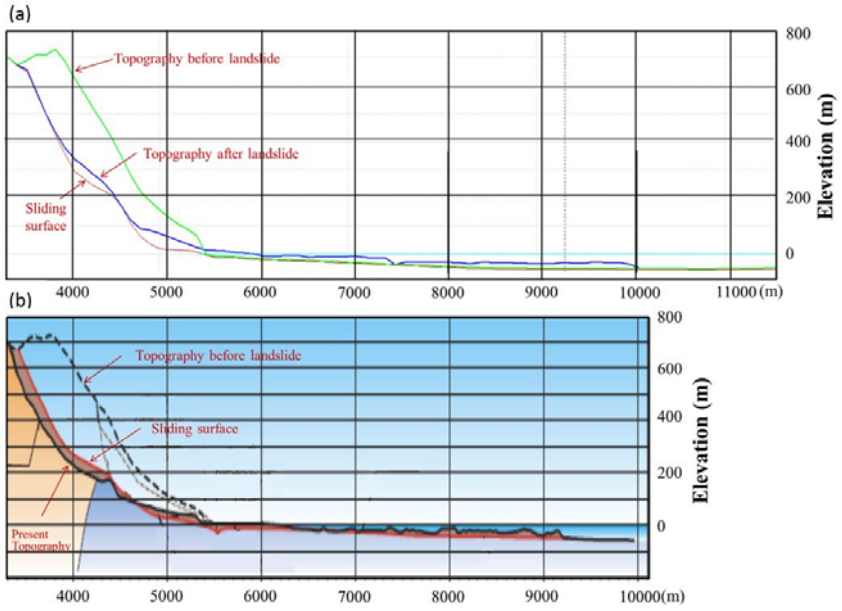

Fig. 16 Comparison between simulation result of LC_RAPID (a) and topographic map (b)

References (in the alphabetical order)

Araiba K, Nagura H, Jeong B, Koarai M, Sato H, Osanai N, Itoh H, Sassa K (2008) Topography of failed and deposited areas of the large collapse in Southern Leyte, Philippines occurred on 17 February 2006. Proc. International Conference on Management of Landslide Hazard in the Asia-Pacific Region (Satellite Symposium on the First World Landslide Forum). pp. 434-443.

Catane SG, Cabria HB, Tomarong CP, Saturay RM, Zarco MA, Pioquinto WC (2007) Catastrophic rockslide-debris avalanche at St. Bernard, Southern Leyte, Philippines. Landslides 4(1):85-90.

Inoue K (1999) Shimabara-Shigatusaku Earthquake and topographic changes by Shimabara catastrophe. Journal of Japan Society of Erosion Control Engineering 52(4):45-54.

Inoue K (2000) Shimabara-Shigatusaku earthquake and topographic change by Shimabara Catastrophe in 1792. Geographical Reports of Tokyo Metropolitan University, No. 35, pp.59-69.

Konagai K, Johansson J, Tajima Y, Fujita T, Tomimasu Y, Nomura F, Date M, Katagiri T (2008) Provisional report of the damage caused by the June 14th 2008 Iwate/Miyagi Prefectures Earthquake. Seisan Kenkyu (Institute of Industrial Science, University of Tokyo), 60 (6): 531-535.

Miyagi T, Yamashina S, Esaka F, Abe S (2011) Massive landslide triggered by 2008 Iwate–Miyagi inland earthquake in the Aratozawa Dam area, Tohoku, Japan. Landslides, 8 (3):99-108.

Nakada S, Suzuki H, Furuya T (1992) Volcanic hazard at Unzen, Japan. International Newsletter Landslide News, No.6, pp.2-6.

Nakada S, Suzuki H, Furuya T (1999) Volcanic hazard at Unzen, Japan. Landslides of the World (editor: Kyoji Sassa), Kyoto University Press, pp. 311-316.

Sassa K (1988) Geotechnical model for the motion of landslides. In: Proc. 5th International Symposium on Landslides, “Landslides”, Balkema, Rotterdam, vol. 1. pp 37-56.

Sassa K (1992) Access to the dynamics of landslides during earthquakes by a new cyclic loading high-speed ring-shear apparatus. 6th International Symposium on Landslides. “Landslides”, A.A. Balkema, Vol. 3, pp. 1919-1937.

Sassa K (1996) Prediction of earthquake induced landslides. Proc. of 7th International Symposium on Landslides, A.A. Balkema, Trondheim, Vol.1, pp.115-132.

Sassa K, Fukuoka H, Wang G, Ishikawa N (2004) Undrained dynamic-loading ring-shear apparatus and its application to landslide dynamics. Landslides, 1 (1):7-19.

Sassa K, He B, Dang K, Nagai O, Takara K (2014) Plenary: Progress in Landslide Dynamics. Landslide Science for a Safer Geoenvironment, Proceedings of the Third World Landslide Forum, Springer, Vol.1, pp.37-67.

Sassa Kyoji, Khang Dang, Bin He, Kaoru Takara, Kimio Inoue, Osamu Nagai (2014) A new high-stress undrained ring-shear apparatus and its application to the 1792 Unzen–Mayuyama megaslide in Japan. Landslides, published online (DOI 10.1007/s10346-014-0501-1).

Sassa K, Nagai O, Solidum R, Yamazaki Y, Ohta H (2010) An integrated model simulating the initiation and motion of earthquake and rain induced rapid landslides and its application to the 2006 Leyte landslide. Landslides, 7 (3): 219-236.

Schuster R, Alford D (2004) Usoi Landslide dam and Lake Sarez, Pamir Mountains, Tajikistan. Environmental & Engineering Geoscience, 10 (2): 151-168.

Stone R (2009) Peril in the Pamir. Science, 326, pp.1614-1617.

Unzen Restoration Office of the Ministry of Land, Infrastructure and Transport of Japan (2002) The Catastrophe in Shimabara -1791-92 eruption of Unzen-Fugendake and the sector collapse of Mayu-Yama. An English leaflet (23 pages).

Unzen Restoration Office of the Ministry of Land, Infrastructure and Transport of Japan (2003) The Catastrophe in Shimabara-1791-92 eruption of Unzen-Fugendake and the sector collapse of Mayu-Yama. A Japanese leaflet (44 pages).

Usami T (1996) Materials for comprehensive list of destructive earthquakes in Japan. University of Tokyo Press.

Proceedings of the SATREPS Workshop on Landslides in Vietnam, 2016

Initiation and motion of the Hai Van landslide by computer simulation based on measured parameter of the drilled core samples

Lam Huu Quang [1], Doan Huy Loi [2], Kyoji Sassa [3], Kaoru Takara [4], Khang Dang [5], Shinro Abe [6], Shiho Asano [7].

1), 2) Institute of Transport Science and Technology, Hanoi, Vietnam.

3), 4), 5), 6), 7) International Consortium on Landslides, Japan.

Abstract This report is written as a research result of the Working Group 3 of Vietnam-Japan SATREPS Project, which is a manuscript submitted to an international journal.

Haivan station is an important station on the North-South railway line at the central of Vietnam. A precursor stage of landslide has been identified to threaten this railway through the field investigation. Therefore, the landslide risk assessment in the Haivan station is urgently needed to protect passenger' safety and national railway. A set of detailed field investigations including drillings, and laboratory testing as well as air photo interpretation was conducted. Sassa and others have developed a new high-stress undrained ring-shear apparatus with the undrained capacity of 3MPa (ICL-2) in the Japan-Vietnam Joint project of the International Programme on Landslides (Sassa 2014a). A set of ICL-2 apparatus was donated to Vietnam in 2015. Undrained dynamic-loading ring-shear apparatus since the development in 2004 were applied to various landslides (Sassa et al., 2004, 2010, 2012, 2014a and Boldini et al., 2009, Yin et al., 2015, Dang et al., 2016 and others). All samples except the study for a hypothetical submarine landslide in 2012 (Sassa et al., 2012) were taken from the ground surface of landslide areas. This research is the first application of the undrained dynamic loading ring shear apparatus to the sample drilled and cored from a precursor stage of landslide. Three loose sand layers were found from the boring log at the depths of around 21 m, 31 m, and 50 m. They were assumed to be the potential sliding surfaces of the landslide. All drilling cores were tested by this apparatus. However, the boundary between the strong weathered rock and bedrock is about 50 m depth, and the inclinometer measurement detected a slight movement at this depth. In addition to this, landslide risk for the case of the sliding surface at 50 m is higher than the cases of both 21 m and 31 m. The landslide dynamics parameters obtained from the ring shear test of 50 m depth samples were input to an integrated simulation model (LS-RAPID). The simulation result presented the critical pore pressure ratio for the landslide occurrence, and the maximum speed, the total volume of the landslide, and the depth of landslide mass covering the railway. These scientific analyses in this paper are expected to contribute for warning and raising awareness of Vietnam railway administration towards potential landslide hazard impact on national railway sector.

Keywords Haivan station, Rainfall, Ring-shear apparatus, Computer simulation, LS-RAPID.

Introduction

Vietnam is one of the countries strongly affected by landslide phenomena. In 2010, Professor Sassa and his team in International Consortium on Landslide (ICL) investigated landslide areas in Vietnam, such as Son La area, Ho Chi Minh Route and Haivan Pass located between Danang and Hue. Based on this joint research in Vietnam, ICL and Vietnam' s Institute of Transport Science and Technology (ITST) applied for SATREPS project from Japan and Vietnam. The Vietnamese - Japanese joint research SATREPS' s project "Development of landslide risk assessment technology along transportation arteries in Vietnam" was divided into 4 working groups: (WG1) Preparation of integrated guidelines for the application of developed landslide risk assessment technology; (WG2-mapping group) Wide-area landslide mapping and identification of landslide risk area; (WG3-testing group) Development of landslide risk assessment technology based on soil testing and computer simulation; (WG4-monitoring group) Risk evaluation and development of early warning system are based on landslide monitoring (Lam 2014).

Globally, there have been many historical megaslides; however, they do not occur frequently in the same area. The 2006 Leyte landslide in the Philippines (Sassa et al. 2010; Catane et al. 2007) was triggered by a very small, but nearby earthquake after a long period of rain. This landslide resulted in 154 confirmed fatalities, and 990 other people are missing in debris. The 2008 Iwate–Miyagi inland earthquake (magnitude 7.2) in Japan caused a megaslide adjacent to the Aratozawa dam reservoir (Miyagi et al. 2011). The volume of this landslide

is 67 million m^3. The maximum height of the head scarp is over 150 m. Only 10 % of the landslide mass (1.5 million m^3) entered the dam reservoir. This landslide mass caused a maximum of 7 to 9 m high tsunami adjacent to where the landslide entered the water (Konagai et al. 2008). The greatest landslide disaster in the history of Japan is the 1792 Unzen–Mayuyama megaslide (Nakada et al. 1992, 1999). Its volume was 3.4x108 m^3 and the maximum depth was 400 m; around 15,000 people were killed by the landslide and its resulting tsunami (Unzen Restoration Office of the Ministry of Land, Infrastructure and Transport of Japan 2002; 2003). The ring-shear simulator was applied to study the landslide initiation and post-failure motion of the above landslides. All samples used for ring-shear tests were taken from ground surface of landslide areas.

To research the deep landslide, Sassa and others have developed a new high-stress undrained ring-shear apparatus (ICL-2) for the projects of the International Programme on Landslides. This project is supported by the Science and Technology Research Partnership for Sustainable Development Program (SATREPS) of Japan. ICL-2 was developed in 2012–2013 to simulate the initiation
and motion of megaslides of more than 100m in thickness. The successful undrained capacity of ICL-2 is 3MPa.

In this paper, the authors present the main results of testing group for one project pilot area: a precursor stage of landslide of the Haivan railway station in Vietnam. Within the project framework, Haivan Pass station on National railway was installed monitoring system and drilled the soil samples with the depth of 80 m. Three samples were taken from the loose sand layers of the drilling cores at the depth of 21 m (sample S3), 31 m (sample S2) and 50 m (sample S1). In order to investigate the motion of the landslide, we collected another drilling core (S4) from 5.6 to 6.0 m depth. We assumed that S4 could represent soils in the lower slope. Then the ring-shear apparatus was used to obtain main soil parameters of those drilling cores. The first application of ring-shear simulator using samples collected from a borehole drilled in a precursor stage of landslide body are reported in this paper.

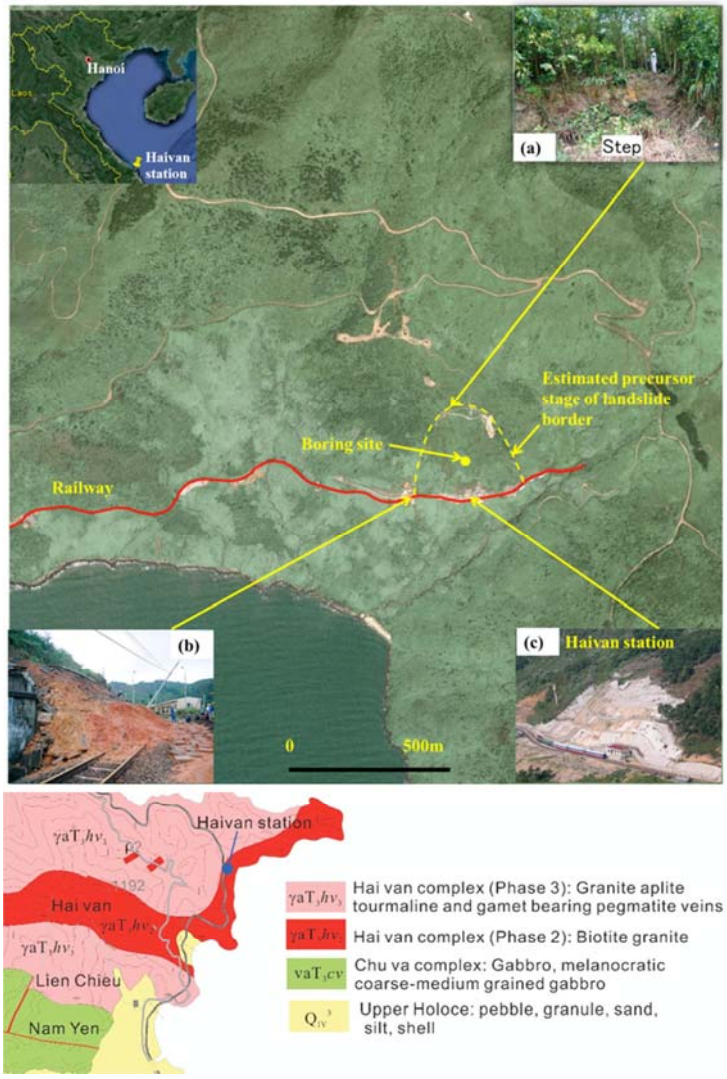

Fig 1. Location, topography, landslide border and geological structure of Haivan station landslide, Danang city, Vietnam (a: a small step where a head scarp of a landslide may be formed; b: previous landslide in 2007; c: Haivan station

The Study Area

Figure 1 presents the location and topography of this landslide study site. Haivan station is located on the sea side-slope of Haivan pass which is the provincial border between Hue and Da Nang. It contributes a great significance to traffic flow efficiency along the national railway. It is estimated that over 30 trains pass through this station each day and Vietnam has only one railway from Hanoi to Ho Chi Minh. However, this area is often affected by landslides, for example landslides in the years of 1999, 2005, and 2007. In particular, the landslide in 2007 (Figure 1b) damaged seriously the Haivan station and stopped its operational process several days. According to field investigations, geological map (Figure 1), and lithological description (Figure 2), geological structure of this study area is mainly composed of granite, called Haivan complex intruded in Triassic period of Mesozoic Era (from 200 million to 250 million years ago). The Haivan complex includes two phases: phase 2 (γa T3 hv2) is biotite granite and phase 3 (γa T3 hv3) consists of granite aplite, tourmaline-and garnet-bearing pegmatite veins. The boundary of those rocks is very clear. Granitic rock is highly and completely weathered until a certain depth under surface due to deep weathering. The vertical geological section at the bore hole was described as: depth 0 to 51 m is a strong weathered coarse granite layer includes clay sand, loose sand and solid granite; depth 51.0 to 54.0 m is a weathered fine granite layer includes hard, dark reddish-brown rock with cracks; and from depth 54 m is granite bedrock. The loose sand layers (20.4-21 m, 30.5-31 m and 49.15-51 m) were expected to be the sliding surfaces of the landslide. Ring-shear apparatus was used to study the initiation of landslide at assumed sliding surfaces.

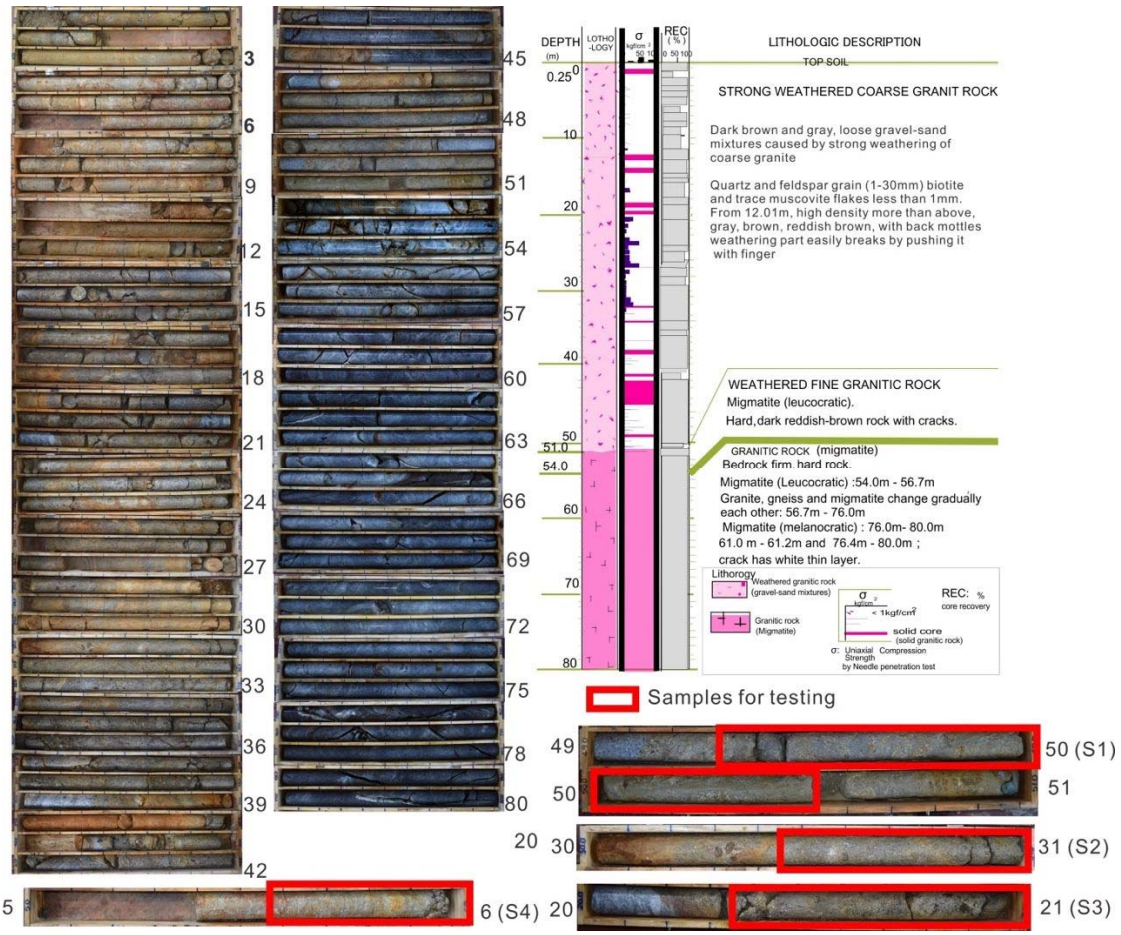

Fig. 2 Lithological description of the Haivan station slope collected from the bore hole and the sampling parts (red color parts) from weathered layers of the drilling cores.

Inclinometer result

Inclinometer was used to measure slope displacement at various depths along bore hole. After drilling, inclinometer casing was installed in the bore hole. The vertical deviation at each measurement interval is the lateral position of the casing relative to the bottom of the casing because the bottom of the casing remains fixed and does not move laterally. The deviation values can be plotted as an incremental displacement or slope change profile (i.e., slope change vs. depth) to show

movement at each measurement interval. The incremental displacement profile is useful to dramatize the location of the deformation zone. A spike in this plot indicates the location of movement, i.e., the failure plane (Stark, 2008) (see Figure 3). The inclinometer measurement was conducted two times per month. Figure 3 shows the inclinometer result data from 15 September 2015 to 15 March 2016. This result indicates that from 20 m to 70 m, displacement around 50 m is largest.

Ring-Shear Apparatus

Ring-shear apparatus has been widely used in the slope stability analysis, because the device can simulate of landslides with unlimited shear displacement (Bishop 1971, Sassa 2004). Sassa and colleagues have developed a series ring-shear apparatus since 1984. The latest version of these devices is a high-stress dynamic-loading undrained ring-shear apparatus ICL-2. Although the dimension of ICL series is smaller than previous generation (DPRI1-7), ICL-2 has high performance. The shear box is smaller than the previous DPRI versions. ICL-2 can maintain undrained condition up to 3000 kPa of pore water pressure (Sassa 2014). This special design allows simulating the large-scale and deep-seated landslides. The volume of the shear box is 300 cm^3. Therefore, ICL-2 is also suitable for testing in laboratory when the drilling cores are limited.

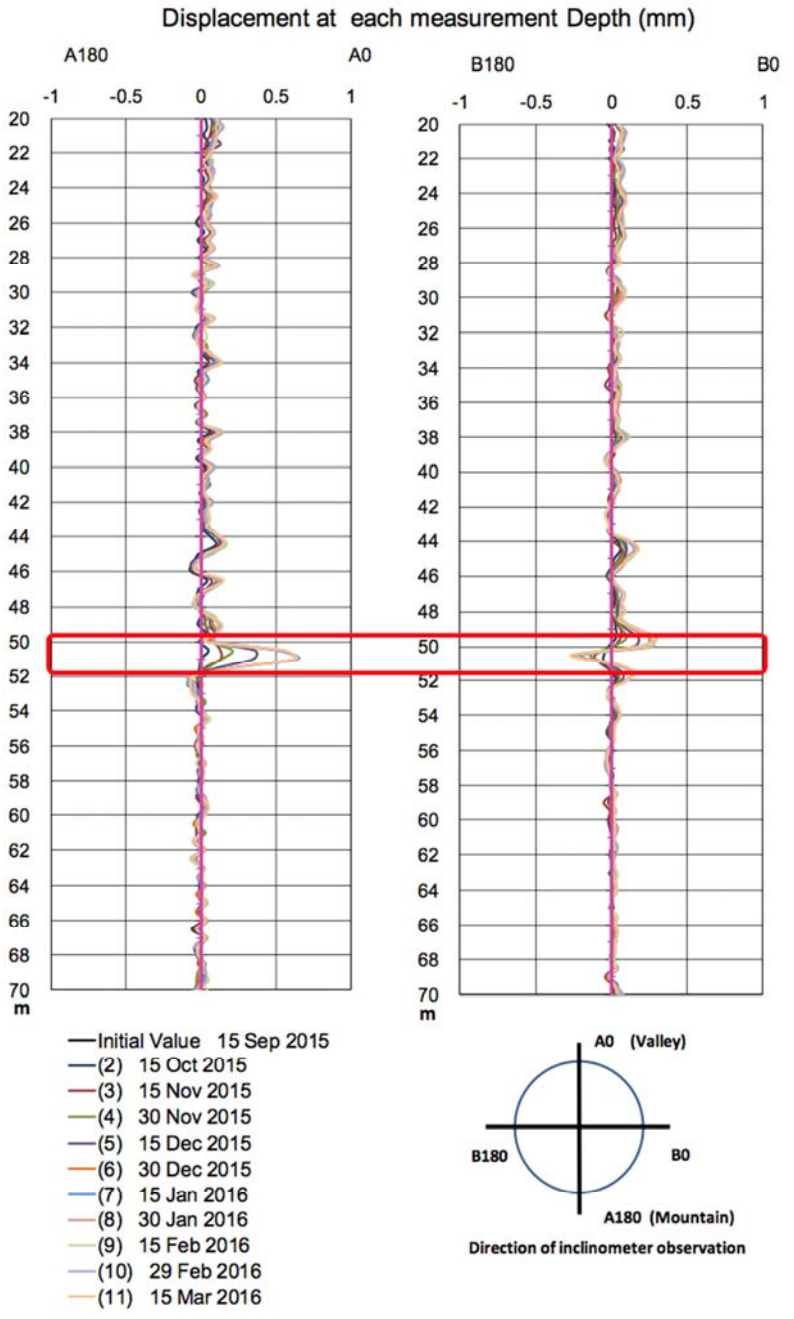

Fig.3 Inclinometer measurement at each depth from 15 September 2015 to 15 March 20

The testing procedure consists of the following steps: gap adjustment, sample saturation, sample consolidation and loading (by shear speed control; stress control – either cyclic or seismic loading). Firstly, the gap value should be adjusted to avoid leakage of water and sample, by applying vertical load. Then, it is kept constantly during the test by an oil piston. Shear box without sample is filled with CO_2 and de-aired water. Then, sample saturated by de- aired water could be slowly placed in the shear box. After that, the water circulation could start to enable full saturation of the sample. De-aired water is slowly supplied through the lower drainage line, and discharged from the upper drainage line until all air bubbles are expelled. The saturation degree of samples is then checked by measuring B_D value that for fully saturated samples should be greater than 0.95. B_D is a pore pressure parameter in direct shear state, related to the degree of saturation that was proposed by Sassa, and is formulated as:

$$B_D = \Delta u / \Delta \sigma$$

Where Δu and $\Delta \sigma$ are increments of pore pressure and normal stress, respectively.

For Haivan core samples, we prepared with B_D = 0.95-0.99, namely the samples were fully saturated.

After samples were fully saturated, the initial stress state of soil layer only due to gravity should be created. The sample was normally consolidated under normal and shear stress, depending on the sample depth and slope angle. After the consolidation, shearing was applied by stress control or speed control test.

Change of mobilized shear resistance is measured by two load cells. Pore pressure, resulting shear displacement, and shear speed are also monitored. The shear resistance mobilized during shearing is obtained by subtracting the rubber-edge friction from the monitored shear resistance. This friction is not constant. The smaller rubber-edge friction is preferable. Therefore, in each test, a minimum gap pressure at which water leakage proof is ensured to be checked and used.

Testing result

Basic tests were carried out to obtain mechanical parameters of the three collected drilling cores. From the grain size distribution (Figure 4), samples are considered as a good graded soil. We consolidated the sample in the ring-shear apparatus under different normal stresses from 0 to 1 MPa in a saturated condition. The saturated unit weight of sample was 21.2 kN/m^3 and the dry unit weight was 18.8 kN/m^3 at 1 MPa normal stress. In shallower areas, the value would be smaller and we assumed a single value of 19 kN/m^3 for the entire area.

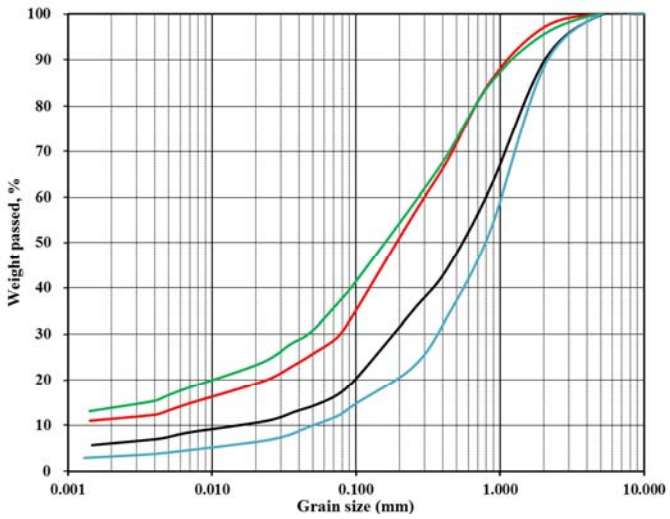

Fig. 4 Grain size distribution of Haivan drilling cores taken from the depths of 50 m (S_1), 31 m (S_2), 21 m (S_3) and 6 m (S_4).

Drained Shear Speed Control Test

The drained test is a basic test and the best method to determine the friction angle and test the ability of the device when not considering the influence of pore water pressure. The experiments were performed with the saturation of sample B_D = 0.96-0.99. When normal stress closes to 780, 520, 350 kPa, corresponding to the landslide depths of 50, 31 and 21 m (Figure 5), the samples were sheared at 0.1 cm/sec in drained conditions. After the shear stress reached to the maximum shear resistance, the drained normal stress was reduced to zero at a rate of $\Delta\sigma$=1 kPa/sec to obtain drained stress path and friction angle of the samples. The maximum friction angle of the sample S_1, S_2, S_3 were 39.0°, 38.7°, 39.8° and the friction angle during motion were 37.7°, 36.8°, 36.6°, respectively. The stress path and the friction angles were reasonable for the nature of the sample.

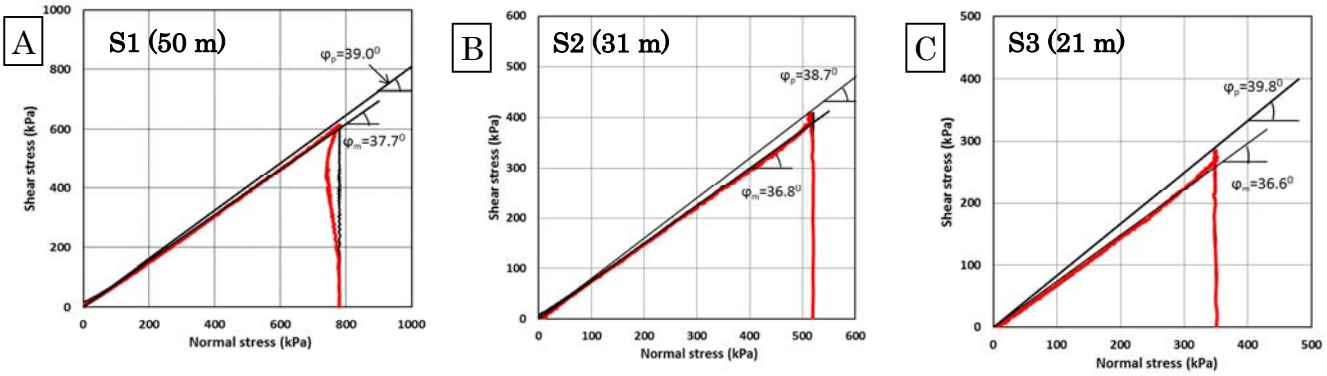

Fig. 5 Stress paths of drained shear-speed control tests on the three drilling cores (A: Sample S1; B: Sample S2; C: Sample S3, B_D = 0.96-0.99).

Undrained Shear Stress Control Test

After consolidation of the samples (by applying normal stress of 780 kPa, 520 kPa, and 350 kPa), the shear boxes were changed to the undrained condition, and shear stresses were loaded gradually at a rate of Δτ=1 kPa/sec. Samples were sheared until steady state obtained. In undrained conditions, the pore water pressures increased during testing and the effective stress paths closed to failure lines.

When the effective stress paths reached the failure lines, they began to decrease due to pore-pressure generation along the failure line until the steady-state shear resistance reached. In Figure 6, the red line is an effective path; the black line is the total stress path. From the graphs, values of the friction angle were determined of 39.8° (S1), 39.7° (S2), 38.7° (S3), and the steady-state shear resistance were 116, 240 and 56 kPa. The peak friction angles are almost the same, however the steady-state shear resistance value at 31 m is highest

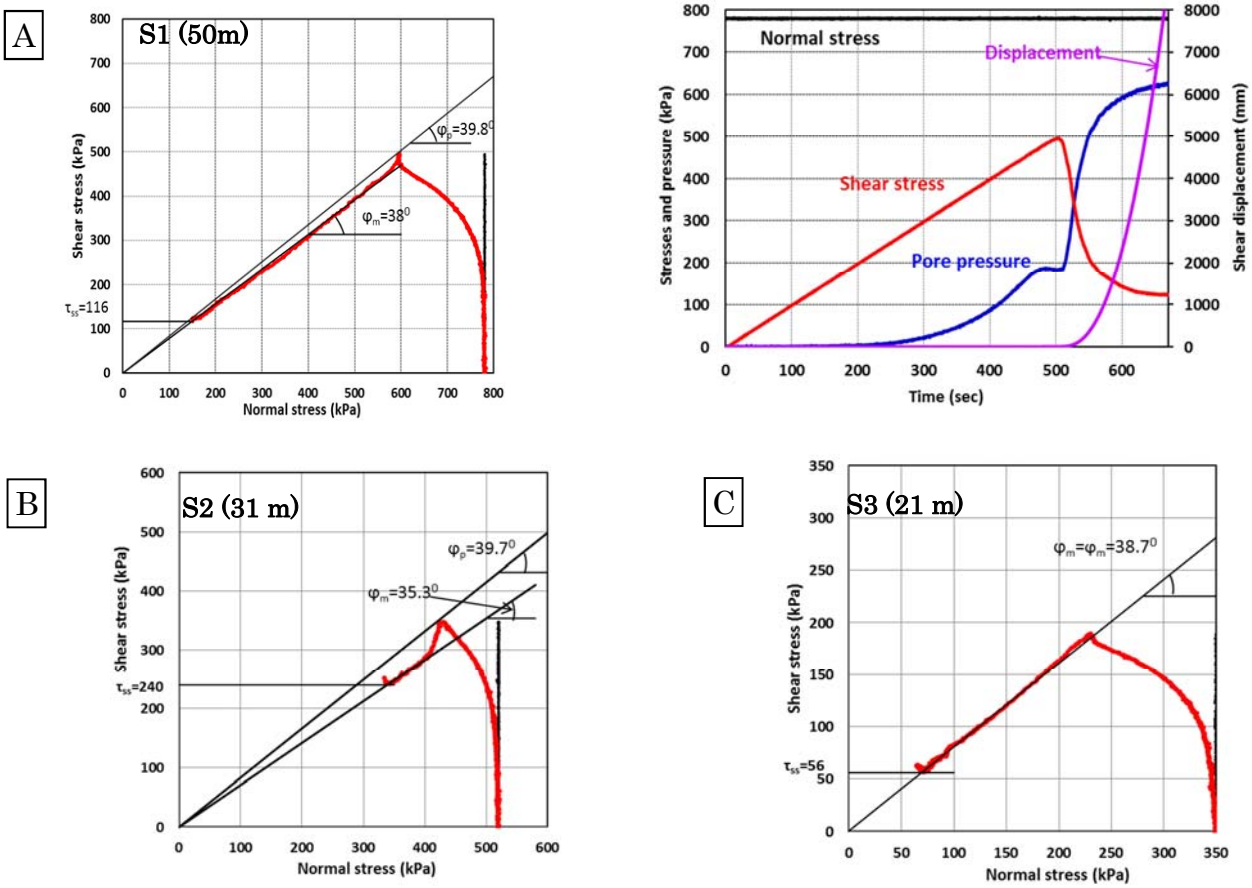

Fig. 6 Undrained shear stress control tests on Haivan drilling cores (A: Sample S1, Normal stress=780 kPa, B_D=0.96, Δ τ /s=1 kPa/s; B: Sample S2, Normal stress=520 kPa, B_D=0.95, Δ τ /s=1 kPa/s; C: Sample S3 Normal stress=350 kPa, B_D=0.96 , Δ τ /s=1 kPa/s).

Pore-Water Pressure Control Test

Pore-water pressure control test is the most appropriate experiment to simulate the effect of rain to landslide. First, the samples (S1, S2, S3) were saturated (B_D = 0.95 - 0.99) and consolidated close to 780 kPa (S1), 520 kPa (S2), 350 kPa (S3) and then sheared with 360, 200, 150 kPa in undrained condition. Initial stress state corresponded to the slope of tangent 24.8°, 21.0°, 23°. This is approximate the actual slope of landslide blocks (about 25o). To simulate the effects of pore-water pressure caused landslides phenomena, the pore water pressure increased with speed of 1kPa/sec, friction angle was 39.5o, 39.8°, 38.9° (Figure 7). Failure occurred when the pore water pressure increased up to 360, 297, 175 kPa, namely, a pore-water pressure ratio r_u = 360/780 = 0.46 for sample at 50 m, r_u = 297/520 = 0.57 for sample at 31 m, and r_u =175/350 = 0.50 for sample at 21 m.

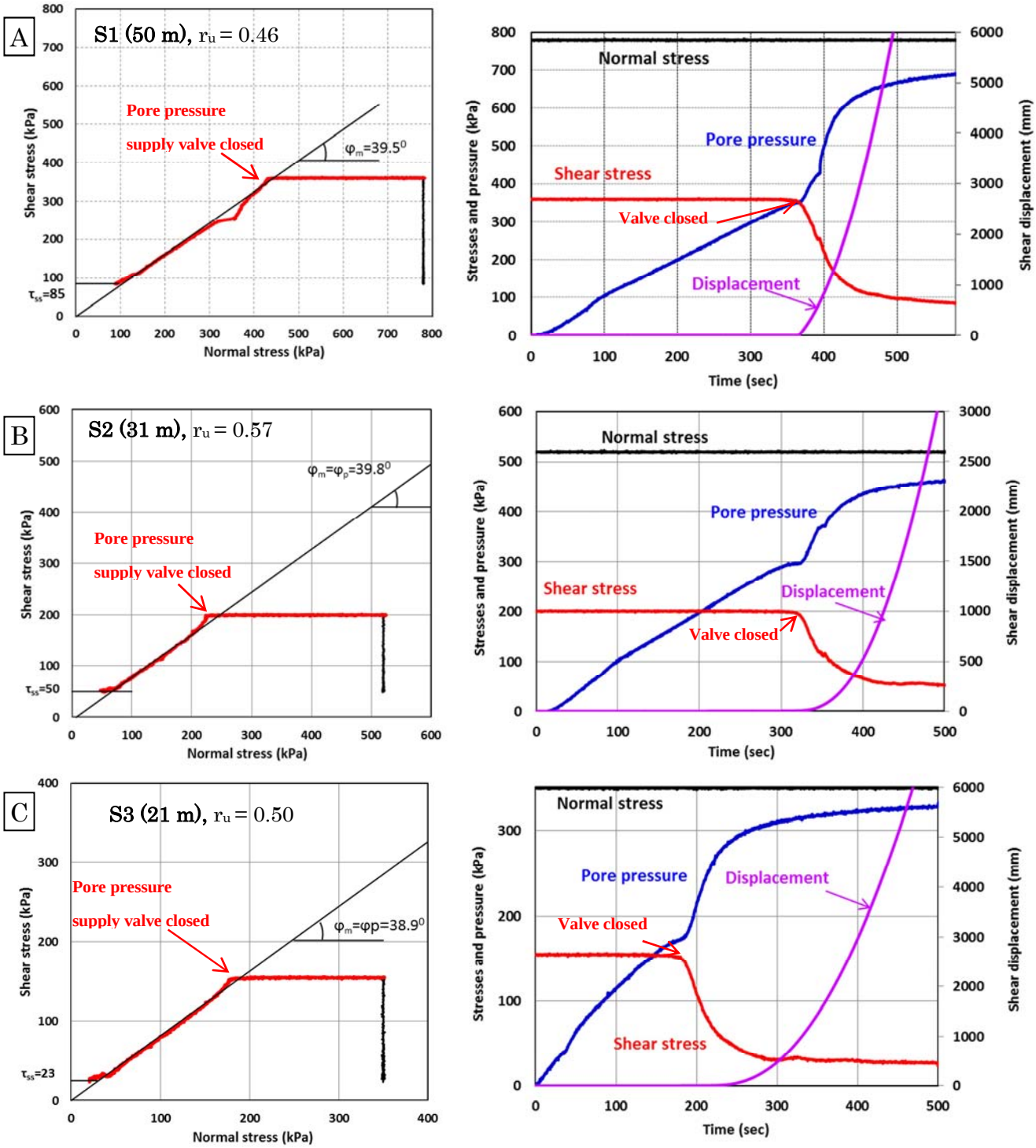

Fig. 7 Pore pressure control test on Haivan drilling cores (A: Sample S1 Normal stress=780 kPa, Shear stress=360 kPa, B_D=0.99, Δu/s=1 kPa/s; B: Sample S2 Normal stress=530 kPa, Shear stress=200 kPa, B_D=0.96, Δu/s=1 kPa/s; C: Sample S3 Normal stress=350 kPa, Shear stress=150 kPa, B_D=0.97, Δu/s=1 kPa/s).

Ring-shear tests to simulate the motion of Haivan landslide

In order to investigate the motion of the landslide, we collected another sample (S4) from 5.6 to 6.0 m depth. We assumed that S4 could represent soils in the lower slope. From figure 5, the peak friction angles of three samples were around 40°, so we assumed that sample S4 was the same value. When a landslide mass on the upper slope moves, it applies undrained loading to the soil mass on the lower slope and initiates motion of the lower slope in addition to the motion from the upper slope. A study of a landslide-induced debris flow, where the landslide mass in the slope moved onto and mobilized a torrent deposit, was reported by Sassa et al. (2004). Figure 8 presents the test result of an undrained dynamic loading test simulating this scenario. Firstly, the initial normal stress and the initial shear stress (σ_o=100 kPa, τ_o=27 kPa, corresponding to around 6 m deep and an 15° slope) were loaded in the drained condition to reproduce the initial stress. The normal stress was increased to 500 kPa as undrained load, corresponding to the depth of 28 m. If the lower slope mass can resist the undrained load from the upper slope without raised pore-water pressure, it may resist around 420 kPa (500 kPa × tan (40°) in this dynamic loading. However, as seen in Figure 8, a high pore-water pressure was generated in the undrained loading. The sample failed at 82 kPa and its steady state stress was 22 kPa. The landslide mass from the upper slope should scrape off a layer of the lower slope and move together as a combined greater mass toward the seaside

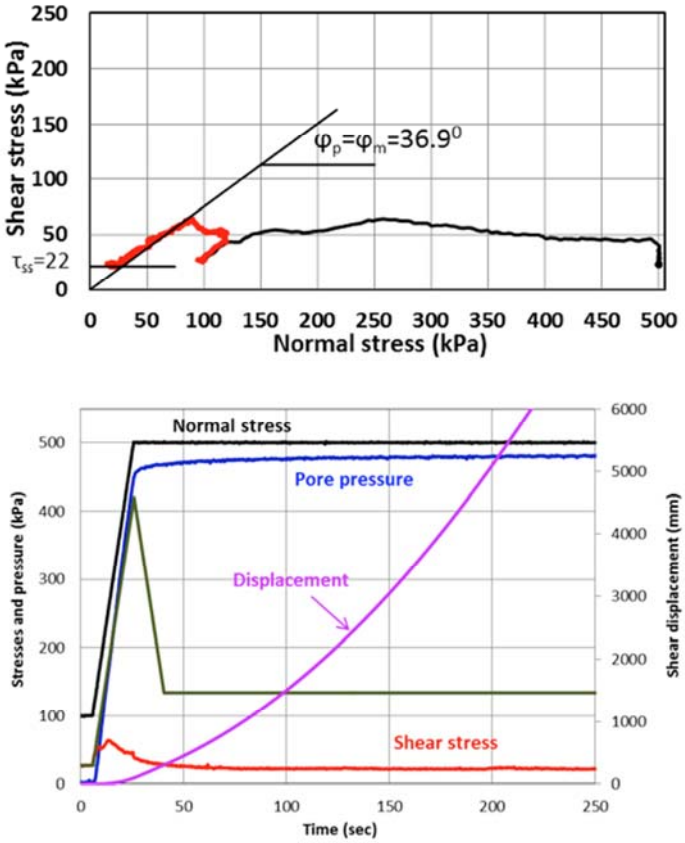

Fig. 8 Undrained dynamic loading test on sample S4 (6 m). B_D=0.98, initial stresses (σ_o=100 kPa,τ_o=27 kPa).

Application for Landslide Hazard Assessment of the Haivan Station

According to the lithological description (Figure 2), pore water pressure test results (Figure 7), and inclinometer measurement (Figure 3), the most serious case is that landslide sliding surface at around 50 m. Therefore, the authors performed the landside simulation with test results on drilling core S1 at the depth of 50 m.

There is no earthquake occurred in the study area and landslides are often triggered by rainfalls. The simulation of the Haivan station landslide was conducted by increasing the pore-water pressure ratio (r_u) as the triggering factor. The shape and the depth of Haivan landslide were created based on the results of drilling and investigation.

The parameters used in the computer simulation were achieved mainly from test results of the ring-shear apparatus (ICL-2), others were obtained from field investigation. Those data are listed in the Table 1.

(1) The steady-state shear strength (τ_{ss}) of sample S1 obtained from the pore water pressure control test under

normal stress of 780 kPa (Figure 7A) is 85 kPa. For the landslide moving area τ_{ss} =22 kPa (Figure 8).

(2) Peak friction angle (φ_p) obtained from undrained stress control test under normal stress of 780 kPa (Figure 6a) is 39.8°. Friction angle during motion (φ_m) is 38°.

(3) Lateral pressure ratio k: 0.4–0.9. We assumed the ratio to be 0.9 under the sea. Outside of the landslide, it was 0.4 (unsaturated). It was 0.6 in the source area.

(4) The shear displacement of shear strength reduction was estimated from undrained shear stress control test. Figure 9 shows the critical shear displacement for starting of strength reduction (DL) is 6 mm and the starting of steady state (DU) is 900 mm.

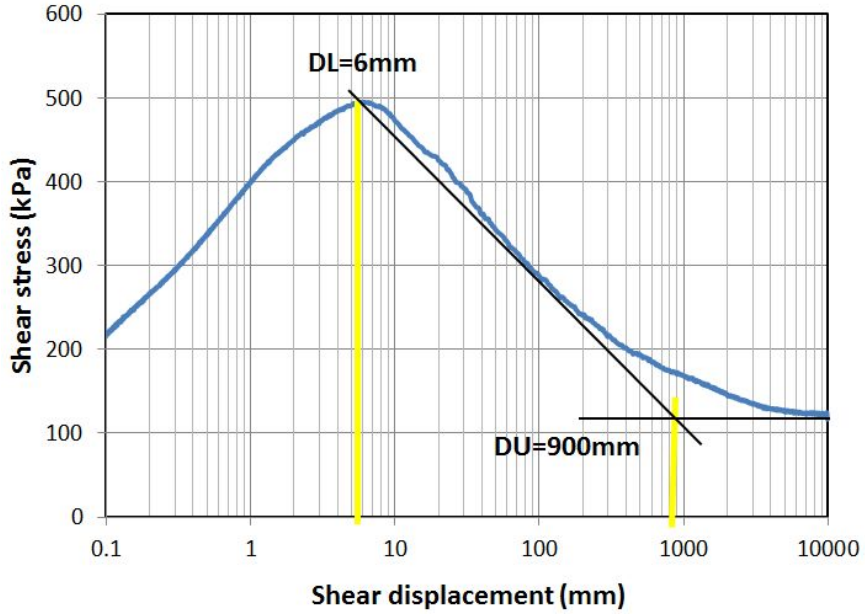

Fig. 9 Shear displacement and shear resistance path of undrained stress control tests on Sample S1 (50 m)

(5) Pore-pressure generation rate Bss was 0.7 – 0.9 in the source area and moving area. Outside of the landslide, it was 0.3 (unsaturated).

(6) The saturated unit weight of sample was 21.2 kN/m^3, and the dry unit weight was 18.8 kN/m^3 at 1 MPa normal stress. In shallower areas, the value would be smaller and we assumed a single value of 19.0 kN/m^3 for the entire area.

(7) The pore water pressure control ring-shear test on sample S1 (Figure 7a) indicated that pore pressure ratio r_u = 0.46 would trigger the landslide in Haivan area. Therefore, the value of r_u was increased from 0 to 0.5 in the computer simulation as the triggering factor of the landslide.

To assess the risk in the Haivan station landslide in the most serious case (τ_{ss}=85 kPa), four computer simulations were performed with different values of pore-water pressure ratio as 0.25, 0.30, 0.45 and 0.50. In the case of r_u=0.25, pore-water pressure ratio pore pressure was increased from r_u=0.0 at the beginning of the simulation to r_u=0.25 with Δr_u=0.01/s and keep constant of r_u=0.25. The same processes were conducted with r_u of 0.30, 0.45 and 0.50. The computer simulations were conducted until the zero velocity for all meshes appeared (Sassa 2010). The simulation results of the landslide were presented in Figure 10. Yellow line is the potential landslide border, blue color balls present the current state of the Haivan slope, and red color balls represent the moving mass. In the computer simulation, no landslide occurs in the case of pore pressure ratio r_u=0.25 (Figure 10a). Figure 10b, c, present the cases with local failure are observed, but those stop without further progressive failure. In the case of maximum r_u of 0.30, local failures occurred but limited, in mostly the right side of the slope. When r_u of 0.45, local failures occurred at the right side, in the central and in the upper part of the slope. When r_u was given as 0.5 (Figure 10d), the whole landslide mass was formed and moved over the railway. The total volume of the landslide is 3.53 x 10^6 m^3.

Table 1 Parameters of Haivan landslide used in LS-RAPID simulation

Parameters	Value	Source
Parameters of Soil in the source area (deeper area)		
Steady state shear resistance (τ_{ss}, kPa)	85	Test data
Lateral pressure ratio ($k=\sigma_h/\sigma_v$)	0.4-0.9	Estimated
Friction angle at peak (ϕ_p, degree)	39.8	Test data
Cohesion at peak (c, kPa)	20	Estimated
Friction angle during motion (ϕ_m, degree)	38.0	Test data
Shear displacement at the start of strength reduction (DL, mm)	6	Test data
Shear displacement at the start of steady state (DU, mm)	900	Test data
Pore pressure generation rate (B_{ss})	0.7-0.9	Estimated
Total unit weight of the mass (γ_t, kN/m^3)	19	Test data
Parameters of Soil in the moving area (shallower area)		
Steady state shear resistance (τ_{ss}, kPa)	22	Test data
Lateral pressure ratio ($k=\sigma_h/\sigma_v$)	0.8-0.9	Estimated
Friction angle at peak (ϕ_p, degree)	39.8	Test data
Cohesion at peak (c, kPa)	20	Estimated
Friction angle during motion (ϕ_m, degree)	38.0	Test data
Pore pressure generation rate (B_{ss})	0.7-0.9	Estimated
Total unit weight of the mass (γ_t, kN/m^3)	19.0	Test data
Triggering factor		
Pore pressure ratio changing during rain in the potential shear zone (r_u)	0-0.50	Test data
Other factors		
Slope angle (θ, degree)	20-25	Investigated
Unit weight of water (γ_w, kN/m^3)	9.8	Normal value

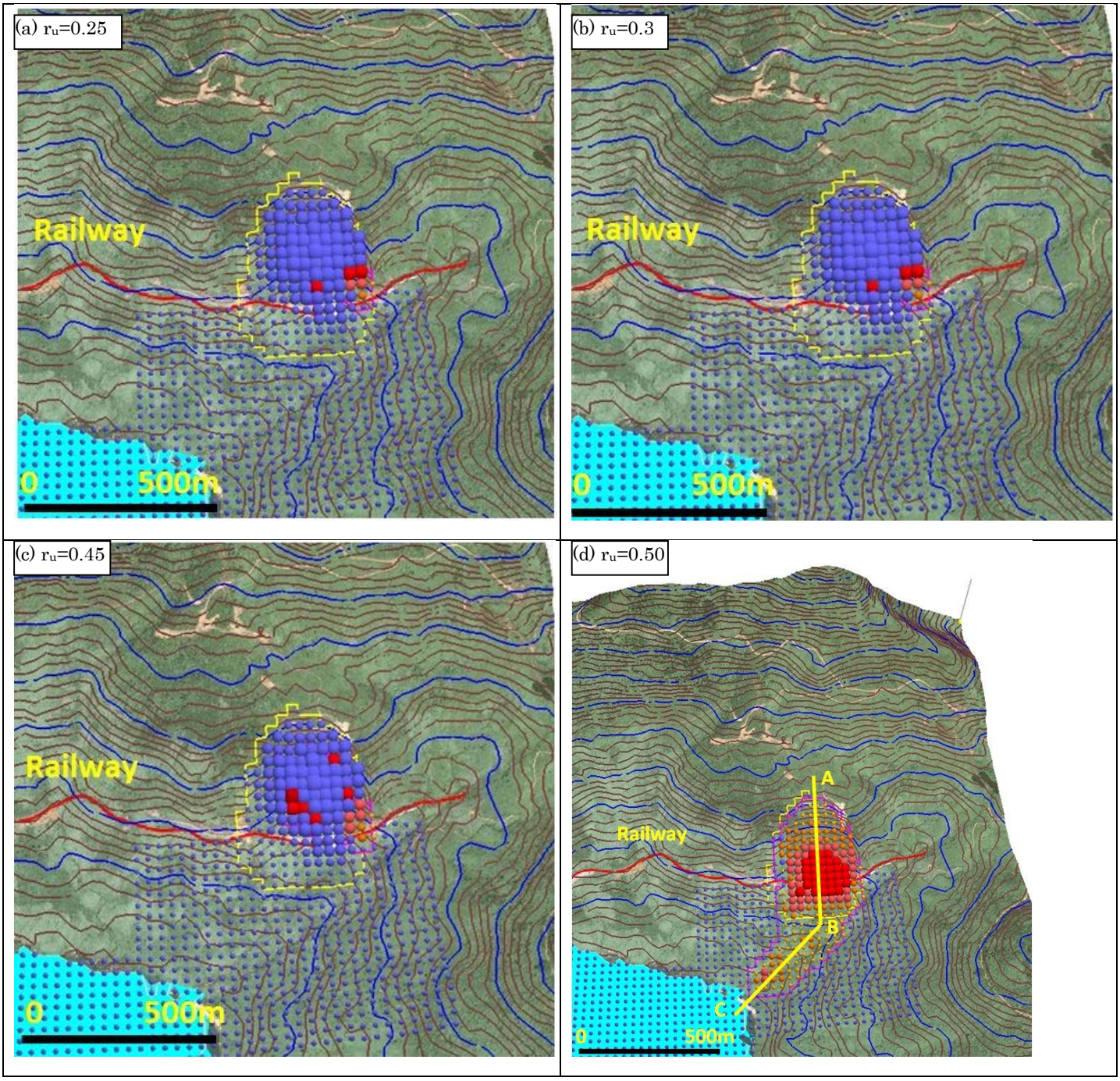

Fig. 10 Landslide deposits (a,b,c,d. landslide deposits with r_u=0.25, 0.30, 0.45 and 0.50; e. Haivan landslide (Google earth photo); f. A-B-C section of Haivan landslide).

Figure 7a shows that failure will be occurred when the pore water pressure increased up to 360kPa, a pore-water pressure ratio r_u = 360/780 = 0.46 for sample at 50 m. In addition, the above simulation results show that local failure occurred when r_u = 0.45 and landslide formed when r_u = 0.46. Therefore, the value of pore water pressure ratio r_u = 0.46 was expected to cause failure of the landslide. To study the landslide development process in detail and assess the exact value, computer simulation was performed with pore-water pressure ratio pore pressure going up from r_u=0.45 at the beginning of the simulation to r_u=0.46 in 100 seconds (incensement pore water pressure ratio is 0.0001) and keep constant of r_u=0.46. The result was shown in Figure 11a, b, c, d. At 1 s, the pore-water pressure reached 0.4501, failure was started at the middle part of the slope and at the right side of the slope. At 10 s, r_u reached 0.4510 failure spread the lower half of the slope with velocity of 2.0 m/s. At 47 s, r_u reached 0.4547 whole landslide mass was formed and moved down with the velocity of 12.7 m/s. At 89 s, the landslide mass stopped and deposited.

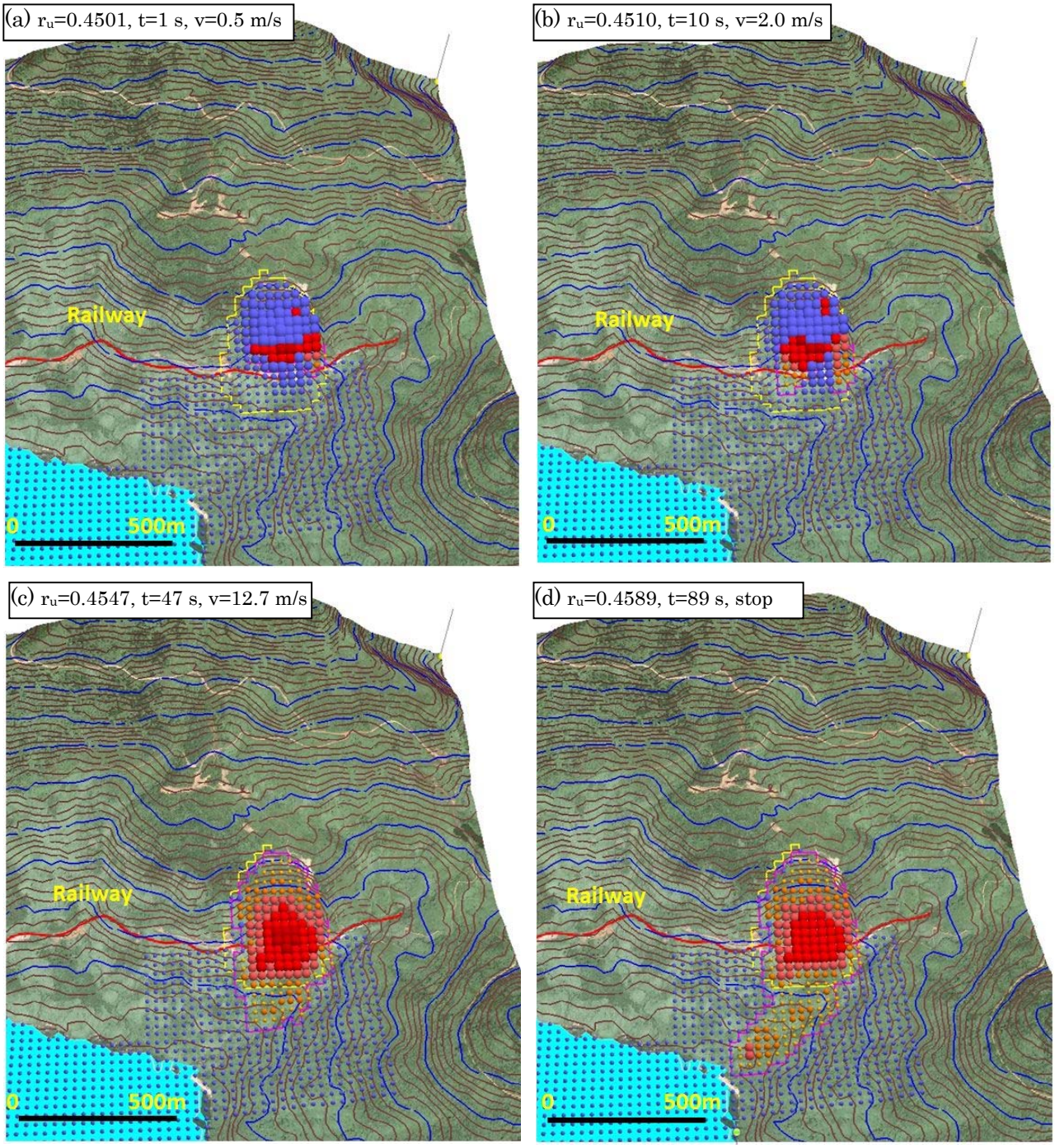

Fig. 11 Landslide development process (τ_{ss}= 85 kPa, DU= 300 mm, DL =3000 mm) (a. r_u=0.4501, t=1 s; b. r_u=0.4510, t=10 s; c. r_u=0.4547, t=47 s; d. r_u=0.4589, t=89 s)

The LS-RAPID results indicated the landsides area (Figure 12a) that was similar to those estimated by site investigations (Figure12b). As shown in the simulation results, the national railway line will be destroyed when the landslide occurs (Figure 12c). The overburden height is about 16.4 meters above the railway.

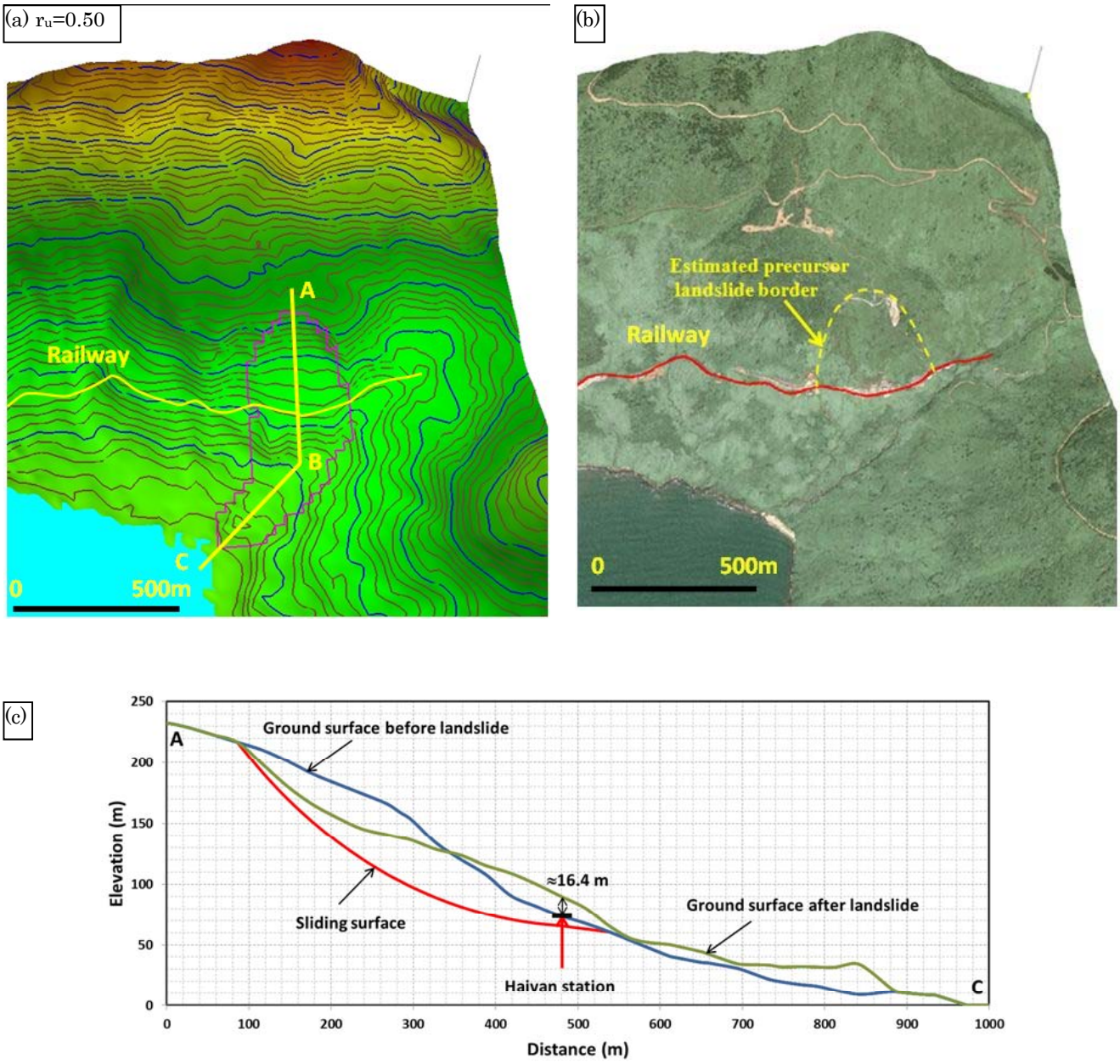

Fig. 12 Risk assessment of the precursor stage of landslide in Haivan station (a: Landslide deposit; b: Google earth photo; c: A-B section of the precursor stage of landslide in Haivan station.

Conclusion

This research is the first application of the undrained dynamic loading ring shear apparatus to the sample drilled and cored from a precursor stage of landslides. According to the results of the ring-shear tests and computer simulation on the samples taken from Haivan Landslide area, the conclusions can be described as follows:

1) Undrained tests with ICL-2 were success in the monotonic speed-control test, monotonic stress-control test, pore-pressure control test on the drilling cores.

2) The results of the pore-pressure control tests on the drilling cores for simulating the initiation of the rainfall-induced landslide indicated that a minimum pore-pressure ratio of 0.46 could cause the landslide with the depth of the sliding surface of 50 m. This is consistent with the obtained data from the inclinometer measurement and the lithological description of the boring log. Other soil parameters of the samples, such as peak friction angle, friction angle during motion, were gained from the drain speed control tests, and undrained shear-stress control test. They are all reliable with the nature of the sample. Then, these parameters were input to the LS-RAPID software to simulate the process of a precursor stage of landslide in Haivan station.

3) To assess the risk in the Haivan station landslide, four computer simulations were performed with different values of pore-water pressure ratio (r_u=0.25, 0.30, 0.45 and 0.50) as the triggering factor. A detailed simulation process was also carried out to assess the exact value of the triggering factor. All the simulation results presented that the local landslide occurred from a middle point of the slope when the pore water pressure r_u reached the value of 0.3. The whole Haivan station landslide mass was formed after r_u reached 0.4547 with the maximum velocity of 12.7 m/s and the national railway line was destroyed. The total landslide volume of the landslide was estimated to be 3.53 x 10^6 m^3. The overburden height is about 16.4 meters above the railway.

Acknowledgments

The design and construction of the ring-shear apparatus ICL-2, was conducted under the support of SATREPS (Science and Technology Research Partnership for Sustainable Development) program of the Government of Japan. This research is a part of the project for Development of Landslide Risk Assessment Technology along Transport Arteries in Vietnam signed on July 27, 2011 between ITST of MOT Vietnam and JICA.

References (in the alphabetical order)

Bishop AW, Green GE, Garge VK, Andersen A, Brown JD (1971) A new ring shear apparatus and its application to the measurement of residual strength. Geotechique 21, pp 273–328

Catane SG, Cabria HB, Tomarong CP, Saturay RM, Zarco MA, Pioquinto WC (2007) Catastrophic rockslide-debris avalanche at St. Bernard, Southern Leyte, Philippines. Landslides 4(1), pp 85–90

Lam HQ, Dang K, Pham VT, Doan HL, Nguyen KT (2014) Recent development of the new high stress undrained ring-shear apparatus (ICL-2) and its application. Proceeding of SATREPS 2014 Workshop "Landslide Risk Assessment Technology", 29-30 July 2014 in Hanoi, Vietnam, pp 168-173

Miyagi T, Yamashina S, Esaka F, Abe S (2011) Massive landslide triggered by 2008 Iwate–Miyagi inland earthquake in the Aratozawa Dam area, Tohoku, Japan. Landslides 8(1), pp 99–108

Nakada S, Suzuki H, Furuya T (1992) Volcanic hazard at Unzen, Japan. Int Newsl Landslide News 6, pp 2–6

Nakada S, Suzuki H, Furuya T (1999) Volcanic hazard at Unzen, Japan. Landslides of the world (editor: Kyoji Sassa). Kyoto University Press, pp 311–316

Sassa K, Fukuoka H, Wang G, Ishikawa N (2004) Undrained dynamic-loading ring-shear apparatus and its application to landslidedynamics. Landslides 1(1), pp 7–19

Sassa K, Nagai O, Solidum R, Yamazaki Y, Ohta H (2010) An integrated model simulating the initiation and motion of earthquake and rain induced rapid landslides and its application to the 2006 Leyte landslide. Landslides 7(3), pp 219–236.

Sassa K, He B, Miyagi T, Konagai K, Ostric M, Setiawan H, Takara K, Nagai O, Yamashiki Y, Tutumi S (2012) A hypothesis of the Senoumi submarine megaslide in Suruga Bay in Japan—based on the undrained dynamic-loading ring shear tests and computer simulation. Landslides 9(4), pp 439–455.

Sassa K, Dang K, He B, Takara K, Inoue K, Nagai O (2014a) A new high-stress undrained ring-shear apparatus and its application to the 1792 Unzen–Mayuyama megaslide in Japan. Landslides 11 (5), pp 827-842.

Sassa K, Bin H, Dang K, Nagai O, Takara K (2014b) Plenary: Progress in Landslide Dynamics. Landslide science for a safer geoenvironment, Vol. 1, Springer, pp 37-67.

Stark TD, Choi H (2008) Slope inclinometers for landslides. Landslides 5(3), pp 339–350.

Unzen Restoration Office of the Ministry of Land, Infrastructure and Transport of Japan (2002) The Catastrophe in Shimabara—1791–92 eruption of Unzen–Fugendake and the sector collapse of Mayu-Yama. An English leaflet (23 pages)

Unzen Restoration Office of the Ministry of Land, Infrastructure and Transport of Japan (2003) The Catastrophe in Shimabara—1791–92 eruption of Unzen–Fugendake and the sector collapse of Mayu-Yama. A Japanese leaflet (44 pages)

Yin Y, Xing A, Wang G, Feng Z, Li B, Jiang Y (2016) Experimental and numerical investigations of a catastrophic long-runout landslide in Zhenxiong, Yunnan, southwestern China. Landslides (2016). doi:10.1007/s10346-016-0729-

Proceedings of the SATREPS Workshop on Landslides in Vietnam, 2016

The influence of rainfalls on the potential of landslide occurrence on Hai Van Mountain in Vietnam

Pham Van Tien[1), 3)], Kyoji Sassa[2)], Kaoru Takara[3)], Doan Minh Tam[1)], Lam Huu Quang[1)], Khang Dang [2), 4)], Le Hong Luong[1)], Doan Huy Loi[1)]

1) Institute of Transport Science and Technology, Hanoi, Vietnam, e-mail: Phamtiengtvt@gmail.com

2) International Consortium on Landslides, Kyoto City, Japan

3) Disaster Prevention Research Institute, Kyoto University, Kyoto City, Japan

4) VNU University of Science, Hanoi, Vietnam

Abstract Granite rocks are vulnerable to progressive physical, chemical and biological weathering processes in tropical and humid regions. As a result, innumerable landslides have been frequently triggered in granite areas by rainfalls worldwide. Located in the Central Region of Vietnam, Hai Van Pass is one of the highest risk areas prone to rainfall-induced landslides that threaten frequently to safe traffic operations of the national transport systems. The area suffered to several serious damages caused by landslides to infrastructures and environment in the past. This paper presents a preliminary investigation on the influence of rainfalls on the potential of landslide occurrence on Hai Van Mountain in Vietnam through rainfall analysis and ring shear experiments. A detailed analysis indicated that rainfalls are mainly a significant trigger that driven landslide occurrence. An extreme precipitation in 1-day period that has triggered a series of large-scale landslides in 3rd November 1999 has been indicated to reach a 92-year return period value. Whereas, low and medium rainfall events with short-return period like 2005 and 2007 could induce landslides in smaller scale. The simulation result of rainfall-induced landslides on two landslides suspected samples by ring shear apparatus showed that only less/moderate weathered granitic soil samples experienced liquefaction behavior at sliding surface while such a phenomenon has not manifested on strongly weathered granitic rock samples. It means that landslides of weakly weathered granite material (sample 2) are very mobile and highly susceptible to rapid sliding. Conversely, the strongly weathered granite material (sample 1) is not apt to move at the high speed. In addition, sample 2 is more vulnerable to rainfall-induced landslides because its shear resistance strength was weaker than that of sample 1 under the rainfall impact (Tien et al., 2015). Understanding the influence of rainfalls to landslides is very helpful to conduct risk assessment of potential landslides in the study area as an output of the SATREPS project on Development of Landslide Risk Assessment Technology along Transport Arteries in Viet Nam.

Keywords SATREPS project, Hai Van, landslides, rainfalls, ring shear apparatus, liquefaction, mobility

Introduction

The case study is Hai Van Mountain as a pilot area of the SATREPS project on Development of Landslide Risk Assessment Technology along Transport Arteries in Viet Nam (the SATREPS project). The area is located in the north of Da Nang City, central region of Vietnam with the geographical position at 16°11' N of north latitude and 108°7' E of east longitude in a transition zone of the northern and southern climate (Fig. 1). The mountain belongs to Annamite Mountain Range in Indochina Peninsula and stretches to the sea with height ranging from 500 m to 1,500 m above sea level. The range divides the Mekong drainage on the west from the Southeast Asia Sea drainage on the east.

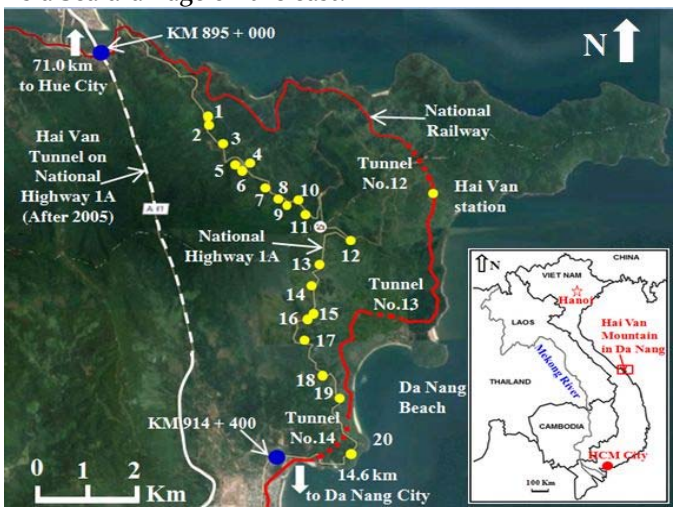

Figure 1 Location of Hai Van Mountain and landslides along National Highway 1A and landslides near Hai Van Station in 1999 (Tam et al., 2008)

Hai Van Mountain is crossed by two main transport lifelines, including Vietnam's main north–south highway, National Route 1A, and the North–South Railway. Those are very important lifeline systems for developing of economic activities between the Northern and the Southern provinces. The road crosses over the mountain more or less directly, while the railway across closely the coastline, passing through a series of tunnels along the way. Hai Van Mountain is also a tourist ecological zone of Da Nang city and it is well known for its scenic beauty as the most beautiful mountain pass of Vietnam. Currently, some ecological tourist project has been doing in this mountain to promote culture activities and economic development in the area.

Table 1 Typical landslide events recorded by years from 1999 to 2010

Year	Time	Trigger/ duration	Type of events	Location	Volume of failed mass (m^3)	Description of impacts	Economic loss and Cost of measures
1999[(1)]	Nov. 3 - Nov. 4	The 1999 historic storm (1 Nov. 1- Nov. 6)	Landslides, debris flows	In the wide area of Hai Van Mountain and along 20 segments of national highway and on railway near Hai Van Station (See Table 2)	Total volume in the Hai Van Mountain about 2 million m^3	Traffic jam in 8 days, traffic lifeline destroyed severely	30 Billion VND (2.7 Million USD)
2004[(2)]	1:00 am to 2 am, 26 Nov.	Intensive rainfall (Nov. 24- Nov. 27)	Landslides	- Hai Van Station - 14 landslides points on the highway (KM905+500 - KM906 and KM 908+500)	- Total 30,000 m^3 - 5,000 m^3 at Hai Van station	Traffic jam for 2 days	22 Billion VND (2 million USD)
2005[(3)]	Nov. 1	Typhoon No. 8 (Oct. 31- Nov. 1)	Landslides and debris flows	- Tunnel No.12 (KM907+250) - Other points on the road	- 7,000 m^3(only at the Tunnel)	Traffic jam for 2 days	1.2 Billion VND (80,000 USD)
2007[(4)]	Nov. 11 and Nov. 12	Typhoon No.5 (Lekima), Sep. 30- Oct. 3	Landslides, debris flows and rock avalanche	- On railway: Tunnel No. 13 (KM 770+830) and KM 757+100 - Along highway (Km 905+250, 907+300, etc): 20 points > 100 m^3 and 100 points < 50 m^3	- Total 32,000 m^3 - 13,000 m^3 (only at the Tunnel)	- Damaged to highway - Destroyed 88 m of the railway - The tunnel buried, traffic jam in railway for 6 days/ delayed 10,000 passengers	80 billion VND (4.9 million USD)
2008[(5)]	Oct. 25	Heavy rainfalls Oct. 24- Oct. 25	Landslides	- Tunnel No.10 on the national railway - Along highway	- Total < 100 m^3 - 30 m^3 of soils covered the tunnel No. 10	- Traffic jam - Several small landslides	Undefined
2010[(6)]	Oct. 17	Heavy rainfall (Oct. 16- Oct. 17)	Landslides, rockfalls	- On highway: KM 910 +600 and others	Undefined	- Several small landslides	Less impact

Retrieved from online sources:
[(1)]Wikipedia, Tienphong (2005); [(2)]Vietbao (2004), Vnexpress (2005), Tienphong (2005), Nguoilaodong (2005); [(3)]Vietbao (2005), Tienphong (2005); [(4)]Ministry of Transport (2008), Tienphong (2005), Vnexpress (2007), Tuoitre (2007), Saigongiaiphong (2008); [(5)]Nhandan (2008); [(6)]Dantri (2010)

The study area suffered extensive damages to transportation infrastructures from a numerous landslides and reactive landslides induced by rainfalls. Such landslide phenomena often occur from October to December in rainstorm season. Most of monitored data with regard to landslides was recorded along two main North-South transport lifelines, namely a segment of about 22 km (from Km 894+000 to Km 916+000) on the national route 1A (a total length 2,301 km), and near 21.6 Km (from Km 755+410 to Km 777+500) on the national railway (total length 1,132 km) (Tam et al., 2008). Here, the national route 1A start with Km 0 post begins in Lang Son Province, northern region while the Km 0 point for

national railway is located at Ha Noi Capital in northern region. And a Km post is sited every 1,000 meters.

According to statistical data of Management Unit for roads, landslide phenomena in Hai Van Mountain such as debris flow, sliding, earth flows and earth/rock falls took place in many time in years of 1999, 2004, 2005, 2007, 2010 (Table 1 and 2). Numerous landslides were mostly triggered by long-term period rainfall in weeks or short time high intensive rainfalls deriving from rainstorms/typhoons in last recent years. All above, extreme rainfall-induced landslides occurred most severely in the years of 1999 in a wide area of Hai Van Mountain and along 20 segments of national highway and railway. The total volume of landslides in Hai Van Mountain was about 2 million cubic meters total volume (Tam et al., 2008). Continuously 3-day rainfalls with high intensity resulted from the historical storm triggered extensive landslides. The volume of landslides varied from 100 m^3 to 10,000 m^3 and the biggest one is a landslide near the Hai Van station (Tam et al., 2008). The detail of past landslide events in Hai Van Mountain is presented in Table 1 while the locations and detailed historical record of the 1999 landslide disaster that occurred along the national highway 1A are shown in Fig. 1 and Table 2. Photos of several landslides and its impacts are illustrated in Fig. 2 below.

Table 2 Historical data of landslide events along National Highway 1A in 1999

No.	Location of road segment	Total volume (m^3)	Types and Descriptions
1	KM 898+000 - KM 899+000	3,600	Landslides were distributed sparsely
2	KM 899+100	500	Landslides
3	KM 900+000 - KM 901+000	350	Landslides + Rockfalls
4	KM 901+100 - KM 901+300	5,000	Surface water caused erosions + landslides caused traffic congestion seriously.
5	KM 901+300	28,000	Landslides and falling of foot-slope next to a stream, causing a traffic jam
6	KM 901+500	700	Landslides
7	KM 902+150	1,500	A reinforced concrete pile culvert damaged partly, eroded embankment bed and 0.4 m height of earthflows on the road
8	KM 902+550	130	Eroded embankment bed and soil falls
9	KM 902+700	40,000	Landslide destroyed and dissected a section 33m of the road completely, a traffic congestion of 5 days
10	KM 898+000 - KM 899+000	3,000	Water runoff caused erosion of slopes
11	KM 903+100 - KM 903+300	50	Landslides nearby the peak of Hai Van Pass
12	KM 905+600 - KM 905+650	200	Several erosions of embankment bed and landslides
13	KM 906+900 - KM 907+000	400	Erosion-induced landslides, rockfalls and earthflow on the road
14	KM 907+500 - KM 907+550	2,000	Large landslides along 50m length of the road caused a traffic jam seriously
15	KM 908+000	< 50	Landslides sparsely and causing a traffic jam partly
16	KM 908+200 - KM 908+250	< 50	Eroded embankment bed
17	KM 909+100	1,000	Landslides buried a reinforced concrete pile culvert
18	KM 910+150 - KM 910+200	100	Eroded embankment bed and a part of road dissected
19	KM 911+000 - KM 912+000	Undefined	Several small landslides on the slope along the road sparsely
20	KM 912+500 - KM 914+000	Undefined	Several small landslides on the slope along the road sparsely

(Sources: Tam et al., 2008)

Damages to countermeasures on landslides after Typhoon in November 2005 (Photo courtesy)

Rockfalls at Km 908+250 on highway (Tienphong, 2005)

Rock avalanche 2005 (Tienphong, 2005)

Rock avalanche destroyed the railway near Hai Van station (Tuoitre, 2007)

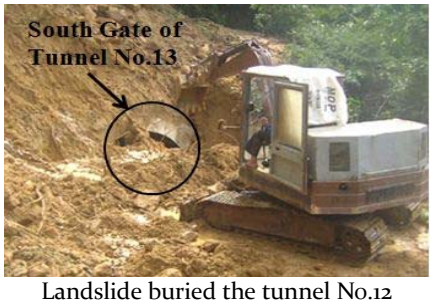

Landslide buried the tunnel No.12 (Vnexpress, 2007)

Rockfalls on highway (Dantri, 2010)

Figure 2 Photos of several landslides and its impacts

Although engineering countermeasures were employed to prevent landslide impacts in this area, such disasters still take place during the rainstorm season in tropical monsoon central region of Vietnam. The SATREPS project targeted to Hai Van landslides for risk assessment, landslide mapping, and monitoring and early warning that will contribute to reduce hazard levels and potential impacts of landslide to the safe operation of Hai Van station and railway system. As a project member, my research on Hai Van landslides aims to investigate the influence of rainfalls on the potential of landslide occurrence through rainfall analysis and laboratory experiment with ring shear apparatus ICL-1.

Soil sampling

A site survey for exploring geological and morphological characteristics of Hai Van landslides was conducted in cooperation with Japanese and Vietnamese experts of the SATREPS project in May 2014. The main finding is that Hai Van Mountain is covered by materials of weathered granitic rocks and debris, which is also described in the geological map of the area (Fig. 3). We selected took two samples with different level of weathering; 1) white less weathered granitic sands and 2) well weathered brown granitic sands from the excavated slopes along a road in the study area (Fig. 4). Those samples are mostly distributed in the wide area of Hai Van Mountain. The materials of specimens were chosen and assumed to be very similar to materials at the sliding surfaces of potential landslides. The first one is a strong weathered granitic rock sample like brown soil sample (hereinafter called as sample 1). Another is a less weathered granitic rock sample like white sand sample (hereinafter called as sample 2. Ring shear tests were performed on those typical samples of Hai Van landslides. The location of two samples and its grain size distribution are shown in Fig. 4&5.

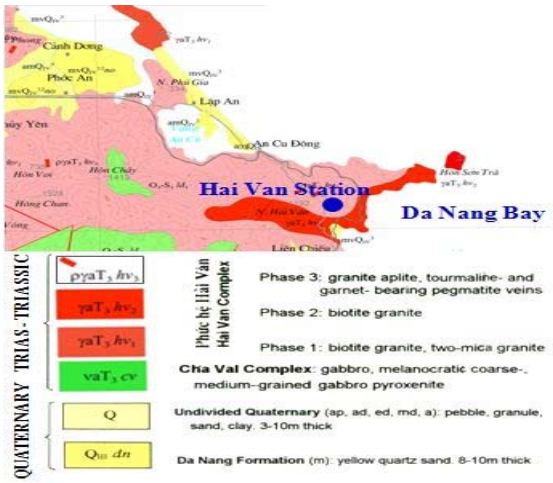

Figure 3 Geological structure of Hai Van Mountain (Geological Survey of Vietnam, 1995)

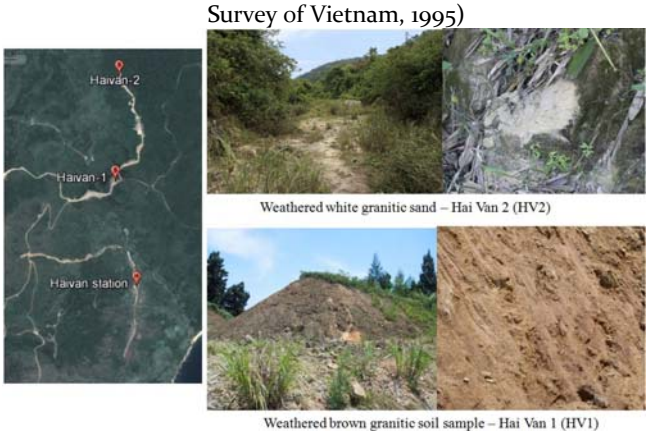

Figure 4 Location of two landslide prone soil samples

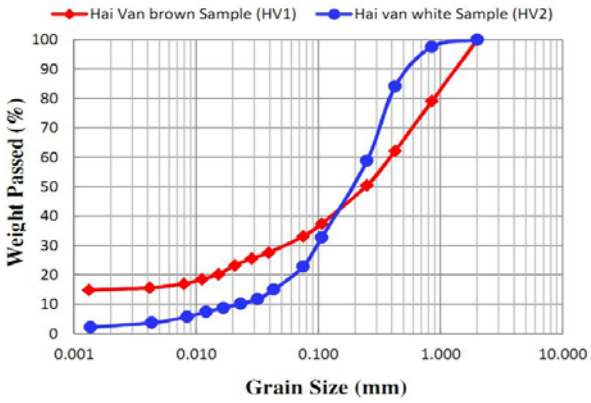

Figure 5 Grain-size distributions of two samples

Ring shear apparatus ICL-1

The un-drained portable ring shear apparatus, ICL-1, was developed by Prof. Sassa and his colleagues in International Consortium on Landslides in 2010 (Maja et al., 2013). The capacity of ICL-1 to keep un-drained condition is up to 1 MPa of normal stress and pore-water pressure, that is almost double than in previous versions (up to 500 kPa in DPRI 5, 6 and 7). The maximum shear velocity is only 5.3 cm/sec, which is smaller than that in previous versions due to a reduction in dimensions. The apparatus has high capacity and reliability to perform the simulation of rainfall-induced landslides through pore-water pressure controlled tests to simulate the failure resulted from an increase of groundwater level. The apparatus has three main components separately, including: (1) Instrument box, (2) Monitoring box and (3) Control box (as shown in Fig. 6).

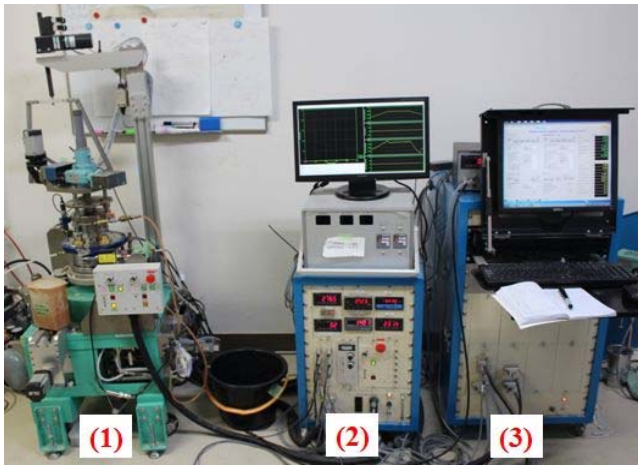

Figure 6 Portable Ring Shear Apparatus, ICL-1 with its instrument box (1), monitoring box (2) and control box (3)

Testing procedures

Firstly, the landslide prone samples were prepared to fully saturate with de-aired water in a vacuum tank. Next, the gap adjustment was conducted by giving an initial contact pressure from 0.8 kN to 1 kN between the upper pair of rings and the rubber edges using the gap control. The gap value was constant during the test to maintain un-drain conditions and to prevent leakage of water and samples during high-speed shearing.

After installing the shear box, the CO_2 and de-aired water circulation were executed to let all bubbles of air come out from the shear box. Next, water leakage and rubber edge friction tests were also made for checking un-drained condition of all tests before building saturated samples inside the shear box. The degree of saturation was checked indirectly by calculating the ratio (BD) of excess pore-pressure increment and normal-stress increment under un-drained condition, the term of BD ratio was proposed by Sassa (1988). In this study, un-drained tests were usually carried out with BD ≥ 0,95.

Landslide prone samples of the sliding surface were normally consolidated to an initial stress condition before testing. The initial shear stress and normal stress is due to the weight of the soil mass above the sliding surface, which was applied slowly to reproduce the initial stress state the same to field conditions. Finally, the simulation of rainfall-induced landslides was carried out by conduct pore water pressure control test. By site survey and based on historical data of landslides recorded, shallow landslides are dominantly distributed in the wide area of Hai Van mountain and the depth of the suspected sliding plane of potential landslides is estimated from 5 m to 20 m. Therefore, the parameters of 230 kPa for normal stress and 120 kPa for shear stress were used in ring shear tests that correspond to 15 m of a depth and a slope angle of 26 degrees.

Rainfall Analysis

Hai Van Mountain is located in the region that dominated by severe tropical monsoon climate with the annual precipitation mostly ranging from as much as 2,000 mm to 3,500 mm. The rain and storm season lasts 4 months, from September to December, but it provides with about 70-80 % of the total precipitation. According to statistical data mentioned above, most of landslides in Hai Van Mountain were triggered by extreme rainfall events with high intensity and short duration during the period of tropical storms and typhoons. In order to understand how rainfalls impacted on landslides in the region, data of daily precipitation at Da Nang Meteorological Observatory in Da Nang city were employed for rainfall analysis. This rain gauge station is about 20 km southeast of Hai Van Mountain. Rainfall data that covers daily rainfall from 1985 up to 2013 (38 years) was provided by Centre of Meteorology and Hydrology in Ha Noi, Vietnam.

The time occurrence of landslides corresponding to high accumulative precipitation is presented in (Fig. 7- a, b, c) that show landslides almost triggered by a long period rainfalls coupled with short-time medium rainfalls providing from typhoons in 2004, 2005 and 2007.

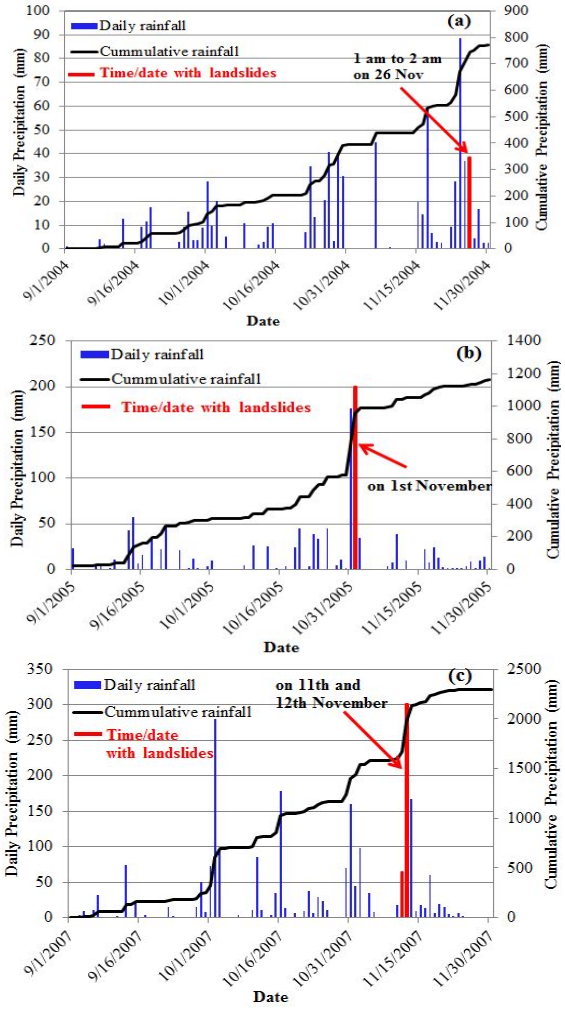

Figure 7 Accumulative precipitation and landslide occurrence in the years of 2004, 2005 and 2007

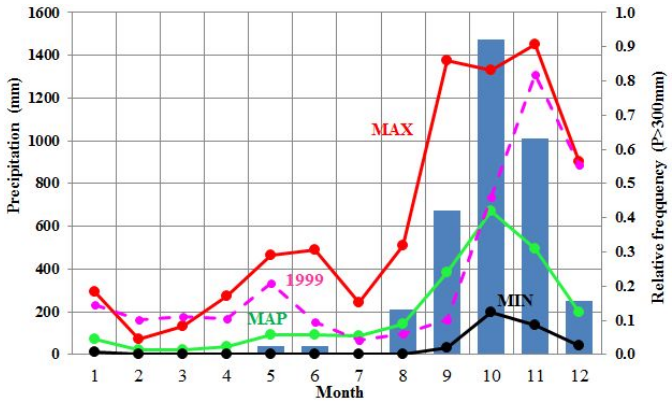

Figure 8 Monthly distribution of rainfall at Da Nang Meteorological Observatory in the 1976-2013 periods

The mean annual precipitation (MAP) in a green color line, minimum annual precipitation (MIN) in a black color line and maximum annual precipitation (MAX) in a red color line are shown for the period from 1976 to 2013 recorded at Da Nang rain gauge station (Fig. 8). As illustrated in the Fig. 8, the available historical record indicates that from September to November in the period (38 years) monthly rainfalls exceeded 300 mm are as much as 75 times (of 114 in a total) and a monthly maximum value is 1,453 mm in November 2011. The dot pink line shows monthly precipitation for 1999 (the left axis). The bar graph shows relative frequency of monthly events when rainfall exceeds 300 mm (the right axis). About 92% of monthly rainfalls are larger than 300 mm in October. A relative frequency is calculated by dividing the number of events exceeded 300 mm in each month by the observed period (38 years).

Annual maximum precipitation of 1-day, 2-day and 3-day in the period of 29 years was employed as an analysis of accumulative rainfall. Events of rainfall-induced landslide were matched with historical record of precipitation in the years 1999, 2005 and 2007 (Fig. 9- a, b, c). As can be seen in Fig. 9, 1-day, 2-day and 3-day accumulative precipitations triggered landslides in 1999 prior to the occurring date are mainly maximum annual 1-day, 2-day and 3-day precipitations in the period from 1985 to 2013. These shows the 1999 extreme rainfalls are the largest events that induced numerous landslides with great destructive impacts on transport systems (seriously destroyed infrastructures along the national highway and railway causing 8 days traffic congestion and a big loss of economic). In comparison with the maximum annual 1-day, 2-day and 3-day precipitations in the period, rainfalls in the years 2005 and 2007 were high, so that triggered small landslides.

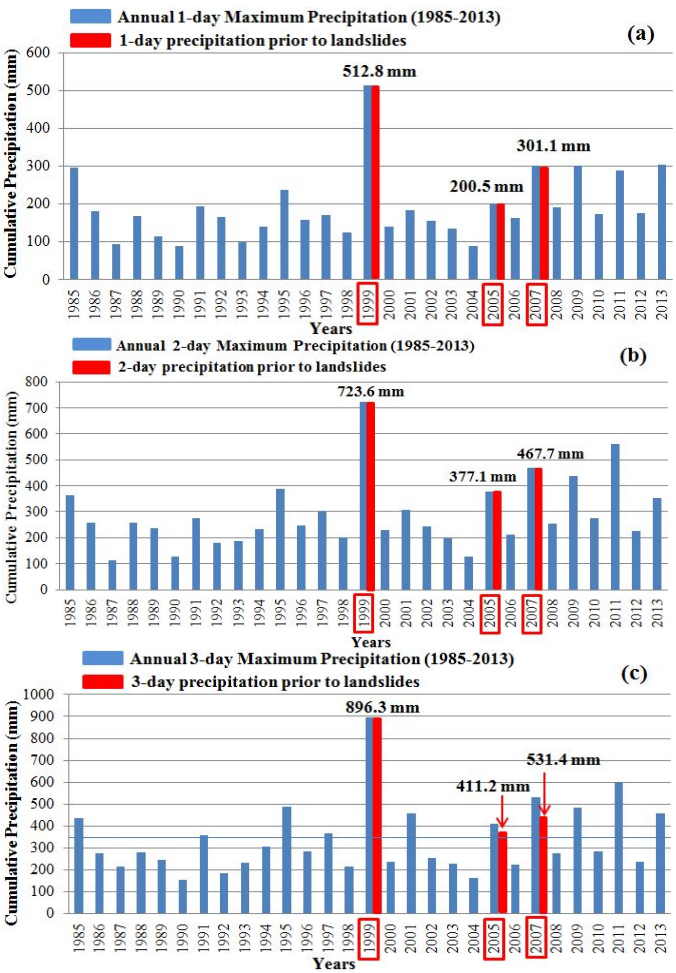

Figure 9 Annual maximum precipitation for a) 1-day, b) 2-day and 3-day in the period from 1985 to 1999 (29 years) at Da Nang station and precipitations triggered landslide occurrences

For a comprehensive analysis of short-term precipitation data, a probability analysis of the cumulative daily rainfall for a 1-day period, 2-day period and 3-day period were done in order to calculate the rainfall probability during the observed period in 1999, 2005 and 2007. In this analysis, six probability distribution functions were used (including Log-normal 3P, Gumbel Max, Frechet, Weibull, Gamma 3P and Log Pearson III) together with the Smirnov Kolmogorov test to estimate goodness of fit (Alias and Takara, 2011). The analysis was supported by using software Easyfit 5.5. The results of rainfall analysis are shown in Table 3.

Table 3 Results of the analysis of cumulative precipitation for the selected periods of 1-day, 2-day and 3-day and occurrence probability

Analyzed Period (days)/ Distribution	Po (mm)[a]						Pc (mm) - RP (year)[b]					
	Av	MIN	MAX	1999	2005	2007	2	5	10	20	50	100
1-day/ Log-Pearson III	191.6	0	512.8	512.8	200.5	301.1	170	246	303	364	451	525
2-day/ Frechet (3P)	287.8	0	723.6	723.6	377.1	414.8	260	370	450	533	649	744
3-day/ Frechet (3P)	337.2	0	896.3	896.3	388.3	433.1	291	421	534	667	888	1096

Where: a Observed Precipitation, b Calculated Precipitation for the 2/5/10/20/50/100-year Return Periods (RP), analysed periods are 1-day, 2-day and 3-day period prior to the date landslide occurrence

Table 3 summarizes the results of the analysis, showing the basic statistical indicators of the analyzed data series (average, maximum and minimum as well as the annual data in 1999, 2005 and 2007) and the values calculated for the characteristic return periods (2 to 100 years). According to the results of the analysis, the observed cumulative values of 1-day, 2-day and 3-day of rainfall in 1999 matches the rainfall with a 92, 89 and 52 year return period (RP), respectively. While, those observed values of 1-day, 2-day and 3-day of rainfall in 2005 are corresponding to 4, 5.5 and 4-year return period. In 2007, the calculated values of rainfall for 1-day, 2-day and 3-day period are characterized by 10, 8 and 5.5 year. From those analysis results, it can be said that the 1999 rainfall event is extreme event that is relatively rare. While the 2005 and 2007 events is not so severe rainfall event. The landslides occurred in the 1999 was strongly influenced by the extreme rainfall. As for rainfall events with return period ranging from 5-10 years, rainfall could trigger landslides in small-scale.

To examine the landslide temporal occurrence and trigger factor of extreme rainfall event, landslide record and accumulative precipitation in the 6-day period from 1st to 6th November 1999 are presented in Fig. 10 clearly. The large-scale 1999 landslide events triggered in the midnight of 3th and the dawn of 4th, November by very heavy rainfall. This extreme rainfall was provided by historic storm in the early period of November. Hai Van landslides were induced in corresponding with over 800 mm of 3-day cumulative rainfall approximately from the beginning of 1st to the end of 3rd. As seen on the graph, the accumulative precipitations for 1-day, 2-day and 3-day prior to the date of landslide occurrence (512.8, 723.6 and 896.3, respectively) are approximately 250% to 270% higher compared to the average accumulative precipitations of 1 day, 2 days and 3 days (191.6, 287.8 and 337.2 mm, respectively) in the period from 1985 to 2013 (29 years).

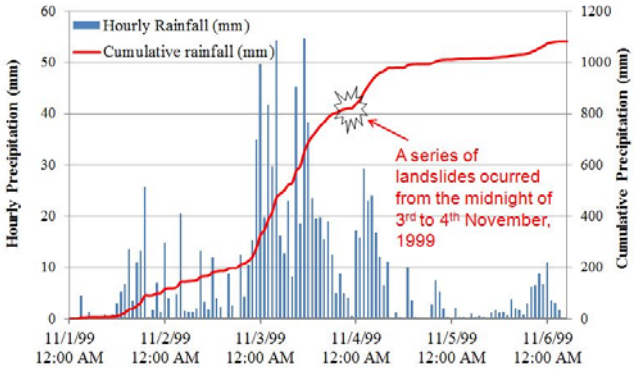

Figure 10 Cumulative precipitations at the Da Nang Meteorological Observatory for the period from Nov 1 to Nov 6, 1999 and landslide occurrences

Test results

The simulation results of rainfall-induced landslides

Analysis of precipitation data showed that rainfall is a main trigger of most of landslides in Hai Van Mountain. To understand characteristics of rainfall-induced landslides, pore-water pressure control test was performed on sample 1 and sample 2. Both samples were consolidated to 230 kPa in normal stress and 120 kPa in shear stress as initial stress condition of the sliding surface. Then power-water pressure was increased up to 200 kPa at a rate of 1.5 kPa/sec for Sample 2 and at a lower rate of 0.2 kPa/sec for sample 1 due to its low permeability. The test results of two landslide samples are shown in Figure 11 & 12.

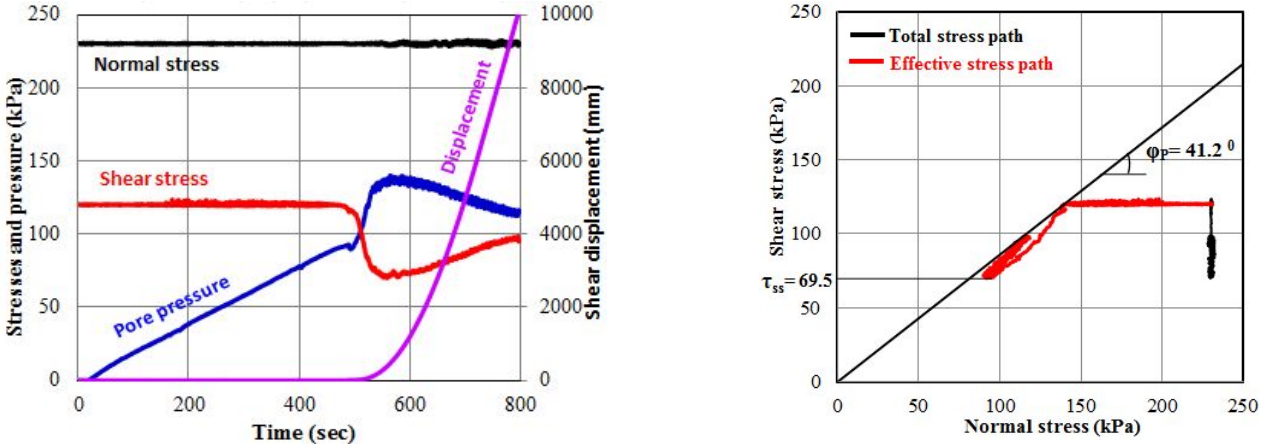

Figure 11 Time series data and effective stress path of pore-water pressure control test on sample 1

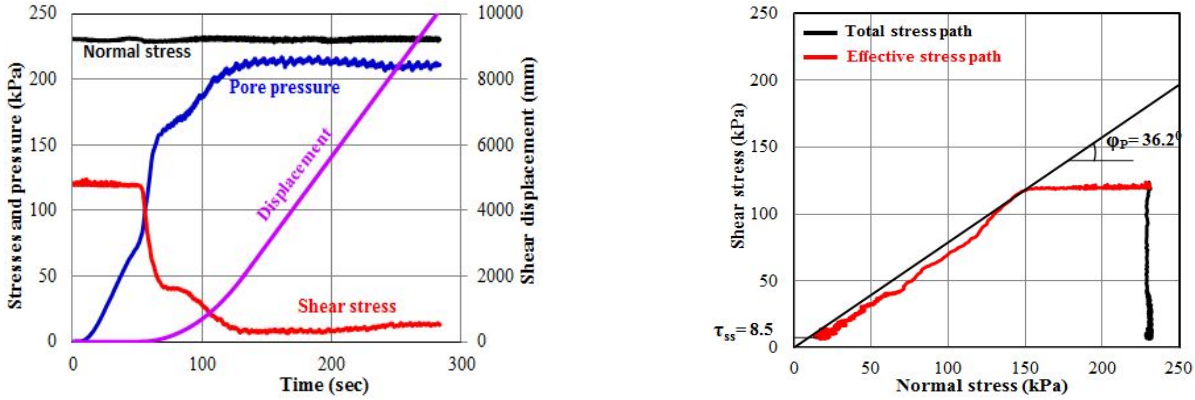

Figure 12 Time series data and effective stress path of pore-water pressure control test on sample 2

Test results show that sample 1 failed around 95 kPa of pore-water pressure increment while failure occurrence of sample 2 occurred at about 80 kPa of additional pore-water pressure value. The critical pore pressure ratios of sample 1 and sample 2 (r_{u1} and r_{u2}) are corresponding to 0.41 and 0.34. For the sample 1, the friction angle at peak stayed at about 41.3° and for sample 2, this angle value was only 36.4°. Steady-state shear resistances of Sample 1 and Sample 2 are 69.5 kPa and 8.5 kPa, respectively. Those soil parameters mean sample 1 shows a greater shear resistance to the sliding and its shear resistance is stronger than that of sample 2. . In addition, the failure of sample 2 resulted from sliding surface liquefaction that generates much excess pore-water pressure, while sample 1 did not have the same behavior. The failure of sample 2 triggered a rapid motion and great loss of shear resistance.

Sliding surface liquefaction behavior of the samples

To assess how grain crushing of samples occurred at sliding surfaces, after the shear test was finished, both disturbed and undisturbed samples were collected from the shear zone and other than sliding zone of the shear box; then grain-size analysis was performed on these samples (Fig. 13).

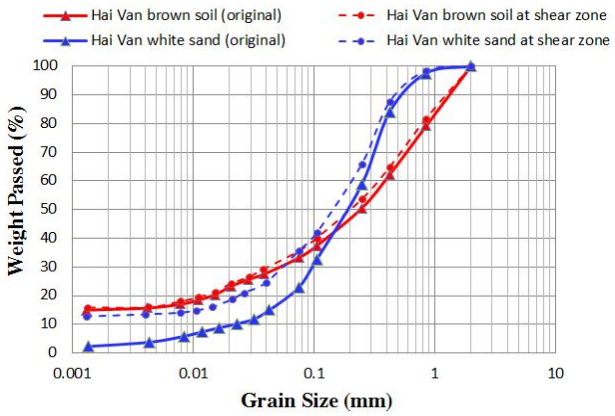

Figure 13 Grain-size distribution of two samples at the sliding surface after shearing until 10 m in compared with two original samples

As seen in Fig. 13, the sample 2 from the shear zone was much finer than its original grain size. This difference is due to the occurrence of grain crushing at sliding surface during shearing. Sample 1 behavior to grain crushing is opposite to sample 2. The sample 2 is higher prone to grain crushing than sample 1. After shearing, sample 2 was crushed into silts or clays with finer grains. In addition, another evidence of grain crushing of sample 2 was also observed visually in a photo taken immediately at a shear zone of the sample

after undrained shearing at a larger shear displacement of 10,000mm in Fig. 14.

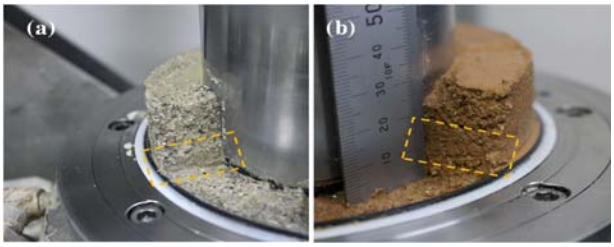

Figure 14 Photograph of the two samples after failure

As seen in these photos, sliding zone can observed clearly for sample 2 but it seems to be difficult to observe sliding zone of sample 1. The shear zone of sample 2 became more silt after shearing at large displacement of 10 m. This change was due to progressive grain crushing. The finer particles resulting from grain crushing and sliding surface are easily to recognize. In contrast, grains of sample 1 seem not to be crushed much and it is very different to observe sliding surface after shearing.

Moreover, in order to examine volume reduction of samples during shearing, drained shear speed controlled tests were conduct to measure change of the volume. In this regard, both samples are tested under drained condition with the same stress state of slope. The change volume of two samples was presented in Fig. 15.

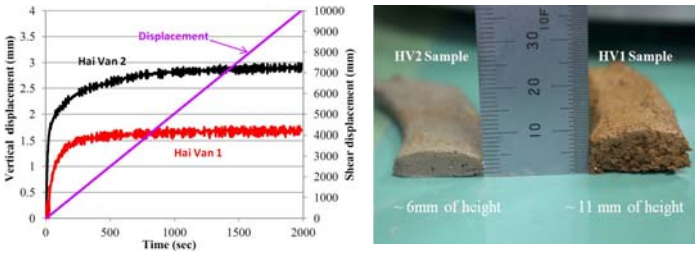

Figure 15 Volume change in drained testing (left) and the different height of the sliding zones of two samples (right)

As seen, the value of vertical displacement for sample 2 is larger than that for sample 1 during testing (as shown in left side of Fig. 15). The larger vertical displacement is a main evidence of grain crushing occurred for sample 2. Consequently, the height of sliding zone of sample 2 is smaller than the sliding zone's height of sample 1.

In this point of view of liquefaction behavior at sliding surface, sample 2 completely experienced with such mechanism due to significant loss of shear resistance, excess pore-water pressure generation and reduction of sample volume. In contrast, for sample 1, the pore pressure continued to increase only until it created a certain value of effective normal stress under which no further grain crushing occurred during shearing. Or it can be said that Sample 1 might be not prone to liquefaction or the sample seems to be slightly liquefied.

As results, grain crushing generated pore water pressure along with acceleration of shear displacement leading to reduce shear resistance to very a lower value τ_{ss} = 8.5 kPa for sample 2 while possibly the Hai Van brown was sheared without liquefaction at sliding surface resulting in no more pore water pressure generated and also shear stress reduced very little.

Discussions and Conclusions

The influence of rainfalls on the potential of landslide occurrence on Hai Van Mountain in Vietnam was examined in this study. The following are some conclusions:

1. Rainfall analysis presented that an extreme precipitation in 1-day period (512.8 mm) that has triggered a series of large-scale landslides in 3rd November 1999 has been indicated to reach a 92-year return period value. Whereas, rainfall events with short-return period like 2005 and 2007 could induce landslides in smaller scale.

2. The simulation of rainfall-induced landslides with ring shear apparatus ICL-1 indicated that sample 2 experienced sliding surface liquefaction completely triggering a loss of shear resistance and increment of pore water pressure as well generation of rapid motion, while sample 1 possibly did not liquefy or partly liquefied as sliding surface softening during slow motion. Liquefaction behavior at sliding surface is a very important factor for assesses Hai Van landslides.

3. Assessment of potential occurrence of landslides induced by rainfalls could be based on shear behavior as well as landslide mechanism of two suspected landslide samples in ring shear simulations. Test results show that the shear strength of the sample 1 is stronger than that in the sample 2 because Sample 1 has a higher shear resistance at the peak, friction angles and residual strength at steady state. In addition, the critical pore-water pressure ratio of sample 1 (r_{u1} = 0.34) is smaller than that value for sample 2 (r_{u2}= 0.41). Those imply that landslides are easier to occur during rainfall condition if the potential sliding surface of landslide mass forms on the layer of sand sample (sample 2). Rainfall-induced landslides are not so high prone to sliding zone of clayed soil layer (sample 1). So it is concluded that landslides are at high risk to occur on slopes of less weathering granitic rocks than their occurrences in slopes of strong weathering granitic rocks due to smaller shear strength parameters of the sample in the less weathering granitic rocks region. This is a very typical characteristic of Hai Van landslides. In fact, this finding was also found in researches of Durgin (1977) and Oyagi (1968). Both authors reported that landslides occur more frequently in areas of moderately weathered granite than in areas of strongly weathered granite.

The understanding of failure mechanism of landslide prone samples and the influence of rainfalls on the occurrence of landslides has a significant importance on assessing landslide risk in Hai Van Mountain. The results of this study much contribute to the output and the success of the SATREPS project between Japan and Vietnam.

Acknowledgments

The study was conducted as a part of the SATREPS project on Development of Landslide Risk Assessment Technology along Transport Arteries in Viet Nam, which is financed by the Japan Science and Technology Agency (JST) and the Japan International Cooperation Agency (JICA). The authors specially thank Prof. Toyohiko Miyagi (Tohoku Gakuin University) and Dr. Tatsuya Shibasaki (Kyoto University) for giving excellent discussions and comments to my research. We deeply acknowledge both agencies and all experts for their important supports during this study.

References

Journals and proceedings

Alias, N.E., Takara, K. (2011): Probability Distribution for Extreme Hydrological Values-Series in the Yodo River Basin, Japan and Kuala Lumpur, Malaysia. International Conference on

Durgin, P.B. (1977): Landslides and the weathering of granitic rocks. Geological Society of America Reviews in Engineering Geology, 3, pp. 127-131.

Geological Survey of Vietnam (1995) Geological map of Huong Hoa-Hue-Da Nang, E-48-XXXV & E-48-XXXVI & E-49-XXXI, Scale 1:200,000.

Miyagi, T. (2015) Landslide classification map in Hai Van Mountain. An output of the SATREPS project in Vietnam.

Ostric, M. (2013): Development of portable un-drained ring shear apparatus and its application. Doctoral Thesis, Graduate School of Engineering, Kyoto University.

Oyagi, N. (1968): Weathering-zone structure and landslides of the area of granitic rocks in Kamo-Daito, Shimane Prefecture. Reports of Cooperative Research for Disaster Prevention, National Research Center for Disaster Prevention, vol.14, pp. 113-127

Sassa K (1988) Geotechnical model for the motion of landslides. Special Lecture of 5th international symposium on landslides, Landslides, Balkema, vol 1. pp 37–55

Sassa, K., Fukuoka, H., Wang, G., Ishikawa, N. (2004): Un-drained dynamic loading ring shear apparatus and its application to landslide dynamics. Landslides 1, (1):7-19.

Tam, D.M, Hanh, N.H, Hung, N.Q, Viet, N.B, Hung, N.V, Thao, P.T, Anh, T.T.V. (2008): Research on Selection and Application Conditions of the New Technologies for Landslide Risk Prevention along National Highways. Research project in transportation sector, Ministry of Transport, 2008, 396 pages (in Vietnamese).

Tien P.V., Sassa, K., Takara, K., Khang D., Loi D. (2015): Analyzing Failure Characteristics and Potential of Landslides in Hai Van Mountain, Vietnam. Proceedings of the 10th Asian Regional Conference of IAEG, Kyoto, Japan, pp. 586-591.

Websites

Dantri (2010) Seriously traffic jams along Hai Van Pass due to heavy rainfalls. http://dantri.com.vn/xa-hoi/giao-thong-nhieu-vung-ach-tac-deo-hai-van-sat-lo-do-mua-lon-1287736827.htm

Ministry of Transport (2009) A state fund of VND 30 billion for structural countermeasures on Hai Van station. http://www.mt.gov.vn/matgt/tin-tuc/988/30846/tcty-duong-sat-vn--dau-tu-them-30-ty-dong-gia-co-duong-sat-qua-deo-hai--van.aspx

Nguoilaodong (2005) Potential hazards on Hai Van Pass. http://nld.com.vn/thoi-su-trong-nuoc/hiem-hoa-lo-lung-tren-dinh-deo-hai-van-133374.htm

Nhandan (2008) Countermeasure Work Completed for the Tunnel No. 10 on Hai Van Pass. http://nhandan.com.vn/xahoi/item/13125202-.html

Saigongiaiphong (2008) National Railway in rainy seaon: Landslide disasters. http://www.sggp.org.vn/xahoi/2008/6/155891/

Tienphong (2005) Rockfalls hazard on the Hai Van Pass. http://www.tienphong.vn/xa-hoi/bay-da-tren-deo-hai-van-28363.tpo

Tienphong (2007) A large landslide burried the Tunnel No. 3 of Hai Van Pass. http://www.tienphong.vn/xa-hoi/mot-duong-ham-deo-hai-van-bi-khoi-dat-da-khong-lo-bit-kin-101981.tpo

Tuoitre (2007) Openning the railway on November 18, 2007. http://tuoitre.vn/tin/chinh-tri-xa-hoi/20071116/18-11-moi-thong-doan-duong-sat-hai-van/229574.html

Vietbao (2004) Thousands of cars in a traffic jam due to landslides on Hai Van Pass. http://vietbao.vn/Xa-hoi/Deo-Hai-Van-Hang-ngan-o-to-bi-ket-duong-do-lo-nui/40057575/157/

Vietbao (2005) Natural hazards on Hai Van Pass. http://vietbao.vn/Xa-hoi/Hiem-hoa-lo-lung-tren-dinh-deo-Hai-Van/30087809/157/

Vietnamnet (2004) Another traffic jam due to rainfalls and floodings on Hai Van Pass. http://vnn.vietnamnet.vn/xahoi/doisong/2004/11/350198/

Vietnam Express (2005) Rockfall hazards on Hai Van Pass. http://vnexpress.net/tin-tuc/thoi-su/hiem-hoa-da-roi-duong-sut-tren-deo-hai-van-2062025.html

Vnexpress (2007) Photos of the railway tunnel buried by landslides on Hai Van Pass. http://vnexpress.net/tin-tuc/thoi-su/anh-ham-duong-sat-hai-van-chim-trong-dat-da-2095718.html

Wikipedia. Flooding in the 1999 historical storm. https://vi.wikipedia.org/wiki/L%C5%A9_l%E1%BB%A5t_mi%E1%BB%81n_Trung_Vi%E1%BB%87t_Nam_th%C3%A1ng_11_n%C4%83m_1999

Proceedings of the SATREPS Workshop on Landslides in Vietnam, 2016

The 28 July 2015 rapid landslide at Ha Long city, Quang Ninh, Vietnam

Doan Huy Loi[(1)], Lam Huu Quang[(1)], Kyoji Sassa[(2)], Kaoru Takara[(3)], Khang Dang[(2,4)], Nguyen Kim Thanh[(1)], Pham Van Tien[(1)]

(1) Institute of Transport Science and Technology, Vietnam

(2) International Consortium on Landslides, Japan

(3) Disaster Prevention Research Institute, Kyoto University, Japan

(4) VNU University of Science, Hanoi, Vietnam

Abstract This report is written as a research result of the Working Group 3 of Vietnam-Japan SATREPS Project, which is a manuscript submitted to an international journal.

From 26 -28 July, heavy rainfall occurred in Quang Ninh province causing serious flooding debris flows and landslides. According to the report of the Central Committee for National Disaster Prevention and Control (CNNDPC-Vietnam) 17 persons were killed, 1,459 households were evacuated and at least 30 houses were fully damaged. Particularly, 8 of the victims died when a landslide buried three houses at Cao Thang ward, Ha Long City. Total initial economic lost in Quang Ninh was estimated about VND 2,000 billion (US$92million). It was the biggest disaster triggered by torrential rains in Vietnam in 2015. Field investigation and ring shear simulation were used to study the initiation mechanism and behavior of the landslide in Ha Long triggered by heavy rainfall. Pore-water pressure changing during rain was estimated by using the Slope-Infiltration-Distributed Equilibrium (SLIDE) model that developed by Montarasio 2008 and Liao 2010, 2012. Ring-shear apparatus (ICL-1) was used to simulate the failure of soils, the formation of sliding surfaces and the steady-state motion of landslides. Landslide dynamic parameters obtained and estimated from ring-shear tests were input to an integrated simulation model (LS-RAPID) to simulate the landslide motion in Ha Long. The simulation results indicated the hazard area that was quite similar to those determined field investigation. In addition, the time of landslide occurrence estimated from rainfall record and LS-RAPID simulation is closed with actual occurrence that was reported by local inhabitants.

Keywords Rapid landslide, Rainfall, Undrained ring-shear test, Computer simulation, SLIDE model, Ha Long, Vietnam

Introduction

Quang Ninh's coordinates are longitude 106º25' to 108º25' east and latitude 20º40' to 21º40' north. Its width from east to west is 195 km (at the widest part) (Wikipedia). Ha Long city is located in the center of province with the complex and diverse topography including mountains, delta, coastal and islands. The North and North East are covered by mountains, containing 70% city's area, the average altitude ranges from 150-250 m, the highest is 504 m. Ha Long' climate is symbolic of the climate of coastal region, the year is divided into two seasons, the winter season and the summer season. The summer season lasts from May to October from November. The average annual precipitation is 1800mm with 80 - 85 % of the annual average falling in the summer season, especially in July and August.

Ha Long is already a highly urbanized and rapidly growing city. Due to the urbanization, many people live in hazard prone areas such as mountainous areas prone to landslides and debris flows in Ha Long city. On 28 July 2015, around 1AM local time, a catastrophic landslide occurred at Cao Thang ward, Ha Long city, Quang Ninh, Vietnam. This disaster claimed 8 deads, 3 houses damaged (Figure 2). It was the biggest disaster triggered by torrential rains in Vietnam in 2015. Total recorded rainfalls in a number of gauging stations in Quang Ninh during 26-30 July were historically highest in the last 40 years (CNNDPC).The cumulative rainfall from 19 PM of 27 July until 7 AM of 28 July reached 296 mm at Bai Chay weather station in Ha Long city (CNNDPC). This is main reason caused the Ha Long disaster. Figure 1 presents the location of landslide study site. Figure 2a,b presents the UAV photo of landslide area and the longitudinal A-B section of the Ha Long landslide. This section based on the digital surface model (DSM) generated by UAV photos after landslide and the 5-m topographical map before landslide. The maximum vertical depth is 6.0 m. The objective of this research is to understand the

initiation mechanism and behavior of the landslide triggered by extreme rainfall in Ha Long. This paper will present the occurrence and landslide motion using ring shear apparatus (ICL-1) and computer simulation.

Fig.1 Location map of Ha Long landslide

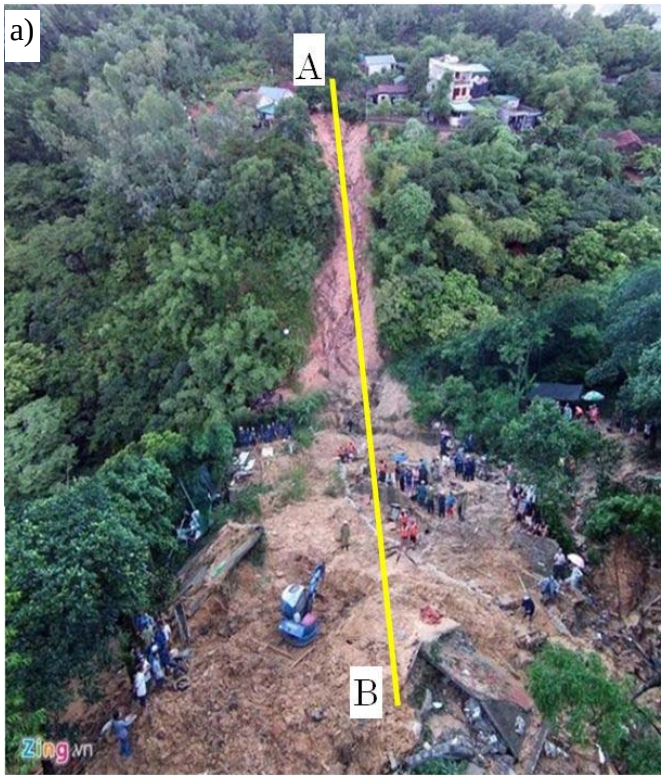

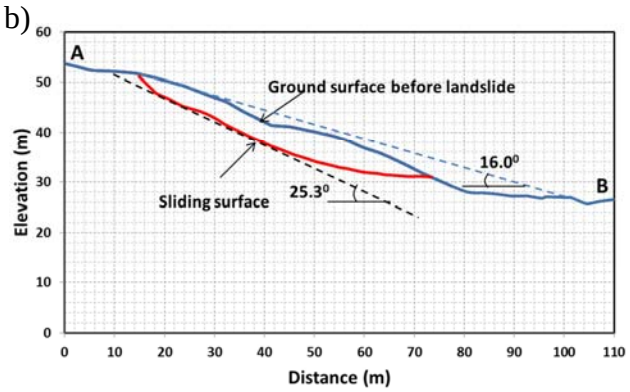

Fig.2 UAV photo (Taken by Zing) (a) and A-B longtitudinal cross section of Ha Long landslide (b)

Geological setting and Sampling

Figure 3 shows the geological map of the Ha Long disaster. In geological characteristics, study area consists of conglomerates, gritstones, sandstones and thin lenses of coal and are formed in Trias formation.

On 10 September 2015, Japanese and Vietnamese researchers investigated the landslide area. Two samples were taken in the source head as shown in Figure 3 and sent to International Consortium Landslide (ICL) laboratory in Kyoto University. Both samples were tested to study characteristic of soil in the source and represented the initiation and motion of Ha Long landslide. Basic geotechnical test results were shown in table 1. Permeability of black sample and brown sample are 4.50×10^{-7} and 3.62×10^{-3} m/s, respectively. Due to permeability changing of two layers, the sliding surface may occur in bottom of brown sand layer. Brown sand sample was used for ring shear tests to find the initiation mechanism and motion behavior of the landslide in Ha Long triggered by heavy rainfall.

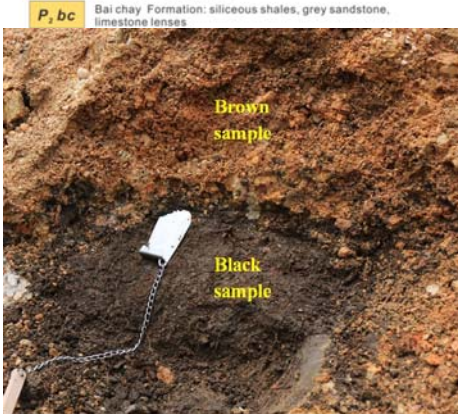

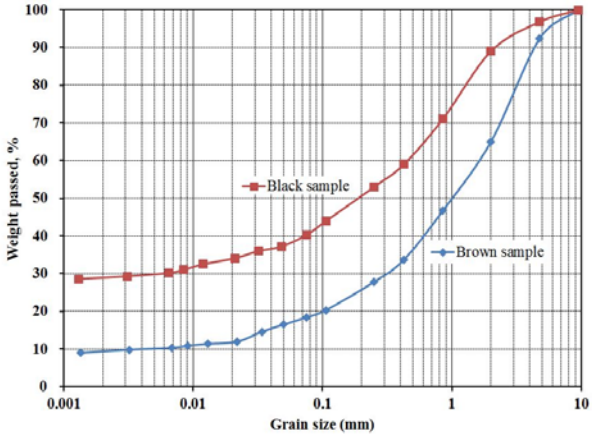

Fig.3 Geological map of study area and sampling

Table 1 Basic geotechnical test results of two samples

Sample	Moisture (%)	Unit weight (kN/m3)	Density (kN/m3)	Permeability m/s
Black sample	26.6	18.7	26.5	4.50x10-7
Brown sample	21.2	19.2	26.7	3.62x10-3

Triggering factors

The Bai Chay weather station in Ha Long city recorded a total rainfall of 387mm between August 27th and 28th. Especially, the cumulative rainfall from 19 PM of 27 July until 7 AM of 28 July reached 296 mm. The main triggering factor of Ha Long landslide is intense rainfall in the short time period.

To simulate the landslides caused by rainfall, pore-water pressure changing during rain needs to be estimated. Based on the research of Montarasio L & Valentino R (2008) and Liao & Hong et al (2010), the SLIDE model can be estimated pore-water pressure changing from rainfall intensity. The assumption is simple that the water depth in a column in the infinite slope is changed by the balance of rainfall infiltration (assumed all rains will infiltrate in to the ground) and the drainage flow from the column. Figure 4 presents the concept of SLIDE Mode. Rainfall penetrates into the soil layer and a saturated layer is formed above the bedrock layer. Then, groundwater will flow along the slope. When the water supply penetrated from the ground surface is greater than the ground-water discharge within the saturated layer, the ground water level will rise, namely the pore water pressure will increase. On the contrary, the groundwater level (pore water pressure) will decrease when the infiltration of rains is smaller than the ground water discharge within the saturated layer.

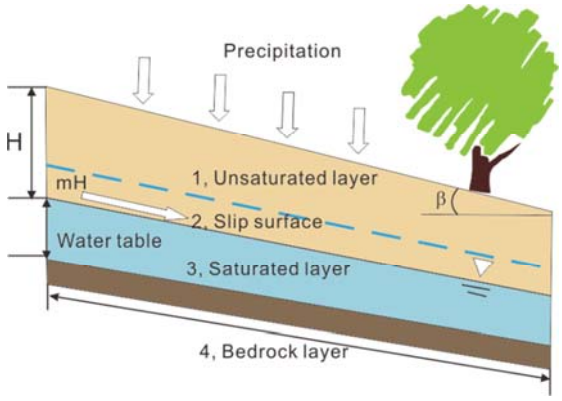

Fig.4 Schematic illustrating the water infiltration the infinite slope (from Liao et al 2010)

According to Liao et al 2010 pore pressure (ΔU) acting at the sliding surface is expressed by equation 1:

$$\Delta U = m.H.\gamma_n.\cos^2\beta \qquad (1)$$

And, changes in the ratio of groundwater layer to the soil layer pressure (m) is calculated by equation 2

$$\begin{cases} m_1 = 0 \\ O_t = K_t.\sin\beta.m_t.H.\cos\beta.\Delta t \\ \Delta m_t = \dfrac{(I_t - O_t)}{n.H.(1-S_r)} \\ m_{t+1} = m_t + \Delta m_t \end{cases} \qquad (2)$$

Where ΔU is pore-water pressure, m is the ratio between the depth of soil layer and the depth of ground water layer, t is time, Δt is time interval, m1 is initial value of m, and mt is calculated at each time-step. Ot represents the water outlet of a finite portion of a slope of finite length L. It is rainfall intensity, and Kt is Average permeability of the soil layer, H is Landslide depth, n is Porosity; β is Slope angle; α is sliding surface angle; Sr is degree of saturation (Liao 2010).

SLIDE model is a simple model neglecting effects of evaporation from trees and vegetation, and also the initial unsaturated infiltration process. However, a simple model is better to use for computer simulation.

The author collected the rainfall intensity at the Bai Chay weather station to identify the landslide occurrence on 28 August 2015. Pore-water pressure rise during the heavy rainfall period was calculated using the SLIDE model. The numbers were used, the average permeability of the soil layer of 0.00362 m/s, degree of saturation of 0.83, thickness of the soil layer of landslide was investigated as 6 m, slope angle was measured approximately 160, porosity was calculated as 0.41.

Excess pore-water pressure ratio (ru) changing during the heavy rainfall period was calculated as trigger factor in LS rapid simulation. It was expresses as: ru = Δu/σ

Where: σ is total normal stress acting on the potential sliding surface $\sigma = H.\gamma.\cos^2\beta$ (γ is unit weight of soil γ=19.2 kN/m3).

Figure 5 shows the relationship between rainfall intensity and pore-water pressure ratio from 0 AM on 26 July 2015. The maximum pore pressure ration is 0.41.

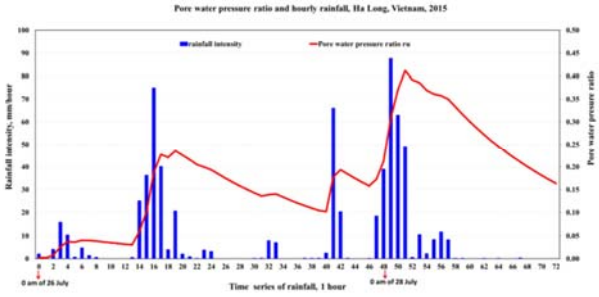

Fig.5 Pore-water pressure calculation by the SLIDE model from the rainfall record monitored at the Bai Chay weather station for each 1 hour from 0 AM on 26 July 2015

Ring shear simulator

Samples are taken from landslide area and set into the shear box. All stresses acting on the potential sliding surface; normal and shear stresses can be reproduced in the shear box. When stresses are high enough to trigger sample failure, a shear surface will be developed within the shear box, and the rotary lower half of the shear box will start turning. During the shearing process, ring shear apparatus measures excess pore water pressure, shear resistance mobilized and shear displacement.

Portable undrained ring shear apparatus ICL-1 was developed for Croatia that is a part of the Croatia-Japan Joint Project "Risk identification and land-use planning for disaster mitigation of landslides and floods in Croatia". It reproduced successfully the high normal stress and an undrained condition up to 1 Mpa. To study the shallow landslide, the capacity of normal stress was decreased to 200 kPa.

Ring shear test results

Undrained monotonic shear stress control test

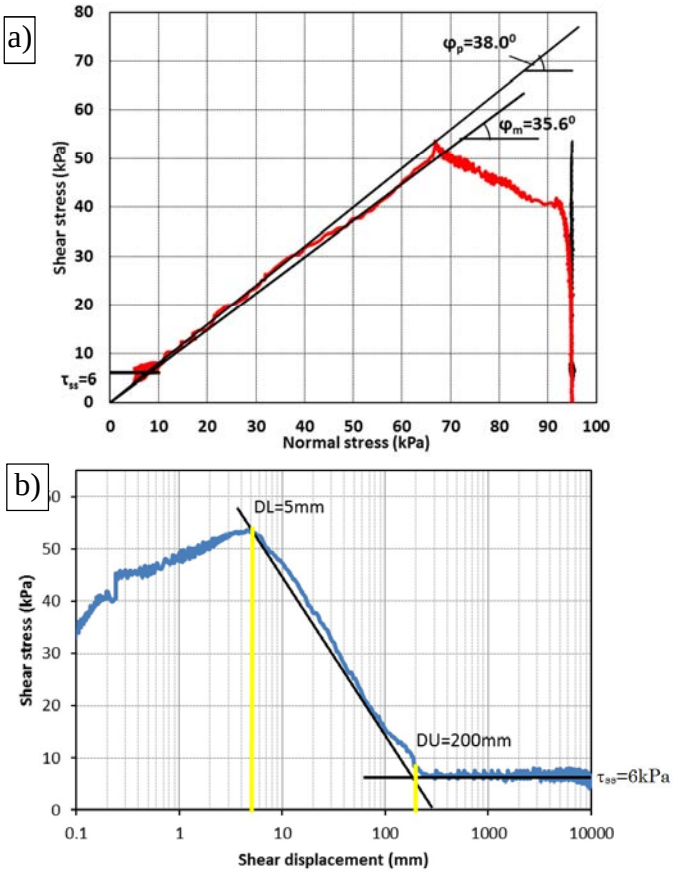

Fig.6 Undrained monotonic stress control test on brown sample (Bd=0.95, normal stress=95 kPa, Δτ/s=0.5 kPa/s). Stress path and time series data (a), Relationship between shear stress and shear displacement (b).

Undrained monotonic shear stress control test was conducted under normal stresses of 95 kpa. This corresponds to the landslide initiation in the field. Normal stress was increased to 95 kPa with a rate of Δσ = 1 kPa/s in the drained condition. After the consolidation, the shear box was then changed to the undrained condition, and shear stress was loaded gradually at a rate of Δτ = 0.5 kPa/s. When the effective stress path reached the failure line, the lower haft of shear box will start to rotate until 10 m of shear displacement. Figure 6 presents the stress paths and time series data of brown sand sample. The steady-state shear resistance was 6 kPa. The friction angle of the peak failure line and friction during motion were 38.0° and 35.6, respectively.

Pore-water pressure control test

Ha Long landslide was triggered by heavy rainfall that can be simulated using ring shear apparatus. The initiation of landslide is caused by pore water pressure increase. In the gentle slope, a high pore pressure is necessary to cause landslide. In order to observe effect of pore-water pressure generation carefully, the initiation of the slope was simulated. Firstly, the sample was saturated (Bd = 0.98), then consolidated to 95 kPa normal stress and 45 kPa shear stress in a drained condition. This preparatory stage was to reproduce the initial stress on the slope (the corresponding slope angel of 25.30), and is shown as a black line in Figure 7.

In order to simulate the pore-pressure induced landslide process, the pore-water pressure was gradually increased at a rate of Δu=0.3 kPa/s up to 95 kPa. Failure occurred at a pore-water pressure of 32 kPa namely, a pore-water pressure ratio ru =32/95=0.34. The friction angle at failure was 36.3°. To monitor the pore-water pressure during shearing, the pore-water pressure supply valve was closed after the failure occurred. Figure 6 shows the stress path go down the failure line during motion and the friction angle during motion of 32.0°

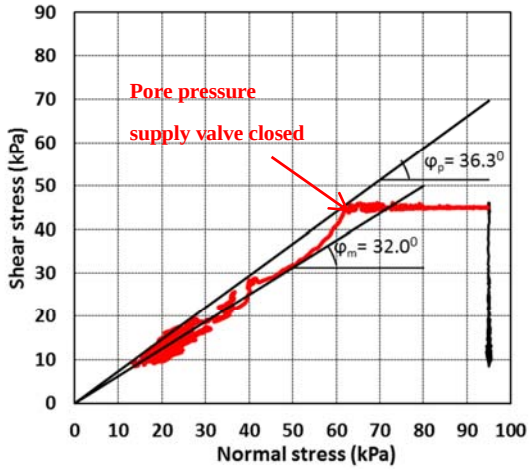

Fig.7 Pore presure control test on brown sample (Bd=0.98)

Application of LS-RAPID and SLIDE model to the 2015 Ha Long landslide

LS-RAPID is a new integrated computer model that can be simulated the initiation and motion of a landslide using soil parameter obtained from ring shear apparatus. This simulation model LS-RAPID was developed from the

geotechnical model for the motion of landslides (Sassa,1988) and its improved simulation model and new knowledge obtained from a new dynamic loading ring shear apparatus (Sassa et al., 2004).

Triggering factors

The 2015 Ha Long landslide was triggered by heavy rainfall. This was calculated by using the SLIDE model. This pore-water pressure ratio was input to LS-RAPID as a graph of triggering factor.

Landslide dynamics parameters

The parameters used in the computer simulation are listed in the table 2.

(1) The steady-state shear strength (τss) of brown sample obtained from the undrained stress control test under normal stress of 95 kPa (Figure 6) is 6 kPa.

(2) Peak friction angle (ϕp) obtained from undrained stress control test under normal stress of 95 kPa (Figure 6a) is 38.00. Friction angle during motion (ϕm) is 35.60.

(3) Lateral pressure ratio k: 0.5 – 0.7. The authors assumed the lateral ratio to be 0.5 in the top of slope, 0.6 in the landslide body and 0.7 in the lower part.

(4) The shear displacement of shear strength reduction was estimated from undrained stress control tests. Figure 6b shows the critical shear displacement for start of strength reduction (DL) is 5 mm and the start of steady state (DU) is 200 mm.

(5) Pore-pressure generation rate Bss was 0.8-0.9 in the landslide area, and 0.3 outside the landslide area. It was 0.95 in the marsh area (inside of yellow line in Figure 9a)

(6) The unit weight of brown sample was 19.2 kN/m3.

The simulation result of the Ha Long landslide is presented in Figure 9. The pink line is the calculated sliding mass distribution area. Then, pore-water pressure ratio was increased and local failure started from the middle of the slope when ru reached 0.34 at 1:30′:00″ (28 July). At 1:55′:39″, ru reached 0.36 and the whole landslide mass was formed and moved down. At 1:55′:49″, landslide mass reached maximum velocity of 13.3 m/s. At 2:10′:19″, movement was stopped. In comparison with the image taken by UAV (Figure 9f), the movement of Ha Long landslide deposit in the computer simulation is similar to the real case. Based on the information from local inhabitants, the Ha Long landslide took place on 28 July, around 1AM local time. Figure 9b shows that the landslide occurred at 1:30′:00″. It indicated the estimated time of landslide occurrence from LS-RAPID simulation is closed with actual occurrence.

Table 2 Parameters used in LS-RAPID simulation

Parameters	Value	Source
Steady state shear resistance (τss, kPa)	6	Test data
Lateral pressure ratio (k=σh/σv)	0.5 - 0.7	Estimated
Friction angle at peak (ϕp, degree)	38.0	Test data
Cohesion at peak (c, kPa)	5	Estimated
Friction angle during motion (ϕm, degree)	35.6	Test data
Shear displacement at the start of strength reduction (DL, mm)	5	Test data
Shear displacement at the start of steady state (DU, mm)	200	Test data
Pore pressure generation rate (Bss)	0.3-0.95	Estimated
Total unit weight of the mass (γt, kN/m3)	19.2	Test data
Unit weight of water (γw, kN/m3)	9.8	Normal value
Triggering factor		
Pore-water pressure ratio in the potential shear zone (ru) during rain	0-0.45	Estimated from SLIDE model

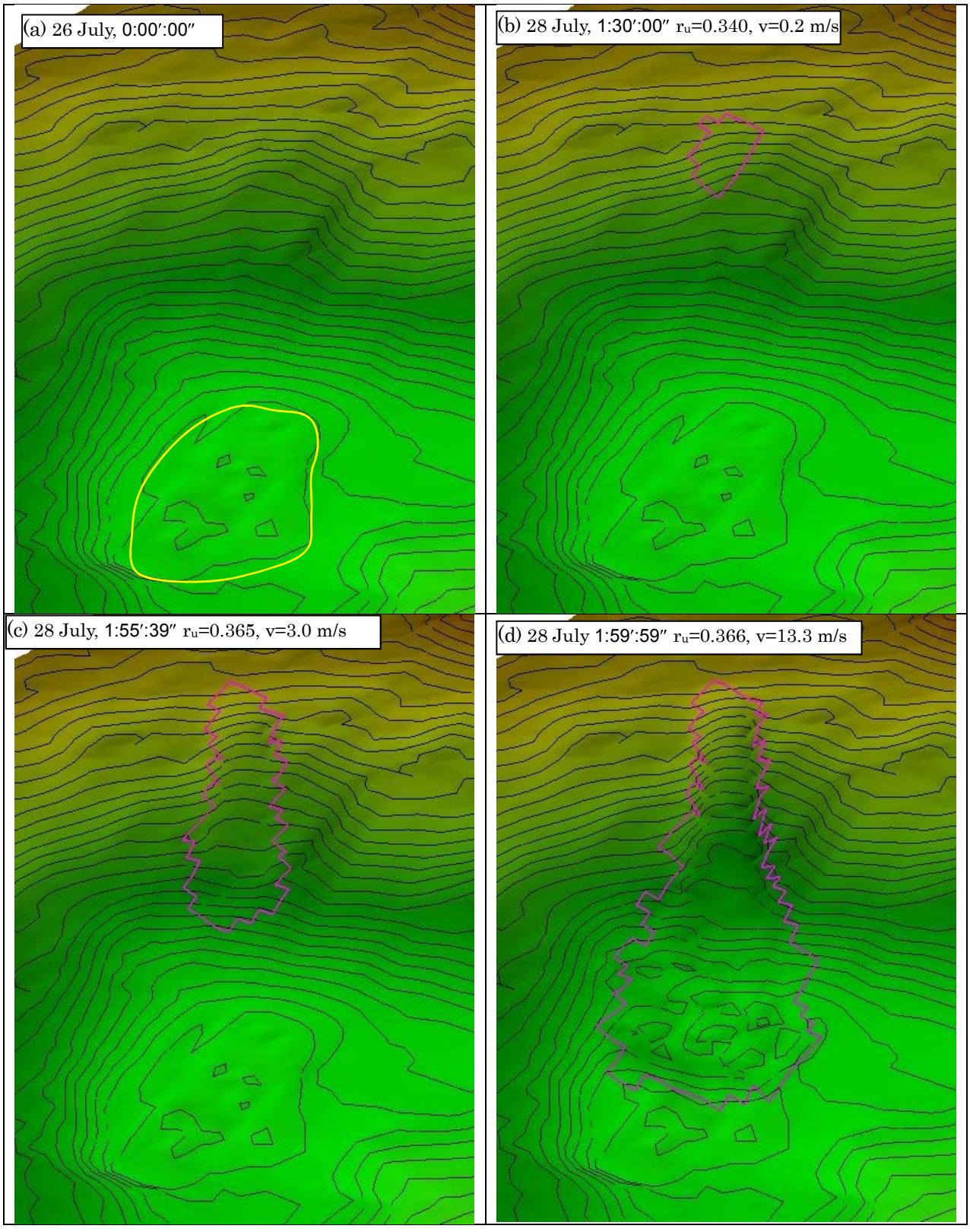
(a) 26 July, 0:00′:00″
(b) 28 July, 1:30′:00″ ru=0.340, v=0.2 m/s
(c) 28 July, 1:55′:39″ ru=0.365, v=3.0 m/s
(d) 28 July 1:59′:59″ ru=0.366, v=13.3 m/s

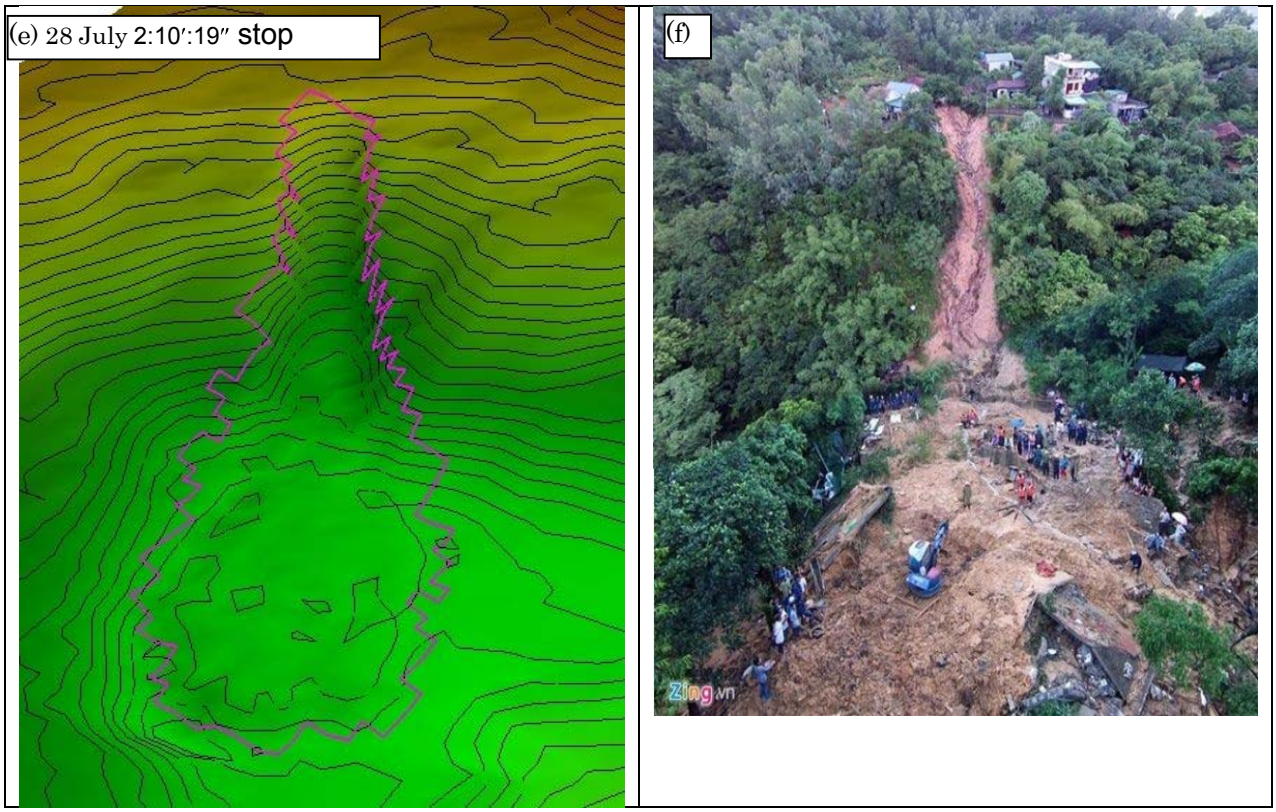

Fig. 9 Simulation result of Ha Long landslide

Conclusion

Landslide and debris flow have caused great disasters as Ha Long case. The main objectives of this research are to study the initiation mechanism and behavior of the Ha Long landslide triggered by heavy rainfall through laboratory testing using ring shear apparatus (ICL-1) and using an integrated simulation model (LS-RAPID) and the SLIDE model. This research examines the influence of rainfall which could trigger the rapid landslide.

From field investigations, the ring shear test results and the Ha Long landslide simulation using LS-RAPID, the conclusions can be described as follows:

The main factor of Ha Long landslide is heavy rainfall in a short time. The cumulative 12 hour rainfall was 296 mm at Bai Chay weather station.

The SLIDE model is simple model to calculate pore-water pressure from rainfall intensity that could be accepted for shallow landslide.

The LS-RAPID results indicated the landside area that was similar to those determined field investigation. In addition, the time of landslide occurrence is closed with actual occurrence that was reported by local inhabitants.

Ha Long landslide is small, however it cause great disaster. This research will contribute to understanding the mechanism of rapid landslide during heavy rainfall as a basic knowledge for disaster prevention. It may be useful information for local governments in Ha Long city to change the land used planning for mountainous area.

Acknowledgment

This research is a part of Vietnamese - Japanese joint research SATREPS'project "Development of landslide risk assessment technology along transportation arteries in Vietnam" The project is financed by the Japan Science and Technology Agency (JST) and the Japan International Cooperation Agency (JICA). The authors appreciate the cooperation from Vietnam Institute of Geosciences and Mineral Resources for their support during investigation of the Ha Long landslide.

References

Central Committee for National Disaster Prevention and Control (CCNDPC-Vietnam) (2015), Report on natural disaster in Quang Ninh. http://www.dmc.gov.vn/chi-tiet-thien-tai/mua-lu-mien-bac-viet-nam-lu-tai-quang-ninh-dis156.html?lang=vi-VN#prettyDetail[gallery1]/2/

Liao, Z., Hong, Y.,Wang, J., Fukuoka, H., Sassa, K., Karnawati, D. and Fathani, F. (2010). Prototyping an experimental early warning system for rainfall induced landslides in Indonesia using satellite remote sensing and geospatial datasets. Landslides, Vol.7, No.3: 317-324.

Liao, Z., Hong, Y., Kirschbaum, D. and Liu, C. (2012) Assessment of shallow landslides from Hurricane Mitch in central America using a physically based model. Environmental Earth Sciences 55:1697-1705.

Montarasio, L. and Valentino, R. (2008) A model for triggering mechanisms of shallow landslides. Natural Hazards and Earth Sciences 8:1149-1159.

Sassa K, Fukuoka H, Wang G, Ishikawa N (2004) Undrained dynamic-loading ring-shear apparatus and its application to landslide dynamics. Landslides 1(1):7–19.

Sassa K, Nagai O, Solidum R, Yamazaki Y, Ohta H (2010) An integrated model simulating the initiation and motion of earthquake and rain induced rapid landslides and its application to the 2006 Leyte landslide. Landslides 7(3):219–236.

Sassa K, Dang K, He B, Takara K, Inoue K, Nagai O (2014) A new high-stress undrained ring-shear apparatus and its application to the 1792 Unzen–Mayuyama megaslide in Japan. Landslides 11 (5):827-842.

Proceedings of the SATREPS Workshop on Landslides in Vietnam, 2016

Experience of Trainees in Japan – Vulnerability of landslide hazard in tropical region

Dinh Van Tien

Institute of transport science and technology, Viet Nam, e-mail: Dvtien.gbn@gmail.com

Abstract

Like other South-East Asia countries, Vietnam is the country with mountainous terrain, complicated geological structure and high rainfall, and as the result, landslides occur regularly and seriously on mountainous road network in rainy season. Study for Vulnerability of landslide hazard is requirement of fact. The contends of dissertation mainly focus on (1) a new strategy for landslide prevention and mitigation for road in humid tropical region; (2) A prediction of landslide type classification by pattern recognition of fuzzy inference method (3) Geological mechanisms of landslide generation in the study area ; (4) Landslide susceptibility mapping along the Ho Chi Minh route in central Vietnam – an AHP approach applied to a humid tropical area and (5) Mitigation landslide hazard vulnerability Guideline. The studies in this dissertation will contribute to understand and mitigate the vulnerability of landslide hazard disaster in center area of Vietnam particular and humid typical tropical region in general.

Keywords, Landslide, Vulnerability, Risk Assessment, Susceptibility, Classification

Introduction

Landslides are considered as a persistent problem in mountainous regions, especially distribute along transportation corridors. Landslides not only cause damages to properties (houses, buildings, vehicles, etc.) and large numbers of casualties but also disrupt utility services and economic activities. Located on the Eastern Indochina Peninsula, Vietnam has a rate of mountainous terrain up to 3/4 area of its territory with a steep sloped terrain due to earth's crust powerful tectonics . Moreover, it also has a complex geological structure and a tropical monsoon climate with the average annual rainfall from as much as 3,000-4,500mm/year in some regions. Consequently,Vietnam is a typical tropical country with the most serious landslide disaster in Southeast Asia and the Mekong subregion.

Concept of Vulnerability of landslide hazard

Vulnerability of landslide hazard is refferred as the portability of slopes by landsliding. There are many causes of landslide vulnerability such as conditions of topography, geomorphology, geology, climate and artificial activities. Landslide vulnerability assessment is a large concept concerning to risk assessment on re-active landslides and landslide susceptibility. For mitigation Effection of this fenomenamce to human life , landslide vulnerability assessment is requirement of fact.

The dissertation purpose is to develop a comprehensive method for the assessment of vulnerablity to landslide risk in tropical regions based on providing a significant method for landslide classification, analyzing relationship of landslide phenomena with causative factors and creating a landslide susceptibility map for vulnerability of landslide hazard. Methodology of the dissertation is based on the conclusion as " for the landslides, the past and the present are the key to the future" (Varnes, 1984; Carrera et al., 1991, Hutchinson, 1995). In some cases together with others topography and slope formation processes, the cover of vegetation in tropical forest could delete their signals for recognition. So by this principle, occurred landslides will be recognized as much as possible, depending on capacity of human recognition. Under this hypothesis, landslides in the future may occur in the same geological conditions, geomorphology and hydrogeology as it happened before. Therefore, to understand clearly about the movement of landslide in the past is very importance to assess landslide causes. From

discovered landslides, the rules for landslide appearance will be studied, then the prediction to land sliding sensitiveness is evaluated and forcasted.

The study area is a zone limited by a distance of 20 km offset to both sides from the center-line of HCM route, extending northwest and southeast between the latitudes of 16° 40'N and 15° 30'N and longitudes of 106° 15'E and 106° 50'E; extends to three provinces of Quang Binh, Hue, and Quang Nam of Vietnam. Through collecting occured landslides along 300km of the route since 2006 to 2015, in the Central of Vietnam.The research for vulnerability of landslide hazard was carried out through 16 reports and publisments. Five new report and recently publishments are presented and discussed here for the dissertation.

The contends of dissertation includes (1) a new strategy for landslide prevention and mitigation for road in humid tropical region; (2) A prediction of landslide type classification by pattern recognition of fuzzy inference method (3) Geological mechanisms of landslide generation in the study area ; (4) Landslide susceptibility mapping along the Ho Chi Minh route in central Vietnam – an AHP approach applied to a humid tropical area and (5) Mitigation landslide hazard vulnerability Guideline.

A new strategy for landslide prevention and mitigation . (Tien.DV, 2014)

From the damages of typical landslides in Vietnam on highway No. 37 (at Chen Pass), Son La Province; the Nam Non Bridge on the Western Route, Nghe An Province; at Hai Van Pass Station; on Highway No. 6 and along the Ho Chi Minh route in the central area, it is able to be recognized that the responding in face to this dangerous phenomenon seems to be quite passive. In the dissertation, a general method to prevent and mitigate landslides actively along roads in humid tropical region was also proposed. The core of the study is a new strategy for reduction affection of vulnerability of landslides, which was discussed by combination of the landslide risk assessment map, which is developed from risk assessment to occured landslides and the landslide susceptibility map, which is developed from the evaluation the sensitiveness to sliding of natural slope from landslide causative factors. The general method can contribute to the forecast, prevent and mitigate the negative impact of the landslide phenomenon for planning, land use, construction of infrastructure, ensuring the safety of existing traffic roads and mountainous residential areas in Vietnam. It can be applied to areas with similar conditions to the study area.

A prediction of landslide type classification by pattern recognition of fuzzy inference method. (Tien DV 2016)

From 2012 to 2015, multi landslide investigations have been taken along Ho Chi Minh route in order to collect as many as occured landslides for assessment . According to Varnes classification, the occured landslides were classified. However because of complicated phenomena and depending on point of observations, there were some landslide cases which had a non-consensus for classification. For landslide mitigation, a degree of risk valuation and the construction of prevention measures are necessary to prevent these landslide disaster. So it is necessary to execute a pattern recognition of different type classification. Cause of landslide having a various moving styles, but the analysis of this type classification is affected by the various factors therefore we examine this analysis method of landslide type classification in consideration of fuzzy nature. From results of study, we show that the weathering of the ground, a geological features and landslide scale are important factors through these analysis . The propose method is high technique analysis precision and could be applicated for similar assessment application.

Geological mechanisms of landslide generation in the study area (Tien DV ,2015)

In central Vietnam, Ho Chi Minh Route (HCMR) runs from south to north along the border with Laos. In this area, HCMR is often closed due to numerous landslides during the rainy season. Thus, there is an urgent need to determine the generation mechanism of landslides and to conduct risk assessment. For this purpose, the area was chosen as one of the study areas for this project. This study focuses on landslides occurring at approximately 180 locations along the 150 km distance (linear distance) from Thanh My (west of Da Nang City) and the intersection with National Route 9 (west of Quang tri). The landslides are

classified based on the type of movement in order to determine the triggering mechanism. The survey was conducted from 2012 to 2014. The type of landslide movement in this area differs significantly depending on whether if the area is Paleozoic metamorphic zone or Mesozoic sedimentary zone. The type of landslide movement in this area differs significantly depending on whether if the area is Paleozoic metamorphic zone or Mesozoic sedimentary zone. In metamorphic area, weak aspect such as schistosity, beddings, faults, and joints associated with geological structures become shear planes. Translational slides (wedge type) and rotational slide/flow (gulley type) occurs often in this area, with the infiltration of surface water and breaking of rocks by weathering as the cause. On the other hand, in Mesozoic sedimentary area, translational rock slides are most common, where coal layers disrupted by fold structures function as the slip surface. It was shown that these landslides are not simply caused by heavy rain and weathering typical of the tropics, but are closely associated with geology, geological structure, development of rivers, and cuesta topography. This result shall be an important indicator in future study of vulnerability of landslide hazard

Landslide susceptibility mapping along the Ho Chi Minh route in central Vietnam – an AHP approach applied to a humid tropical area. (Tien DV, 2016)

To assessment the sensitiveness to vulnerability of the slope by sliding a landslide susceptibility mapping along the Ho Chi Minh route in central Vietnam, was created. Ingeneral there are various possible causes for land sliding with complex inter–relationships. However, in practice a detailed assessment to find the main causes of each landslide is not feasible in most cases. The selection of causative factor for landslide susceptibility map is usually base on expert's subjective experience. In this study, to analyse landslide manifestation, causative factors are derived of slope angle, type of rock, fault density, distance to the road, land used and precipitation. Maps for causative factors were created, in which each one was divided in to classis. From position of 604 artificial slope failures appeared along the Ho Chi Minh route a landslide distribution was build up. The sensitiveness to landslide of each classis zone of causative factor maps is calculated and then evaluated thought the value of number occurred landslide -NOL and density of occurred landslide DOL. These values were the result of comparison of landslide distribution map and each causative factor maps using GIS application. An analytical hierarchical process (AHP) is used to combine these maps for landslide susceptibility mapping. As the result, A landslide susceptibility zonation map with 4 landslide susceptibility classes, i.e low, moderate, high and very high susceptibility for land sliding, is derived based on the inventory map of observed landslide from 2006-2009. This map indicates that 82.66% total number of occurred landslide, which have been reported fall into highly and very highly susceptible zone. Even there was limited matter concerning relevant, scale and available data, the landslide susceptibility map of this study for corridor along this road is credible for landslide mitigation.

Mitigation landslide hazard vulnerability Guideline (Tien DV, 2016)

For landslide prevention, response and mitigation, a Landslide Hazard Vulnerability in tropical region a Guideline was proposed. The author approach is to answer for questions " What-Where-When-How"to landslides. Concept and classification of landslide in study area will be discussed for "What" question. Landslide moving mechanism is mentioned, in which the effect of the pore-pressure rise by raining is confirmed then the relationship between dynamic factor and displacement (signal of landslide recognition) is tagged for observation. As the result, basic data for landslide management and regional monitoring system are advised that will answer for "When" question. The integrated maps for landslide hazard vulnerability such as landslide inventory map, landslide risk assessment map, landslide susceptibility map and landslide hazard map are presented as basic tools to answer for "Where" question as site prediction. The application of research for landslide prevention, response and mitigation plan, in which metioned landslide knowlerges and tools used will discuss for question "How". This guideline will contribute for landslide hazard management as a basic document in center of Vietnam.

Conclusions

Vulnerability of Landslide Hazard assessment is one very important issue in the "proactively

prevent natural disasters" strategy of Vietnamese government. From landslides survey data in corridors of Ho Chi Minh route in center area of Vietnam, a basic data for occurred landslide was created base on three basic methods, which is commonly used for inventory maps as field recognizance to investigate landslide occurrences, collection of historic information of landslide and interpretation of landslide occurrences from aerial photographs. The relation of occured landslides distribution to causative factors such as topography, geomorphology, geology, climate and Artificial activities were studied. During the research time, the following matters including: new strategy for Landslide prevention and mitigation for road; the prediction of landslide type classification by pattern recognition of fuzzy inference method; Geological mechanisms of landslide generation ;Landslide susceptibility and Mitigation landslide hazard vulnerability Guideline for tropical region were disscussed. The results of above studies could apply to similar tropical zone. However, vulnerability of landslide hazard assessment is large matters. Beside of above studies, Creation of Landslide Risk Assessment to occured landslidesd that using AHP or Fuzzy method has not mentioned in this study should be the targget of furture reseachs. The studies in this dissertation will contribute to understand and mitigate the vulnerability of landslide hazard disaster in center area of Vietnam particular and humid typical tropical region in general.

References

Tien D. V. (1) Toyohiko Miyagi (2), Shinro Abe (3), Eisaku Hamasaki (4), Hiroyuki YOSHIMATSU (5) - Landslide susceptibility mapping along the HCMR in central Vietnam - an application of an AHP approach to humid tropical area - Transactions, Japanese Geomorphological Union, vol.37-1; January, 2016;

Tien D. V. (1), Hiroyuki Yoshimatsu (2), Kazunari Hayahi (3), Toyohiko Miyagi (5), - A prediction of landslide type classification by pattern recognition of fuzzy inference method along the HCMR in central zone of Vietnam - Transactions, Japanese Geomorphological Union, vol.37-1; January, 2016;

Tien D. V. (1), Shinro Abe (2), Hiroyuki YOSHIMATSU (3), Toyohiko Miyagi (4),- Geological mechanisms of landslide generation along HCMR in central Vietnam -Journal of Japan Landslide Society - Vol .52, No4 (226) July 2015;

Tien D. V.(1), Toyohiko Miyagi(2),Eisaku Hamasaki (3), Shinro Abe(4), Nguyen Xuan Khang (5)- Landslide prevention and mitigation for road in humid tropical region - The 4th volume of World Landslide Forum 3 (WLF3) -2-6 June 2014, Beijing;

Tien D. V. (1). Vulnerability of landslide hazard in tropical region – dissertation, 2016

Proceedings of the SATREPS Workshop on Landslides in Vietnam, 2016

The Integrated Approach of Landslide Hazard Mitigation along the Roadside in Central Viet Nam

Ngo Doan Dung [(1)], Tatsuya Shibasaki [(2)], Eisaku Hamasaki [(3)], Toyohiko Miyagi [(4)]

1) Institute of Transport Science and Technology, Hanoi, Vietnam, Vietnamese member of WG2, short term trainee and Doctoral candidacies in Japan, e-mail: ngodoandung@gmail.com

2) Japan Conservation Engineers Co.,Ltd, Japan, e-mail: shibasaki@scs.dpri.kyoto-u.ac.jp

3) Advantechnology Co., Ltd, Aoba, Sendai, 0081, Japan, e-mail: hamasaki@advantechnology.co.jp

4) Tohoku Gakuin University, Izumi Campus/2-1-1 Tenjinzawa, Izumi-ku, Sendai, 0081, Japan, e-mail: miyagi@izcc.tohoku-gakuin.ac.jp

Abstract The landslide phenomenon is the cause of economic damages up to 0,1 % of total GDP and about 30 persons fatal every year in Vietnam. However, it can easily recognize that control and mitigation of damages caused by landslides current in Vietnam seems to be quite difficult and passive. Lack and limited in guidelines and standards for field survey, collecting soil data, simulation and calculate the safe factor, countermeasures; lack of professional engineers and the budget for landslides, lack of forecasting technology and awareness of local people are reasons.

In the framework of The SATREPS project titled "Development of evaluation techniques for slope vulnerability to disasters along the axis transportation network in Vietnam" by JICA/JST/ITST, a lot of knowledge and technological in the field of landslides, which has obtained from reality and long historical studies on landslide in Japan such as field survey, collecting soil data, simulation and calculate the safe factor, early warning, countermeasures to be introduced and transferred to young engineers of ITST.

This paper focuses presented a research proposal in the Integrated Approach of Landslide Hazard Mitigation along the Roadside in Central Viet Nam.

Keywords Landslide mapping, field survey, risk evaluation, AHP, slip surface, weathered, Vietnam

Landslides distribution mapping by ALOS W3D data

The aerial photographic interpretation is ordinarily the first step in creating distribution data of landslide topography. In most regions of Vietnam, aerial photographs taken are "mostly of a scale of 1:33,000, and have been taken only once in the past with black-white". In many other regions are difficult to undertake aerial photography.

NIED of Japan has usually used aerial photographs of a scale of 1:40,000 in the Landslide Distribution Maps project, in which the minimum scale of landslide topography extracted by aerial photographic interpretation is specified as width of about 100 m (Oyagi et al., 2014). Therefore, stereopticon interpretation of images of a scale of 1:30,000 would provide nothing more than a basic image of the outline of landslide topography.

Moreover, the landslide reactivation risk evaluation is based on a micro-landform interpretation using aerial photographs of a scale of about 1:10,000. It is difficult to evaluate a micro landform with aerial photography of a scale of about 1:30,000 (Luong et al., 2015). However taking aerial photographs again by airplane requires huge expenses. Such circumstances are common in many states worldwide, as well as in Vietnam.

The Advanced Land Observing Satellite "DAICHI" (ALOS) launched by JAXA has captured 2 million Earth images. Three organizations, ERSDAC, NTT Data, and JAXA, conducted processing for these images jointly, and built up digital information of a 5-m mesh and orthographic images that cover the entire world. However, these 3D data are not perfect because they are DSM data: to the degree that they are DSM, they are not representative of information acquired by direct measurement of the topography. Because they are originally created from ALOS images, nothing can be done but inferring the tree height of the region and subtracting it from Z value to generate a Digital Elevation Model (DEM). However, image information covered by vegetation is obtained by reading recognition from aerial photographic interpretation conventionally, so that it is presumably possible to attain the same accomplishment from DSM as the topographical analysis by stereopticon interpretation of aerial photographs. Therefore, it is regarded as meaningful to examine the possibility of analysis using W3D data in various regions in the world. Five ground meters corresponds to 0.15 mm on the contact printing of an aerial photograph of a scale of 1:33,000, so that the precision of W3D data of a 5-m mesh is almost equivalent to that of aerial photographs that are

actually used in Vietnam. Consequently, it is natural to infer that an accomplishment equivalent to landslide topography distribution data based on aerial photograph interpretation can be acquired from W3D data using a topographic map with an appropriate contour interval. It is also considered possible to obtain finer relief information by selecting an appropriate interval of contour lines.

Based on the ALOS W3D data combination with field investigation, the landslide distribution maps is established along the National Road No. 7 is completed and more than 1000 landslide areas are identified (Dung et al, 2016).

Fig. 1 Landslide field survey along the National Road No. 7 (May, 2016)

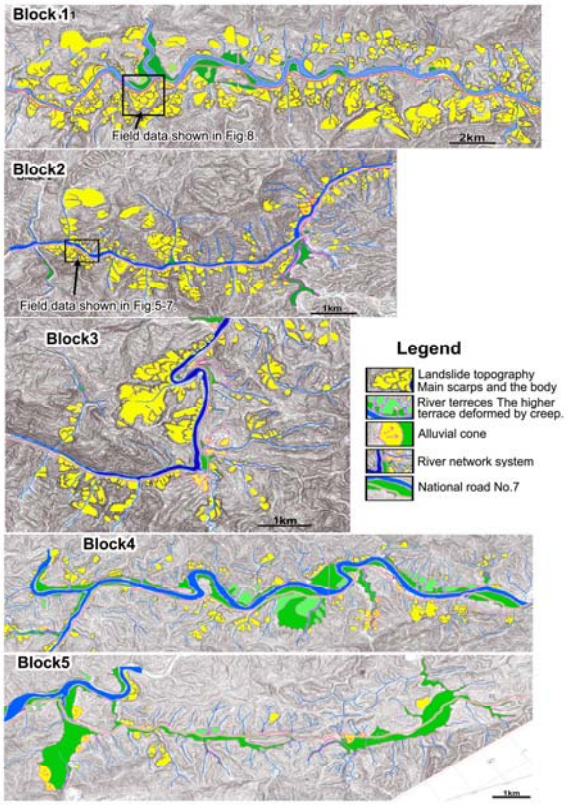

Fig. 2 Landslide distribution maps along the National Road No. 7 (Dung et al, 2016).

Field investigation for landslides and soil testing

Field investigation for landslides

After analysis of aerial photographs, field investigation work will be very important to develop and clarify the results from analysis of aerial photographs.

From 2011 to 2016, a series of field investigation were conducted along the corridor of Ho Chi Minh road, National road No. 6 (section Hoa Binh province), National road No. 7 and Hai Van pass area.

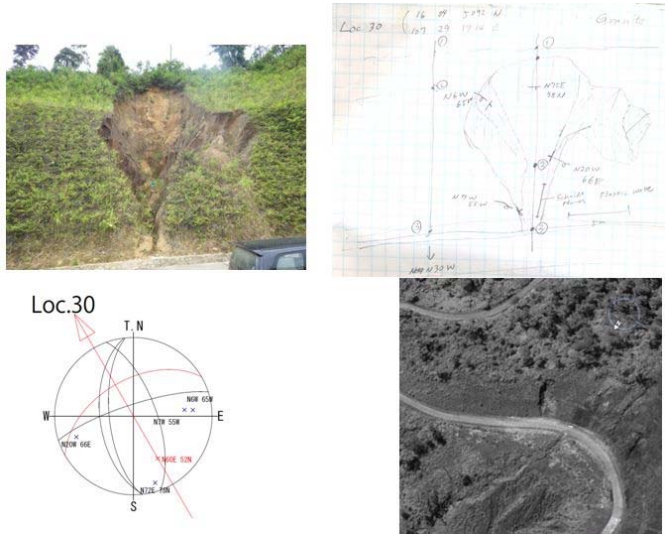

Fig. 3 Sketch a shallow landslide during field surveying along Ho Chi Minh Road (Aug, 2013)

During field investigation, slip surface, geological features, geology and weathering, type of landslides along road have been discussed and clarified by Vietnamese engineers and Japanese experts (Fig.1, Fig. 3, Fig. 4).

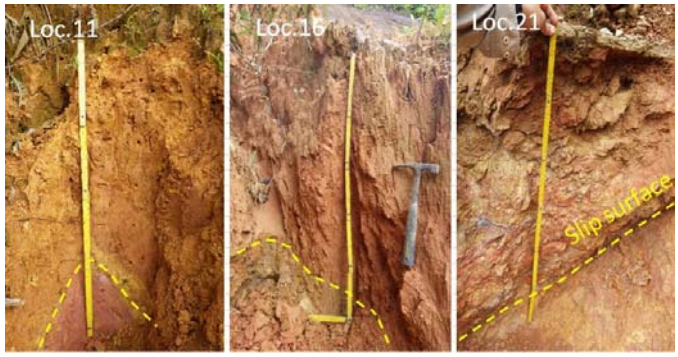

Fig. 4 Identify slip surface at the landslide site along Ho Chi Minh Road (Aug, 2013)

Field test

Some soil test at field such as Elastic wave velocity test (by Handy seismograph), Schmidt Rock-hammer test and Yamanaka-type Soil Hardness test have been conducted. Fig. 6 show results of soil hardness profiles at the

excavated outcrops. Data were measured by Yamanaka-type soil hardness tester at landslides along HCM road.

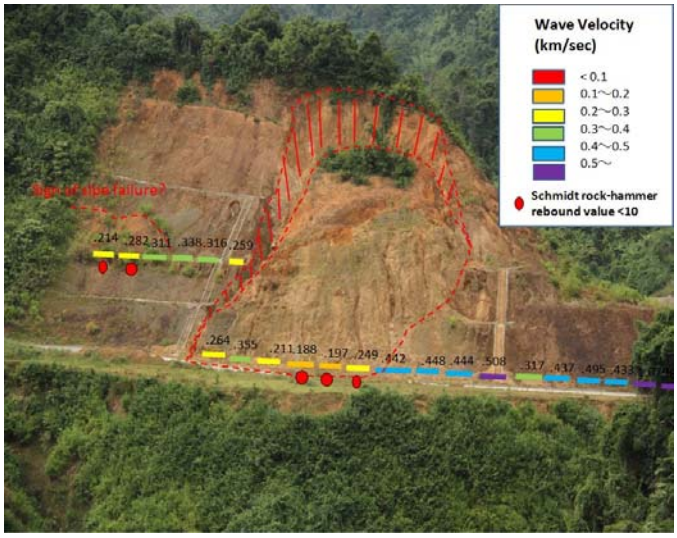

Fig. 5 Elastic wave velocity test (by Handy seismograph) and Schmidt Rock-hammer test at the landslide No.29 along HCM road (Dung et al., 2016 submitting).

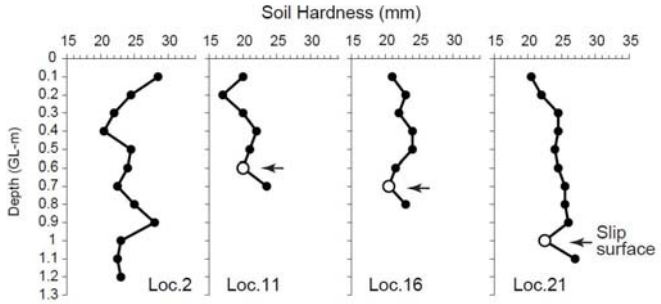

Fig. 6 Soil hardness profiles at the excavated outcrops. Data were measured by Yamanaka-type soil hardness tester at landslides along HCM road (Dung et al., 2016 submitting).

Physical properties and X-ray diffraction analysis and Ring shear and box shear tests

Besides, a lot of soil and rock samples have been collected to perform the experiments determining mechanical properties of soil. The experiments identified physical properties of soil have conducted at ITST's laboratory. X-ray diffraction analysis and Ring shear and box shear tests for residual strength characteristics of weathered rocks were conducted in the laboratory in Japan by ring-shear apparatus.

Clay mineral characteristics of the weathered materials are examined by X ray analyser. Soil faces are categorized to crack rock, laminated rock, strongly weather rock and soil. The result is very clear. That is, relatively flesh rocks include iolite. But according to the weathering advance, kaolinite getting appears.

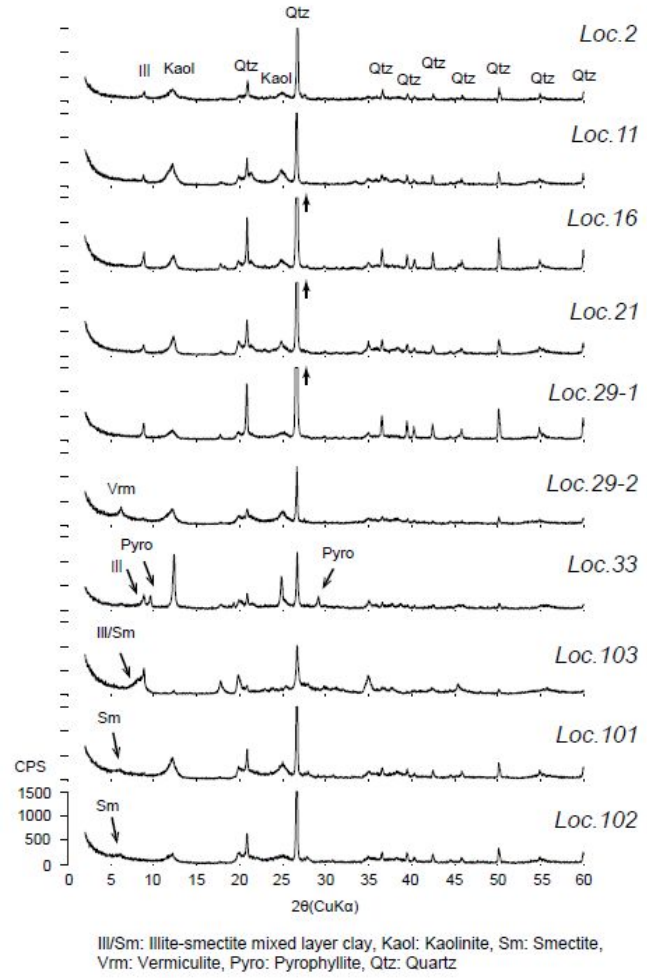

Fig. 7 X-ray diffraction patterns of soil samples subjected to ring shear test (Dung et al., 2016 submitting).

Fig. 8 Residual strength characteristics of weathered rocks were conducted in the laboratory in Fukushima, Japan (Dung et al., 2016 submitting).

Table 1. Physical and mineralogical properties of tested soils (Dung et al., 2016 submitting).

Sample No.	Location	Geology	Grain Size (<425 μm)			Index Property			Mineral Assemblages
			Sand 63-425 μm	Silt 2-63 μm	Clay <2 μm	LL (%)	PL (%)	PI	Ill/Sm: Illite-smectite mixed layer clay, Kaol: Kaolinite, Sm: Smectite, Vrm: Vermiculite, Pyro: Pyrophyllite, Qtz: Quartz
1	Loc.2	Paleozoic, Mylonite	28	57	15	44.5	29.5	15.0	Qtz>Kaol>Ill
2	Loc.11	Paleozoic, Schist	13	72	15	44.4	29.8	14.6	Qtz>Kaol>Ill
3	Loc.16	Paleozoic, Schist	34	49	17	44.9	29.8	15.1	Qtz>Kaol>Ill
4	Loc.21	Paleozoic, Schist	20	64	16	43.5	29.3	14.2	Qtz>Kaol>Ill
5	Loc.29-1	Paleozoic, Schist	31	54	15	40.2	27.1	13.1	Qtz>Kaol>Ill
6	Loc.29-2	Paleozoic, Schist	16	68	16	43.5	29.0	14.5	Qtz>Kaol,Vrm>Ill
7	Loc.33	Mesozoic, Coaly Shale & Sandstone	29	55	16	31.3	19.9	11.4	Qtz,Kaol>Pyro
8	Loc.103	Mesozoic, Tuff, Mudstone & Sandstone	5	51	44	52.1	22.9	29.2	Qtz>Ill,Ill/Sm>Kaol
9	Loc.101	Cenozoic, Basalt & River Deposit	15	53	32	65.4	35.5	29.9	Qtz>Kaol>Sm
10	Loc.102	Cenozoic, Basalt & River Deposit	17	49	35	79.1	37.9	41.2	Qtz>Kaol>Sm

Safety factor evaluation by ADCALC3D

The combination works with contour from W3D data, field investigation data and simulation lead us the presence of real phenomenon and will suggests the alternative countermeasure strategy setting up. Fig. 10 is one of results of study. The case study is Loc. 101 on Ho Chi Minh road in Kham Duc area, central of Vietnam.

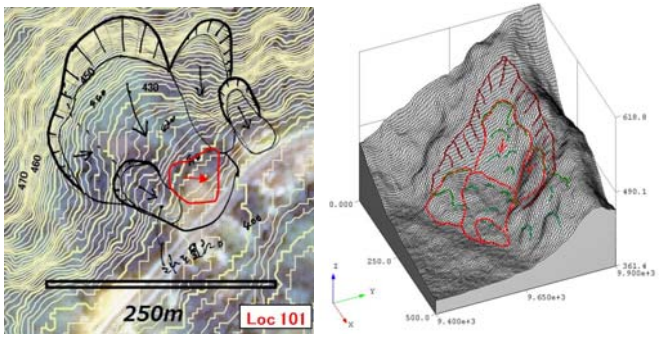

Fig. 9 Simulation the slip surface on the contour from W3D data for safety factor evaluation by ADCALC3D (Dung et al., 2016 submitting).

The results of estimations carried by the 3 dimensional landslide stability analysis by ADCALC3D showed on Table 2. This is very clear result. When the ground water level lower slip surface (Void), the safety factor Fs= 1.4097 and the slope is stable. But when the ground water level full, the safety factor Fs= 0.9832 and landslide occurs.

Table 2 The results of estimations carried by the 3 dimensional landslide stability analysis by ADCALC3D (Dung et al., 2016 submitting).

Test			Result	Fs (Void)	Fs (Full)
Ring shear	Fully softened strength	Cs(kPa)	13.2	-	-
		ϕs(deg.)	24.3		
	Residual strength	Cr(kPa)	6.7	1.4097	0.9832
		φr(deg.)	8.3		

Landslide risk evaluation

Landslide risk evaluation by AHP approach (Saaty, 1980) has been carried long time in Japan by Japanese scientists (Miyagi et al, 2004). But in Vietnam, this method is still fairly new. The question is how application this method in Vietnam? Japanese experts and engineers Vietnam have discussed and agreed to that could apply in Vietnam but need to consider characteristics of landslide in Vietnam. Then based on the basic AHP inspection sheets have been prepared by Japanese scientists, the modify AHP sheet for Landslide risk evaluation in Vietnam should be recommended as below.

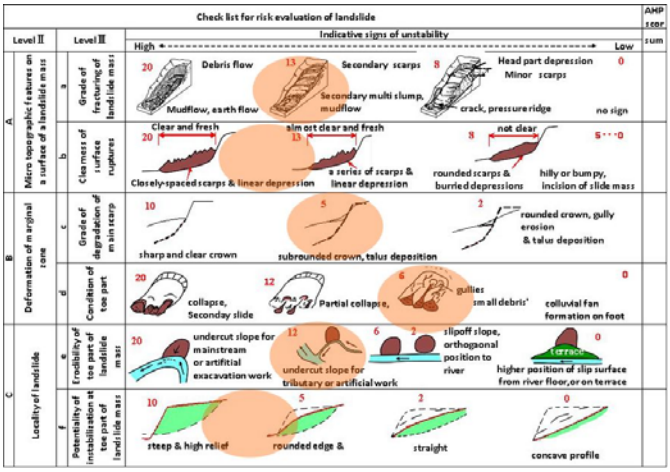

Fig. 4 New inspection sheet for calculation of Landslide AHP score (Dung, et al., submitting).

The Integrated Approach of Landslide Hazard Mitigation along the Roadside

The trial covers almost of all area of landslide management in the field. Actually there is poor advancing or the improvement of landslide management technology yet (Dung et al, 2016). The new framework of landslide investigation and the management for landslide disaster prevention, mitigation and the control along the Roadside in Vietnam have been suggested as show in Fig.10.

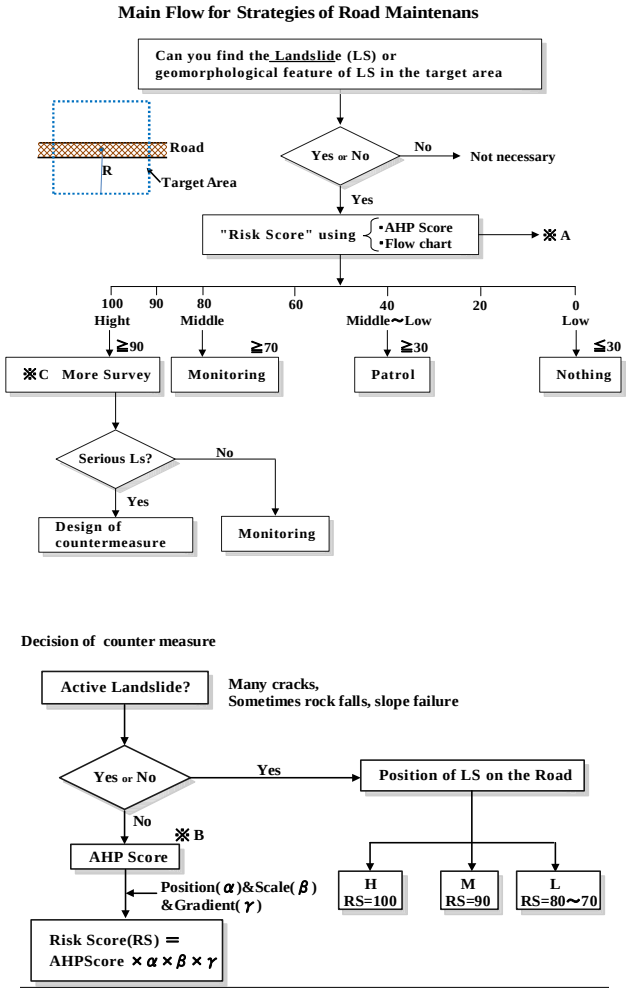

Fig.10. Main flow of landslide management (above) and sub flow (below) along the roadside (Dung et al. 2016)

Study experience in Japan

Lecture about Landslide Mapping:

The lectures about Landslide mapping were carried out at Tohoku Gakuin University by Prof. Miyagi (Fig. 11). The topics of lectures were "how should we observe the landform and understand it", based on this understanding, "how high risk slope, particularly landslide topography should be distinguished from other slopes of normal process" and "what can be known by classifying and understanding the characteristics of the slopes geomorphological."

Outcome of these lectures could be concluded as (1) How to deduce the landslide topography through the aero photos interpretation and mapping and (2) How to detect the slip surface structure by aero photos interpretation combined with field investigation.

Fig.11. Lecture on Landslide mapping by Prof. Miyagi

Lecture about Risk evaluation technique:

The lectures about Risk evaluation technique also were carried by Prof. Miyagi. Landslide is a domain clearly distinguished from the surrounding slope. That is, it regards as a landslide topography is has a feature with very clear unit. Here, the landslide as the research object is a typical landslide phenomenon which has three the geomorphic and geological elements called the "Main Scarp", "Landslide Body" and "Slip Surface (Surface of Rapture)". As an important characteristic of a landslide, some part of destructed moving body which remains on a slope as a movable body, and it mentions the point that this movable body has the characteristic which works again. When this point is identify, it has the potential of reactivation repeatedly and it is necessary to note the point that it causes a disaster. That is, it is necessary for the land formed of the landslide to evaluate a possibility remove. This is the landslide risk evaluation.

On the other hand, it may also be called risk evaluation of landslide generating to give the aim also including the place which the landslide has not generated "whether a landslide occurs at what kind of place." This is called susceptibility evaluation in many cases. In order to evaluate Susceptibility, it is necessary to grasp where the actual landslides are distributed fundamentally. However, it performs now at Susceptibility evaluation tried in various places in many cases only by operation of the parameter considered to be concerned with landslide generating generally considered as the distribution actual condition of landslide geographical feature is not grasped.

Creation of landslide distribution map is a fundamental procedure which leads to slope disaster mitigation. The places which the landslide occurring is grasped correctly and are figure-sized. The possibility of the re-activation which this landslide place each that was figure-sized has is grasped. Techniques, such as AHP are used for this works. In this SATREPS project, the landslide topographic area distribution map was created in two areas of Central Vietnam. Based on these pieces of distribution maps, a field survey is performed rationally, and the movement characteristic of the landslide itself will be grasped, the mechanism of generating is also will considered.

Lecture about how to take sample in the field and soil test method:

The lectures about how to take sample in the field and soil test method were carried out at Tohoku Gakuin University by Mr. Shibasaki. The lectures have clarified “How to categorize the C and Phi by soil testing data ?”. Outcome of this lectures could be concluded as slope failures occurring on cutting slopes are strongly controlled by discontinuities of rocks. They sometimes contain very weak clay layers. Residual friction angle is an important parameter for considering potentials of reactivation of landslides and mechanical properties of discontinuities of weathered rocks.

Lecture about Modelling the factor of stability estimation by the Adcalc 3D:

The lectures about Modeling the factor of stability(FS) estimation by the Adcalc 3D was carried out at Tohoku Gakuin University by Dr. Hamasaki. Outcome of this lectures could be concluded asADCALC3D offers a variety of options for 3-D slope stability analysis of the landslides. This program has an easy data compute/input operation which can provide full 3-D images and solid viewer functions.This is a simulation software program calculates the factor of stability of slope with highly intuitive. Simulation terrain data input from many different formats such as DWG, dng, jpg, ….

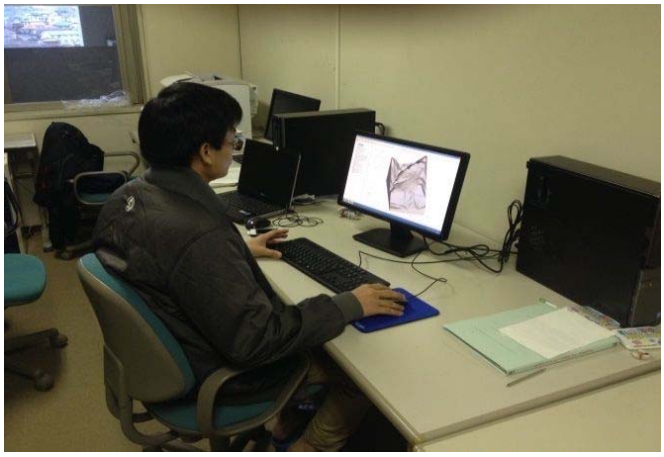

Fig.12. Lecture on Modelling the FS estimation by the Adcalc 3D by Dr. Hamasaki

Landslide survey (at Tozawa Landslide, Bandai mountain landslide, and.Sunakozawa dam landslide)

Landslide survey trip guided by Prof. Miyagi, Dr. Abe and Mr. Shibasakihave been carried out as mentioned above schedule. During this site trip, there were some small snow on surface of landslide, but could see many characters of landslide and factors influencing the slope movement haven discussed.

Land sliding involves the down slope movement of soil and rock under the direct influence of gravity, but combined with several factors such as geology, geomorphology, human impact, rainfall, snow smelt…From the site investigation, many factors have been pointed out and to be subject of discussion.

There are many factors contributing to the large landslides in Japan: Earthquakes and precipitation are two importance factors.It is differentin Vietnam.The movement of the slope along roads in the mountainous area of Vietnam is mainlycaused by high precipitation. In Vietnam, the landslide is recorded and divided into four phenomenon: landslides, topples, earth flows/ erosions or rock falls, and the causes are (1) slope angle, (2) weathering, (3) geomorphology, (4) fault density, (5) geology, (6) drainage distance, (7) elevation, (8) precipitationand (9) land use.

From (1) to (8) are natural conditions such as topographic, geology, and hydrology and climate that we have to accept them as initial data for studying but (9) land useis a factor that we have to do some adjustment.

Fig.13. Site visit at Tozawa landslide and Sunakozawa landslide

Acknowledgments

First of all, I pay my sincere gratitude to ITST leaders, Prof. Kyoji SASSA and the honourable every renowned Professors of different University in Japan many officers and engineers from Government and private sectors, field officers and Japanese coordinators, who give us some chances to study in Japan, many research experiences.

I would especially like to thank Dr. Shinro ABE, Dr. Daimaru, Mr. Uchiyama, Dr. Hayashi, Prof. Noriyuki CHIBA, Dr. Hiroyuki YOSHIMATSU, Mr. Katoh and the other members of WG2 of Vietnam project, who have contributed their outstanding efforts through their presentations, lectures, site visits and laboratory testing for the support to writing this article.

References

Dung, N.D., T. Shibasaki, T. Miyagi and E. Hamasaki (2016), Residual strength characteristics of weatherd rocks in Central Vietnam. (Submitting now)

Dung, N.D., T. Miyagi and E. Hamasaki, T. Shibasaki,K. Hayashi, Tien, D.V., and Luong, L.H. (2016), Study of new road side landslide disaster management structure in Vietnam. (Submitting now)

Dung N.D, Tien D. V., Khang N.X (2016), The current manual and standards for the survey and design works for Landslide prevention in Vietnam - Transactions, Japanese Geomorphological Union, vol.37-1, pp. 5-31.

Dung N.D., T. Miyagi, L.H. Luong, E. Hamasaki, K. Hayashi, Tien D.V (2016), Trial of landslide topography mapping using W3D data – Case study along the National Road No. 7 in central Vietnam, Transactions Japanese Geomorphological Union, p.127-140, vol.37-1.

Dung N.D., T. Miyagi, L.H. Luong, E. Hamasaki, K.Hayashi, D. V. Tien - Trial of landslide topography mapping using W3D data – Case study along the National Road No. 7 in central Vietnam, Transactions Japanese Geomorphological Union, p.127-140, vol.37-1; January, 2016;

Hamasaki E., TAKEUCHI Norio, OHNISHI Yuzo, (2006) Development of simplified discrete limit analysis for three-dimentional slope stability problem. Landslide – Journal of the Japan Landslide Society Vol.42. No.5 (2006), January, pp.389-397

Hamasaki E., MIYAGI Toyohiko, TAKEUCHI Norio, OHNISHI Yuzo, (2007) Risk evaluation of the earthquake triggered landslide on the land reclamation slope by three dimentional instability analysis of simplified RBSM. Landslide – Journal of the Japan Landslide Society Vol.43. No.5 (2007), January, pp.251-258

Luong L.H, T. Miyagi, Tien P.V (2016), Mapping of large scale landslide topographic area by aerial photograph interpretation and possibilities for application to risk assessment for the Ho Chi Minh route – Vietnam. Transactions, Japanese Geomorphological Union, pp. 97-118.

Miyagi T., G.B. Prasada, C. Tanavud, A. Potichan, E. Hamasaki (2014), Landslide Risk evaluation and Mapping - Manual of Aerial photo Interpretation for Landslide Topography and Risk Managemen. Reprinted from Report of the National Research Institute for Earth Science and Disaster Prevention No.66.

Tien D. V., S. Abe, Dung N.D, Ha D.N, T. Miyagi (2016), Outline, typology and the causes of landslides disasters in Vietnam - Transactions, Japanese Geomorphological Union, vol.37-1.

Tien D. V., T. Miyagi, S. Abe, E. Hamasaki, H. Yoshimatsu, (2016), Landslide susceptibility mapping along the HCMR in the Central of Vietnam - an application of an AHP approach to humid tropical area - Transactions, Japanese Geomorphological Union, vol.37-1.

Proceedings of the SATREPS Workshop on Landslides in Vietnam, 2016

Do Ngoc Ha – Experience of Landslide Trainees in Japan

Do Ngoc Ha[(1)(2)]

1) Member of WG4, Institute of Transport Science and Technology, Research & Development – Standards and International Cooperation Department, Hanoi, Vietnam

2) Master Student Graduated from Shimane University, Shimane, Japan, e-mail: hangoc910@gmail.com

Abstract As a member of Working Group 4 (WG4), I passed entrance exam to participate in Master Course at the graduate school of Science and Engineering of Shimane University, Japan from October 2012 to September 2014. During the long-term training course, I learned about the principle subjects of geology, geotechnical instructed by Japanese professors. Moreover, I had chances to survey sites at many landslide areas in Shimane and others. In the final presentation of the course, I wrote thesis about Mihata landslides in Izumo City, Shimane, Japan which occurred on 6 August 2012. My thesis paper was well recognized by Shimane University professors. During master course, I registered as a member of Japan Landslide Society and joined some its annual meetings. Especially, I regularly contact and work with WG4's members to execute group activities in Japan and Vietnam. After completion of the course, I was back to Vietnam and have continued to work at ITST and SATREPS project. The knowledge that I got from training course has been applied effectively for the project activities in Hai Van landslide and at landslide flume laboratory at ITST. In this report, I summarized my main activities within the SATREPS project period in Vietnam.

Keywords Working group 4, Shimane University, Mihata landslide, monitoring, flume experiment

Introduction

The SATREPS Project on Development of landslide risk assessment technology along transportation arteries in Vietnam is from the year of 2011 to the year of 2016. There are four working groups. I am a member of Monitoring Group (WG4). The main activities of WG4 are setting the monitoring system in Hai Van Station Landslide and conducting the flume experiment in laboratory. As a member of WG4, I was a long term trainee in Shimane University for two years. My site research was Mihata landslide in Izumo city, Shimane Prefecture, Japan. . Field investigations and landslide monitoring were conducted to examine the mechanical characteristics of this landslide. Samples were collected from the sliding zone in the main scarp. A series of direct shear tests, triaxial tests, and ring shear tests were conducted to analyze the shear behavior of the soil material from the Mihata landslide. The results of my research was presented in the 11th International Symmposium on Mititgation of Geo-disasters in Asia hold in Kathmandu, Nepal and in World Landslide Forum 3 in Beijing, China. The knowledge that I studied in Japan was applied effectively in SATREPS project in Vietnam.

Research results on Master course in Shimane University about Mechanical Characteristics of the August 6, 2012 Mihata landslide, Shimane Prefecture, Japan

Introduction

Shimane Prefecture is located along the western coast of Shimane Prefecture is one of the three areas in Japan strongly affected by landslides. In the early morning of 6 August 2012, the Mihata landslide occurred in Izumo city, Shimane Prefecture, Japan. The landslide was not triggered by obvious rainfall, nor by an earthquake. However, a high-precipitation event was recorded in the Sada district of Izumo city on 6 July 2012, one month before the landslide occurred (Fig. 1).

Figure 1 Side-view of the Mihata landslide (taken by Do N.H., 26 Nov. 2012)

A field investigation was conducted to examine the mechanical characteristics of this landslide. Samples were collected from the sliding zone in the main scarp. A series of direct shear tests, triaxial tests, and ring shear tests were conducted to analysis the shear resistance behaviour of the Mihata landslide's samples. The results show that a high pore-water pressure developed because of the shearing effect, which may explain the sudden collapsed of the landslide. LS-RAPID software was used to simulate the initiation and movement of the landslide.

Features of the Mihata landslide

The Mihata landslide occurred in in the early morning of 6 August 2012. The landslide was not triggered by obvious rainfall, or by an earthquake. However, a high-precipitation event was recorded in the Sada district of Izumo city on 6 July 2012, exactly one month before the landslide. The maximum hourly precipitation recorded was 74 mm, with a 10-minute maximum of 21.5 mm. Although smaller than the Tsuwano and Gotsu events described above, this was also a 37-year record rainfall for Izumo city. Light rain fell for a few days after the main event, and all rainfall ceased on 21 July. At that time the Mihata slope did not show any obvious signs of deformation. On 26 July 2012, a small collapse occurred at the right end of the slope, near the Mihata River. A main scarp with a height of 3 m was detected in the Mihata landslide on 2 August 2012. A large and sudden deformation then occurred on 6 August 2012, creating a main scarp 20 m in height (Fig. 2).

Figure 2 Main scarp of 20 m in height (taken by Do N.H., 15 Oct. 2012)

Ring shear test results

The ring shear test apparatus (ICL-2) was used to simulate the landslide dynamics. The apparatus is the latest model of undrained dynamic-loading ring shear apparatus developed by Sassa et al. (2013) in conjunction with SATREPS project in Vietnam. To examine the shear behaviour of the samples from the Mihata landslide, two tests were conducted: (a) undrained shear speed control and (b) pore water pressure control. In the undrained shear speed control test, the sample was first fully saturated and consolidated at 1,000 kPa normal stress. Then, it was sheared in the shear speed control mode at 2 kPa/sec. The effective stress path reached to the failure line, then the stress path went down until reaching a certain value. The final state was the steady state of the sample (Sassa et al., 2013). When shear stress was increased, pore-water pressure started to increase immediately. When the shear resistance reached to peak value, pore-water pressure was 250 kPa and still increasing as shear displacement increasing. This test result presents that the samples were high generated excess pore water pressure (more than 200 kPa) during shearing. It can be calculated as the ground-water level rising 21 m. Combining this result with the calculation in the triaxial test result, it may possibly explain the trigger and the process of the Mihata landslide.

Simulation the initiation and motion of the landslide by the integrated computer model

We used the LS-RAPID software to simulate the initiation and motion of the landslide. The soil parameters including internal friction angle, excess pore pressure, lateral earth pressure coefficient, shear resistance of sliding surface at steady state were measured in triaxial test and ring shear test as above. The values of $\tan\phi_p$ = 0.75, c_p = 20 kPa, τ_{ss} = 280 kPa, k = 0.55 were used as input data of the LS-RAPID software to simulate the initiation and motion of the landslide. Simulation stopped when the zero velocity for all meshes appeared. Time in the figure 14 (b) shows the time from the start to the end of motion. The air photo taken from a helicopter and the simulation results presented in the 3D view from a similar angle are presented (Fig. 3).

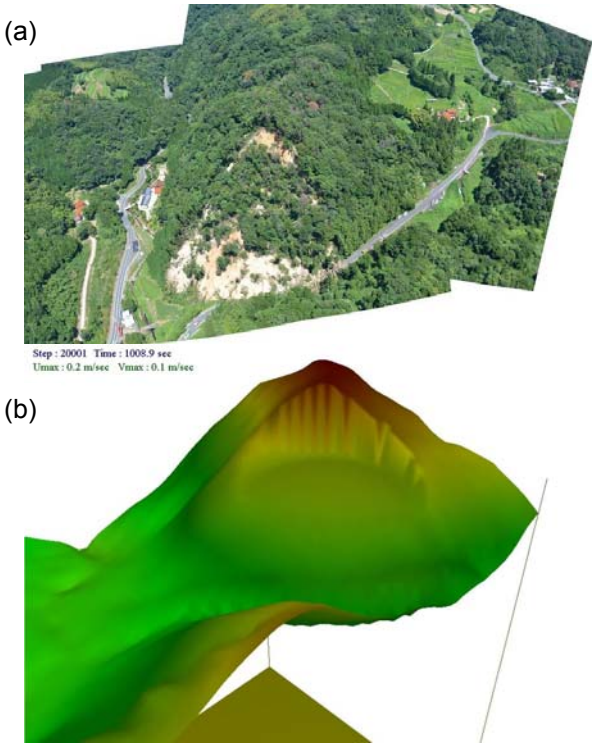

Figure 3 Air photo by Fujii et al., 2013 (a) and the result of computer simulation (b) of the Mihata landslide

Discussion and conclusions

Through field investigation and direct shear tests, triaxial tests, ring shear tests on the motion mechanism of the Mihata landslide, a possible explanation for the Mihata landslide is concluded as follows:

1. Historical heavy precipitation within 37 years on 6 July 2012 (one month before Mihata landslide occurred on 6 August 2012) infiltrated into the soil which has low permeability, causing ground-water level to rise, leading to initial movement.
2. During the initial movement of some weak zones within the sliding mass, high excess pore water pressure was generated in shearing zone.
3. The sliding mass moving slowly, leading the excess pore water pressure to increase slowly until reaching the failure value. Then whole landslide mass rapidly collapsed.
4. The sliding mass did not move for a long distance after the failure because of a high residual strength, or high steady state of Mihata landslide soil.
5. Higher precipitation due to climate changing, global warming, more frequently the risk of landslides occur in Shimane Prefecture, Japan. Monitoring and early warning systems are necessary and important in the potential landslide areas, even in the day without rainfall or earthquake activities.

Participated on The Japan Landslide Society Annual meeting

During my study in Japan, I participated 4 times on The Japan Landslide Society Annual meeting in Matsue city (2013), in Tsukuba city (2014), in Yamagata city (2015), and in Kochi city (2016). In 2013, I participated as a staff of the meeting. In 2014, I participated as a student presented our my research in Shimane University. In 2015 and 2016, I participated as a cooauthor and a member of SATREPS project in Vietnam presented our research in Haivan Station Landslide in Vietnam.

Figure 4: Japan Land Society Annual meeting in 2013 in Matsue, Shimane Prepecture, Japan

In these meeting, reports and exhibitions about research on landslide in Japan were presented by researchers and students of Japan Landslide Socity. These is a very good annual activity so that the reseachers on landslide field can exchange thier experience on there reseach. In near future, the Vietnam Landslide Association on Transport (VLAT) may has the same activity for reseacher on landslide in Vietnam.

Attending International Conference on Landslide

In October 2013 I participated in the 11th International Symmposium on Mititgation of Geo-disasters in Asia hold in Kathmandu, Nepal. I attend the field trip to visit some landslide and debris flow cause by heavy rain and earthquake in Kathmandu and Pokhara in Nepal. I presented my research in Shimane University in this Symmposium and got the Award of Best Student Presentation.

Figure 5: Landslide and debris flow cause by heavy rain and earthquake in Pokhara, Nepal

In June 2014 I participated in the World Landslide Forum 3 hold in Beijing, China. There were many researchers around the world attended and presented their research about landslide. I attend the student section to presented my research on Mihata landslide in Japan.

Figure 6: I presented my research on Mihata landslide in World Landslide Forum 3 in Beijing, China

Training on Activities of SATREPS Project in Vietnam

Training on using Ring shear apparatus

In order to measure apparent friction angle of the Mihata landslide material during a long shear displacement in the laboratory, the undrained dynamic-loading ring shear apparatus (ICL-2) was used to simulate the landslide dynamics. The apparatus is the latest model of undrained dynamic-loading ring shear apparatus developed by Sassa et al. (2013) in conjunction with SATREPS project in Vietnam.

Figure 7: Training on using ring shear apparatus in Kyoto University, Japan

Training on using Landslide flume experiment

To investigate the mechanisms of landslides caused by rainfall, large-scale model slopes have been used to induce shallow landslides. In 2013, landslide experiment facilities were designed and the building was made in ITST. The landslide flume was designed based on the soil properties of the weathered granite of Hai Van area. In 2015 and 2016, four experiments to induce in a large-scale model slope by artificial heavy rainfall were conducted on landslide flume experiment in ITST. Two river sand samples and two weathered granite sand samples were used. The river sand samples were taken from Red River in Hanoi, Vietnam. The two others weather granite sand samples were excavated from Haivan landslide in Danang city in Central of Vietnam

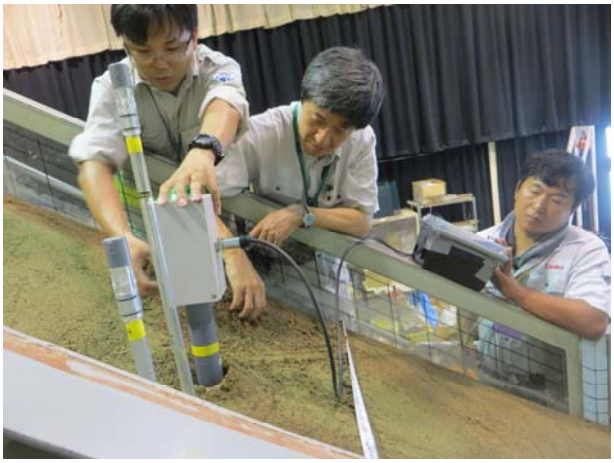

Figure 8: Training on using landslide flume experiment in Forestry and Forest Products Research Institute, Japan

Training on using Landslide monitoring system

This monitoring system is consisted by some kinds of sensors and these are installed at the whole landslide area. The five extensometers are used for alarm and they are installed nearby railway track. Others are used for clarification of mechanism of landslide for early warning. The position of each sensor is decided in consideration of the characteristics. All observation sensors are networked by cable or wireless LAN connection. And all data is transferred to computers in ITST office automatically.

Figure 9: Training on using Total station - Monitoring system in Haivan Station landslide, Da Nang, Vietnam

Acknowledgments

At first I am grateful to the leaders and colleagues of Institute of Transport Science and Technology, Ministry of Transport, Vietnam, for their support my study in this project.

I would like to express my deep appreciation and thanks to all Professors and Experts from Japan in our SATREPS project for their guide and support me in my study.

I also would like to acknowledge with thanks all Professors and friends in the Department of Geosciences, Faculty of Science and Engineering, Shimane University, Japan for their teaching and support me in my Master's course.

I acknowledge financial support from Japan International Cooperation Agency (JICA) and International Consortium on Landslides (ICL) for my training in Japan.

Proceedings of the SATREPS Workshop on Landslides in Vietnam, 2016

Landslides on the road in Vietnam - Monitoring and solutions for landslide risk reduction

Huynh Thanh Binh[(1)], Huynh Dang Vinh[(1)], Do Ngoc Ha[(1,2)]

1) Institute of Transport Science and Technology, Hanoi, Vietnam, e-mail: thanhbinh166@gmail.com (WG4)

2) Shimane University, Project Center on Natural Disaster Reduction, Shimane, Japan (WG4)

Abstract Landslide is one of the disasters caused by natural and human activities. To assess the cause of the landslide, we need to conduct the survey and monitoring which can suggest the appropriate solutions.

Keywords landslide, monitoring, Ho Chi Minh route

Introduction

In Vietnam, the landslide is one of the most popular natural disaster occurring on the road systems. Every year, Landslide usually occurs in the rainy season with more than one million m^3 of volume and damage property about hundreds of billions VND. In the early on October 2007, 60 dead and 13 missing in the storm number 5. The storm also causes long -term traffic congestion in some nation roads.

Figure 1 Landslide in Nghe An province, 2007

According to statistics of Directorate For Road of Vietnam in 2007, the road network has about 223.059 Km length. In particular, up to 3/4 of the total length roads cut through hilly terrain, that has many slopes with 60-70m high, especially some slopes are more than 100m high. According to the general report of Institute of Transport Science and Technology, the region usually occurs landslides in Vietnam, mainly in the roads, mountainous northwest and the route along or cross Truong Son range from Quang Binh to Kontum, Gia Lai such as Nation road No.6, No.70, No.279, No.7, No.14 and Ho Chi Minh route. In summary, Vietnam has a tropical monsoon climate with average rainfall about 2000 mm, a local individual to reach 4000 mm/year (Northwest and Central of Vietnam). Therefore, due to high rainfall, high terrain and complex geological structures, landslide phenomena usually happen and impact on the stability of roads and life of people along the roads.

The classification of landslide in transportation

There are many landslide classifications in the world. It depends on characteristic of climate, geology and hydro geological. In order to identify the reason of landslide phenomena and proposal approximate solutions to reduce the impact of landslides, Institute of Transport Science and Technology has proposed division landslide in 04 typical forms that describe as follows:

Type 1: Landslide

Landslide that the material slid along the surface is curved upward (in the soil embankment or in the homogeneous structure slopes) or break into several sections of the surface depended on bedrock.

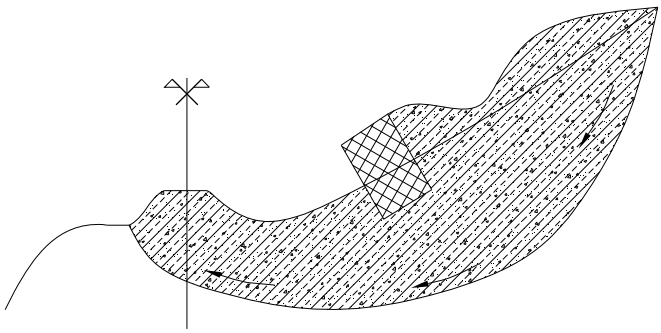

Figure 2 The schematic of landslide

When landslides occur almost materials inside the sliding mass will move simultaneously. On the surface, trees and infrastructures are tilted. Its bent toward the vertical. We

will easily see the scrap and cracks in the top of sliding mass.

Figure 3 Landslide on Ho Chi Minh route

Type 2: Erosion

Erosion is the process by which soils are removed from the Earth's surface by exogenitic processes such as water flow and the effect of ground water.

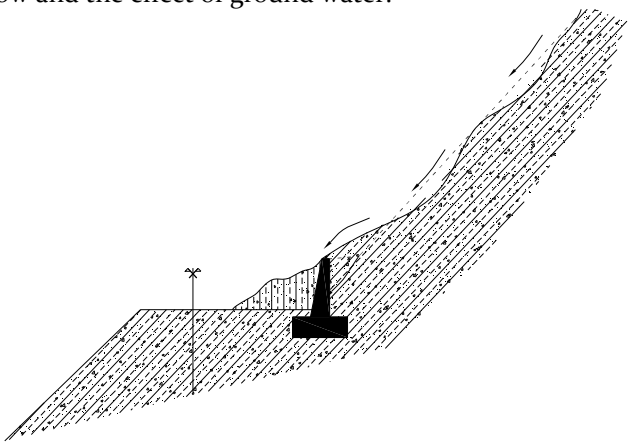

Figure 4 The schematic of erosion on talus.

The final result of this phenomenon is gullies or caves. A other form of erosion is debris flow stream from a cliff or from the watershed to the road.

Figure 5 Erosion in Ho Chi Minh route.

Debris flow occurred in January 2000 on national road No.27 has caused serious consequences for agricultural production, damaging dozens of kilometres of roads and cause damage to tens of billions VND.

Type 3: Topple

A topple is the final period of erosion phenomena. In the field investigation, it is difficult to identify scarp and sliding surface. The material in sliding mass is disturbance and tree collapse. Topples usually occur quickly and makes the soil around warped, cracked and affect the stability of the soil next to it.

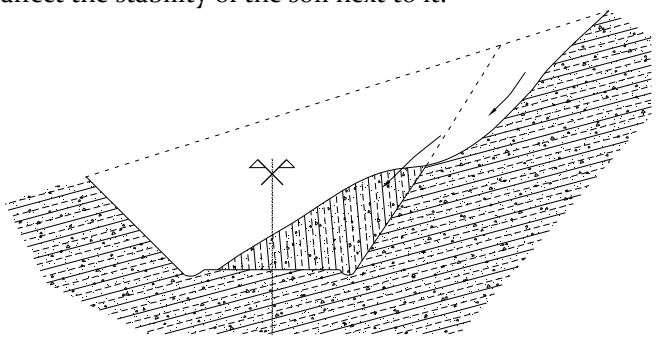

Figure 6 The schematic of topple

Figure 7 The topple in national road No.6

Type 4: Rock fall

Rock falls are abrupt, downward movements of rock or earth, or both, that detach from steep slopes or cliffs. Rock fall can occur in the rainy season or sunny day. The material volume is not so high, but it is dangerous for people and affect on the transportation system.

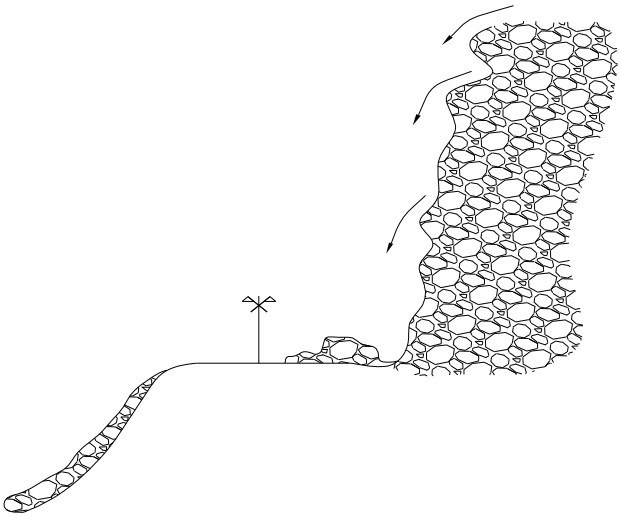

Figure 8 The schematic of rock fall

Figure 9 Rock fall on national road No.37

In summary, landslides phenomenon usually occurs roads network, especially during rainy seasons. Landslides damage roads, threatening the lives of the residential areas along the route, causing damage to life and property every year hundreds of billions VND. We have a national standard TCVN 9861:2013 about the investigation and design for landslide mitigation on the road. However, the landslide study in Vietnam is limited and has some problems. So, to assess the cause of landslide we need investigation experience and using the monitoring methods.

Some monitoring instrumentations for landslide

In recent year, we installed some monitoring instrumentations to observe and forecast landslides. In this part, we will introduce some instrumentations that have been used in Vietnam as follows:

Rain gauge

Figure 10 Rain gauge installed in Hai Van station

Landslides are related to rainy season (rainfall and rainy time). So, rain gauge usually uses for landslide monitoring and early warning. The rain gauge can connect to the siren system to warn the community if the precipitation reaches a certain value.

Inclinometer

Inclinometers are used for monitoring deformation normal to the axis of a pipe by means of a probe passing along the pipe. Inclinometers are installed to exceed the expected depth of sliding surface. So, the inclinometer provides data for defining sliding surface. At present, Institute of Transport Science and Technology is building the national standard for inclinometer.

Figure 11 Inclinometer system

Monitoring instrumentations for surface movement

One of the methods of landslide monitoring is to install posts that can be sequentially measured for landslide movement. However, these surface posts can be damaged by animals or people. Wooden, concrete or metal posts in the ground can be directly installed into a landslide. In addition, some stable reference points beyond the boundary of the moving landslide are needed.

Figure 12 Concrete post for landslide monitoring

Figure 13 Geodetic measurement for landslide movement

Figure 14 Checking the data of extensometer

Installation of extensometers is similar to establishing movement posts except for the wire connection between the landslide and the stable location adjacent to the landslide. For slow-moving landslides, it may be difficult to determine the location for installing a stable base for the extensometer. Additionally, if the ground is generally creeping outside of the landslide, then the measurement of landslide movement will not be accurate.

Piezometers

Piezometers are instruments that are installed within the ground to measure the groundwater pressure at specific depths.

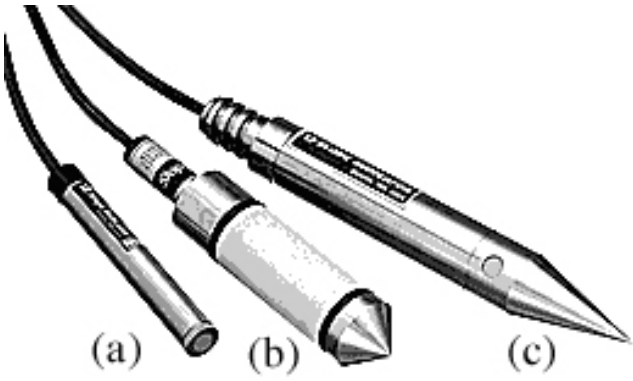

Figure 15 Probe piezometers
a- for bore hole, b- for embankment, c- for pressing into the soil

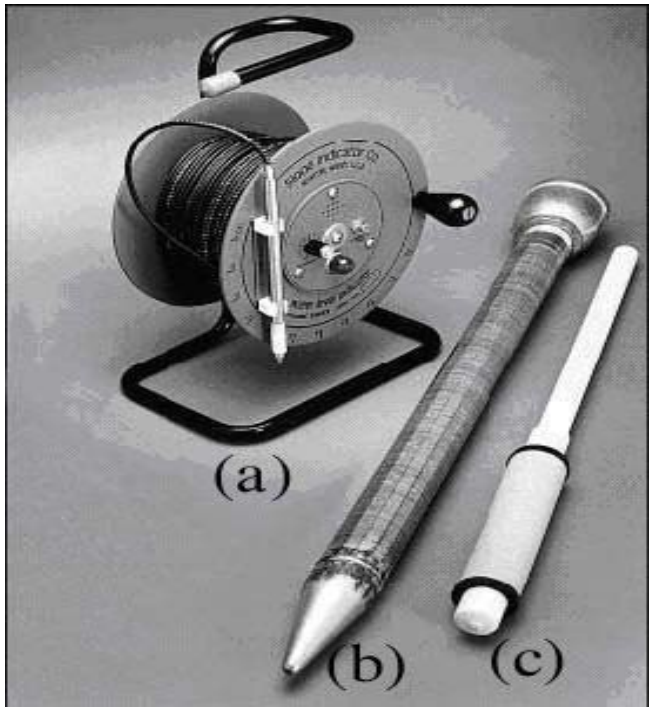

Figure 16 Groundwater measurement device

In addition, we need to measure the ground water level. Those information are useful for detailed long term monitoring of ground water level fluctuation and landslide movement.

Some Solutions for landslide mitigation

The group of structural solutions

In the structural solutions, we need to flexibly apply solutions to enhance the stability of the slope as:

Geometry modification measures, in which the geometry of the hillside is changed (in general the slope).

This method easily to construct and is low cost but it need wide space.

Drainage measures aim to made lower ground water level or to reduce the water content of material. Drainage can be either surface or subsurface. Surface drainage measures require minimal design and costs and have substantial stability benefits. We applied the various methods of drainage such as: site levelling, ditches drains and drain pipes, deep drainage trenches.

Reinforcement measures aim to increase landslide resisting forces. It is a expensive measure and consists of two different approaches: insertion of reinforcement elements in the ground (anchor, nailing, geogrids, retaining walls, micro piles) and the improvement of the mechanical characteristics of the ground (chemical, thermal or mechanical treatment).

The group of non-structural solutions

Propagate widely to people to realize the importance of threats from natural hazards and specially landslides hazards caused in particular for preventive measures.

Conclusions

Vietnam is located in tropical monsoon climate and topography and geology condition are complicated. So, landslides usually occur especially during rainy seasons. Therefore, we need the promotion of research and apply measures to prevent landslides efficiently on transport routes and in residential areas in the local mountains. In Vietnam, we study the reason of landslide and design the solution after the landslide happens but some landslides still occur. The monitoring system only install after we construct some structural solutions. It is problem in Vietnam. In the future, we will study some new technology for landside monitoring such as Hai Van station case to observe the slope movement and develop the early warning system in Vietnam.

Reference

Doan Minh Tam (2013) Research ground prestressed anchors technology on the road, Research project

ITST (2005-2010) Investigation and design for landslides on Ho Chi Minh road, Results project

ITST (2008) Research technology choices and conditions apply new technologies to combat soil loss on the road, Research project

ITST (2006) Research technology anchors for landslide on the road, Research project

Lomtadze V.D. (1982) Geological Engineering (in Vietnamese language - translation from Russian). Publisher College and Technical secondary schools in Hanoi

Vietnam National Standard TCVN 8869 (2011) Method for measurements of pore pressures in soil

Proceedings of the SATREPS Workshop on Landslides in Vietnam, 2016

Experience of Landslide Trainees in Japan – proposal for application of unmanned aerial vehicle (UAV) for landslide survey along transport arteries in Viet Nam

Nguyen Kim Thanh

Institute of transport science and technology, Viet Nam, e-mail: nguyenkimthanh.itst@gmail.com

Abstract Project for ''Development of Landslide Risk Assessment Technology along Transport Arteries in Vietnam" is not only expected to provide new technologies and research facilities in landslide risk assessment but also to develop the human resources of the Institute of Transport Science and technology though Long-term training and Short-term training. This project is considered as a success of a new landslide - training tool in the cooperation with Asia members of International Consortium on Landslides (ICL), especially South-East Asia countries in terms of mitigation of natural disaster.

This paper summarizes my studying results from short-term training in Japan, self-orientation on research in the future, and received of new technology under Japanese experts' instruction.

Keywords, Landslide, RSA, UAV, Viet Nam...

Introduction

Currently, the Institute of Transport Science and Technology (ITST) under the Ministry of Transport of Vietnam has been assigned as Project Owner of an ODA project with Japanese Government's fund assistance by JICA titled 'Development of Landslide Risk Assessment Technology along Arteries in Vietnam'. The purpose of this project is to reduce landslide disasters along main transport arteries and on residential areas and education and capacity development for the effective use of this technology which is implemented in Viet Nam. The expected outputs of project are (1) Preparation of integrated guidelines for the application of developed landslide risk assessment technology and capacity development by WG1 Joint Team of all groups, (2)Wide-area landslide mapping and identification of landslide risk area by WG2 Mapping Group, (3)Development of landslide risk assessment technology based on soil testing and computer simulation by WG3 Testing Group and (4) Risk evaluation and development of early warning system based on landslide monitoring by WG4 Monitoring Group.

Author join project play in role, (1)Project Secretary; (2) Member of ODA Project Management Unit; (3) Member of Work Group (WG) 3- Development of landslide risk assessment technology through laboratory soil testing & Computer simulation. Some main tasks are as follows:

- To support legal matters and link the communication between ITST with JICA Project office and JICA Vietnam Office contributing to the development of the Project.
- To participate frequently or occasionally counterpart tasks assigned by the Project Director and ODA Project Manager
- To join with team for site survey, relevant data collection, making reports for the Project purpose.
- To join and support Vietnam's and Japan's expert survey trips for the Project purpose in Vietnam.
- To work on main activities of WG 3: Development of landslide risk assessment technology through laboratory soil testing & Computer simulation
- To participate training program tutored by JICA/JST experts.
- To participate the business trip and training to Japan 4 times.

Experience of Landslide Trainees in Kyoto, Japan 2014

Business trip To check the JICA/JST project equipment, 16-29 June 2014, Kyoto. Japan

The Business trip "to check the JICA/JST project equipments " was held at 16-29 June 2014 at ICL Laboratory, Kyoto University, Kyoto. Japan, under the Jica assistance.

This was the content of program in the framework of project for ''Development of Landslide Risk Assessment Technology along Transport Arteries in Vietnam" with purpose to reduce landslide disasters along main transport arteries and on residential areas and education and capacity development for the effective use of this technology which is implemented in Viet Nam. The outputs of this checking and training program are (1) checked the JICA/JST project equipments for the Ring shear apparatus (the version of ICL2-Verson No3) (2) Learned how to operate the shear test apparatus (the

equipment will be installed in ITST later for the project use) and how to analyze the data, (3) After studying to operate the shear test apparatus, participant can promote Landslide study and share the skill with ITST staff in future.

This checking and training program was assigned for WG3, Development of landslide risk assessment technology based on soil testing and computer simulation. The objective of the checking and the training the training program includes:

- The participants would check the manufacture for ring shear apparatus before they were transferred to Vietnam including: checking about operation the stabilities, some changes or adjustment needed during manufacturing, checking some technical factors of RSA as testing the samples.
- The participants would have opportunities to learn how to operate the shear test apparatus (the equipment will be installed in ITST later for the project use) and how to analyze the data.
- After studying to operate the shear test apparatus, participants can promote Landslide study and share the skill with ITST staff in future.

Figure 1. The first testing RSA with Hai Van sample

Experience on the result of training course direct shear test, 29 August to 30 September 2014, Kyoto. Japan

This training program was assigned for WG3. The objective of the training program includes:

- The participants would check the manufacture for ring shear apparatus before they were transferred to Vietnam including: checking about operation the stabilities, some changes or adjustment during manufacturing, checking some technical factors of RSA as testing the samples
- The participants would have opportunities to learn how to operate the direct shear test apparatus (the equipment would be installed in ITST later for the project use) and how to analyse the data.
- After studying to operate the direct shear test apparatus, participants can promote Landslide study and share the skill with ITST staff in future.
- Training result, I proposed to PMU have official letter to ICL for begin manufacture Ring shear apparatus for Project.

Figure 2. testing RSA with Hai Van sand and potable direct shear test.

Experience on the Business trip 8 April to 21 April 2016, Sendai. Japan

This Business trip is under Project for Development of landslide risk assessment technology based on mapping. The objective of the business program includes:

- The participants had training UAV including: Guide to UAV to fly and take photo, guide to analyzing photo by software.
- The participant had opportunities to learn how to operate the UAV and how to analyze the data by Photoscan Pro Software.
- The participants discussed with Prof. Miyagi for analyzing results.
- The participants discussed with Prof. Miyagi for outline of guideline for DSM establishing by UAV-SFM.

The future plan of actions of the training the training programs are:

- To participate to carry out of the ODA Project with technical assistance funded of JICA titled 'Development of Landslides Risk Assessment Technology along Transport Arteries in Vietnam'.
- Senior management as functions and tasks in ITST.

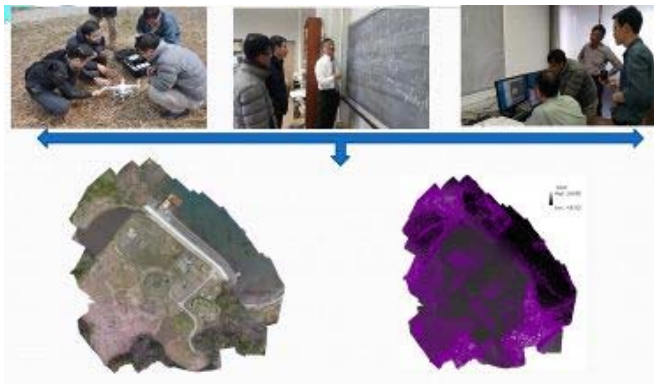

Figure 3. Training UAV in sendai, Japan

After Business trip to Tohoku-Gakuin University, the participants have some conclusions:

- We received a new technology for survey and mapping Landslide.
- Apply UAV for landslide survey results are useful for quickly, cost photographed by UAV cheaper than ordinary air photos

Field Trip to Landslides and Debris Flows of Japan 11th to 15th September 2016

Objective: to visit several types of landslide and debris flows sites
To observe the monitoring system and disaster reduction measures at each site
To utilize the knowledge and experience of this trip for establishing Vietnamese National Standard of Landslide Prevention

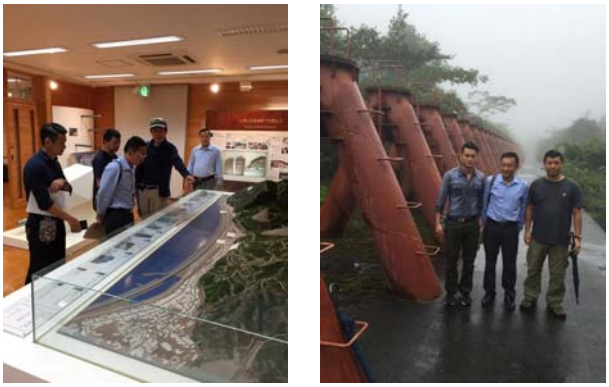

Figure 4. Field Trip to Landslides and Debris Flows of Japan

The business trip provided information and insights to Vietnamese Group about structure and operation of Landslide Disaster Management unit of Japan as well as the Morden solutions, new texture types in reducing the effects of landslide on transportation construction.
The solution to prevent and reduce disaster of Japan are varied and efficiency, especially with many solutions using new technology and materials such as pile foundation retaining wall, steel pile, system of stabilization of slope anchor, underground drainage works such as water well, horizontal drainage drilling or drainage tunnel or monitoring system of early warning. To apply these solutions, need to understand about the types, causes mechanism of landslide occurring. Based on experience be used at Japan, these solutions can be applied to prevent landslides along the transportation routes in Vietnam. However, we need to research construction and promulgate standards for effective application.
The business trip completed purpose and requirement set out initially. Through the survey trip and research results in the frame work of Project "Development of technology risk assessment due to landslides along the main transportation routes in Vietnam", Institute of Transport Science and Technology will build research plans, standards to advise the Ministry of Transport in the prevention and reduction of damage caused by landslides on transportation construction consistent with the conditions of Vietnam.

Experience of Landslide Trainees in Japan – proposal for application unmanned aerial vehicle (UAV) for landslide survey along transport arteries in Viet Nam

Landslide is one of the most serious geotechnical disasters in Vietnam tropical monsoon regions, which often leads to the loss of lives and socio-economic impacts. Since the global trend of climate change and rapid urbanization growth are likely to further increase the occurrence of landslide disasters, research on landslides is always considered as an urgent issue for finding appropriate countermeasures in order to prevent and mitigate its impacts.
With nearly 9-year experience of working as a research staff as well as an engineer at Institute of Transport Science and Technology (ITST) in Viet Nam as well as Project secretary of project for "Development of landslide risk assessment technology along transport arteries in Viet Nam", I have executed a lot of works related to engineering geotechnical fields, including site surveys on slope failure, laboratory tests using ring shear apparatus, analysis of slope stability to design safe solutions to sliding surfaces, in-situ geological investigation for construction of traffic infrastructures at the first stage. I have taken part in several research projects in co-operation with ITST's members, including research on landslide characteristics on National Highway No. 6 in Hoa Binh province, Yen Bai province, Ha Long city investigation some sliding surface on Ho Chi Minh Road and research on investigation and analysis of triggering factors for occurrences of slope failures on Hai Van Pass in Da Nang province. These researches showed that mostly landslide occurrence is due to a very complex topography and geological condition (with strong weathered soils or rocks) and impacts of tropical monsoon climate condition in regions. Specifically, prolonged and heavy rainfall is characterized as a key factor causing the events. The typical characteristic of such landslides is reduction of soil strength parameters due to the generation of pore water pressure in slopes. Additionally, I clarified the current stage and failure features of slopes along arterial transport roads in Viet Nam. This is really useful to further propose for appropriate solutions for landslide countermeasures.
Aerial photo technology application has been conducted in Vietnam in various sectors but mainly in military. This technology is recently applied in Vietnam for landslide analysis by Japanese experts via ODA landslide project. Unmanned Aerial Vehicles (UAV) has been used widely in many countries applying in different sectors. Photo shots, as a result of UAV, could be used for DSM making..
At the present, I am proposing a research under MOT for year 2016-2017, the title is: *research application take photo remote sensing technology using unmanned aerial vehicles (UAV) for landslide survey along transport arteries in Viet Nam*.
This proposal includes 5 parts
Chapter 1. research application take photo remote sensing technology using unmanned aerial vehicles (UAV) for landslide survey in the world
1.1 Overall research on remote sensing photo shoot technology in the world.
1.2. Analysis of features and technology of remote sensing photo shoot in Vietnam.
1.3. Analys of features and actual application of UAV in landslide survey works in Vietnam.

1.4. Analysis of requests for geology survey in landslide.
Chapter 2 Research and proposal type of UAV conform landslide survey in Viet Nam
2.1. Operation principal research for various UAV devices.
2.2. Proposal of UAV devices suitable for landslide survey in Vietnam.
Chapter 3 Research process for UAV application for landslide survey point on transport arteries
3.1. Research processes and technical requirements with UAV flight take photos
3.2. Study of data processing method for UAV
3.3. Technical creation of surface models DSM and DEM digital elevation model data with UAVs
3.4. Analysis of landslide point identification from results of surface modelling
3.1. Research on process and technical requirement for UAV photo shooting.
3.2. Research of data analysis method with UAV.
3.3. Methods to establish DSM surface model and DEM digital elevation model by using UAV data.
3.4. Analysis to identify landslides from surface modelling results.
Chapter 4 Case study about UAV application for landslide survey in Highway No. 06; No 07 and Ha Long city.
4.1. Survey report, landslide point choosing on NH No.6-Hoa Binh, NH No.7- Nghe An and Ha Long City- Quang Ninh.
4.2. Application example of UAV in landslide survey on NH No.6- Hoa Binh.
4.3. Application example of UAV in landslide survey on NH No.7-Nghe An.
4.4. Application example of UAV in landslide survey in Ha Long City- Quang Ninh.
Chapter 5 Guideline making for landslide survey using UAV
5.1. Guideline making for landslide survey using UAV

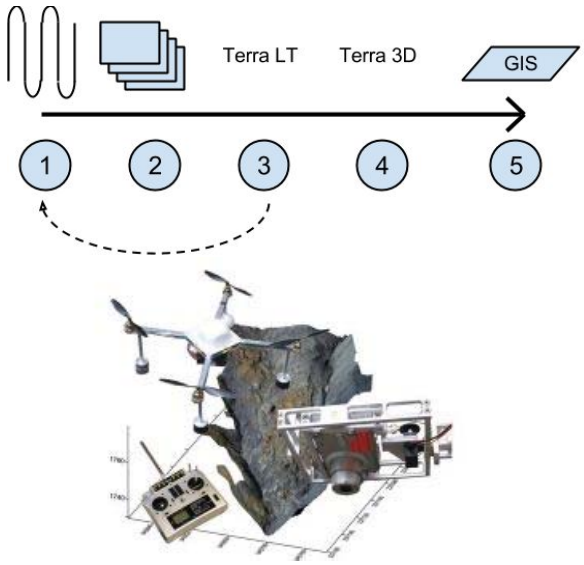

Figure 5. Proposal build process to capture photo by UAV and analysing for landslides survey

Acknowledgments

I pay our sincere gratitude to Professors and of ICL member, in Japan who jointed to this project, many Officers and engineers from ICL, JICA, and Japanese coordinators and especial thanks to Professor. Sassa, Professor Miyagi, Professor. Fukuoka, Dr. Dinh Van Tien who have contributed their outstanding efforts to make training program meaningful.

References

Report on the Business trip To check the JICA/JST project equipment, 16-29 June 2014, Kyoto. Japan, Nguyen Kim Thanh.
Report on the result of training course direct shear test, 29 August to 30 September 2014, Kyoto. Japan, Nguyen Kim Thanh.
Report on the Business trip 8 April to 21 April 2016, Sendai. Japan
Field Trip to Landslides and Debris Flows of Japan 11th to 15th September 2016, Nguyen Kim Thanh.
Report Field Trip to Landslides and Debris Flows of Japan 11th to 15th September 2016, Nguyen Kim Thanh.
Outline research under MOT, research application take photo remote sensing technology using unmanned aerial vehicles (UAV) for landslide survey along transport arteries in Viet Nam, DT164057, Nguyen Kim Thanh

Proceedings of the SATREPS Workshop on Landslides in Vietnam, 2016

Experience of Landslide Trainee in Japan – A case study of Sorayama landslide, Shimane prefecture, Japan

Pham Thi Chien[(1)(2)]

1) Member of WG4, Institute of Transport Science and Technology, Hanoi, Vietnam

2) Master Student Graduated from Shimane University, Shimane, Japan, e-mail: chienpham1612@gmail.com

Abstract

I had been studying for the master course at Shimane University in Japan from 1st October, 2013 to 24th September, 2015. The time when I studied in Japan is one of the best memories in my life. I learned a lot of things during I studied in there including knowledge, experience, making friends and be more confident. In this article, I would like to share my experience during I studied in Japan.

Keywords experience, landslide, laboratory test, field study, conference

Acknowledgment

I would never have been able to complete the master course without many people's support. I would like to express my sincere thanks to my supervisors, Prof. Fawu Wang and Assistant Prof. Toshihide Shibi as well as all of the Professors in Department of Geosciences, Faculty of Science and Engineering, Shimane University for their support and guidance. I am particularly grateful to Prof. Kyoji Sasa of International Consortium on Landslide (ICL) for supporting me to go and study in Japan, Ms. Akemi Yoda and Ms. Kondo Yuko (JICA staff) for their help for my daily life. I would like to thank Japan International Cooperation Agency (JICA) and International Consortium on Landslide (ICL) for their financial support and Institute of Transport Science and Technology for their encouragement so that I could have been studying in Japan. I also would like to thank all of my colleagues at Shimane University for their support for my study. Last but certainly not the least, special thanks goes to my family and my friends who are always beside me.

Introduction of my study in Japan

The objectives of my study are to evaluate the effect of heavy rainfall on the stability of slopes considering variations in groundwater level. A landslide which occurred in 2013 near Matsue city in Shimane prefecture of Japan was chosen as a typical case study. My study has three main parts: field investigation, laboratory tests, and simulation of change in groundwater level and slope stability of a representative landslide using Vadose/W and Slope/W software. In the first part, field investigations were carried out to examine the general properties of the landslide. Some investigation methods were applied such as microtremor survey method, self-potential method and 1-m depth temperature method to understand the geological structure and groundwater flow within the landslide. In the second part, disturbed samples were taken from the landslide to determine the mechanical and physical properties of soil layers. These tests are water content test, specific gravity test, Atterberg limits test, grain size distribution test, direct shear test and triaxial shear test. In the last part, firstly, Vadose/W was used to analyze the infiltration process and variation of groundwater level in the slope due to rainfall, as well as considering transpiration, evaporation and runoff on the surface. A two dimensional model was set up to simulate the longitudinal section of the slope before the landslide occurred. The input data included basic soil parameters, climatic data, initial piezometric head and vegetation condition. Finite element method (FEM) was used to simulate the soil behavior. Furthermore, Slope/W was used to evaluate the stability of the slope during groundwater level change from results in Vadose/W.

Figure 1 Sorayama landslide, Shimane prefecture, Japan

From the series of field and laboratory investigations conducted, it can be inferred that the probable cause of the landslide was due to rapid rise in the groundwater level caused by heavy rainfall that adversely affected the stability of the slope. The events that led to the triggering of the Sorayama landslide can be ascribed to the rainfall events that occurred several days before the day the

landslide was triggered. These rainfall events infiltrated into the soil and raised the groundwater level. However, the 4 September 2013 heavy rainfall with peak value of 85 mm caused rapid rise in the groundwater level which also increased the pore water pressure within the slope and changed the soil slope from unsaturated to fully saturated state. Hence, the reduction of the effective stress of the soil caused by rise in pore water pressure led to the destabilization of the slope and mass failure.

Experience of Landslide trainee in Japan

Firstly, I would like to share the experience to use effectively laboratory and communicate well with professors and colleagues. As you know, soil tests are very important for landslide research. Before I study in Japan, I do not have so many experiences to do the soil tests. However, day by day, my test skill was improved with my professor's support and colleague's support. The experience to use effectively laboratory is practice as more as possible. I am very lucky to have two supervisors Prof. Fawu Wang and Assistant Prof. Toshihide Shibi. Therefore, I joined two groups which belong to my supervisors. I learned a lot about soil test, how to do one research on the landslide, presentation skill and writing an article and a thesis. In my groups, there were many foreign students so my English had been improving by communication with them. Do not be shy when discussing with professors and friends. Be confident, we can learn a lot of things from them and improve ourselves.

Figure 2 A laboratory test in Shimane University

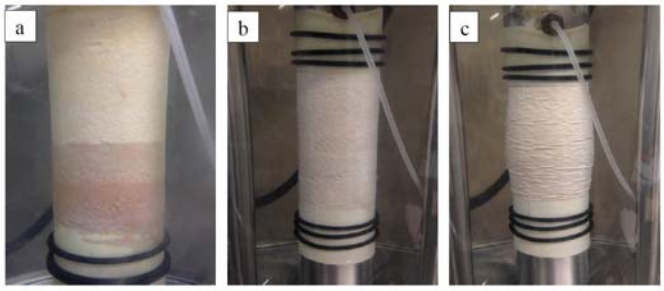

Figure 3 Specimen of triaxial tests (a) when apply de-aired water, (b) before loading and (c) after loading

Secondly, I want to share experience for the study field trips. I had many field trips during I had been studying in Japan. We went to the real landslides to investigate and take soil samples. For my master thesis, I worked on Sorayama landslide which is located Shimane prefecture. We applied some method to investigate this landslide such as microtremor survey method, self-potential method and 1-m depth temperature method to understand the geological structure and groundwater flow within the landslide. Thus, let go to the field trip as much as possible.

Figure 4 An investigation in Ohnan town, Shimane

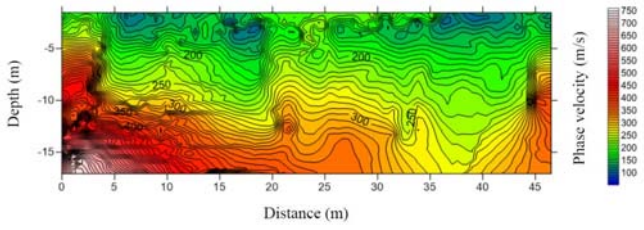

Figure 5 Microtremor survey in Sorayama landslide

Thirdly, it is a great experience when attending conferences in Japan as well as in the world. I joined some conferences during I studied in Japan. I attended the World Landslide Forum 3 in Beijing, China in June 2014. I am also a participant in the 54th annual meeting of the Japan Landslide Society. In the conferences, I had

chances to listen to the research results from experts on the landslides, their research experience and getting their advances for my study. You can ask any question about the subject that you are interested. It will make you more confidence and make you understand deeply on the subjects which you are interested.

Figure 6 World Landslide Forum 3

Moreover, I am also a member of the project for Development of Landslide Risk Assessment Technology Along Transport Arteries in Vietnam. Therefore, I have been participating this project activity. It is a chance for me to apply the knowledge that I studied in Japan in Vietnam.

Figure 7 Group 4 activity in the project for Development of Landslide Risk Assessment Technology Along Transport Arteries

Experience in daily life in Japan

In addition, living in Japan is a wonderful experience in daily life. Please enjoy the life in Japan and do not worry so much before you go to live in Japan. In the first days in Japan, everything there is new for me. I could not speak Japanese, transport system is different and some troubles came to my life. But it did not disappoint me. Through these, I have many good friends who help me to integrate in Japan. I am very interested in the Japanese culture. I love Japanese people. They are very kind and polite. They supported me so much when I live in Japan.

Figure 8 International student activity in Shimane University

Figure 9 Kansai trip of Shimane University

In Japan, I had wonderful experiences and understanding more Japanese and other countries culture. It became a memory that I never forget in my life. Likewise, it makes me improving myself as well as giving me more opportunity in my career. Thank you, Japan!

Proceedings of the SATREPS Workshop on Landslides in Vietnam, 2016

Study on the 2014 Hiroshima Landslide Disasters and Study Experience in Japan

Doan Huy Loi

Institute of Transport Science and Technology, e-mail: doanhuyloidkt@gmail.com

Abstract In this paper, the author presented two parts: the first part is the main content of master thesis, the second part is some experiences during two years study in Japan. On August 20, 2016 many landslides and debris flows occurred in Hiroshima city during the heavy rainfall. Ring shear apparatus (ICL-1) was used to simulate the failure of soils, the formation of sliding surfaces and the steady-state motion of Hiroshima landslide disasters. Samples were taken from source area in Midorii and Yagi district. The ring shear tests on Midorii and Yagi samples were carried out under the normal stress of 50 and 100 kPa that assumed the landslide depth from 4 to 8 m. The triggering factor such as pore-water pressure was calculated by using the Slope-Infiltration-Distributed Equilibrium (SLIDE) model that developed by Liao and Hong et al., (2010, 2012). The rainfall record monitored at the Miiri JMA station for each 10 minutes from 8:30 PM on August 19, 2014 was used to calculated pore-water pressure and landslide occurred when pore-water pressure reached 15.2 kPa. All test results were input to an integrated simulation model (LS-RAPID) as dynamic parameter of landslide. The combination of landslide ring shear simulator and integrated landslide simulation model provides a new tool for landslide assessment. The hazard area and time of occurrence in Hiroshima disaster were estimated by LS-RAPID. The estimated hazard area is similar with landslide moving area reported by Geospatial Information Authority of Japan (GSI). This research will contribute to understanding the mechanism of landslide and debris flow during heavy rainfall as a basic knowledge for disaster prevention.

Keywords Hiroshima landslide, SLIDE model, undrained ring shear apparatus, integrated simulation model, rainfall

Ring shear simulator

Ring shear apparatus was designed initially to investigate the residual shear resistance along the sliding surface at large shear displacement in landslides because it is unlimited for shear displacement (Sassa et al., 2004). The ring shear test was introduced by Hvorslev (1939) and improved by Bishop (1971), Bromhead (1979), Savage and Sayed (1984), Sassa (1984), Hungr and Morgenstern (1984), Tika (1989), and Garga and Sendano (2002). Ring shear apparatus (ICL-1) was developed for Croatia with maximum normal stress in undrained condition is up to 1 Mpa. Fig.1 present the general view of the portable ring shear apparatus.

Fig 1. General view of the portable ring shear apparatus, ICL-1

Debris flows can develop during heavy rainfall but in most cases, they were mobilized from landslides (Sassa, 1998; Iverson et al., 1997). When the initial landslide mass rides on the torrent bed deposits, an undrained loading process may generate a high pore-water pressure within torrent deposits and this helps incorporate those deposits into moving mass (Sassa, 2004).

Fig. 2 illustrates the model for undrained loading of saturated deposits by a displaced mass. Landslide takes place at the head scarp and the displaced soil mass slide down the slope (step I) and then ride onto debris deposit at the toe of the slope (step II). The debris deposits were sheared and moved together with displaced soil mass (step III). In the initial state (step (I)), it is assumed that

applied stress on the torrent deposits was self weight of the column of the debris deposit, W and is expressed by the point "A". If no excess pore pressure gene is generated during the step (II), the initial point moves to point (C) by plus static stress (ΔW) to the initial stress. When sliding mass ride on the debris deposits with a certain velocity, it caused a dynamic stress (Fd). Here, assume the applied stress as the sum of static stress (ΔW) and dynamic stress (Fd). So, by adding applied stress to the initial stress, total stress move to point (B) as is expressed the stress path in the field

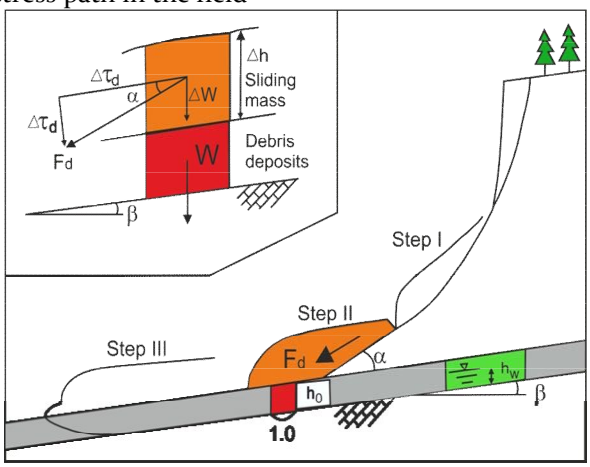

Fig. 2Model for undrained loading of saturated deposits by a displaced mass (Sassa et al., 2004).

The main text of the paper should be formatted using Normal Style according to the Template Style List. The first paragraph of each Section should not have right indentation whilst following paragraphs should, as in the following.

Right indentation is of .8 cm (as per Template Style Normal). The Normal style is based on the Constantia font, available within Microsoft Word software in all recent rheleases, size 10. Line spacing is single. The page format must be strictly respected as per Template Page Format. In particular, two columns formatting with column width of 8.85 cm and column spacing of 0.8 cm should be used. Page margins are: Top 2.5 cm; bottom 2 cm; Internal side 1.5 cm; External side 1.0 cm. Please ensure to respect the paper template which has different margins for right and left pages to allow for double-sided printing.

Test result

Undrained shear stress control and Pore-water pressure control

To study the initiation of landslide, undrained shear stress control and pore-water pressure control were conducted. The dynamic parameters were obtained to simulation Hiroshima landslide disasters. In this paper, the author only introduced the most important test is undrained dynamic loading test.

Undrained dynamic loading test

To examine the model in Fig. 2 for Hiroshima landslides, Midorii sample was used to simulate landslide triggered debris flow. The test parameters were: $\Delta h = 3.5m$, $h_0 = 3m$, $\beta = 150$, $\alpha = 0^0$. The unit weight of Midorii sample was $\gamma = 20$ kN/m. The initial stress due to $W_o$were $\sigma_o = 56$ kPa, $\tau_o = 15$ kPa, the increase of static loading due to ΔW of displaced mass were $\Delta\sigma_o = 66$ kPa, $\Delta\tau_o = 20$ kPa, and the dynamic stresses caused by displaced mass were assumed to be $\sigma_d = 0$ kPa, $\tau_d = 75$ kPa. The slide mass moves quickly, so the test was carried out under the undrained condition. The test result was shown in Fig. 3. When shear stress increases only 26 kPa, the torrent deposits will shear and move together with the original slide mass. The peak friction angle was 48.1° and the motion friction angle was 39.8°. The steady state shear resistance reached 2.9 kPa and the apparent friction angle at the steady state was 1.4°. Therefore, rapid motion could continue in a torrent bed steeper than 1.4°.

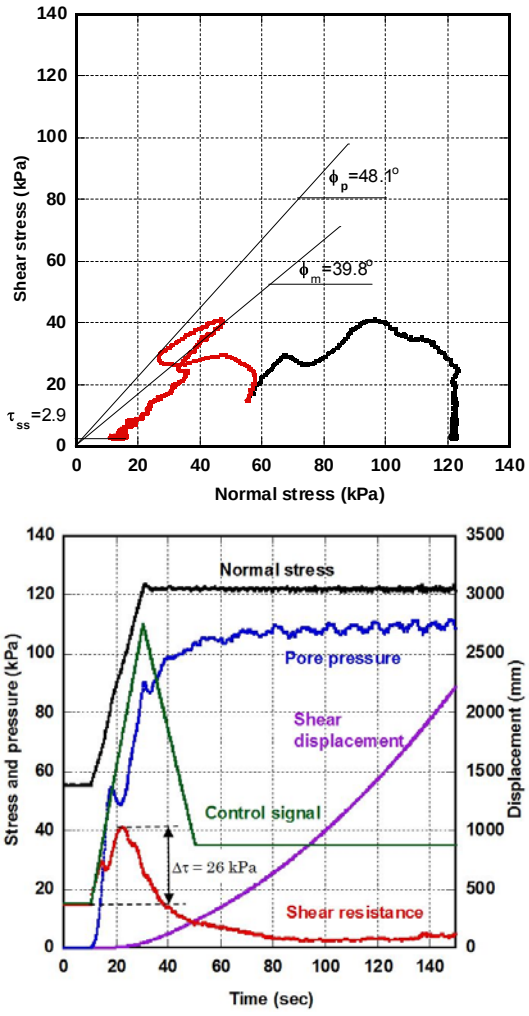

Fig. 3 Stress path and time series data of undrained dynamic loading test on Midorii sample.

Simulation result

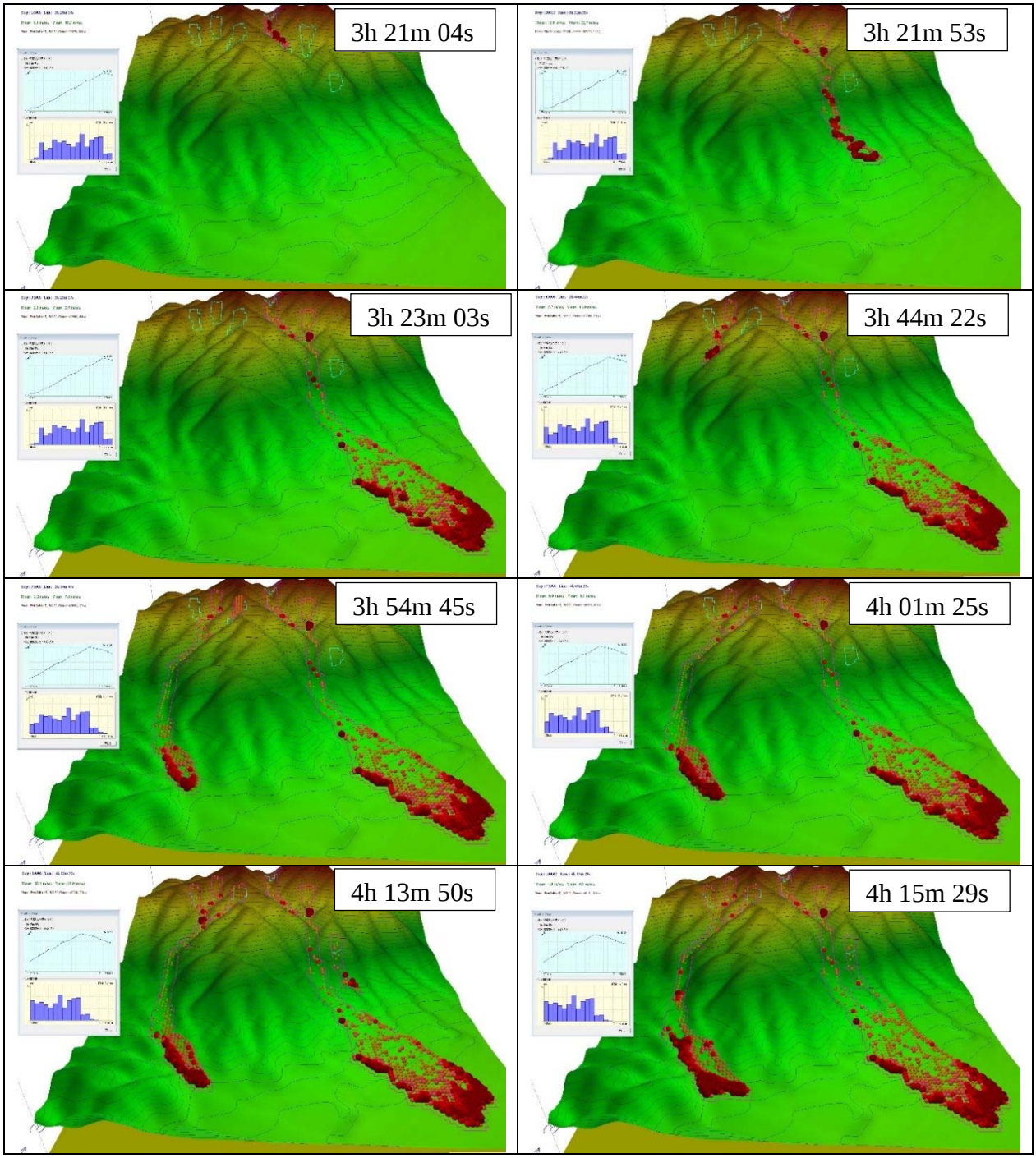

The simulation results are presented in Fig. 4:

Red colour balls represent the moving mass, while blue balls represent the stable mass.

At 3h21m04s, landslides occurred in the top of Yagi district (Yagi-1. At 3h21m53s, Yagi-1 and Yagi-2 flowed together to residential areas. At 3h23m03s, the displacement mass reached residential areas in Yagi district. At 3h44m22s, failure occurred in the central of Midorii (Midorii-2). At 3h54m45s, failure occurred in the other part of Midorii district (Midorii -3). At 4h01m25s, two landslides in Midorii district (Midorii -2, -3) flowed into the residential area. At 4h13m50s, Midorii -3 and Yagi -3 started to move. At 4h15m29s, the landslide mass stopped moving.

Study experience in Japan

First impression after arrival in other countries for school and conduct a research is to study the language and culture of the country first. I am ready to enter this stage when arrived in Japan. I can obtained a lot of knowledge related to the Japan's culture and language. This was be interesting . To study Japanese culture, I jointed some events. I also introduce the vietnamese culture to Japanese people and other foreign student. During 2 years

in Japan, I think the most important that Vietnam must study Japan is everything is always on time.

Fig.5 Sustainability Week event in Kyoto University

Fig. 6 student exchange Vietnam – Japan

Fig. 7 Introduction Vietnamese foods

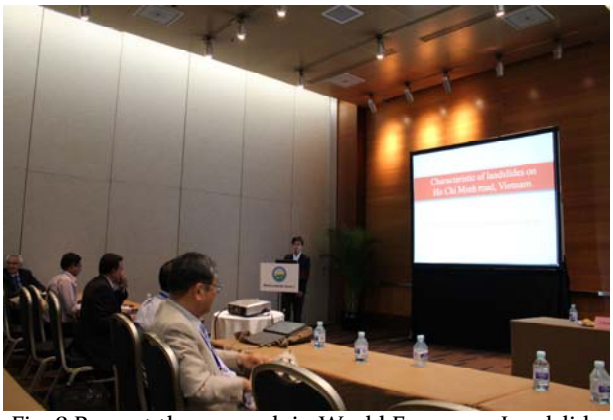

Fig. 8 Present the research in World Forum on Landslide

Fig.9 Shinkansen in Kyoto

Acknowledgments

This research is a part of Vietnamese - Japanese joint research SATREPS'project "Development of landslide risk assessment technology along transportation arteries in Vietnam" The project is financed by the Japan Scienceand Technology Agency (JST) and the Japan International Cooperation Agency (JICA).

References

Liao, Z., Hong, Y.,Wang, J., Fukuoka, H., Sassa, K., Karnawati, D. and Fathani, F. (2010). Prototyping an experimental early warning system for rainfall induced landslides in Indonesia using satellite remote sensing and geospatial datasets. Landslides, Vol.7, No.3: 317-324.

Liao, Z.,Hong, Y., Kirschbaum, D. and Liu, C. (2012) Assessment of shallow landslides from Hurricane Mitch in central America using a physically based model. Environmental Earth Sciences 55:1697-1705.

Montarasio, L. and Valentino, R. (2008) A model for triggering mechanisms of shallow landslides. Natural Hazards and Earth Sciences 8:1149-1159.

Sassa K, Fukuoka H, Wang G, Ishikawa N (2004) Undrained dynamic-loading ring-shear apparatus and its application to landslide dynamics. Landslides 1(1):7–19.

Sassa K, Nagai O, Solidum R, Yamazaki Y, Ohta H (2010) An integrated model simulatingthe initiation and motion of earthquake and rain induced rapid landslides and itsapplication to the 2006 Leyte landslide. Landslides 7(3):219–236.

Sassa K, Dang K, He B, Takara K, Inoue K, Nagai O (2014) A new high-stress undrained ring-shear apparatus and its application to the 1792 Unzen–Mayuyamamegaslide in Japan. Landslides 11 (5):827-842.

Proceedings of the SATREPS Workshop on Landslides in Vietnam, 2016

Experience of Landslide Trainees in Japan - Shallow landslide disaster in Izu-Oshima island caused by the typhoon Wipha, 2013

Vu The Truong [(1)(2)]

1) Member of WG4, Institute of Transport Science and Technology, Hanoi, Vietnam

2) Master Student Graduated from Shizuoka University, Japan, e-mail: thetruong01@yahoo.com

Abstract I am a member of Working Group 4 (WG4). In 2013, I passed entrance exam to participate in Master Course at Shizuoka University, Japan from October 2013 to September 2015. During the long-term training course, I learned about the principle subjects of geology, geotechnical instructed by Japanese professors. I also had chances to survey sites at many landslide areas in Japan and Vietnam. My thesis talking about shallow landslide in Izu-Oshima island, Japan which occurred in October 2013. In this paper, I would like to talk about the main objective of my research and to show some activities on survey sites at many landslide areas in Japan and Vietnam during the long-term training course.

Keywords Working group 4, Shizuoka University, Rainfall, Shallow landslide, Flow-type, Saturated-unsaturated.

Introduction

Heavy rainfall can lead to shallow landslide in slopes that are initially in a state of partial water saturation. The failure surface of shallow landslide is commonly situated between 0.5 and 3 meters in soil depth and runs subparallel to slope surface along an interface between soil cover and bedrock. The whole sliding mass is often several meters to tens of meters wide, several tens of meters long and sums up to a couple of hundred to thousand cubic meters in volume (Dai et al. 1999). Shallow landslide in steep slopes (30 to 400), composed of loose colluvial deposits mostly mobilize completely to form debris flows. Actually, flow-type failures such as debris flows and flowslides are reported to result most often from shallow landslide (Iverson et al. 1997). Although landslides under the action of variations of positive (compressive) pore pressures are well documented and probably most recurrent, they may also happen in unsaturated conditions. Such is the case for slopes where the substratum is not in particular less permeable than the soil cover and the contribution of capillary forces to slope stability is substantial (Godt et al. 2009).

Significant disasters are systematically recorded in Izu-Oshima island, Japan where pyroclastic deposits overlie carbonate massifs. In this study, the groundwater level rising during the typhoon event in the western site of Mt. Mihara in Izu-Oshima island is estimated using combined saturated–unsaturated flow analysis by finite elements method. In the estimation of groundwater level rising, the effect of rainfal boundary condition on the rainwater infiltration into the slope was also investigated.

Outline of Izu-Oshima disasters

Izu-Oshima is a volcano island, which has a 3-4 km across summit caldera and a central cone, in Izu Islands about 100km east of Shizuoka. A major eruption from Izu-Oshima volcano in 1986 produced spectacular lava fountains up to 1600 m height and a 16-km-high subplinian eruption column.

In October 2013, typhoon Wipha passed over the island of Izu-Oshima, bringing strong winds and heavy rainfall (more than 800 mm in 24 hours) that triggered shallow flow-type landslides along the slopes of the western side of Mihara Mountain. Thirtynine people died and missing, and more than 70 houses destroyed in the resulting extensive shallow landslides and following debris flow. The trees, surface soil and volcanic ash deposition becomes debris flow reached the sea.

Cumulative rainfall observed at 9:00 on 15th October in Oshima observatory was about 20 mm. Then rainfall intensity started to increase at around 0:00 on 16th, and reached 118 and 118.5 mm at 3:00 and 4:00 of the same day, respectively. After 24-hours, total rainfall was 824 mm. On the other hand, the interviews from the local residents were carried out and estimated the occurred time of shallow landslides at from 2:30 to 3:00 on 16th October.

The research activities and results obtained

The field investigation were carried out in the collapse area. An average depth of the surface slope collapse was evaluated of 0.92 m by Cone Penetration Test. This test is

a method used to determine the geotechnical engineering properties of soils and delineating soil stratigraphy.

Figure 1 Field investigation in the collapse area

Hydraulic properties of soil samples were investigated by the experiment.

Figure 2 The laboratory activities

A slope in the sediment movements area of western side of Mihara mountain was selected with a distance of 600 m, the depth of the analytical domain is 30 m from ground surface for seepage flow analysis and simulation. The finite element mesh was designed for slope and was composed of 7968 nodes and 8250 elements. Based on the geotechnical engineering properties of soils and the results of the cone penetration test, the slope was divided into 3 layers for saturated–unsaturated flow analysis. The governing flow equation for saturated–unsaturated flow analysis was the two-dimensional form of the Richards equation. The limit equibrium method was applied for slope stability analysis, such as the Ordinary method of slices. Process of groundwater level rising was simulated based on the analysis of transient infiltration of rainwater into the soil during the rainfall duration. And then, the estimated groundwater level changes were applied to the slope stability analysis.

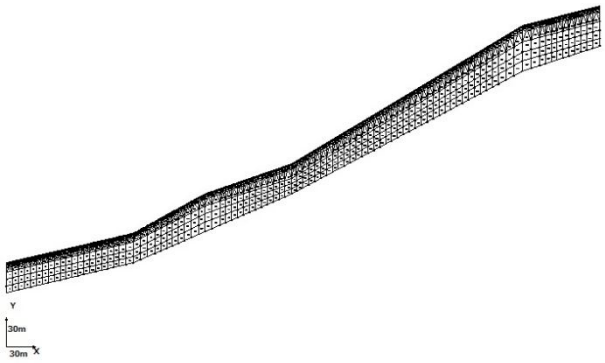

Figure 3 Model slope and finite element mesh (Scale 1:3500)

The main objective of this research is to study the influence on the infiltration of heavy rainfall and the resulting in groundwater level rising, and to estimate the generated location of shallow landslide. With the actual rainfall data and slope material properties, the numerical simulation by the saturated-unsaturated flow theory was conducted to estimate during rainfall infiltration in this research.

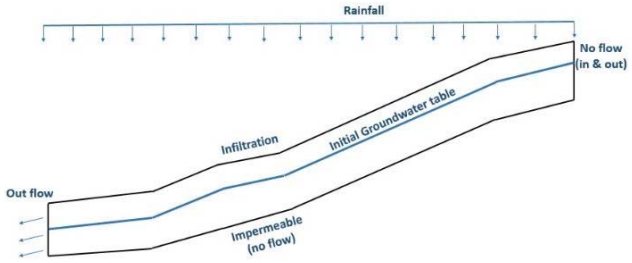

Figure 4 Boundary condition for flow calculation

Factor of safety and the location of shallow landslide in both case without groundwater and with groundwater level after 20 hours of rainfall duration were obtained. The location of shallow landslide with groundwater level rising accorded with the location of the actual failed slope of the site. This result is important for explaining the initiation mechanism of the shallow landslides in Izu-Oshima island.

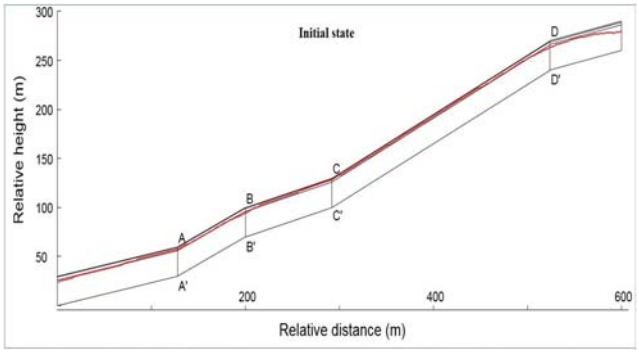

(a)

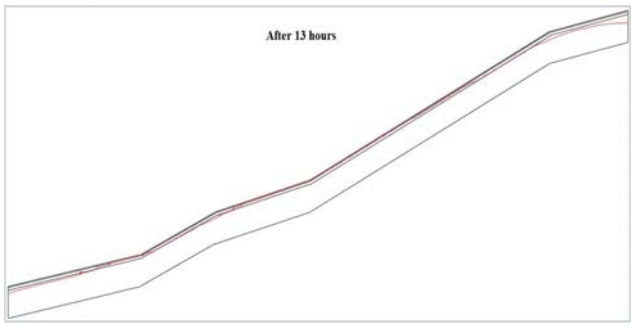

(b) (Scale 1:4500)

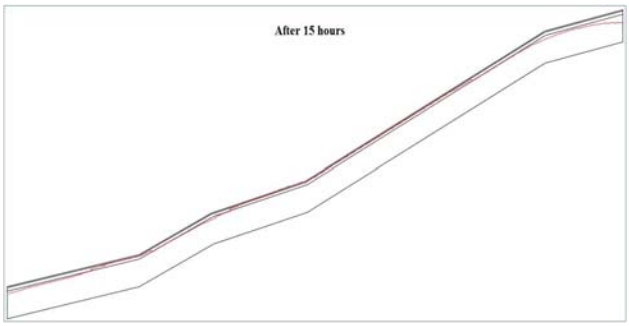

(c) (Scale 1:4500)

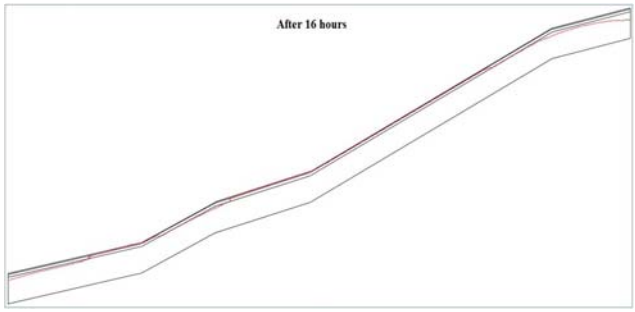

(d) (Scale 1:4500)

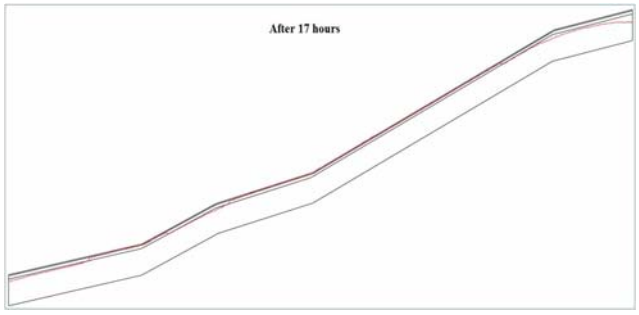

(e) (Scale 1:4500)

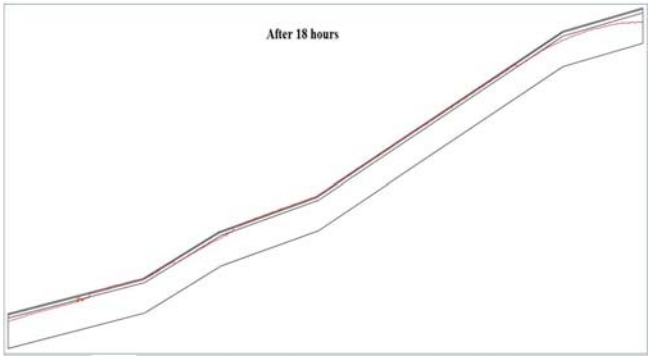

(f) (Scale 1:4500)

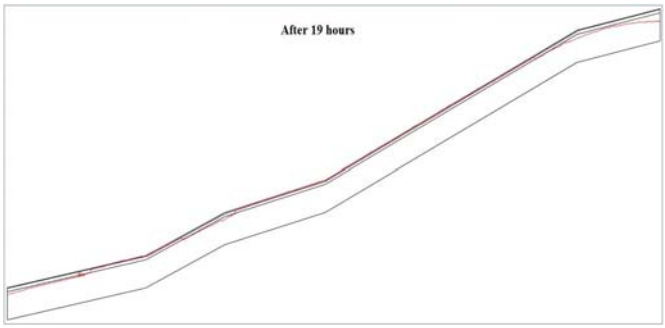

(g) (Scale 1:4500)

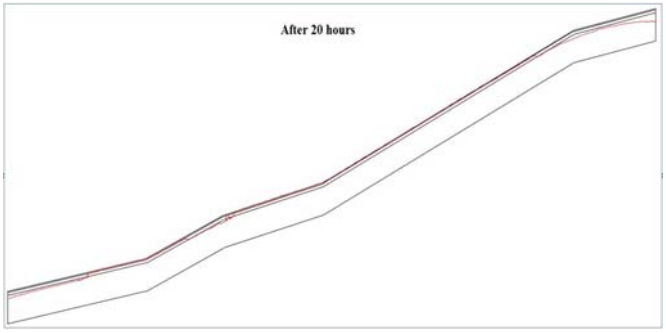

(h) (Scale 1:4500)

Figure 5 State of groundwater level rising in the red colour line (Scale 1:4500); (a) initial state, (b) after 13 hours of rainfall duration, (c) after 15 hours of rainfall duration, (d) after 16 hours of rainfall duration, (e) after 17 hours of rainfall duration, (f) after 18 hours of rainfall duration, (g) after 19 hours of rainfall duration, (h) after 20 hours of rainfall duration.

Survey sites at landslide areas in Vietnam

Figure 6 Survey sites at landslide areas in Hai Van with Japanese professors

Figure 7 Survey sites at landslide areas in Ho Chi Minh Road with Japanese professors

Figure 8 Survey sites at landslide areas in Ho Chi Minh Road with Japanese professors

Figure 9 Survey sites at landslide areas in Highway No 6 (Hoa Binh province) with Japanese professors

Acknowledgments

I am grateful to the leaders and colleagues of Institute of Transport Science and Technology, Ministry of Transport, Vietnam, for their support my study in this project.

I also would like to acknowledge with thanks all Professors and members of Laboratory of Forest Hydrology and Erosion Control Engineering – Department of Environment and Forest Resources Science – Shizuoka University, Japan for their support me in my Master's course.

I acknowledge financial support from Japan International Cooperation Agency (JICA) and International Consortium on Landslides (ICL) for my training in Japan.

ITST-ICL GUIDELINE FOR LANDSLIDE RISK ASSESSMENT

GL 01:2016

First edition

Landslide mapping through Aerial Photograph Interpretation

HA NOI – 2016

Abstract

The production of a landslide inventory map is a very important and preliminary step to determine landslide susceptibility, hazard, and risk assessment. There are a number of methods for producing land-slide inventory maps, such as geomorphological field mapping and visual interpretation of stereoscopic aerial photographs, lidar... The exact choice of method depends on the quality of collected data, type of data, purpose of the map, map scale and availability of aerial photographs etc. In this guideline visual interpretation of stereo-scopic aerial photography is used to prepare an inventory map because of the type of data collected on landslide occurrence. These features are clearly discernible in terms of morphological features that manifest as changes in the form, shape and appearance of the topographic surface. Most of these features can be recognized and appropriately classified through the interpretation of aerial photographs.

Recognizing and mapping of landslide topographic area using aerial photograph interpretation remains a challenging task. Formal standards for identification as yet do not exist, and the interpreter classifies landslide morphological forms based on experience and on the analysis of a set of characteristics (signatures) that can be identified on the images.

Table of contents

Landslide mapping through Aerial Photograph Interpretation

1. Scope

Landslides can be recognized and mapped using various techniques and tools. In this guideline, interpretation of stereoscopic aerial photographs is used to identify and map landslides because it is an intuitive process that requires no sophisticated technological skill; and the technology and tools necessary to interpret aerial photographs are simple and inexpensive compared to those of other methods.

This guideline is performed to guide how to recognize landslide topographic area from aerial photograph interpretation.

2. List of references

Miyagi Toyohiko, Gyawali B. Prasad, Charlchai Tanavud, Aniruth Potichan and Eisaku Hamasaki, (2004). Landslide Risk Evaluation and Mapping - Manual of Aerial Photo Interpretation for Landslide Topography and Risk Management. Report of the National Research Institute for Earth Science and Disaster Prevention.

Guzzetti Fausto, 2005. Thesis - Landslide hazard and risk assessment. Rheinischen Friedrich-Wilhelms-Univestität Bonn.

Rib, H.T., Liang, T., 1978. Recognition and identification. In: Schuster, R.L., Krizek, R.J. (Eds.), Landslide Analysis and Control. Transportation Research Board Special Report, 176. National Academy of Sciences, Washington.

Hansen, A., 1984a. Engineering geomorphology: the application of an Evolutionary model of Hong Kong. Zeitschrift für Geomorphologies 51.

Hansen, A., 1984b. Strategies for classification of landslides. In: Brunsden, D., Prior, D.B. (Eds.), Slope Instability. Wiley, New York.

Hutchinson, J.N., 1988. General report: morphological and geotechnical parameters of landslides in relation to geology and hydrology. In: Bonnard, C. (Ed.), Proceedings 5th International Symposium on Landslides, Lausanne, Switzerland. Balkema, Rotterdam, Netherlands.

Baum, R.L., Schuster, R.L., Godt, J.W., 1999. Map showing locations of damaging landslides in Santa Cruz County, California, resulting from 1997 to 1998 ElNino rain-storms. U.S. Geo-logical Survey Miscellaneous Field Studies Map, MF-2325-D, scale 1:125,000.

Guzzetti Fausto, Alessandro Cesare Mondini, Mauro Cardinali, Federica Fiorucci, Michele Santangeloa, Kang-Tsung Chang, 2012. Landslide inventory maps: New tools for an old problem. Earth-Science Reviews 112.

Varnes, D.J, 1978. Slope movements: types and processes. In: Schuster, R.L. and Krizek, R.J. (eds.) Landslide analysis and control, National Academy of Sciences, Transportation Research Board Special Report 176, Washington.

Karl W. Wegmann, 2006. Digital Landslide Inventory for the Cowlitz County Urban Corridor,

Washington. Washington division of Geology and Earth resources - Report of Investigations 35 – Washington State department of Natural Resources.

Oldrich Hungr, Serge Leroueil, Luciano Picarelli, 2013. The Varnes classification of landslide types, an update. Landslide journal april 2014, pp. 167-195. Doi 10.1007/s10346-013-0436-y.

Soeters, Cees Van Westen, 1996. Slope instability recognition, analysis, and zonation. In: Landslides, investigation and mitigation / ed. by. A.K. Turner and R.L. Schuster. Washington, D.C. National Academy Press, 1996. ISBN 0-309-06151-2. (Transportation Research Board, National Research Council, Special Report; 247).

3. Stereoscopic equipment and photograph requirements

Usually equipment are used for interpreting is mirror stereoscope or pocket stereoscope. This equipment (Figure 1) will create the illusion of three-dimensional depth from given two-dimensional photographs.

For purpose of interpreting: place the pair of photographs on a flat surface; then place the stereoscope over the photographs so that the left lens is over the left photograph and the right lens is over the right photograph. Separate the photographs along the line of flight until two-dimensional photographs are then combined in the brain to give the perception of 3D depth. Finally, sketch the boundary of landslide directly to the photographs base on features recognizing from aerial photographs.

There are no requirements for aerial photographs but remember that interpretation quality depends on the quality of aerial photographs; aerial photography in large scale will give out more detail of result of interpretation.

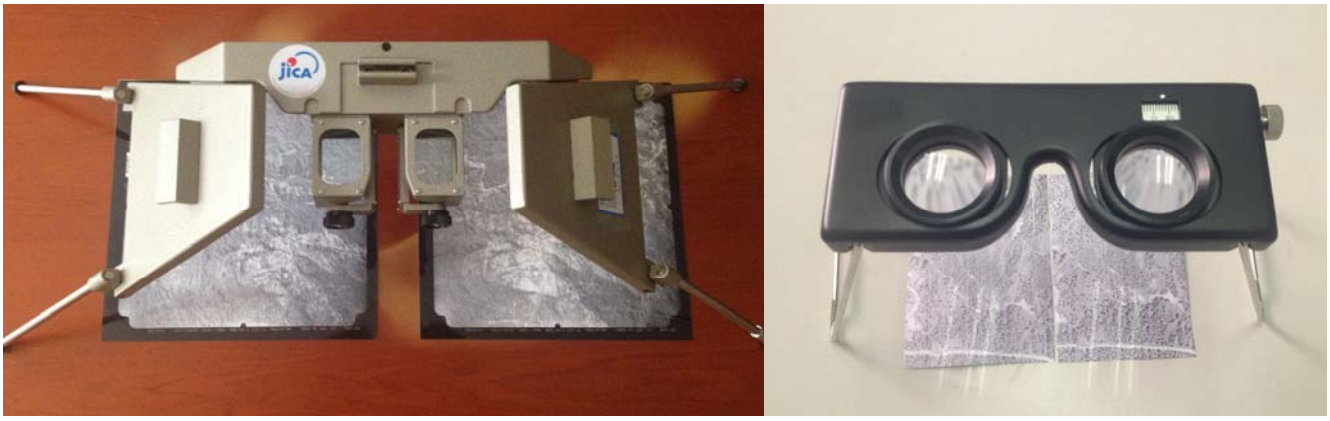

Figure 1 Mirror and pocket stereoscope for interpreting stereoscopic pairs of aerial photographs

4. Theoretical framework

According to Guzzetti (Guzzetti, 2005), identification and mapping of landslides should derive from all of the following assumptions:

i) When landslides occur, they leave discernible signs, most of which can be recognized, classified, and mapped from aerial photograph interpretation. These morphological signs refer to changes in form, position or appearance of the topographic surface. Other signs induced by a slope failure might reflect lithological, geological, land use, or other types of surface or sub-surface changes.

ii) Morphological signs of landslide depend on the type and rate of movement. In general, the same type of landslide will produce similar signs. The morphological signs left by a landslide can be

interpreted to ascertain the extent of slope failure and to infer the type of movement. From the appearance of a landslide, an expert or morphologist can also infer qualitative information of the probability of landslide re-occurrence.

iii) Landslides do not occur randomly. Slope failures represent the result of the interplay of physical process.

iv) For landslides, we can adopt a principle that follows from uniformitarianism. The principle implies that slope failures in the future will be more likely to occur under the conditions which led to past and present instability. Mapping recent slope failures is important to elucidate the geographical distribution and arrangement of past landslides. Landslide inventory maps are fundamental information to help forecast the future occurrence of landslides

5. Landslide recognition

When landslides occur, they alter the local topography of the land surface and leave discernible signs in comparison to the surrounding areas. Most such signs are morphological, involving changes in the shape or appearance of the topographic surface. They can be recognized, classified and mapped through the interpretation of (stereoscopic) aerial photographs (Rib and Liang, 1978; Hansen, 1984a, 1984b; Hutchinson, 1988; Baum, 1999; Guzzetti et al., 2012). A skilled aerial photograph interpreter, by observing various elements on a photograph, can identify numerous ground conditions (e.g., material type, drainage) that are indicative of potential or present landslides.

Numerous features discernible on aerial photographs also aid in the identification and interpretation of landslides and landslide processes. Some of these are the following: scarps; irregular or hummocky topography below scarps, at the body; bare linear tracks oriented downslope; fresh rock exposure; fresh rock accumulation at the slope base; disordered vegetation and disarranged drainage. Aerial photograph examples and a list of basic features are useful for identifying landslides and terrain that might slide.

Figure 2 presents typical aspects of each part constituting the landslide topography. They help interpreters and morphologists can understand and interpret the morphological signature left by the landslide. Of course, landslide topography is diverse and is adjusted by time and erosion processes (Figure 2). Observational data from aerial photograph interpretation range from obvious to subtle. Interpreters and morphologists must classify landslide morphological forms based on experience and based on the analysis of characteristics (signatures) that are identifiable on the images.

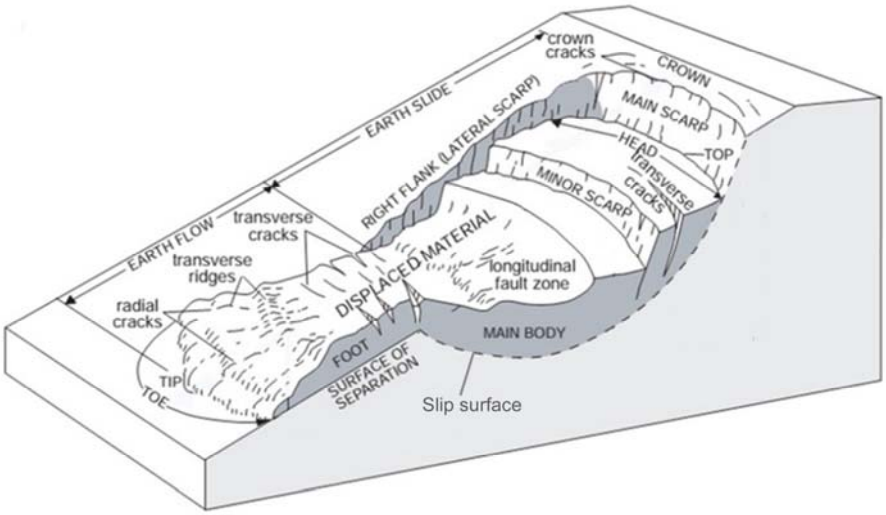

Figure 2 Typical of each part which constitutes landslide topography (Varnes, 1978): This figure shows typical aspects of each part constituting landslide topography

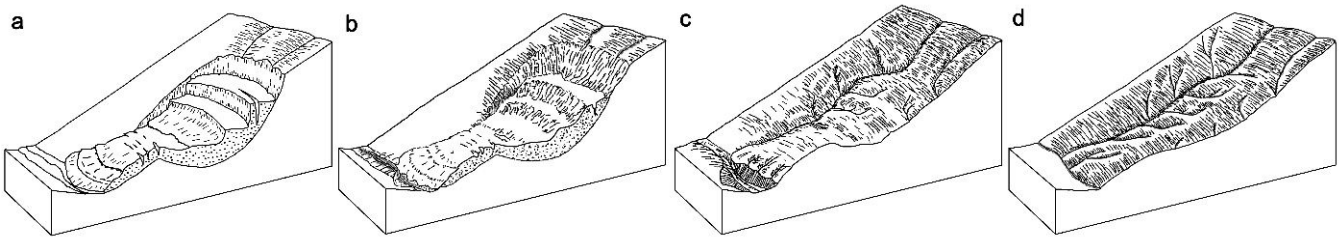

Figure 3 Landslide topography was adjusted by time and erosion process (Karl, 2006). Morphological changes of landslide topography over time, at the first stage when landslide occurred morphological features are very clear (a), and by time and erosion process morphological features become to be more vague (b→d)

Herein, we will outline the basic features used for identifying landslides and potential terrain slides. Interpretation will begin with observation, identification, and measurement of features on photographs. When examining aerial photographs, the significant recognition elements are the relative photographic tone, color, texture, pattern, and shape, in addition to the association of features. Therefore, we must use these elements to recognize existing landslide topographic areas. They are commonly identified based on morphology, vegetation cover characteristics and drainage characteristics.

Regarding morphology: Identifying the landform-morphology commonly identifies the natural process that formed it. It is the first element used to recognize existing landslide. Features related to these elements are concave–convex slopes, hummocky relief, step-like morphology, back tilting of slope faces, semicircular niches, and steep slopes (Figure 4). For example, in a plan including landslide blocks, clear scarp and depressions behind blocks, a block may be back-tilted with an intermediate scarp or cracks in the middle of the body (Figure 4-c); in profile, it is a concave–convex slope (Figure 4-a). Therefore, it must be a rotational slide. When a landslide occurs, landforms at the landslide body are disordered, producing hummocky relief. These features are extremely important to recognize existing landslides. Alternatively, when there is a sudden change in gradient of slope (Figure 4-f); it might be a scarp: a landslide feature. Cracks might be observed on aerial photograph interpretation (Figure 4-e) based on changing of the graphic color and tone.

Vegetation characteristics: These include disorder of vegetation, partly dead vegetation,

differences of vegetation inside and outside of the landslide area, and disrupted vegetation across a slope. Compared with morphology and drainage characteristics, vegetation as an element has been regarded as difficult to interpret because it is influenced by climatic factors and the soil type. For example where abrupt changes in soil conditions exist, vegetation changes will also occur. However, distribution patterns of trees and shrubs contribute to landslide interpretation. These characteristics demand attention when interpreting aerial photographs: disorder of vegetation, partly dead vegetation, differences of vegetation inside and outside of landslide, and disrupted vegetation cover across a slope.

Drainage characteristics: These include disarranged drainage and anomalies in a drainage patterns, zones with stagnated water, seepage zones or well appearance, excessively drained masses. These are easy to recognize from aerial photographs because they contrast with not failed slopes. At first, we view the drainage arrangement, a drainage line broken or a zone of stagnated water making pond at slope means that the area probably is a landslide. Another example is slopes dissected by gullies or canyons, which usually indicates linear features. Such areas are susceptible to debris flows.

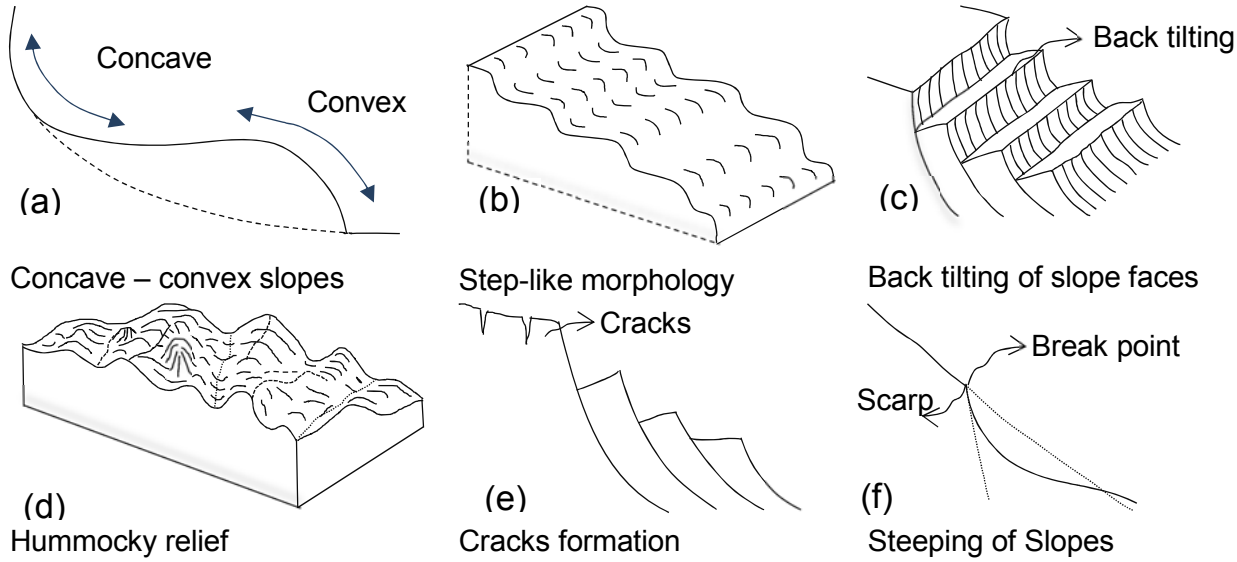

Figure 4 Morphological characteristics of landslides (modified from referenced data)

In the area of Prao and Kham Duc (central province Vietnam), over 100 monochrome aerial photographs in scale of 1/33.000 were used for interpreting. Five types of mass movements were recognized and classified: (i) rotational slide (RS), (ii) translational slide (TS), (iii) complex/compound slide (CS), (iv) debris slide (DS), and (v) debris flow (DF). Among these types, there are three types (rotational slide, translational slide, compound slide) that are classifiable by their topographic features: main scarp, lateral scarp, and landslide body. Two other types (debris slide, debris flow) can be identified only by the topographic features of the body of the feature.

Here are examples that we will describe the geomorphological features of five types that have enabled us to classify mass movements of different types.

5.1. Rotational slide

Rotational slide: A rotational slide is defined as a sliding of a mass of weak rock, soil on a cylindrical or other rotational rupture surface (Oldrich Hungr, 2013). The slide movement is more or less rotational about an axis that is parallel to the contour of the slope. The body is formed by blocks and is generally easily recognizable. There is no disintegration of blocks in the flow lobes and they include spoon-shaped irregular landforms. The morphology is character-ised by a prominent main scarp and a

characteristic back-tilted bench formed at the head of the slide. In the stereo-pair image from the aerial photographs (shown in Figure 6), the block is very clear, hits and blocks the stream. There are depressions behind the block and ponding in niches of the back-tilting area.

Of course, not all of landslides have these features due to post-event weathering, erosion processes and the type of landslide material. In the case of landslide at Figure 7, this has a semi-lunar crown and lobate frontal part, the scarp is curved and slightly concave upward and the slope is characterized by concave (niche) - convex (run-out lobe) forms. These morphological features are specific characteristics of a rotational slide.

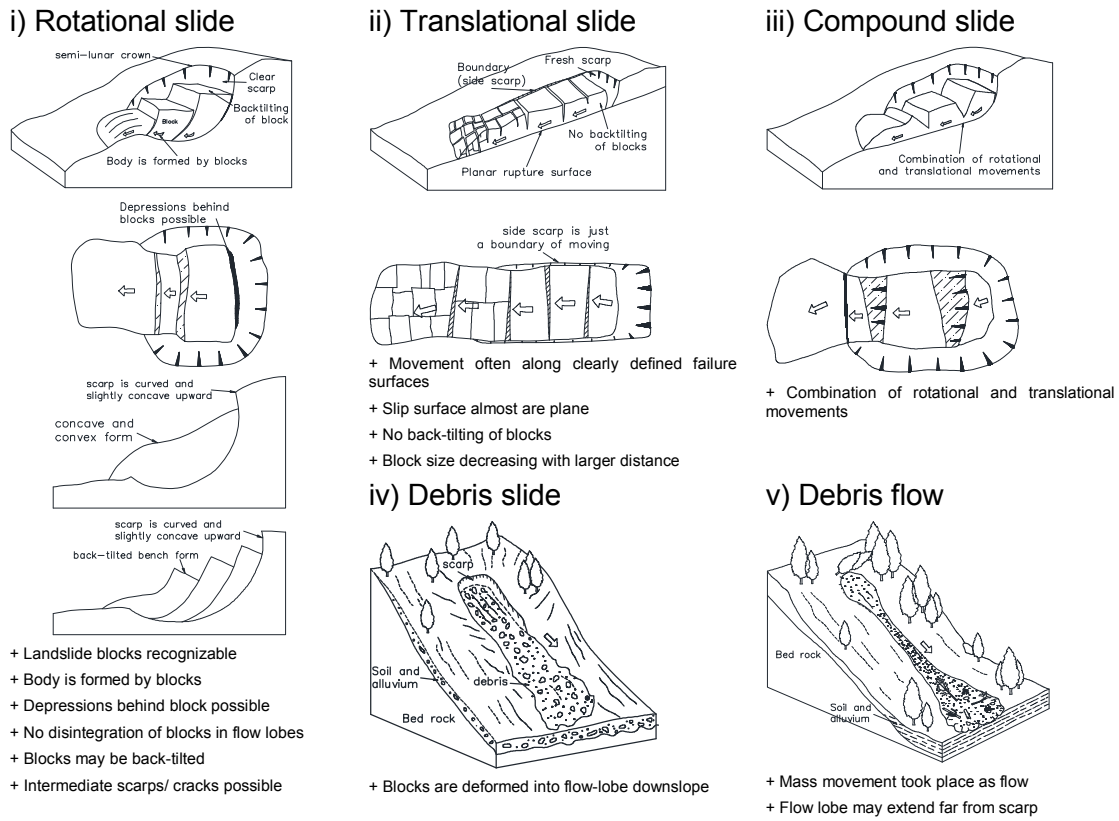

Figure 5 Features of landslide typology for photograph interpretation

Figure 6 Stereo pair aerial photograph (D2-99-06-415 & 416) showing a typical rotational slide

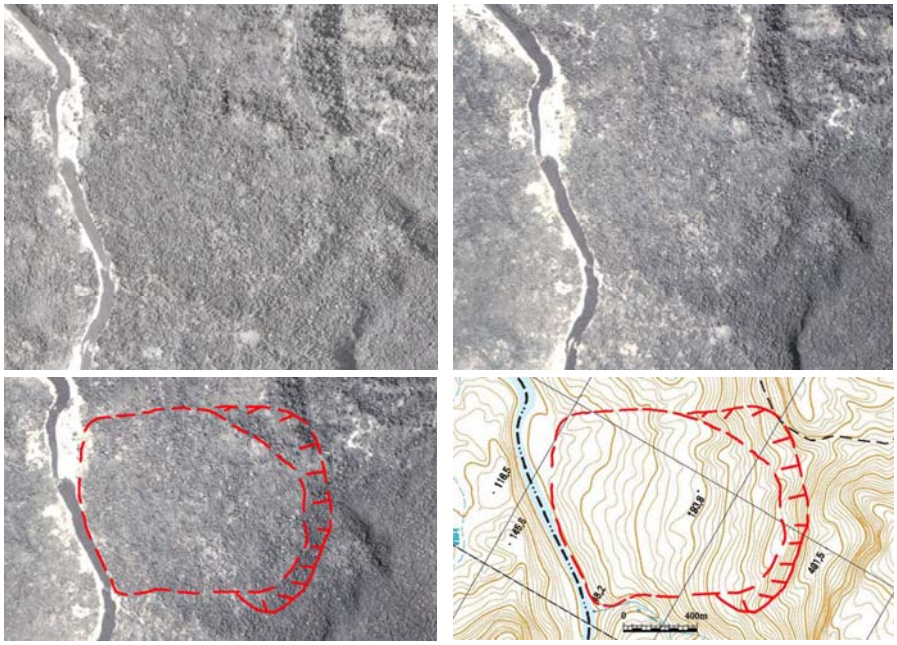

Figure 7 Stereo aerial photo pair(D2-99-05-168 & 169) showing a typical rotational slide

3.2. Translational slide

Translational slide: a translational slide is a sliding mass of rock or block of cohesive soil that moves across one or more inclined planar rupture surfaces (Oldrich Hungr, 2013). In the case of rock, planar slides usually involve dip slopes that have been undercut by erosion or excavation. The slide head may be separating from stable rock along a deep vertical tension crack. In the case of a soil planar slide, it is likely controlled by a weak layer, inclined at an angle exceeding the angle of repose. Before total failure, tension cracks often form during initial disturbance. During and after the failure event, the sliding mass separates from stable soil along these tension cracks and leave a fresh scarp, forming a graben.

The main scarp is not a slip surface, side scarp is just a boundary of moving because that is detachment between body and stable zone (Figure 5-ii). The slip surface is relatively shallow, the run-out hummocky rather chaotic relief, with block size decreasing with larger distance.

In the source area and along the movement pathway, the vegetation is denuded, often with lineation in the direction of movement. In comparison with a rotational slide, there is no ponding below the crown, and surface drainage is either disordered or absent on the body (Soeters, Van Westen, 1996); the scarp is clear and often elongated with no back tilting of blocks. Figure 8 shows a typical translational slide in which a weak layer overlays a planar rock formation. At the head of slide, the separate stable soil and sliding area can easily be recognized. The slip surface is almost planar and the debris accumulates at the bottom of slope deforming the river.

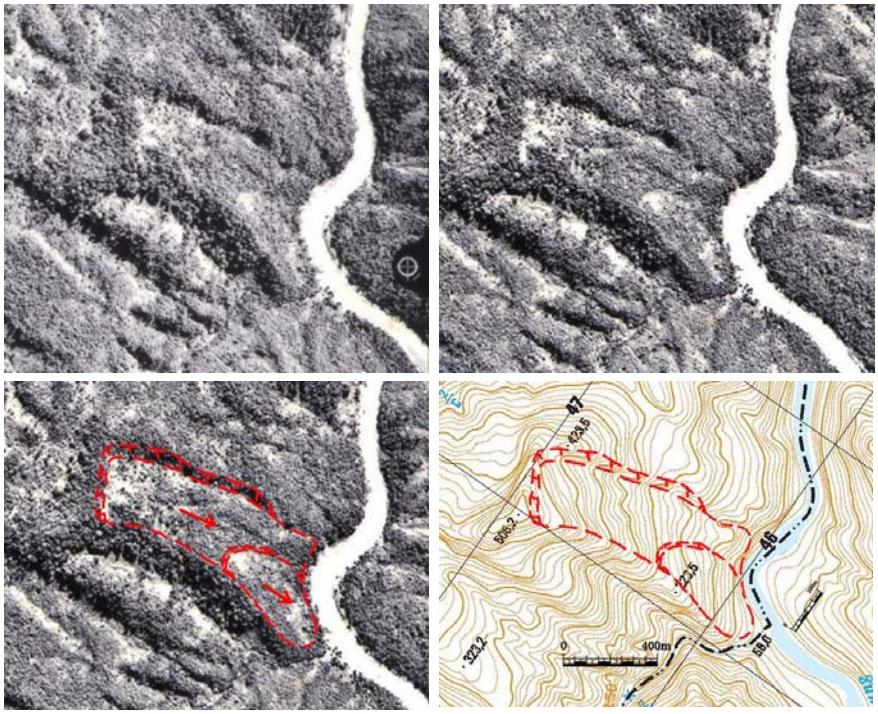

Figure 8 Stereo aerial photo pair (D2-99-06-415 & 416) showing a typical translational slide

3.3. Compound slide

Compound slide: acompound slide is a sliding mass of rock, soil on a rupture surface consisting of several planes or an irregular rupture surface consisting of a number of randomly oriented joints. When a landslide occurs as a compound slide, it creates a concave-convex slope morphology. Concavity is often associated with a linear graben-like depression. There is no clear run-out but there is a gentle convex/bulging frontal lobe. Back-tilting facets are associated with (small) antithetic faults (Soeters, Van Westen, 1996). Figure 9 illustrates typical features of this type of slide.

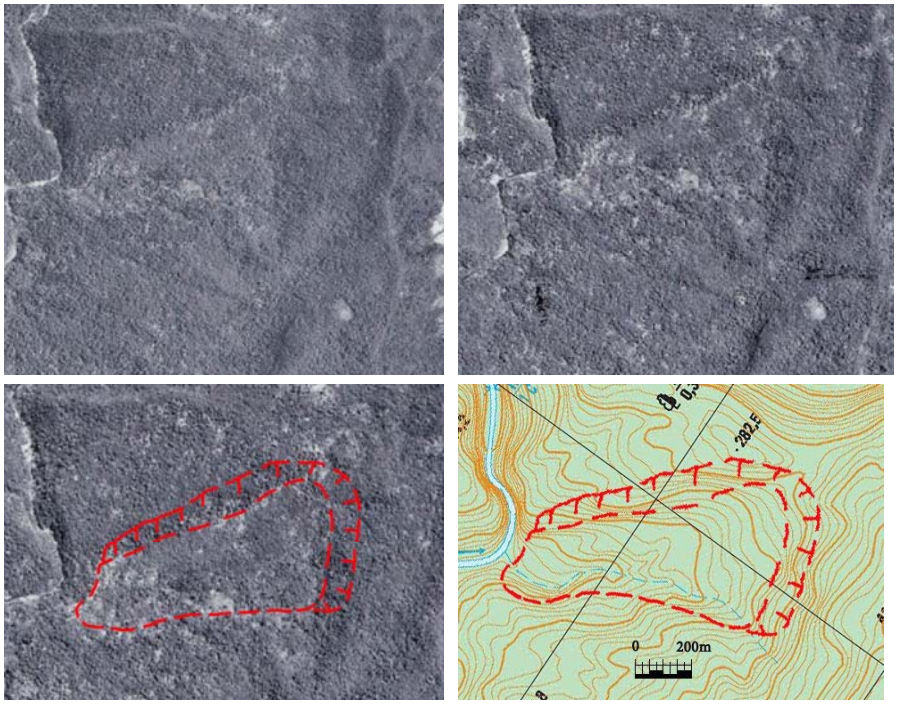

Figure 9 Stereo pair aerial photo (D2-99-04-226 & 227) show typical of compound slide

3.4. Debris slide

Debris slide: a debris slide involves the movement of a mass of unconsolidated material along a steeply-sloping, planar surface parallel to the ground. Usually, the sliding mass is a veneer of colluvium, weathered soil or pyroclastic deposits sliding over a stronger substrate. Many debris slides become flow-like after moving from tens to hundreds of meters and may transform into extremely rapid debris avalanches (Oldrich Hungr, 2013) and accumulate downslope. Based on this definition, we can deduce morphological character-istics belonging to this type; blocks (landslide body) are deformed into flow-lobes downslope, and display clear flow-structures with a lobate convex frontal section. The flow-lobe is usually larger than the initial blocks (landslide body). Figure 10 shows these features.

Vegetation on the scar and body is highly disturbed and clearly distinguishable from the surroundings. Drainage conditionsinclude ponding or disturbed drainage towards the rear and deflected or blocked drainage at the frontal lobe.

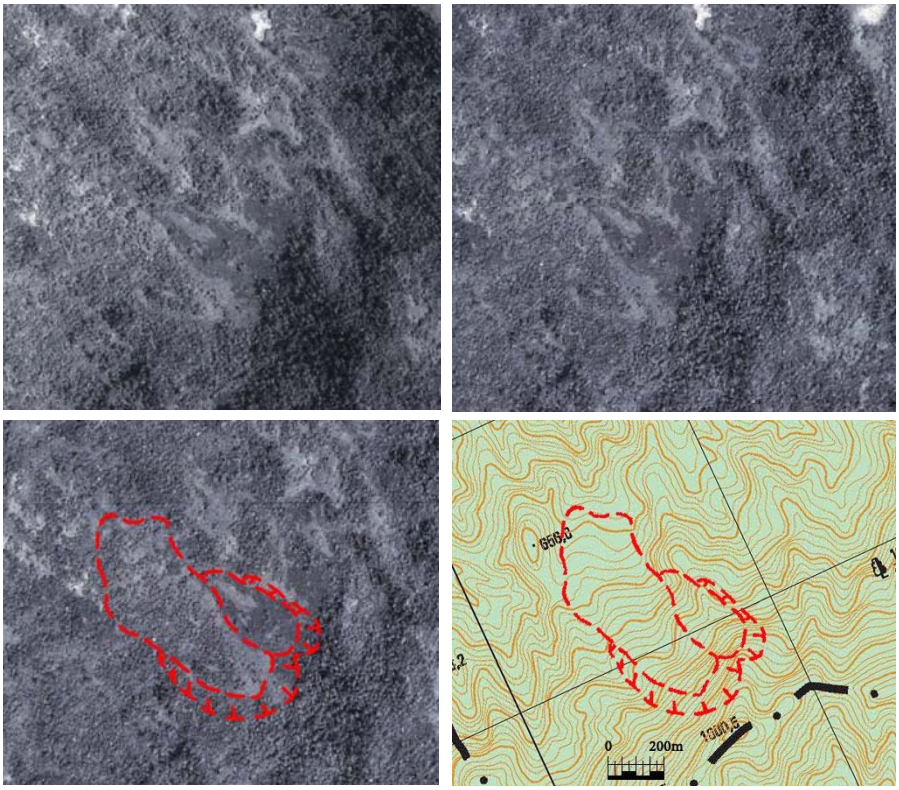

Figure 10 Stereo pair aerial photo (D2-99-03-244 & 245) show typical of debris slide

3.5. Debris flow

Debris flows: A debris flow involves movement of loose soil or gravel on a steep slope. It often occurs simultaneously with heavy rainfall and initiate by a slide, debris avalanche or rock fall from a steep bank or spontaneous instability in a steeply sloping stream bed (Oldrich Hungr, 2013). Under such conditions, these materials can liquefy or be subject to a significant increase in pore-pressure and flow downslope. Morphological features associate with this type of landslide typically include large numbers of small concavities) or one major scar characterizing source area. There is almost complete destruction along the movement pathway, sometimes marked by depositional levees. Figure 11 shows a typical debris flow feature in the study area.

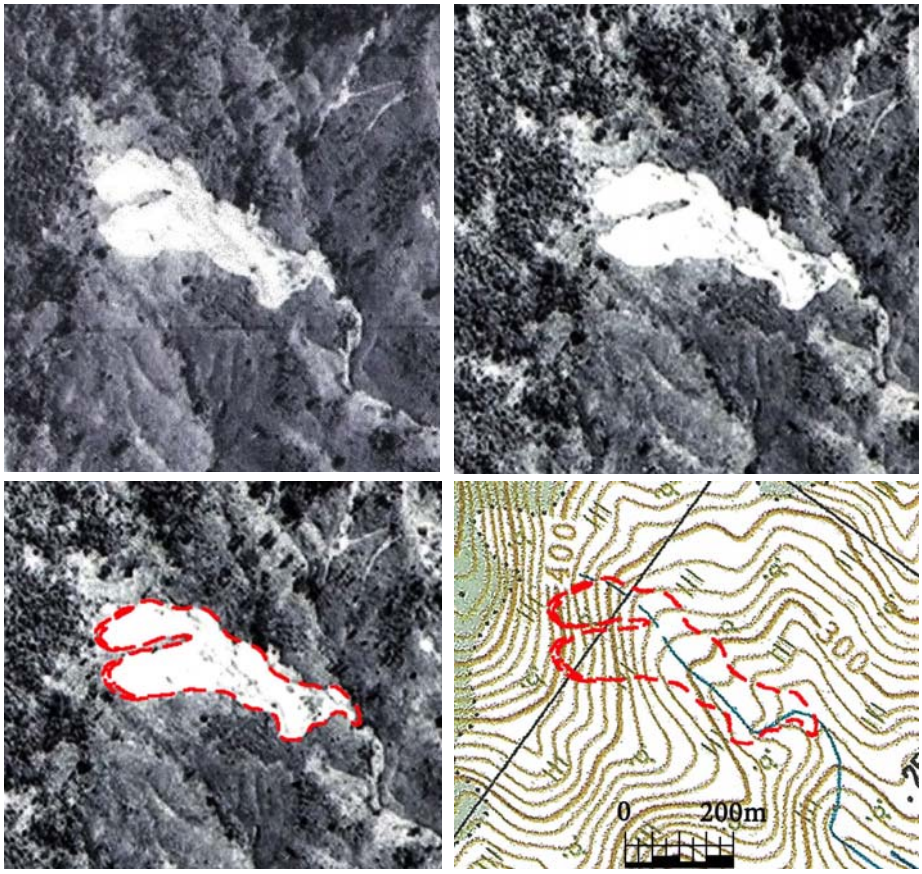

Figure 11 Stereo pair aerial photo (D2-99-06-127 & 128) show typical of debris flow

5. Landslide inventory mapping

A result of aerial photograph interpretation is presented by landslide inventory map. A map, that is defined as a terrain map showing the distribution of existing landslides. They can contain diverse data on past landslide occurrence, such as location, date of occurrence, activity and physical properties of landslides in a region… Most important in landslide mapping is the identification of and representation of the main boundary structure for a unit landslide landform (Miyagi et al., 2004). Therefore, it is drawn with thick lines (curves). General rules for the symbols on landslide maps are shown in Figure 12. The crown of a main scarp and its extension flank or lateral scarps are shown by thick lines. A fresh and continuous crown is drawn by a continuous thick line (Figure 12-I.A.1). If a crown is discontinuous with dissection by gullies or small valleys in the case of a somewhat aged landslide which has been more or less eroded, lines must be broken with intervals of the same lengths on the map as the widths of the dissected parts of the crown (I. A. 2). A crown dissected by many gullies or small valleys in an advanced stage of erosion is shown by a thick dashed line (I. A. 3). Rounded and/or vague crowns in more advanced stages of erosion are depicted by a single-dot-dash-line (I. A. 4), if landslide deposit remain on the downward slope.

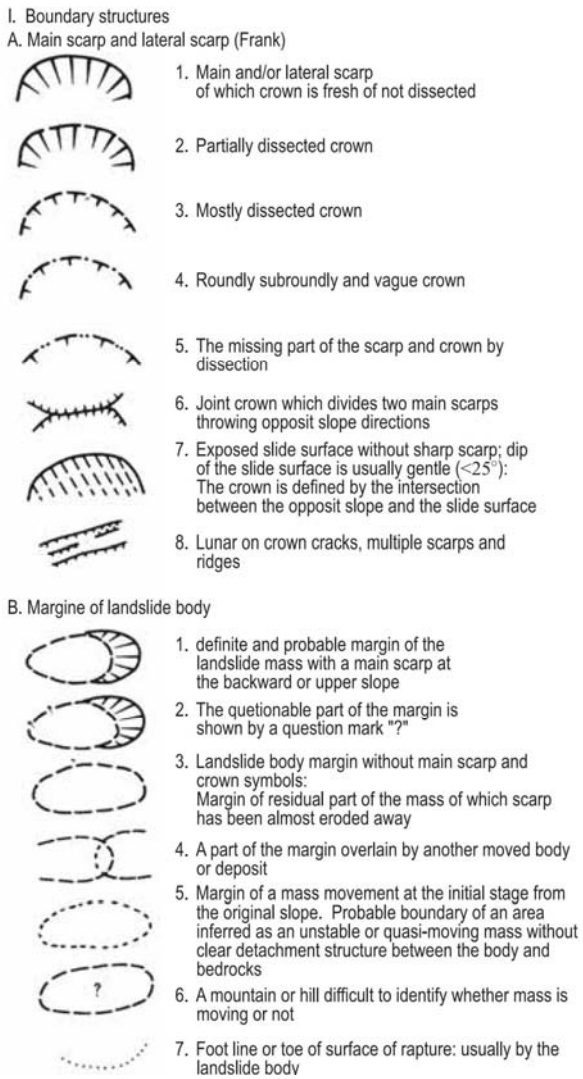

Figure 12 Symbols of the boundary structure for landslide inventory map (Miyagi et al., 2004)

Here is an example of landslide inventory map

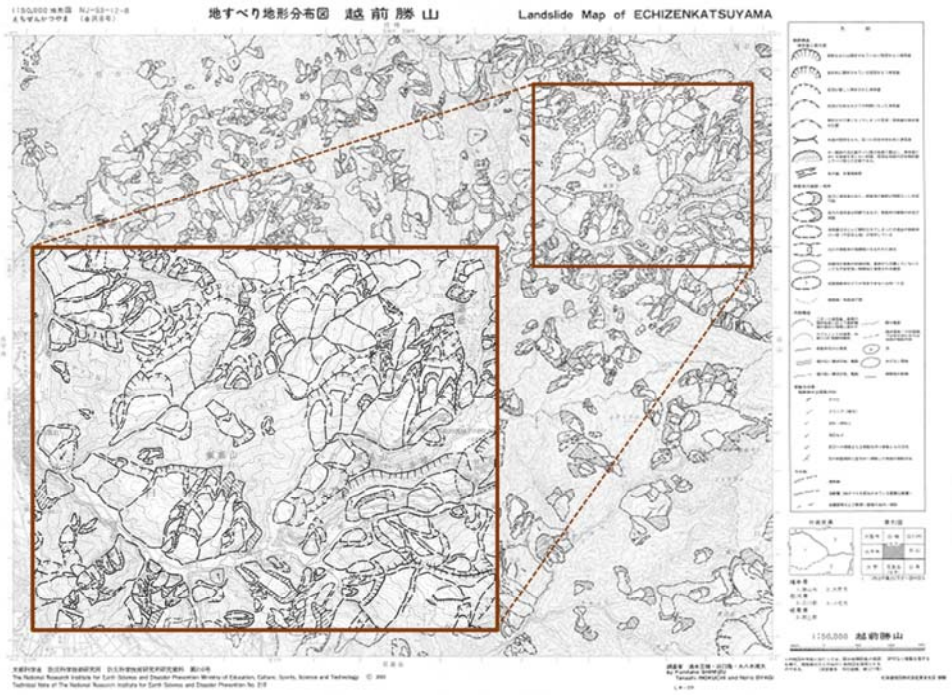

Figure 13 Example of landslide inventory map at Echizenkatsuyama (NIED, 2000)

ITST-ICL GUIDELINE FOR LANDSLIDE RISK ASSESSMENT

GL 04:2016

First edition

Landslide risk evaluation by using AHP (Analytic Hierarchy Process) approach

HA NOI - 2016

Abstract

In Vietnam, landslides occur frequently; most of them was recognized after they occurred. Countermeasures must be quite simple because of lack of funds including retaining walls, surface water drainage works, and earth removal works... Although these countermeasures are simple but they require large budgets, the government cannot supply them sufficiently because lack of budget and disasters increase year by year. Therefore, risk evaluation is extremely important. We must ascertain the probability of landslide occurrence and take time to prepare sufficient necessary sources for reduction. In this case, Analytic Hierarchy Process (AHP) method is used to evaluate the risk. It aims to rank decision alternatives and select the best one for a complex multi-criteria decision-making problem using pairwise comparison of those criteria. This work will be implemented through several times discussion at the working groups. Each person in the working group implements AHP evaluations. The score is calculated intuitively based on the experiences of a geomorphologist. In this way, landslides are classified from special high risk to low risk based on the AHP score evaluation.

Table of contents

Landslide risk evaluation by using AHP (analytic hierarchy process) approach

1. Scope

This guideline is performed to guide how to evaluate possibility of landslide re-occurrence by AHP approach.

2. List of references

Hamaski Eisaku, Miyagi Toyohiko, 2013. Risk Evaluation using the Analytic Hierarchy Process (AHP) - Introduction to the process concept. ICL Landslide Teaching Tools, pp36-49.

Miyagi Toyohiko, Gyawali B. Prasad, Charlchai Tanavud, Aniruth Potichan and Eisaku Hamasaki, (2004). Landslide Risk Evaluation and Mapping - Manual of Aerial Photo Interpretation for Landslide Topography and Risk Management. Report of the National Research Institute for Earth Science and Disaster Prevention.

Saaty, T., 1980. The Analytic Hierarchy Process. McGraw Hill International.

Zhang L, 2010. Thesis-Comparison of classical analytic hierarchy process (AHP) approach and fuzzy AHP approach in multiple-criteria decision making for commercial vehicle information systems and networks (CVISN) project. University of Nebraska-Lincoln.

3. AHP methodology

Analytic Hierarchy Process (AHP) method is multiple-criteria decision-making method proposed by Thomas Saaty in 1980. In that time, Saaty was directing research projects for Arms Control and Disarmament at the US State Department. He had to surmount communication difficulties between scientists and lawyers with an apparent lack of practical systems for priority-setting and decision-making. After noting these difficulties, he attempted to develop a simple means of helping ordinary people make complex decisions (Saaty, 1980), choosing among a set of pre-specified alternatives. The decision-making process relies on information related to alternatives.

This method is useful where teams of people are working on a complex problem involving judgment. It aims to rank decision alternatives and select the best one for a complex multi-criteria decision-making problem using pairwise comparison of those criteria.

The decision situation to which AHP is applicable includes the following six aspects (Zhang, 2010):

- Choice – Selection of one alternative from a given set of alternatives, usually with multiple decision criteria involved
- Rank – Arranging a set of alternatives from most to least desirable
- Priority – Determining the relative merit of members of a set of alternatives, as opposed to selecting a single one or merely ranking them
- Resource allocation – Apportioning resources among a set of alternatives

- Benchmark – Comparing the processes in one's own organization with those of other best-of-breed organizations
- Quality management – Dealing with the multidimensional aspects of quality and quality improvement

4. AHP theory and calculations

AHP provides a comprehensive and rational framework for structuring a decision problem. The essence of AHP process is to create a hierarchy based on the decomposition of a complex problem, with a goal at the top, criteria and/or sub-criteria at different levels, and decision alternatives at the bottom of Figure 1 Therefore, AHP was proposed. It is a simple method: people with no formal training can understand and participate in activities using it.

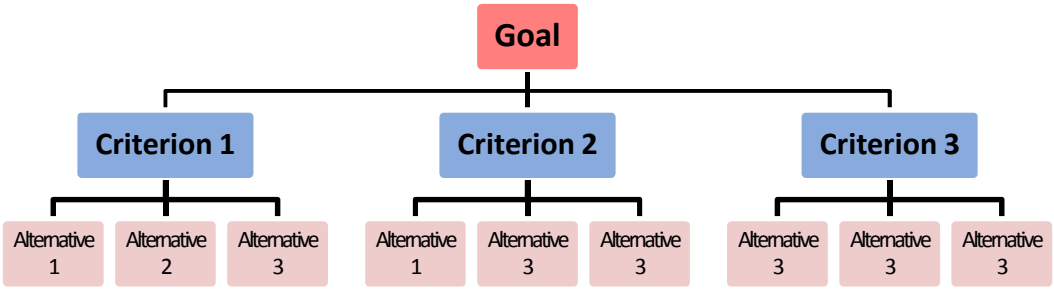

Figure 1 Structure of AHP method (Zhang, 2010)

In this method, the number of criteria and the corresponding relative priority form judgment matrix A (reciprocal matrix), which contains pairwise comparison values.

$$A = \begin{bmatrix} a_{11} & a_{12} & \dots & a_{1n} \\ a_{21} & a_{22} & \dots & a_{2n} \\ \vdots & \vdots & \ddots & \vdots \\ a_{n1} & a_{n2} & \dots & a_{nn} \end{bmatrix} = \begin{bmatrix} 1 & z_1/z_2 & \cdots & z_1/z_n \\ z_2/z_1 & 1 & \cdots & z_2/z_n \\ \vdots & \vdots & \ddots & \vdots \\ z_n/z_1 & z_n/z_2 & \cdots & 1 \end{bmatrix}$$

Therein, z_i denotes the element/criterion to be compared, a_{ij} is the pairwise comparison value of criteria z_i and z_j; $a_{ij} = 1/a_{ji}$ for $i \neq j$, and $a_{ii} = 1$. These values, which are given by each decision-maker, form a square matrix.

A priority vector can be calculated using the following formula:

$$w = \begin{bmatrix} w_1 \\ w_2 \\ \vdots \\ w_n \end{bmatrix} = \begin{bmatrix} (\prod_j^n a_{1j})^{1/n} \\ (\prod_j^n a_{2j})^{1/n} \\ \vdots \\ (\prod_j^n a_{nj})^{1/n} \end{bmatrix}$$

To check the consistency of the answer, it is necessary to calculate the principal eigenvalue (λ_{max}). The principal eigenvalue is obtained from the summation of products between each element of eigenvector and the sum of columns of the reciprocal matrix.

$$\lambda_{max} = w_1 * b_1 + w_2 * b_2 + \cdots + w_n * b_n$$

Therein, the following variables are used:

$$b_1 = a_{11} + a_{21} + \cdots + a_{n1}$$

$$b_2 = a_{12} + a_{22} + \cdots + a_{n2}$$

$$b_1 = a_{1n} + a_{2n} + \cdots + a_{nn}$$

Saaty proved that, for consistent reciprocal matrix, the largest eigenvalue is equal to the

comparison matrix size, or $\lambda_{max} = n$. For a measure of consistency, called Consistency Index as deviation or degree of consistency using the following formula:

$$CI = \frac{\lambda_{max} - n}{n - 1}$$

Saaty also proposes consistency ratio, which is a comparison between the Consistency Index and the Random Consistency Index, as in the following equation:

$$CR = \frac{CI}{RI}$$

The inconsistency is acceptable if the value of the consistency ratio (CR) is less than or equal to 10%. It is necessary to revise the subjective judgment if the consistency ratio is greater than 10%. The Random Consistency Index can be referred from Table 1:

Table 1 Random Consistency Index (RI)

n	1	2	3	4	5	6	7	8	9	10
RI	0	0	0.58	0.4	1.12	1.24	1.32	1.41	1.45	1.49

5. Using AHP for landslide risk evaluation

Japan landslide society (JPS) first used AHP for landslide risk evaluation in 2002. At that time, they wanted to evaluate the probability of landslide occurrence by interpreting aerial photographs (Hamasaki, 2013). This work was implemented through several times discussion at the working group according to the following flowchart (Figure 2):

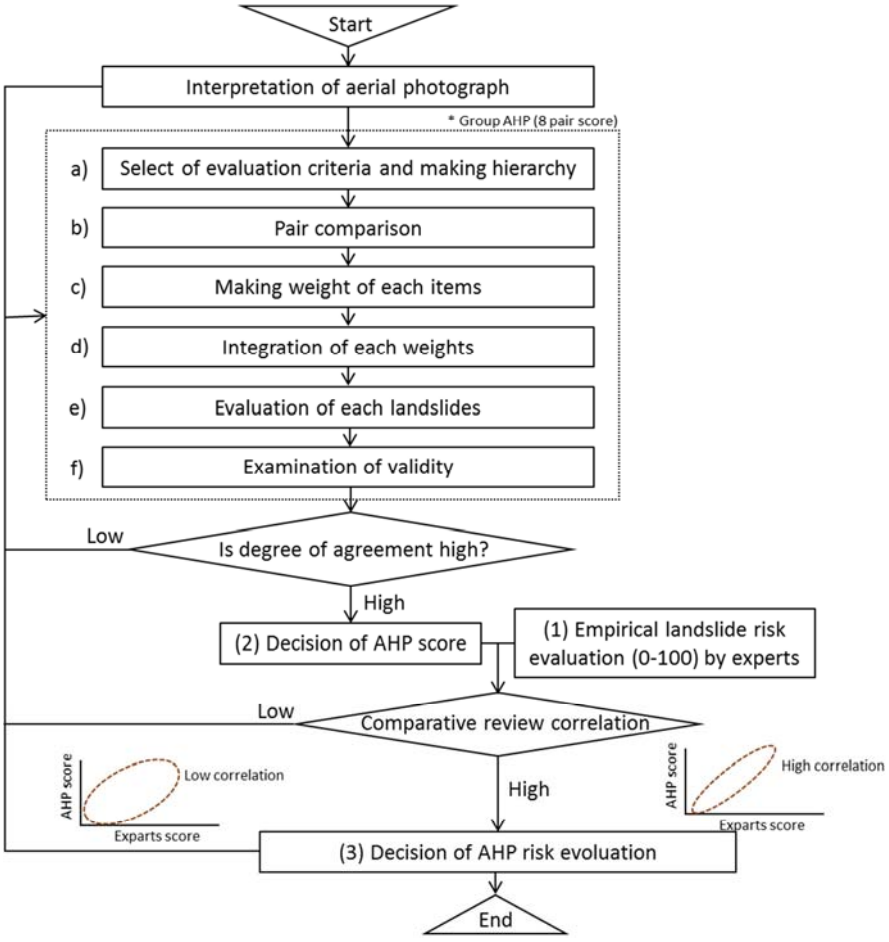

Figure 2 Flow chart showing determination process for AHP score (Hamasaki, 2013)

According to Miyagi (Miyagi et al., 2004) various stages exist in a sequence of a landslide development: the primary stage, the active stage and periods of differentiation, the expansion stage, and the suspension and the dissolution stage. The series of these stages is presented in Figure 23. The micro-topography of each stage reflects the characteristics of autonomous destruction processes and comprises distinct micro-landform units. Each stage is made up of distinct micro-landform units. In the initial (stage) period of occurrence, a landslide has been gradually differentiated, becoming vulnerable because some internal transformation is deformed repeatedly. However, variation processes proceed intermittently and repeatedly over time. Geomorphologic processes of two types occur: an intermittent landslide action and a normal process in landslide area. The landslide hazard risk evaluation must distinguish these two processes. Determining the stage of a landslide activity and interpreting direct indexes of the risk and landslide risk evaluation will be the following (Miyagi et al., 2004):

- Landslide topography is identified and illustrated through aerial photograph interpretation and through development of the landslide topography distribution map.

- Micro-topographies are identified through photograph interpretation. The items are checked on a card. The card is constructed on the system of item arrangement.

- The total score of the checked items indicates the risk level. The score of items is estimated by AHP. Each landslide topography is identified as high risk (70–100), moderate risk (30–70), and low risk (0–30).

In addition, risk evaluation is based on the following assumptions (Miyagi et al., 2004):

- Fundamental factors for the evaluation are limited to topographical information interpreted from aerial photographs.

- Scale or characteristics of interpretable landforms and landslide phenomena are often affected by the aerial photograph accuracy.

- Factors such as rainfall are not objects for evaluation.

Risk evaluation is a probability of landslide re-occurrence within a given area. Risk evaluation can be conducted by analyzing landslide topographies because most landslide processes result from reactivity of aged landslide topographies. Wherever landslides occur, the unit of risk evaluation should be the whole area of the landslide topography. When conducting risk evaluations, the following points should be noted:

- Occurrence of landslides caused by artificial influences such as anthropogenic alternation is not an object for evaluation.

- Risk is a probability of landslide occurrence. It is not a magnitude of occurrence or behavior of destruction on the surrounding area in movement.

- If the whole area of a landslide topography is evaluated based on an unstable area within it, then an interpretation map should represent the area and mention the existence of such an area, its position within the landslide topography and relative relation to other.

For purposes of systematic and objective risk evaluation, the Japan landslide society has developed an inspection sheet (Figure 4) incorporating geomorphic factors within and beyond landslides (Miyagi et al., 2004): First, the working groups separate evaluation criteria items into three main categories: (1) “Micro landform features in landslide body” as an index related to characteristics of movement; (2): “The boundary of major landslide landform” as an index related to the time process;

and (3) “Landslide topography and adjoining environment” as an index related to geomorphic setting. Further subdivision can be made into nine intermediate elements: A: Type of movement; B: Level of clearness and micro landform components within landslide body; C: Level of instability of landslide body; D: Direct features of movement; E: Between top edge of main scarp and upper slope; F: Between main scarp and body; G: Between landslide body and frontal slope; H: Toe part of landslide body; I: The lower part of landslide body (Hamasaki, 2013).

Characteristics and features of each small classification are described as follows by Miyagi et al. (2004):

A) Type of movement: Movement of each type will produce a distinct micro-landform, such as flow mound, pressure ridge which caused by mud flow and debris flow. Clay debris flows to mud flow type landslide are fairly unstable because of the strongly weathered clayey materials. It will increase the recurrence of landslides (Miyagi et al., 2004).

B) Level of clearness and micro landform components within landslide body: By processes occurring over time, weathering and erosion, micro-landform units within the landslide body (e.g., cracks, minor scarps, graven, depression, and pressure ridge) have been modified and have lost their original shape. The landslide body is divided into small parts changing toward the active stage. The micro-landform density indicates some level of destruction (Miyagi et al., 2004).

C) Level of instability of landslide body: The landslide body often becomes unstable by sustaining head block separation from the lower part and slight failure at the toe and lateral portions. Such inversion phenomena often become triggers of a large slide reoccurrence. If the landslide faces a suspended stage, the process that causes the invasion of gullies and erosion valleys can be regarded as an erosion process leading to its disappearance (Miyagi et al., 2004).

D) Direct features of movement: Generally, if a crack is clear, then it can be inferred that little time has passed after the landslide occurrence. Sometimes, it is difficult to recognize the crack existence from aerial photographs. However, cracks are often recognized as an indirect feature such as a systematic deformation of the forest crown (Miyagi et al., 2004).

E) Between top edge of main scarp and upper slope: At the top edge of a main scarp after landslide action that includes lateral stress situation, there remain some unstable materials. Consequently, several echelon cracks and lateral cracks develop at the top edge of the main scarp. After the action, the stability increases gradually and is modified by creep. Furthermore, the weathering process deforms the initial topography and decreases the edge sharpness. If the suspending condition holds for a long time, then the area of creep and gully erosion will develop. Typical topographic characteristics of the landslide main scarp will disappear (Miyagi et al., 2004).

F) Between main scarp and body: This boundary is very clear, like an edge of the main scarp, which is formed immediately after the action. Plenty of materials fall from the scarp and accumulate at the boundary. Such materials develop talus topography. The development of talus accompanies aging. The spatial ratio of the talus indicates the time process after the event (Miyagi et al., 2004).

G) Between landslide body and frontal slope: This boundary is very clear after the action. The landslide body is deformed and dissected by weathering process and linear erosion such as gully erosion, which leads to the development of a gully, a channel at the body and small alluvial cones develop in front of the landslide body. Therefore, such components of micro-landforms are also indicators of time processes after the landslide action (Miyagi et al., 2004).

H) Toe part of landslide body: If a mountain stream creates an erosion situation, then it will be

identified as equal to attack the face to a river. However, the front part of a body might become unstable by the partial abutment to the opposite bank of the mountain stream (Miyagi et al., 2004).

I) The lower part of landslide body: An increase or decrease of relief energy will engender a change of the potential of the landslide body (Miyagi et al., 2004). Although we can recognize multiple items in a landslide body, we must mark only one item at each category box. In such cases we should mark those items as much unstable ones.

Table 2 Weight value of each morphological item for risk evaluation (Miyagi et al., 2004)

Major classification	Medium classification	Small classification		Weight value
(1) Micro landform features in landslide body (as an item of characteristics of movement)	A: Type of movement	1	Flow mound and pressure ridge	12.5
		2	Minor scarp	4.9
		3	Separation scarp, Depression, Trenches	2.0
	B: Level of clearness and micro landform components within landslide body	1	Huge no. of deformed blocks and clear micro topographic boundary	19.5
		2	Clear micro-topography of smooth boundary	12.5
		3	Unclear deformed block	6.0
		4	Smooth boundary	5.5
	C: Level of instability of landslide body	1	Head block separates from the lower part	13.9
		2	Gullies development	3.6
		3	Linear erosion development	1.5
	D: Direct features of movement	1	Cracks and scares	18.8
		2	Tree crown deformation	6.3
(2) The boundary of major landslide landform (as an item of the time process)	E: Between top edge of main scarp and upper slope	1	Echelon	3.8
		2	Main scarp	3.2
		3	Creeping slope	1.8
		4	Gullies extension	1.5
		5	Modified to smooth slope	1.3
	F: Between main scarp and body	1	Non deposition	3.1
		2	Talus	1.8
		3	Large-scale talus	1.1
		4	Smooth deformed by creeping and talus development	0.6
	G: Between landslide body and frontal slope	1	Non deformed landslide body	1.0
		2	Gully, debris cone	0.5
		3	Smooth surface topography	0.4
		4	Disappeared surface	0.3
(3) Landslide topography and adjoining environment (as in index of geomorphic setting)	H: Toe part of landslide body	1	Face to the undercutting slope of river	8.6
		2	Face to the river	4.4
		3	On the flat plain	1.6
		4	Hit to opposite slope	0.9
	I: The lower part of landslide body	1	Increasing toward the active condition	19.2
		2	Moderate the change of relief energy	9.2
		3	Decreasing	2.7

.

Analytic Hierarchy Process (AHP) method is used to make paired comparisons for each of the major elements, intermediate elements, minor elements and score system was created for all elements as mentioned in Table 2 and Figure 3. All the items above were put into a card (Figure 3). For convenience of practices, the categories are arranged to decrease the risk from the left to the right, enabling clarification of the landform formation mechanisms. In addition, a category can be checked between some categories. For example, in Figure 3, if item F was determined to be between " Non deposition " and "Talus," then a check can be placed between the two. The score of the card is calculated intuitively based on the experiences of a geomorphologist. In this way, landslides are classified from special high risk to low risk (high probability of landslide occurrence) based on the AHP score evaluation. The landslide's morphometric signs appeared fresh on aerial photographs if the score's evaluation is high. In contrast, morphometric signs are extremely vague. A score of 70–100 signifies high probability of landslide occurrence; 30–70 stands for the probability of landslide occurrence; and 0–30 denotes no probability of landslide (Miyagi et al., 2004).

Figure 3 depicts an example of inspection sheet for risk evaluation. In this case, AHP score is 70; it means that this landslide has high possibility of landslide re-occurrence.

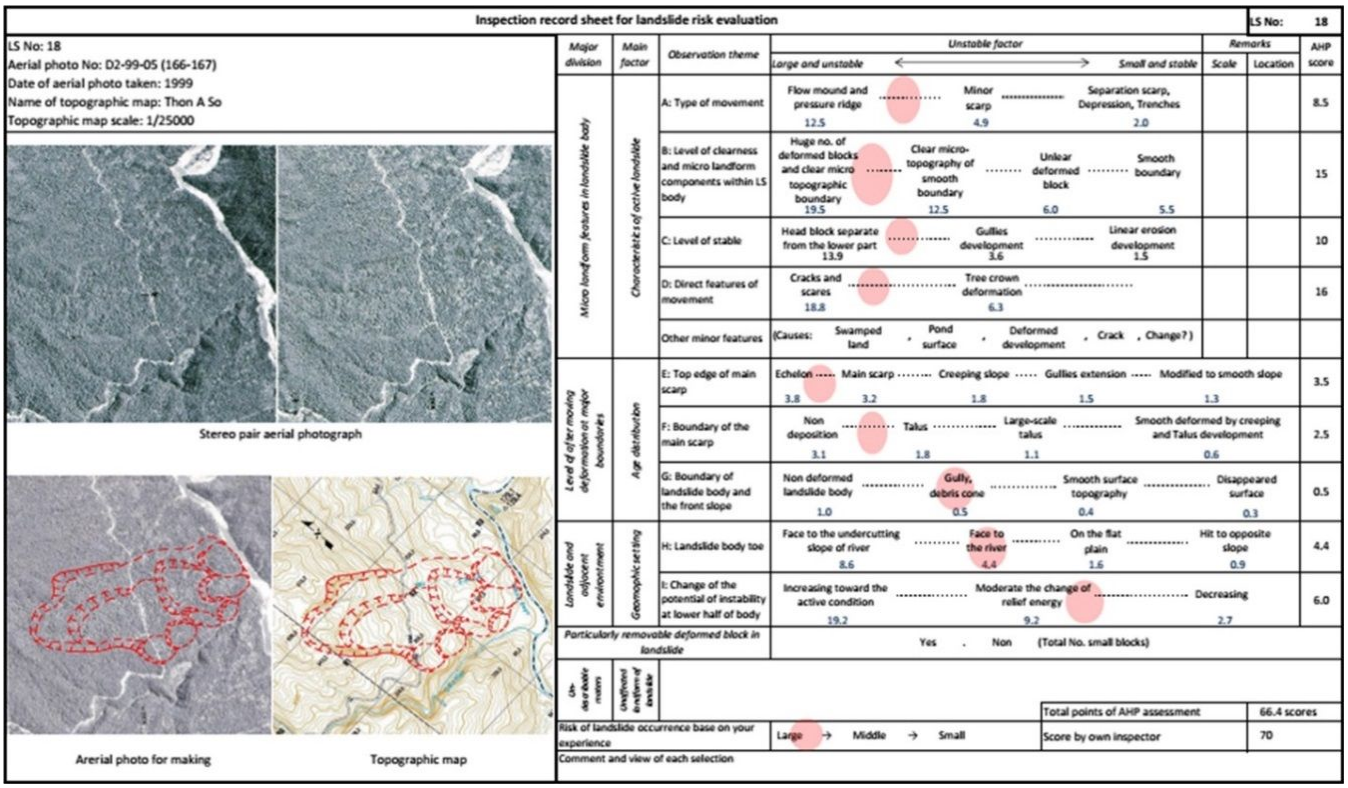

Figure 3 Example of inspection sheet for risk evaluation; in this sheet total AHP score is 70; it means that this landslide has high possibility of landslide re-occurrence

6. Example of AHP score of each morphological item for risk evaluation

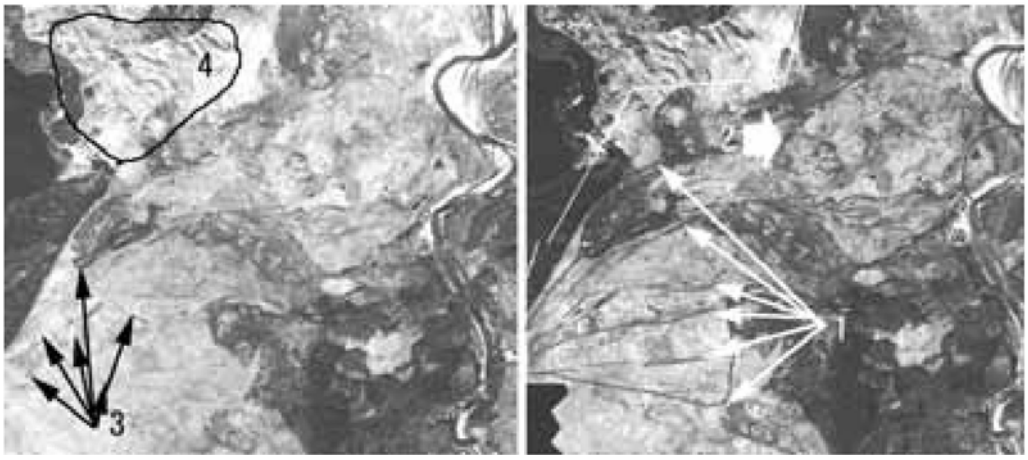

Figure 4 Flow mounds, small but sharp scarp and lateral ridge of clayey debris flow, pressure ridge. Weight value: 12.5. Such micro topographies characterize the clayey flow type landslide. The plan is long and oval, size is small and shallow, usually high water contains, very unstable. 1; Lateral ridges at the rims of landslide. 2; Flow mounds distribute at the lower part of body. 3; Crown of landslides are connect to rims smoothly. 4; Lamina shape hammocky topography is called pressure ridge (Miyagi et al., 2004).

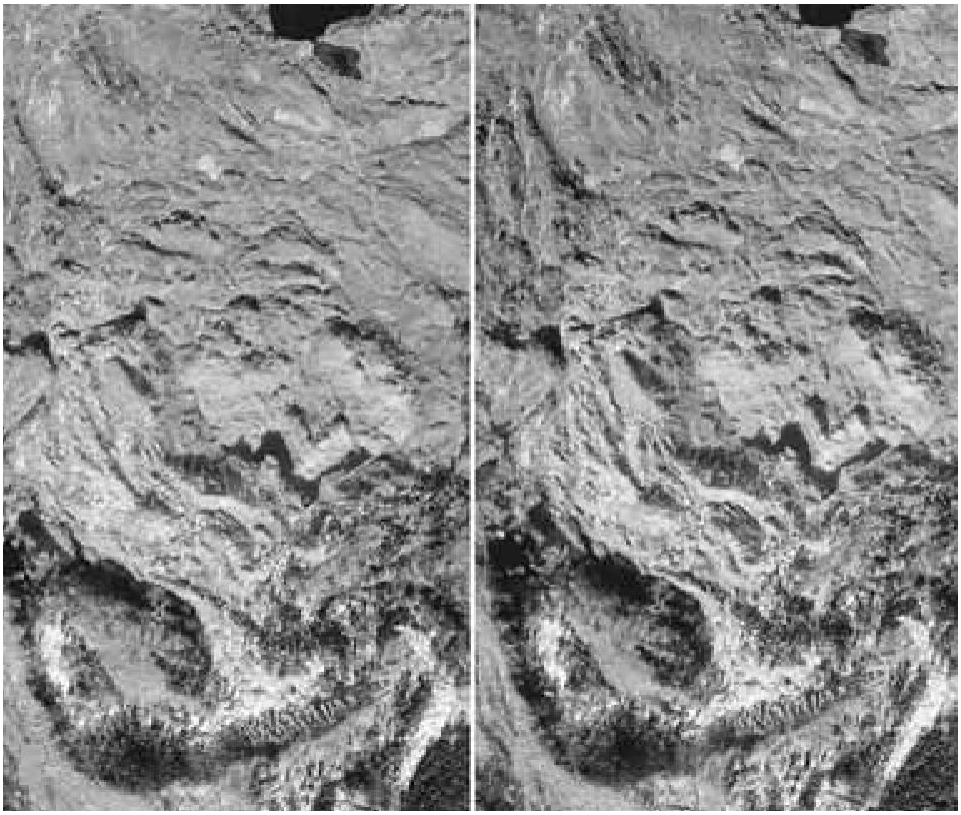

Figure 5 Huge number of deformed blocks and clear micro topography. Weight value: 19.5. The number of micro topography in the body which is an indicator of the extent of destruction (Miyagi et al., 2004).

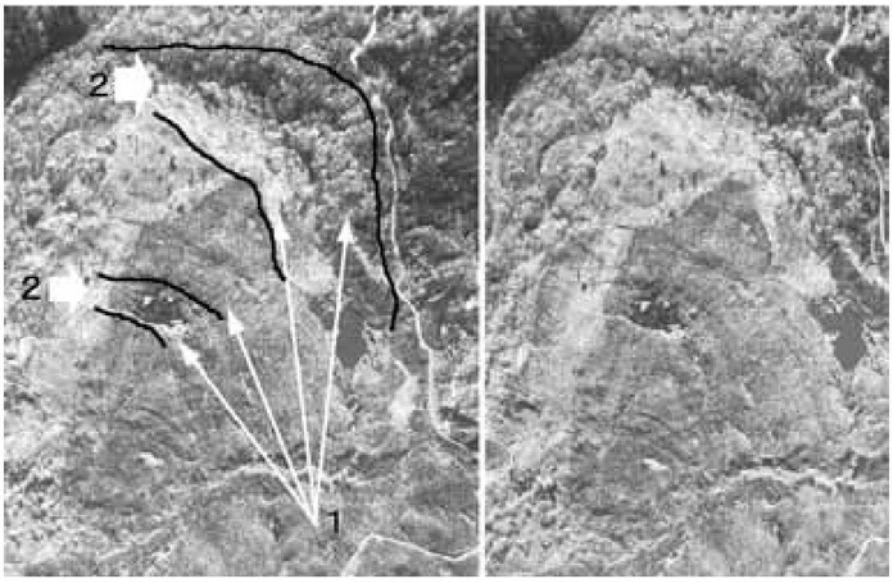

Figure 6 Minor scarp. Weight value: 4.9. Minor scarps are typical feature of rotational slump type destruction. 1; Sharp main scarp 2; Minor scarps develop in front of the main scarp (Miyagi et al., 2004).

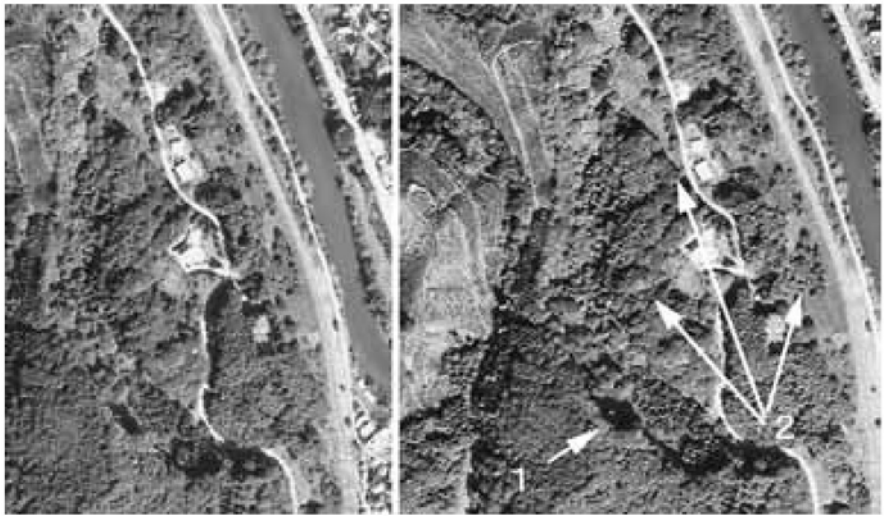

Figure 7 Separation scarp. Weight value: 2.0. Separation scarp are typical feature of the glide type, spreading type landslide. It makes a graben or trench depression between the facing scarps. 1; Separation scarps. 2; Trench (Miyagi et al., 2004).

Figure 8 Major boundary of landslide. This is the case of suspended landslide. There is talus topography (1) developed between the main scarp and the body. The weight value is 1.8 (Miyagi et al., 2004).

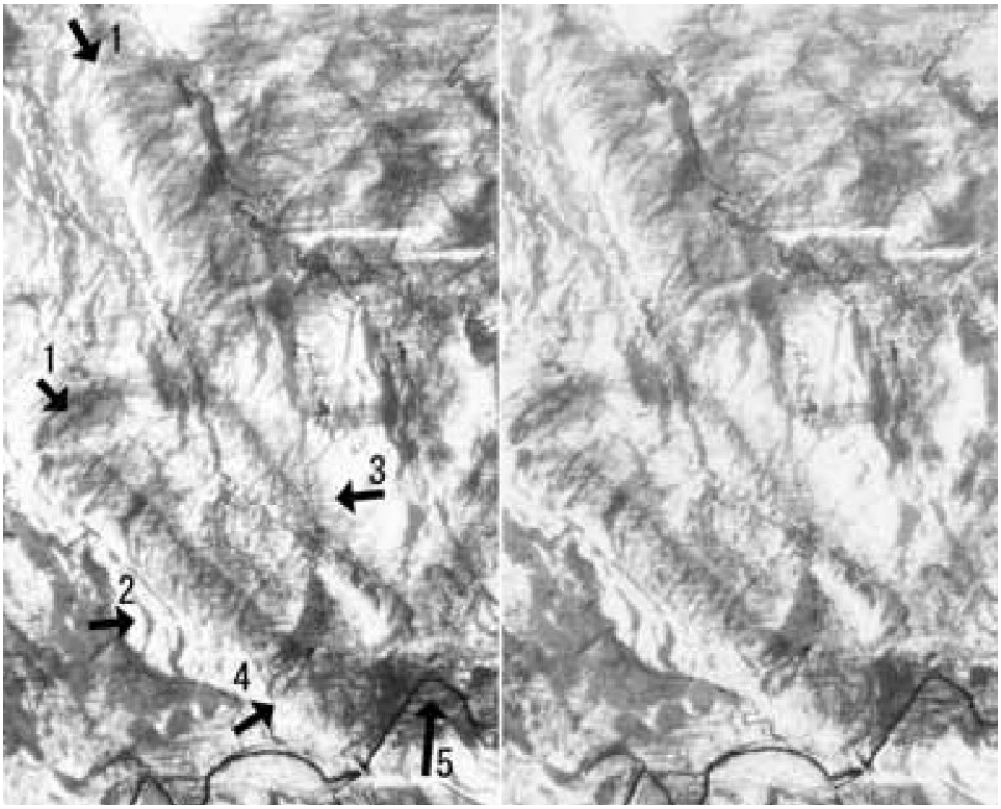

Figure 9 Huge number of deformed blocks and clear micro topography. Weight value: 19.5. A number of parallel and small scarps are the feature of the destruction. Number and clearness its self means the high activity. 1; Parallel minor scarps. 2; Parallel scarp deforms the direction to downward with the release of compression force. 3; Large landslide block (between 1 and 3) moved to down ward but the toe is shuttered by adjacent blocks. 4; Toe part face to the river which deformed the stream to south (down) ward by sharp sliding block. 5; Toe slope attacked by stream will become slope failure and small landslide occur (Miyagi et al., 2004).

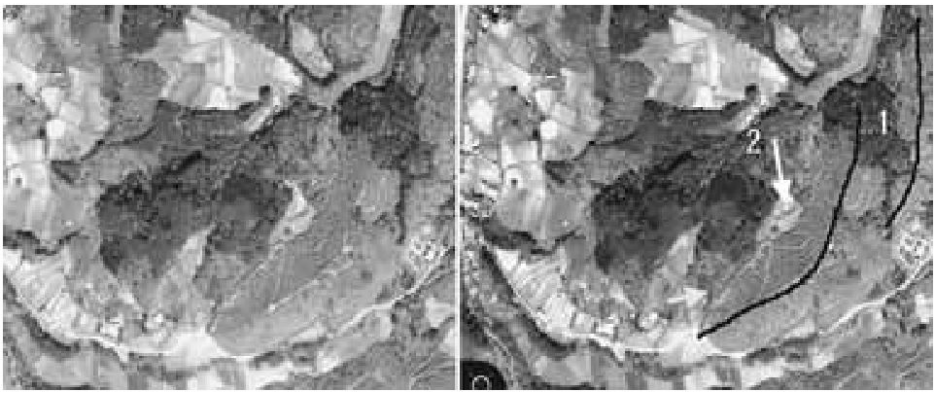

Figure 10 Smooth boundary. Weight value: 5.5. Micro topography by the landslide action will diminish by the normal geomorphic process while the suspended stage of landslide development. The small micro topography is easy to diminish and the boundary of the blocks changes to smooth by talus and weathering the original shapes. 1; Edge of minor scarp modified by weathering. 2; Boundary of the minor scarp and sub block is modified by talus material accumulation (Miyagi et al., 2004).

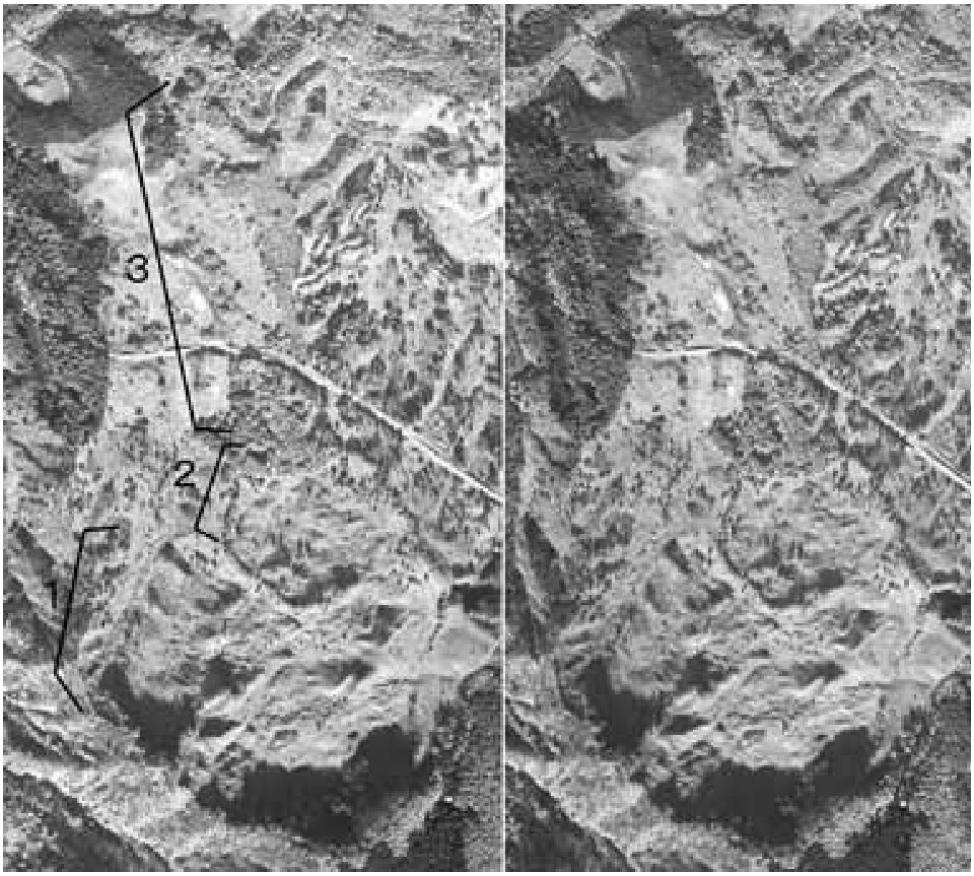

Figure 11 Clear to unclear micro topography and boundary. Weight value of clear micro topography and smooth boundary: 12.5. Weight value of the unclear deformed block: 6.0. 1; Is also an example as same as Fig.6.7.a & Fig.6.7.b. 2; Micro topography of the part is slightly deformed and thus the boundary of the blocks change to smooth. 3; The landslide feature mostly diminish. Unclear micro topography and smooth boundary is almost same value as the indicator of the suspended stage (Miyagi et al., 2004).

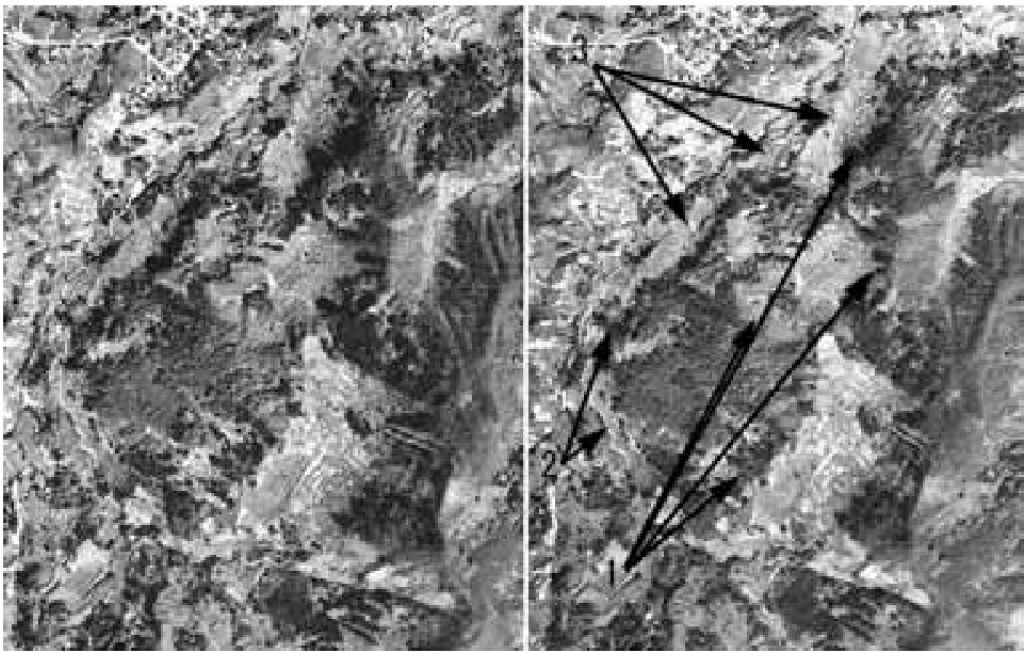

Figure 12 Head block separation from the lower part. Weight value: 13.9. Front part of the body received the number of landslide action, thus the material crushed and deformed from the consolidated one to weathered clayey one. The instability increases especially in a front part of the

body. This is a typical process of autonomous destruction process. Small scale landslide and slope failure, flow type shallow landslide getting frequently. This photo shows a part of large scale landslide topography. 1; Minor scarps. 2 and 3; Small landslides occur at the toe part of the blocks (Miyagi et al., 2004).

Figure 13 Gullies development. Weight value: 3.6. The normal erosion processes will appear at the suspended stage. Gully erosion is one of the clear and easy to interpretational features. 1; Lateral erosion by stream cut the toe part of the body. 2; Gullies start the dissection to the toe part of body (Miyagi et al., 2004).

Figure 14 Major boundary of landslide. This is the case of suspended landslide. There is talus topography (1) developed between the main scarp and the body. The weight value is 1.8 (Miyagi et al., 2004).

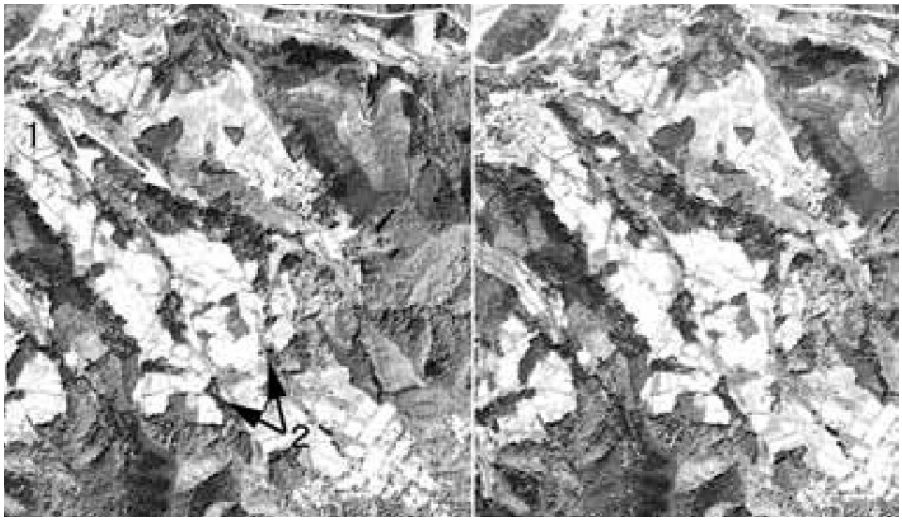

Figure 15 Linear erosion development. Weight value: 1.5 Gully will change to channel by the suspended stage continue long time. 1; Two small river dissected the body widely. 2; Upper stream intrude near the boundary of the body and main scarp (Miyagi et al., 2004).

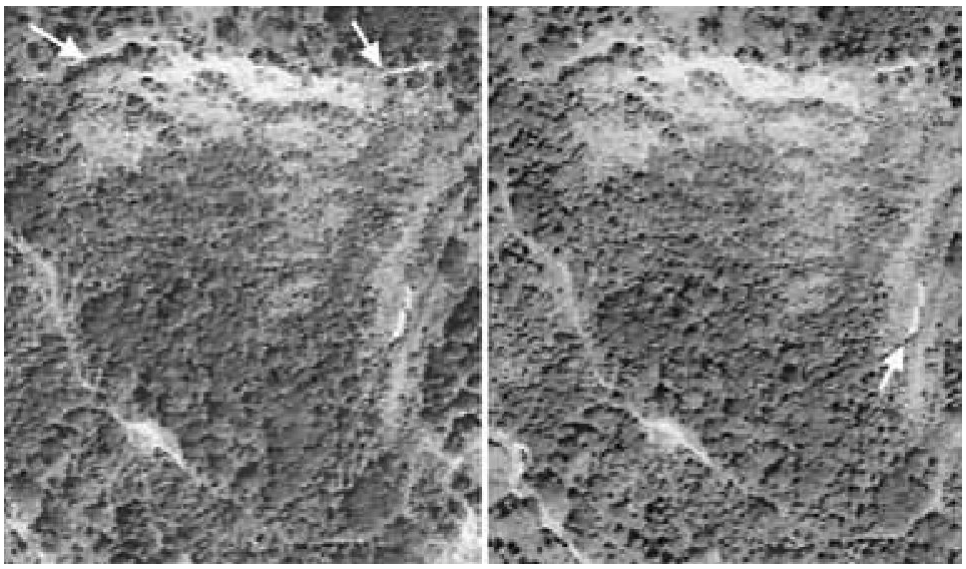

Figure 16 Crack and scar. Weight value: 18.8. Cracks and some scars are direct indicators of the landslide action. Arrows in figure are typical cracks in a very active landslide (Miyagi et al., 2004).

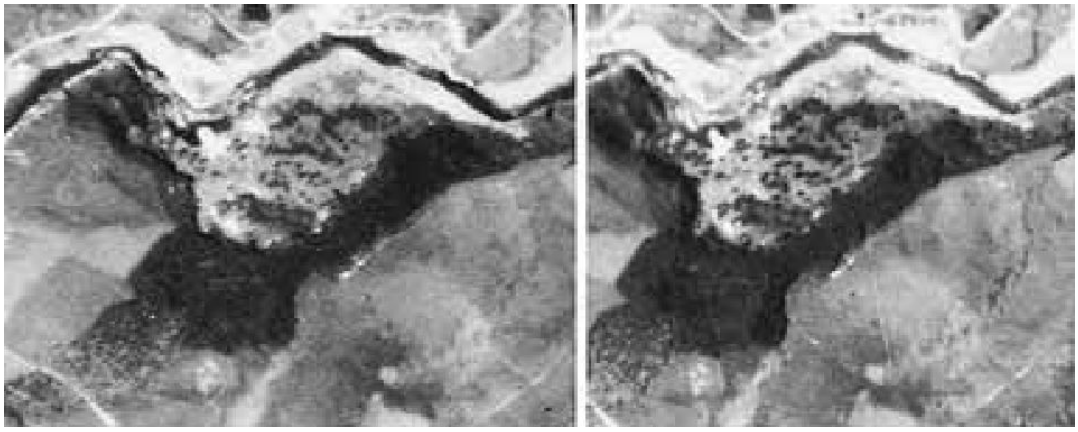

Figure 17 Tree crown deformation. Weight value: 6.3. Crack is very important feature but sometimes it is difficult to identify trough photo interpretation. The deformation of the forest canopy is a indirect sign of crack. Although, such deformation appears by artificial land deformation too. By the reason the score is much poor (Miyagi et al., 2004).

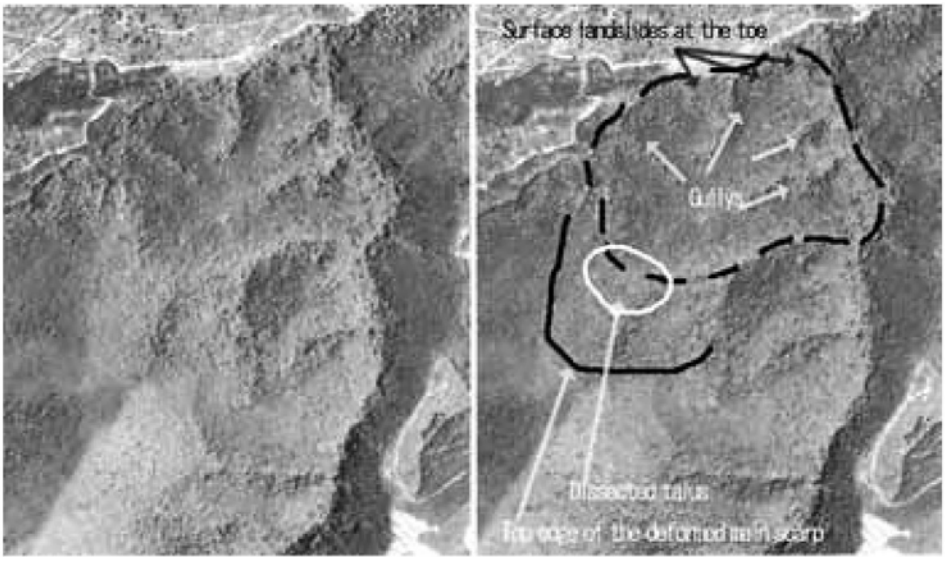

Figure 18 Major boundary of landslide. This photo is the typical non active landslide topography. The major landform of landslide still remain but all of the major boundaries are smoothly modified by talus

accumulation and weathering, The body dissected mostly by gullies. The weight value of the top edge of main scarp is 1.3, boundary of main scarp and the body is 0.6, boundary of landslide body and the frontal slope is 0.3 (Miyagi et al., 2004).

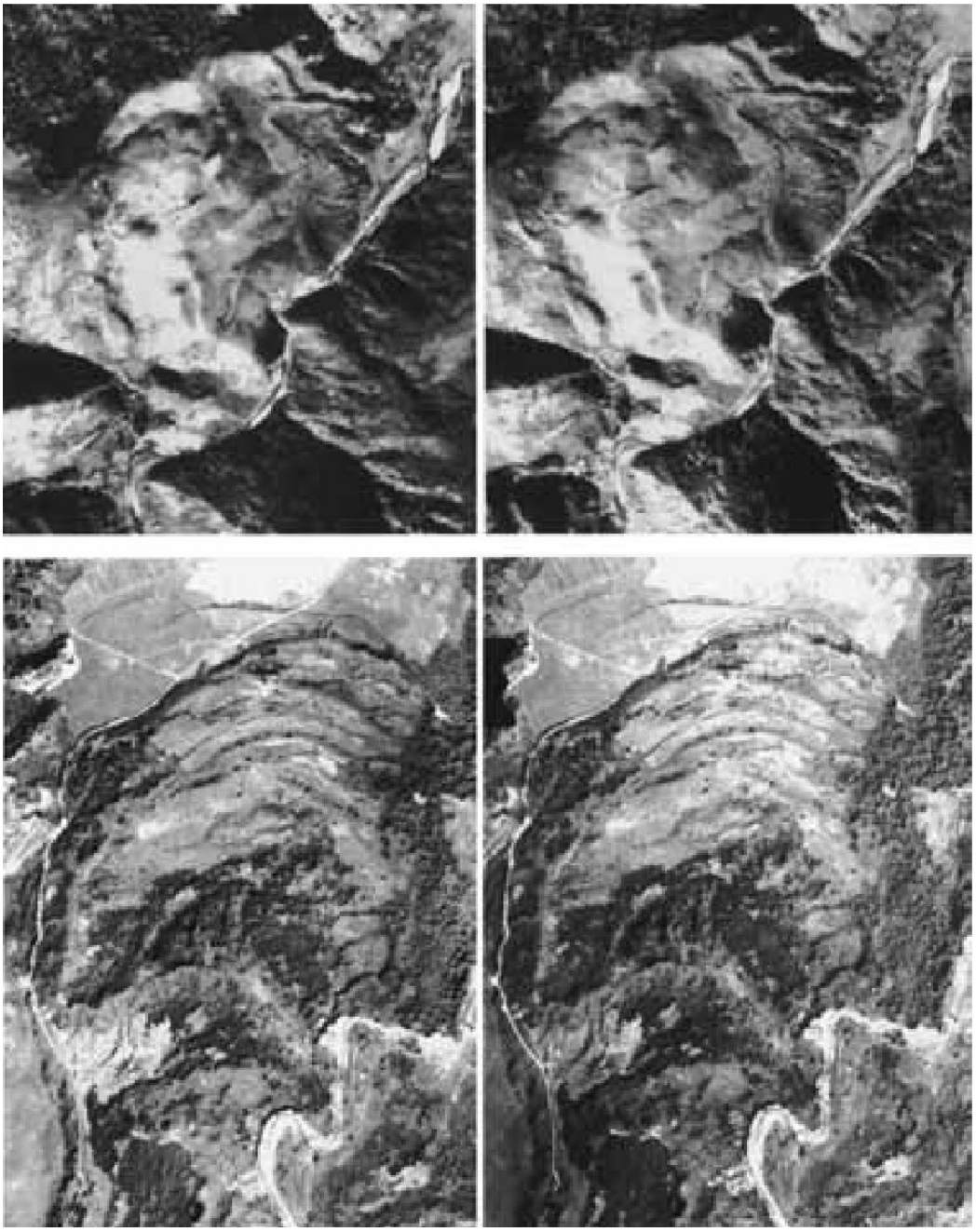

Figure 19 Major boundary of landslide. These two landslides are very recently moved. The major boundary such as top edge of main scarp, boundary of main scarp and landslide body keep the original topographic features. Above 1; Top edge of main scarp. 2; Boundary of main scarp and the body. 3; Boundary of the body and frontal slope. Below 1; Top edge of main scarp. 2; Boundary of main scarp and the body. Weight value in this case, the edge of main scarp is 3.2 (above) and 3.8 (below), The boundary of main scarp and the body is 3.1 each (Miyagi et al., 2004).

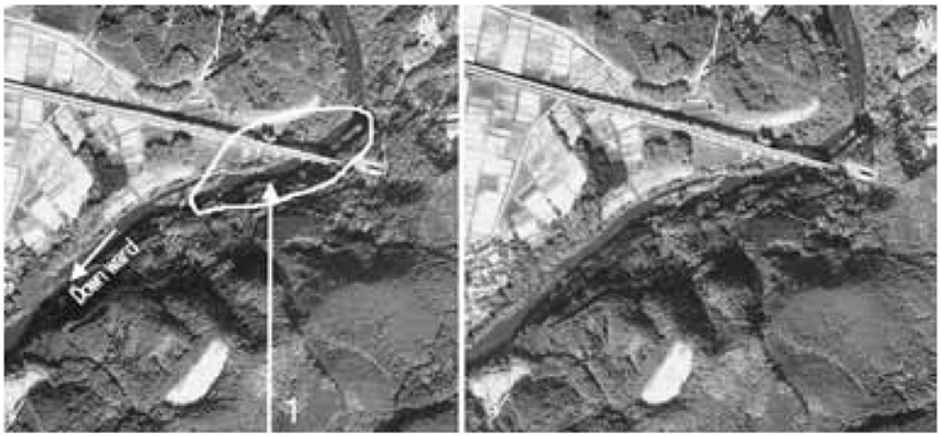

Figure 20 Landslide body and adjacent environment. Landslide body at lower face to the other near. Increase toward the active condition. Weight value: 8.6. Landslide body face to the undercutting slope of river stream has very high potential of landslide (Miyagi et al., 2004).

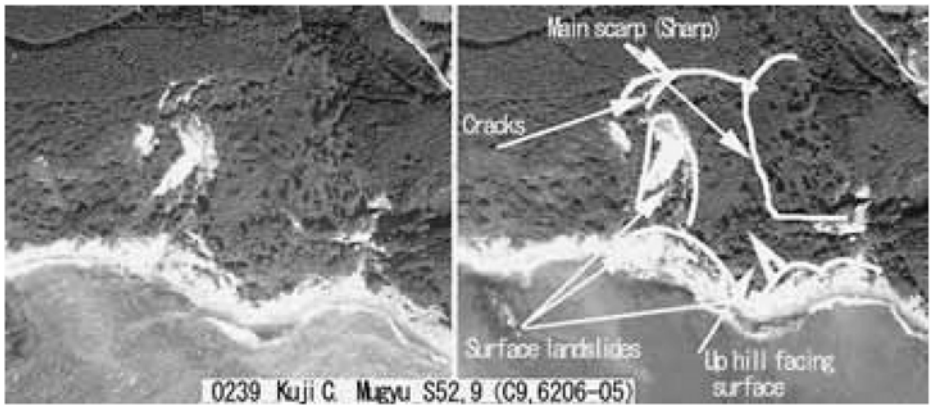

Figure 21 Landslide body and adjacent environment. Landslide body at lower face to the other near. Increase toward the active condition. Weight value: 8.6. Landslide body face to coast is also very unstable because of the coastal erosion by wave and coastal sea current (Miyagi et al., 2004).

Figure 22 Landslide body and adjacent environment. Landslide body at lower face to the other near. Decreasing (stabilizing order). Weight value: 0.9. The landslide body moved but if it stop by any barrier the potential of reoccurrence should be decrease (Miyagi et al., 2004).

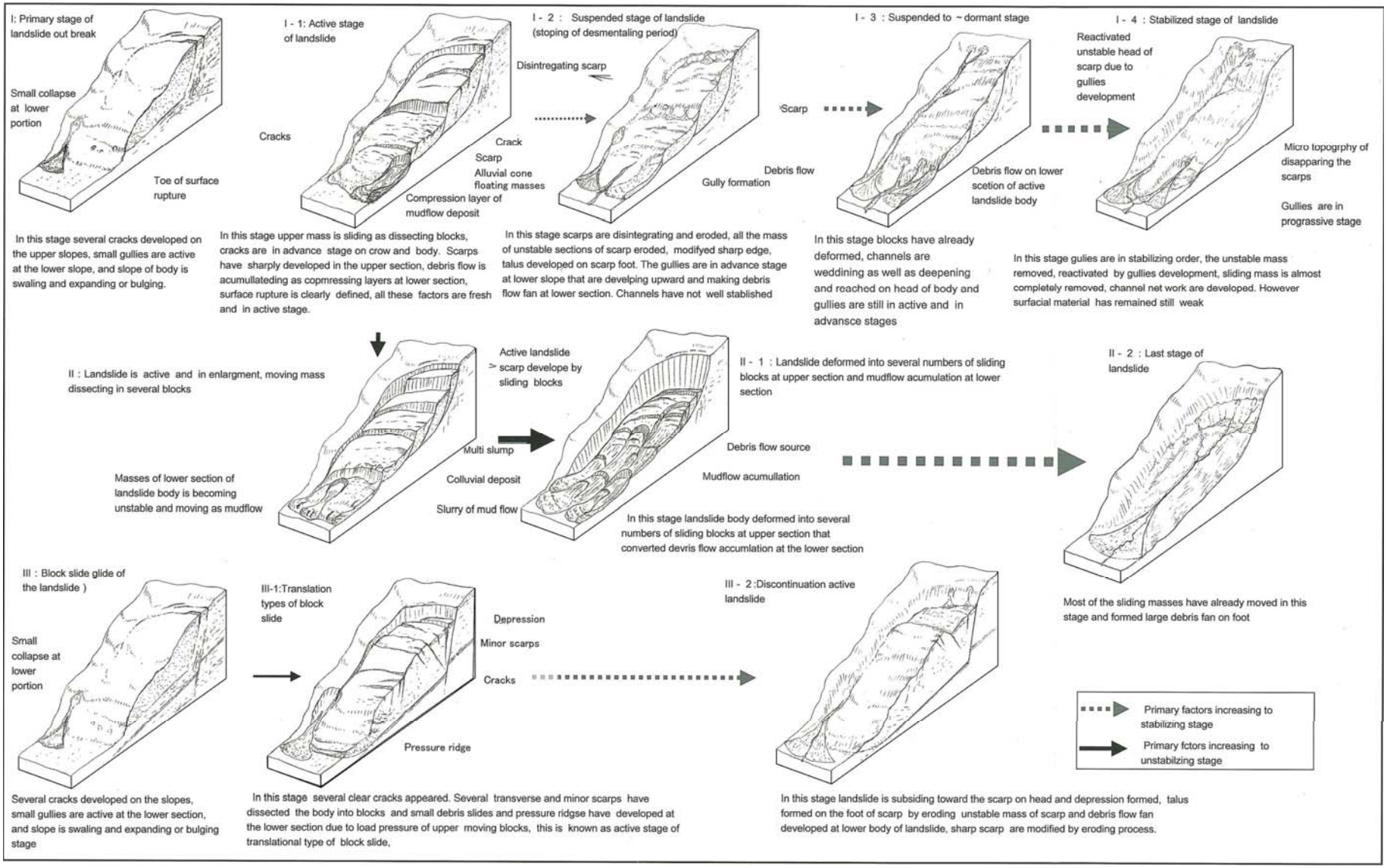

Figure 23 Model of changing process of outline and interior of landslide topography based on autonomous landslide destruction with the suspended stage (Miyagi et al., 2004)

GL 08: 2016

First edition

Guideline for vulnerability of Landslide mitigation in humid tropical region

HA NOI - 2016

Abstract

For landslide prevention, response and mitigation, a Landslide Hazard Vulnerability in tropical region a Guideline was proposed. The author approach is to answer for questions " What-Where-When-How''to landslides. Concept and classification of landslide in study area will be discussed for "What" question. Landslide moving mechanism is mentioned, in which the effect of the pore-pressure rise by raining is confirmed then the relationship between dynamic factor and displacement (signal of landslide recognition) is tagged for observation. As the result, basic data for landslide management and regional monitoring system are advised that will answer for "When" question. The integrated maps for landslide hazard vulnerability such as landslide inventory map, landslide risk assessment map, landslide susceptibility map and landslide hazard map are presented as basic tools to answer for "Where" question as site prediction. The application of research for landslide prevention, response and mitigation plan, in which metioned landslide knowlerges and tools used will discuss for question "How". This guideline will contribute for landslide hazard management as a basic document in center of Vietnam.

Table of contents

Guideline for vulnerability of Landslide mitigation in humid tropical region

1 Scope

This document was create as the results of the project experience. Beside supply for readers the updated classification of landslide phenomenon regarding the character of geometry, geology in study area, which is very necessary for consideration of landslide countermeasures, The signals of development of movement is explained for understanding. The concepts of landslide tools for prevention, mitigation was mentioned in order to giving out the general guide for landslide management of region. Depending the classification, main solutions for prevention, response and mitigation were advised. This document is useful for student, engineers involved to landslide study, mitigation and management.

2 Reference documents

Varnes, D. J. (1978). Slope Movement Types and Process. In Transport research board, *Landslides,* Analysis *and Control, Special report176* (pp. 11-33). Washington, D.C.: National Academy of Sciences.

Oldrich, H. (2014). The Varnes classification of Landslide type, an update. Landslides, 167-194.

Kyoji, S. and Bin HE. (2012). TXT-tool 3.081 -1.1 Landslide Initiation Mechanism. In ICL, Landslide teaching tools (pp. 205-214). Tokyo: ICL.

Toyohiko, M. (2004). Landslide Risk Evaluation and Mapping – Manual of Landslide Topography and Risk Management. The national Research Institute for earth Science and Disater Prevention.

Eisaku H. and Toyohiko M.i. (2012). TXT-tool 1.081-2.3 Abstracting unstable slopes (landslide topography) using aerial photos and topographic maps:Concept and frameworks. In ICL, Landslide teaching tools (pp. 22-35). Tokyo: ICL.

Eisaku HAMASAKI1 and Toyohiko MIYAGI. (n.d.). Risk Evaluation using the Analytic Hierarchy Process (AHP) – Introduction to the process concep. In ICL, Landslide teaching tools (pp. 36-49). Tokyo: ICL.

Wieczorek, G.F. (1996). Landslide triggering mechanisms: Investigation and Mitigation. Washington D.C.: Transportation Research Board.

Hansen, A. (1984). Landslide Hazard Analysis. In D. B. (editors), Slope Instability (pp. 523-602). New York: John Wile & Sons.

3 Terms, definitions

- Landslide data collection: Landslide data collection is considered as the basic document (landslide data base) for creation of regional landslide management tools. Landslide data collection is assemblage landslide information, which occurred in each region. With objective of information providing such as landslide classification type, location, boundary and size, including width, height and depth as well as the moving statute of landslide, it should be named or coded for reference.

- Regional monitoring system: Propose of regional monitoring system is predicted the relation ship between precipitation of rain with displacement of landslides in target region.

- Landslide inventory map: For development of the landslide hazard or risk assessment, the collection of information is considered as first step. This is the goal of landslide collection of information is creation of Landslide inventory map. It records many information as the location, where known, the date of occurrence and types of landslides that have left discernible traces in an area (Hansen, A., 1984). A detail landslide inventory map could shows landslide boundary, shape, combine parts, topographical micro-features, direction of moving...Beside this landslide inventory map usually presented on the base of topography map which supplied for user surrounding information regarding geomorphology such as landform, stream network (gully/rill), convex breakline , concave

- Landslide risk assessment map: Landslide risk evaluation aims to determine the “expected degree of loss due to a landslide (specific risk) and the expected number of live lost, people injured, damage to property and disruption of economic activity (total risk)” (Vaners, 1984).There are two possible approaches as quantitative (probabilistic) and qualitative approaches. Quantitative risk assessment aims to establish the probability of occurrence of a catastrophic event. However, the method requires a catalogue of landslides and their consequences. Because lack of the data of lost by landslide this evaluation is not discussed in this study.

- Landslide susceptibility map: Landslide susceptibility maps describe the relative likelihood of future landsliding based solely on the intrinsic properties of a locale or site. Some organizations use the term “landslide potential map” for maps of this kind.

- Landslide hazard map: Landslide hazard maps indicate the possibility of landslides occurring throughout a given area. An ideal landslide hazard map shows not only the chances that a landslide may form at a particular place, but also the chance that it may travel downslope a given distance.

4. Targets for landslide hazard vulnerability management for humid tropical regions

To Landslide hazard vulnerability management for region in order to natural disaster prevention, response and mitigation the author approach is to answer for questions “ What-Where-When-How’’to landslides. Concept and classification of landslide in study area will be discussed for “What” question. Integrated maps for landslide hazard vulnerability for mitigation will present to answer for “Where” question as site prediction. Setting up local regional monitoring and Material testing reference are applied for “When” question as time prediction. The application of research for landslide prevention, response and mitigation plant will discuss for question “How”.

This guideline for Landslide hazard vulnerability management for region is one of 34 of landslide integrated guidelines of landslide risk assessment, which was developed by the cooperation research project ‘’Development of landslide risk assessment technology along transport arteries in Vietnam’’. The integrated guidelines includes 5 parts, covers on (1) Mapping and site

prediction, (2) material tests, (3) monitoring,(4) landslide flume experiment, (5) softwares and simulations. The detail list of landslide-integrated guideline set list is presented in table 6.3 for reference.

5. Landslide types and moving mechanism

5.1 Landslide classification in region and recognition signal

Landslide is complicated movement of slope. According to type of movement, it was classified in to seven types as fall, topple, translational slide, rotational slide, lateral spreading, flow and complex by (Varnes, 1978). The classification was updated (presented in table 6.1) and landslide types were classified in to 29 types depending movement and material (Oldrich, H., 2014). In the study area, the landslide classification is carrying base on Varnes' 1978 classification system. However, most of landslidesare classified based on remaining signals after movement, so in some case the classification was non-consensus form researchers.

Table. 5.1 A summary of Vanners' 1978 classification system (Varnes, 1978)

Movement type	Rock	Debris	Earth
Fall	1. Rock fall	2. Debris fall	3. Earth fall
Topple	4. Rock topple	5. Debris topple	6. Earth topple
Rotational sliding	7. Rock slump	8. Debris slump	9. Earth slump
Translational sliding	10. Rock slide	11. Debris slide	12. Earth slide
Lateral spreading	13. Rock spread	-	14. Earth spread
Flow	15. Rock creep	16. Talus flow	21. Dry sand flow
		17. Debris flow	22. Wet sand flow
		18. Debris avalanche	23. Quick clay flow
		19. Solifuction	24. Earth flow
		20. Soil creep	25. Rapid earth flow
			26. Loess flow
Complex	27. Rock slide-debris avalanche	28. Cambering, valley bulging	29. Earth slump - earth flow

In the study area, beside 5 typical classes as rock fall, debris rotational slide, translational rockslide, translational shallow debris slides, gully type slides and flows, which were classified, the following translational wedge type slides was added. Here after, typical landslide types in study area will be discussed for clear understand for classification.

5.1.1 Rock fall

A rockfall or rock-fall refers to quantities of rock falling freely from a cliff face. A rockfall is a fragment of rock (a block) detached by sliding, toppling, or falling, that falls along a vertical or sub-vertical cliff, proceeds down slope by bouncing and flying along ballistic trajectories or by rolling on talus or debris slopes," (Varnes, 1978). In the study area, rock-fall was found in some cases, where is in granitic rocks slide as rock falls of granite core stones formed at shallow layers effected by weathering. However, the number of this phenomenon is small. At the site, after cutting natural

slope for road construction, the remaining talus, which were step and some cases were nearly vertical created high potential energy for slope failure to continue development.

At most those locations, the dip of geological slope layer, which was strong weathering, was reverse with the dip of cutting slope surface of the road. As the result, rock fall occurred. Rocks falling from the cliff may dislodge other rocks and serve to create another mass wasting process. Pictures of Phenomenon of rockfall on HCMR – Quang Nam section is presented in Fig 5.1

Fig. 5.1 Rockfall on HCMR– Quang Nam section – Vietnam

5.1.2 Translational shallow debris slides

Landslide in which the sliding surface is located within the soil mantle or weathered bedrock (typically to a depth from few centimeters to some meters) is called a shallow landslide. They usually include debris slides and failures of road cut-slopes. The survey and study records showed that the most landslide phenomenon in study area had character of sallow landslide, largely related to heavy raining fall to the surface of the terrain, which was strong weathering. In the study area landslides occur in sedimentary rocks with bedding and schistosity, weakly converted crystalline schist, and granitic rocks. Landslides move as a translational slide when the beds are gently sloping, and otherwise as a wedge type slide at an intersection with a crack.

Fig. 5.2 (a)Debris Shallow landslide and (b), (c)Translational wedge type slides in HCMR -Hue section-Vietnam

Pictures of Translational type slides in HCMR -Hue section-Vietnam is presented in Fig 5.2.(a) (on left side). Typical slope in study area was discovered with silt and sand as its top soil and

bedrock as its bottom soil. During an intense rainstorm, the bedrock will keep the rain trapped in the top soils of silt and sand. As the topsoil becomes saturated and heavy, it can start to slide over the bedrock and become a shallow landslide.

The slip surfaces usually have the same direction of geological slope layers or cutting slope of the road. Slip surface usually appeared at the position of interface geological or different weathering layers. In those cases, slip surface usually shallow and toe of surface of rupture usually ended up at middle or end of the cutting slope of the road taluy. Accumulation of landslide was soil or debris greatly influenced by surface water and ground water, moved following stream over the road surface.

5.1.3 Translational wedge type slides

Beside typical landslide as shallow, one more type of landslide was found as translational wedge type slides. Translational wedge type slides has the characters of translational slide as mentioned. Beside it, moving mass slides has shape in a triangular form. Gully type slides and flows, and translational wedge type slides usually occurs in metamorphic rocks have fundamentally the same occurrence mechanism. Translational wedge type slides have a side scrap or a base that matches a weak surface such as schistosity, faults, and joints. In the study area, it was usually located in the rock with middle weathering. Pictures of Translational wedge type slides in HCMR - Hue section-Vietnam is presented in Fig 5.2 (b), (c); (Right side)

5.1.4 Translational rock slide

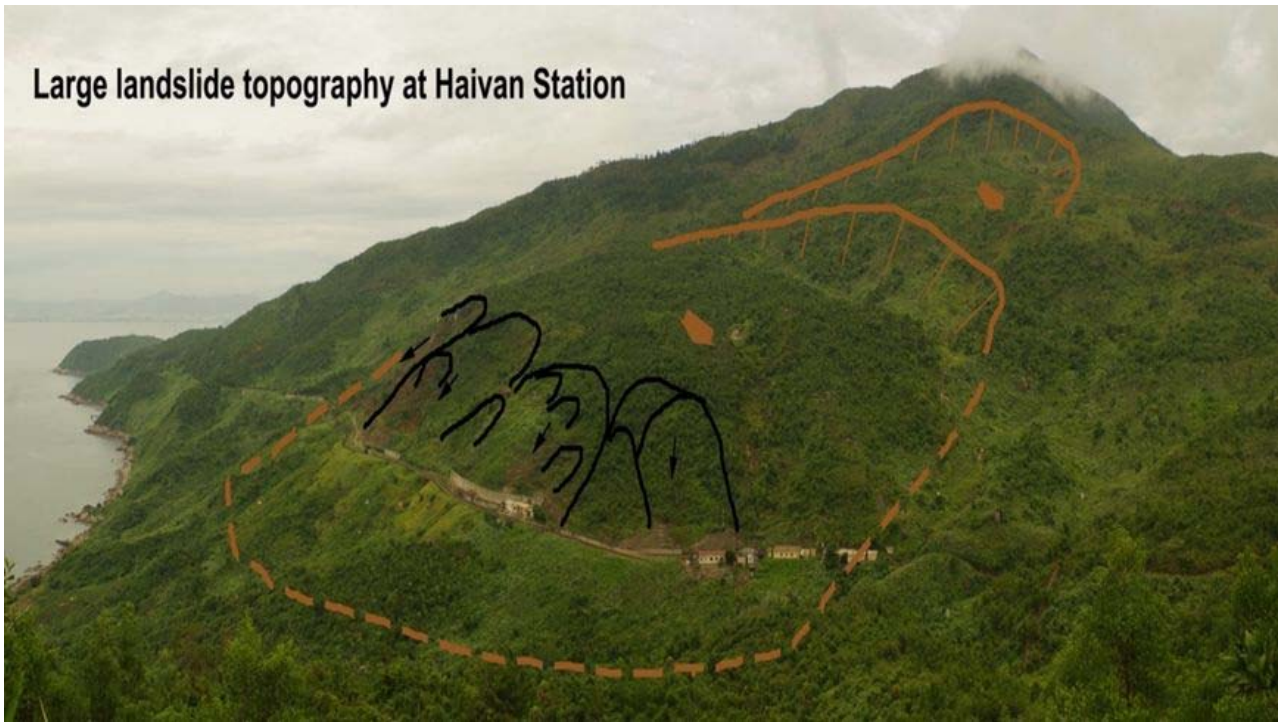

Fig. 5.3 Deep seated Landslide on Hai Van pass - Da Nang –Vietnam

Translational rockslide has the sliding surface mostly deeply located below the maximum rooting depth of trees (typically to depths greater than ten meters). Translational rockslide usually occurred in relation with the geological structure. This type of landslides are potentially occur in a tectonic active region. They tend form along a plane of weakness such as a fault or bedding plane. Some landslide cases, the depth of slip surface is located over hundred meter on deep, with the size is over several square kilometers and usually is considered as deep-seated landslide. In many cases,

the organic layers, such as crushed coal bed, black mudstone, black shale, and black schist, act as a slip plane in sedimentary rocks with developed bedding.Some landslides in areas distributed by limestone occur with limestone as a cap rock. A slip plane is formed in the bedding plane of shale as the underlying layer of limestone and the schistosity plane of weakly converted crystalline schist. All landslides have occurred on a large scale as rockslides.

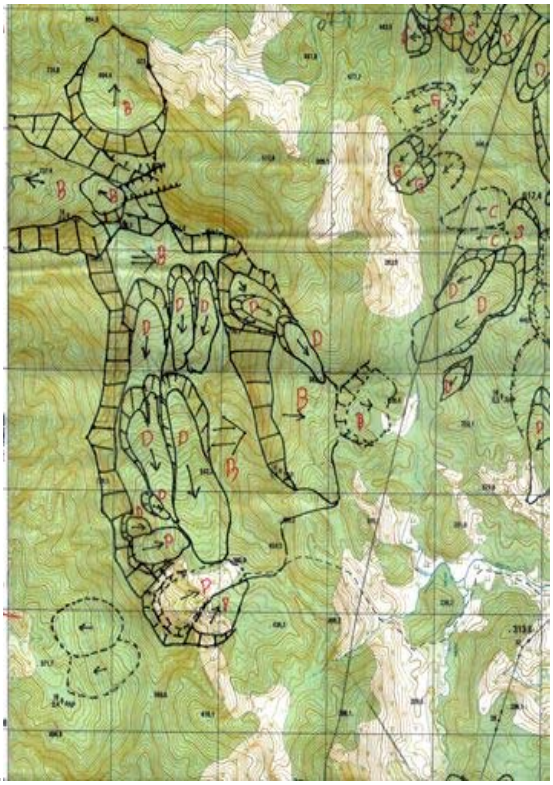

Fig.5.4 Photo of Translational rock slideNorthwestward of Thach My town

Fig.5.4.aTopography of Translational rock slide on Khom9-Kham Duc

A deep seated Landslide original form changes to many minor debris flow inside its landslide body. B means block slide; D means debris flow

In the study area, a number of topographic area of deep-seated landslide distributed. Among of them, the huge landslide distributed at the west point of Kham Duc town, Northwestward of Thach My town and Hai Van pass. The huge landslide distributed at the west point of Khom 9 - Kham Duc My cause by the relationship with the characteristic of ultra-basic rock. Topography map of this Translational rockslide is presented in Fig. 5.4-b.Regarding landslide Topography map, a deep seated landslide original form changes in to many minor debris flows inside its landslide body. B means block slide; D means debris flow.The cause of the one near the Thach My town on HCMR was relation of existance of coal layer between rock layers. The photo of translational rockslide North West ward of Thach My town is presented in Fig. 5.4-a.

Hai Van landslide is special remarkable huge landslide that the real cause is unknown up to now. The land mass of the Hai Van mountains consist with granite. In the granitic area, deeply sheeted landslide is seldom discovered. Pictures of deeply seated Landslide on Hai Van pass - Da Nang - Vietnam is presented in Fig. 5.3.

5.1.5 Rotational debrisslide

Rotational slides occur when a slump block, composed of sediment or rock, slides along a concave-upward slip surface with rotation about an axis parallel to the slope. Rotational movement causes the original surface of the block slipping down, breaking in to many parts with scraps. The top of the slump is rotated backward. In the study area rotational landslides was discovered in deep weathering sedimentary rocks with bedding and schistosity, weakly converted crystalline schist, and granitic rocks. A small number of slip surface with middle to large radius, which was predicted as old landslides, located under the road embankment.

Fig. 5.5-a Photo of landslide body of a rotational landslide in HCMR (Quang Nam section)

Fig. 5.5-b Photo of main scarp of a rotational landslide in HCMR (Quang Binh section)

The sliding movement of the deflection and accumulation zone of deep landslide created cracks and in some cases put up pavement or facilities of road over and they is continues to move with slow velocity depending on the water absorption of the sliding block. Fig. 5.5-a presented main scarp of a rotational landslide and Fig. 5.5-b presented the body a rotational landslide and in HCMR (Quang Binh section).

5.1.6 Gully type slides and Debris flow

Debris flowsare geological phenomena in which water-laden masses of soil and fragmented rock rush down mountainsides, funnel into stream channels, entrain objects in their paths, and form thick, muddy deposits on valley floors. Slope material that becomessaturated with water may develop into a debris flow.

Fig. 5.6 Debris Flow and gully on HCMR-Hue Section-Vietnam

In study area, gully type slides and debris flows, by which an arc-shaped sliding mass originating at the upper area of a slope slides down the slope surface, and the morphology resembles an erosional gully. The development of the small gullies is the initial manifestation of the phenomenon due to the movement of soil particles or fragments of weathering surface, which has resource from broken type of geology wedge structure running follow surface water stream. The small gullies develop larger and larger, and created deep gullies on the surface of slopes, and in some cases, they link together and as the result the slopes failure occurred. Pictures of debris flow and gully on HCMR-Hue section-Vietnam is presented in Fig 5.6.

5.2 Landslide moving mechanism

To landslide, classification types that are discussed above, the mechanism of rock fall is very simple and clear. We concentrated in explanation for Landslides phenomenon include debris flow.

In the case that we studied a unit of soil mass in water on a slope. Under the pressure of ground water rise, the pore water pressure rise respectively. The stress reaches the failure line expressed by equation (1), then the initiation mechanism of sliding starts. There are two factors, that make the pore water pressure rise are ground water rise by heavy rain and earthquake. So the main factor triggered the movement of unit soil mass in water on a slope is the increase of pore-water pressure to make shearing stress equal or larger a shearing stress at failure shear strength of material of each slope.

As discussed above, to contribute for landslide movement there are many causative factors, which are classifiable as dynamic factors (e.g. pore water pressure) and passive factors (e.g. rock structure, land form, slope anger ...).The passive factors take a roll as preparatory factors and nearly unchanged. In the pact, shear strength of material is one of preparatory factors that has small change such as the reduction of value of cohesion (C) depend of content moisture.

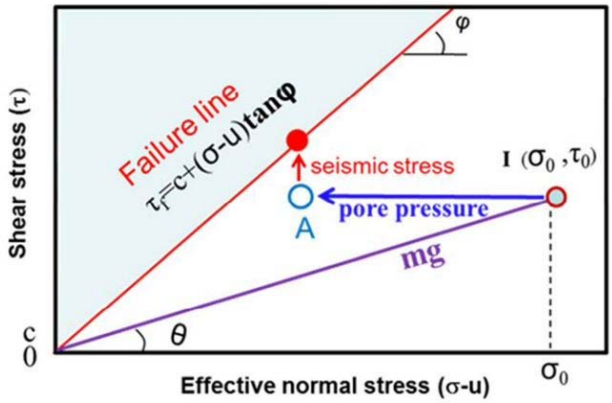

Fig. 5.7 Landslide-initiation mechanism by the combined effect of earthquake and pore -pressure rise (Kyoji, S. and Bin HE, 2012)

Rain is a normal natural phenomenon that we usually meet, especially in rain and storm season. A part of the volume of water from precipitation falls on the slope creates water stream on the surface of slope. The rest penetrates into slope that makes the underground water and increasing the pore water pressure, depending the capacity for discharge of inside contented slope water. Therefore, the change value of pore water pressure depends on slope itself (such as slope gradient, material, etc) which is stable during process of rain and depend on precipitation as well as interval time between each of each rains. While keeping the water content in slope material if the

slope meets the earthquake phenomena, the vibration force will make the pore water pressure increasing in a short time. This will easily trigger rapid slope movement. In other hand, most of soil is not sand absolutely, so value of cohesion (C) of soil exists. Cohesion depend on type of soil as well as its moisture. It makes delay speed of landslide block. This explains for moving phenomenon with slow and middle speed of landslide. The landslide-initiation mechanism by the combined effect of earthquake and pore-pressure rise is presented in Fig. 5.7 for sand material.

However, the study area located in the area that have frequency of earthquake is small. So the main active factor triggered most of landslide in the area is high precipitation. Difference from earthquake action, which brings pore water pressor rise over failure line in very short time, the rain action can make pore water pressor rise very slow, depending water keeping capacity of soil. That can explain for character of the most landslide occurred in Vietnam with middle and slow speed.

5.3 Therelationship betweent dynamic factor and displacement / signal of landslide recognization

To find the explanation for the signal of landslide movement with the change of pore-water pressure, the relationship of integrated factors triggered of landslide surface of the 1792 Unzen earthquakes in Japan (Fig 5.8) is studied for an example.

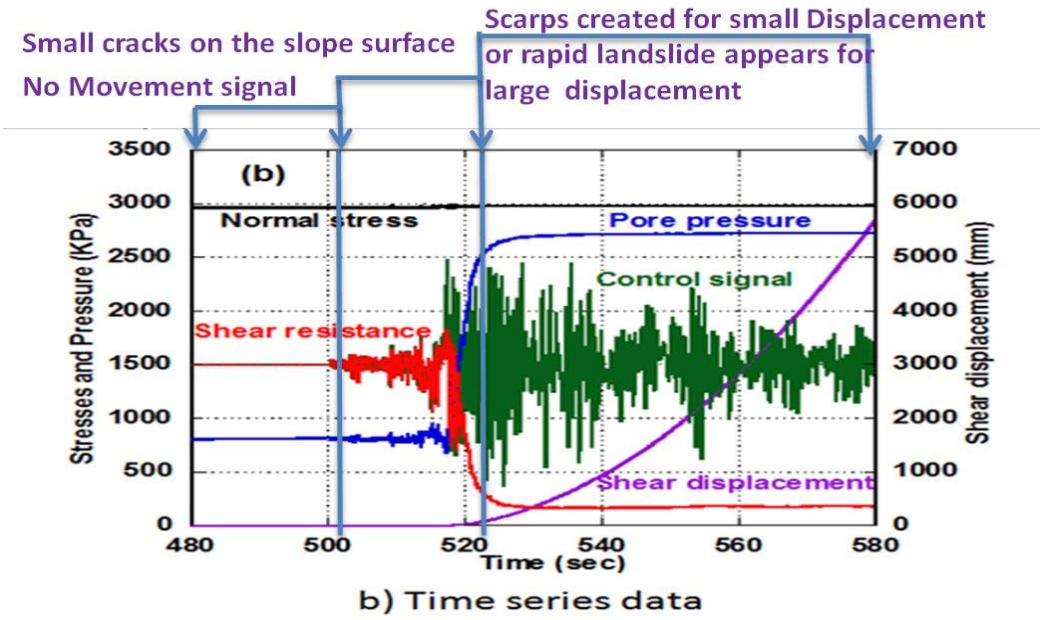

Fig. 5.8 The samples were taken from the landslide surface of the 1792 Unzen earthquakes in Japan

The Fig. 5.8 presented relative parameters of a rapid landslide from initial stage to failure. It will be recognised that on the first zone when the pore water pressure is stable (non change) and shear displacement is zero and It means no signal of landslide is found on the slope. On the second zone of chart, when pore water pressure starts increasing, small shear displacement appears. The landslide starts moving and displacement signal usually found is cracks on the surface of slope. In some cases small main scraps of landslide may be found.

On the third zone , when the pore water pressure increases and gets high value and lasts for a time , shear displacement was increasing. The cracks and small scrap was opened and developing.

The signal usually found in large scraps and clear other micro features. The landslide changes in to rapid movement.

However, In fact, except the earthquakes which can make pore water pressure increasing rapidly, the speed of pore water pressure increasing by the rain usually rises slowly, and repeatedly depending water absorption and discharge underground water of the slope.When pore water pressure increases closely to failure line of slope material then reduces, stage of movement is just around second zone and first part of third zone.The change of pore pressures repeatedly makes the change speed of movement of moving block. The process of “moving and stop” of slope is considered as reactive landslide. It will be answer for the survey landslide results in study area, in which the most of reactive landslides was found in the area.

To abstract an unstable slope in a landslide, it is important to understand how the topography changes. Landslide processes (from beginning to eternal stop) are not limited to a single pattern. Depending on impact of dynamic factor, a landslide is in stage of moving or pause stage along to the length of slip surface and at last, moving to termination stage. For example, landslide displacement can increase or change the initial micro topography structure by continually expanding. Or, if the landslides stopped state continues for a long time, its micro topography, such as scrap and fissures, undergo moderate sloping, and are gradually lost by impact of other morphology phenomenons. Transitions in landslides from occurrence to termination is presented in Fig 5.9 (Toyohiko, M., 2004). So for forecast of landslide disaster , it is necessary to create the relationship between dynamic factors and displacement / signal of landslide . To study area , dynamic factors here is pore water pressure which is variable from landslide to landslide. However, the indirect factor relating directly to it is rain fall. It should be recorded during landslide moving signal investigation.

Fig. 5.9 Transitions in landsides from occurrence to termination (Toyohiko, M., 2004)

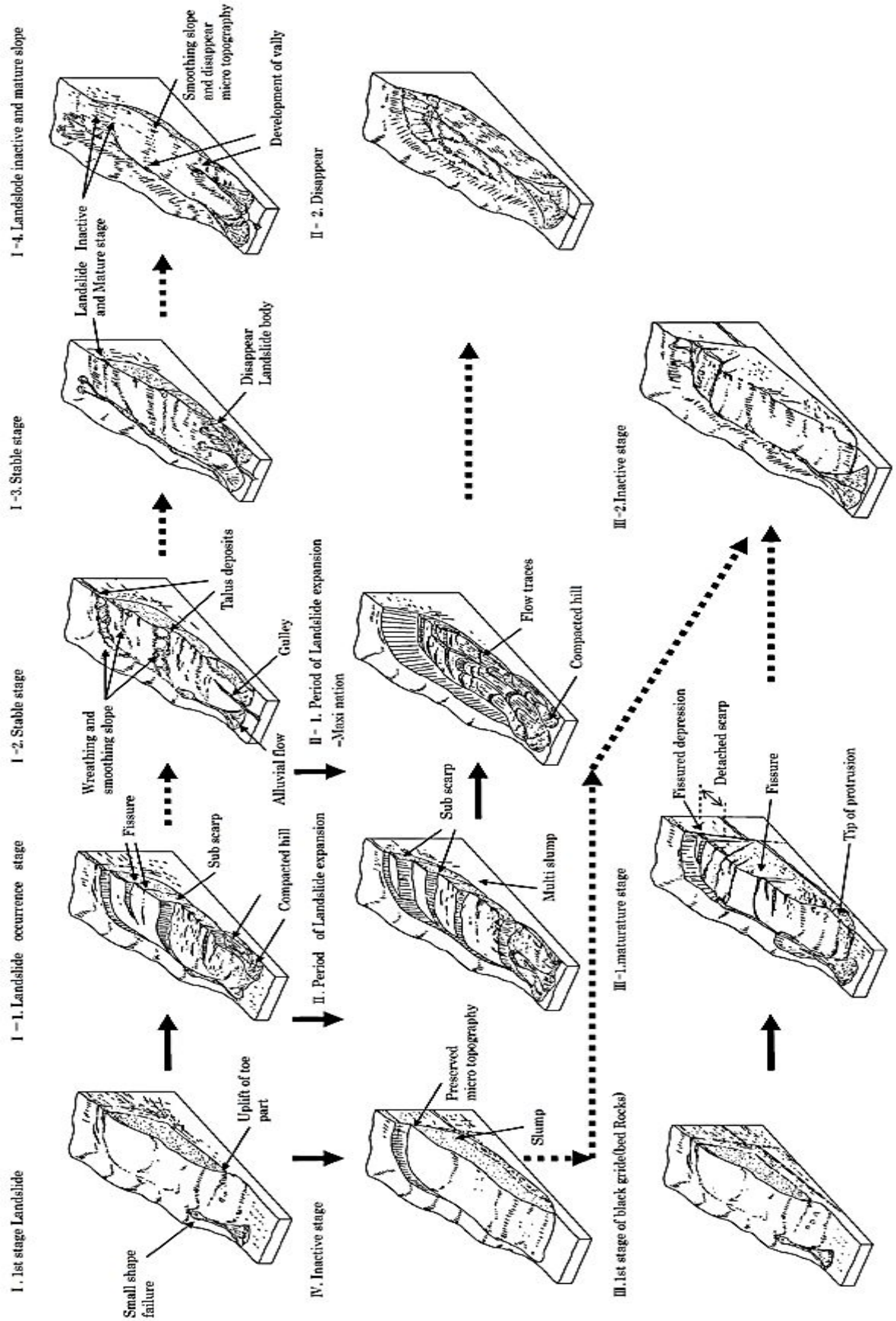

6 Tools for Landslide management for region

6.1 Basic data for landslide management

6.1.1 Landslide data collection

Landslide data collection is considered as the basic document (landslide data base) for creation of regional landslide management tools. Landslide data collection is assemblage landslide information, which occurred in each region. With objective of information providing such as landslide classification type, location, boundary and size, including width, height and depth as well as the moving statute of landslide, it should be named or coded for reference.

In general, there are three basic methods commonly used for landslide data collection were employed as field recognizance to investigate landslide occurrences, collection of historic information of landslide and interpretation of landslide occurrences from aerial photographs.

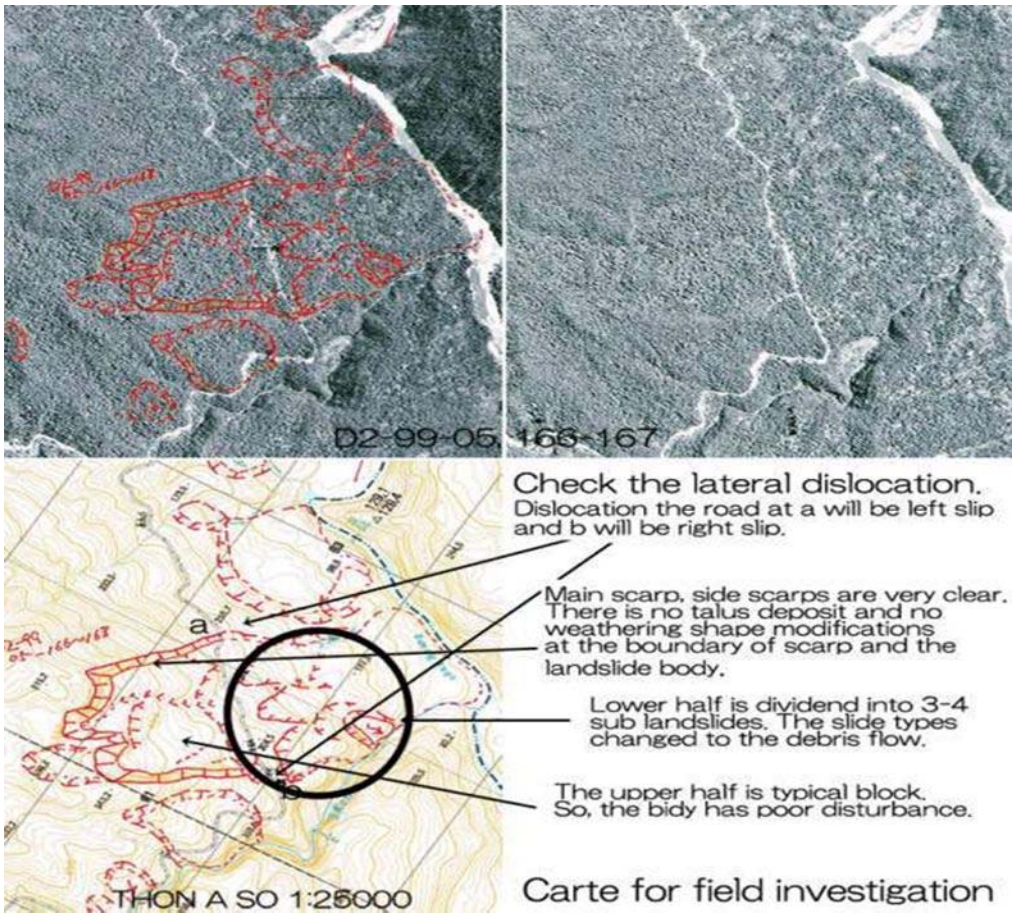

Fig. 6. 1 Landslide interpretation of LS No.18 – HCMR – Vietnam

Interpretation of landslide occurrences from aerial photographs is overall method for recognition. Depending on scale and quality of air photo, geomorphology knowledge combining with possible causative factors concerning to each landslide is employed, the information of each landslide could be identified. From results of landslide interpretation, landslide inventory map will be developed. Fig 6.10 presented the landslide interpretation result of LS No. 18 on HCMR, Vietnam as an example of result of landslide from aerial photographs interpretation.

Field recognizance to investigate occurred landslide is direct and detail for landslide data collection. From site survey, information of micro features of landslide could be recorded including :

(i) General information

- Name or code

- Air Photo code reference

- Topographic map reference

- Landslide overview figure, an aerial photo and topographic map interpretation and real site pictures

- Coordination of position

- Date and name of investigator.

(ii) Landslide and landslide topography micro features information (Pattern diagram of landslide topography is presented in Fig 6.2).

-Type of landslide: (landslide, topple, fall, spread, flow….)

- Landslide scale (shape, ratio of height, length, width, estimated depth)

- Landslide topography micro features (scrap zone : degree of dissection, shape of crown; middle zone : dhape of middle; toe zone : shape of toe)

- Landslide activity stage (cracks, opening crack, moving, flowing signals …)

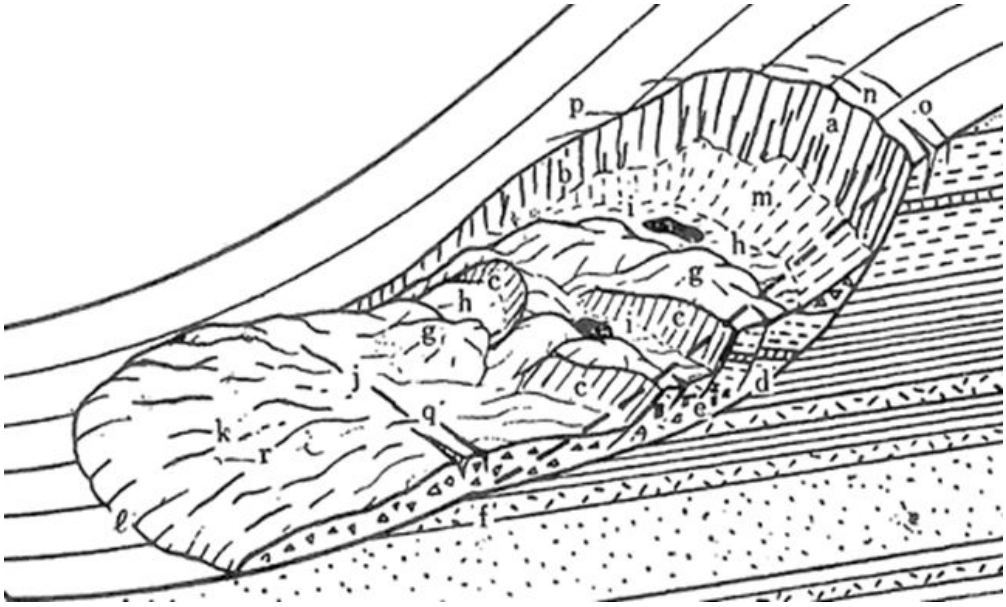

Fig. 6.2 Pattern diagram of landslide topography (Eisaku H. and Toyohiko M.i, 2012)

a. Main scarp, b. Lateral scarp, c. Secondary scarp, d.Main slide surface, e.Secondary slide surface, f.Toe part, g.Small prominence, h.Depression, pond (bog), j.Uplifted area, k. tongue, l.Tongue line, m.Talus, n.Crown, o.Crown fissures, p.Lateral (echelon) fissures, q.Fissures on uplifted area, r.Tongue fissures (collectively, g - l are called the landslide bank)- (Eisaku HAMASAKI1 and Toyohiko MIYAGI)

(iii) Causative factors information

- Topography information (slope anger, topographic type , position with beside objects such as road, residential house, stream ..)

- Geomorphology information (surrounding landslide natures, land form, plain view, knick line …)

- Geographical information (type of rock, weathering, dip and strike, special geographical character if any.

- Climate information (recently maximum precipitation …)

Collection of historic information is very important method for landslide data collection. Historical information could suplied us the landslide information regarding historical classification, boundary, micro-feature and movement stage under the types of document such as report, drawings, pictures or maps. Landslide inter-phases interpretation is one of example of collection of historic information . Using formed inventory map is one of very useful document for landslide investigation information.

6.1.2 Regional monitoring system

Causative factors that contribute to landsliding should divided into four categories: geological causes, morphological causes, physical causes and human causes. While there may be multiple causes for a landslide, there can be only one trigger (Varnes, 1978). (Wieczorek, G.F., 1996) stated that a trigger is “an external stimulus that causes a near-immediate response in the form of a landslide by rapidly increasing the stress or reducing the strength of slope material”. For study area, trigger factor is high pore water pressor, which is result from high precipitation and directly relating to slope displacement. A full landslide monitoring system could measure many moving sensitive factors of landslide on site as full and muntil drection displacement of the vulnerable slope, moving directional displacement, slip displacement, precipitation, pored water pressor... Depending on propose of monitoring, sensitive factors selected are difference. Propose of regional monitoring system is predicted the relationship between maximum precipitation of rain with displacement of landslides in target region.

Principle for regional monitoring system is “the conditions have led to past and present landslides can be used to identify cases likely landslides occur in the future.” Actual landslide is full scale landslide experiment for monitoring. As dissucusing above, landslide-initiation mechanism is the effect of pore-pressure rising, that cause directly by rain. The precipitation of rain is absolutely measured and forecasted. The displacement signals of a slope were presented by pattern diagram of landslide topography, especially the landslide scarps (vertical displacement) and opening cracks (horizontal displacement). Both landslide displacement and rainfall parameters can be identificable by measurement.

For a given region, from investigation and mapping, landslide high risk and high succepsibile locations will be marked as typical control points. The regional monitoring system should be set up for those in this region. The real signals of slope displacement and precipitation after rain could be recorded then the possibility of slope movement will be predicted from precipitation forecast. However, because of impossible agrangement of too many control points so the number of control points should be suitable with economical condition of mountainous region. For this reason, the real time or full monitoring system for landslide warning is not discussed in this guideline. There are 2 common monitoring equipments for precipitation and displacement of surface of slope is mentioned.

6.1.3 Rain gauge -Rainfall Monitoring

Fig. 6.3-a shows a picture of a rain gauge, wich is often used to measure the amount of precipitation. The rain gauge consists of a funnel that collects and channels the precipitation into a small container.

Fig. 6.3 Rain gauge

Fig. 6.3-a Extensometer

After a pre-set amount of precipitation falls, the lever tips, dumping the collected water and sending an electrical signal. A rain gauge can be used for measurement of precipitation of a region.

6.1.4 Extensometers – displacement monitoring

Extensometers are devices used to measure the changing distance between two points. They are commonly used in the monitoring of landslides. Fig.6.4-b presented an arrangement of an extensometer for slope movement measurement in HaiVan landslide. Measurement points may be located on the surface of a landslide to measure the surface movements, for example, spanning a tension crack to monitor its rate of opening, or in a borehole to measure differential displacements at depth for instance to identify active landslide shear surfaces. However, it will not feasible to set up extensometer for every landslide. So the simple way for record displacement is multi observation and manual measurement of signal of displacement such as width of crack, then opening of the crack, scarps opening scarps of landslide or the signal of rapid landslide movement, especially after rain.

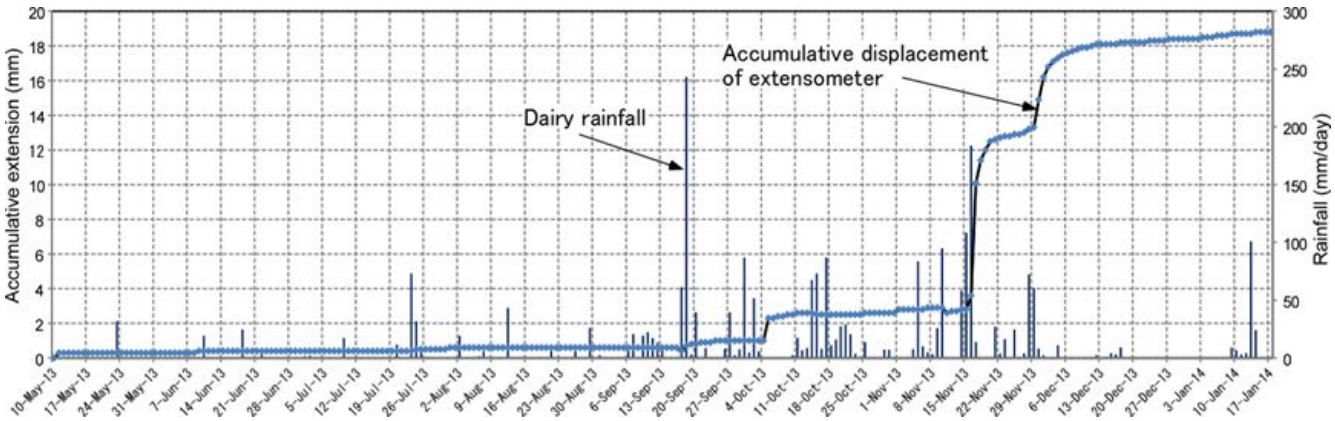

Fig. 6.4 The results of monitoring the relationship between precipitation and displacement at Hai Van landslide – Vietnam

The result of relationship between precipitation of rain and displacement signal should be done for creation the response plan to landslide.The results of monitoring relationship between

precipitation (by Rain gauge) and displacement (by mono extensometer) at Haivan landslide – Vietnam in scope of ’Development of landslide risk assessment technology along transport arteries in Vietnam’’ is presented in Fig 6.4 for reference.

6.2 Integrated maps for landslide hazard vulnerability mitigation

6.2.1 Landslde inventory map

For development of the landslide hazard or risk assessment, the collection of information is considered as first step. The goal of landslide collection of information is creation of Landslide inventory map. It records many information as the location, where known, the date of occurrence and types of landslides that have left discernible traces in an area (Hansen, A., 1984). A detail landslide inventory map could shows landslide boundary, shape, combine parts, topographical micro-features, direction of moving...Beside this landslide inventory map usually presented on the base of topography map which supplied for user surrounding information regarding geomorphology such as landform, stream network (gully/rill), convex breakline , concave

Inventory maps can be prepared by different techniques, depending on their scope, the extent of the study area, the scales of base maps and aerial photographs, and the resources available to carry out the work. In this area , Inventory maps was prepared by Air Photo scale 1: 33000 (one phase) and topo-map, which was extracted form DEM scale 1: 25000.

As they are prepared by interpreting one or more sets of aerial photographs and correcting the results by field investigation, landslide inventory maps tend to be subjective. Reliability, completeness and resolution are issues to be considered when preparing and using an inventory map. An incomplete or unreliable inventory may result in erroneous hazard or risk assessments. Many factors affect the reliability, completeness and resolution of an inventory map. Beside factors regarding to availability of input data such as landslide freshness and age, the quality and scale of aerial photographs and base maps, factors concerning to natural condition of area as the morphological and geological complexity of the study area, land use types and alterations, the human factor like degree of experience of the geomorphologist, who completes the inventory take a very important role. Good quality event inventories should be reasonably complete, at least in the areas for which aerial photographs were available and where it was possible to perform field work.

As a drawback, inventory map often covers only a part of the total geographic area associated with a landslide triggering event. For the rest sensitive area, we have no information. In other hand, historical inventory landslide is never complete. Evidence for the existence of landslides is rapidly removed by erosion,growth of vegetation and human activity. And with time landslide boundaries become fuzzy, making it difficult to map the landslide precisely. However, because the synthesis and sufficiency regarding landslide information, landslide inventory Map is used for many propose of regional management.

6.2.2 Landslide risk assessment map

Landslide risk evaluation aims to determine the “expected degree of loss due to a landslide (specific risk) and the expected number of live lost, people injured, damage to property and disruption of economic activity (total risk)” (Vaners, 1984).There are two possible approaches as quantitative (probabilistic) and qualitative approaches. Quantitative risk

assessment aims to establish the probability of occurrence of a catastrophic event. However, the method requires a catalogue of landslides and their consequences. Because lack of the data of lost by landslide this evaluation is not discussed in this study.

A qualitative approach can be pursued in such a way as to establish qualitative levels of landslide risk. The landslide risk assessment map in this study was established based on interpretation of geomorphology-topography-airphoto. The landslide risk assessment map was developed from inventory map. In the process of air-photo interpretation, causative factors concerning to geological features, land used was considered together with characters of landslide topography micro features. An analytical hierarchical process (AHP) was used for evaluation the sensitiveness of reactive landslide by weight. As the results, a landslide risk assessment map is created, in which each landslide is coded. The risk level of each landslide is classified and divided in grades as low, middle, high and very high depending the sensitiveness evaluation to movement of each landslide.

Landslide risk assessment map is useful for ceration the landslide priority courtemeasures plan as well as other applications for management of region.

6.2.3 Landslide susceptibility map

Landslide susceptibility maps describe the relative likelihood of future landsliding based solely on the intrinsic properties of a locale or site. Some organizations use the term “landslide potential map” for maps of this kind.There are various possible causes for land sliding with complex interrelationships. However, in practice a detailed assessment to find the main causes of each landslide is not feasible in most cases. The selection of causative factor for landslide susceptibility map is usually based on experts subjective experience. In this study, to analyse landslide manifestation, causative factors are derived of slope anger, type of rock, fault density, distance to the road, land used and precipitation. The maps for causative factors were created, in which each one was divided in to classes. From occured landslide distribution on the space from classes of causative factors map, the relation rule is concluded for future landslide prediction.

The sensitiveness to landslide of each classes zone of causative factor maps is calculated and then evaluated thought the value of number occurred landslide (NOL) and density of occurred landslide (DOL). These values were the result of comparison of landslide distribution map and each causative factor maps using GIS application. An analytical hierarchical process is used for evaluation. The combination these causative maps with difference evaluation weigh is carried out for landslide susceptibility mapping. As the result, a landslide susceptibility zonation map with 4 landslide susceptibility classes, i.e low, moderate, high and very high susceptibility for land sliding, is derived.

Landslide susceptibility maps are useful for disaster respond and mitigation plan, creation development master plan regarding with plan for land use, construction of infrastructure

.6.2.4 Landslide hazard map

Landslide hazard maps indicate the possibility of landslides occurring throughout a given area. An ideal landslide hazard map shows not only the chances that a landslide may form at a particular place, but also the chance that it may travel downslope a given distance. Landslide hazard maps is developed base on landslide information of inventory map, risk evaluation map and landslide susceptibility map. To a concrete landslide or high susceptibility slope, the tests

for material for causative factors which triggered landslide will be done. A model experiment may invest for predict influence boundary of landslide when it would able to happen.

However, because it concerns to establish landslide hazard zone so concept of acceptable risk zone was discussed and not yet get the same point of view for every field. So landslide hazard maps is usuaslly developed and applied for concrete sensitiveness landslides or region depending on the purpose of regional manager.

6.3 Planning for landslide prevention and mitigation

To landslide prevention and mitigation, depending strategies as prevention, response and mitigation, the following plans/program should be carry out.

6.3.1 Landslide prevention strategies

Landslide prevention concerning to understanding of landslide and potential of sliding. To prevent landslide hazard, a long-term strategies must be build as followingadvocacy, training and knowledge of landslide disaster prevention for the community. Main contend of Landslide prevention strategies includes (1) Building up landslide data base and (2) creation and application of inter-grade landslide hazard maps.

- Building up alandslide basic data , which was disscussed above(refer to iterm 6.1 for details) for landslide management.

- Creation inter-grade landslide hazard maps as Landslide inventory map, landslide risk assessment map, landslide hazard map and landslide susceptibility map. The concept of them have been discussed above section. (refer to iterm 6.2 and table 6 landslide integrated guideline list for details). Using inter-grade landslide hazard maps for planning new residential development areas, land use and infrastructure development. For landslide prevention, the high susceptibility zone from landslide susceptibility map and high risk landslide from landslide risk assessment map should be avoided. Middle susceptibility zone or middle risk assessment should be considered for use . In case of inevitability, the strategies for landslide mitigation must be given out. To the new development area, which be located nearby easy landslide hazard vulnerability zone should be targeted for landslide predict calculation of stable factor and landslide hazard map for safety boundary.

6.3.2 Landslide respone trategies

- Establishing a public-domain information systems regading landslide disaster to forecast andwarningto community effectively. Information about the weather focast regading landslide such as locations, respone solutions, evacuation locations, waning sign, grade of risk assessement shoud be shared to each family in sensitive area. Trial evacuation is nessessay for action of community.

- Establishing regional monitoring system. There are many sensitive factor should be the target of monitoring. Depending on condition of each region, necessary factors is chosen. However, for the each region, 2 parameters including landslide displacement and precipitation of rain must be monitored for muntil sensitive locations in the region (Regional monitoring system is

discussed in 6.1.2). Please refer table 6.2 for landslide integrated guideline list for details of other real time monitoring parameters.

- Creating respone solutions and evacuation plans base on integrated landslide maps and analyze results of sensitive factors from regional monitoring system. For example, from distribution of displacement of typical occurred landslides on precipitation chart, the reliability grade will be selected and evacuation plan is created. The safety area for evacuation will be selected based on inter-grade landslide maps on the low risk assessment and susceptibility zone.
- Establish the search and rescue force, which is ready for landslide occurring in order to rescue and mitigate the damage of phenomenon when disater occures.
- Setting up the early warning system. In case of tagget such as local residents still stays on high potential of landslide moving area, a monitoring and early warning system should be set up. The training to people to understand and recognized emergency situation from the system is necessary. Please refer table 6.2 for landslide integrated guideline list for details of landslide warning system.

6.3.3 Typical mitigation strategies

There are 2 basic strategies to mitigate for a particular landslide, that are (1) stabilization and protection countermeasures, which seeks to counter one or more key failure mechanisms and improve stability of the slope and (2) Maintenance and monitoring, which is applied when landslide countermeasures are ineffective. In this section, we do not dissuss deeply for each countermeasures but guide for application scope.

- Stabilization and Protection countermeasures

Depending on type of material as well as type of movement, landslide stabilization and protection countermeasures is divided into 3 categories as countermeasures for earth slope, rock slope and debris-flow. Table 6.1 present the matrix of typical landslide countermeasures for mitigation strategies.

Countermeasures for Earth Slope Stabilization

Excavation is common and quite low investment countermeasure for earth slope stabilization. Depend situation of landslide, following solutions will be applied as removal of soil from the head of a slide, reducing the height of the slope, backfilling with lightweight material, benches, reducing slope angle, or other slope modification. Before and during process of excavation, landslide movement stage must be considered carefully for safety.

Strengthening slopes is countermeasure that increasing the bearing capacity of the slope to unstable stage. The solutions include plastic mesh reinforcement, rockfill buttresses, stream channel linings or check dams to prevent check dam failure. Local available material should be used for those solutions.

As discussed above, water takes a very important role to stable stage of a slope by changing pore water pressure. Discharge water from potential slope or landslide body is a very effective solution to stable stage .The drainage techniques includes site leveling, ditches and drains, drain pipes, straw wattles and straw bales, retaining walls, timber crib, steel bin wall, reinforced earth wall, gabion walls, piles. It could be combined with other solutions in order to

get the targets of prevent water erosion and infiltration connecting with reduction of ground water.

For longterm and enviromental family countermeasure, slope stabilization using vegetation such as types of seeds, mulching or biotechnical slope protection solutions shoud be advised.

Countermeasures for Rock Slope Stabilization

To rock slope, typical landslide that usually meet, especially on the cliff face or cutting taluy along the road is rockfall. For that kind of phenomenon, safe catching techniques countermeasure used will be simplest and the most effective. The catch ditches; cable, mesh, fencing, and rock curtains are solutions usually applied for rock fall or rock rolling.The retaining walls rock, sheds/shelters or rock ledge reinforcement are solutions that are built over the road or railway to prevent rock rolling or avalanches. They are usually relate to strong and heavy structure and take a large money for investment.

Excavation of rock countermeasure includes benches ; scaling and trimming solutions. Benches solution is applied on rock cliff with high potential of translational slide. It also reduce tensional force in the surface and reduce surface erosion rates. In cases of rock cliff face with loose, unstable or overhanging blocks, scaling and trimming solution is advised as an initiative one. Beside mentioned countermeasure, rock cliff could be reinforced in place by application of shotcrete and gunite ;anchor, bolt, and dowel solution.

Countermeasures for Debris-Flow

As discussed in last part, the initial manifestation of the phenomenon of a debris-flow is erosion and erosional gully on the easy vulnerability slope by weathering, rain and other physical abrasion. Strengthening slopes for erosion/debris flows countermeasure could be used for strengthening as soil to resist erosion; proper planting of vegetation on slopes; keeping slopes free from fuel for wildfires solutions are considered as good one to prevent the possibility to make soil slope more prone to debris flow.

Structures for mitigating debris flows such as debris-flow basins, check dams, debris-flow retaining walls are solutions that can reduce the power of debris-flow by device it in to many portions and reducing its velocity. They could be built to stop or diverting it around a vulnerable area. In case debris flows make landslide dam, the following measure can be implemented as diversion of inflow water before it reaches the lake formed by landslide dam ; temporary drainage from the impoundment by pumps and siphons ;construction of an erosion-resistant spillway or drainage tunnel through an abutment.

- **Maintenance and monitoring**

To the slope that has very large scale and high risk landslides,to which the using landslide countermeasures are ineffective, there are two solutions that are usually applied. They are (1) keep away from landslide and (2) Maintenance and monitoring.

Keep away from landslide solution often applies to large and very dangerous landslide. That is isolated landslide potential hazard area. Resident is not access or limited access to the landslide area for living. Landslide fences should be set up around the boundary. The boundary of limited assessment is divided depend the reliability of landslide hazard map.

In case of keep away from landslide solution becomes infeasibility, maintenance and monitoring should be applied combining with early warning system. (refer guide line list for Early warning system) Generally, these measures are relatively low cost and can be highly

effective in reducing public exposure to slide risk. Resident who live inside sensitive of landslide hazard map should be well trained for response evacuation when waning signal works.

Table. 6.1 Matric of typical landslide countermeasures for mitigation strategies

Countermeasures for Earth Slope Stabilization	Excavation	-Removal of soil from the head of a slide, -Reducing the height of the slope, -Backfilling with lightweight material, -Benches, -Reducing slope angle, -Other slope modification.	Countermeasures for Rock Slope Stabilization	Safe Catching Techniques	-Catch Ditches Cable, Mesh, -Fencing, and Rock Curtains -Retaining Walls, Rock Sheds/Shelters -Rock Ledge Reinforcement	Countermeasures for Debris-Flow	Strengthening Slopes for Erosion/Debris Flows	-strengthening the soil to resist erosion -Proper planting of vegetation on slopes can prevent erosion -Keeping slopes free from fuel for wildfires
	Strengthening slopes	-Lastic mesh reinforcement, -Rock-fill buttresses, - Stream channel linings -Check dams to prevent check dam failure.		Excavation of Rock	-Benches -Scaling and Trimming		Structures for Mitigating Debris Flows	.-Debris-flow basins -Check dams -Debris-flow retaining walls
	Drainage techniques	-Site leveling, -Ditches and drains, -Drainpipes, -Straw wattles and straw bales, -Retaining walls, -Timber crib, -Steel bin , reinforced earth , gabion walls, -Piles.		Reinforcing Potential Rockfall Areas	-Shotcrete and Gunite -Anchors, Bolts, and Dowels		Landslide Dam Mitigation	.-Diversion of inflow water before it reaches the lake formed by landslide dam -Temporary drainage from the impoundment by pumps or siphons -Construction of an erosion-resistant spillway -Drainage tunnel through an abutment
	Green	-Types of seeds, -Mulching -Biotechnical Slope Protection						

Table. 6.2 Landslide intergraded guideline list

Code	No.	Name of guideline
Part	I	Mapping and Site Prediction
GL1	1.1	Landslide topography mapping through aerial photo interpretation
GL2	1.2	Field Work for Landslide Engineers
GL3	1.3	SFM base DSM establishing
GL4	1.4	Risk Evaluation of occurred landslide using the Analytic Hierarchy Process (AHP)
GL5	1.5	Landslide susceptibility mapping along the HCMR in central Vietnam
GL6	1.6	Hazard zonation for Landslide Risk Reduction
GL7	1.7	Geological survey for landslide
GL8	1.8	Vulnerability of landslide hazard mitigation for humid tropical region
Part	II	Material Tests
GL9	2.1	High Stress Un-drained Ring Shear Apparatus (RSA) Introduction
GL10	2.2	Drained shear speed control test using RSA
GL11	2.3	Un-drained shear stress control test using RSA
GL12	2.4	Pore water pressure control test using RSA
GL13	2.5	Cyclic stress control test using RSA
GL14	2.6	Un-drained pore water pressure and seismic loading test using RSA
GL15	2.7	Soil shearing test in lab – Direct shear test
GL16	2.8	Portable Direct shear apparatus and testing
Part	III	Monitoring
GL17	3.1	Landslide Monitoring Systems
GL18	3.2	Measurement of slope surface displacement using Robotic total station
GL19	3.3	Measurement of slope surface displacement using Global Navigation Satellite System (GNSS)
GL20	3.4	Measurement of slope surface displacement using Extensometer
GL21	3.5	Measurement of slip surface displacement in borehole using Inclinometer
GL22	3.6	Measurement of slip surface displacement in borehole using Vertical extensometer
GL23	3.7	Rainfall gauge and others Meteorological equipment
GL24	3.8	Groundwater observation using water pressure gauge
GL25	3.9	Early warning system
Part	IV	Landslide experiment
GL26	4.1	Outline of landslide experiment
GL27	4.2	Infiltration properties of testing material – for permeameter
GL28	4.3	Testing method (displacement measurement, porepressure measurement)
GL29	4.4	Analysis of measured data (Landslide motion and porewater pressure)

Code	No.	Name of guideline
GL30	4.5	Mechanism of landslide initiation
Part	V	Softwares and Simulations
GL31	5.1	Alcalc 3D Software
GL32	5.2	3D Analysis
GL33	5.3	Arc View Software - Arc GIS10.1/ Spatial Analysis Software
GL34	5.4	LS rapid

ITST-ICL

GUIDELINE FOR LANDSLIDE RISK ASSESSMENT

GL 11: 2016

First Edition

Testing Method of Undrained Shear-Stress Control Test

HA NOI – 2016

Abstract

A new high stress undrained ring shear apparatus ICL-2, which has been newly developed as a part of the SATREPS and ICL/JST project in Vietnam, has applied to study the initiation and motion mechanism of large-scale and deep-seated landslides in Vietnam in May 2015. This apparatus is suited for undrained shear tests under various types of loading such as rainfalls and earthquakes. Specifically, the device enables observing the undrained shear behaviors of soil samples at unlimited shear displacement and under undrained high stress condition. The undrained capability is up to 3.0 MPa of normal stress and pore pressure that correspond to 100-200 m deep landslides. Undrained shear stress control test is employed to determine the physical properties of soil samples, namely steady state residual strength (τ_{ss}), friction angle at peak (ϕ_p), the angle of friction during motion (ϕ_m). This guideline presents the procedure for undrained shear-stress control test using the new high-stress ring-shear apparatus (ICL-2).

Table of contents

Testing method of undrained shear-stress control test

1. Scope

This guideline covers a procedure for undrained shear-stress control test using the new high-stress ring-shear apparatus (ICL-2).

Undrained shear-stress control test is used to determine the technical specifications of the soil: steady state shear strength (τ_{ss}), friction angle at peak (ϕ_m), the angle of friction during motion (ϕ_p).

2. Reference documents

MARUI & CO., LTD, Operation Manual For Undrained Ring-Shear Apparatus Data Acquisition & Control Software.

MARUI & CO., LTD, OPERATION MANUAL (Main Unit) For Undrained Ring Shear Apparatus

Kyoji Sassa, Bin He, Mauri McSaveney, Osamu Nagai, ICL Landslide Teaching Tools.

3. Apparatus

Ring shear apparatus is designed to quantitatively simulate the entire process of failure of a soil sample, from initial static or dynamic loading through shear failure, pore pressure changes and possible liquefaction, to large-displacement, steady state shear movement. A series of ring shear apparatus (DPRI-3,4,5,6,7, ICL-1 and ICL-2) was developed by Sassa and his colleagues since 1984, in which, the ICL-2 has a high capability to reproduce large-scale and deep-seated landslides. The introduction and description of the ICL-2 (Fig. 1) is referred to Guideline 9 for High Stress Un-drained Ring Shear Apparatus (RSA) Introduction.

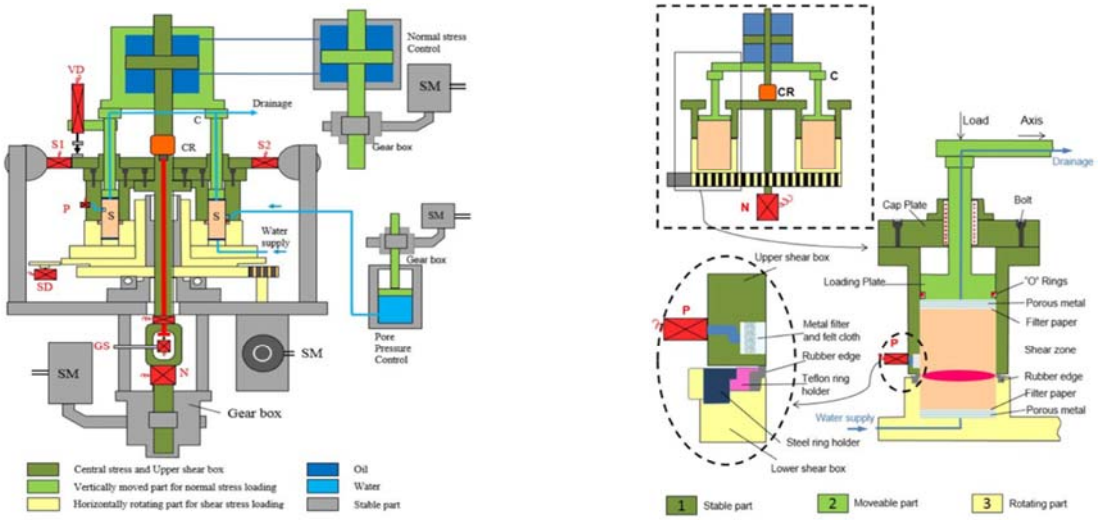

Fig. 1 The new high-stress dynamic-loading ring- shear apparatus (ICL-2)

4. Testing procedure

This part describes the testing procedure for undrained shear stress control test using the ring shear apparatus, ICL-2 in detail. Bassically, the testing procedure is followed by steps as mentioned in Guideline 9 for High Stress Un-drained Ring Shear Apparatus (RSA) Introduction.

4.1 Apparatus Preparation

Teflon is sprayed separately with three times to protect the rubber edges, in which, the time of each Teflon spray is about 10 minutes to dry Teflon coats (Fig. 2).

Fig. 2 Teflon Spay

Silicon grease is coated on the inner and outer rings of upper shear box in order to reduce the friction and to prevent water leakage during shearing (Fig. 3).

Fig. 3 The inner and outer rings are covered in grease

4.2 Sample preparation

Soil specimens required for ring shear tests have particle sizes smaller than 2 mm in diameter and to be fully saturated before building in shear box. The following procedure is carried out for sample preparation (Fig. 4).

• Firstly, after sieving the in-situ taken sample by the sieve of 2.0 mm in diameter, the sample are slowly poured into a plastic container with de-aired water (about 300 ml to 400 ml of deaired water and 500 grams of soil sample). Then this container with sample and de-aired water is put in the vacuum tank and leave them over night.

• Next day, the specimen is saturated by using a vibrator in combination with a vacuum pump. In order to finish this step, leave the sample in the vacuum tank without further vibrations during night. Depending on types of sample, it will take several hours to make air bubbles inside soil particles come out. Even it may take some days to saturate samples that have a very low permeability like clays and silts.

• After the sample is fully saturated on which no any air bubbles is observed, the sample is ready for test. Release the vacuum tank slowly by opening the upper valve, then take the saturated sample out of the water tank.

Fig. 4 Vacuum tank

4.3 Gap Adjustment

Fig. 5 Switch on GAP control

First, a defined gap value, which corresponds to a vertical force (contact force), must be given to avoid leakage of water and sample through a servo control motor. The defined gap value is determined in advance by an adjustment of gap value in order to prevent water leakage as presented in the Guideline 9. Gap value is kept constant during the test.

Main steps for gap adjustment are presented as follows:

- Firstly, run Ring Shear Simulator Software on PC and switch on Gap control (Fig. 5).

- Secondly, screw the inner ring and adjust vertical load to 0 by reset the value of normal stress (Fig. 6). Normally, vertical load is always to be zero at the neutral position of Gap control button.

Fig. 6 Reset Gap value to zero

- Next, after putting the outer ring, Helping Ring is put and connected with the inner and outer rings by 6 screws and 3 Helping Screws (golden screws). At the beginning, 3 Helping Screws is to adjust position of shear box only, so it is required to leave them loose (Fig. 7).

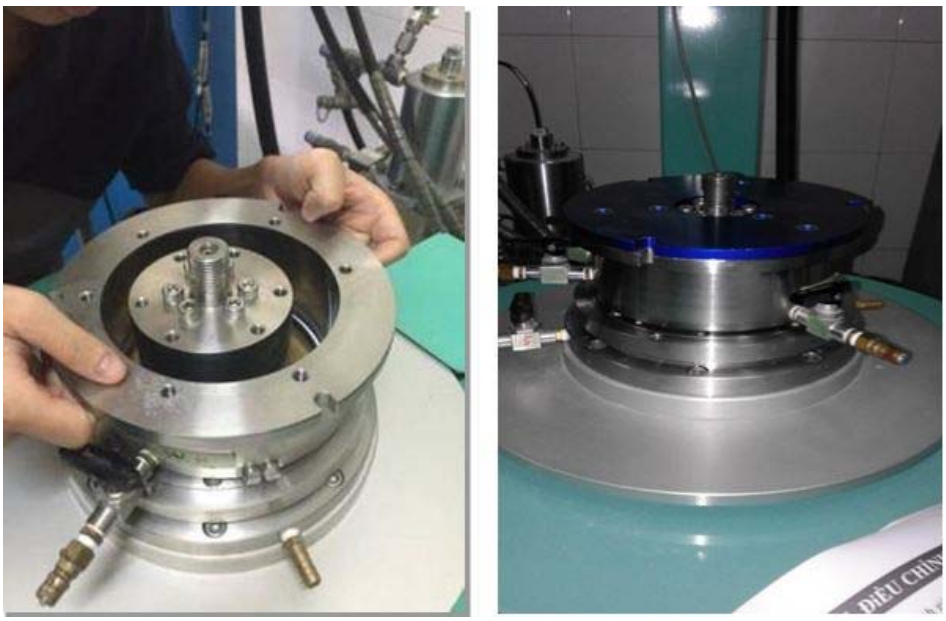

Fig. 7 Putting outer ring and helping ring

- Once contact force is increased to a designed pressure of Gap value, Helping Screws are screwed tightly and then remove the Helping Ring (Fig. 8).

Fig. 8 Increasing Contact pressure and removing the Helping Ring

- Finally, Loading Plate is installed with the help of all 9 screws (Fig. 9). In this step, it is not necessary to tighten 9 screws.

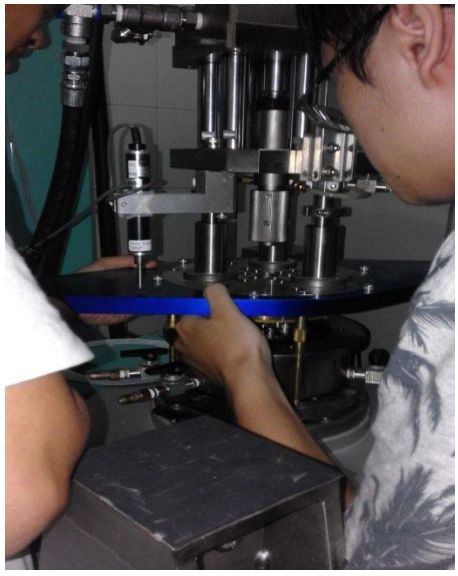

Fig. 9 Installing Loading Plate

4.4 CO_2 and H_2O (de-aired water) saturation

Shear box without sample is filled with CO_2 and de-aired water. Then, saturated sample that is prepared by de- aired could be slowly placed in shear box. After that, the water circulation could start to enable full water saturation of the sample. De-aired water is slowly supplied through the lower drainage line, and discharged from the upper drainage line until all air bubbles are expelled. Valves 2, 3, 4a and 4b are de-aired by CO_2, respectively (as shown in Fig. 10).

Fig. 10 Procedure of CO2 and H2O Saturation

After de-airing water, PPT-1 and PPT-2 are installed to Valve 4a and Valve 4b, these valves are drained to exclude air bubbles from the inside (Fig. 11).

Fig. 11 A photograph of pore water pressure transducers PPT-1, PPT-2

4.5 Sample setting

After putting a filter paper, the sample could be slowly built in shear box (Fig. 12).

Fig. 12 Putting a filter paper and building the sample

After building the sample, loading plate is set up and fixed by 12 screws (Fig. 13). The contact of loading plate and the sample should be given by a small amount of vertical load ranging from 20 kPa to 30 kPa).

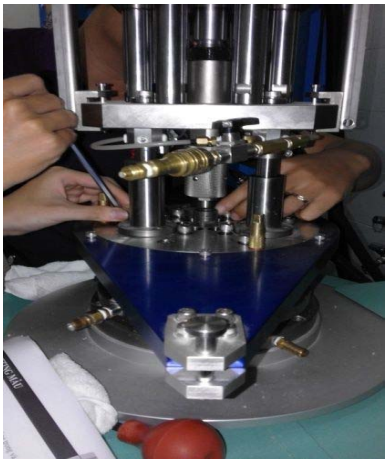

Fig. 13 Setting up loading plate

Fig. 14 Installing Shear Load Cells

Once two shear load cells are set up after installing shear box and loading plate (as presented in Fig. 14), 12 screws must be screwed tightly. Later on, the lifter of upper loading plate is returned back to neutral position and to be locked.

After screwing 12 screws on LP, Vertical Load Cylinder (VLC) is lowered to connect to the central axis of the apparatus (Fig. 15). In addition, one important thing needs to do is that the fixer which prevent the drop of the upper loading part by self-weight must be unlocked and removed from the pillars after sample setting. Fixers are only fixed until sample setting and those should be unlocked during loading. Otherwise, normal stress can not load and it may lead to some damages to the apparatus.

Fig. 15 Installing VLC and unlocking the fixers

Next, Vertical Displacement Sensor (VDS) that measures the vertical displacement of the sample under consolidation loadings is connected to main control unit.

Finally, a water circulation by gravity can start to fully saturate shear box and the sample. In water circulation, de-aired water is supplied through the lower drainage line (valve 5), and discharged from the upper drainage line (valve 2) until all air bubbles are expelled (Fig. 16).

Fig. 16 De-aired water flow to valve 5 and discharge at valve 2

4.6 Saturation checking

To check the saturation degree of the sample, BD parameter (proposed by Sassa 1988) is used for ring-shear tests. The sample is firstly consolidated under normal stress of 30 kPa in drained condition to make contact between sample and porous metal of the loading plate. Then shear box is changed to the undrained condition. In this condition, the normal stress begins loading with an increment of 50 kPa in each step ($\Delta\sigma$=50 kPa while the increment of pore pressure generation is measured (Δu). The degree of saturation (BD) is calculated by the ratio of pore pressure increment and normal stress increment ($\Delta u/ \Delta\sigma$). Specimens with BD greater than 0.95 could be considered as a full saturation. In drained tests and pore water control tests, it is not necessary to check BD value.

4.7 Sample consolidation

Sample consolidation is carried out in order to reproduce the initial stress condition of the sample. The initial stress state of soils only due to gravity is created by loading normal stress and shear stress that depend on the depth of samples at the suspected sliding surface, slope angle and unit weight of the sample. After making input data form panel for Data acquisition with appropriate parameters, data acquisition is switched on and stress loading can be apply while Valve 02 is opened. The rate of normal stress and shear stress increasing ranges from 1 kPa to 5 kPa per second for ICL-2 tests. When shear stress and normal stress reach to designed values and pore water pressure dissipates completely (values at u_1, u_2 is zero), valve 02 is closed to turn shear box to undrained condition. Fig. 17 illustrates the input data window for normal stress and shear stress of the ring shear tests.

Fig. 17 Photograph of input data window for sample consolidation

4.8 Undrained shear stress control test

After the consolidation, values of shear displacement should be reset back to zero and removing of helping screws and water pipe of valve 5 must be done to avoid any damages during shearing. Then, input data setting on the control screen is carried out with appropriate parameters for this specific test including a defined shear stress, shear slope and a defined value of shear displacement. Immediately, undrained shear stress control test can start by applying monotonic shear stress control mode after starting the data acquisition, switching on “Start” button and selecting “Static” button of normal stress or shear stress for such kind of tests. A screen-print of the ICL-2 Application Software for undrained shear stress control test is shown in Fig. 18.

To perform this test, after normal stress reaches designed value in the consolidation step and pore pressure is zero approximately, the sample is sheared by applying shear stress control mode in undrained conditions. In this condition, shear stress is gradually increased at a rate from 1 kPa to 5 kPa per second. The failure will occur when the shear stress reached to a failure line at the maximum shear resistance with friction angle at peak (ϕ_p). Then the effective shear resistance path go down along the failure line with a friction angle during motion (ϕ_m) Fig. 19.

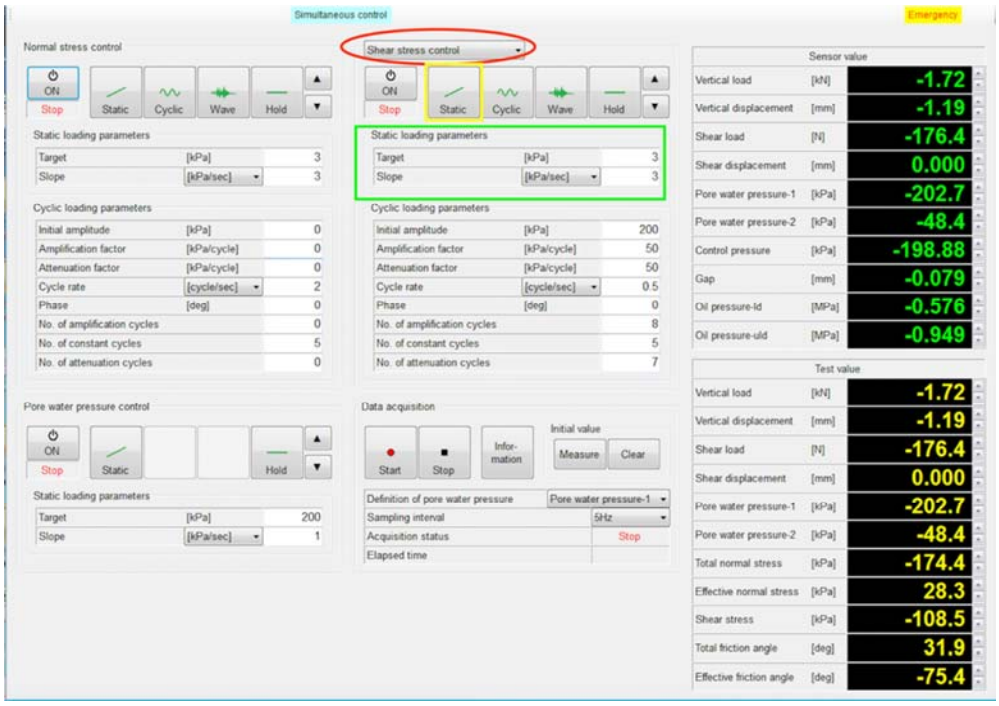

Fig. 18 Print screen of the ICL-2 Application Software showing Shear Speed Control (in red frame) and shear speed parameters (in green frame)

The change of mobilized shear resistance is measured by two shear load cells. Mobilized friction angle, effective friction angle and pore pressure generation in progress with shear displacement are also monitored. The shear resistance mobilized during shearing is obtained by subtracting the rubber-edge friction from the monitored shear resistance. The rubber-edge friction value is not constant, which depends on contact force, normal stress and shear velocity. However, for practical purposes, rubber-edge friction can be regarded as constant throughout the test and it can be calculated as the mean value from rubber edge friction tests under different normal stresses. The smaller rubber-edge friction is preferable. Therefore, in each test, a minimum gap pressure at which water leakage proof is checked and used carefully.

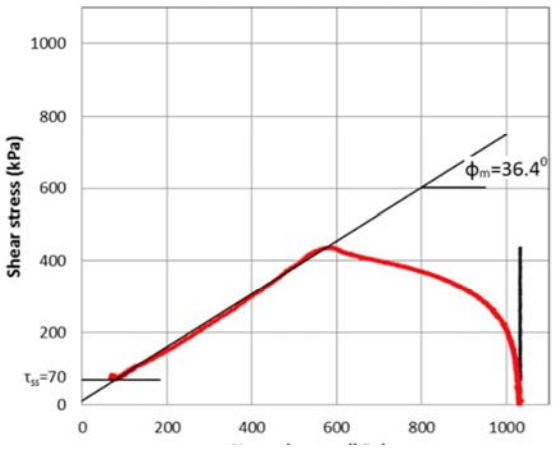

Fig. 18 Undrained shear stress control test result

4.9 Reinstallation and cleaning of ring shear apparatus

Before starting reinstallation of ring shear tests, it is necessary to release stress and pressure, either manually or by computer. In case of releasing by computer, it is better to release up to 100 kPa of normal stress and then unload manually or using lower slope until 0 in order to avoid decreasing normal stress to 0. This makes to avoid the piston of normal stress cylinder to be sucked.

After shear stress and normal stress is back to zero, stress control must be switched off and valve 2 should be open. Later on, reinstallation and cleaning of ring shear apparatus are made in the order of putting helping screws (Fig. 20), uplifting loading plate, disconnecting VDS, PPT-1 and PPT-2, disconnecting VLC and locking fixer along the pillars, taking out of the sample, and cleaning the shear box and apparatus. Finally, the lower part of shear box is turned to the initial position as marked by arrows. The detail is described as follows:

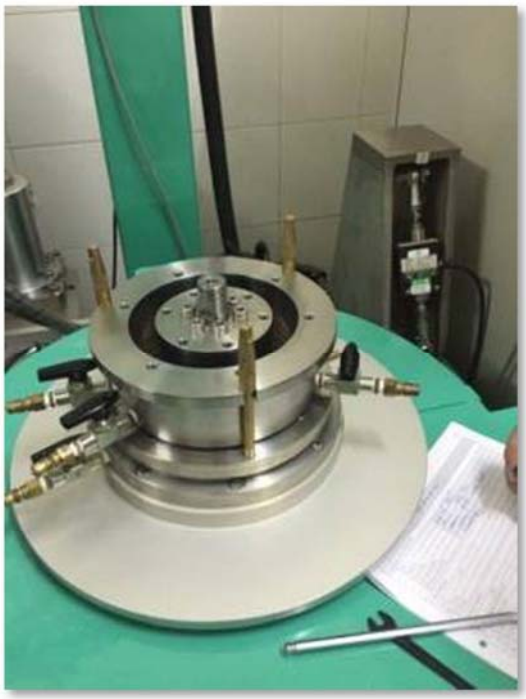

Fig. 20 Helping Screws (yellow screws)

- Disconnection of monitoring equipments: including Shear Load Cells (Fig. 21), Vertical Displacement Sensor from the Vertical Load Cyllinder, and reinstalling VLC (Fig. 22), the piston is returned to initial position, then lock protection screw.

Fig. 21 Shear Load Cells

Fig. 22 Disconnection of VLC and central axis

- Removal of Loading Plate: Firstly, fix the shear box with 3 helping screws, then unscrew 12 connected screws between Loading Plate and shear boxes, finally remove Loading Plate from shear box and put Loading Plate back the neutral position (Fig. 23). When pulling Loading Plate, drain valve should be opened to let airs enter or get out of shear box. This work enables to release pressure within SB for smoothly reinstalling Loading Plate.

Fig. 23 Reinstalling Loading Plate (the plate in dark blue color)

- Removal of outer shear box: Firstly, remove the water from the Shear Box by opening lower drain or by vacuum cleaner, then take out outer shear box for removing the sample easily.

- Removal of the sample: If some parts of the sample are going to be used for other tests, make sure to remove the shear zone. Otherwise, all samples will be disposed. In case of determining saturated unit weight, dry weight and the water content of the sample, after doing the test, all sample including filter paper and tissues should be weight. The sample and sliding surface after testing is presented in Fig. 24.

Fig. 24 Shear zone is presented by a black arrow

- Removal of inner shear box and Gap adjustment: When sample is removed, finish reinstalling by removing the Inner ring (unsrew 6 screws) and then decreasing the gap value by gap control button to 0. Later on, stop the gap and lock the control button at the neutral position.

- Cleaning of the apparatus: After all parts are reinstalled, cleaning of ICL-2 requires to use water, acetone, vacuum cleaner and brush. Firstly, rubber edge needs to be carefully cleaned with acetone in order to remove all layers of Teflon spray and grease used in test. Next, clean shear boxes with grease by using Acetone. After all, shear box is cleaned, the most sensitive parts are left in water (upper- outer part of SB and Loading Plate).

Noted that, it is necessary to carefully clean the RSA in order to prevent damage. This is especially important for the upper-outer part of SB and its gutter that can be blocked with fine grained material used in tests. Since the gutter is very sensitive and the most important part for pore pressure measurement, special attention should be given to cleaning and maintaining of that part. This also refers to parts with metal filters, namely Loading Plate and the base of Shear box.

5 Testing results

5.1 Processing test results

After completing, the experiment data recorded over time parameters is saved in the file format "file.Dat" (Fig. 25).

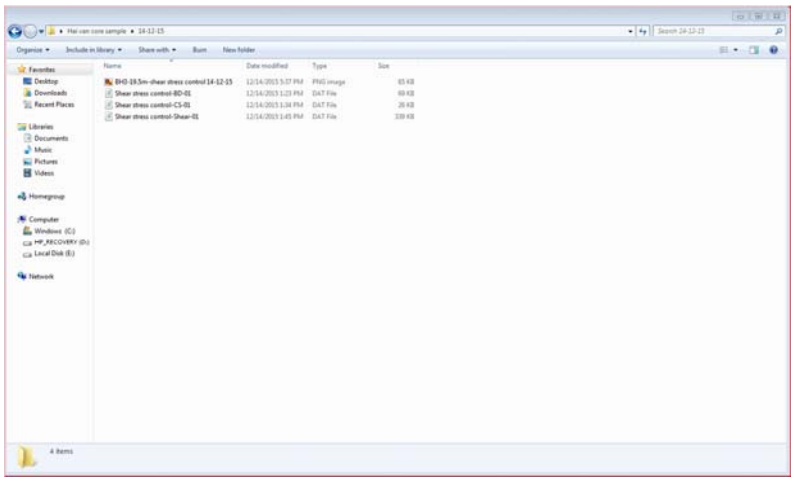

Fig. 25 Files of testing results

Using Excel program to open files of testing result. Finding and Deleting two column ”Oil pressure – id” and “Oil pressure – uld”.

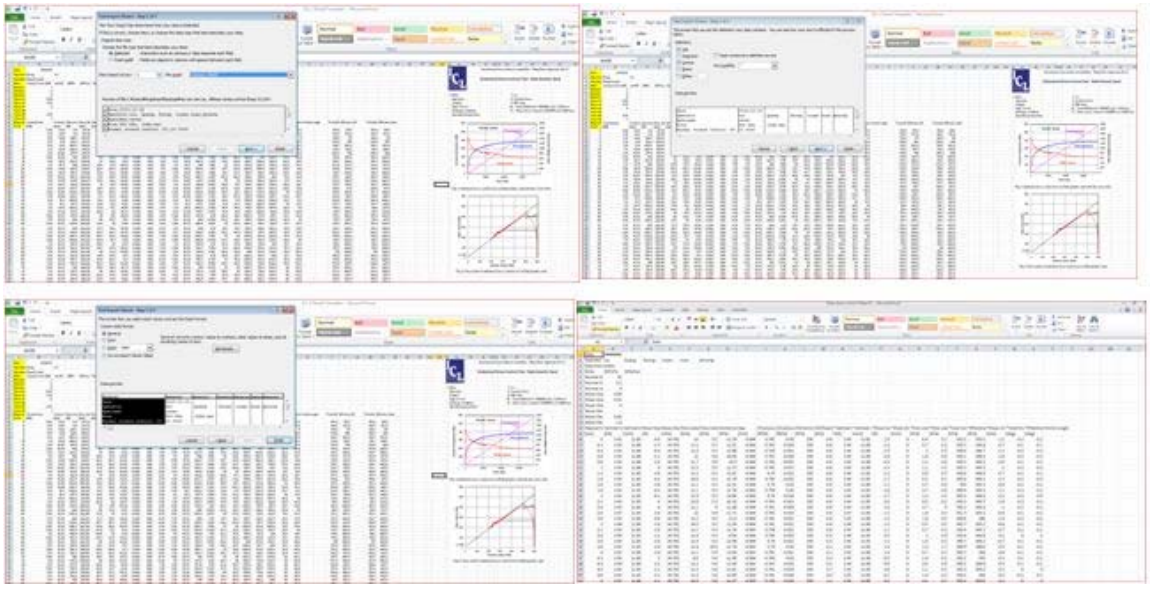

Fig. 26 Opening the testing result

Copy the data in columns from ”Elapsed time” to the ”Effective friction angle” in the file test results to colums respectively in file ”Test result” for making the charts.

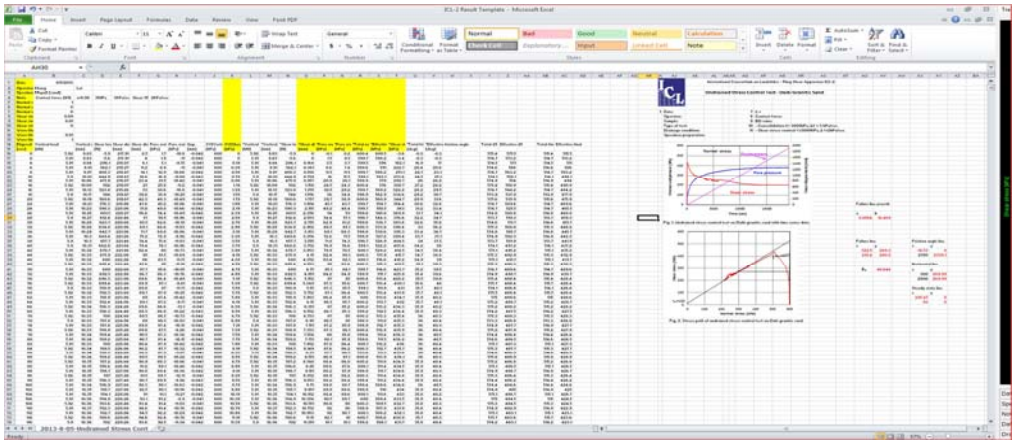

Fig. 27 The Chart of test results

The types of chart of the undrained shear stress control test as below:

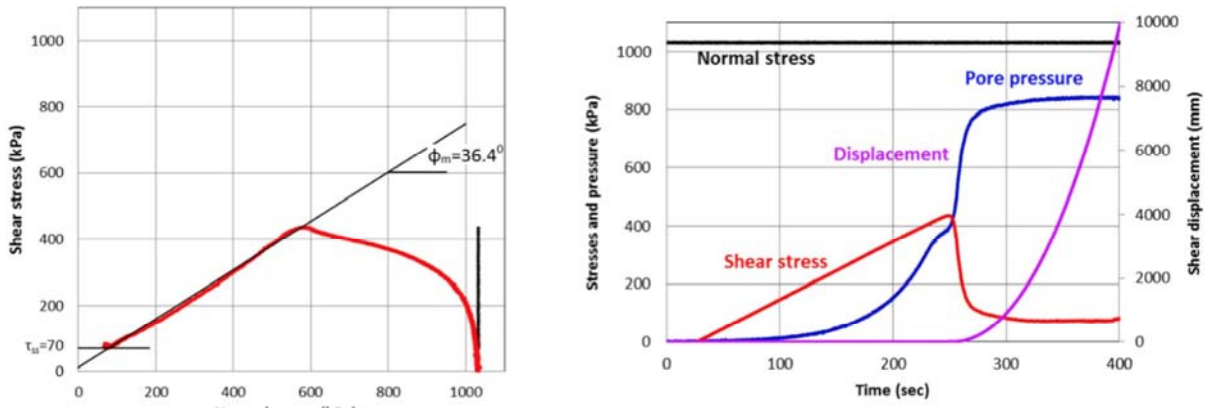

Fig. 28 Stress paths (left side) and time series data (right side) of the Undrained shear stress control test

5.2 Result of Undrained shear stress control test on Haivan drilling core sample depth 20m.

After consolidation of the sample (by applying normal stress of 350 kPa), the shear box was changed to the undrained condition, and shear stress was loaded gradually at a rate of $\Delta\tau$=1 kPa/sec. Samples were sheared until steady state obtained. In undrained conditions, the pore water pressure will increase during testing and the effective stress path closed to failure line. When the effective stress path reached the failure line, it began to decrease due to pore-pressure generation along the failure line until the steady-state shear resistance reached. In the Fig. 29, the red line was an effective stress path; the black line was the total stress path. From the graph, we can determine the value of the friction angle is 41.6° and the steady-state shear resistance were 55 kPa.

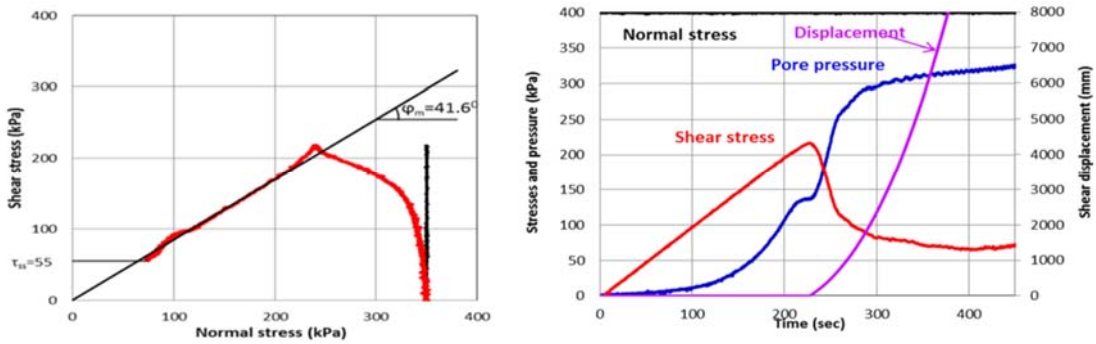

Fig. 29 Result of Undrained shear stress control test on Haivan drilling core sample depth 20m

GL 12: 2016

First Edition

Testing Method of Pore-Pressure Control Test

HA NOI – 2016

Abstract

A new high stress undrained ring shear apparatus ICL-2, which has been newly developed as a part of the SATREPS and ICL/JST project in Vietnam, has applied to study the initiation and motion mechanism of large-scale and deep-seated landslides in Vietnam in May 2015. This apparatus is suited for undrained shear tests under various types of loading such as rainfalls and earthquakes. Specifically, the device enables observing the undrained shear behaviors of soil samples at unlimited shear displacement and under undrained high stress condition. The undrained capability is up to 3.0 MPa of normal stress and pore-pressure that correspond to 100-200 m deep landslides. The ICL-2 shears the sample under a high-speed motion at a maximum shear speed of 50 cm/s to an unlimited shear displacement. Pore-pressure control test is used to determine the largest value of pore-pressure that induces landslides. In addition, this kind of test is also to determine the technical parameters such as friction angle of the peak failure line φ_p, friction angle during motion φ_m and steady state shear resistance τ_{ss}. This guideline covers a procedure for performing pore-pressure control test by using the new high-stress ring-shear apparatus (ICL-2).

.

Table of contents

Testing method of pore-pressure control test

1. Scope

This guideline covers a procedure for pore-pressure control test using the new high-stress ring-shear apparatus (ICL-2).

Pore-pressure control test is conducted to determine the largest value of pore water pressure that induces landslides. In addition, this kind of test is also to determine the technical parameters such as friction angle of the peak failure line φ_p, friction angle during motion φ_m and steady state shear resistance τ_{ss}.

2. Reference documents

MARUI & CO., LTD, Operation Manual For Undrained Ring-Shear Apparatus Data Acquisition & Control Software.

MARUI & CO., LTD, OPERATION MANUAL (Main Unit) For Undrained Ring Shear Apparatus

Kyoji Sassa, Bin He, Mauri McSaveney, Osamu Nagai, ICL Landslide Teaching Tools.

3. Apparatus

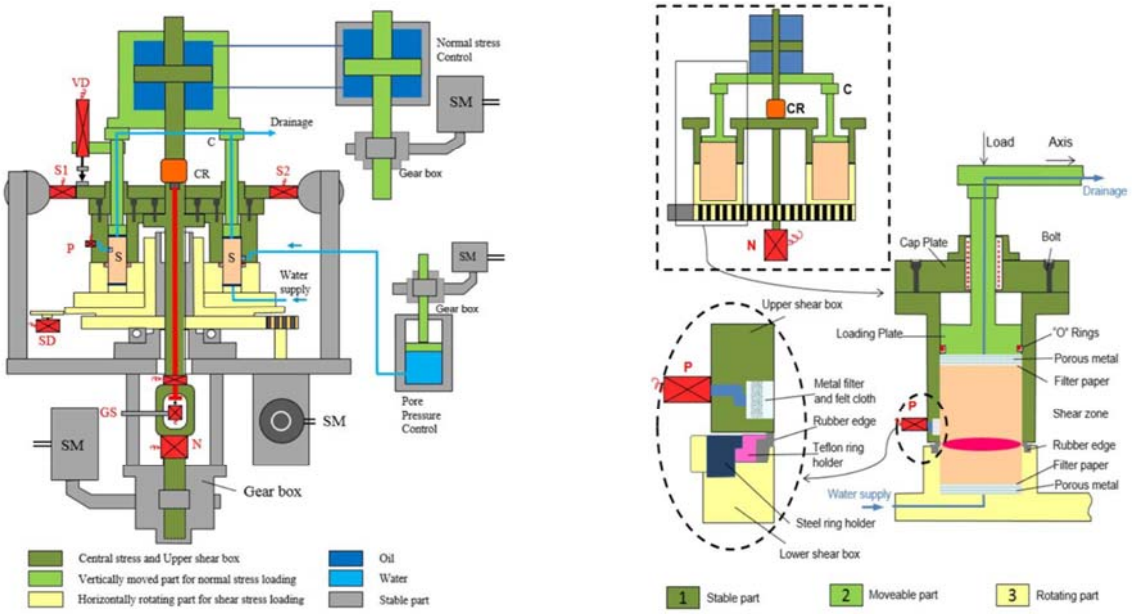

Fig. 1 The new high-stress dynamic-loading ring- shear apparatus (ICL-2)

Ring shear apparatus is designed to quantitatively simulate the entire process of failure of a soil sample, from initial static or dynamic loading through shear failure, pore-pressure changes and

possible liquefaction, to large-displacement, steady state shear movement. A series of ring shear apparatus (DPRI-3,4,5,6,7, ICL-1 and ICL-2) was developed by Sassa and his colleagues since 1984, in which, the ICL-2 has a high capability to reproduce large-scale and deep-seated landslides. The introduction and description of the ICL-2 (Fig. 1) is refered to Guideline 9 for High Stress Un-drained Ring Shear Apparatus (RSA) Introduction.

4. Testing program

This part describes the testing procedure for undrained pore pressure control test using the ring shear apparatus, ICL-2 in detail. Bassically, the testing procedure is followed by steps as mentioned in Guideline 9 for High Stress Un-drained Ring Shear Apparatus (RSA) Introduction.

4.1 Apparatus Preparation

Teflon is sprayed separately with three times to protect the rubber edges, in which, the time of each Teflon spray is about 10 minutes to dry Teflon coats (Fig. 2).

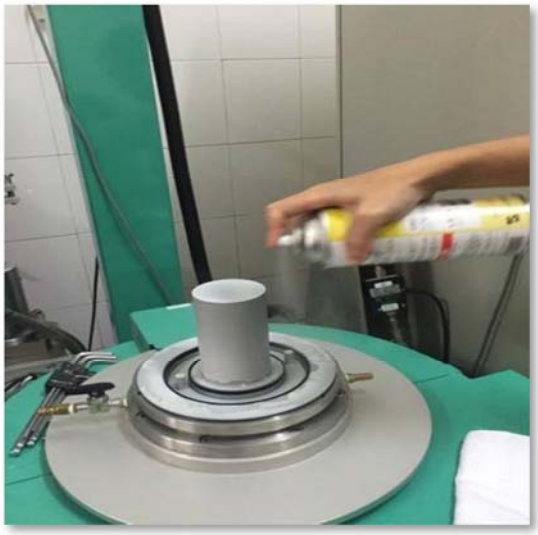

Fig. 2 Teflon Spay

Silicon grease is coated on the inner and outer rings of upper shear box in order to reduce the friction and to prevent water leakage during shearing (Fig. 3).

Fig. 3 The inner and outer rings are covered in grease

4.2 Sample Preparation

Soil specimens required for ring shear tests have particle sizes smaller than 2 mm in diameter and to be fully saturated before building in shear box. The following procedure is carried out for sample preparation (Fig. 4).

• Firstly, after sieving the in-situ taken sample by the sieve of 2.0 mm in diameter, the sample are slowly poured into a plastic container with de-aired water (about 300 ml to 400 ml of deaired water and 500 grams of soil sample). Then this container with sample and de-aired water is put in the vacuum tank and leave them over night.

• Next day, the specimen is saturated by using a vibrator in combination with a vacuum pump. In order to finish this step, leave the sample in the vacuum tank without further vibrations during night. Depending on types of sample, it will take several hours to make air bubbles inside soil particles come out. Even it may take some days to saturate samples that have a very low permeability like clays and silts.

• After the sample is fully saturated on which no any air pubbles is osbserved, the sample is ready for test. Release the vacuum tank slowly by opening the upper valve, then take the saturated sample out of the water tank.

Fig. 4 Vacuum tank

4.3 Gap Adjustment

First, a defined gap value, which corresponds to a vertical force (contact force), must be given to avoid leakage of water and sample through a servo control motor. The defined gap value is determined in advance by an adjustment of gap value in order to prevent water leakage as presented in the Guideline 9. Gap value is kept constant during the test.

Main steps for gap adjustment are presented as follows:

Fig. 5 Switch on GAP control

- Firstly, run Ring Shear Simulator Software on PC and switch on Gap control (Fig. 5).

- Secondly, screw the inner ring and adjust vertical load to 0 by reset the value of normal stress (Fig. 6). Normaly, vertical load is always to be zero at the neutral position of Gap control button.

Fig. 6 Reset Gap value to zero

- Next, after putting the outer ring, Helping Ring is put and connected with the inner and outer rings by 6 screws and 3 Helping Screws (golden screws). At the beginning, 3 Helping Screws is to adjust position of shear box only, so it is required to leave them loose (Fig. 7).

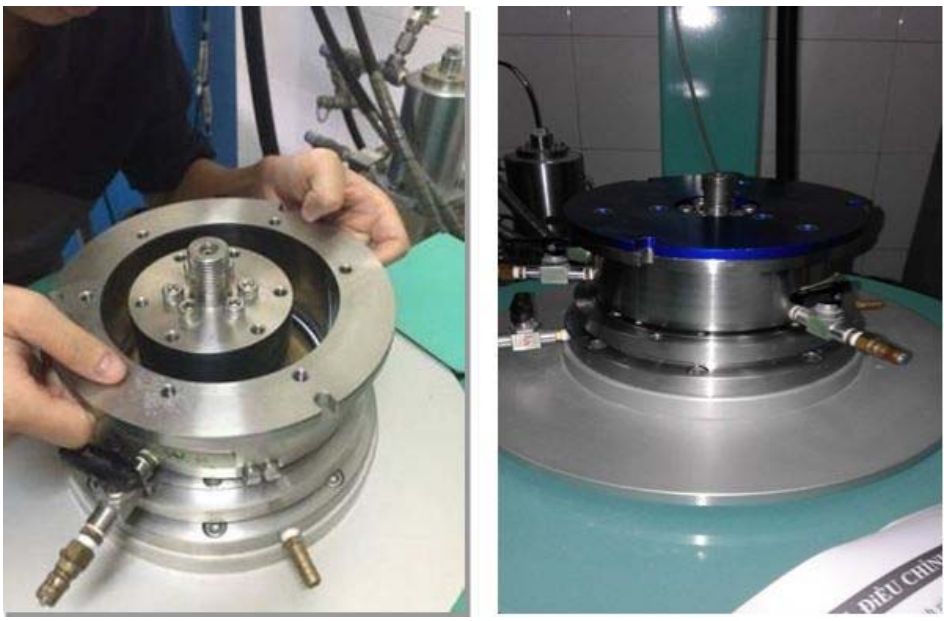

Fig. 7 Putting outer ring and helping ring

- Once contact force is increased to a designed pressure of Gap value, Helping Screws are screwed tightly and then remove the Helping Ring (Fig. 8).

Fig. 8 Increasing Contact pressure and removing the Helping Ring

- Finally, Loading Plate is installed with the help of all 9 screws (Fig. 9). In this step, it is not necessary to tighten 9 screws.

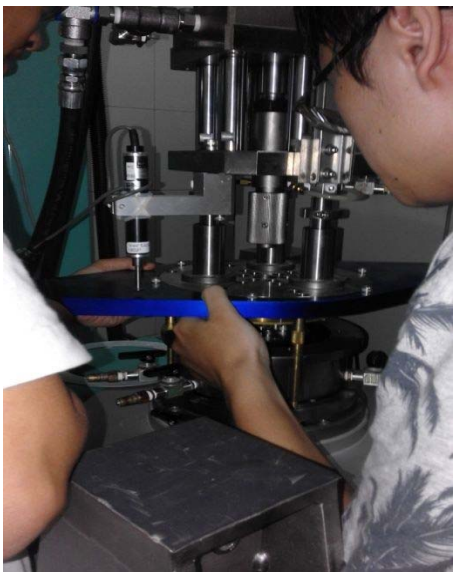

Fig. 9 Installing Loading Plate

4.4 CO_2 and H_2O (de-aired water) saturation

Shear box without sample is filled with CO_2 and de-aired water. Then, saturated sample that is prepared by de- aired could be slowly placed in shear box. After that, the water circulation could start to enable full water saturation of the sample. De-aired water is slowly supplied through the lower drainage line, and discharged from the upper drainage line until all air bubbles are expelled. Valves 2, 3, 4a and 4b are de-aired by CO_2, respectively (as shown in Fig. 10).

Fig. 10 Prodecure of CO2 and H2O Saturation

After de-airing water, PPT-1 and PPT-2 are installed to Valve 4a and Valve 4b, these valves are drained to exclude air bubbles from the inside (Fig. 11).

Fig. 11 A photograph of pore water pressure transducers PPT-1, PPT-2

4.5 Sample setting

After putting a filter paper, the sample could be slowly built in shear box (Fig. 12).

Fig. 12 Putting a filter paper and building the sample

After building the sample, loading plate is set up and fixed by 12 screws (Fig. 13). The contact of loading plate and the sample should be given by a small amount of vertical load ranging from 20 kPa to 30 kPa).

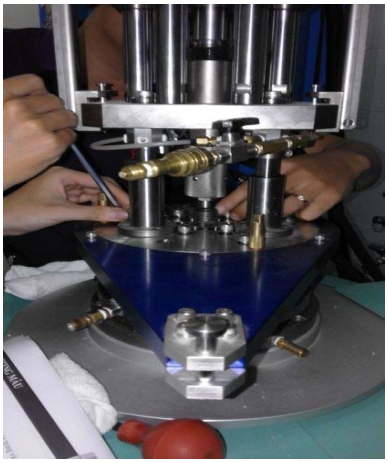

Fig. 13 Setting up loading plate

Fig. 14 Installing Shear Load Cells

Once two shear load cells are set up after installing shear box and loading plate (as presented in Fig. 14), 12 screws must be screwed tightly. Later on, the lifter of upper loading plate is returned back to neutral position and to be locked.

After screwing 12 screws on LP, Vertical Load Cylinder (VLC) is lowered to connect to the central axis of the apparatus (Fig. 15). In addition, one important thing needs to do is that the fixer which prevent the drop of the upper loading part by self-weight must be unlocked and removed from the pillars after sample setting. Fixers are only fixed until sample setting and those should be unlocked during loading. Otherwise, normal stress can not load and it may lead to some damages to the apparatus.

Fig. 15 Install VLC and unlocking the fixers

Next, Vertical Displacement Sensor (VDS) that measures the vertical displacement of the sample under consolidation loadings is connected to main control unit.

Finally, a water circulation by gravity can start to fully saturate shear box and the sample. In water circulation, de-aired water is supplied through the lower drainage line (valve 5), and discharged from the upper drainage line (valve 2) until all air bubbles are expelled (Fig. 16).

Fig. 16 De-aired water flow to Valve 5 and discharge at Valve 2

4.6 Saturation checking

To check the saturation degree of the sample, BD parameter (proposed by Sassa 1988) is used for ring-shear tests. The sample is firstly consolidated under normal stress of 30 kPa in drained condition to make contact between sample and porous metal of the loading plate. Then shear box is changed to the undrained condition. In this condition, the normal stress begins loading with an increment of 50 kPa in each step ($\Delta\sigma$=50 kPa while the increment of pore pressure generation is measured (Δu). The degree of saturation (BD) is calculated by the ratio of pore pressure increment and normal stress increment ($\Delta u/ \Delta\sigma$). Specimens with BD greater than

0.95 could be considered as a full saturation. In drained tests and pore water control tests, it is not necessary to check BD value.

4.7 Sample consolidation

Sample consolidation is carried out in order to reproduce the initial stress condition of the sample. The initial stress state of soils only due to gravity is created by loading normal stress and shear stress that depend on the depth of samples at the suspected sliding surface, slope angle and unit weight of the sample. After making input data form pannel for Data acquisition with appropriate parameters, data acquisition is switched on and stress loading can be apply while Valve 02 is opened. The rate of normal stress and shear stress increasing ranges from 1 kPa to 5 kPa per second for ICL-2 tests. When shear stress and normal stress reach to designed values and pore water pressure dissipates completely (values at u_1, u_2 is zero), valve 02 is closed to turn shear box to undrained condition. Fig. 17 illustrates the input data window for normal stress and shear stress of the ring shear tests.

Fig. 17 Photograph of input data window for sample consolidation

4.8 Pore water pressure control test

After the consolidation, values of shear displacement should be reseted back to zero and removing of helping screws and water pipe of valve 5 must be done to avoid any damages during shearing. Then, input data setting on the control screen is carried out with appropriate parameters for this specific test including a pre-defined value of pore water pressure, slope for pore pressure increasing and a defined value of shear displacement. Immediately, undrained pore water pressure control test can start by applying pore pressure control mode after starting the data acquisition, switching on “Start” button and selecting “Static” button in the control unit for pore water pressue. A screen-print of the ICL-2 Application Software for undrained pore pressure control test is shown in Fig. 18.

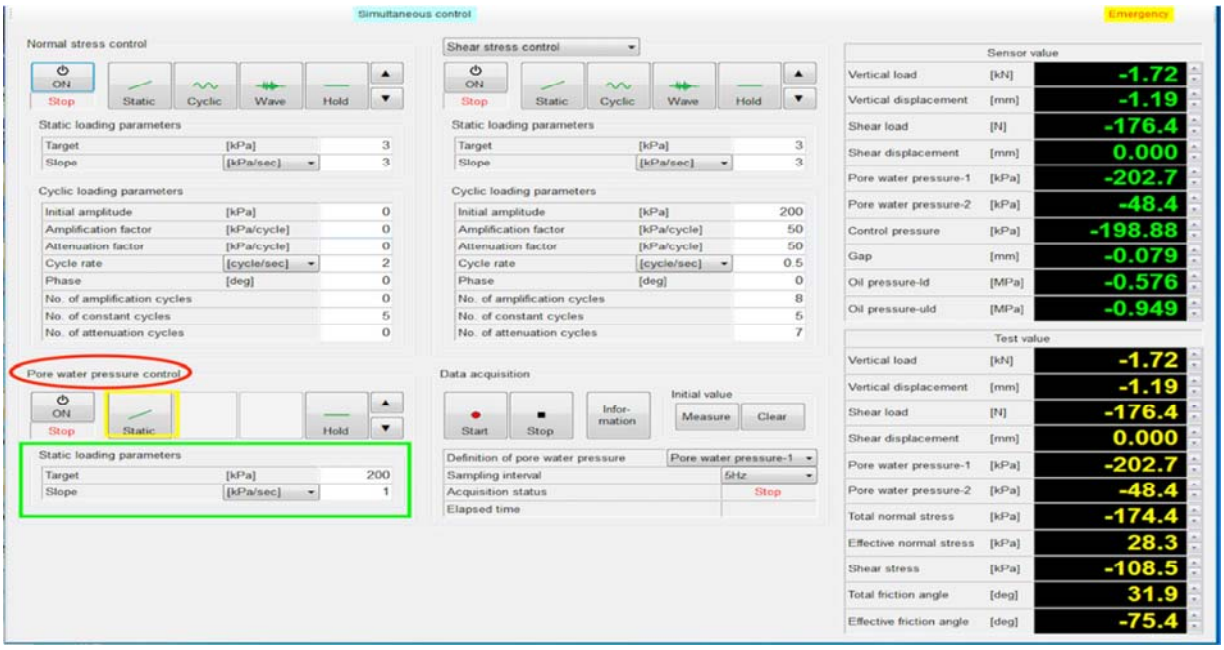

Fig. 18 Print screen of the ICL-2 application software showing Pore water pressure Control (in red frame) and Pore water pressure parameters (in blue frame)

Before testing, the shear box must be changed to the undrained condition and pore water pressure is then loaded gradually at a rate of Δ τ=1-5 kPa/sec. The sample is sheared until the steady state obtained at large displacement. In undrained conditions, due to an increasing of pore water pressure, the effective stress path shift to failure line. Consequently, a rainfall-induced landslide is reproduced under which excess pore water pressure continues to generate in progress with shear displacement. The effective stress path moves down along the failure line until a certain value of residual strength of the sample at steady state. In Fig. 19, the red line denotes an effective path and the black line illustrates the total stress path. From the graph, we can determine the value of the friction angle and the steady-state shear resistance.

The change of mobilized shear resistance is measured by two shear load cells. Mobilized friction angle, effective friction angle and pore pressure generation in progress with shear displacement are also monitored. The shear resistance mobilized during shearing is obtained by subtracting the rubber-edge friction from the monitored shear resistance. The rubber-edge friction value is not constant, which depends on contact force, normal stress and shear velocity. However, for practical purposes, rubber-edge friction can be regarded as constant throughout the test and it can be calculated as the mean value from rubber edge friction tests under different normal stresses. The smaller rubber-edge friction is preferable. Therefore, in each test, a minimum gap pressure at which water leakage proof is checked and used carefully.

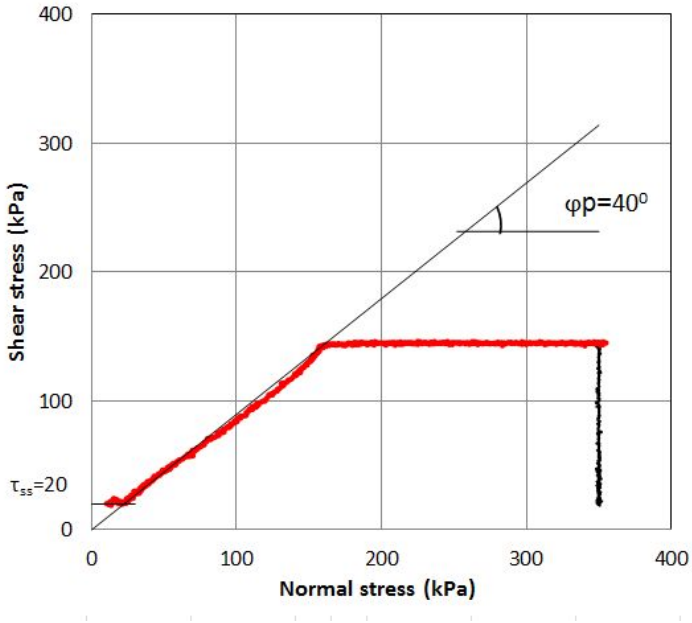

Fig. 19 Pore water pressure control test result

4.9 Reinstallation and cleaning of ring shear apparatus.

Before starting reinstallation of ring shear tests, it is necessary to release stress and pressure of normal stress, shear stress and pore pressure, either manually or by computer. In case of releasing by computer, it is better to release up to 100 kPa of normal stress and then unload manually or using lower slope until 0 in order to avoid decreasing normal stress to 0. This makes to avoid the piston of normal stress cylinder to be sucked.

After shear stress and normal stress is back to zero, stress control must be switched off and valve 2 should be open. Later on, reinstallation and clearning of ring shear apparatus are made in the order of putting helping screws (Fig. 20), uplifting loading plate, disconnecting VDS, PPT-1 and PPT-2, disconnecting VLC and locking fixer along the pillars, taking out of the sample, and cleaning the shear box and apparatus. Finally, the lower part of shear box is turned to the initial position as marked by arrows. The detail is described as follows:

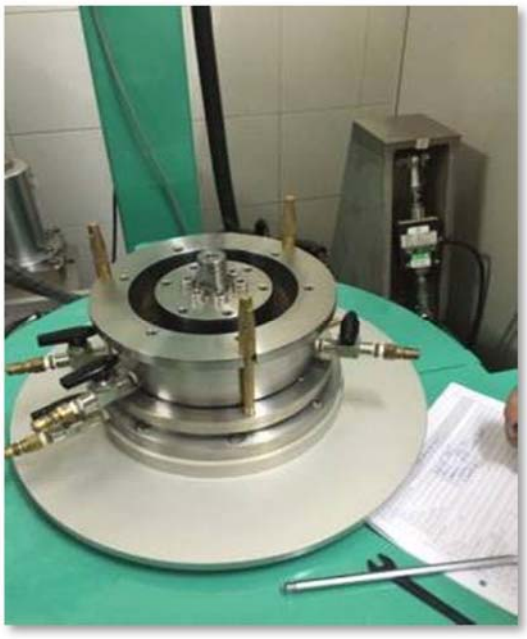

Fig. 20 Helping Screws (yellow screws)

Disconnection of monitoring equipments: including Shear Load Cells (Fig. 21), Vertical Displacement Sensor from the Vertical Load Cyllinder, and deinstall VLC (Fig. 22), the piston is returned to initial position, then lock protection screw.

Fig. 21 Shear Load Cells

Fig. 22 Disconnection of VLC and central axis

- Removal of Loading Plate: Firstly, fix the shear box with 3 helping screws, then unscrew 12 connected screws between Loading Plate and shear boxes, finally remove Loading Plate from shear box and put Loading Plate back the neutral position (Fig. 23). When pulling Loading Plate, drain valve should be opened to let airs enter or get out of shear box. This work enables to release pressure within SB for smoothly deinstalling Loading Plate.

Fig. 23 Reinstalling Loading Plate (the plate in dark blue color)

- Removal of outer shear box: Firstly, remove the water from the Shear Box by opening lower drain or by vacuum cleaner, then take out outer shear box for removing the sample easily.

- Removal of the sample: If some parts of the sample are going to be used for other tests, make sure to remove the shear zone. Otherwise, all samples will be disposed. In case of determining saturated unit weight, dry weight and the water content of the sample, after doing the test, all sample including filter paper and tissues should be weight. The sample and sliding surface after testing is presented in Fig. 24.

Fig. 24 Shear zone is presented by a black arrow

- Removal of inner shear box and Gap adjustment: When sample is removed, finish deinstalation by removing the Inner ring (unsrew 6 screws) and then decreasing the gap value by gap control button to 0. Later on, stop the gap and lock the control button at the neutral position.

- Cleaning of the apparatus: After all parts are reinstalled, cleaning of ICL-2 requires to use water, acetone, vacuum cleaner and brush. Firstly, rubber edge needs to be carefuly cleaned with acetone in order to remove all layers of Teflon spray and grease used in test. Next, clean shear boxes with grease by using Acetone. After all, shear box is cleaned, the most sensitive parts are left in water (upper- outer part of SB and Loading Plate).

Noted that, it is necessary to carefully clean the RSA in order to prevent damage. This is especially important for the upper-outer part of SB and its gutter that can be blocked with fine grained material used in tests. Since the gutter is very sensitive and the most important part for pore pressure measurement, special attention should be given to cleaning and maintaining of that part. This also refers to parts with metal filters, namely Loading Plate and the base of Shear box.

5 Testing results

5.1 Processing test results

After completing, the experiment data recorded over time parameters is saved in the file format "file.Dat" (Fig. 25).

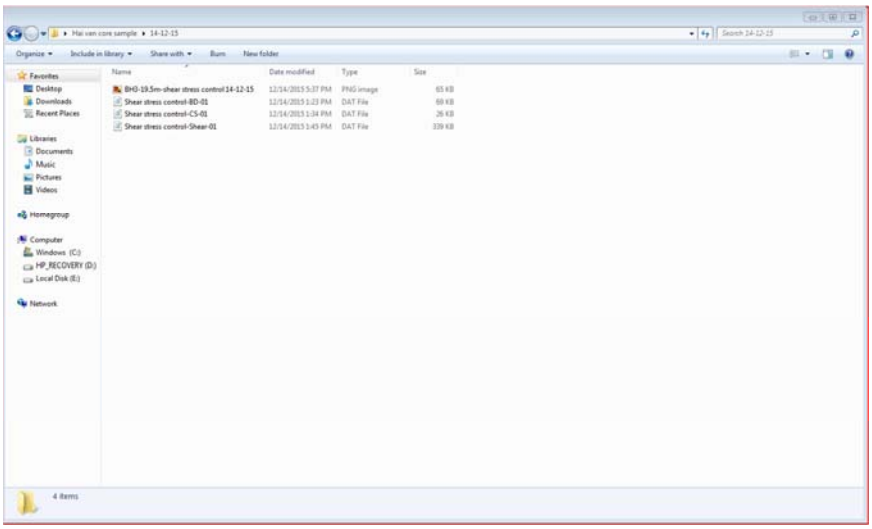

Fig. 25 Files of testing results

Using Excel program to open files of testing result. Finding and Deleting two column ”Oil pressure – id” và “Oil pressure – uld”.

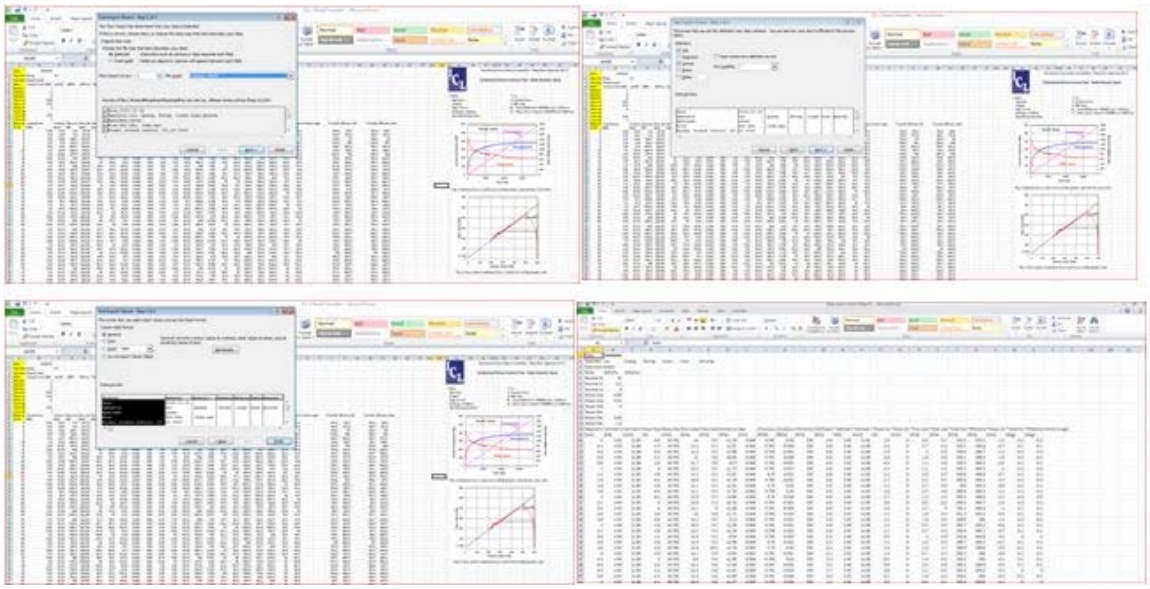

Fig. 26 Opening the testing result

Copy the data in columns from ”Elapsed time” to the ”Effective friction angle” in the file test results to colums respectively in file ”Test result” for making the charts.

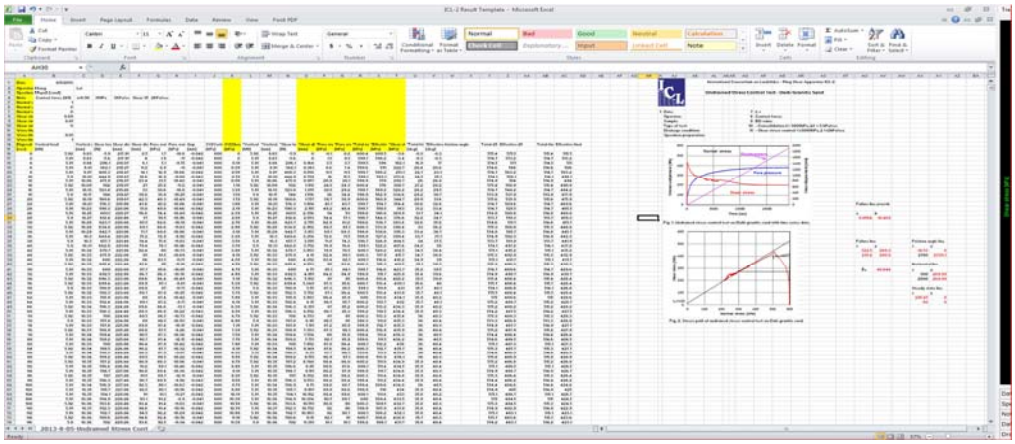

Fig. 27 The Chart of test results

The types of charts of the Pore water pressure control test:

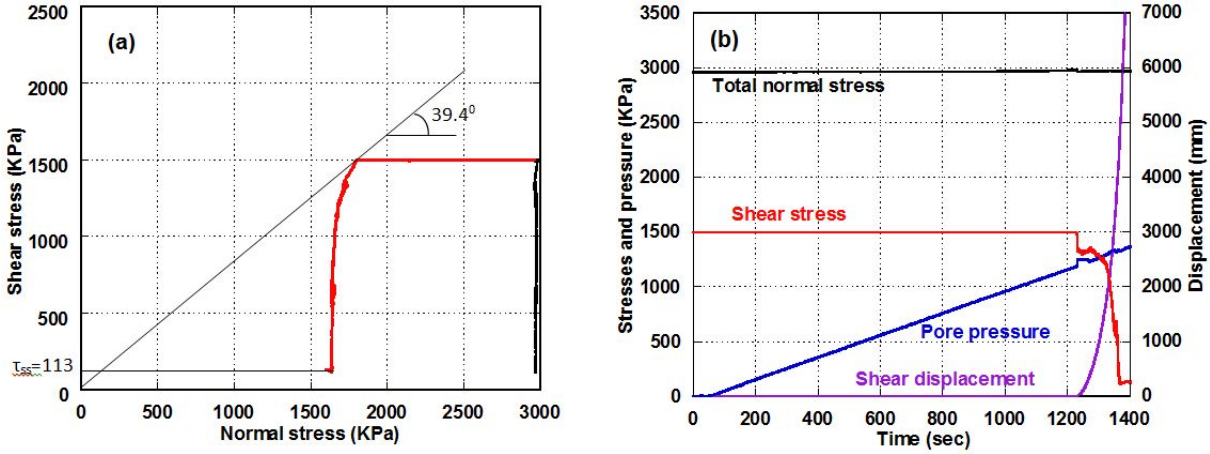

Fig. 28 Stress paths (left side) and time series data (right side) of the Pore water pressure control test

5.2 Result of Pore water pressure control test on Haivan drilling core sample depth 20m.

First, the saturated sample (BD = 0.99) was consolidated close to 350 kPa of normal stress and 145 kPa of shear stress in undrained condition. The initial shear stress state corresponds to the slope of tangent = 20.4°. This is approximate the actual slope of landslide blocks (about 20-25°). To simulate the effects of pore water pressure caused landslide, the pore water pressure was increased to a designed value at speed 1kPa/sec. Test result presented that the failure occurred at the pore water pressure about 195 kPa and friction angle of the sample was 40° as shown in Fig. 29.

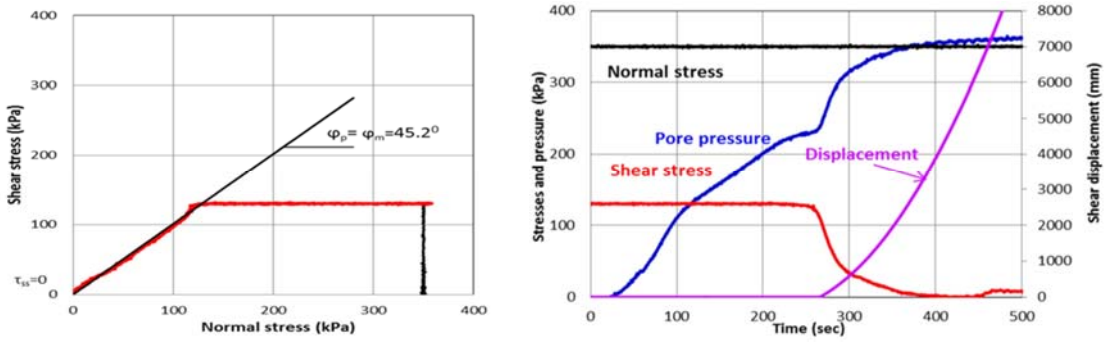

Fig. 29 Result of Pore water pressure control test on Haivan drilling core sample depth 20m.

ITST-ICL

GUIDELINE FOR LANDSLIDE RISK ASSESSMENT

GL 17: 2016

First edition

Landslide Monitoring Systems

HA NOI – 2016

Abstract

Landslide monitoring system is important for clarification of landslide mechanism and early warning for landslide prevention. The monitoring system has various types and should be adapted to the purpose and environmental conditions. When it is planned, the landslide characteristics should be imaged by previous investigation. The items of monitoring system such as the kinds of sensors, setting location, data collection, maintenance, data analysis and the way of handling of these data should be decided according to the purpose.

Table of Contents

Landslide Monitoring Systems

1. Scope

This guideline explains the purpose, design method and notes for the landslide monitoring system for early warning. The monitoring system is applied to the specific landslide which is clarified the activity and is caused a final slope failure after accumulative displacement for a long time. There are other landslide disasters which the activity was not clarified in past, and was difficult to estimate the active area and mechanism and suddenly occurred without precursory phenomena under heavy rain. It is necessary to examine other observation methods.

2. Reference documents

Kyoji Sassa, Bin He, Mauri McSveney, Osamu Nagai (2012), ICL Landslide Teaching Tools

Tsuchiya et al. (2012), Landslides in Japan (The Seventh Revision), Japan Landslide Society

Shiho Asano, Shinro Abe, Osamu Nagai (2014), Development of landslide monitoring and data transfer system in the Hai van station landslide and the initial extensometer monitoring result behind the station, Proceeding of the SATREPS Workshop on Landslides in Vietnam

Shiho Asano, Do Ngoc Ha, Huynh Dang Vinh (2016), Landslide monitoring and web observation system in Hai van st. landslide, 2016 Vietnam-Japan SATREPS report meeting.

Shiho Asano, Hirotaka Ochiai, Huynh Dang Vinh (2015), Landslide monitoring and early warning of landslides and its application to Vietnam, Landslide technical forum.

3. Purpose and outline of planing of landslide monitoring systems

The goal of landslide monitoring system is the identification of the cause(s) of an unstable slope or the scientific investigation of an earlier landslide. This goal can be difficult and sometimes impossible to accomplish, because of the time involved and sheer scale of the dimensions of a landslide.

There are two kinds of purpose of landslide monitoring. One is to clarify the landslide mechanism and other is to keep watch for warning of disaster. Clarifying the mechanism isn't only important for countermeasure, but also for warning of disaster. The warning of disaster by the monitoring data without understanding mechanism is baseless.

When the monitoring method is planned, it is necessary to examine the selection of monitoring items and equipment, accuracy and arrangement of equipment, method of measurement and method of management and maintenance of system according to the purpose of monitoring.

Deciding the way of analysis and evaluation of data is necessary for the monitoring. And it is essential to decide the standard value of monitoring item and the procedure for warning of disaster when monitoring data exceed to the standard value beforehand.

4. Previous investigation

When the landslide monitoring system is planned, it is necessary to examine the actual condition of targeted landslide, purpose and method of monitoring and handling of the result beforehand.

For understanding the actual landslide condition, Three dimensional figure and direction movement of landslide should be estimated by field survey and geographical analysis beforehand. Monitoring data complements the estimated landslide conditions.

5. Planning of monitoring system

5.1 Monitoring method type

The monitoring method is different according to the purpose. The observation data is collected by manual monitoring or semi-automatical monitoring when the countermeasure is planned and evaluated, Low cost payment and a level of emergency is lower in small-scale landslide. When a level of emargency and the importance is high and real-time observation is needed, the automatical monitoring system is sometimes selected.

The manual monitoring is the observation method that engineers or scientists go to site and measure by handy equipment. It is advantageous that the measurement can be started earlier and the landslide and measurement condition can be visually checked. However, it is recommended to be not used many times except emergency situation such as just after disasters, because it takes long interval time and it is difficult to catch the peak value.

Semi-automatical monitoring is a method that the equipment with data logger measures the landslide condition automatically and human collect the data from data logger by hand. The data is analysed in the office. It can start to monitor in a short time because it doesn't need data transfering system. And it can measure the peak value. Because the situation of the measurement can be checked when data is collected, it helps to decrease the error data.. However, real-time monitoring under emergency condition is difficult.

The automatic monitoring is the method that all data are automatically measured and transfered to database in a remote office. All data in database are automatically analysed and observed real-time under the emargency situation. Recently, the surveillance camera is popular to be used with the monitoring. It is necessary to construct the stable measurement and communication conditions to observe automatically. Especially, a stable power supply and comunication line is required. Therefore, the construction of system needs enough time and cost and the maintenance is important. When the

system is operated well, attention for monitoring will not cost so much. However, system should be sometimes checked and maintained to keep the quality of data.

Monitoring method should be planned according to the consideration of the purpose, the importance, the time for preparation and cost of construction and maintenance of system.

5.2 Selection of monitoring sensors

Variety of monitoring items can be divided roughly into slope surface displacement, underground soil mass displacement and hydrological environment. If there are some constructions in the area, the behavior of them should be monitored also. And other items should be measured also if they may affect to the landslide.

The monitoring items include some physical component. For example, surface displacement has the lateral movement and surface inclination, Monitoring sensor is selected for measurement of physical component. The sensor of each monitoring items should be selected according to targeted physical compornent. The detail of sensors which are often used for automatical monitoring in landslide is explained from GL18 to GL25,

5.3 Arrangement plan of sensor location

When monitoring system is planned, it is considered with the characteristics of landslide based on previous investigations. The arrangement plan of sensors should be suitable for the landslide characteristics.

The main observation line is arranged in the center of area along the direction of landslide displacement in general. The landslide moving direction is paralell in the maxmum inclination direction of slope in many times. But the previous investigation is important because some landslides moved to other directions of maxmum inclination. The landslide observation is planned based on these lines. The sensors are evenly arranged along these lines. In the boundary area like head and toe of landslide, the sensors are often arranged by high density.

There are some landslides that the direction movement winds during the slope. In this case, the observation line is often winded along accordingly.

It is necessary to decide the installation depth of the sensor that is installed under ground. The installation depth is considered with the geological structure and groundwater aquiferred by the geological survey and boring survey. Boring survey is important because of decision of slip surface of landslide. Since the landslide slope is usually received the disturbance, the boring survey should be carefully made to ensure the accuracy.

In a large-scale landslide, the direction of the displacement is often complex. In these cases, some observation lines are set at cross direction of main line and observation points are arranged at intersection of lines.

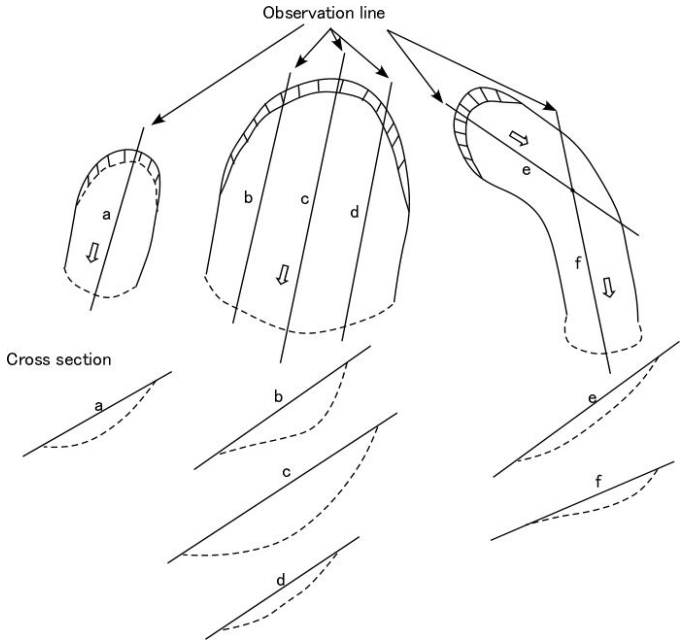

Fig.1 Schematic map of observation line

5.4 Data tranfering method

In the automatic monitoring, the system that the output signal of sensor is set to the office automatically is necessary. There are two ways of transmitting data including using signal cable and using wireless signal. The way of using cable is able to send the signal under communication stability in stead of the setting and maintaining the long cable. It can supply the electroric power to sensors using cable. The way of using wireless is able to start in short time because the long cable isn't necessary to set on the ground. On the other hand, the power supply component is necessary in each sensors because it needs a lot of power consumption and it is sometimes affected by environmental noise. It is suggested to note the wireless useage because the regulation is different among countries.

5.5 Maintenance of monitoring equipment

The sensor transmits from physical value to electroric signal and is recorded in the memory. They are weak to electroric troubles like water and lightning in general. Those kinds of trouble cause a big problem of monitoring especially auto and semi-auto monitorings. A variety of accident is occurred during monitoring; deteriorated equipment by rain, strong wind and sun ray and breakdown by animals and flying objects. Therefore, regular maintenance is indispensable to keep the monitoiring system. In case of automatic monitoring, the person doesn't often check it in the field if the problem isn't recognized. In that case, the problem may be occured that decrease of data accuracy and lack of data. If the monitoring system has troubles when the landslide disaster is occurred, it isn't possible to achieve its duty.

5.6 Handling of monitoring data

It is necessary to clarify the landslide mechanism using the monitoring data. When sensors are arranged a lot of points in a landslide, the landslide mechanism should be considered using the trend of

changing of all sensors but not only one sensor. The data should be observed based on the mechanism in the monitoring for warning.

When the signal of landslide activity is appeared, the disaster should be estimated by the actual data. In that case, the data should be shared with the related organizations. It is necessary to decide the corresponding methods of each risk level of landslide disaster for preparation in related organizations. The monitoring system only provides the data for concluding the risk levels. Because the data contain various errors and noises, scientists have to conclude the risk levels with considering the meaning of each data.

6. A case study of landslide monitoring system at Hai van station landslide

6.1 Introduction of Hai Van station landslide

This study was conducted in Hai Van station landslide area. This area located near Danang city in the central part of Vietnam. Because the national railway of Hai Van station is one of the most important lifelines, the safety management of landslide disaster is required.

Fig.2 Landslide slope in Hai van Station (Asano et.al.2016)

6.2 Previous investigation

There are some signals of slope deformation and small landslides. Small landslides were occurred near railway. The previous investigation was conducted on this slope before installation of system. There was a landslide topography larger than previous small landslides. Some steps on the ground and deformation of gabion slope and small concrete channel were found. As a result, this slope seemed to be gradually deformed but active area wasn't clearly shown.

Boring investigation was conducted on the middle part of area. Strong weathered sandy granite were layed on granite layer in this slope. The thickness of sandy layer was about 50m and there wasn't remarkable disturbance.

6.3 Monitoring plan

(1) Survey lines

Recent active area of the landslide wasn't clearly shown. The main surveying line was set the middle part of landslide topology along longitudinal direction. The monitoring on main line was focused on the clarification of mechanism of landslide. And sub surveying line was set near railway. it was focused on the warning of railway. And many monitoring points were set around main line. They were used to identify the active areas.

Fig. 3. Map of landslide monitoring system in Hai Van landslide

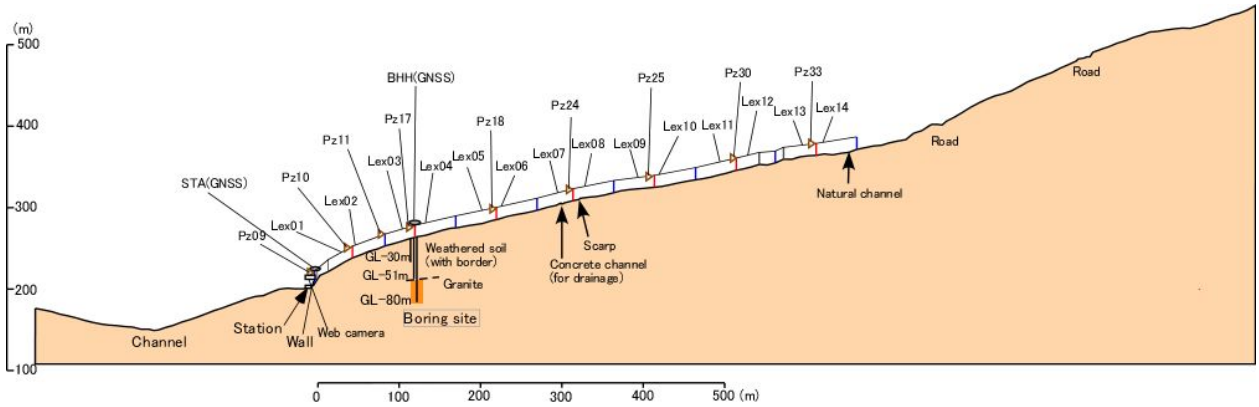

Fig. 4. The main surveying line was set in the middle part of landslide topology along longitudinal direction

:

(2) Monitoring equipments

The monitoring items should be selected based on the phenomena and inducement of the landslide. In this area, heavy rain may incude the slope displacement. The monitoring items were rainfall , groundwater and displacement of ground in this case. Displacement is important for warning. But the magnitude of displacement wasn't clear so the mesurement equipment of displacement was necessary to be high acurate.

Monitoring	Apparatus	Number	Reference Guideline
Deformation of ground surface	Total station and prisms	40	GL 18
Deformation of ground surface	GNSS	3	GL 19
Deformation of ground surface	Long span Extensometer (Lex)	14	GL 20
Deformation of ground surface	Short span Extensometer (Sex)	5	GL 20
Deformation of underground of landslide soil mass	Inclinometer	1	GL 21
Deformation of underground of landslide soil mass	Vertical Extensometer (Vex)	2	GL 22
Weather	Rain Gauge, Temprate, Wind speed, Air pressure sensors	1	GL 23
Underground water	Underground water level sensor	2	GL 24

Table 1: Number of landslide monitoring apparatus apply in Hai Van landslide system

(3) Data transferring and observating system

The landslide was located in important area for tranportation system in Vietnam. In this case, automatic monitoring system was selected. Small hut (BHH) was constructed on the boring site in landslide slope and signal cables from all sensors were connected to it. Another small monitoring station (TSH) was constructed on the stable slope on opposite from landslide slope and all data in BHH were transmitted by WIFI to TSH. The control PC that was installed control softwares of each equipment in TSH collected all data and all data were transmitted to the database PC in the office in Hanoi using virtual private network(VPN) on mobile phone.

Fig. 5. Monitoring hut (BHH) in landslide slope and momitoring station (TSH) in opposite stable slope (Asano et.al 2016)

All data of database at office were analysed and displayed on Web site. The information about time changing of data, the prediction of landslide occurrence based on displacement and status of transmitting condition were able to shered wite related organization.

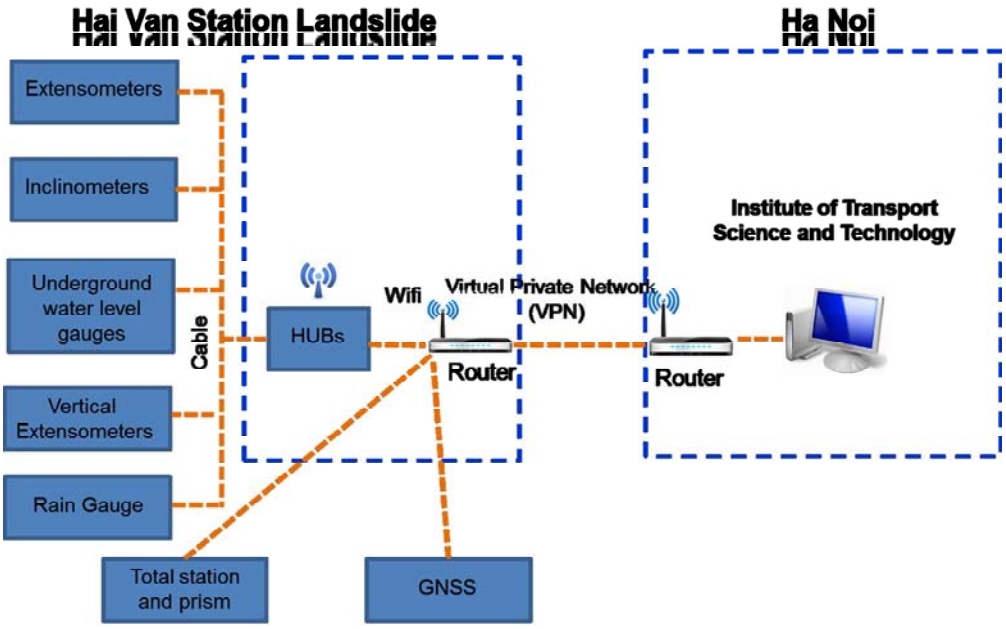

Fig. 6. Schematic map of monitoring system in Hai Van Station landslide and transfer data system from Hai Van Station to Ha Noi

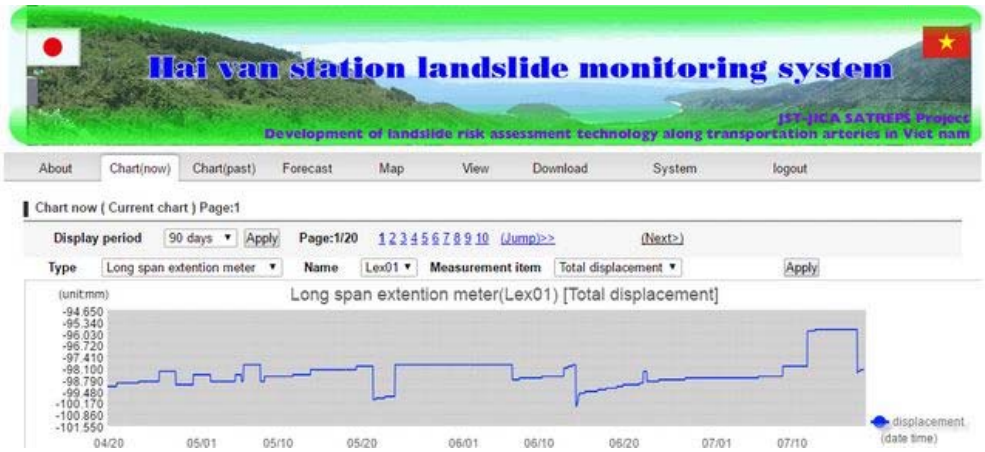

Fig. 7. Display of the data on web observation system (Asano et.al. 2016)

Structure of the web observation system

- About: General information of the monitoring system in Hai Van Station landslide
- Chart (now): To see the trace back data in past from recent
- Chart (past): To see the past data since specific date
- Forecast: To see the estimation of the slope collapse time after the start of landslide movement
- Map: To see the location of each sensors
- View: To see the photo of landslide slope by interval camera
- Download: To collect the all data in database to analyze the mechanism of the landslide
- System: To check the condition of devices for data transfering

GL 21: 2016

First edition

Measurement of Slip Surface Displacement in Borehole Using Inclinometer

HA NOI – 2016

Abstract

Inclinometer was used to measure slope displacement at various depths along bore hole. Those data can obtain automatically and manually. The manual inclinometer was used to determine the depth of landslide surface. The automatic inclinometer was used for early warning system and studying the relationship between the movement and landslide trigger factor.

Table of Contents

Measurement of Slip Surface Displacement in Borehole Using Inclinometer

1. Scope

1.1 This guide defines the sequence of installation, monitoring horizontal displacement of soil in depth by inclinometer probe device

1.2 This guide are used to monitor serves to determine the distance of the horizontal displacement sliding on a slope, excavation, building vertical, wall of deep foundation pit.

2. Referenced documents

TCVN 2682:2009 Portland cements - Specifications;

TCVN 6260:2009 Portland blended cement- Specifications;

TCVN 9395-2012 Bored pile-Construction, check and acceptance;

AASHTO T254 - 2000: Standard Test Method Installing, Monitoring, and Processing Data of the Traveling Type Slope Inclinometer.

ASTM D6230 - 98 (2005), Standard Test Method for Monitoring Ground Movement Using Probe – Type Inclinometers;

ASTM D7299-2006, Standard Practice for Verifying Performance of a Vertical Inclinometer Probe.

3. Terminology and definitions

In this standard, apply the following terms and definitions

3.1 Inclinometer device

Include: Inclinometer casing , inclinometer, signaling cable, data reading (see Fig B.2, Appendix B)

3.2 Inclinometer casing

Vertical Inclinometer casing at locations to monitoring, internal structure 4 guide slot forming 2 perpendicular planes to control the direction of the inclinometer and create a standard plane along the tube for repeated measurements.

3.3 Lateral movement

Move in a direction perpendicular to the gravitational.

3.4 Twist inclinometer casing

The standard deviation of guide slots in Inclinometer casing by the tube turn around the axis.

3.5 Direction A_0-A_{180}

Direction parallel with the direction largest displacement predicted of the ground.

3.6 Directions B_0-B_{180}

Direction perpendicular to the direction largest displacement predicted of the ground.

3.7 Initial readings

Include: Inclinometer casing location coordinates (x,y,z) determined by total station. The position of Inclinometer casing s under the direction of the A_0-A_{180}, B_0-B_{180} at each depth, determined by Inclinometer Device the Inclinometer casing has stabilized after installation.

3.8 The inclinometer

Include: two pairs of wheels, each pairs has two wheels symmetrical through the inclinometer. The inclinometer has two sensors. An inclinometer sensor of plane containing the wheel called axis sensor A_0-A_{180}. An inclinometer sensor of the plane perpendicular to the plane containing the wheel called axis sensor B_0-B_{180}.

3.9 Automatic inclinometer

The inclinometer installed fixed in the inclinometer casing, data monitoring automatically recorder at preset cycle time and transmit to center station.

3.10 Spacing shift

The horizontal movement of Inclinometer casing s at a depth compared to gravitational at the time of measurement.

4. Principle

The inclinometer probe device used to determine the size, the speed and the horizontal displacement of the ground. Inclinometer casing s fixed in the ground, Inclinometer casing will show the horizontal displacement of the environment around it. Inclinometer probe pulled by hand and measure the inclination of the probe compared to gravitational. Using algebraic function to transfer data inclinometer to distances. Calculate the sum of the distances to determine position over time. Comparing the data of monitoring the next time cycle with initial readings will indicate the different positions of the tubes, thereby determining the lateral movements perpendicular to the axis of the tube. On that basis, automatic inclinometer device will be permanently installed in the borehole to measure the movement with time served for the early warning system and studies the relationship between movement and the factors causing landslides.

5. Required material

5.1 Backfill between wall of borehole and inclinometer casing

Backfill between wall of borehole and inclinometer casing have to meet state principle similar to the soil around the inclinometer casing and avoid the creation of voids thus using composite material cement – mortars suitable.

Cement – mortar used to fill the middle of wall of borehole and inclinometer casing includes: poor cement mortar; clay cement mortar and cement – mortar.

Poor cement mortar includes: cement, water, betonies in proportion: 1: 2,5: 0,3 for sand has density state, cohesive soil has soft hard – hard . The strength of mortar at 28 days is at least 70 kPa.

Clay cement mortar includes: cement, water, betonies in proportion: 1: 6,5: 0,4 for sand has flexible state, cohesive soil has soft plastic – plastic liquid . The strength of mortar of testing at 28 days at least 28 kPa

Cement mortar includes: cement, water in proportion: 2,5:1 for weathered rock. The strength of mortar is at 28 days at least 30Mpa.

Soil around inclinometer casing differs from state of materials equivalent quality.

Portland cement or a mixture of Portland cement meets technical requirements TCVN 2682: 2009 and TCVN 6260: 2009.

Betonies meets technical requirements TCVN 9395-2012

NOTE: cement used for rate on the PCB 30, if another need to test.

5.2 Inclinometer casing

Inclinometer casing (Figure 1) made of durable molded plastic, aluminum or steel. Cross section of inclinometer casing is circle or square, suitable for each type of inclinometer. Inside inclinometer casing have four grooves evenly spaced along the tube 900 to the wheel of the inclinometer moves adjoining the tube. The length of inclinometer casing is meeting the depth installation and minimize coupling. The inclinometer is undistorted of diameters under the pressure of external load installation depth. Head of inclinometer have a section to associate with tube.

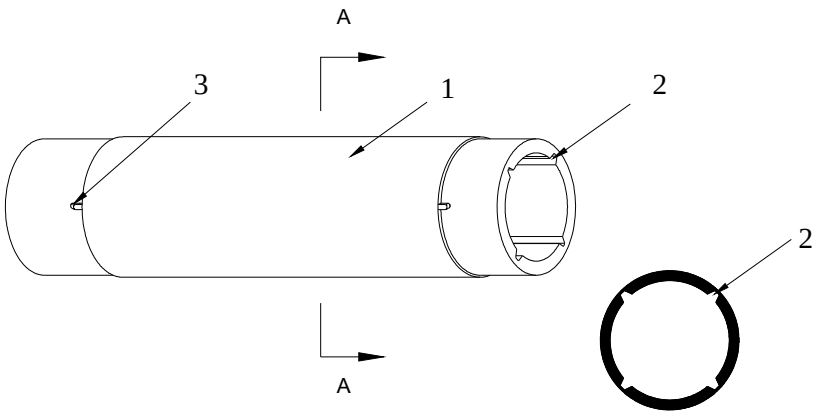

Section A-A

NOTE:
1. Inclinometer casing
2. Orientation grooves of wheel
3. Cottar locate inclinometer casing with coupling

Figure 1 – Inclinometer casing

5.3 The coupling inclinometer casing

The coupling inclinometer casing (Figure 2) made from high-strength plastic, aluminum or metal with evenly spaced grooves, diameter of the coupling inclinometer casing to fit inclinometer casing . Inclinometer casing should be hard to not be deformed in diameter under the pressure of external load installation depth. Couplings must have a part to link the two inclinometer casing fixed not move during installation and monitoring

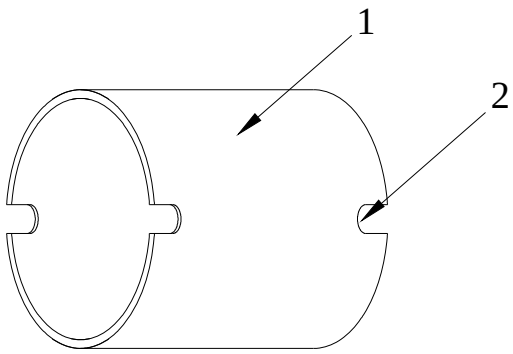

NOTE:
1. The coupling inclinometer casing
2. Orientation grooves of the coupling inclinometer casing

Figure2 - The coupling inclinometer casing

5.4 Lid, sealing of inclinometer casing

Lid, sealing of bottom inclinometer casing (Figure 3) must fit on diameter of the inclinometer casing to protect the top and bottom of the pipe, prevent drill cutting and debris into the pipe. For bottom sealing contacted bottom boreholes should use cone sealing for easy lowering borehole inclinometer casing .

.

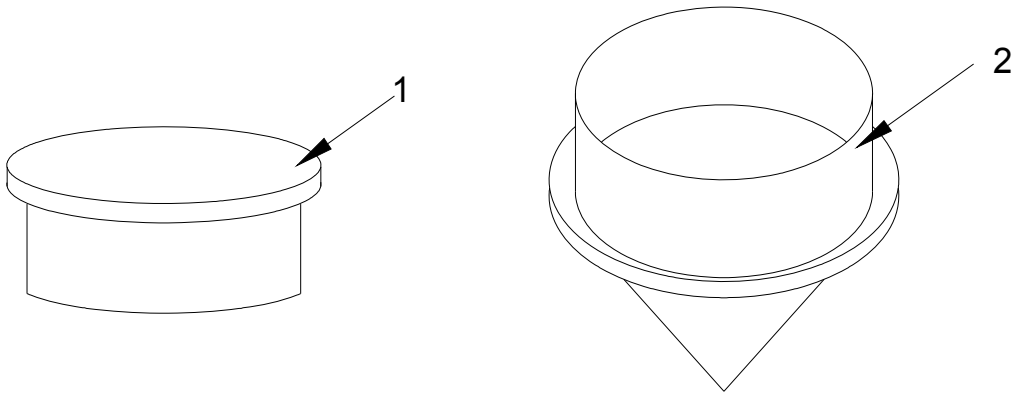

NOTE:
1. Lid of top inclinometer casing
2. Sealing of bottom inclinometer casing

Figure3 –Lid, Sealing of bottom inclinometer casing

6. Required equipment

6.1 Equipment borer

- Drilling equipment must be able to create a borehole with diameter, depth fitting the diameter of the inclinometer casing and installation, geological conditions of the ground. Usually the hole diameter is not less than 110 mm.

- Drilling equipment must be calibrated parts for drilling boreholes are vertical and firmly anchor must not movement during the drill.

6.2 Inclinometer

6.2.1 The inclinometer

The inclinometer must be calibrated for at least 1 year. In the process used to regularly test follow Appendix C.

The inclinometer must be synchronized with the read data specified in 6.3. Two sensors in the probe simultaneously measured the movement of inclinometer casing under the perpendicular direction each other at the same time compared to the gravitational.

Wheels of the pipe move in the grooves in the inclinometer casing and must always adjoin along the inclinometer casing (Figure 5).

Specifications shown in Table 1:

Table 1: Specifications shown

Specifications	Value
1. Measurement range	± 15^0
2. Display resolution	0.001^0
3. The repeatability of probe	$\pm 0.003^0$ or ± $5x10^{-5}$ radian
4. Measurement accuracy	±0.1[%FS]
5. Spacing of wheel	50cm
6. Depth	150m

6.2.2 Automatic inclinometer (Figure 4)

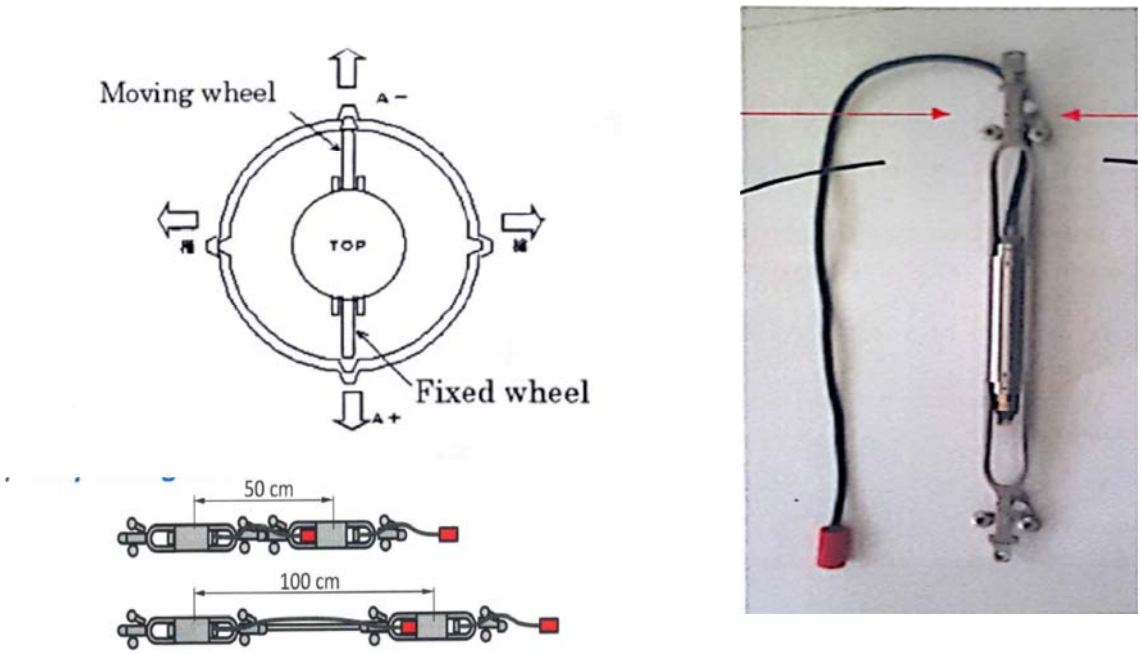

Figure 4- Automatic inclinometer

The structural of the inclinometer automatically like the inclinometer. The device include many inclinometer connected together. Quantity of the probe depend on the quantity of monitoring position in the pore hole. The probe installed fixed in the inclinometer casing, cable connect of the probe lead to the ground and connect with data reading and recording automatically.

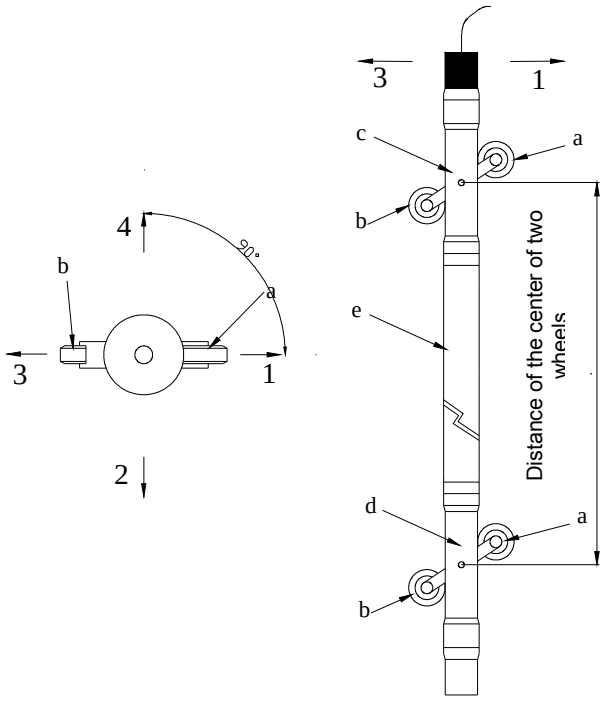

NOTE

a - wheel on the top

b - wheel on the bottom

c - String on the top

d - String on the bottom

e - Probe

$\overleftarrow{A_0}$ directions No. 1

$\overleftarrow{B_0}$ directions No. 2

$\overleftarrow{A_{180}}$ directions No. 3

$\overleftarrow{B_{180}}$ directions No. 4

Figure 5 – Typical of inclinometer

6.3 Logger

The functions of logger are reading, record and save measured values during measurement connect to probe with interconnecting cable reel. The measured values are: Number measurement points, measurement date, depth, horizontal displacement of inclinometer casing at measurement locations.

The logger can connect to a computer, the results calculated through data software measurement.

6.4 Interconnecting cable

Interconnecting cable reel connect the inclinometer with data reading, together hang and kept probe during the probe in the inclinometer casing .

Interconnecting cable has to ensure uninterrupted signal and tenacity to hang the probe during measurement and used to test the depth of the probe tilt. Cable marked equally spaced points depending on the distance of two-wheels center measured (Figure 6).

Figure 6 – Interconnecting cable

7. Inclinometer casing installation

Inclinometer casing installation includes: borer, Inclinometer casing installation and Backfill between wall of borehole and inclinometer casing (Figure 7)

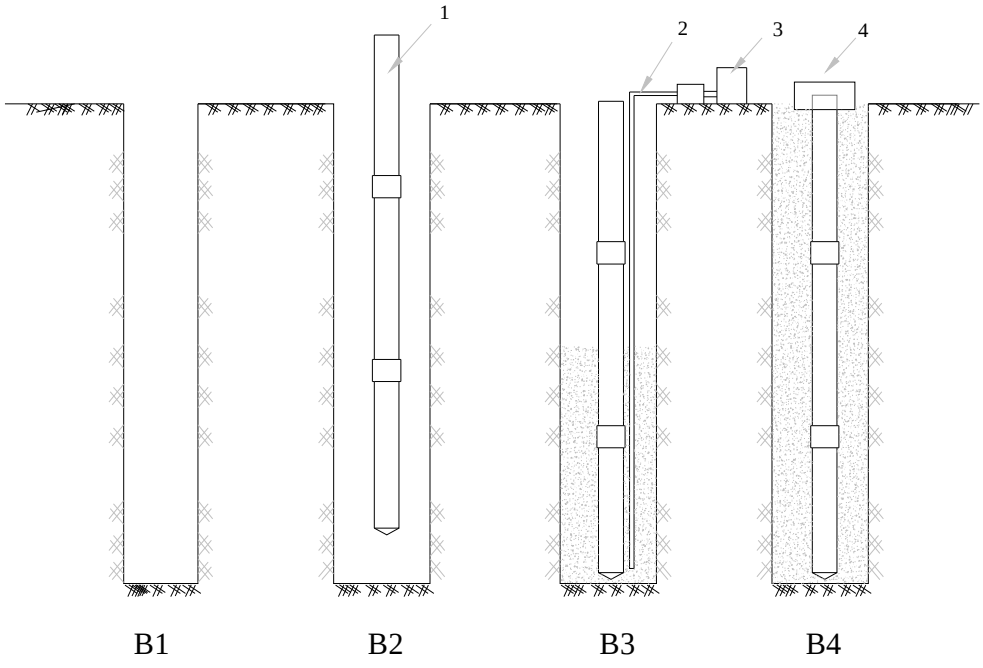

NOTE

B1 - Borer
B2 - Inclinometer casing installation
B3 - Grouting between wall of borehole and inclinometer casing
B4 - Inclinometer casing installation complete

1 - Inclinometer casing
2 - Grouting pipe
3 - Mortar pump
4 - Lid protective

Figure 7 – Typical diagram of Inclinometer casing installation

7.1 Borehole

7.1.1 Position of borehole

Borehole locations have been determined exactly in the field in accordance with design documents prior to drilling. All borehole coordinates (X, Y, Z) must be recorded and presented in the data report.

7.1.2 Diameter of borehole

Diameter borehole should be large to fit the size of the inclinometer casing and depends on the construction drill borer but not less than 110 mm.

7.1.3 Depth of drill hole

The depth of the borehole depends on the depth of monitoring and the bottom of inclinometer casing with a length not less than 2 m in soil with hard plastic state to hard or sandy layers.

NOTE: Drilling deeper when drill cuttings cannot remove from the borehole when the inclinometer casing dropped, ensure depth of monitoring by design.

7.1.4 Clean of drill hole

Borehole after drilling to a depth of regulation should be cleaned by washing to remove drill cuttings. Time for cleaning boreholes must be fast, avoid borehole wall collapsed.

NOTE: inspect the borehole to determine the borehole wall not collapsed for the installation of inclinometer casing

7.2 Installation of inclinometer casing

Set the direction standard for inclinometer casing , the direction of grooves in the tube will be parallel and perpendicular to the predicted movement. Direction of parallel with the predicted movement largest of the ground is defined as the A_0-A_{180}.Direction of Perpendicular with the predicted movement largest of ground is defined as the B_0-B_{180} (Figure 8).

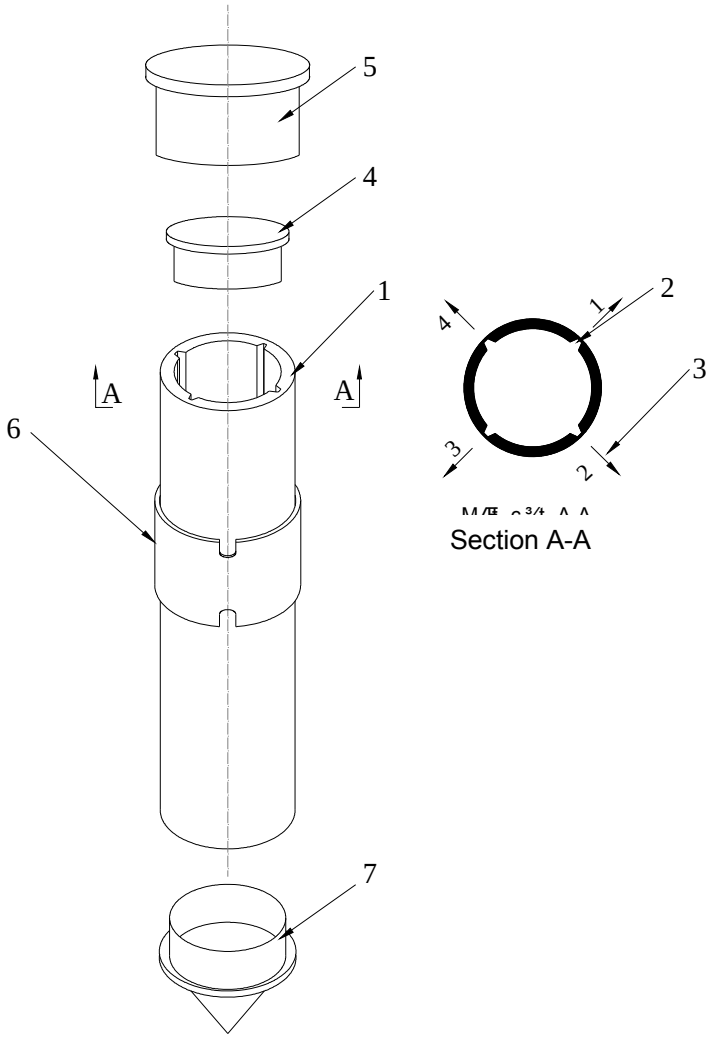

NOTE

1. Inclinometer
2. Orientation grooves of wheels
3. Direction of movement
4. Lid of inclinometer casing
5. Protection cap after installation
6. Substitute
7. Bottom sealing

Figure 8 - Typical diagram of structure of Inclinometer casing

7.2.1 Set the sealing into the bottom of inclinometer. Bottom sealing must be connected to the tube by the manufacturer

7.2.2 Insert the substitute on the top of the inclinometer casing ; connect the substitute with the inclinometer casing by the manufacturer.

7.2.3 Lower the first tube with bottom sealing of inclinometer towards the bottom to drill hole

7.2.4 Use tools to keep the inclinometer casing not falling into the drill hole. Always keep the Orientation roves in the inclinometer casing was set in place during installation.

7.2.5 Set the second inclinometer casing into the head of the first substitute, adjust the groove of two tube are aligned.

NOTE: Absolutely not press inclinometer casing by the drill cause the inclinometer casing has twisted.

7.2.6 Continue connecting the inclinometer casing in 7.2.2; 7.2.3; 7.2.4; 7.2.5 until it touches the bottom of the drill hole

NOTE 1: If necessary, proceed to pour clean water into the inclinometer casing to avoid the buoyancy tubes.

NOTE 2: check the inclinometer casing during installation to not twisted.

NOTE 3: To avoid scratching if the inclinometer casing by aluminum.

7.2.7 Use the hacksaw to cut off the excess overhang of the inclinometer casing on the ground by the design documents and fitting the protection cap of the inclinometer casing.

7.3 Backfill between the wall of drill hole and the inclinometer casing

7.3.1 Pump suitable material specified in 5.1 to fill the space between the wall of drill hole and inclinometer casing after having installed inclinometer casing, as follow:

+ Lower pump mortar tube simultaneously with inclinometer casing. Grouting pipe outside pipe direction;

+ Bottom of pump mortar tube 20cm from the bottom. Grouting until the mortar rises and spills over the drill hole to pull up tube.

NOTE: if get the buoyancy during grouting to find appropriate measures to prevent buoyancy, but not affect the inclinometer casing.

7.3.2 When the drill with casing pipe down, when pulling up the casing pipe should be not rotation system to prevent broken inclinometer casing , avoiding fill material to fall into the inclinometer casing

NOTE: if borehole was installed casing pipe, it should be pulled and grouted both.

7.3.3 The space between the wall of drill hole and inclinometer casing backfill material when material spill over drill hole mouth, positioning inclinometer casing and installation of protection cap.

8. Requirements in the installation

8.1 Check while installation

8.1.1 Check the working borer

8.1.1.1 Check the coordinate of drill hole

8.1.1.2 In the drill hole must regularly check core sample to determine the strata graphic and depth installation position. If there are differences compared to the design inform the supervisory consultant engineer to decide.

8.1.1.3 Check wall of the borehole to ensure stability, not collapsed.

8.1.1.4 After the drill, check depth of drill hole with the designs.

8.1.2 Check the inclinometer casing

8.1.2.1 The components of the inclinometer casing include inclinometer casing , substitute, and the bottom sealing. Check whether the parts are damaged or not. Do not use damaged parts so they can cause problems when reading and working hard for analyzing monitoring data. Keep clean these parts and avoid external influence during installation. The process of installation must comply with the manufacturer.

8.1.2.2 Check the Orientation grooves of the inclinometer; it must be concentric grooves, to ensure

the wheels of the inclinometer unhindered.

8.2 Check after installation

8.2.1 Check borehole

The accuracy of boreholes following requirements:

- Discrepancy position <10 cm.
- Diameter of borehole not less than the design requirements.
- The depth of the drill hole should not be less than the depth of design and as follow in 7.1.3

8.2.2 Check the inclinometer casing after installation

8.2.2.1 after installation of the inclinometer casing -conducting test following contents:

- Check length of inclinometer casing by tape measure, tolerance ± 20cm with the designs.
- Use the test probe: probe moves from top to bottom. In the tube has no mud or drill cutting.

8.2.2.2 If the inclinometer casing have drill cuttings or fill material, to conduct pump clean water into the inclinometer casing to clean the groove before freeze.

9. Monitoring of horizontal displacement

9.1 Monitoring procedure

9.1.1 Calibration of Equipment

Equipment is calibrated at the factory. Each equipment has a K factor (see Eq 1). Before conducting monitoring daily to check with the experiments turntable stand and casing (details see Appendix C)

9.1.2 Determine the number of initial reading

9.1.2.1 Conduct initial readings after at least 3 days of installation to be enough time for the grout around the inclinometer casing or fill material was stable. Check the number of reading by taking at least two sets of readings on the same day in depth. Check the stability of the reading by examining the sum of the number of reading and check the movement within the equipment's accuracy. Repeat measurement readings until meet required. From all initial readings will carry out a number of readers chose as the standard for the next reading.

Due to the calculation of all the movement depends on the initial reading, number must be exactly.

Determine the top of position of inclinometer casing (x, y, z) at the same time as the initial measurement readings.

Must be used the same probe during monitoring to minimize systematic errors. If used to replace have to use the same type.

9.1.2.2 Check the set of readings by summing the readings for the A_0-A_{180} and B_0-B_{180} directions at each depth. These summing are called check-sums and should equal a constant value that is a characteristic of the probe.

NOTE: Refer to the manufacture's literature for information on allowable variation in the check-sum.

A single deviation in a check-sum probably indicates a bad reading. Erratic behavior of check-sum generally indicates a poor electrical connection or a malfunctioning probe or readout.

9.1.3 Monitoring procedure

9.1.3.1 Insert the probe in to the inclinometer casing at A_0-A_{180} direction (wheels on the probe into

the groove No.1). The probe was lowered slowly to the bottom of inclinometer casing . Keep the probe about 10minutes to temperature equilibrium than the temperature in the inclinometer casing . Measured by pulling up the probe and keep probe fixed at depth intervals are marked on the Interconnecting cable for stable readings, recording data (depth and reading R) on the data reading . Continue to pull the probe up each about taking the next figures. Do not leave the probe in the tube in free fall during measurement.

9.1.3.2 Repeat the above sequence until the end of the inclinometer casing . Pull the probe out of the inclinometer casing , turning the wheel on 1800 put the wheel into the third groove and lower the probe to the bottom. Take data at the same depth as the first time (see 8.1.3.1).

NOTE: For the biaxial probe for measuring twice just as on the complete of the reading. For an axial probe, both the A_0-A_{180} and B_0-B_{180} directions are measured.

9.1.4 Frequency of monitoring

The frequency of monitoring depends upon the rate of movement when measured by handwork. The frequency of monitoring more increase when slope of movement through other monitoring equipment.

Table 2– Monitoring frequency

Time Monitoring	Monitoring frequency (times)
1. Initial reading	01
2. On the time monitoring	01/ 15 day

NOTE: Frequency of horizontal displacement monitoring with the depth should coincide with other monitoring, such as subsidence measuring table, equipment of depth settlement, horizontal displacement movement on the face.

9.2 Logger

The data were recorded with the initial data include: altitude of the ground surface, installation date, the date of taking the initial reading, the level of the bottom of the inclinometer casing , and coordinate positions monitoring (see appendix A).

Monitoring data at a frequency included: day of monitoring, the direction of monitoring, the monitoring data horizontal displacement (depth and reading R)

10. Calculation and report

10.1 Calculation

Assuming inclinometer casing is vertical for the first reading. All subsequent to readings are compared to the initial reading

10.1.1 Calculation of space movement of inclinometer casing

The displacement of inclinometer casing with standard direction (Vertical direction) is proportional to the readings R, following the Eq:

$$d = \frac{L}{K} \times R \qquad (1)$$

Where:

d – Space of movement of inclinometer casing (m)

L – Reading interval (mm)

K – Instrument constant (supplied by the manufacturer and determined by factory calibration)

R – Reading on the data reading

10.1.2 Compute the increase of movement of inclinometer with two directions

Compute the increase of movement of inclinometer at each depth. Following the Eq:

$$d_{1-3} = \frac{L \times (R_1 - R_3)}{2K} \qquad (2)$$

$$d_{2-4} = \frac{L \times (R_2 - R_4)}{2K} \qquad (3)$$

Where:

dA_0-A_{180}: is the computed incremental casing deflection at one depth in direction A_0-A_{180} (mm)

dB_0-B_{180}: is the computed incremental casing deflection at one depth in direction B_0-B_{180} (mm)

R1,R3: the reading on the data reading in direction A_0-A_{180}

R2,R4: the reading on the data reading in direction B_0-B_{180}

L,K: see the Eq (1)

10.1.3 Compute the displacement one point on the inclinometer casing at the time of measurement (Time t)

The position of the inclinometer casing at any depth (D_n) as the sum of the incremental casing deflection from the end of the inclinometer casing to that depth:

$$D_{n_{1-3}} = \sum_{i=1}^{n} d_{i,t_{1-3}} \qquad (4)$$

$$D_{n_{2-4}} = \sum_{i=1}^{n} d_{i,t_{2-4}} \qquad (5)$$

Where:

$D^{n}{}_{1-3}$ the sum of increase of movement inclinometer casing with standard direction at the depth n in direction A_0-A_{180}(mm);

$D^{n}{}_{2-4}$ the sum of increase of movement inclinometer casing with standard direction at the depth n in direction A_0-A_{180}(mm);

$d_{i,t_{1-3}}$ is the computed incremental casing deflection at one cycle of monitoring in direction A_0-A_{180} (mm);

$d_{i,t_{2-4}}$ is the computed incremental casing deflection at one cycle of monitoring in direction B_0-B_{180}(mm).

NOTE: Equation (4), (5) standard point at the bottom of casing.

10.1.4 Compute the initial value of the inclinometer casing

Use the Eq (4),(5) with initial reading (time t_0) to determine initial reading of inclinometer casing. Two or

more sets of initial readings taken on the same day can be averaged of initial readings.

10.1.5 Compute the displacement of inclinometer casing between two sequence measurement

Use the Eq (6), (7) to compute the displacement of the casing, ∆Dn, between two times of monitoring, this is the changing position of casing.

$$\Delta D_{n_{1-3}} = \sum_{i=1}^{n} d_{i,(t)_{1-3}} - \sum_{i=1}^{n} d_{i,(t-1)_{1-3}} \qquad (6)$$

$$\Delta D_{n_{1-3}} = \sum_{i=1}^{n} d_{i,(t)_{2-4}} - \sum_{i=1}^{n} d_{i,(t-1)_{2-4}} \qquad (7)$$

Where:

$\Delta D_{n_{1-3}}$ is the displacement of inclinometer casing at the point n in direction A_0-A_{180} (mm),between two cycle monitoring;

ΔD_{n2-4} is the displacement of inclinometer casing at the point n in direction B_0-B_{180} (mm),between two cycle monitoring;

$d_{i,(t)_{1-3}}$ is the computed incremental casing deflection at one cycle of monitoring t at any depth in direction A_0-A_{180};

$d_{i,(t-1)_{1-3}}$ is the computed incremental casing deflection at one cycle of monitoring t-1 at any depth in direction B_0-B_{180};

$d_{i,(t)_{2-4}}$ is the computed incremental casing deflection at one cycle of monitoring t at any depth in direction A_0-A_{180};

$d_{i,(t-1)_{2-4}}$ is the computed incremental casing deflection at one cycle of monitoring t-1 at any depth in direction B_0-B_{180}.

- If L and K are constant and the same for all set of readings, Eq (6), (7) can be simplified as:

$$\Delta D_{n_{1-3}} = \frac{L}{2K} \times \left[\sum_{i=1}^{n} (R_1 - R_3)_t - \sum_{i=1}^{n} (R_1 - R_3)_{t-1} \right] \qquad (8)$$

$$\Delta D_{n_{2-4}} = \frac{L}{2K} \times \left[\sum_{i=1}^{n} (R_2 - R_4)_t - \sum_{i=1}^{n} (R_2 - R_4)_{t-1} \right] \qquad (9)$$

Where:

L,K see Eq (1);

$(R_1 - R_3)_t$ is the readings on the set of reading at cycle of monitoring t in direction A_0-A_{180};

$(R_2 - R_4)_t$ is the readings on the set of reading at cycle of monitoring t in direction B_0-B_{180};

$(R_1 - R_3)_{t-1}$ is the readings on the set of reading at cycle of monitoring t-1 in direction A_0-A_{180};

$(R_2 - R_4)_{t-1}$ is the readings on the set of reading at cycle of monitoring t-1 in direction B_0-B_{180}.

10.2 Report

Report of testing result (example for one project with 15m depth) including:

1) Name of project;
2) Coordinates (x,y,z) monitoring point;
3) Type of measuring equipment's;

4) Date of taken initial reading;

5) Read of next time;

6) Date of completion;

7) Table shown displacement with corresponding to the depth, see Appendix A, table A1, A2;

8) The chart indicates the relationship between cumulative displacements with depth in both local time, see Appendix A, Table A2.

11. Installation inclinometer in HaiVan landslide

At the HaiVan landslide, we drilled and installed apparatus to monitor the horizontal displacement of scope with the install depth is 80 m. The installation process as following:

11.1 Material

11.1.1 Fill material between borehole wall and wall of Inclinometer casing

Use cement PCB 40 mixture with the rate water/ cement is =0.4 to full fill the space between drill hole wall and wall of Inclinometer casing .

11.1.2 Inclinometer casing

At this project Inclinometer casing made of aluminum, has round cross – section, suitable with probe ò inclinometer. Inside the Inclinometer casing has four channel with vertical direction, and has event distance is 900to made the wheel of probe of inclinometer move closely to the wall of pipe. The length of Inclinometer casing portion is 3m (Figure 9). Inclinometer casing has no deformation of diameter when applied loading follow the depth.

Figure 9: Inclinometer casing

11.1.3 The cap seal the bottom of Inclinometer casing

This cap aims to avoid drilling dirt insert and debris insert into pipe. Should use the cap has cone geometry to easy lower the Inclinometer casing .

11.1.4 Geo-textile pipe wrap over Inclinometer casing

Geo-textile pipe to protect pipe in installation process and prevent the loss of grout in the cracks of stone.

Geo-textile pipe has diameter 120mm, and has continuous and longer than the depth of drill hole at least 10 m

11.2 Apparatus

11.2.1 Apparatus for making hole

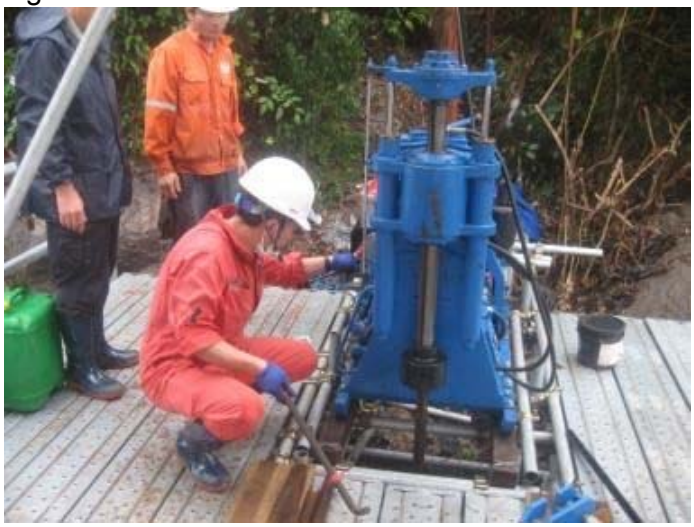

Figure 10: Apparatus for making hole

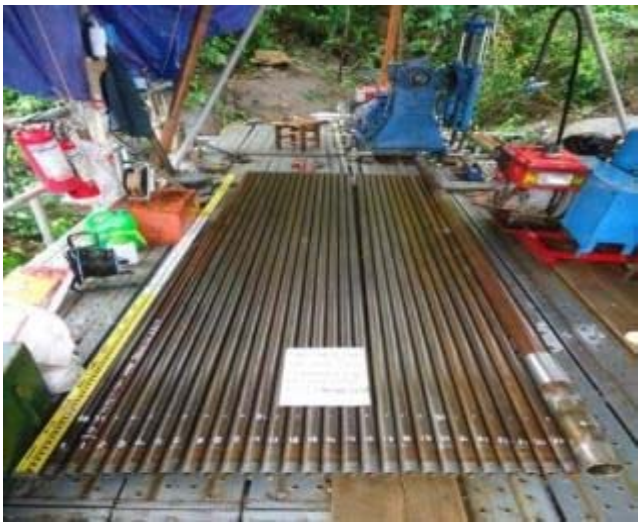

Figure 11: Rod of drill

a) Use rotary drilling machine with ability to drill to depth more than ≥ 120m. Don't use jumper drilling

b) At each position drill, use twin auger has diameter 86 mm to take intact soil and rock and diameter 66 for drill hole not take sample

c) casing – well is used in drill process to ensure vertical direction and stability in casing well 11.2.2 Inclinometer probe

11.2.2 Inclinometer probe

11.2.2.1 Inclinometer probe pull by hand

Inclinometer probe use **Digital Q- Tilt 6000 Model 4470**

Table 3: Technical parameters of inclinometer probe pull by hand

Parameters	**Value**
1 Measurement range	± 15^0
2. - Display resolution	0.001^0
3. Reparation of probe	$\pm 0.003^0$ or ± $5x10^{-5}$ radian
4. Measurement accuracy	±0.1[%FS]
5. Distance of wheels	50cm
6. Measure depth	150m

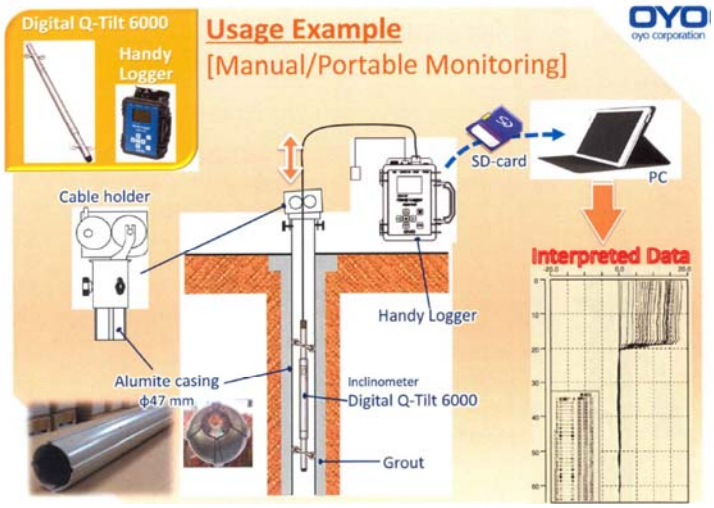

Figure 12: Figure of inclinometer pull by hand of OYO- Japan firm

11.2.2.2 Inclinometer with auto logger

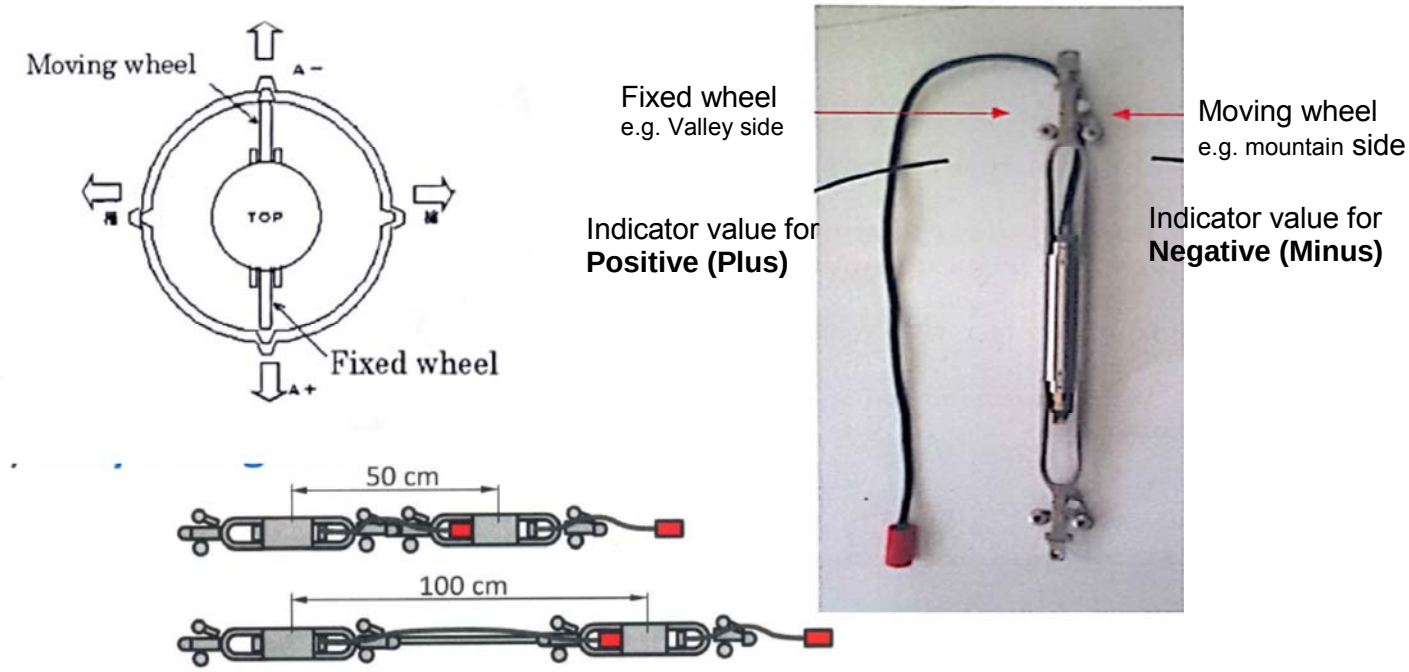

Figure 13: Inclinometer with auto logger

Table 4: Technical Parameters of auto inclinometer probe

The following shows the specification of the stationary inclinometer.

Measurement components	: 2-axis inclination (A-axis and B-axis)
Output data unit	: Angle [°]
Measurement range	: ±15 [°]
Display resolution	: 0.001 [°]
Measurement accuracy	: ±0.1 [%FS]
Operating power range	: DC12 [V] ±20%
Temperature characteristics	: ±0.008 [°/°C] or less
Power supply voltage fluctuation	: ±0.003 [°] or less (DC12V ±20% range)
Communication method	: Serial communication by single cable (RS485)
Maximum connectable number	: 20 sequential connections
Maximum cable length	: 120 [m]
Installation interval	: Standard installation interval: 0.5m or 1m (2m or more is possible by adding equipment)
Cables	: Waterproof construction, Detachable type
Current consumption	: 25 [mA] or less with DC12V supply
Dedicated logger	: i-SENSOR 2

11.2.3 Logger

Figure 14: Logger

11.3 Install

11.3.1 Drill hole

Due to complicated terrain at HaiVan so we need use drilling rig

Figure 15: rig system

Use investigate drill hole to install to measure horizontal displacement. Drill hole has diameter is D=86mm, finish drill process when reach to the depth 80m an drill into (fresh basic rock stratum) with continuous length over 20m with RQD index ≥70%. The depth for install pipe to measure horizontal displacement is 80m.

11.3.2 Clean the drill hole

Clean all dirt and debris in drill hole diameter 86mm by pump with reverse circulation

11.3.3 Install Inclinometer casing and insert tube to pump grout

Determine standard direction for pipe: The channel in Inclinometer casing has parallel and perpendicular with predict displacement direction .Parallel direction with predict max displacement direction is A_0-A_{180}. Perpendicular to max displacement direction is B_0-B_{180}.

Lower the first pipe with attach seal cap at the bottom to under position of Inclinometer casing , the first injection grout is attached to portion of the first Inclinometer casing , the distance from injection grout pipe to the bottom of drill hole is 0.5m. Attach the bottom part of second pipe into the top of the first pipe, adjust channel of each portion tube in alignment. Joint between two pipe made by specific colloid and must ensure no have dirt's outside come in. If the depth more than 80m installs three injections, grout pipe with the distance between each other is 30 m approximately (See Figure 16).

Figure 16: Install inclinometer casing and insert tube to pump grout

Continue joint and lower all portion pile of guide tube as this process until reach to the bottom of borehole. During lower guide, line pipe process pour water into pipe to avoid floating phenomena

Wrap guideline pipe by geo-textile pile and lower into drill hole with Inclinometer casing

11.3.4 Inject grout between space of borehole wall and wall of guideline pile.

Pump grout has mixture follow specification in section 8.1.1.1 to full fill the space between borehole wall and wall of inclinometer casing after finished the process to install Inclinometer casing

Calculate amount of grout for each portion length 30 m to the bottom to the top which ensure injection grout pope always immerse in at least 2m length of grout and avoid unclog the pump pipe . Stop pump until grout full over the top of borehole. After insert grout must verify the unclog of Inclinometer casing by probe, lower the probe from the tip to bottom. No peat or drill cutting in pipe.

If in Inclinometer casing has drill cuttings or material filling hole must clean by pump water combine with suitable tools to clean before material for filling hole become stiff

11.4 Monitoring

11.4.1 Monitoring process with inclinometer pull by hand

Taking at initial reading at least 3 days after completed installation. Taking at least two reading set in one day at the same depth. Check stability of these reading by checking total reading and the displacement in accuracy range of apparatus

Frequency to monitoring: - once time for each 15 days for inclinometer pull by hand in 6 month.
- The auto logger record for each 1 hour.

Monitoring process:

- Insert probe inclinometer in A_0-A_{180} direction (wheel of probe insert in A_0 channel (See Figure 17). The probe goes down gradually to the bottom of Inclinometer casing . The probe keeps in inclinometer casing about 10 minutes balancing with the temperature with temperature in inclinometer casing . Taking measure by pull the probe and maintain the probe fix at the marked depth in cable signal, wait the reading stable , read and record data (depth, reading R) in the reading apparatus. Continue pull probe in specific distance an take the next reading (See Figure 18).

- Repeat this process until the probe reach to the top of Inclinometer casing . Pull the probe out of inclinometer casing and rotary 180^0 to take the wheel on the probe intro channel A_{180} and lower the probe to the bottom if Inclinometer casing . Take to data at specific depth as the first time

Figure 17: Insert probe inclinometer in A_0-A_{180} direction

Figure 18: Rotary 180^0 to teke the Wheel on the probe intro Channel A_{180}

11.4.2 Record data

Table 5: Table record monitoring data

'ID	DATE_TIME	DATA No	REF_DEPTH
18	16/03/17 17:04:57	140	70m

DEPTH (m)	A_0	A_{180}	B_0	B_{180}
0.5	-0.0431	0.0414	-0.0140	0.0121
1.0	-0.0419	0.0402	-0.0127	0.0111
1.5	-0.0411	0.0394	-0.0138	0.0121
2.0	-0.0424	0.0409	-0.0143	0.0128
2.5	-0.0449	0.0432	-0.0155	0.0138
3.0	-0.0500	0.0486	-0.0161	0.0145
3.5	-0.0549	0.0532	-0.0163	0.0146
4.0	-0.0560	0.0543	-0.0165	0.0148
4.5	-0.0458	0.0442	-0.0133	0.0115
5.0	-0.0100	0.0088	-0.0057	0.0041
5.5	0.0092	-0.0111	0.0010	-0.0029
6.0	0.0200	-0.0216	0.0068	-0.0086
6.5	0.0188	-0.0207	0.0065	-0.0083
7.0	0.0125	-0.0139	-0.0097	0.0081
7.5	0.0146	-0.0161	-0.0240	0.0220
8.0	0.0278	-0.0294	-0.0296	0.0278
8.5	0.0344	-0.0359	-0.0107	0.0091
9.0	0.0303	-0.0321	0.0071	-0.0087
9.5	0.0278	-0.0296	0.0114	-0.0133
10.0	0.0246	-0.0263	0.0042	-0.0060
10.5	0.0231	-0.0246	-0.0005	-0.0015
11.0	0.0252	-0.0266	0.0011	-0.0023
11.5	0.0072	-0.0096	-0.0022	0.0001
12.0	-0.0087	0.0072	-0.0066	0.0047
.....	.....	.....	.....	.....
29.5	-0.0111	0.0095	0.0061	-0.0079
30.0	-0.0004	-0.0009	0.0082	-0.0100
....	.....	.....	.....	.....
65.5	0.0468	-0.0487	-0.0269	0.0249
66.0	0.0476	-0.0493	-0.0251	0.0232
66.5	0.0497	-0.0514	-0.0240	0.0221
67.0	0.0504	-0.0522	-0.0228	0.0207
67.5	0.0516	-0.0533	-0.0232	0.0212
68.0	0.0498	-0.0514	-0.0249	0.0228
68.5	0.0494	-0.0511	-0.0274	0.0254
69.0	0.0468	-0.0487	-0.0250	0.0229
69.5	0.0441	-0.0458	-0.0222	0.0201
70.0	0.0423	-0.0450	-0.0180	0.0161

11.5 Calculate

11.5.1 Calculate result

Table 6: Calculate result

Borehole Inclinometer

No. | Number of monitoring: Initial Value

B01-01 | Date: 30 Jun 2015

Depth (m)	A_0	A_{180}	A_0-A_{180}	Section Displace-ment (mm)	Accumulated Displacement (mm)	B_0	B_{180}	B_0-B_{180}	Section Displacement (mm)	Accumulated Displacement (mm)
0.50	-0.0440	0.0430	-0.0870	0.00	0.00	-0.0145	0.0135	-0.0280	0.00	0.00
1.00	-0.0423	0.0414	-0.0837	0.00	0.00	-0.0127	0.0115	-0.0242	0.00	0.00
1.50	-0.0410	0.0404	-0.0814	0.00	0.00	-0.0139	0.0128	-0.0267	0.00	0.00
2.00	-0.0428	0.0418	-0.0846	0.00	0.00	-0.0149	0.0140	-0.0289	0.00	0.00
2.50	-0.0451	0.0443	-0.0894	0.00	0.00	-0.0159	0.0150	-0.0309	0.00	0.00
3.00	-0.0504	0.0493	-0.0997	0.00	0.00	-0.0163	0.0155	-0.0318	0.00	0.00
3.50	-0.0547	0.0538	-0.1085	0.00	0.00	-0.0165	0.0155	-0.0320	0.00	0.00
4.00	-0.0557	0.0546	-0.1103	0.00	0.00	-0.0165	0.0158	-0.0323	0.00	0.00
4.50	-0.0458	0.0448	-0.0906	0.00	0.00	-0.0135	0.0125	-0.0260	0.00	0.00
5.00	-0.0106	0.0095	-0.0201	0.00	0.00	-0.0063	0.0055	-0.0118	0.00	0.00
5.50	0.0090	-0.0097	0.0187	0.00	0.00	0.0000	-0.0009	0.0009	0.00	0.00
6.00	0.0193	-0.0206	0.0399	0.00	0.00	0.0059	-0.0070	0.0129	0.00	0.00
6.50	0.0176	-0.0184	0.0360	0.00	0.00	0.0060	-0.0071	0.0131	0.00	0.00
7.00	0.0120	-0.0129	0.0249	0.00	0.00	-0.0103	0.0091	-0.0194	0.00	0.00
7.50	0.0145	-0.0154	0.0299	0.00	0.00	-0.0235	0.0226	-0.0461	0.00	0.00
8.00	0.0285	-0.0294	0.0579	0.00	0.00	-0.0290	0.0277	-0.0567	0.00	0.00
8.50	0.0335	-0.0345	0.0680	0.00	0.00	-0.0113	0.0104	-0.0217	0.00	0.00
9.00	0.0305	-0.0312	0.0617	0.00	0.00	0.0057	-0.0067	0.0124	0.00	0.00
9.50	0.0273	-0.0283	0.0556	0.00	0.00	0.0104	-0.0115	0.0219	0.00	0.00
10.00	0.0230	-0.0237	0.0467	0.00	0.00	0.0037	-0.0048	0.0085	0.00	0.00
10.50	0.0211	-0.0220	0.0431	0.00	0.00	-0.0013	0.0001	-0.0014	0.00	0.00
11.00	0.0228	-0.0235	0.0463	0.00	0.00	0.0008	-0.0014	0.0022	0.00	0.00
11.50	0.0059	-0.0068	0.0127	0.00	0.00	-0.0028	0.0017	-0.0045	0.00	0.00
12.00	-0.0092	0.0084	-0.0176	0.00	0.00	-0.0064	0.0054	-0.0118	0.00	0.00
.....	.....	.....	.....	.....	.....	.....	.....	.....	.....	.....
29.50	-0.0109	0.0099	-0.0208	0.00	0.00	0.0063	-0.0073	0.0136	0.00	0.00
30.00	-0.0001	-0.0006	0.0005	0.00	0.00	0.0080	-0.0091	0.0171	0.00	0.00
.....	....	.....	.....	.....	.....	.....	.....	.....	.....	.....
65.50	0.0469	-0.0480	0.0949	0.00	0.00	-0.0266	0.0256	-0.0522	0.00	0.00
66.00	0.0480	-0.0489	0.0969	0.00	0.00	-0.0247	0.0237	-0.0484	0.00	0.00
66.50	0.0499	-0.0511	0.1010	0.00	0.00	-0.0238	0.0227	-0.0465	0.00	0.00
67.00	0.0507	-0.0519	0.1026	0.00	0.00	-0.0226	0.0215	-0.0441	0.00	0.00
67.50	0.0519	-0.0530	0.1049	0.00	0.00	-0.0229	0.0218	-0.0447	0.00	0.00
68.00	0.0503	-0.0510	0.1013	0.00	0.00	-0.0244	0.0234	-0.0478	0.00	0.00
68.50	0.0495	-0.0507	0.1002	0.00	0.00	-0.0271	0.0260	-0.0531	0.00	0.00
69.00	0.0472	-0.0482	0.0954	0.00	0.00	-0.0247	0.0235	-0.0482	0.00	0.00
69.50	0.0445	-0.0457	0.0902	0.00	0.00	-0.0221	0.0211	-0.0432	0.00	0.00
70.00	0.0423	-0.0433	0.0856	0.00	0.00	-0.0175	0.0163	-0.0338	0.00	0.00

11.5.2 Report

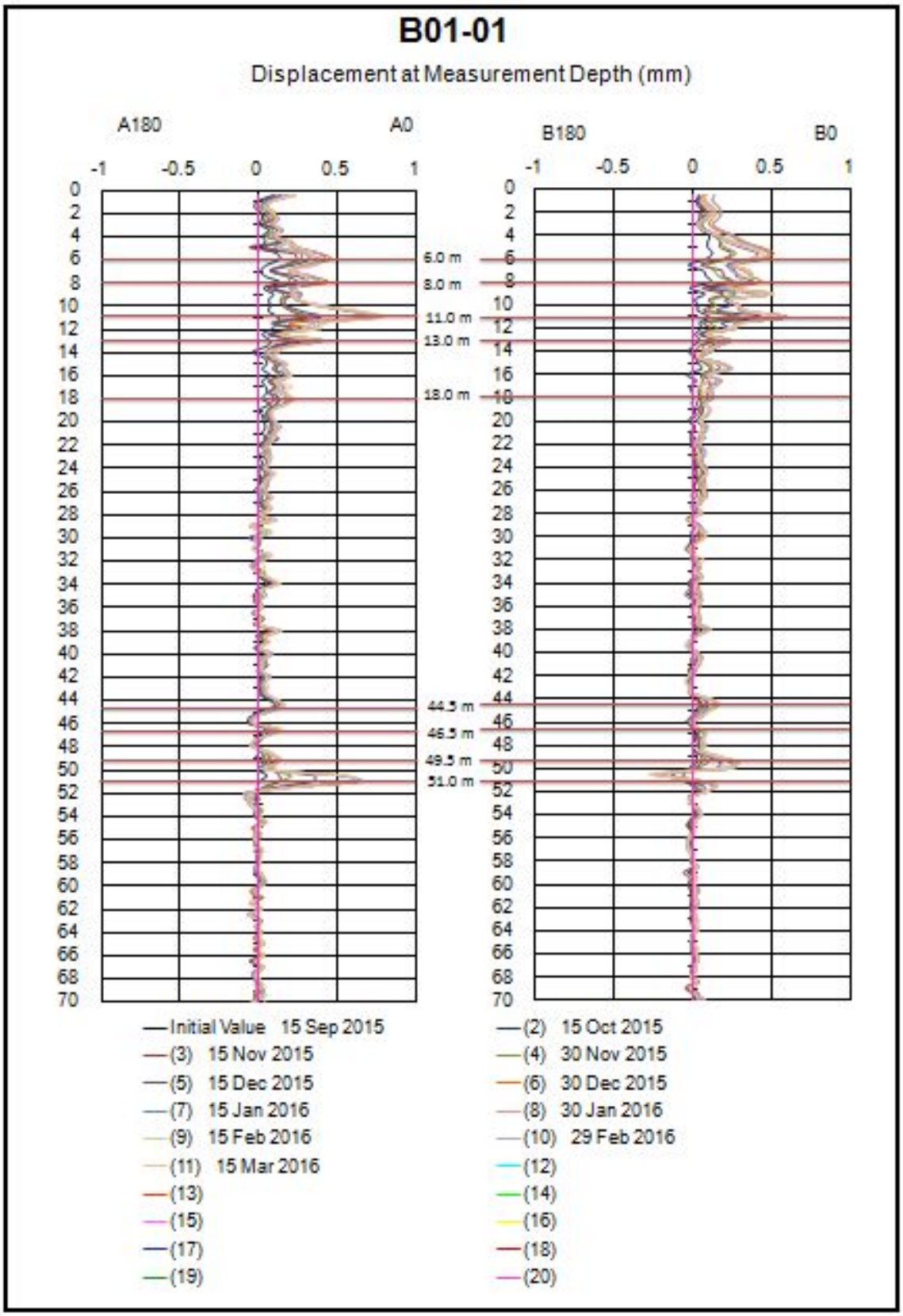

Figure 19: Chart moving

From data of monitoring with inclinometer pull by hand determine which cross-section need to install auto logger at different depth as: 6m; 8m; 10m; 13m; 18m; 44.5m; 46,5m; 49.5m; 51m.

11.6 Installation of inclinometer automatically

The depth was determined in section **11.5**, statistic of quantity equipment and accessories (table 7).

Table 7: Quantity of probe and accessories

No	Apparatus	Unit	Quantity
1	Probe (LinQ-Tilt) 0.5m length	Pcs	9
2	Lead-in cable	m	11
3	Rod holder	Pcs	1
4	Adjustment rod	Pcs	1
5	Rod 0,5m	Pcs	7
6	Rod 1,0m	Pcs	5
7	Rod 2,0m	Pcs	19
8	Joint rod	Pcs	9
9	End cap	Pcs	1

11.6.1 Connection of probe

Signal wire connections with waterproof connectors Probe connects each other by the rod and the pivot joints (figure 20). In the following:

End cap (end cap figure 21) – probe – rod 1m – probe – rod 2m – rod 0.5m – probe – rod 1m – rod 0.5m – probe – 13 rods 2m – rod 0.5m – probe – 2 rods 2m – rod 0.5m – probe – 2 rods 2m – rod 0.5m – probe – rod 1m – rod 0.5m – probe – rod 1m rod 0.5m - probe – 2 rods 2m – rod 1m – rod 0.5m – rod holder (figure 22).

Centre of probes at : 6m; 8m; 10m; 13m; 18m; 44.5m; 46,5m; 49,5m; 51.0m depths

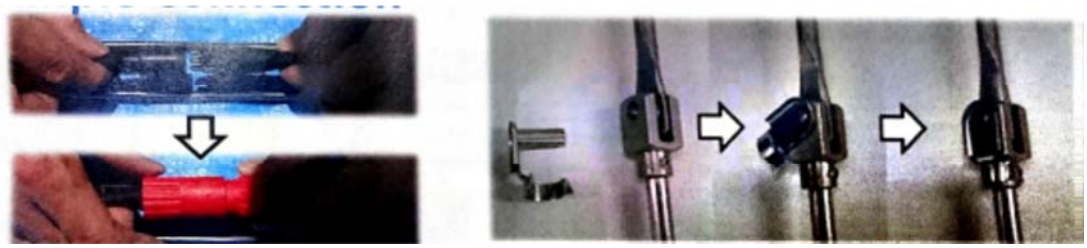

Figure20 : connection of cable and probes

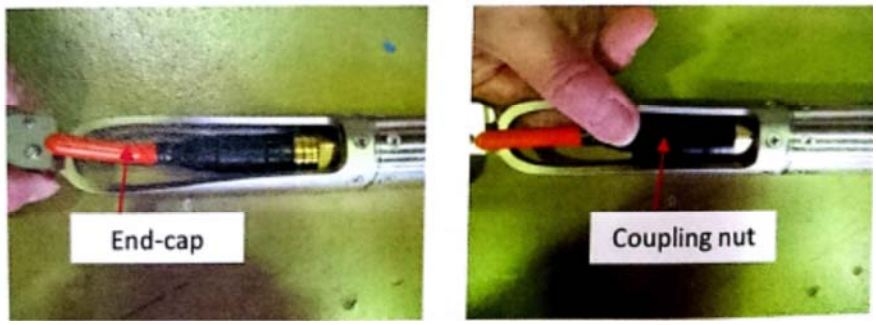

Figure 21 : End cap

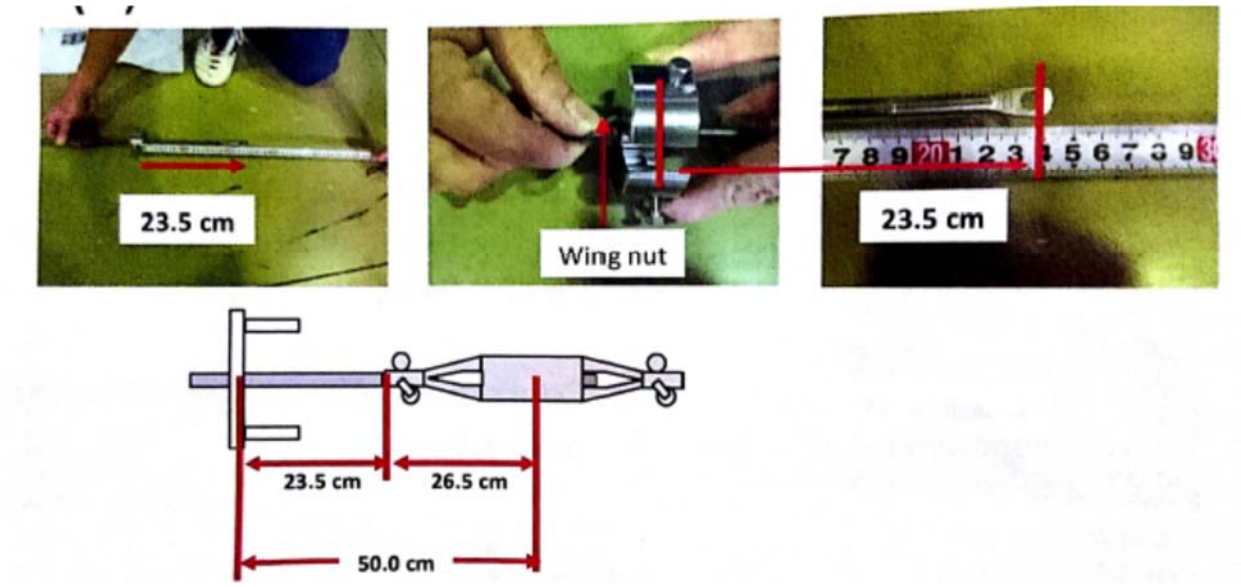

Figure 22: connection of cable with rod holder

11.6.2 Installation of inclinometer automatically in the inclinometer casing

Lower end cap of the inclinometer automatically after connection (section 11.6.1) down inclinometer casing, the plane contain the wheel of the first probe into the groove A_0-A_{180} of inclinometer casing. The wheel above (fixed wheel) in the groove A_0 or A+ (see figure 17).

Continue lower the remainder of the probe of inclinometer automatically in the inclinometer casing in accordance with the above principles. Rod holder was taken to the top of the inclinometer casing, screw connecting up to lock the rod holder with the inclinometer casing.

Note: in the process of lowering inclinometer automatically into the inclinometer casing should be slow down and have to insurance device to avoid free falling.

Connect the cable connection of the inclinometer automatically with the recorder data. The end of the process of the installation.

11.7 Result of the monitoring of the inclinometer automatically

Monitoring data was transmitted the center station via wireless transceiver system. From center station the data transmits the center office in HaNoi with cycle 1 hour for each.

Results of monitoring of the inclinometer automatically (Figure 23).

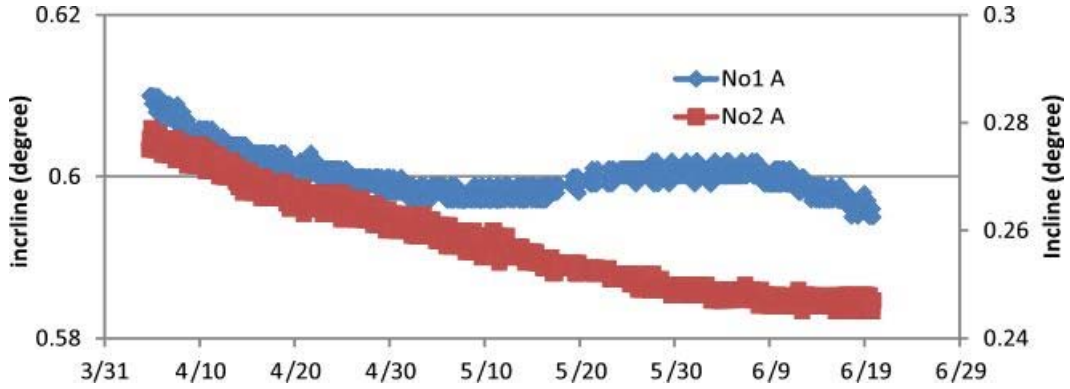

Figure 23: Results of monitoring of the inclinometer automatically

12 Maintenance

Due to the inclinometer has high accuracy and high work- time so need to has strict maintenance .

1- Verify and maintenance probe

Every day before measure, we need verify these following:

- Check tension force of string in guide wheels by press wheels near to the probe the release, the string still good if wheels turn to initial position.

- Verify guide wheel must be smooth in both directions.

After measure must clean the probe by dry cloth and put grease in ball bearing axis.

2- Verify the logger:

Before take, measure must check battery by software of system. After measured need to remove battery out of logger, prevent apparatus

NOTE: Place apparatus in dry place and avoid high temperature, often operate to make apparatus dry

.

Appendix A
(Reference)
Inclinometer Data and Calculations
Table A1 – **Inclinometer Data**

Table of data recorder horizontal displacement in depth using inclinometer								
Project:								
Items:						**Monitoring point number: N1**		
Location:						**Type of equipment:**		
Positions of monitoring point: X: Y:								
Date of installation: 22/7		Date of initial reading: 24/7		Date of monitoring: 18/9				
Altitude of underground water (m):				Altitude of the top of tube (m):			Altitudes of the bottom of tube (m):	
	Direction of measuring: A_0-A_{180} parallel with the direction of movement				Direction of measuring: B_0-B_{180} perpend ocular of the direction movement			
Depth (m)	Direction A_0	Direction A_{180}	The point movement (mm)	The movement of accumulate (mm)	Direction B_0	Direction B_{180}	The point movement (mm)	The movement of accumulate (mm)
0,5	1,68	-1,70	1,69	20,050				
1,0	1,68	-1,69	1,685	18,360				
1,5	1,42	-1,43	1,425	16,675				
2,0	1,42	-1,44	1,430	15,250				
2,5	1,42	-1,43	1,425	13,820				
3,0	1,30	-1,31	1,305	12,395				
3,5	1,24	-1,25	1,245	11,090				
4,0	1,16	-1,17	1,165	9,845				
4,5	0,57	-0,58	0,575	8,680				
5,0	0,42	-0,43	0,425	8,105				
5,5	0,40	-0,41	0,405	7,680				
6,0	1,36	-1,37	1,365	7,275				
6,5	2,20	-2,21	2,205	5,910				
7,0	1,12	-1,13	1,125	3,705				
7,5	0,30	-0,31	0,305	2,580				
8,0	0,10	-0,11	0,105	2,275				
8,5	0,06	-0,07	0,065	2,170				
9,0	0,00	-0,01	0,005	2,105				
9,5	-0,04	0,03	-0,035	2,100				
10,0	-0,13	0,12	-0,125	2,135				
10,5	-0,20	0,19	-0,195	2,260				
11,0	-0,18	0,17	-0,175	2,455				
11,5	-0,28	0,27	-0,275	2,630				
12,0	0,22	-0,23	0,225	2,905				
12,5	0,20	-0,21	0,205	2,680				
13,0	0,29	-0,30	0,295	2,475				
13,5	0,36	-0,37	0,365	2,180				
14,0	0,50	-0,51	0,505	1,815				
14,5	0,56	-0,57	0,565	1,310				
15,0	0,74	-0,75	0,745	0,745				

Table A2 - The table reports the results of monitoring horizontal displacement

Report of result horizontal displacement in depth using inclinometer

Project:

Item: **Monitoring point number: N1**

Position: **Type of equipment:**

Direction of measuring: A_0-A_{180}

Positions of monitoring point:

Date of installation: 22/7	Date of initial reading: 24/7	Depth of the installation (m):	altitude of the bottom of tube (m):
Direction of measuring: A_0-A_{180} parallel with the direction of movement		Altitude of underground water (m):	

Date of monitoring	24/7		21/8		18/9		ĐỒ THỊ ĐỘ DỊCH CHUYỂN
Depth (m)	Initial reading convectional	Initial reading	The movement of accumulate (mm)	Displacement (mm)	The movement of accumulate (mm)	Displacement (mm)	
0,5	0,0	2,20	11,03	8,83	20,05	17,85	
1,0	0,0	2,20	10,19	7,99	18,36	16,16	
1,5	0,0	2,11	9,31	7,20	16,68	14,57	
2,0	0,0	2,01	8,54	6,53	15,25	13,24	
2,5	0,0	1,93	7,79	5,86	13,82	11,89	
3,0	0,0	1,84	7,04	5,20	12,40	10,56	
3,5	0,0	1,76	6,35	4,59	11,09	9,33	
4,0	0,0	1,68	5,69	4,01	9,85	8,17	
4,5	0,0	1,60	5,10	3,50	8,68	7,08	
5,0	0,0	1,53	4,78	3,25	8,11	6,58	
5,5	0,0	1,49	4,54	3,05	7,68	6,19	
6,0	0,0	1,45	4,28	2,83	7,28	5,83	
6,5	0,0	1,41	3,52	2,11	5,91	4,50	
7,0	0,0	1,32	2,47	1,15	3,71	2,39	
7,5	0,0	1,18	1,87	0,69	2,58	1,40	
8,0	0,0	1,14	1,73	0,59	2,28	1,14	
8,5	0,0	1,13	1,68	0,55	2,17	1,04	
9,0	0,0	1,12	1,63	0,51	2,11	0,99	
9,5	0,0	1,09	1,62	0,53	2,10	1,01	
10,0	0,0	1,07	1,63	0,56	2,14	1,07	
10,5	0,0	1,05	1,69	0,64	2,26	1,21	
11,0	0,0	1,03	1,77	0,74	2,46	1,43	
11,5	0,0	1,00	1,84	0,84	2,63	1,63	
12,0	0,0	0,97	1,97	1,00	2,91	1,94	
12,5	0,0	0,94	1,84	0,90	2,68	1,74	
13,0	0,0	0,90	1,73	0,83	2,48	1,58	
13,5	0,0	0,87	1,57	0,70	2,18	1,31	
14,0	0,0	0,83	1,37	0,54	1,82	0,99	
14,5	0,0	0,79	1,10	0,31	1,31	0,52	
15,0	0,00	0,75	0,80	0,05	0,75	0,00	

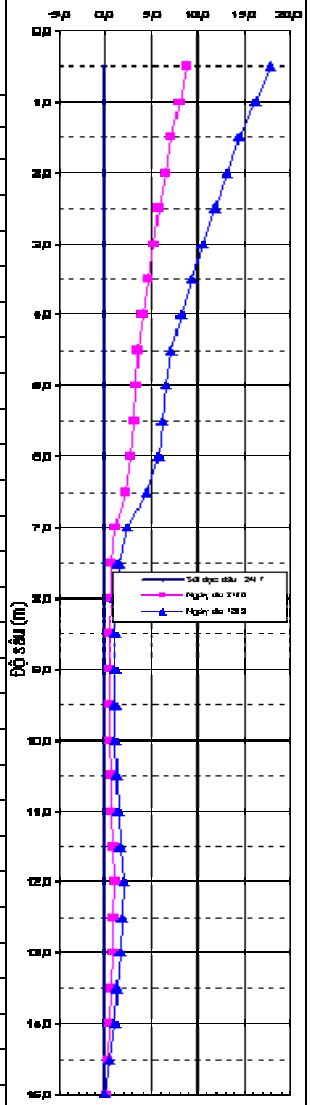

Appendix B
(Reference)
Some typical equipment of illustrations

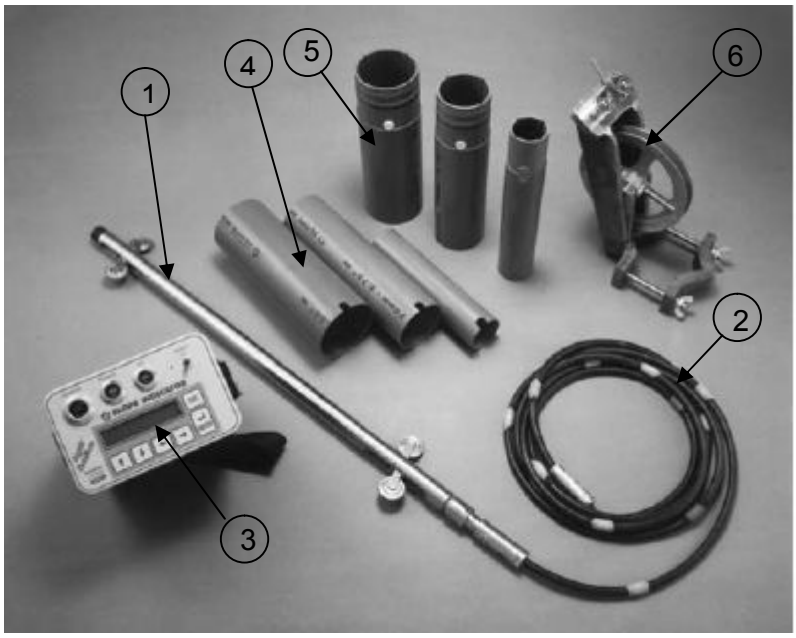

NOTE:

1 Inclinometer
2 Interconnecting cable
3 Data reading
4 Coupling of Inclinometer casing
5 Inclinometer casing
6 Holder Coupling of Inclinometer casing

Figure B.2 - Typical set measurement of horizontal displacement

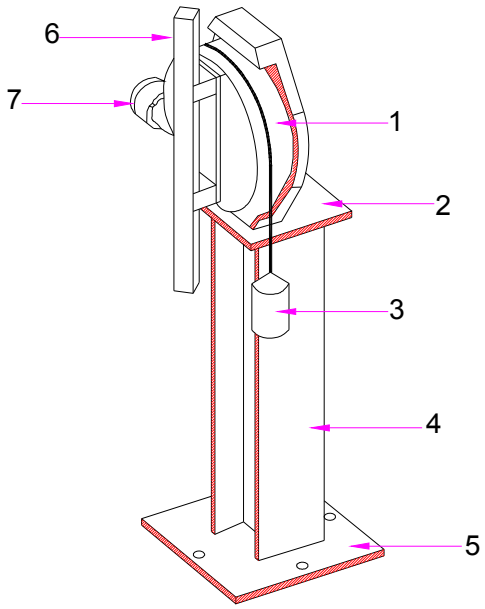

NOTE
1 Turntable
2 Bearing plate of turntable
3 Balance weight
4 Supporting rack of turntable
5 Bearing Plates
6 The probe hinged
7 Adjusting screw rate meter

Figure B.3 – Diagram of vertical turntable checking probe

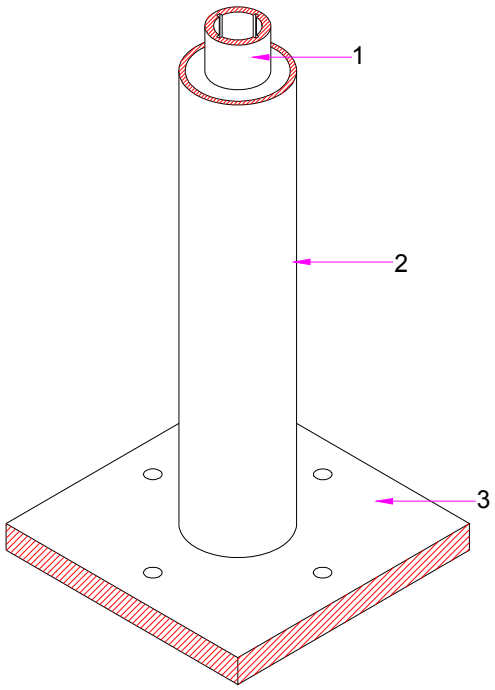

NOTE:
1 Inclinometer casing
2 casing
3 Plate

Figure B.4 – Diagram of equipment checking probe

ITST-ICL

GUIDELINE FOR LANDSLIDE RISK ASSESSMENT

GL 26 : 2016

First edition

Outline of landslide experiment

HA NOI – 2016

Table of Contents

Abstract

In the causes of the shallow landslides in Vietnam, heavy rain is a major cause. To investigate the mechanisms of landslides caused by rainfall, large-scale model slopes have been used to induce shallow landslides. In Japan, there are several landslide experiments conducted in Forestry and Forest Products Research Institute and National Research Institute for Earth Science and Disaster Prevention. A similar landslide flume experiment with artificial rainfall was made in Institute of Transport Science and Technology (ITST), Ministry of Transport, Vietnam in 2016. Four experiments to induce in a large-scale model slope by artificial heavy rainfall were conducted on these landslide flume experiments. Two river sand samples and two weather granite sand samples were used. The river sand samples were taken from Red River in Hanoi, Vietnam. The two others weathered granite sand samples were excavated from Haivan landslide in Danang city in Central of Vietnam. Wire extensometer was installed to detect the surface displacement before the landslide initiation. Time prediction of landslide initiation could be possible from the accumulation and acceleration of slope surface movement.

Outline of landslide experiment

1. Scope

This guideline is described in general about the purpose, the equipment, the method and the results when using the landslide flume experiment to investigate the mechanisms of landslides caused by rainfall.

2. Reference documents

Yoichi Okura, Hikaru Kitahara, Hirotaka Ochiai, Toshiaki Sammori, Akiko Kawanami (2002), Landslide fluidization process by flume experiments, Engineering Geology 66: 65-78

Hirotaka Ochiai, Yasuhiko Okada, Gen Furuya, Yoichi Okura, Takuro Matsui, Toshiaki Sammori, Tomomi Terajima, Kyoji Sass (2004), A fluidized landslide on a natural slope by artificial rainfal, Landslides (2004) 1:211 219, DOI 10.1007/s10346-004-0030-4

Do Ngoc Ha, Huynh Dang Vinh, Huynh Thanh Binh (2014), Landslides on the road in Vietnam – Monitoring and solutions for landslide risk reduction, 2014 Vietnam – Japan SATREPS report meeting.

Hirotaka Ochiai, Do Ngoc Ha, Huynh Dang Vinh (2016), Activities Report of WG4, 2016 Vietnam – Japan SATREPS report meeting.

3. Apparatus and Material

The apparatus include experimental flume and the observation system. The material used in the flume experiment is river sand or materials taken from the actual field.

3.1. Experimental flume

Landslide experiment is an almost real-size slope model to study the initiation process of landslide fluidization during torrential rain. One type is artificial slope named landslide flume experiment. Another type is natural slope in the field. The size of the experiment is as large as similar with the actual slope.

A design diagram of the landslide flume experiment with artificial rainfall is shown in Fig. 1. One side of the flume is covered with reinforced glass to observe material movement, one side is metallic. The inclination of the slope is different between the upper and lower sections to induce collapse at the

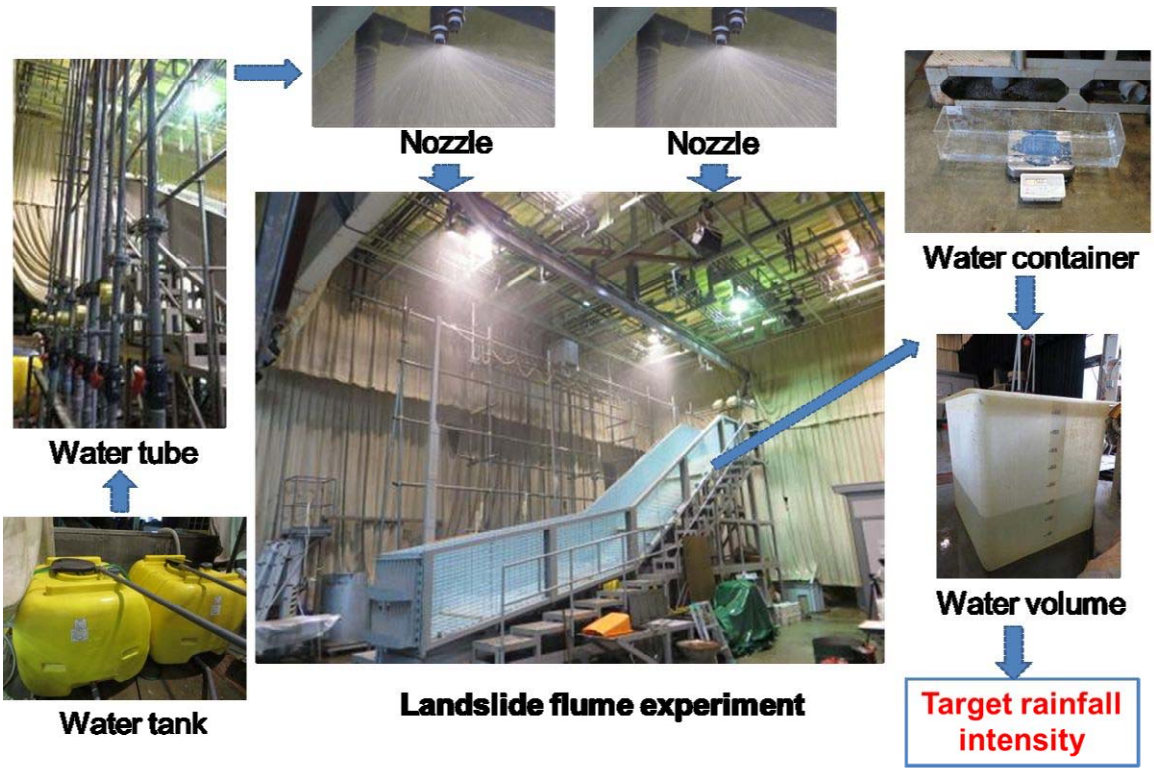

upper part of the slope and observe how the collapsed soil induces new slide on the lower part (Yoichi Okura et al., 2002).

To simulate the artificial rainfall, there are several nozzles on the top of the flume. These nozzles are needed to arrange so that the rainfall will be sprayed uniform along the flume. The valves along the water tube are used to control the rainfall intensity pumped from the water tank to the nozzles.

Fig. 1: The view of the flume and the artificial rainfall system (Do Ngoc Ha et al., 2014)

3.2. Observation system

The concept of the observation system is showed in Fig. 2. The system is designed to monitor the change in pore water pressure and the material movement.

- Monitor the change in pore water pressure at a specific depth: it is recommended to monitor the change in pore water pressure during the rainfall. When the pore water pressure increases, the slope will move to the failure. Small cylindrical pressure transducers are installed within the material mass to measure the pore water pressure changes.
- Monitor of the surface movement of material on the slope: it is needed to monitor the movement of the material on the slope surface using extensometers. The surface displacement and the acceleration in failing masses show a straight line on a full logarithmic graph. Using the inverse curve relationship of the velocity base on the method of Saito (1968) and the Fukuzono (1985), it can predict the time to failure of the landslide.
- Monitor of the mass movement of material on the slope: it is necessary to monitor the mass movement to analyse with the change in pore water pressure. Marker column or colour sands are placed along the flume. The movement of the markers are recorded with three video cameras and three digital cameras located along the glass side of the flume.

- Synchrony of data is attempted by generating time codes from a time-code generator or GPS, recording the codes together with pore water pressure measurements, and displaying them in video camera images of the mass movement.

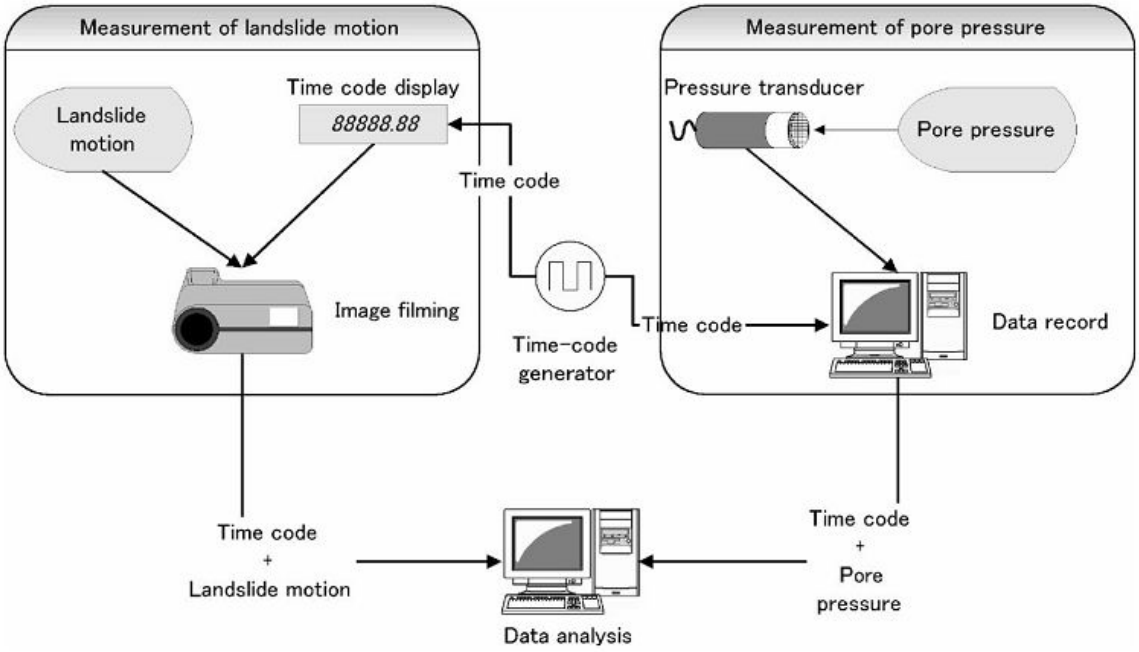

Fig. 2: The measurement system (Yoichi Okura et al., 2002)

3.3. Material mass layer shapes and configuration of the instruments

The material mass is filled on the slope by changing the thickness of the layer at the upper and lower slope. Fig. 3 shows the initial material mass layer and the position of the instruments installed along the slope.

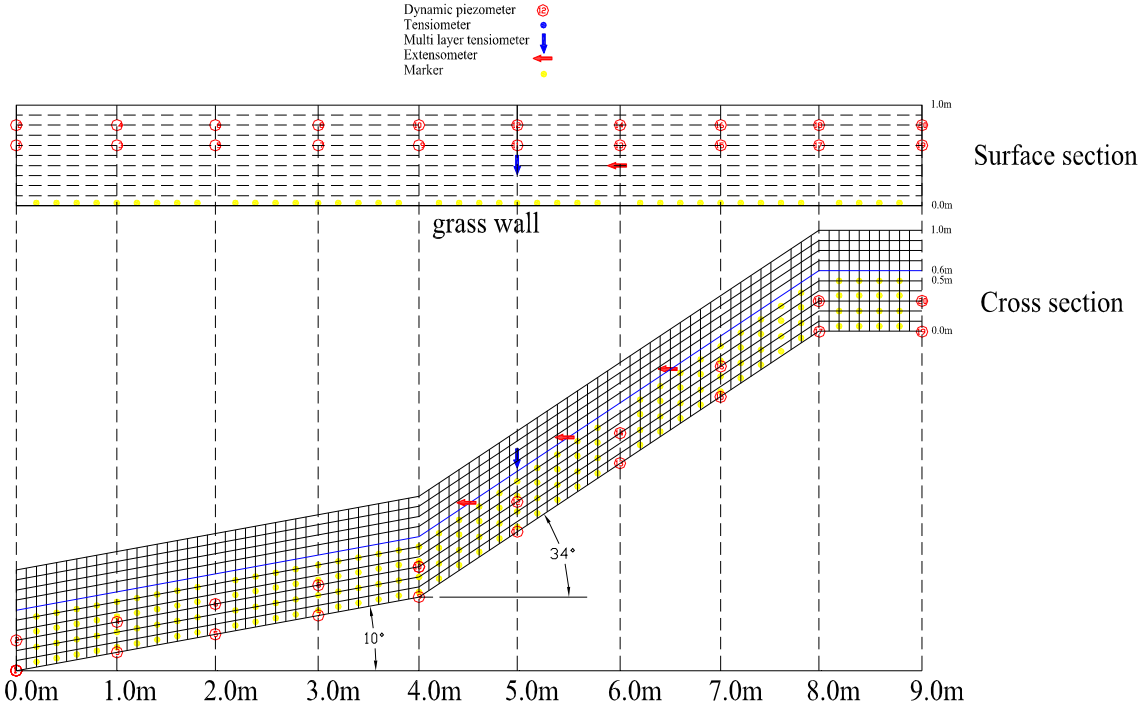

Fig.3: The side view of material mass layer and configuration of instruments (Hirotaka Ochiai et al., 2016)

4. Results from the experiments

4.1. Properties of the material used for the experiments

The properties of the material used for experiment are tested in advance. The results of soil tests are listed as follows:

- Dry density (surface)
- Void ratio (surface)
- Saturated water content
- Internal friction angle
- Cohesion
- 50% diameter of soil particle
- Silt and Clay content
- Uniformity coeffcient
- Coefficient of permeanbility

4.2. Relationship between landslide motion and pore water pressure distribution

The test results show the relationship of parameters as follows:

- The water table within the sand layer immediately before the collapse (? Ko hiểu- thiếu động từ),
- The form of the sand layer surface and the displacement vector of the pressure transducer embedded within the sand before and after the collapse, and
- The pore water pressure distribution within the sand layer immediately after the collapse and sedimentation

4.3. Relationship between volumetric strain, velocity, and pore water pressure fluctuation

The test results show the relationship of parameters as follows:

- The speed of soil movement, volumetric strain, pore water pressure, and
- The change in sand thick-ness all at the compressed soil section.

5. A case study of Landslide experiment in Institute of Transport Science and Technology (ITST)

In 2013, landslide experiment facilities were designed and the building was made in ITST. The landslide flume was designed based on the soil properties of the weathered granite of Hai Van area. In 2015 and 2016, four experiments to induce in a large-scale model slope by artificial heavy rainfall were conducted on landslide flume experiment in ITST. Two river sand samples and two weathered granite sand samples were used. The river sand samples were taken from Red River in Hanoi, Vietnam. The two others weather granite sand samples were excavated from Haivan landslide in Danang city in Central of Vietnam (Fig. 4).

Fig. 4: Slope before failure (left side) and after failure (right side) on flume experiment in ITST (Hirotaka Ochiai et al., 2016)

Detail of this experiment will be continuously written in other guidelines as follows:

- GL 27: Infiltration properties of testing material – for permeameter
- GL 28: Testing method
- GL 29: Analysis of measured data

ITST-ICL

GUIDELINE FOR LANDSLIDE RISK ASSESSMENT

GL 32 : 2016

First edition

Arc View Software - Arc GISI 10.1/ Spatial Analysis Software

HA NOI – 2016

Abstract

This report aims at providing guidelines for Spatial Analysis using Arc Map 10.1 for landslide research. ArcMap is used to view, edit, create, and analyze geospatial data. ArcMap allows the user to explore data within a data set, symbolize features accordingly, and create maps. Up to now, we can order or make the raster data of landslide area. From raster data, we can create slope, contour map, 3D view of landslide area and export the 3D cordinate for making topography in the landslide simulation.

Table of Contents

Arc View Software - Arc GISI 10.1/ Spatial Analysis

1. Scope

The Spatial Analysis functions we have just performed in ArcGIS are based on a vector data structure of points, lines and polygons. As demonstrated, this data model is ideal for elements that have discrete boundaries like airports, highways and landslide areas. But what if our data does not have discrete boundaries and is continuous over space (for example, elevation, slope, aspect or soil type)? The raster data model can be particulary beneficial in analyzing data that is continous. As stated earlier, raster data is composed of a two-dimensional matrix of grid cells, with each cell assigned a numerical value.

2. References

Kyoji Sassa, Bin He, Mauri McSveney, Osamu Nagai (2012), ICL Landslide Teaching Tools

Tsuchiya et al. (2012), Landslides in Japan

U.S. Government Information, Maps & GIS Services, Spatial Analysis Using ArcGIS 10 (2012)

3. Spatial Analysis

3.1. The Spatial Analyst Extension and Toolbar

In order to use the raster model in ArcGIS we need to load the Spatial Analyst extension and activate the Spatial Analyst Toolbar

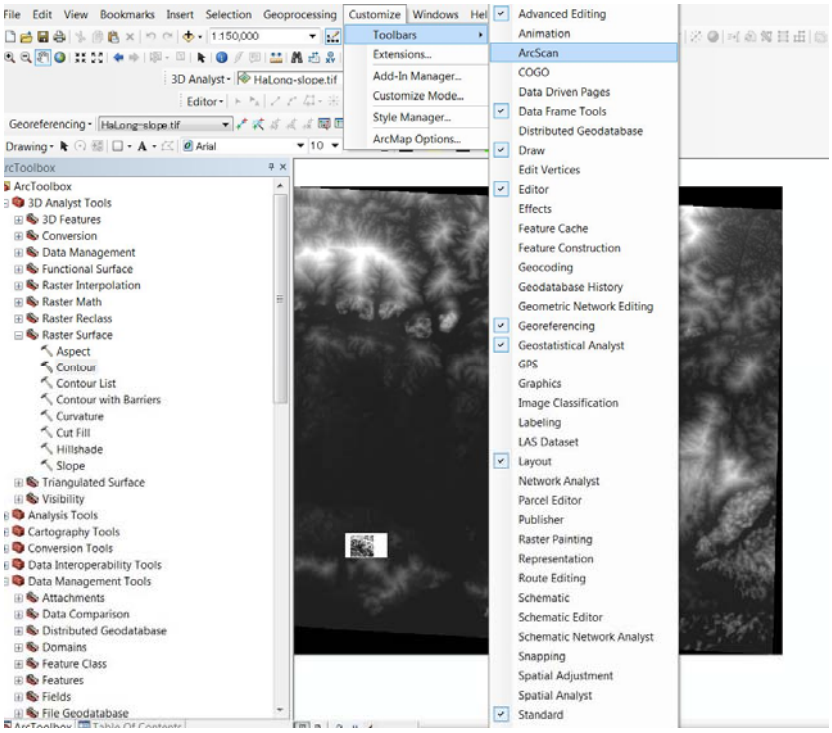

Fig.1 Toolbar in Arc Map 10.2

3.2. Examine raster data

(1). Add an elevation data to ArcMap by clicking on the Add Data icon 

(2). Use the 'identify' tool to get each cell's value

(3). Right click on the DSM/DEM layer and go to 'Properties'.

- Look at the "Source" tab to find the size of the cells, the extent of the data, what spatial reference it is using, and other good information.

- Look at the "Symbology" tab to see some color ramp options for display. Right click on "Color ramp" and uncheck "Graphic view" to see the names of the color ramps—pick.

- Look at the "Extent" tab to see the coordinates of the image's extent.

3.3. Surface Analysis

Surface analysis produces a new dataset—this can help you identify or derive patterns within the original dataset that may not have been evident. We will look at two examples: contour and slope. Contour will produce a vector output, while slope will produce a raster output. The raster output you get from spatial analysis on grid data can be either grid with unique values or Boolean.

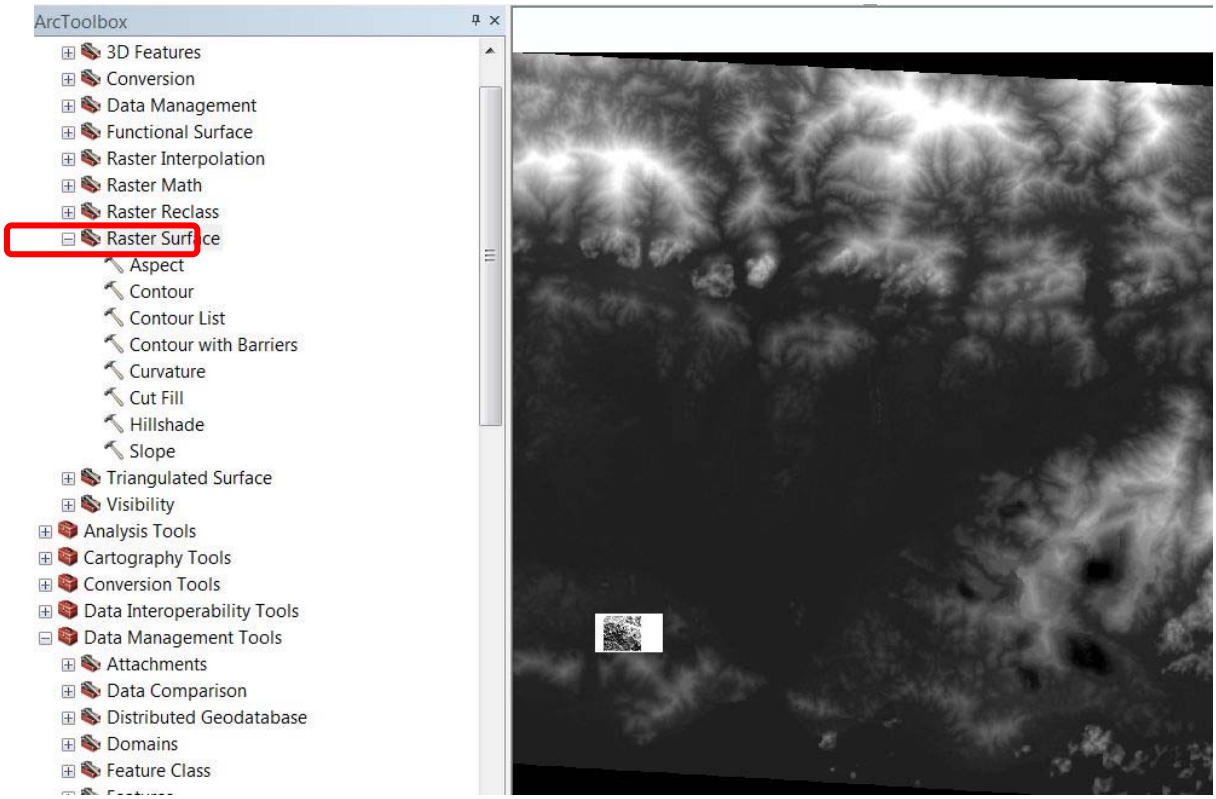

Fig. 2 Surface analysis

3.3.1 Contour (Vector)

Contour is a very good way to look at the overall gradation of the land, and is familiar to the eye. Using contour as an example also illustrates how you can get a vector result from a raster original.

From ArcToolbox,

(1). Left-click on the plus sign to the left of ‘Spatial analyst.’

(2). Left-click on the plus sign to the left of ‘surface’

(3). Double click on ‘Contour.’

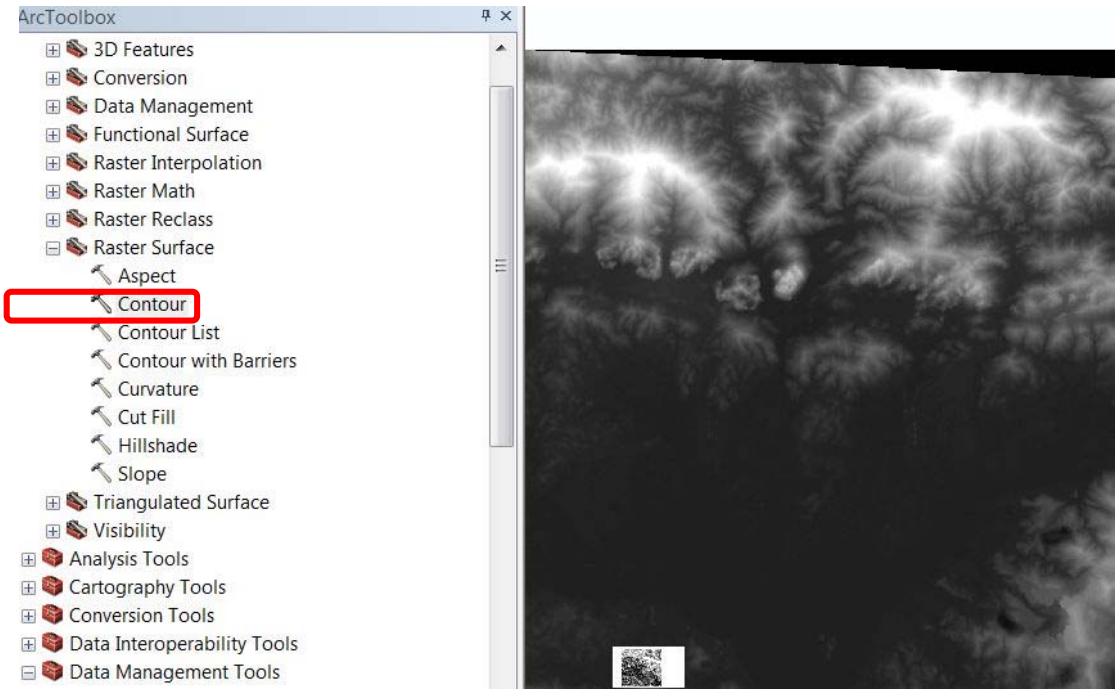

Fig. 3 Making cotour

In the ‘Contour’ box,

(1) Select “your flie” in the drop down box under ‘Input raster’.

(2) Name the file.

(3) Put ‘10’ (or your own choice) in the ‘Contour interval’.

(4) Keep the defaults for the remaining boxes.

(5) Click ‘OK.’

(6) A box showing the progress for the task will appear. When it is finished running, close the programming box.

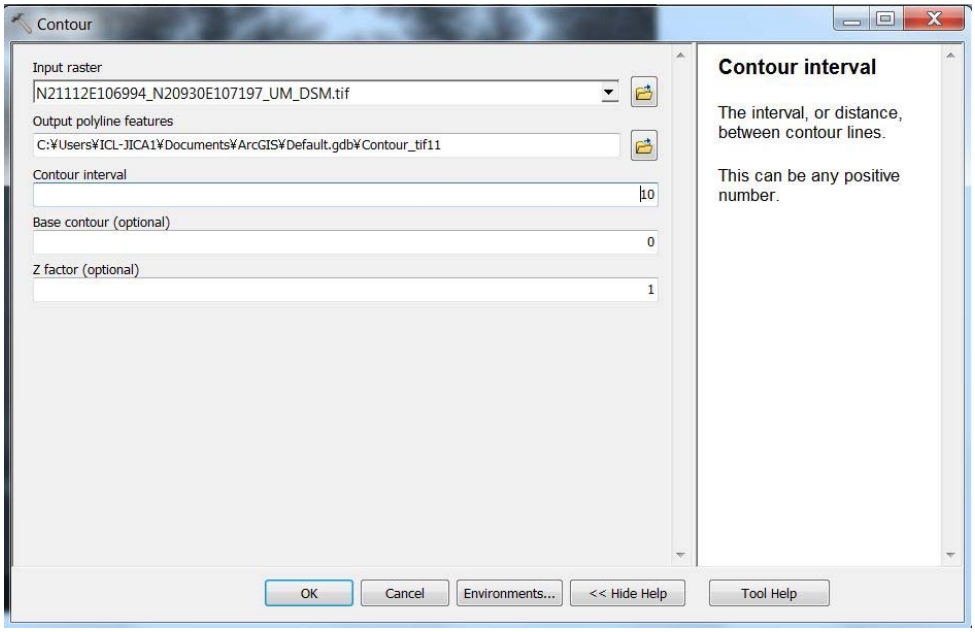

Fig. 4 Cotour information

Raster data is converted into vector data—contour lines.

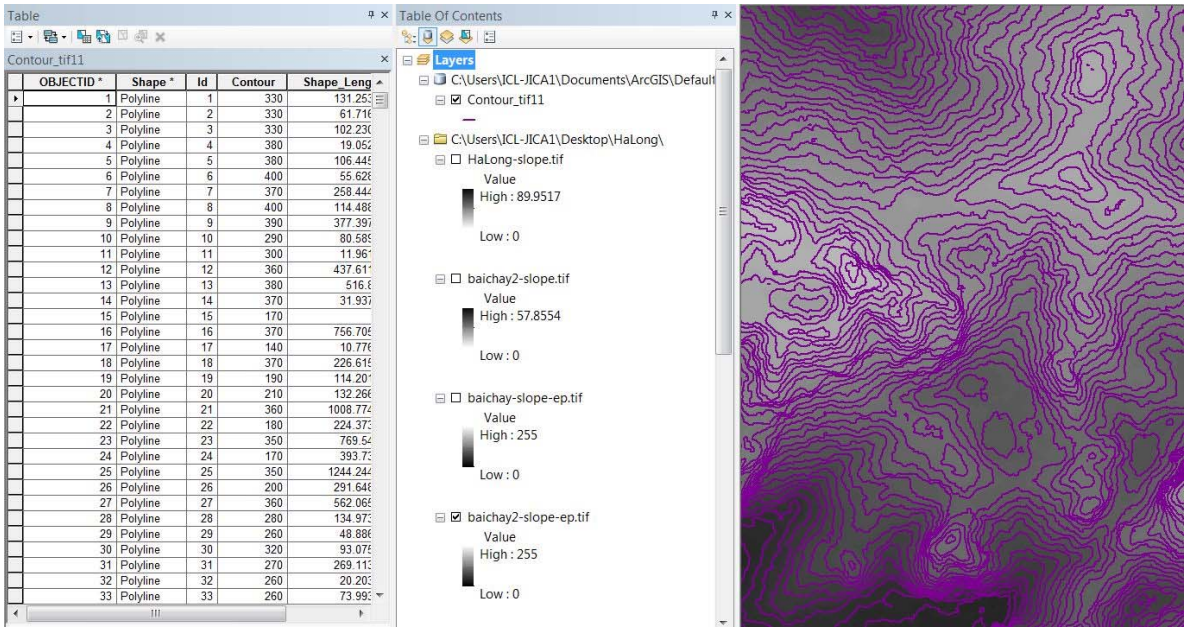

Fig. 5 Cotour map

8. Right click on contour-tif11.shp to open the attribute table.
9. Highlight a line and notice that the corresponding line on the map is highlighted.

3.3.2 Slope (Grid)

Examing slope tells you how steep the terrain is—this kind of output can then be analyzed and used for a variety of determinations such as potential landslide areas, likelihood of flooding, best places to locate buildings, etc. What the software is doing in this case is calculating the maximum rate of change between each raster cell and its neighbors. You can calculate your slope output either as percent slope or degree of slope. We will use percent in this example, and our output will bea raster.

From ArcToolbox,

1. Left-click on the plus sign to the left of ‘Spatial analyst.’
2. Left-click on the plus sign to the left of ‘Surface’
3. Double click on ‘Slope.’

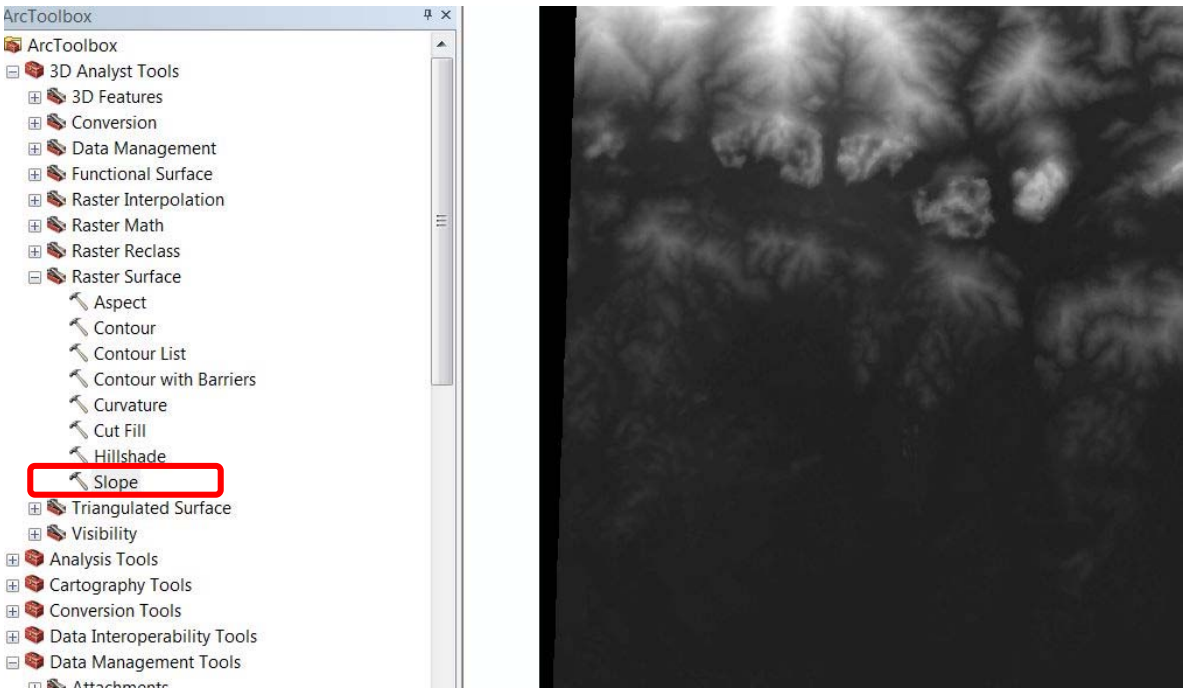

Fig. 6 Making slope

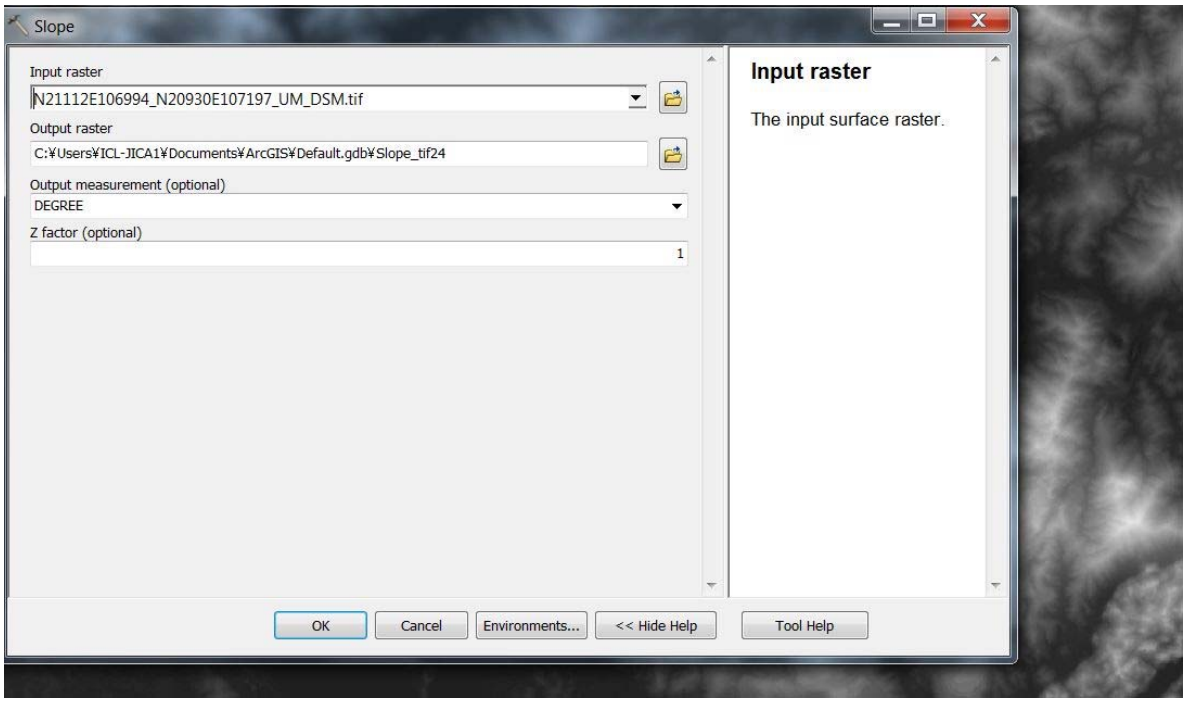

Fig. 7 Slope box

In the ‘Slope box’,

1. Select “your file” in the drop down box under ‘Input raster’.
2. Name the file “your file” .
4. Put “degree or percent rise” in the drop down box under ‘Output measurements’.
5. Keep the defaults for the remaining boxes.
6. Click ‘OK.’
7. A box showing the progress for the task will appear. When it is finished running, close

the programming box.

The resulting output is a slope map of the elevation data. The grid cells have been given new values based on the difference between their elevation value and that of their neighbors. In the example the dark areas are those with the steepest slopes.

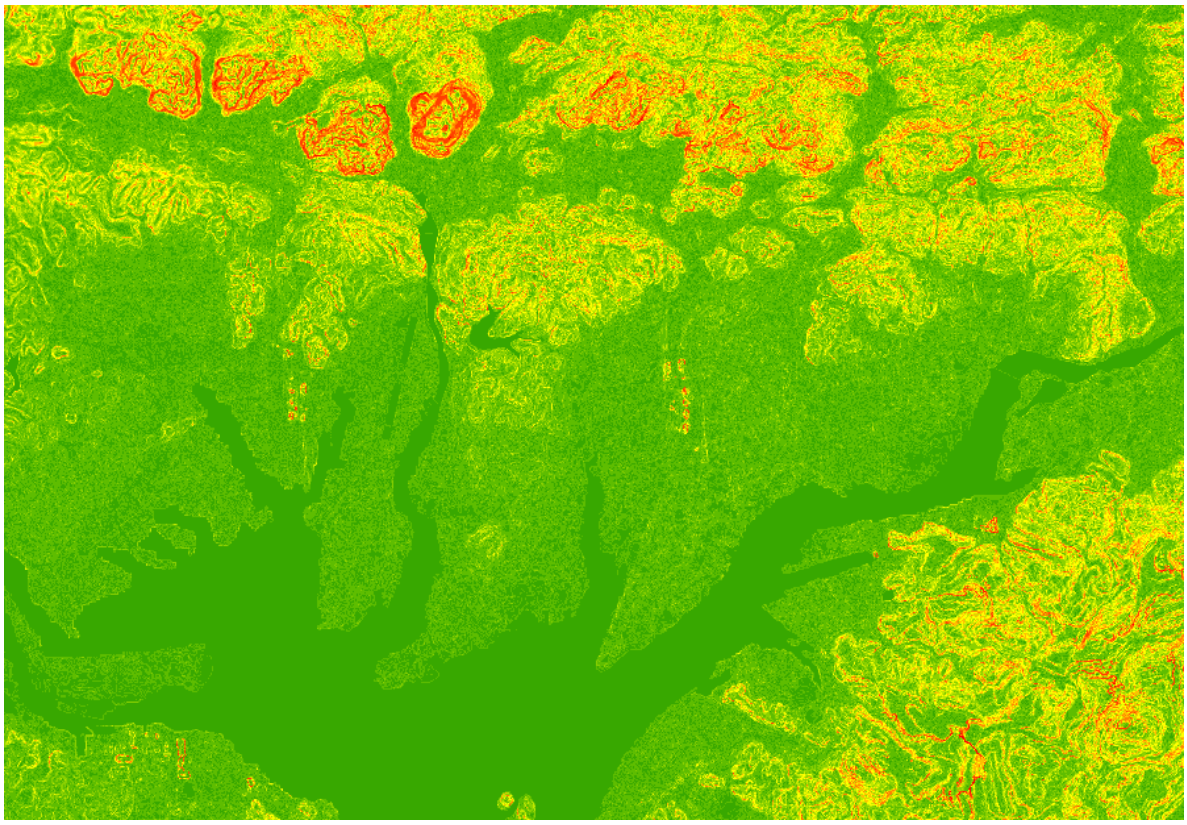

Fig. 8 Slope result of Ha Long area

3.3.3 Hillshape, cutfill, aspect: similar to 3.3.1

3.4. Converstation tool

There are several ways to think about converting raster data in ArcGIS. You may want to convert nonraster data into raster data or vice versa, such as converting a point file into a raster dataset. You may want to convert raster data into another type of raster data, such as changing the file format from .img to .tif, or you may want to change how it's managed, such as converting from a raster catalog to a mosaic dataset.

The majority of the time, you will be using geoprocessing tools to perform your conversion. Sometimes you might be able to interact with the user interface through shortcut menus to access these geoprocessing tools or other menus. For example, you can export raster data from the ArcMap table of contents to another format using the Export dialog box presented via the raster layer's shortcut menu, whereas, in the Catalog window, you can right-click a raster and choose to export it to another format and this will open the Copy Raster tool.

3.4.1 Converting to and from non-raster data

There are a number of core geoprocessing tools that allow you to convert to and from raster data, which are shown in the table below.

Converting data to a raster dataset

Tool	Description
ASCII to Raster	Converts an ASCII file representing raster data to a raster dataset.
Feature to Raster	Converts features to a raster dataset.
Float to Raster	Converts a file of binary floating-point values representing raster data to a rast dataset.
Point to Raster	Converts point features to a raster dataset.
Polygon to Raster	Converts polygon features to a raster dataset.
Polyline to Raster	Converts polyline features to a raster dataset.

Converting data to a raster dataset using tools in the To Raster toolset

3.4.2 Converting a raster dataset to a vector dataset

Tool	Description
Raster to Point	Converts a raster dataset to point features.
Raster to Polygon	Converts a raster dataset to polygon features.
Raster to Polyline	Converts a raster to polyline features.

Converting a raster dataset to a vector dataset using tools in the From Raster toolset

3.4.3 Converting a raster dataset to a file

Tool	Description

Fig. 9 Raster to ASCII

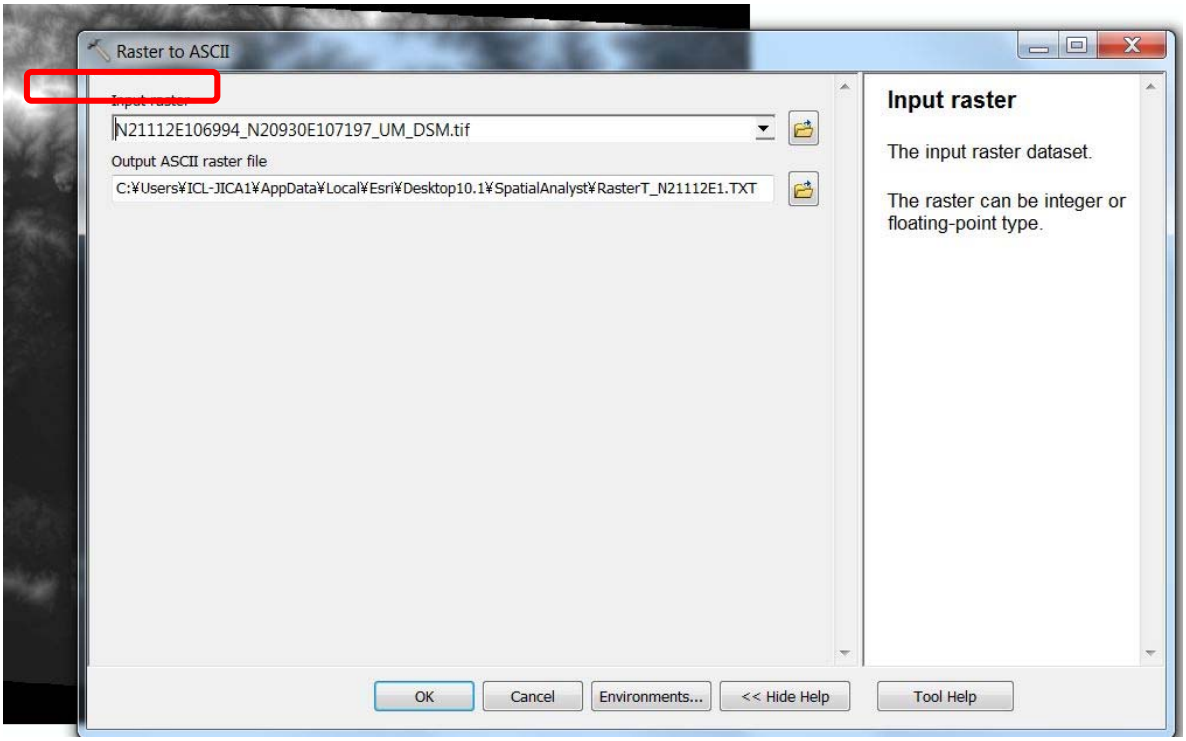

Fig. 10 Raster to ASCII box

4. Application Spatial Analysis for Haivan

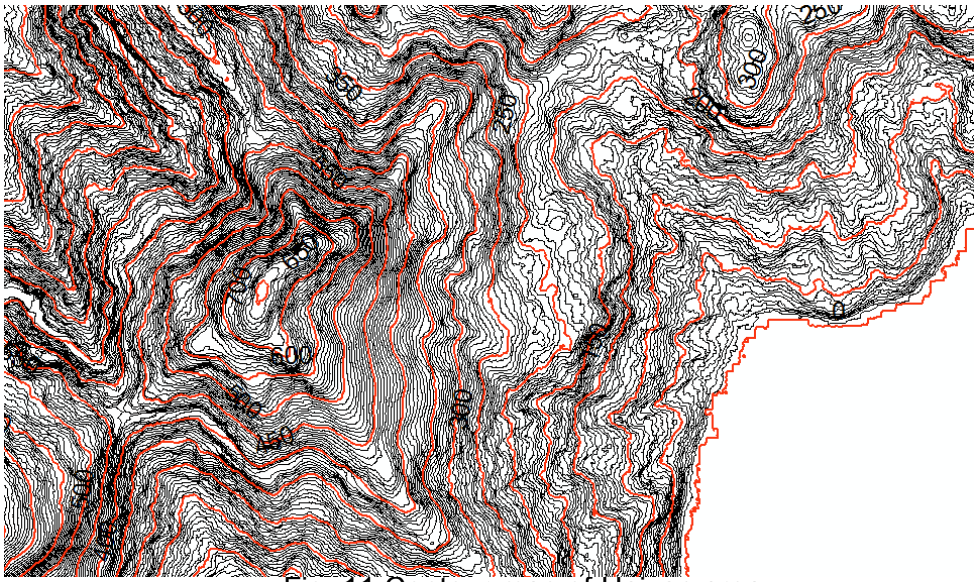

Fig. 11 Contour map of Haivan area

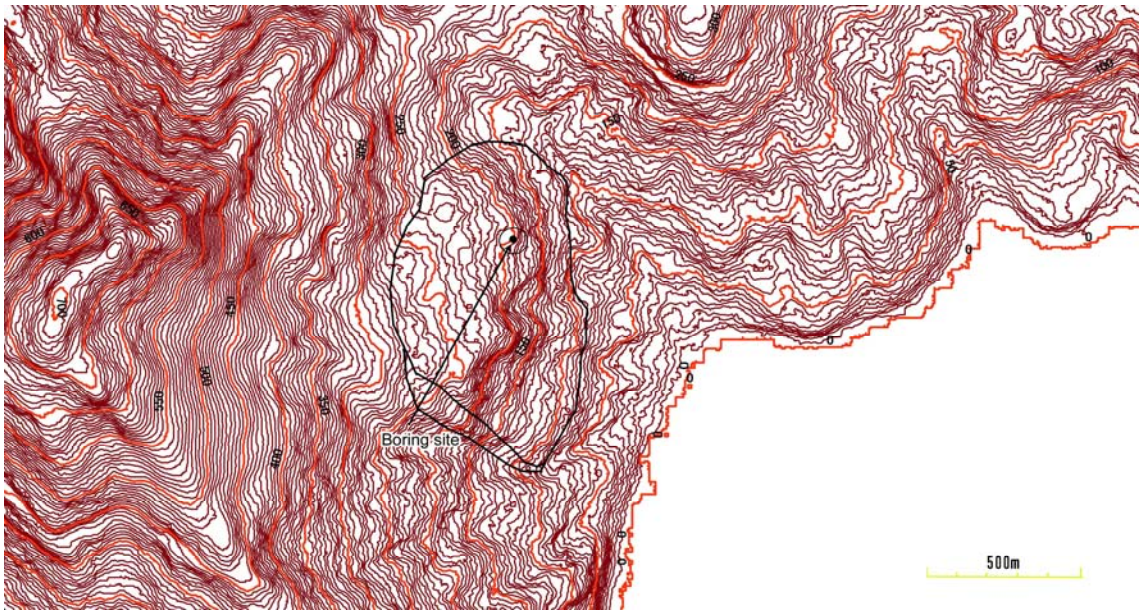

Fig 12. Indentification landslide area based on contour map

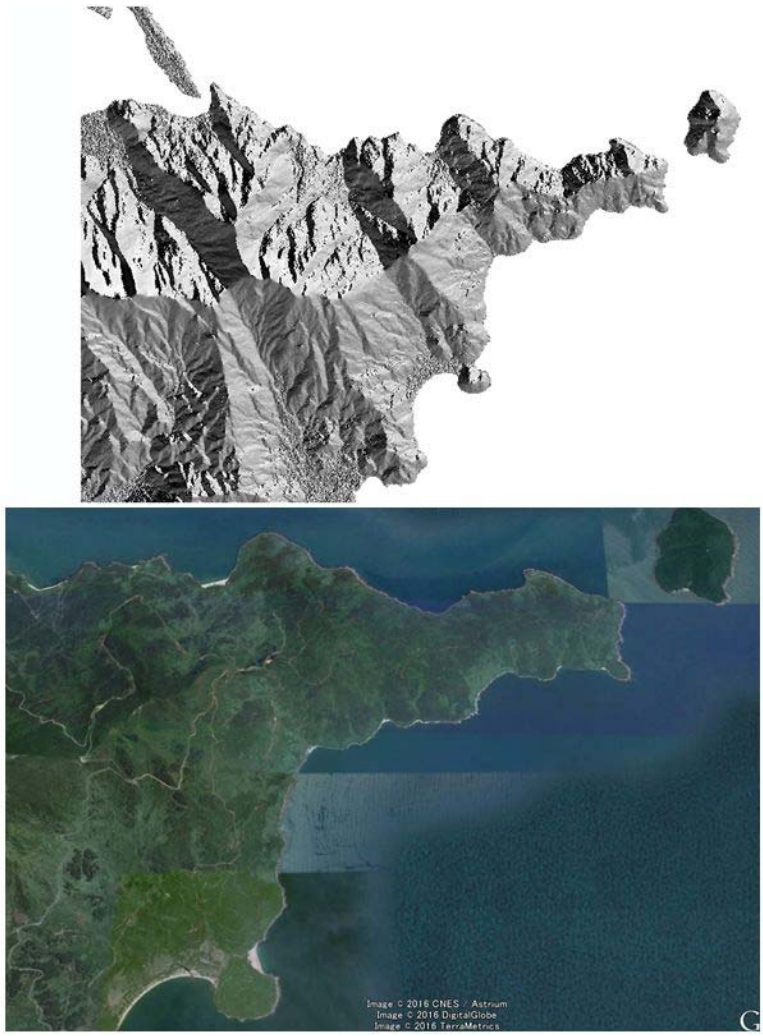

Fig 13. Comparation between google earth and aspect photo in Arc Gis

Capacity Development in SATREPS Project

I. Doctor Degree

1. Le Hong Luong - Doctor of Philosophy (PhD.)

Work Group: WG2
School: Graduate School of Human Informatics, Tohoku-Gakuin University.
Title of Doctor Dissertation: Large scale landslide risk evaluation by aerial photograph interpretation and integrated AHP approach for humid tropical region based on Japan and Viet nam field surveys
Date of certification: 24th March, 2016
Abstract of Dr. Dissertation: He carried the study of landslide mapping and complete the large scale landslide topographic area mapping. On the way of mapping, he had been accumulate the field investigation and photo interpretation skill. The integrated inspection sheet for evaluate the risk of landslide reactivation established. Among the landslide reactivation, geological era, weathering characteristics are very important contributions that is also clarified.

2. Dinh Van Tien - Doctor of Philosophy (PhD.)

Work Group: WG2
School: Graduate School of Human Informatics, Tohoku-Gakuin University.
Title of Doctor Dissertation: Vulnerability of Landslide Hazard in Tropical Region
Date of certification: 30th July, 2016
Abstract of Dr. Dissertation: The comprehensive study for the mitigation of landslide hazard in humid tropical region has been carried. That is the facts finding the actual disasters, the mechanism base typology, the risk and the susceptibility evaluation of landslide hazard by fuzzy and AHP approach. The research is successively completed. The skill and knowledge will be very useful for landslide hazard mitigation in all Humid Tropical Regions.

3. Dang Quang Khang - Doctor of Philosophy (PhD.)

Work Group: WG3
School: Graduate School of Engineering, Kyoto University, Japan
Title of Doctor Dissertation: Development of a new high-stress dynamic-loading ring-shear apparatus and its application to large-scale landslides
Date of certification: 24th September, 2015
Abstract of Dr. Dissertation: The main objective of this research is to develop a new high-stress dynamic-loading ring-shear apparatus for studying deep-seated landslides. There are three specific objectives as follows: (1)Development of the new high-stress dynamic-loading ring-shear apparatus, ICL-2; (2) Application of the new apparatus to conduct tests on samples taken from two real landslides including one case in Japan and one in Vietnam; (3) Application of the measured parameters obtained from ICL-2 for the mechanical modelling to historical 1792 Unzen-Mayuyama megaslide in Japan and landslide hazard assessment of a recent Hai Van station large-scale landslide in Vietnam.

II. Doctor Candidates

1. Ngo Doan Dung

Work Group: WG2
School: Graduate School of Human Informatics, Tohoku-Gakuin University, Japan.
Tentative Title of Doctor Dissertation: The Integrate Approach of Landslide Hazard Mitigation along the Road Side in Central Viet Nam.

Base Reports for Doctor Dissertation:

Dung N.D, Tien D. V., Khang N.X (2016), The current manual and standards for the survey and design works for Landslide prevention in Vietnam - Transactions, Japanese Geomorphological Union, vol.37-1, pp. 5-31.

Dung N.D., T. Miyagi, L.H. Luong, E. Hamasaki, K. Hayashi, Tien D.V (2016), Trial of landslide topography mapping using W3D data – Case study along the National Road No. 7 in central Vietnam, Transactions Japanese Geomorphological Union, p.127-140, vol.37-1.

Dung, N.D., T. Shibasaki, T. Miyagi and E. Hamasaki (2016), Residual strength characteristics of weatherd rocks in Central Vietnam. (Submitting now)

Dung, N.D., T. Miyagi and E. Hamasaki, T. Shibasaki,K. Hayashi, Tien, D.V., and Luong, L.H. (2016), Study of new road side landslide disaster management structure in Vietnam. (Submitting now)

2. Pham Van Tien

Work Group: WG3
School: Graduate School of Engineering, Kyoto University, Japan
Tentative Title of Doctor Dissertation: Failure mechanism and dynamic process of rainfall-induced landslides in Asian Countries
Base Reports for Doctor Dissertation:

Pham Van Tien, Kyoji Sassa, Kaoru Takara, Khang Dang, Le Hong Luong, Nguyen Duc Ha (2016) Simulating the Formation Process of the Akatani Landslide Dam Induced by Rainfalls in Kii Peninsula, Japan. Proceeding of the 4th World Landsides Forum, in Slovenia, June, 2017 (under reviewing).

Pham Van TIEN, Kyoji SASSA, Kaoru TAKARA, Khang DANG, Hendy SETIAWAN, Nguyen Duc HA (2016) Mechanism of large-scale deep-seated landslides induced by rainfall in gravitationally deformed slopes: A case study of the Kuridaira landslide in Kii Peninsula. Landslide Dynamics: ISDR-ICL Landslide Interactive Teaching Tools, Text-tool 5.081-5.22 (Under reviewing).

Pham Van Tien, Kyoji Sassa, Kaoru Takara, Hendy Setiawan, Hiroshi Fukuoka, Khang Dang, Tatsuya Shibasaki, Nguyen Duc Ha, Lam Huu Quang, Doan Huy Loi (2017) Failure mechanim and dynamic process of deep-seated rapid landslides induced by Typhoon Talas (Writting).

Le Hong Luong, Miyagi Toyohiko, Pham Van Tien (2016). Mapping of large scale landslide topographic area by aerial photograph interpretation and possibilities for application to risk assessment for the Ho Chi Minh route – Vietnam. "Transactions, Japanese Geomorphological Union", pp. 97-118.

Khang Dang, Kyo Sassa, Hiroshi Fukuoka, Naoki Sakai, Yuji Sato, Kaoru Takara, Lam Huu Quang, Doan Huy Loi, Pham Van Tien, Nguyen Duc Ha, (2016), Mechanism of two rapid and long-runout landslides in the 16 April 2016 Kumamoto earthquake using a ring-shear apparatus and computer simulation (LS-RAPID). (Online)

Doan Huy Loi, Lam Huu Quang, Kyoji Sassa, Kaoru Takara, Khang Dang, Nguyen Kim Thanh, Pham Van Tien (2016), The 28 July 2015 rapid landslide at Ha Long city, Quang Ninh, Vietnam. (Submitting now)

3. Lam Huu Quang

Work Group: WG3
School: Graduate School of Engineering, Kyoto University, Japan
Tentative Title of Doctor Dissertation: Risk Assessment of a Precursor Stage of Landslide: A case study of the Haivan Station Landslide in Vietnam.
Base Reports for Doctor Dissertation:

Dang K, Sassa K, Fukuoka H, Sakai N, Sato Y, Takara K, Lam H Q, Doan H L, Pham V T, Nguyen D H (2016) Mechanism of two rapid and long runout landslides in the 16 April 2016 Kumamoto earthquake using a ring-shear apparatus and computer simulation (LS-RAPID), Landslides (published online first. DOI: 10.1007/s10346-016-0748-9).

Lam H Q, Doan H L, Sassa K, Takara K, Dang K, Abe S, Asano S (2016) Risk Assessment of a Precursor Stage of Landslide Threatening the Haivan Railway Station in Vietnam (Submitted to Landslides).

Doan H L, Lam H Q, Sassa K, Takara K, Dang D, Nguyen K T ,Pham V T (2016) The 28 July 2015 rapid landslide at Ha Long city, Quang Ninh, Vietnam (Submitted to Landslides).

4. Do Ngoc Ha

Work Group: WG4
Shool: Graduate School of Engineering, Kyoto University, Japan
Tentative Title of Doctor Dissertation: Research on landslide mechanism of weathered granite slope in Hai Van mountain, Central Vietnam
Base Reports for Doctor Dissertation:

Do Ngoc Ha, Hirotaka Ochiai: Flume exeriment to simulate landslide initiation process of weathered granite slopes in Hai Van mountain, Central Vietnam (writing)

Shiho Asano, Do Ngoc Ha: Assessment of landslide using the real-time monitoring on Hai Van Station Landslide, in Central Vietnam (writing)

Shinro Abe, Do Ngoc Ha: Topographic and geological features of weathered granite slope in Hai Van mountain (writing)

Do Ngoc Ha, Masao Yamada, Shiho Asano, Osamu Nishimura, Hirotaka Ochiai: The hydro-geological structure of the weathered granite in Hai Van Station Landslide (writing)

5. Doan Huy Loi

Work Group: WG3
School: Graduate School of Engineering, Kyoto University, Japan
Tentative Title of Doctor Dissertation: Landslide Risk Assessment in urban areas.
Base Reports for Doctor Dissertation:

Khang Dang, Kyo Sassa, Hiroshi Fukuoka, Naoki Sakai, Yuji Sato, Kaoru Takara, Lam Huu Quang, Doan Huy Loi, Pham Van Tien, Nguyen Duc Ha, (2016), Mechanism of two rapid and long-runout landslides in the 16 April 2016 Kumamoto earthquake using a ring-shear apparatus and computer simulation (LS-RAPID). (Online)

Doan Huy Loi, Lam Huu Quang, Kyoji Sassa, Kaoru Takara, Khang Dang, Nguyen Kim Thanh, Pham Van Tien (2016), The 28 July 2015 rapid landslide at Ha Long city, Quang Ninh, Vietnam. (Submitting)

6. Nguyen Kim Thanh

Work Group: WG3, Project secretary
School: Graduate School of Human Informatics, Tohoku-Gakuin University
Tentative Title of Doctor Dissertation: research application unnamed aerial vehicles (UAV) for landslide survey along transport arteries in Viet Nam.
Base Reports for Doctor Dissertation:

Doan Huy Loi, Lam Huu Quang, Kyoji Sassa, Kaoru Takara, Khang Dang, Nguyen Kim Thanh, Pham Van Tien (2016), The 28 July 2015 rapid landslide at Ha Long city, Quang Ninh, Vietnam. (Submitting now)

Nguyen Kim Thanh (2016), Experience of Landslide Trainees in Japan – proposal for application unnamed areal vehicle (UAV) for landslide survey along transport arteries in Viet Nam. Proceedings SATREPS 2016

Dr. Dinh Van Tien, MSC Nguyen Kin Thanh (2016) Vietnam-Japan SATREPS Project `Development of landslide risk assessment technology along transport arteries in Vietnam` and its impact to the Vietnamese society. Proceedings SATREPS 2016

III. Master Degree

1. Vu The Truong

Work Group: WG4
School: Shizuoka University, Japan
Title of Master Thesis: Initiation of shallow landslide using a model for unsaturated infiltration: application to the sediment disaster in Izu-Oshima island caused by the typhoon Wipha, 2013
Date of certification: 18th September 2015
Abstract of Master thesis: In October 2013, typhoon Wipha passed over the island of Izu-Oshima, bringing heavy rainfall (more than 800 mm in 24 hours) that triggered shallow flow-type landslides along the slopes of the western side of Mihara Mountain. Thirty nine people died and are missing, and more than 70 houses were

destroyed in the resulting extensive shallow landslides and following debris flows. Many trees, surface soil and volcanic ash deposition were transported by debris flows and reached the sea. The main objective of this research is to study the influence on the infiltration of heavy rainfall and the resulting in groundwater level rising, and to estimate the generated location of shallow landslide. With the actual rainfall data and slope material properties, the numerical simulation by the saturated-unsaturated flow theory was conducted to estimate during rainfall infiltration in this research. Factor of safety and the location of shallow landslide in both case without groundwater and with groundwater level after 20 hours of rainfall duration were obtained. The location of shallow landslide with groundwater level rising accorded with the location of the actual failed slope of the site. This result is important for explaining the initiation mechanism of the shallow landslides in Izu-Oshima island.

2. Do Ngoc Ha

Name: Do Ngoc Ha – Master of Science & Engineering
Work Group: WG4
School: Geoscience Course at the graduate school of Science and Engineering of Shimane University, Japan
Title of Master Thesis: Mechanical characteristics of the August 6, 2012 Mihata landslide, Shimane Prefecture, Japan
Date of Conferral: September 26, 2014
Abstract of Master Thesis: The study is focus on researching the mechanism of the Mihata landslide in Izumo city, Shimane Prefecture, Japan occurred on 6 August, 2012. Field investigation and setting the monitoring system were conducted to examine the mechanical characteristics of this landslide. A series of direct shear tests, triaxial tests, and ring shear tests were conducted to analysis the shear resistance behavior of the Mihata landslide's samples. LS-RAPID software was used to simulate the initiation and movement of the landslide.

3. Doan Huy Loi

Work Group:3
School: Graduate School of Engineering, Kyoto University, Japan
Title of Master Thesis: Study on the 2014 Hiroshima Landslide Disasters Using Ring Shear Apparatus and an Integrated Simulation Model
Date of certification: 23/3/2015
Abstract of Master thesis:

On August 20, 2014 many landslides and debris flows occurred in Hiroshima city during the heavy rainfall. This disaster claimed 74 dead, 255 houses damage and a total of 4,576 houses were affected (MLIT). The cumulative rainfall from 20:30 PM of 19 August until 04:30 AM of 20 August reached 248 mm at Miiri rain gauge station in Hiroshima. This is main reason caused the Hiroshima disasters.

The main objectives of this research are to study the initiation mechanism and motion behavior of the Hiroshima landslides triggered by heavy rainfall. Ring shear apparatus (ICL-1) was used to simulate the failure of soils, the formation of sliding surfaces and the steady-state motion of landslides. Ring shear apparatus (ICL-1) was developed by the International Consortium of Landslide (ICL) for Croatia. It can reproduce the natural process of landslide with undrained condition up to 1 MPa of pore water pressure and load normal stress up to 1 MPa. Samples were taken from source area in Midorii and Yagi district. The ring shear tests on Midorii and Yagi samples were carried out under the normal stress of 50 and 100 kPa that assumed the landslide depth from 4 to 8 m.

Landslide occurred in head scarp and it rode on the debris deposits. The debris deposits were sheared and moved together with the landslide mass. Landslide triggered debris flow plays a key role on the occurrence and motion of debris flows in Hiroshima disasters. This process can be reproduced using undrained dynamic loading test of ring shear apparatus.

The triggering factor such as pore-water pressure was calculated by using the Slope-Infiltration-Distributed Equilibrium (SLIDE) model that developed by Liao and Hong et al., (2010, 2012). The rainfall record monitored at the Miiri JMA station for each 10 minutes from 8:30 PM on August 19, 2014 was used to calculated pore-water pressure and landslide occurred when pore-water pressure reached 15.2 kPa.

All test results were input to an integrated simulation model (LS-RAPID) as dynamic parameter of landslide. The combination of landslide ring shear simulator and integrated landslide simulation model

provides a new tool for landslide assessment. The hazard area and time of occurrence in Hiroshima disaster were estimated by LS-RAPID. The estimated hazard area is similar with landslide moving area reported by Geospatial Information Authority of Japan (GSI).

From simulation results, three source heads collapse in Yagi district. Local failure of Yagi-1 occurred on August 20, 2014 at 3:18:00. Landslide block was formed and its destruction was expanded, it started to move as a whole at 3:21:02. The mass movement shaved the end of the middle slope in Yagi district (Yagi-2) at 3:21:16 and the collapse was expanded to the upper slope at 3:21:21. The combination of Yagi-1 and Yagi-2 flowed into the residential area. In addition, three landslides occurred at the source head of Midorii. According simulation results, the occurrence period agrees reasonably with the report of Hiroshima city office. This research will contribute to understanding the mechanism of landslide and debris flow during heavy rainfall as a basic knowledge for disaster prevention.

4. Pham Thi Chien

Work Group: Group 4
School: Shimane University, Japan
Title of Master Thesis: Evaluating the effect of heavy rainfall on groundwater level change and stability of the Sorayama landslide, Shimane prefecture, Japan
Date of certification: 24 September, 2015
Abstract of Master thesis:

The objectives of this study are to evaluate the effect of heavy rainfall on the stability of slopes considering variations in groundwater level. A landslide which occurred in 2013 near Matsue city in Shimane prefecture of Japan was chosen as a typical case study. This study has three main parts: field investigation, laboratory tests, and simulation of change in groundwater level and slope stability of a representative landslide using Vadose/W and Slope/W software. In the first part, field investigations were carried out to examine the general properties of the landslide. Some investigation methods were applied such as microtremor survey method, self-potential method and 1-m depth temperature method to understand the geological structure and groundwater flow within the landslide. In the second part, disturbed samples were taken from the landslide to determine the mechanical and physical properties of soil layers. These tests are water content test, specific gravity test, Atterberg limits test, grain size distribution test, direct shear test, triaxial shear test. In the last part, firstly, Vadose/W was used to analyze the infiltration process and variation of groundwater level in the slope due to rainfall, as well as considering transpiration, evaporation and runoff on the surface. A two dimensional model was set up to simulate the longitudinal section of the slope before the landslide occurred. The input data included basic soil parameters, climatic data, initial piezometric head and vegetation condition. Finite element method (FEM) was used to simulate the soil behavior. Furthermore, Slope/W was used to evaluate the stability of the slope during groundwater level change from results in Vadose/W.

5. Pham Van Tien

Work Group: WG3
School: Graduate School of Engineering, Kyoto University, Japan
Title of Master Thesis: Analyzing Failure Characteristics and Potential of Landslides in Hai Van Mountain, Vietnam
Date of certification: March 23, 2015.
Abstract of Master thesis: This study aims: (1) to explore failure characteristics and contributing factors of slope failures in weathering granitic rocks region in Hai Van Mountain, (2) to study landslide mobility for understanding characteristics of landslides through physical simulation of landslide initiation and motion by using ring shear apparatus ICL-1 and (3) to assess potential occurrence of landslides in study area. The followings are some findings in this research.

1. In Hai Van Mountain, slope failures are mostly characterized by rotational-transitional form or slump type with various extents (shallow or large-scale deep-seated landslides). Hai Van landslides were induced by combination of contributing factors including climatic, morphological and geological conditions of weathered granitic area as well as triggering factor (extreme rainfalls).

2. Ring shear test results revealed that the mechanism of rapid motion of the landslides only occurs in the HV2 sample (less weathered granitic rock sample). In contrast, HV1 sample (strong weathered granitic rock sample) has not shown a mobility behavior. So it can be understand that, landslides of HV1 sample cannot

move at a high velocity, while landslides of HV2 sample will be characterized by a high velocity movement during motion.

3. In addition, an assessment of potential occurrence of landslides based on un-drained ring shear simulations shows that failures are more likely to occur on slopes of less weathering granitic rocks than those in slopes of strong weathering granitic rocks, due to lower shear strength parameters of the sample in the less weathering granitic rocks regions.

Ring-shear Apparatus

Landslide Flume

Monitoring Equipment

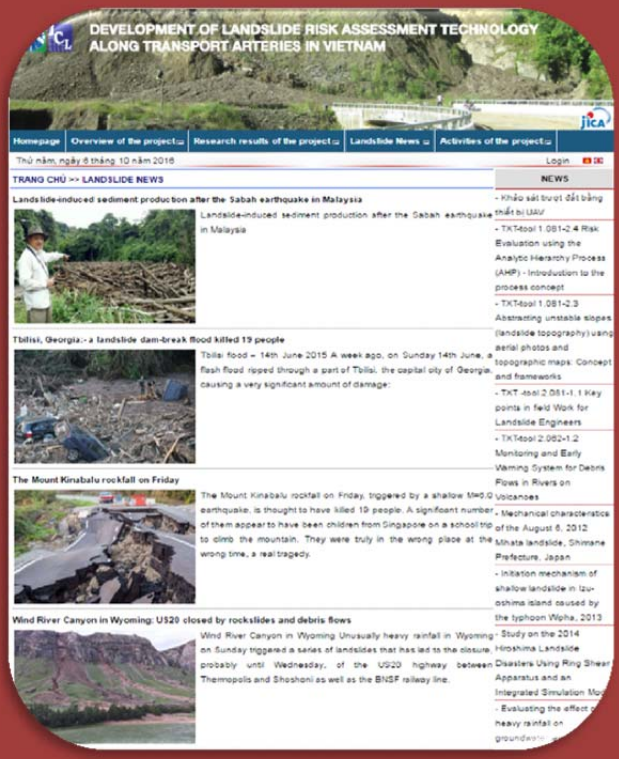

Project Website

ISBN: 978-4-9903382-3-7
October 2016